

I.O.S.

ESTIMATES OF EXTREME CURRENT SPEEDS
OVER THE CONTINENTAL SLOPE OFF SCOTLAND

BY
D.J.T. CARTER, J. LOYNES AND P.G. CHALLENGOR

REPORT NO. 239
1987

NATURAL ENVIRONMENT
INSTITUTE OF
OCEANOGRAPHIC
SCIENCES
RESEARCH
COUNCIL

I.O.S.

ESTIMATES OF EXTREME CURRENT SPEEDS
OVER THE CONTINENTAL SLOPE OFF SCOTLAND

BY
D.J.T. CARTER, J. LOYNES AND P.G. CHALLENGOR

REPORT NO. 239
1987

NATURAL ENVIRONMENT
INSTITUTE OF OCEANOGRAPHIC SCIENCES
RESEARCH COUNCIL

INSTITUTE OF OCEANOGRAPHIC SCIENCES

WORMLEY

Estimates of extreme current speeds
over the continental slope off Scotland

by

D.J.T. Carter, J. Loynes* and P.G. Challenor

I.O.S. Report No. 239

March 1987

The preparation of this report was supported financially by the Department of Energy.

* *Present address:*

*Cranfield Institute of Technology
School of Management
Cranfield
BEDS. MK43 0AL*

CONTENTS

	<u>Page</u>
SUMMARY	5
1. INTRODUCTION	7
2. METHOD OF ANALYSIS	9
2.1 Probability distribution of resolved speed	9
2.2 50-year return value of resolved speed	11
2.3 Probability distribution and extreme value of total speed	11
3. APPLICATION TO THE CONSLEX DATA	13
3.1 General description of the data sets	13
3.2 Maximum observed current speeds	14
3.3 Probability distributions of current speeds and estimates of return values	15
4. CONCLUSIONS	18
REFERENCES	20
TABLES	
1. CONSLEX mooring sites	21
2. CONSLEX current meter records	22
3. Estimates of 50-year current speeds	24
FIGURES	
1. CONSLEX mooring sites	27-29
2. Probability distribution functions of residual and tidal current speeds	31-83
3. Cumulative probability distributions of residual current speed	85-137
4. Joint probability distributions of tidal and residual currents	139-143

SUMMARY

A method for estimating return values of current speed from time-series data, based upon the convolution of tidal and non-tidal (residual) components, is described. It is applied to the CONSLEX data set of measurements obtained over the Continental Slope to the northwest of the UK during 1982-83, to obtain estimates of 50-year return values of hourly mean speed along-slope, cross-slope and omni-directional.

The method depends upon the speed of the tidal component being at least comparable with the residual component. This condition is found to hold at most CONSLEX sites west of 4°W but usually not at sites to the east of 4°W.

Histograms are presented showing the observed probability distributions of tidal and residual components of current speed and their convolutions along- and cross-slope for each CONSLEX current meter data set.

1. INTRODUCTION

As exploration for offshore oil and gas resources moves into deeper waters, so the need for estimates of extreme currents also extends into them. In particular, designers of offshore structures require estimates of extreme speeds over the continental slope to the West and North of Scotland in order to assess the feasibility and design of rigs there, where water depths are between 200m and 1000m.

Estimating extreme values of environmental parameters (such as the 50-year return value of wind speed or wave height) generally requires many years of measurements or the use of a well-validated model. Neither is available for estimating ocean currents on the UK continental slope. Fortunately, the forcing periods of the tides are well-established and extreme tidal speeds can be calculated from considerably shorter series of measurements.

If the tidal component is a significant portion of the extreme total current speed, then - as pointed out by Pugh and Vassie (1980) - estimates of extreme values can be made from relatively short data sets. This report develops a method for doing so, and applies it to estimate 50-year return values of hourly mean current speed from the Continental Slope Experiment (CONSLEX) measurements obtained between August 1982 and April 1983 from twenty moorings laid on the slope to the West and North of Scotland (Gould, 1982). The locations of these moorings are shown in Figure 1. Their co-ordinates are given, along with the water depth at each mooring, in Table 1.

Estimating extremes from records covering only about seven months is clearly unsatisfactory, particularly as we have only a limited understanding of the physics of some components of the total current. However, the tidal constituents are obtainable, with good accuracy, from the CONSLEX data; so, where the tidal stream contributes a significant portion of the total current, we might expect a reasonable estimate for the extreme speed - although it is not possible to put confidence limits upon the value - but at some current meters the tide turns out to be relatively small and here the estimates are questionable.

2. METHOD OF ANALYSIS

2.1 Probability distribution of resolved speed

Given a data series of current speed resolved in a specified direction, such as the easterly component of mean values at hourly intervals, and assuming the series is sufficiently long to estimate the tidal component, then the total speed in the specified direction at any hour, U , can be expressed as a tidal component, U_t , and a residual U_r :

$$U = U_t + U_r$$

and histograms can be constructed showing estimates for the probability distributions of U_t and U_r , p_t and p_r .

Assuming the tidal and residual components are independent, then the probability distribution of U , p_{t+r} , is given by a convolution of p_t and p_r , defined by

$$p_{t+r} = \int_{-\infty}^{\infty} p_t(x-z) p_r(z) dz \quad (1)$$

(Feller, 1971, p.144)

It readily follows that the Fourier transform of p_{t+r} equals the product of the transforms of p_t and p_r , that is:

$$p_{t+r}^* = p_t^* \cdot p_r^* \quad (2)$$

where $*$ denotes Fourier transform. Equation 2 provides an efficient method for calculating p_{t+r}^* from p_t and p_r , and hence, by an inverse Fourier transform, for calculating p_{t+r} .

4. CONCLUSIONS

An inspection of the bracketed (more dubious) estimates in Table 3 for the 50-year return value of hourly mean current speed, U_{50} , indicates that the method proposed in this report might be expected to give reasonable results at CONSLEX sites A to E, but further North at F and G (except at F1 and G1 in less than 200m) the method is less satisfactory; the tidal components are here considerably weaker than the residual currents and often these residuals do not appear to be normally distributed.

The highest estimate for U_{50} from the analysis of the CONSLEX data is 133 cm/s for mooring E4 at 111m, with a water depth of 1015m. This was where the highest recorded current speed of 117 cm/s was obtained. Fig. 3 (E4, 111m) shows apparently anomolous residuals along-slope, towards the North East approaching 100 cm/s, which convolve with the along-slope tidal stream exceeding 30 cm/s. The origin of these anomolous residuals, perhaps associated with the oceanic front separating deep and coastal waters, requires further investigation.

Nearby at E3 at 725m, the estimated value of U_{50} is 94 cm/s while the maximum recorded current speed was 100 cm/s; the greatest recorded residual happened to occur within a few hours of the maximum recorded tide.

At the deep water site of I2, which is off the slope in a depth of 1463m, the method does not give satisfactory estimates of U_{50} at the two current meters below 1000m because the tidal components are small compared to the residuals. The method appears to be reasonable at shallower depths.

2.2 50-year return value of resolved speed

Defining the 50-year return value of hourly mean speed, U_{50} , as that which is exceeded on average once in 50 years, then it is given by

$$\text{Prob}(U_{50} < U) = 1 - 1/(365.25 \times 24 \times 50)$$

ie.

$$\text{Prob}(U_{50} < U) \approx 0.99999772 \quad (3)$$

Hence U_{50} may be calculated given the distribution p_{t+r} - or rather two values, one from each tail of p_{t+r} , giving the 50-year speed in opposite directions.

With the definition for U_{50} , in terms of only the average interval between exceedances, its value is not affected by any correlation between the data. However, given positive correlation between successive hourly mean values, exceedances of U_{50} will tend to come together, while maintaining the average interval between exceedances of 50 years. So if the 50-year return value is defined as that which is exceeded at least once during one year in 50, then it would have a slightly lower value than that given by (3). However, Pugh and Vassie (1980) examined the effect of correlation upon estimates of return values of surface elevation and decided that any such reduction would in practice be insignificant.

2.3 Probability distribution and extreme value of total speed

Suppose U and V are current speeds resolved orthogonally so that total speed W is given by

$$W = \sqrt{U^2 + V^2}$$

Then, the distributions of U and V can be estimated from data as described above. In theory the distributions of U^2 and V^2 can then be estimated and convolved to give the distribution of W^2 and hence of W (assuming U^2 and V^2 are independent). However, the sizes of the arrays to accommodate the histograms for the distributions of U^2 and V^2 are too large for practical FFT procedures. So we estimate the distribution of W using the numerical approximation for

$$\text{Prob}(W < w) = \iint \sqrt{U^2 + V^2} p(U, V) dU dV$$

where integration is over all U, V such that $0 < \sqrt{U^2 + V^2} < w$ and $p(U, V)$ is the joint probability distribution of U and V .

i.e.
$$\text{Prob}(W < w) \approx \sum_{i,j} w_{ij} p(U_i, V_j) \delta U \delta V \quad (4)$$

where δU and δV are the bin sizes of the histogram representation of the distributions of U and V and summation is over all bins (i, j) such that $w_{ij} < w$ where w_{ij} is the speed at the mid-point of the (i, j) bin. Assuming U and V are independent, then

$$p(U_i, V_j) \delta U \delta V = \text{Prob}(U_i < U < U_{i+1}) \text{Prob}(V_j < V < V_{j+1}) \quad (5)$$

The 50-year return value of W , W_{50} , is given by

$$\text{Prob}(W_{50} < w) \approx 0.99999772 \quad (6)$$

An alternative method for obtaining the distribution of W was considered: histograms for the distributions of the tidal and residual components of W , W_t and W_r , could be obtained, where

$$W = W_t + W_r$$

and these histograms convolved to obtain the distribution of W . But this method fails because W_t and W_r are not independent - since W cannot be negative.

3. APPLICATION TO THE CONSLEX DATA

3.1 General description of the data sets

The method of analysis described above was applied to the CONSLEX data set of hourly mean current speeds associated with 'spot' measurements of direction. The data were obtained from the IOS Marine Information and Advisory Service data base, including the results of tidal analysis carried out at IOS (Bidston).

The CONSLEX data consists of 53 sets of recordings made by DAFS, IOS and SMBA from 20 moorings, using Anderaa current meters deployed between 23 August 1982 and 31 April 1983 - measurements at one site (I2) extended into May 1983. The sites of these moorings and the notation identifying them are shown in Fig. 1 together with the approximate orientation, θ , of the maximum variance of current velocity.

This orientation was calculated for each meter by a principal component analysis of the current velocity. In general it was found to lie along the slope; the flow seems to be constrained by topography. The direction of the line of maximum variance is not specified by this analysis. The direction arrows shown in Fig. 1 were specified in order to fix the co-ordinate system. The variation in θ between meters at any one mooring was generally within $\pm 10^\circ$, and an average direction is shown in Fig. 1. Where the spread was greater than $\pm 10^\circ$, the range of θ is shown. The 'cross-slope' axis was taken as positive to the right of the along-slope, ie. up-slope. The data were analysed in a co-ordinate system defined by

the value of θ for the individual meter - thus ensuring zero correlation between resolved current speeds - but directions are referred to as 'along-slope' and 'up-slope'. Further details, including the depth of each instrument and the values of θ , are given in Table 2.

Site I2 is not on the slope, but in the Rockall Trough with a water depth of 1463m. Section D is on the Wyville-Thomson Ridge; currents at D5 in particular appear unlike those on the slope, as indicated by the wide range of θ with depth - similar to that at I2.

Records from the current meter at G4 at 496m cover only 34 days, and at B1 (130m) only 58 days. The other meter at B1 and both meters at B2 had to be replaced during October 1982 - with the loss of some days of records at B2.

3.2 Maximum observed current speeds

The maximum mean hourly current speed recorded by each instrument and associated direction are included in Table 2.

The maximum recorded hourly mean current speed was 117 cm/s at E4 at a depth of 111m. The only other measurement exceeding 100 cm/s was at G2 at 151m. Generally the maximum speeds at each mooring tended to decrease with increasing meter depth; an exception was at E3 where 100 cm/s was recorded at 725m. The direction of the maximum speed was usually within about 20° of the direction given by the principal component analysis; a notable exception was that of 66 cm/s at E4 at 950m which was 79° away (down-slope).

3.3 Probability distributions of current speeds and estimates of return values

Using the data from each meter, except B1 (130m) and G4 (496m) with less than two months data, histograms showing the distribution of tidal and residual current speeds along-slope and up-slope were constructed with a bin size of 1 cm/s, or 2 cm/s if a component speed exceeded 100 cm/s. These histograms, together with their convolution are shown in the set of figures: Fig. 2. (Strictly, the histograms should be drawn as step functions, but joining mid-points of the bin values gives a clearer picture.)

Fig. 2 shows that the along-slope flow is generally considerably stronger than the up-slope. It also shows that the residual current is usually stronger than the tidal component - but not, for example, at A1 (145m) and at D1 and D2. Sometimes the residual is very much stronger than the tidal component particularly for the up-slope flow, and the convolution is then a smoothed version of the residual histogram, so the tails of the convolution are dominated by the few calculated extreme residual values, eg. F3 at 388m. In these cases it seems preferable to fit a distribution to the residual histogram and to convolve this distribution with the tidal histogram. The set of figures, Fig. 3, show the Gaussian and Laplacian fits to the cumulative distribution of residual components - scaled such that the Gaussian distribution is linear. Generally the Gaussian distribution appears to be a reasonable fit to the residuals; occasionally the observations in the tails deviate from the straight line, but these are determined by only a few values so their sampling variance is high. Construction of confidence limits would require an analysis of the

correlation structure of the data; but where the data approaches the long-tailed Laplace distribution the use of the Gaussian distribution must be expected to underestimate extreme values.

The fifty-year return values of current speed up- and down-slope and in both directions along-slope were estimated using equation 3 and the convolutions with the residual histograms and the Gaussian fit. Results are shown in Table 3.

Values are given to the nearest bin size, that is ± 2 cm/s for the higher values and ± 1 cm/s for the lower.

Note that the fifty-year return values are given by interpolation of the convolution. No extrapolation is required.

The convolution only gives the distribution of the sum of the tidal and residual components if these components are independent. There is no entirely satisfactory method for testing independence, but examples of the joint distributions of the tide and residual components plotted in the set: Fig. 4 show no obvious dependence. On physical grounds, one might expect negative correlation between tide and residual in shallow water or at current meters close to the sea bed, but none is apparent in Fig. 4, or in other joint distributions which we examined. If there were negative correlation then the convolution would overestimate the fifty-year return values.

Table 3 also includes fifty-year return values of total speed, U_{50} , calculated from equations (4)-(6), and the maximum observed speeds from

Table 2. The choice of θ from the principal component analysis ensures no correlation between the measured 'up-slope' and 'along-slope' speeds. The requirement of (5) is stronger, requiring independence between the two distributions, but this seems a not-unreasonable assumption.

The values for U_{50} from the residual histogram are given in brackets if Fig. 2 suggests that the dominant tail of the component convolution has a negligible tidal contribution. The value of U_{50} from the Gaussian fit is in brackets if Fig. 3 indicates that the dominant residual component is not Gaussian.

4. CONCLUSIONS

An inspection of the bracketed (more dubious) estimates in Table 3 for the 50-year return value of hourly mean current speed, U_{50} , indicates that the method proposed in this report might be expected to give reasonable results at CONSLEX sites A to E, but further North at F and G (except at F1 and G1 in less than 200m) the method is less satisfactory; the tidal components are here considerably weaker than the residual currents and often these residuals do not appear to be normally distributed.

The highest estimate for U_{50} from the analysis of the CONSLEX data is 133 cm/s for mooring E4 at 111m, with a water depth of 1015m. This was where the highest recorded current speed of 117 cm/s was obtained. Fig. 3 (E4, 111m) shows apparently anomolous residuals along-slope, towards the North East approaching 100 cm/s, which convolve with the along-slope tidal stream exceeding 30 cm/s. The origin of these anomolous residuals, perhaps associated with the oceanic front separating deep and coastal waters, requires further investigation.

Nearby at E3 at 725m, the estimated value of U_{50} is 94 cm/s while the maximum recorded current speed was 100 cm/s; the greatest recorded residual happened to occur within a few hours of the maximum recorded tide.

At the deep water site of I2, which is off the slope in a depth of 1463m, the method does not give satisfactory estimates of U_{50} at the two current meters below 1000m because the tidal components are small compared to the residuals. The method appears to be reasonable at shallower depths.

However, because of our lack of knowledge of all the mechanisms producing extreme currents at sites off the continental shelf including their within-year variability, estimates of the 50-year return value of current speed made from data recorded over only a few months must be viewed with caution. Even where the method suggested in this report appears to be satisfactory, further data are needed to confirm its applicability and to put confidence limits upon the results.

REFERENCES

- Feller, W. 1971. An introduction to probability theory and its applications. Vol. 2 (2nd edition) J. Wiley and Sons.
- Gould, W.J. 1982. Currents on the continental slope. MIAS News Bulletin 5, 3-5.
- Pugh, D.T. 1982. Estimating extreme currents by combining tidal and surge probabilities. Ocean Engng. 9, 361-372.
- Pugh, D.T. and Vassie, J.M. 1980. Applications of the joint probability method for extreme sea level computations. Proc. Instn. Civ. Engrs. Part 2, 69, 959-975.

Table 1: CONSLEX mooring sites

Mooring	Latitude (N)	Longitude	Water depth (m)
A1	57° 20.7'	9° 07.2'W	145
A5	57° 18.6'	9° 40.4'W	1614
B1	57° 56.3'	8° 51.0'W	155
B2	58° 00.7'	9° 07.7'W	193
B3	58° 06.5'	9° 33.1'W	504
B4	58° 08.3'	9° 41.2'W	1082
C2	59° 05.4'	7° 27.0'W	514
C3	59° 08.5'	7° 42.4'W	998
D1	59° 39.8'	6° 02.5'W	237
D2	59° 46.7'	6° 10.8'W	370
D5	60° 09.9'	7° 44.5'W	637
E2	60° 13.3'	4° 31.8'W	478
E3	60° 31.2'	4° 56.8'W	1035
E4	60° 46.4'	4° 49.4'W	1015
F1	61° 09.3'	1° 31.7'W	189
F3	61° 24.8'	2° 06.1'W	995
G1	61° 30.7'	0° 02.5'E	191
G2	62° 06.1'	0° 03.9'E	550
G4	63° 08.8'	0° 00.9'W	1611
I2	60° 12.7'	9° 13.3'W	1463

Table 2: CONSLEX current meter records

Mooring	meter depth (m)	days of records	max. recorded speed (cm/s)	hr mean vely. dir ⁿ towards (° from N)	dir ⁿ princ. component (θ°)
A1	55	106	59	031	046
	120	181	44	307	042
A5	209	179	57	347	333
	510	179	45	340	333
	1111	179	49	186	343
	1562	179	33	339	341
B1	55	173	70	033	032
	130	58	61	194	031
B2	43	120	53	023	036
	168	120	47	033	033
B3	104	172	63	035	025
	257	172	54	028	025
	457	169	50	043	036
B4	169	172	53	023	017
	477	172	50	014	019
	1035	172	38	184	013
C2	115	172	82	043	051
	266	172	77	050	048
	468	172	76	037	035
C3	104	172	58	199	041
	403	172	52	049	046
	951	172	46	027	008
D1	87	136	80	054	049
	212	136	82	227	050
D2	120	169	86	078	061
	270	169	79	074	065
	345	169	69	057	066
D5	510	186	88	208	051
	633	186	85	194	007

Table 2 continued

Mooring	meter depth (m)	days of records	max. recorded hr speed (cm/s)	hr mean vely. dir ⁿ towards (° from N)	dir ⁿ princ. component (θ°)
E2	453	162	77	033	047
E3	120	164	95	92	063
	419	164	83	027	052
	725	164	100	212	055
E4	111	184	117	063	053
	950	181	66	158	057
F1	39	163	88	076	081
F3	79	80	89	084	063
	388	161	66	046	035
	694	161	60	244	049
	945	161	66	030	044
G1	41	117	48	133	108
	166	117	33	117	107
G2	151	162	114	073	073
	299	162	89	069	062
	500	162	84	106	079
G4	195	164	64	98	053
	496	34	26	021	028
	1104	164	32	212	051
	1554	164	34	206	044
I2	251	216	60	331	022
	654	222	45	106	038
	1055	216	67	182	020
	1440	222	75	144	343

Table 3: Estimates of 50-year current speeds (cm/s)

Mooring	meter depth (m)	Residual Histogram				TOTAL SPEED	Gaussian fit				TOTAL SPEED	MAX. OBS. SPEED
		Along-slope +	up-slope -	up-slope +	Along-slope -		Along-slope +	up-slope -	up-slope +	Along-slope -		
A1	55	65	66	51	58	69	62	60	53	54	66	59
	120	52	50	44	47	55	49	51	45	46	54	44
A5	209	58	43	47	29	(63)	75	55	42	36	75	57
	510	47	32	36	23	(50)	63	46	34	29	63	45
	1111	46	50	29	27	50	52	46	28	28	(52)	49
	1562	39	33	27	29	(40)	42	37	27	29	42	33
B1	55	95	75	54	47	96	99	83	45	43	101	70
B2	43	79	69	56	45	81	81	79	55	51	83	53
	168	63	54	34	27	63	60	52	29	30	60	47
B3	104	73	41	32	37	74	77	48	33	36	77	63
	257	59	33	21	28	59	64	38	25	29	65	54
	457	57	36	24	30	58	62	41	25	31	62	50
B4	169	64	48	38	31	65	70	53	32	33	70	53
	477	59	38	26	28	60	62	50	22	24	62	50
	1035	42	44	10	13	44	49	46	10	12	49	38
C2	115	97	45	27	45	97	101	45	25	47	101	82
	266	88	38	24	33	89	93	42	20	35	93	77
	468	90	37	31	32	91	81	44	28	33	(82)	76
C3	104	67	71	52	35	72	80	62	48	49	(80)	58
	403	59	51	29	27	60	61	48	33	34	(62)	52
	951	60	51	41	39	62	63	54	40	39	64	46
D1	87	95	89	49	45	97	107	91	49	43	107	80
	212	82	94	30	41	94	95	83	31	33	(95)	82
D2	120	95	65	57	41	97	99	73	59	43	101	86
	270	95	61	51	39	97	95	73	51	41	97	79
	345	97	65	49	47	99	93	71	49	43	93	69
D5	510	81	101	57	74	102	83	91	65	69	(91)	88
	633	65	103	49	75	(103)	59	102	51	57	102	85

Table 3 continued

Mooring	meter depth (m)	Residual Histogram				TOTAL SPEED	Gaussian fit				TOTAL SPEED	MAX. OBS. SPEED
		Along-slope +	-	up-slope +	-		Along-slope +	-	up-slope +	-		
E2	453	87	64	43	46	88	109	63	37	45	109	77
E3	120	101	84	79	91	113	113	109	99	103	119	95
	419	83	78	51	58	89	87	91	69	71	93	83
	725	58	93	57	37	94	65	78	47	43	(78)	100
E4	111	131	95	79	63	133	115	111	93	85	(119)	117
	950	46	86	77	24	92	60	75	51	39	(75)	66
F1	39	97	53	44	61	98	94	64	42	65	96	88
F3	79*	117	51	48	73	(121)	115	67	63	81	(117)	89
	388	71	71	38	47	(74)	90	70	52	52	91	66
	694	73	69	43	43	(74)	85	111	37	41	(111)	60
	945	78	64	36	40	(78)	89	102	35	37	(102)	66
G1	41	73	65	57	49	75	71	60	59	56	73	48
	166	50	40	40	33	50	47	40	37	36	47	33
G2	151	128	29	67	67	(129)	134	47	61	69	135	114
	299	98	23	53	47	(100)	127	77	47	47	(127)	89
	500	81	31	68	52	(87)	90	46	54	60	92	84
G4	195	58	44	49	57	(71)	78	65	59	63	79	64
	1104	30	31	20	26	(35)	42	37	31	31	(43)	32
	1554	34	35	22	22	(37)	43	36	31	30	(44)	34
I2	251	59	63	103	55	103	61	59	103	51	103	60
	654	46	47	50	41	58	51	48	52	46	(56)	45
	1055	35	71	53	41	(73)	55	71	45	46	(71)	67
	1440	69	85	68	49	(92)	71	86	71	40	(89)	75

* F3(79m): only 80 days of records.

Fig.1: CONSLEX mooring sites and direction of axis determined by principal component analysis of current records. (A range is shown where directions from each meter on a mooring differed by more than 10° .)

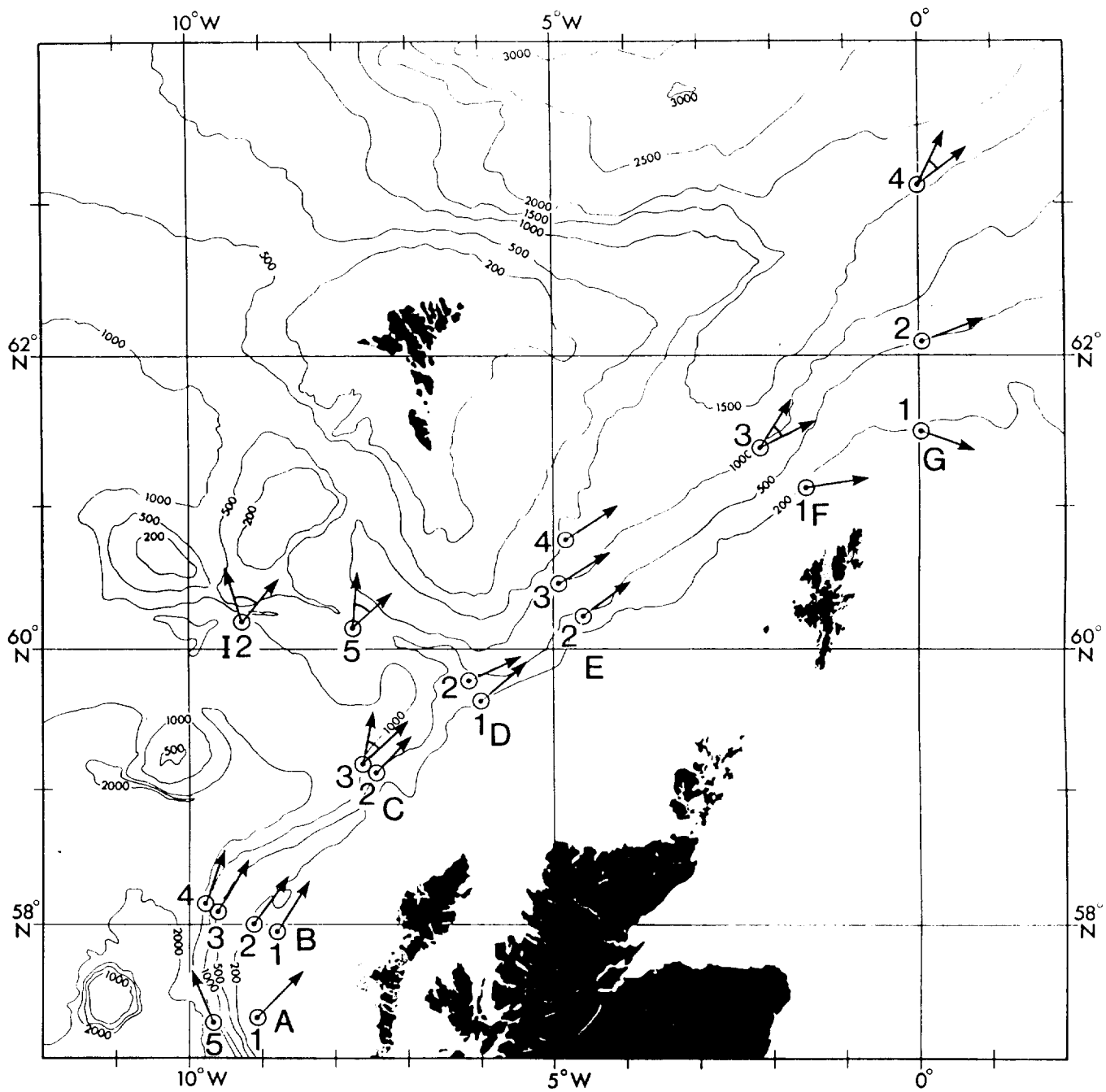
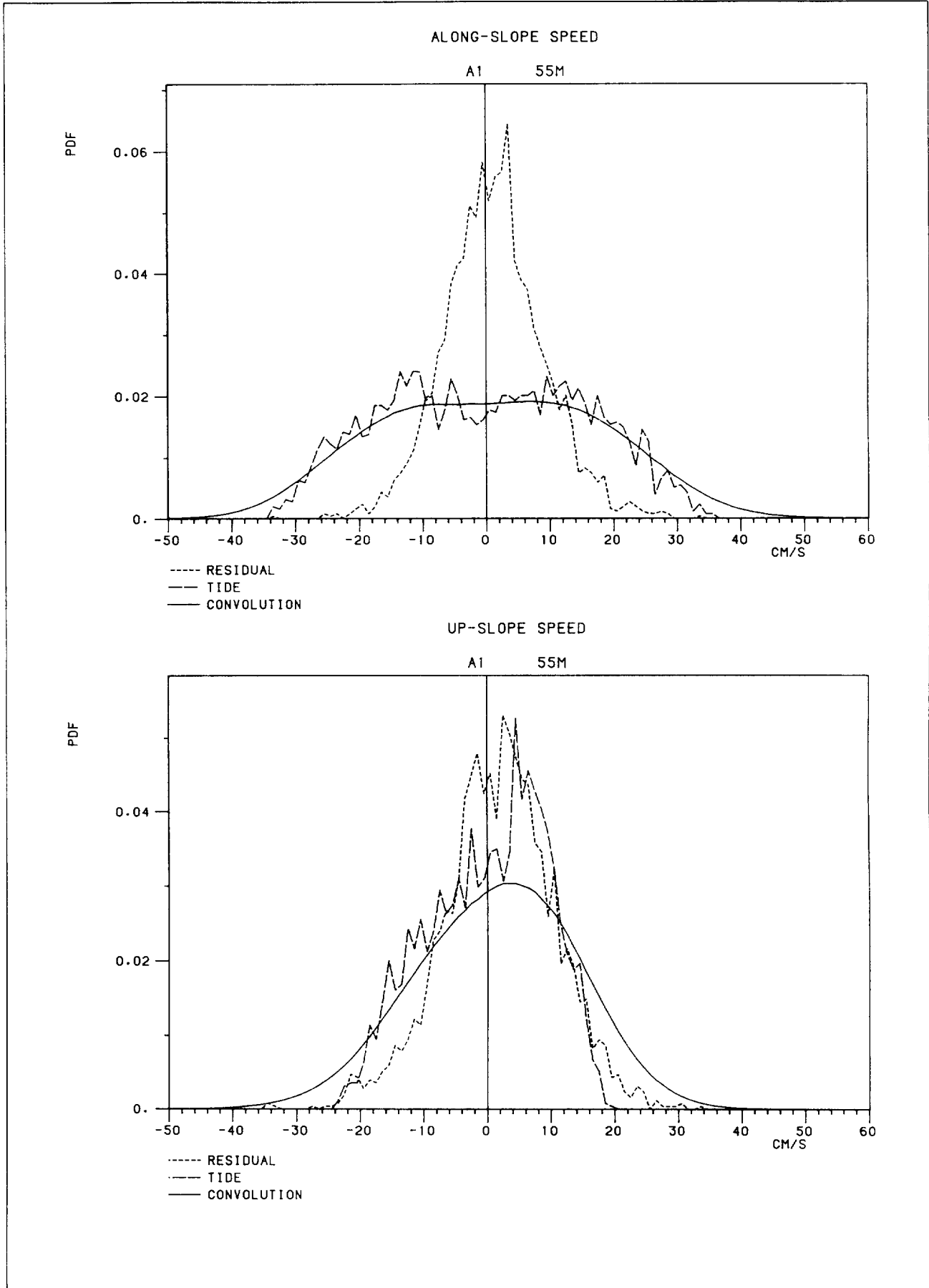
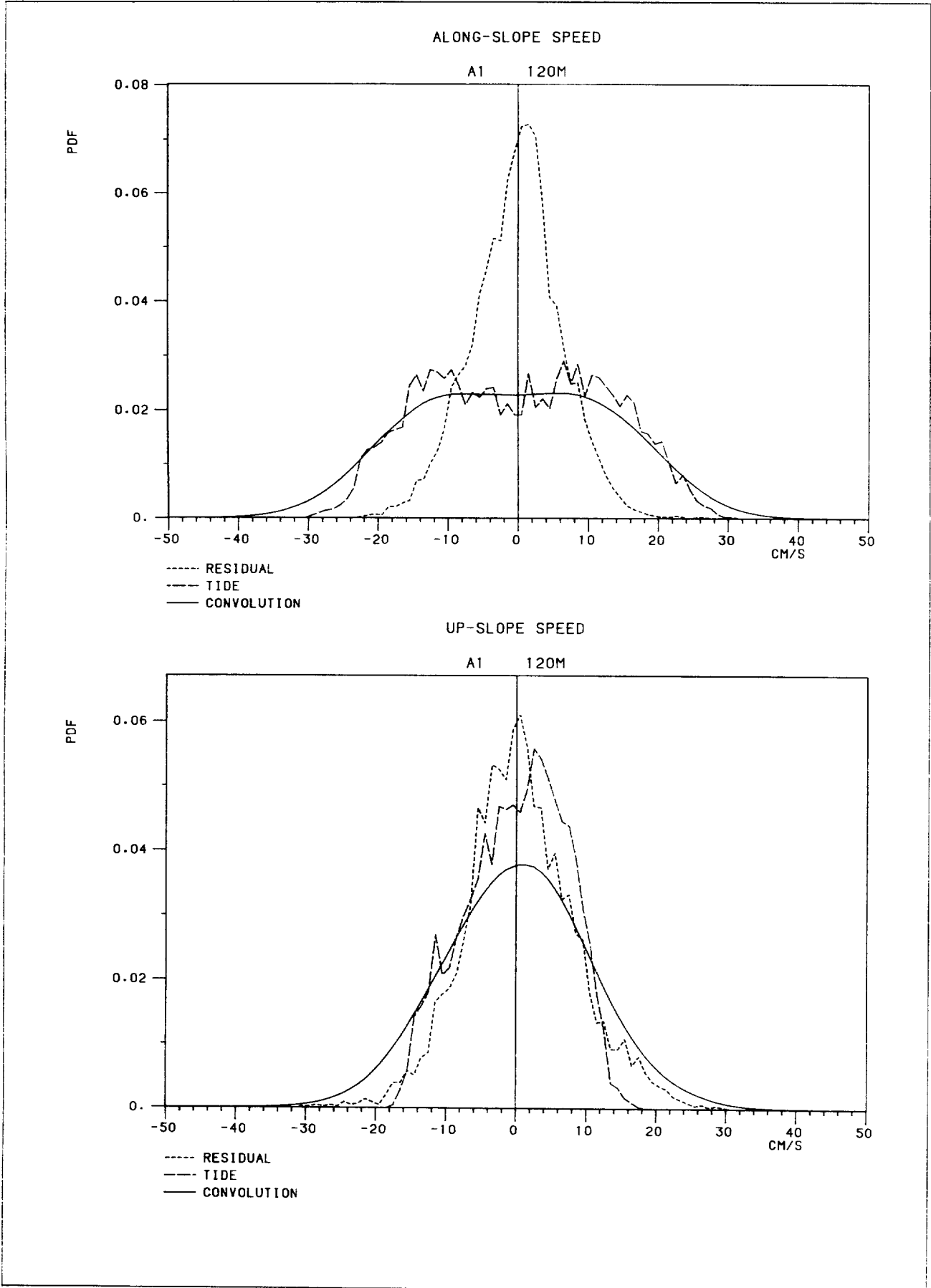
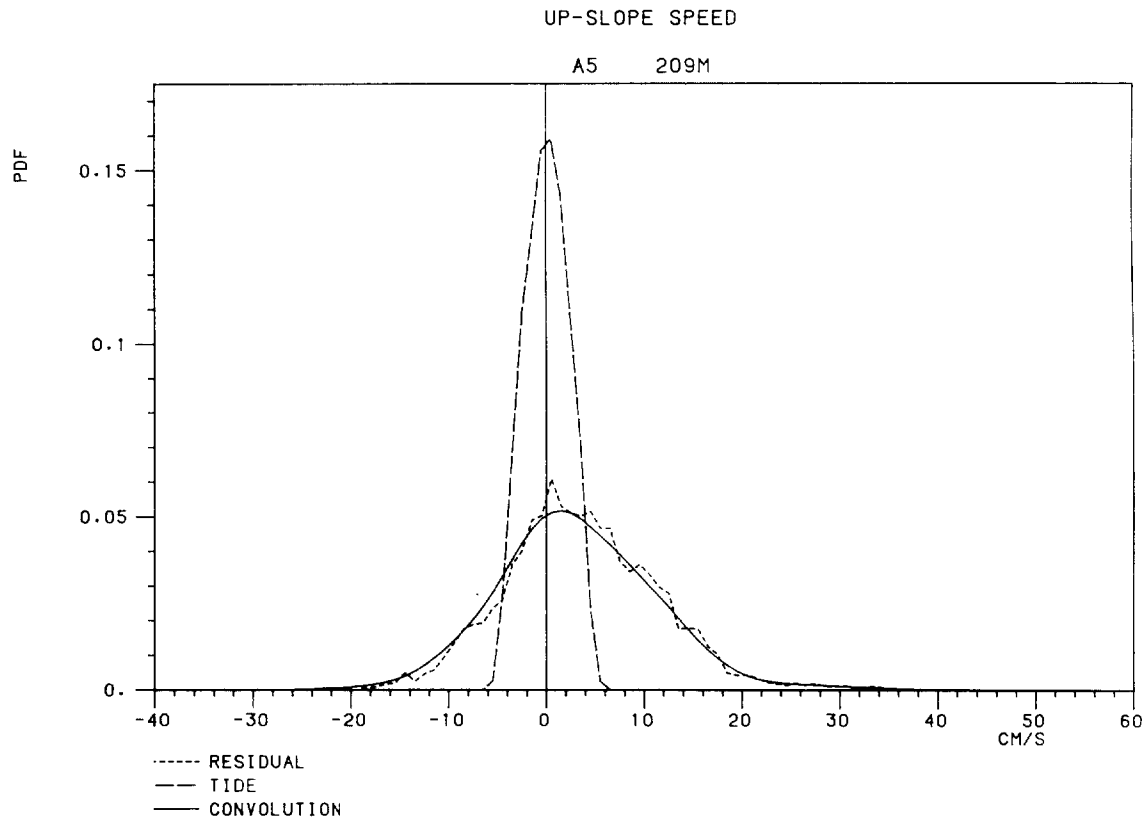
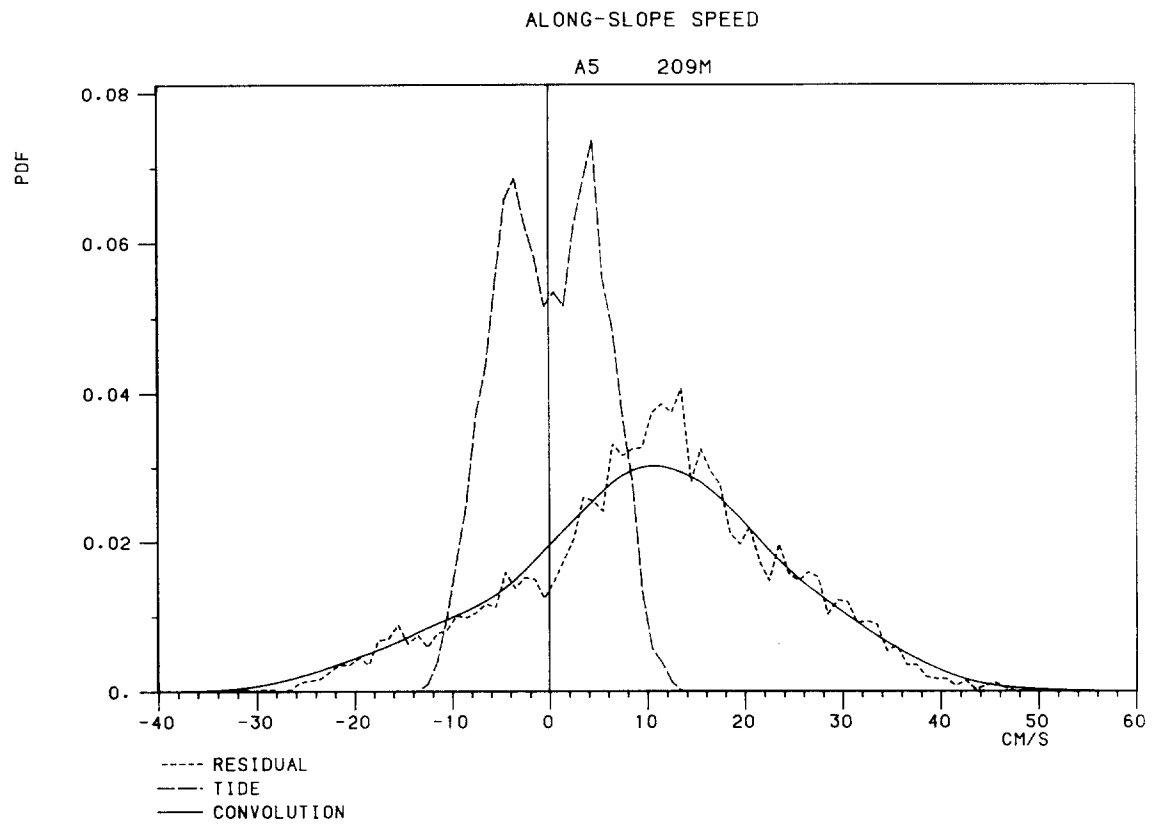


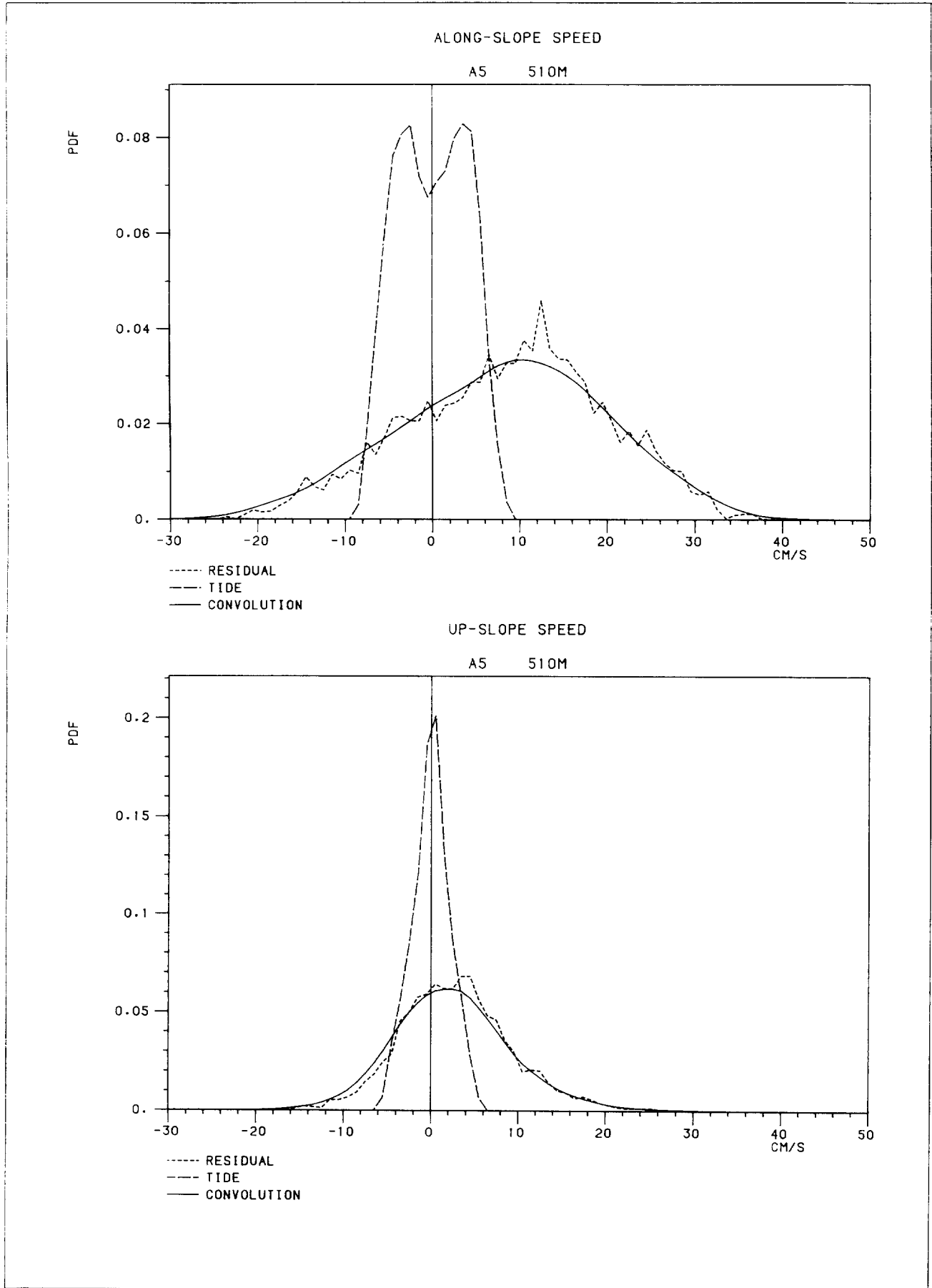
Fig.2: Probability distribution functions of residual and tidal current speeds along- and up-slope from speeds recorded by each current meter and their convolutions. (The meter is identified by the mooring and by the depth of the meter below the sea surface.)





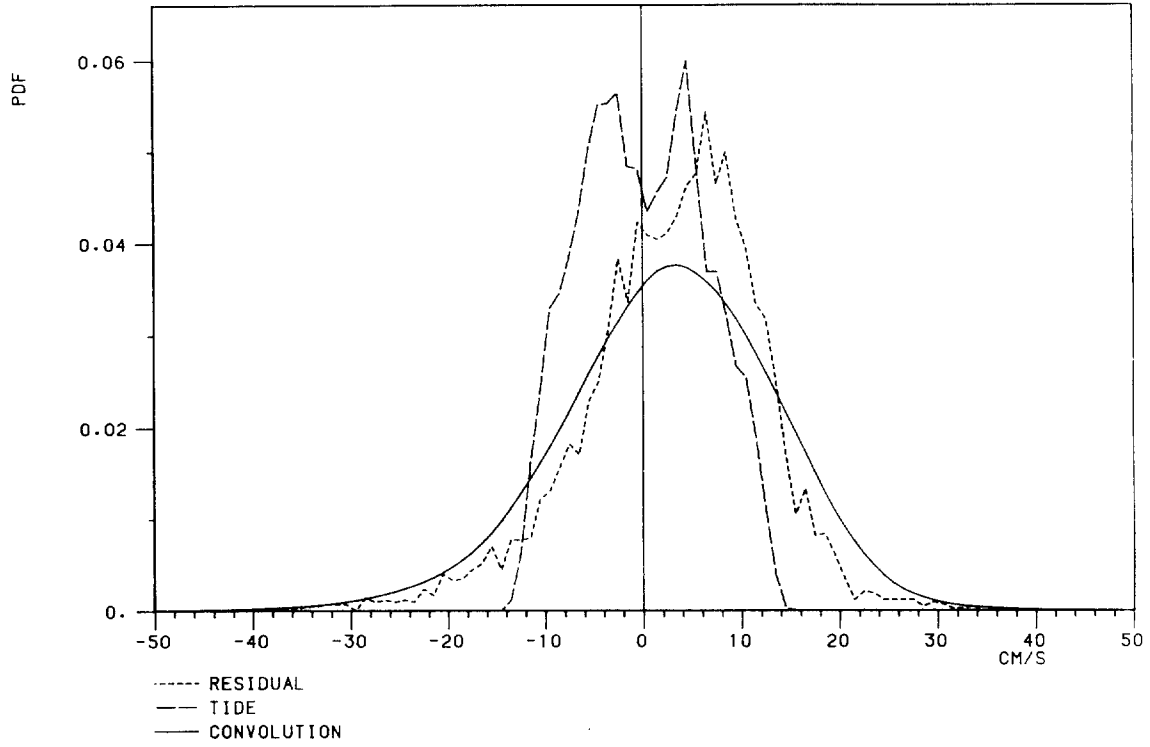






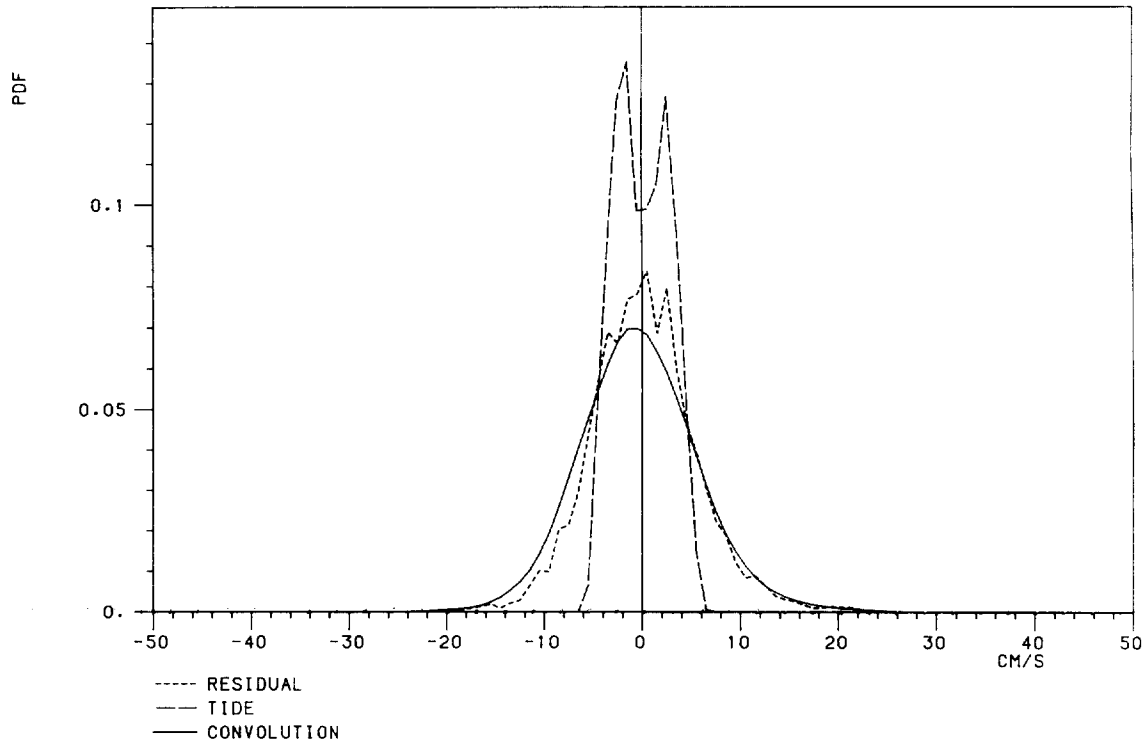
ALONG-SLOPE SPEED

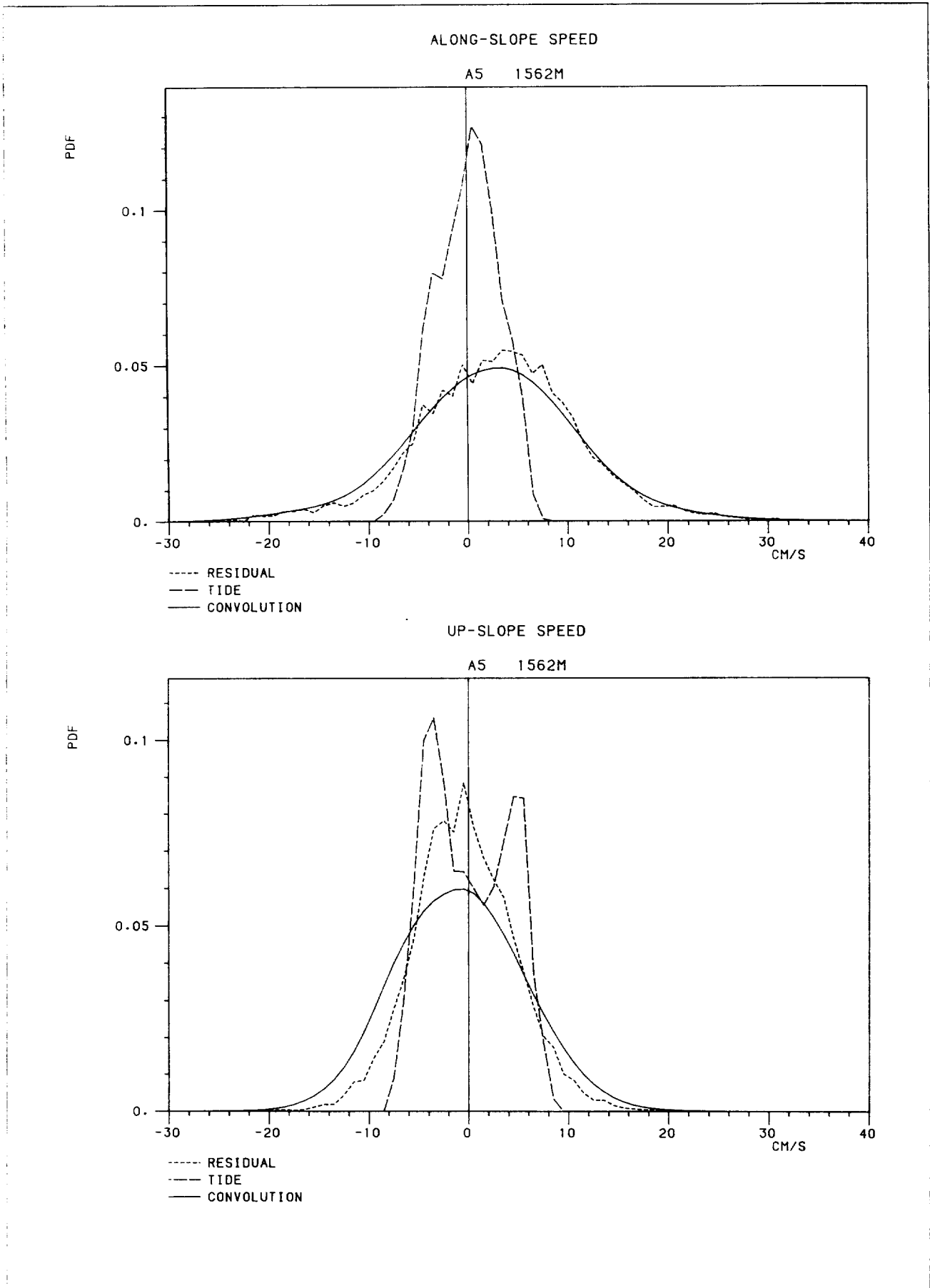
A5 1111M

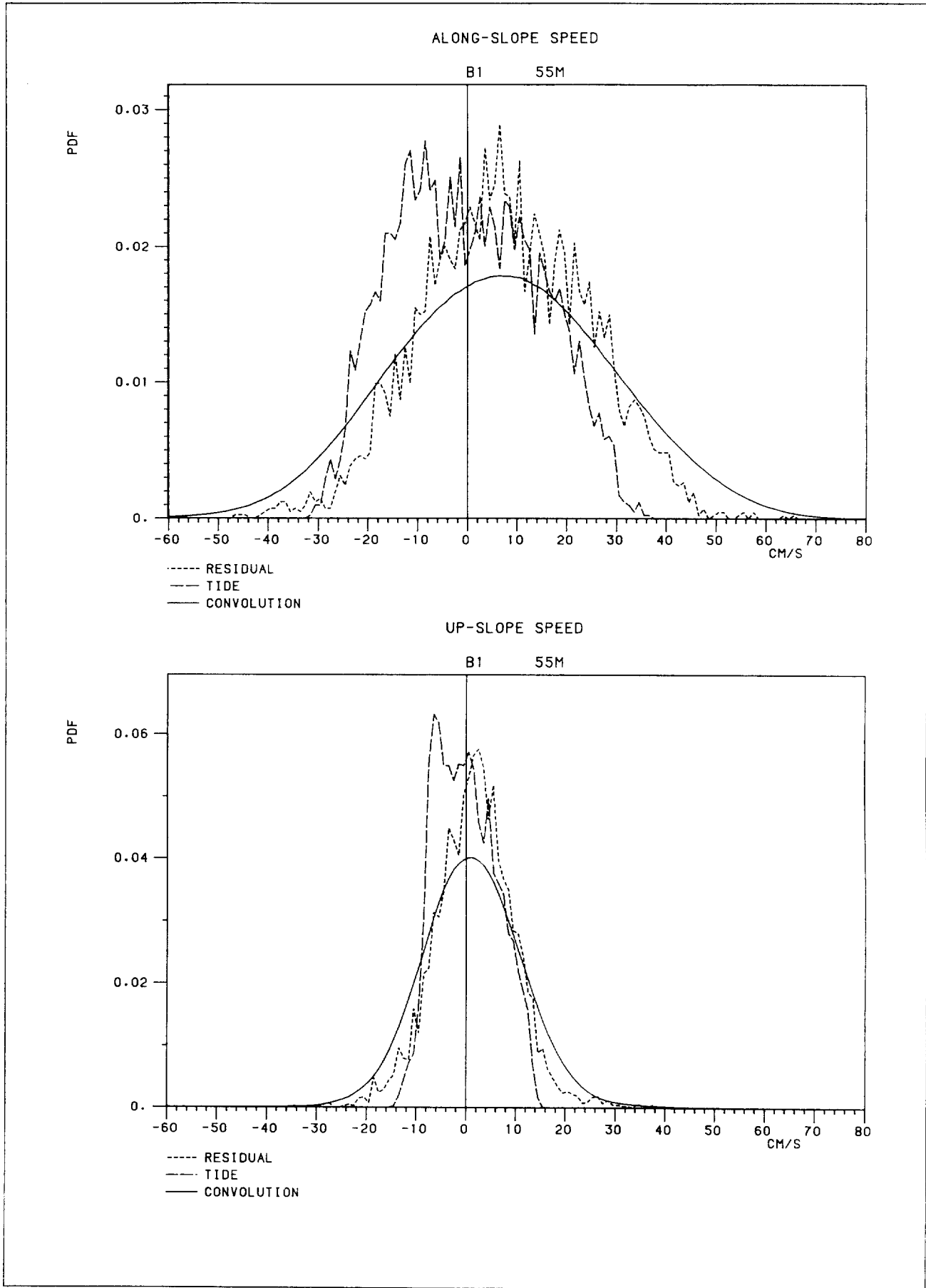


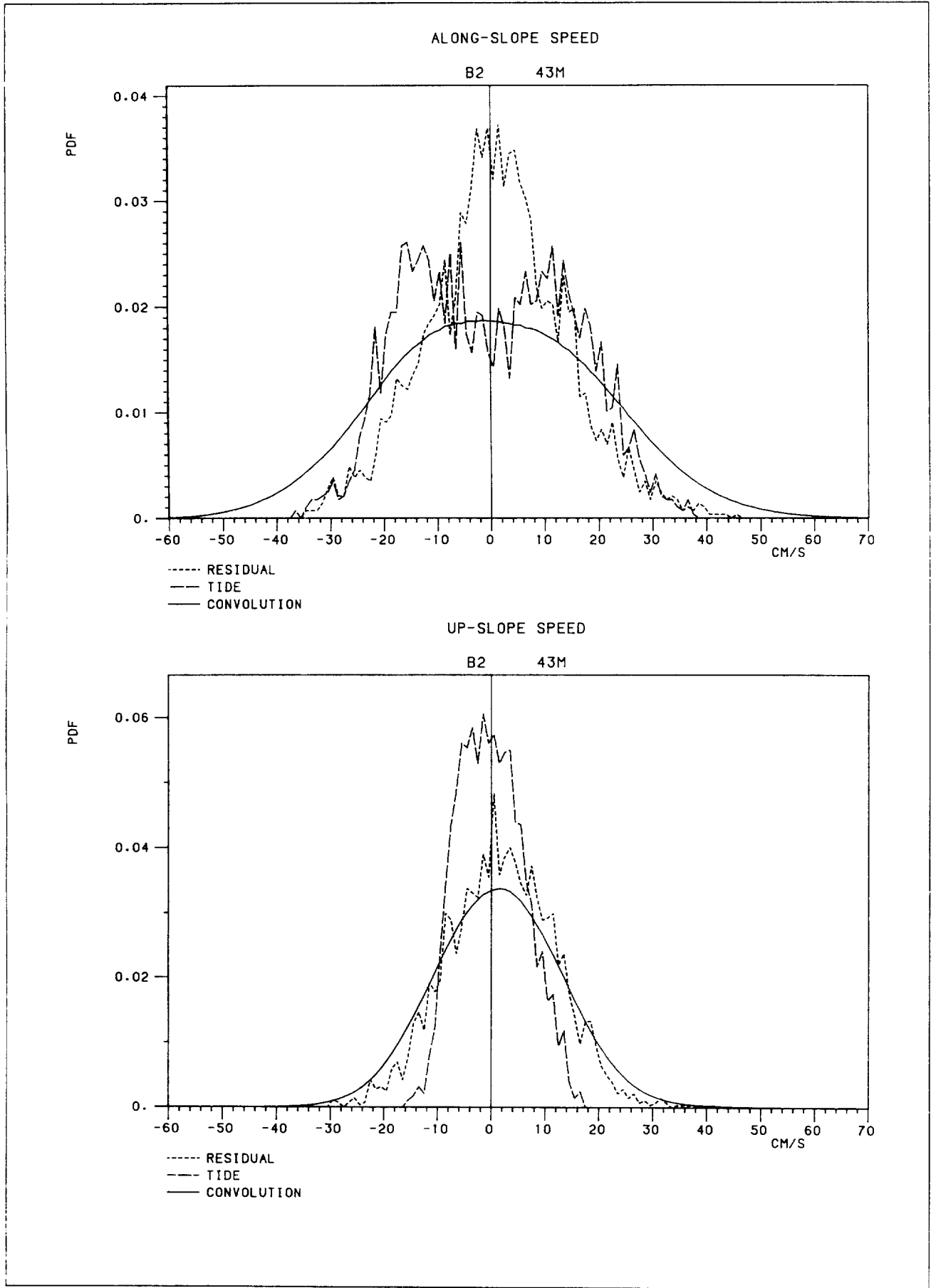
UP-SLOPE SPEED

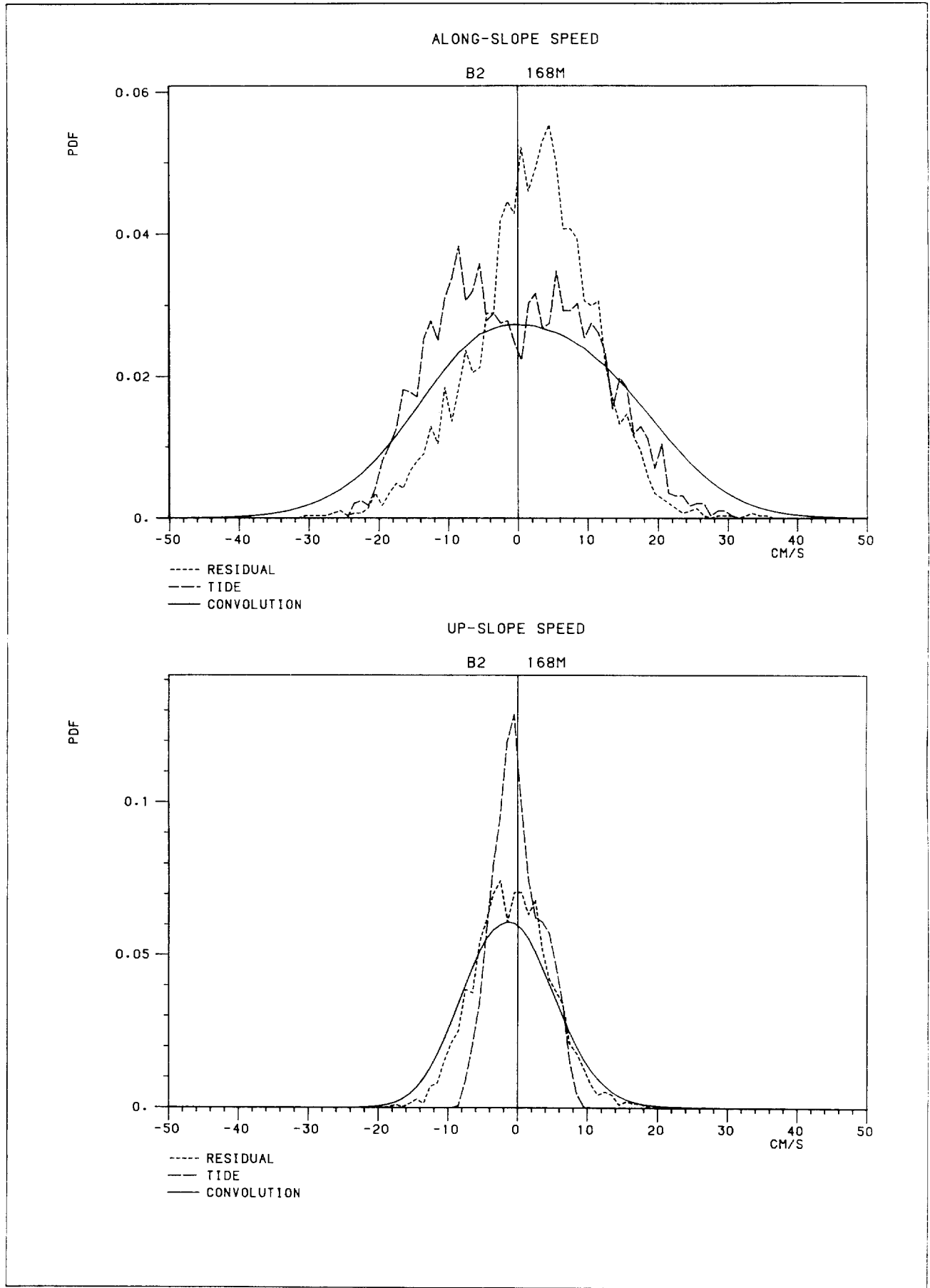
A5 1111M

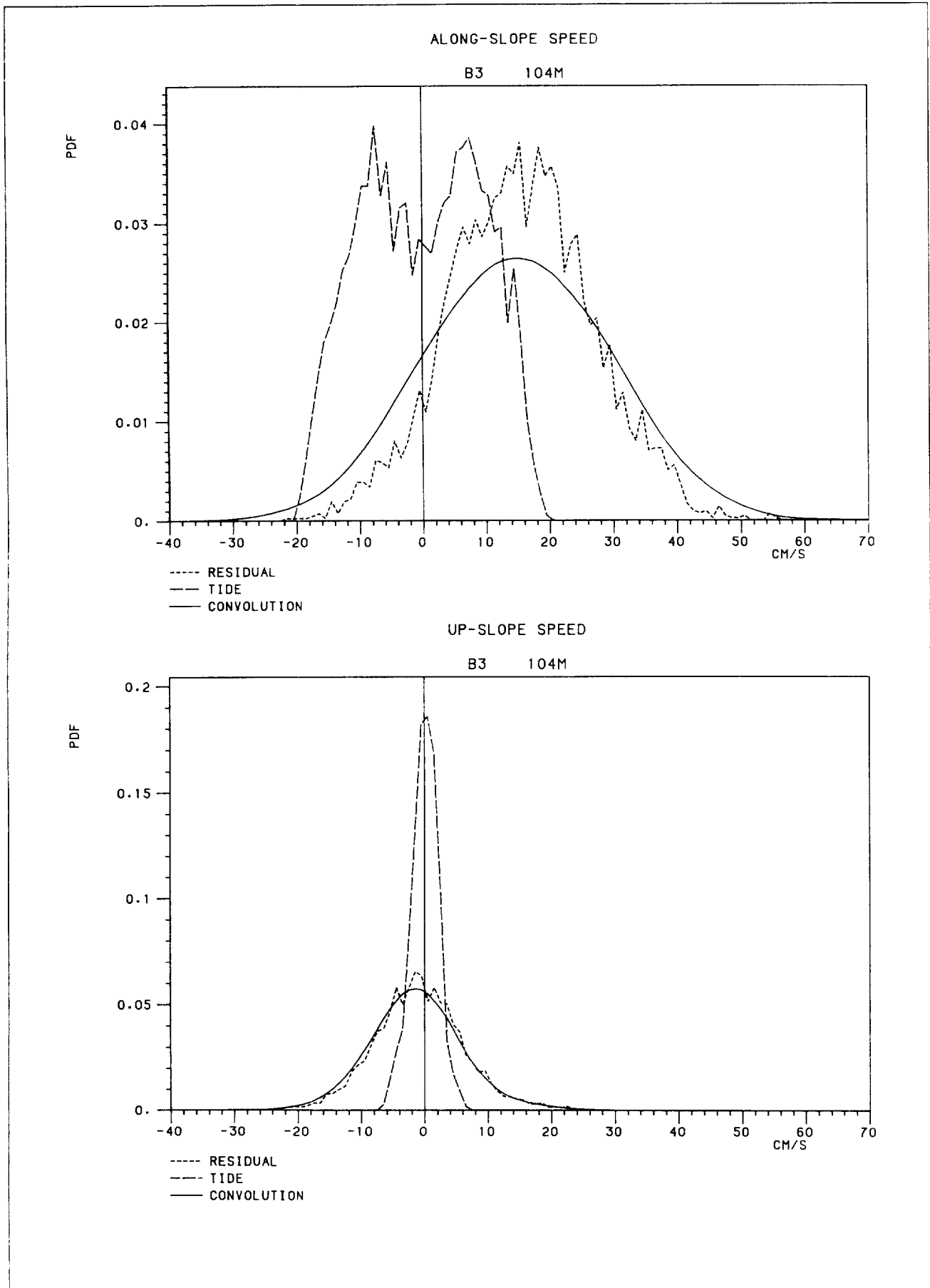


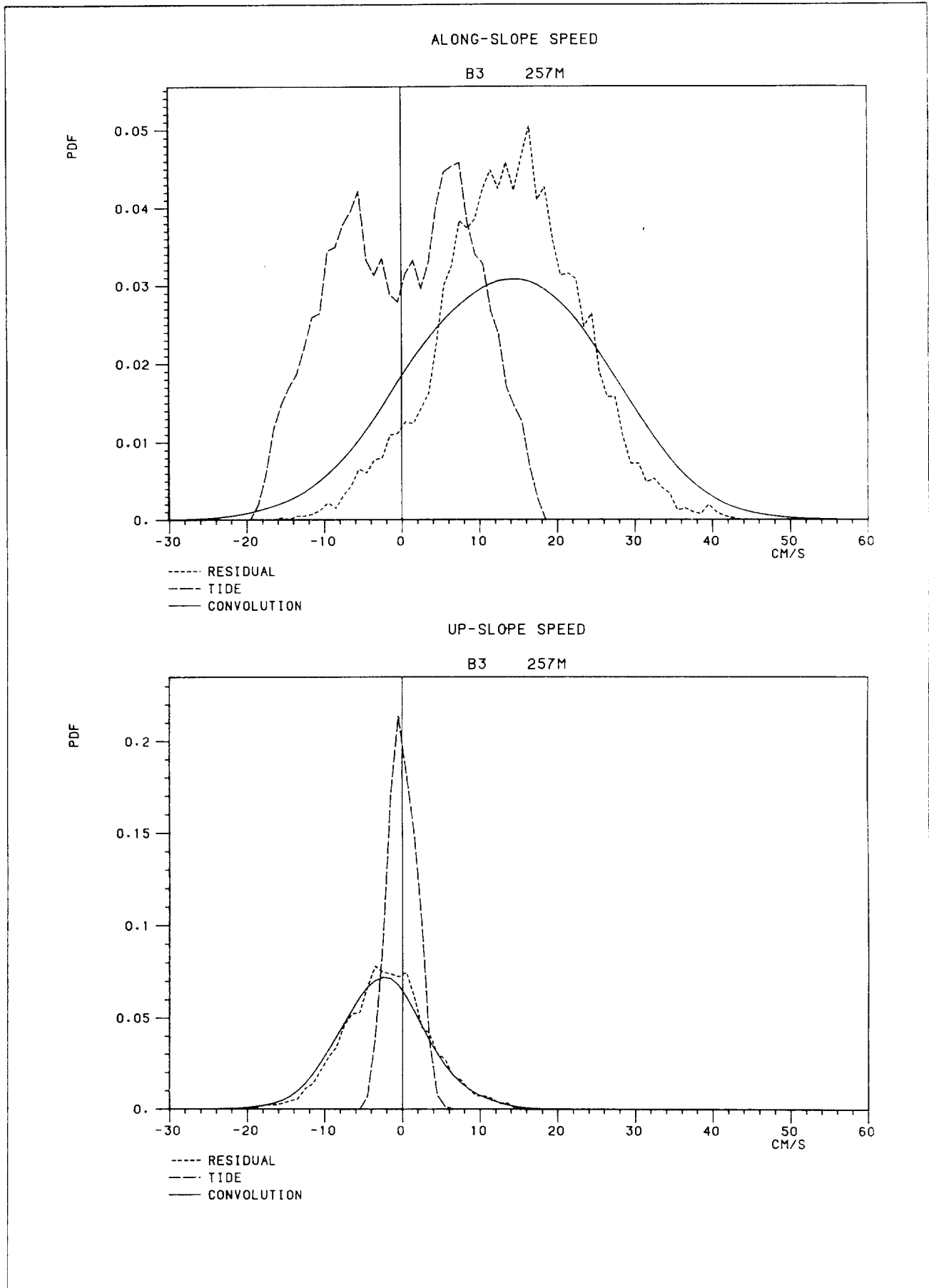


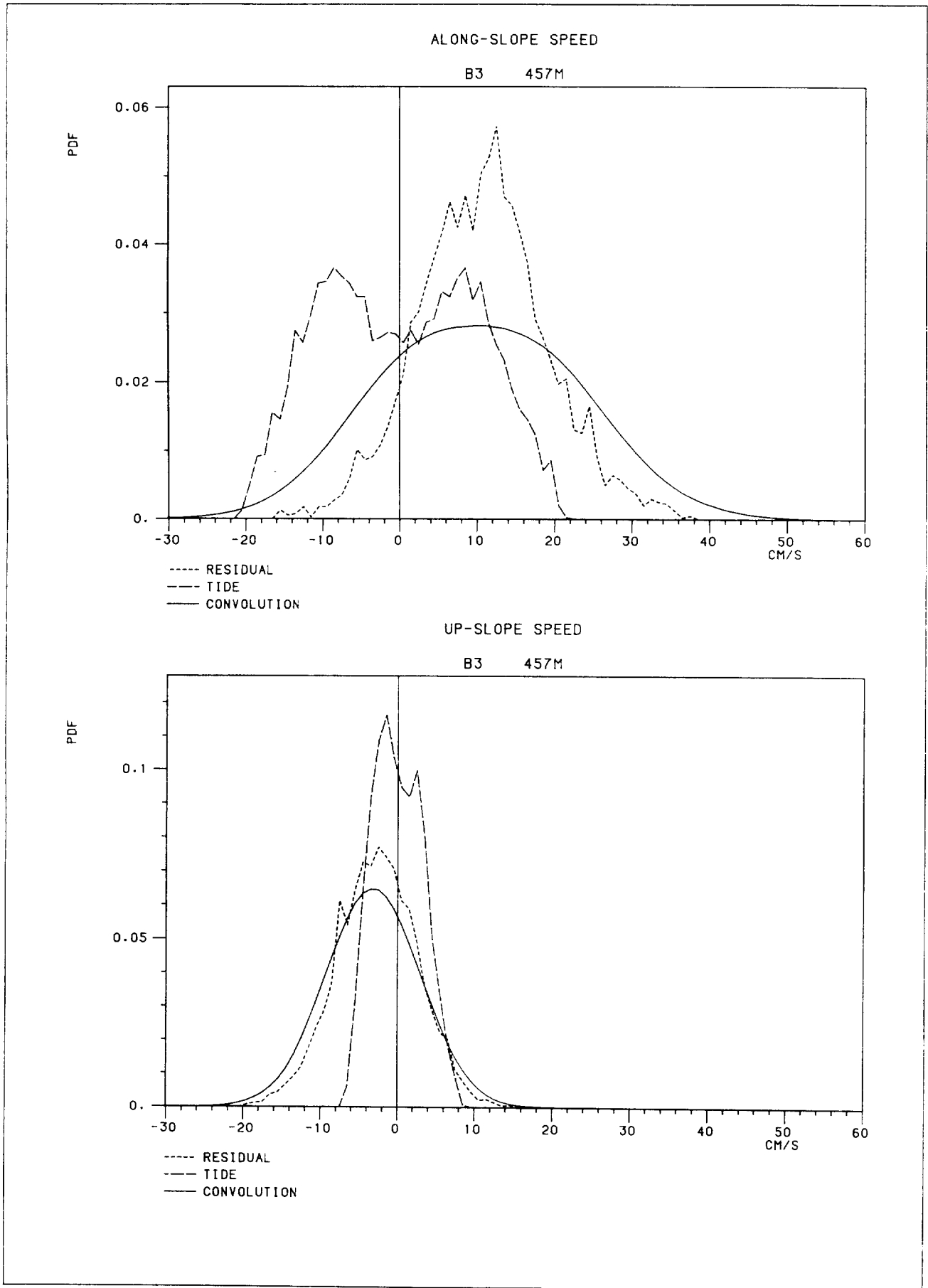


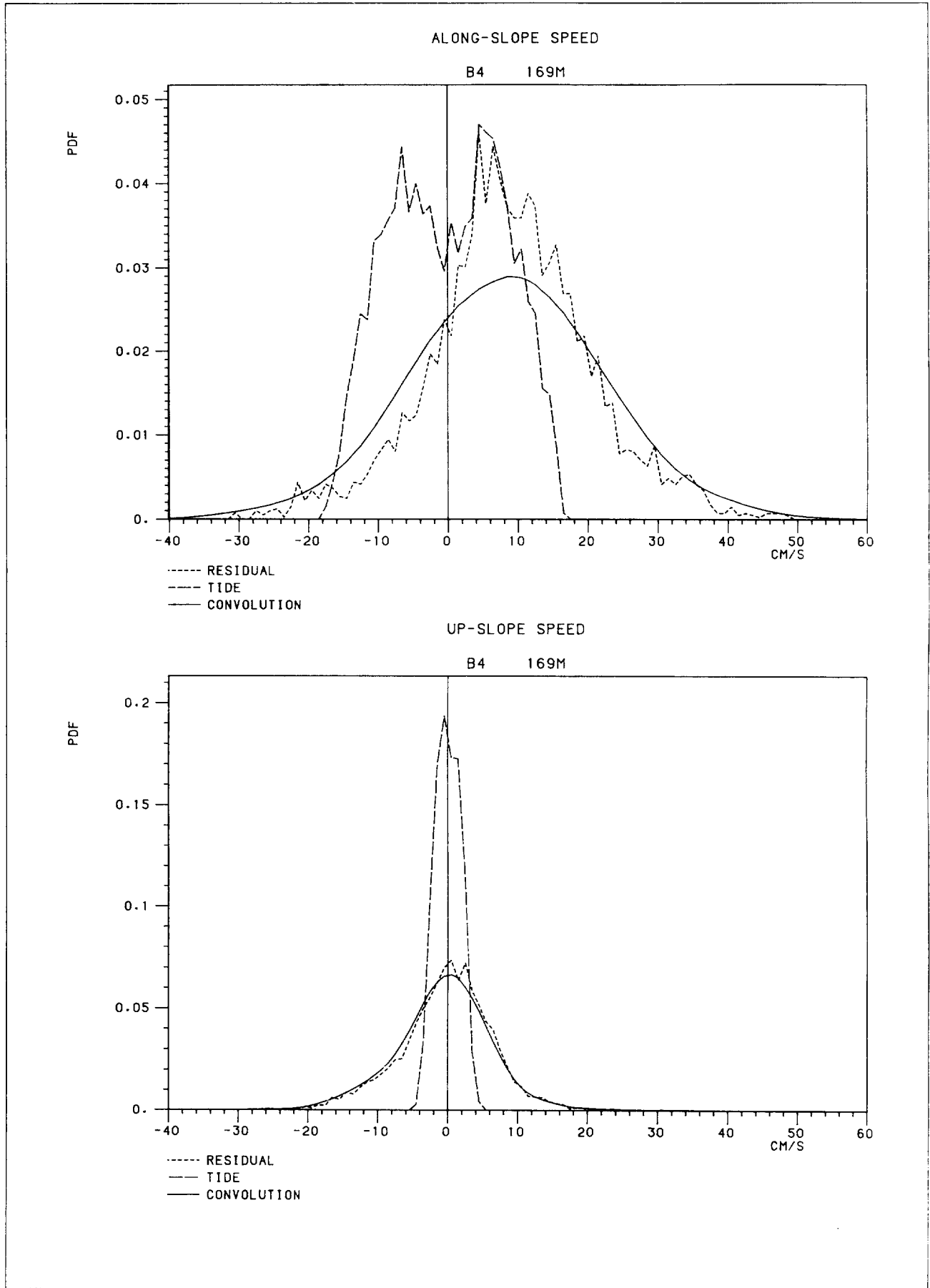






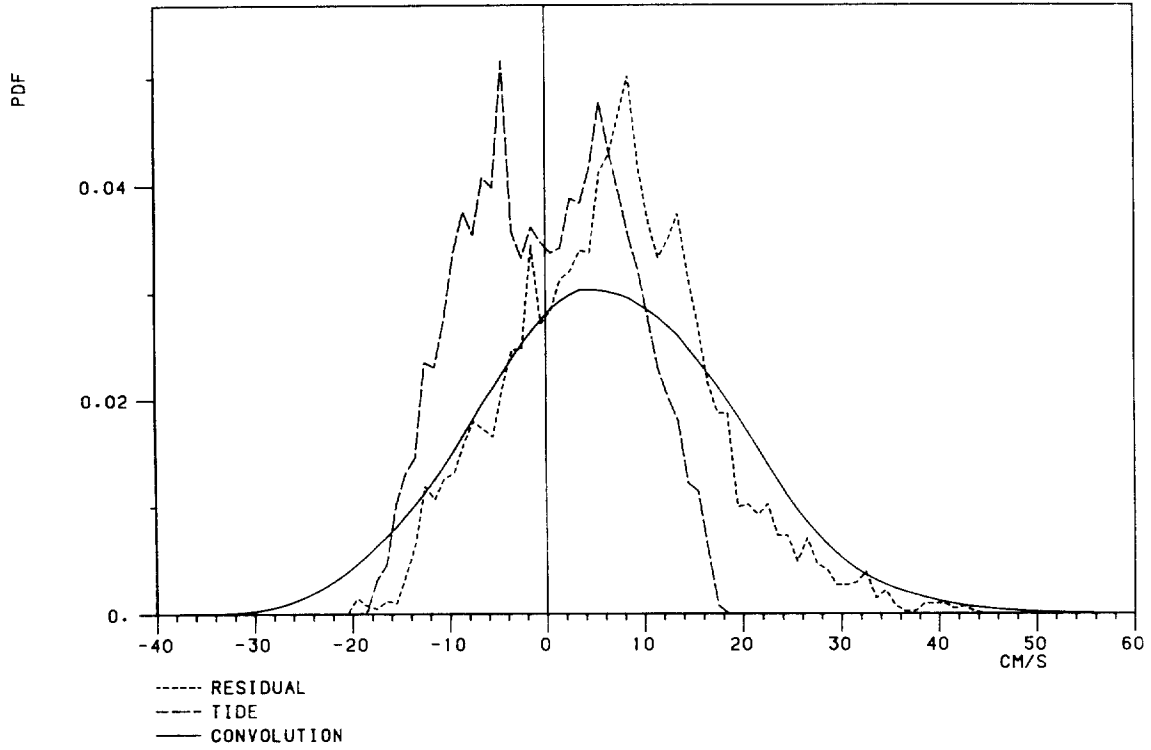






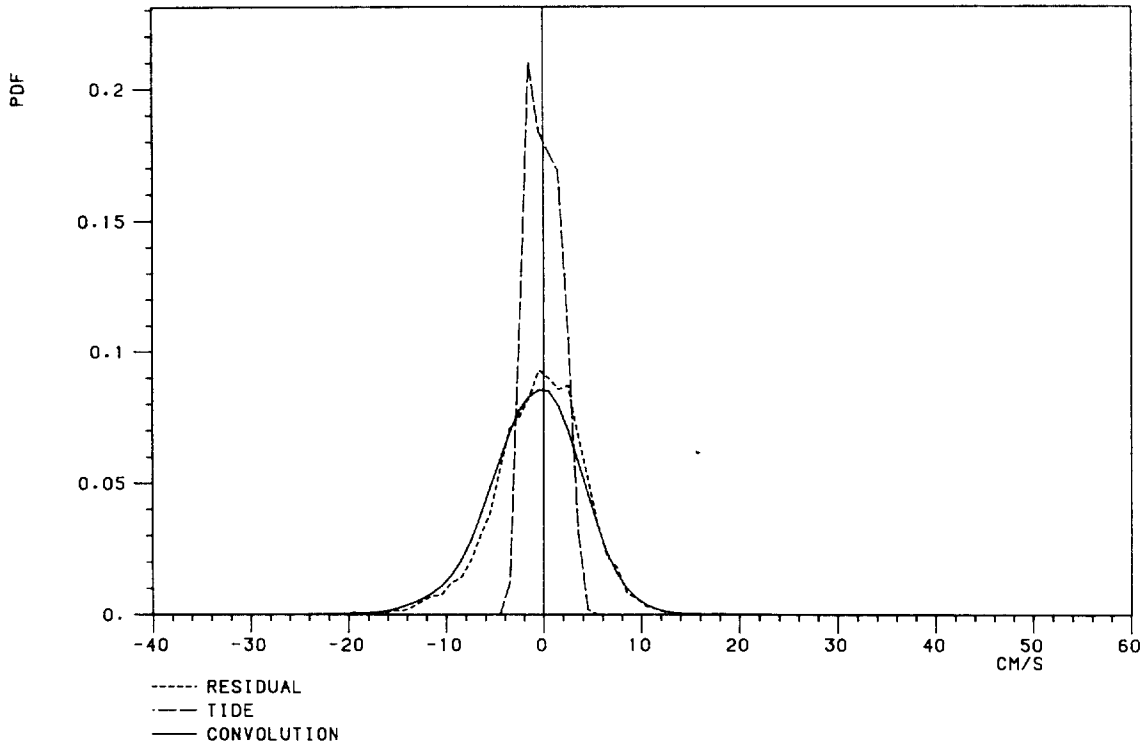
ALONG-SLOPE SPEED

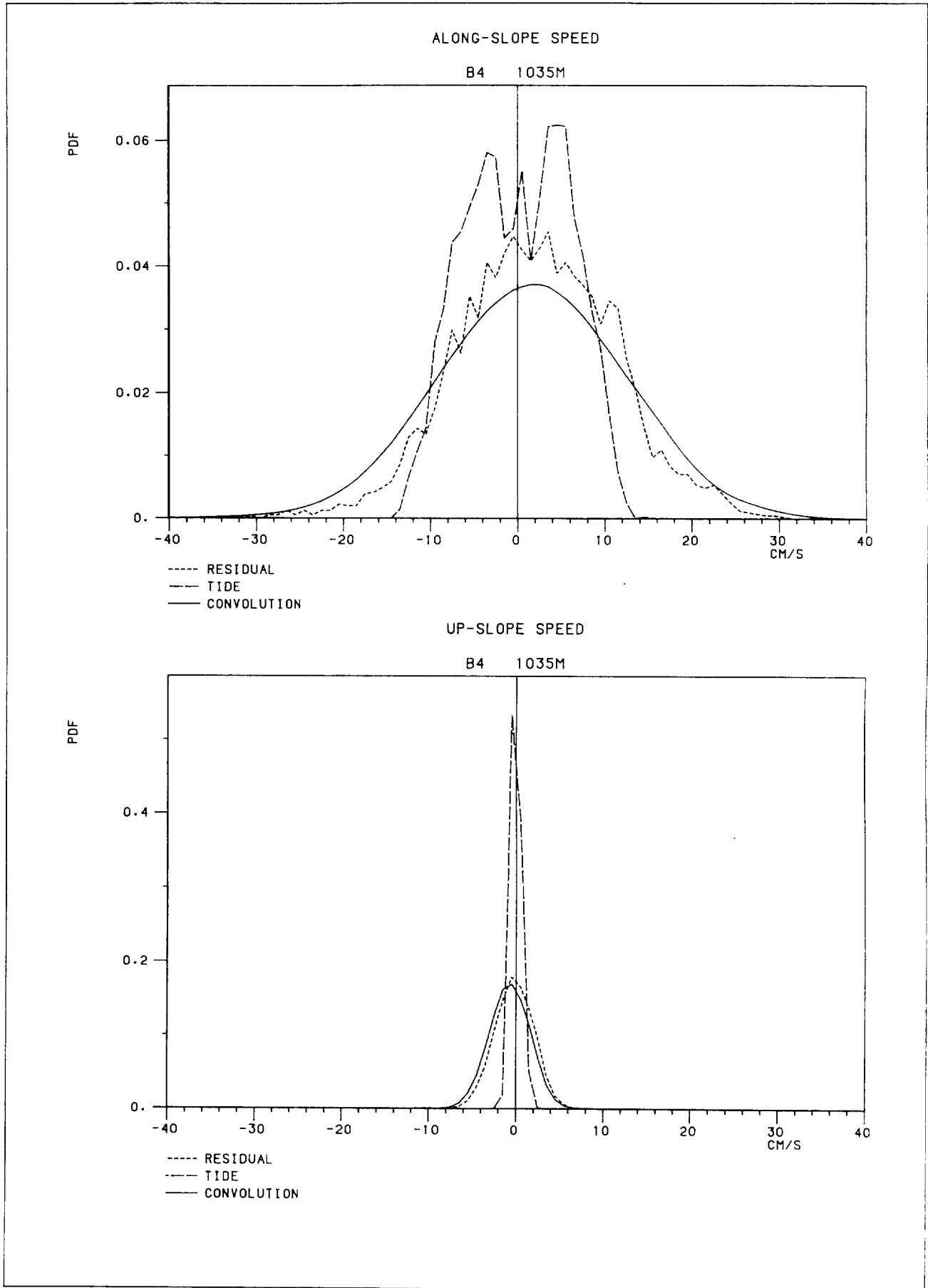
B4 477M



UP-SLOPE SPEED

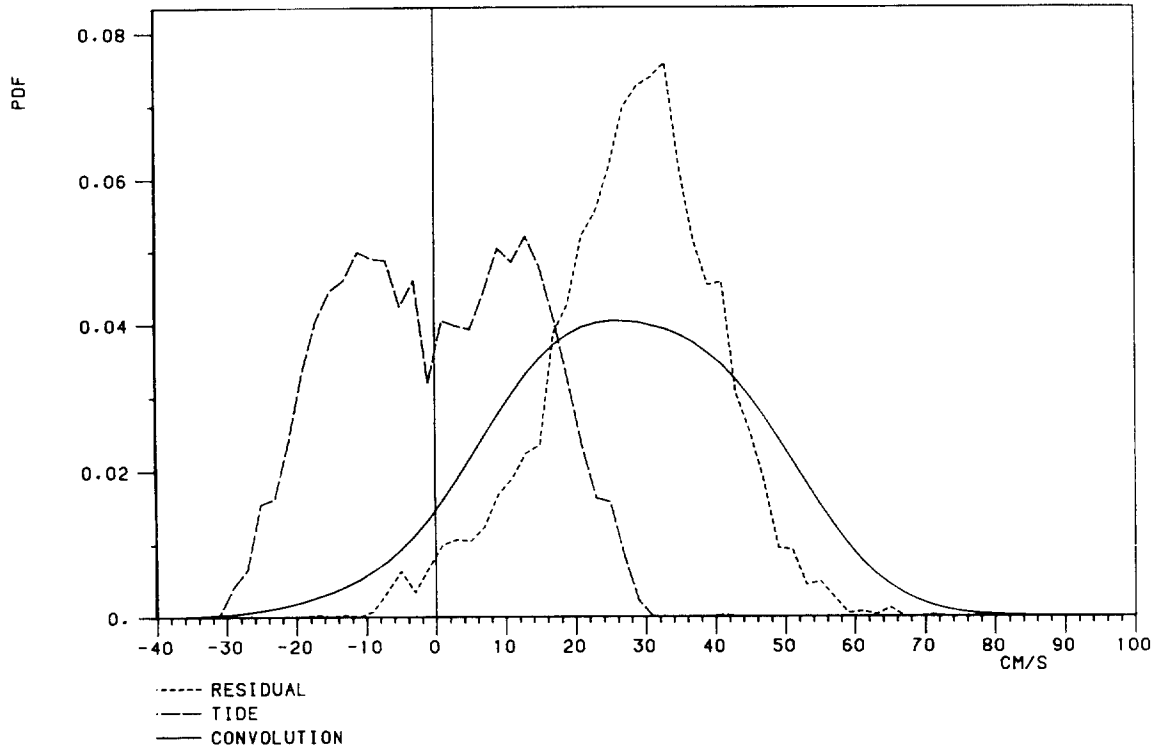
B4 477M





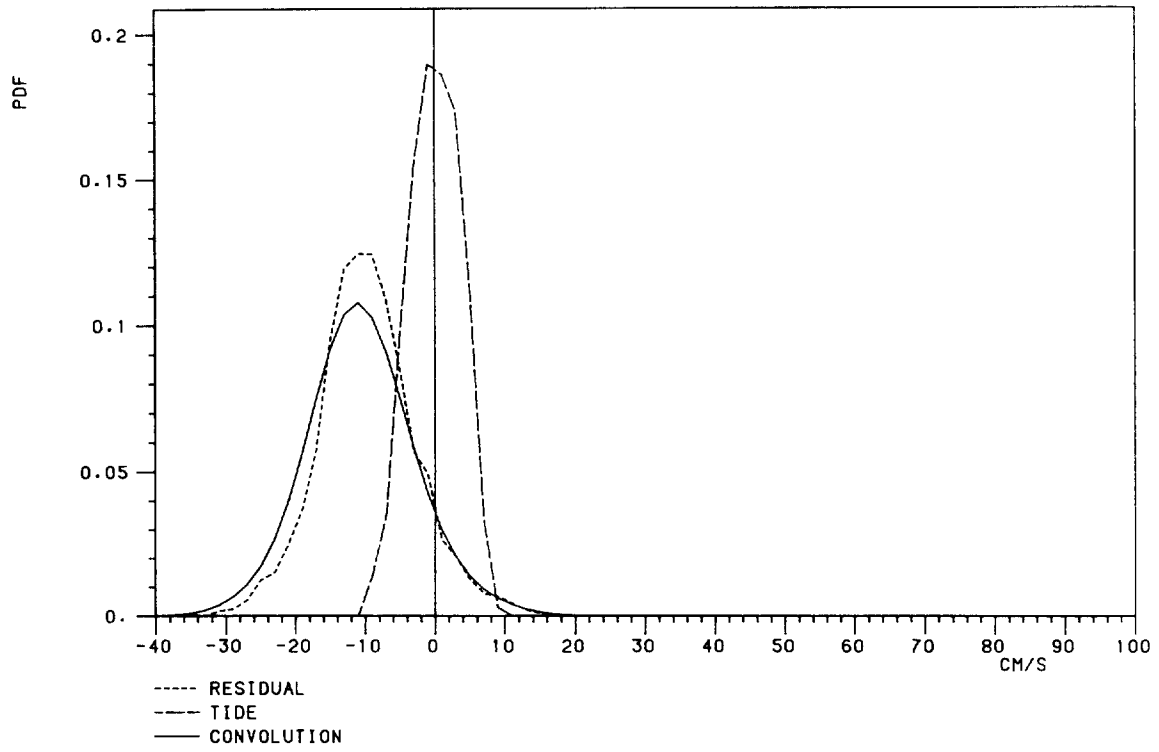
ALONG-SLOPE SPEED

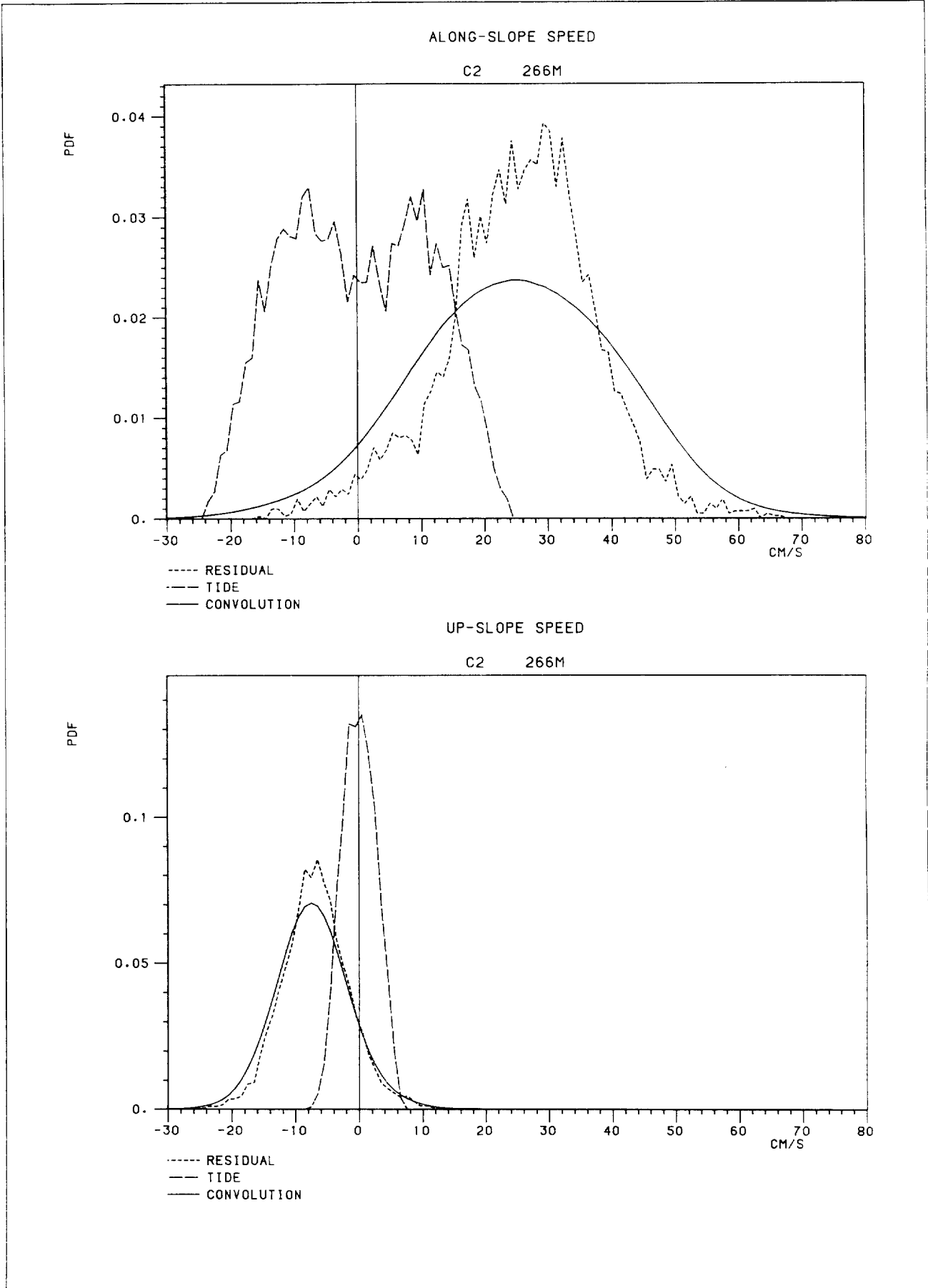
C2 115M

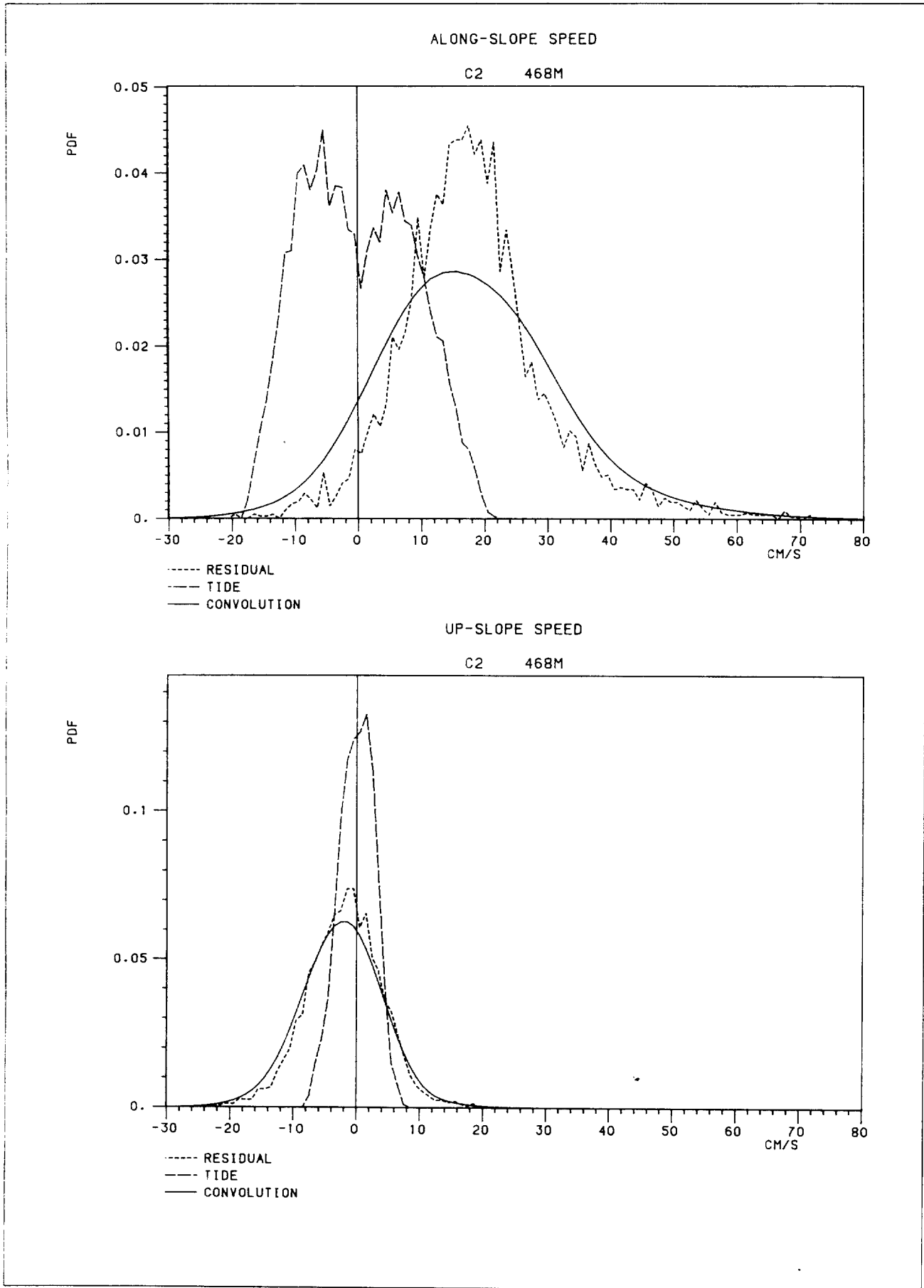


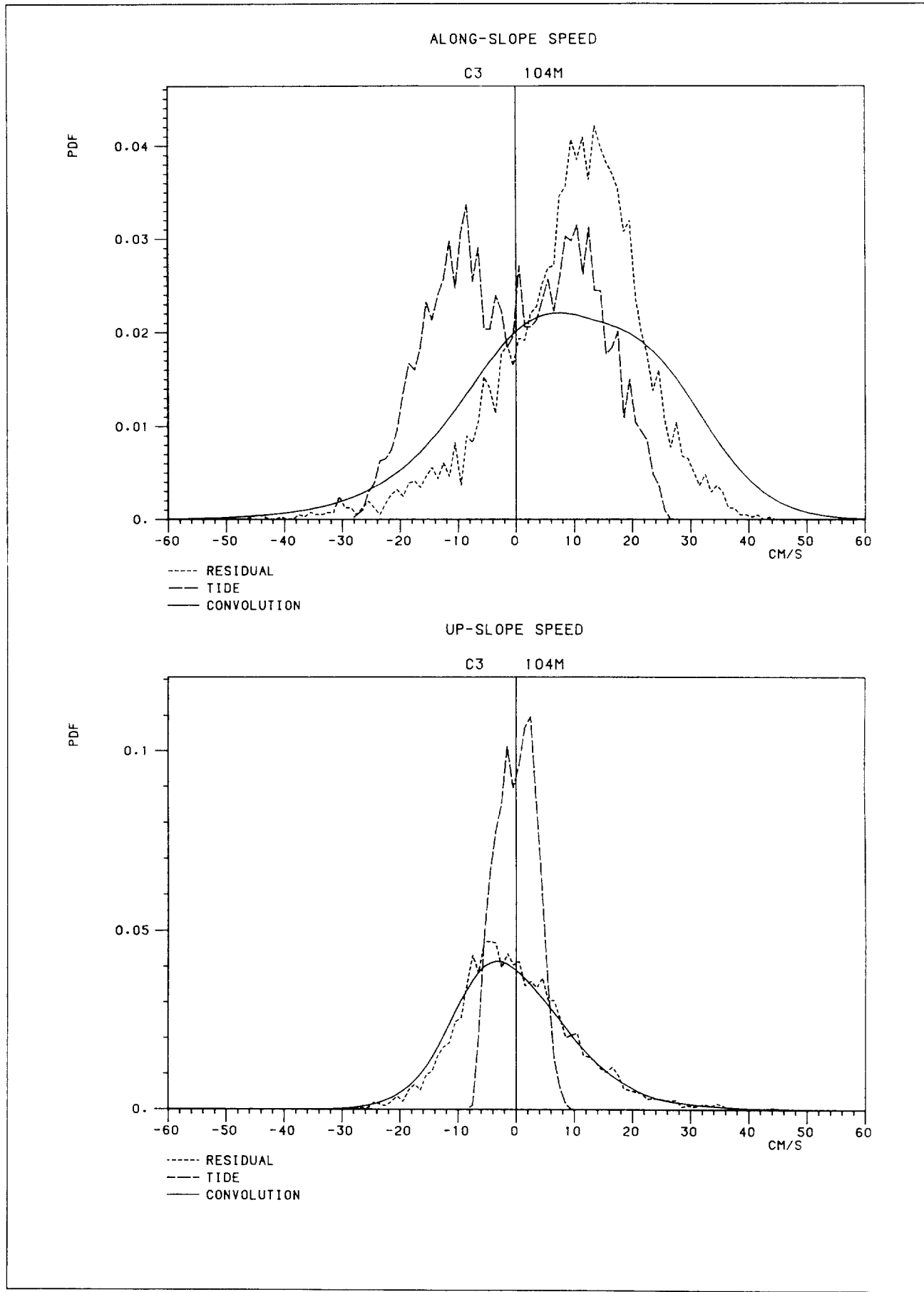
UP-SLOPE SPEED

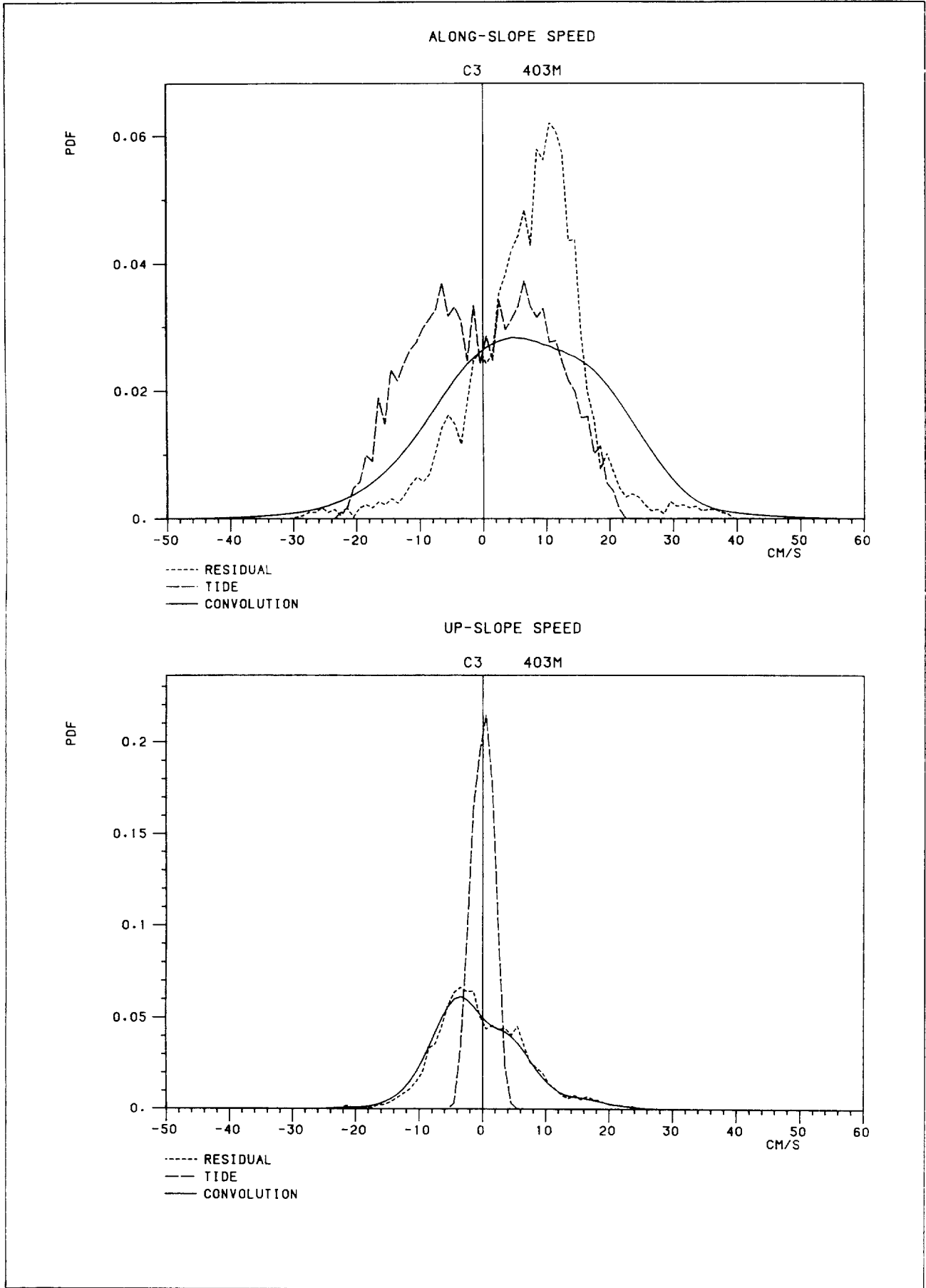
C2 115M

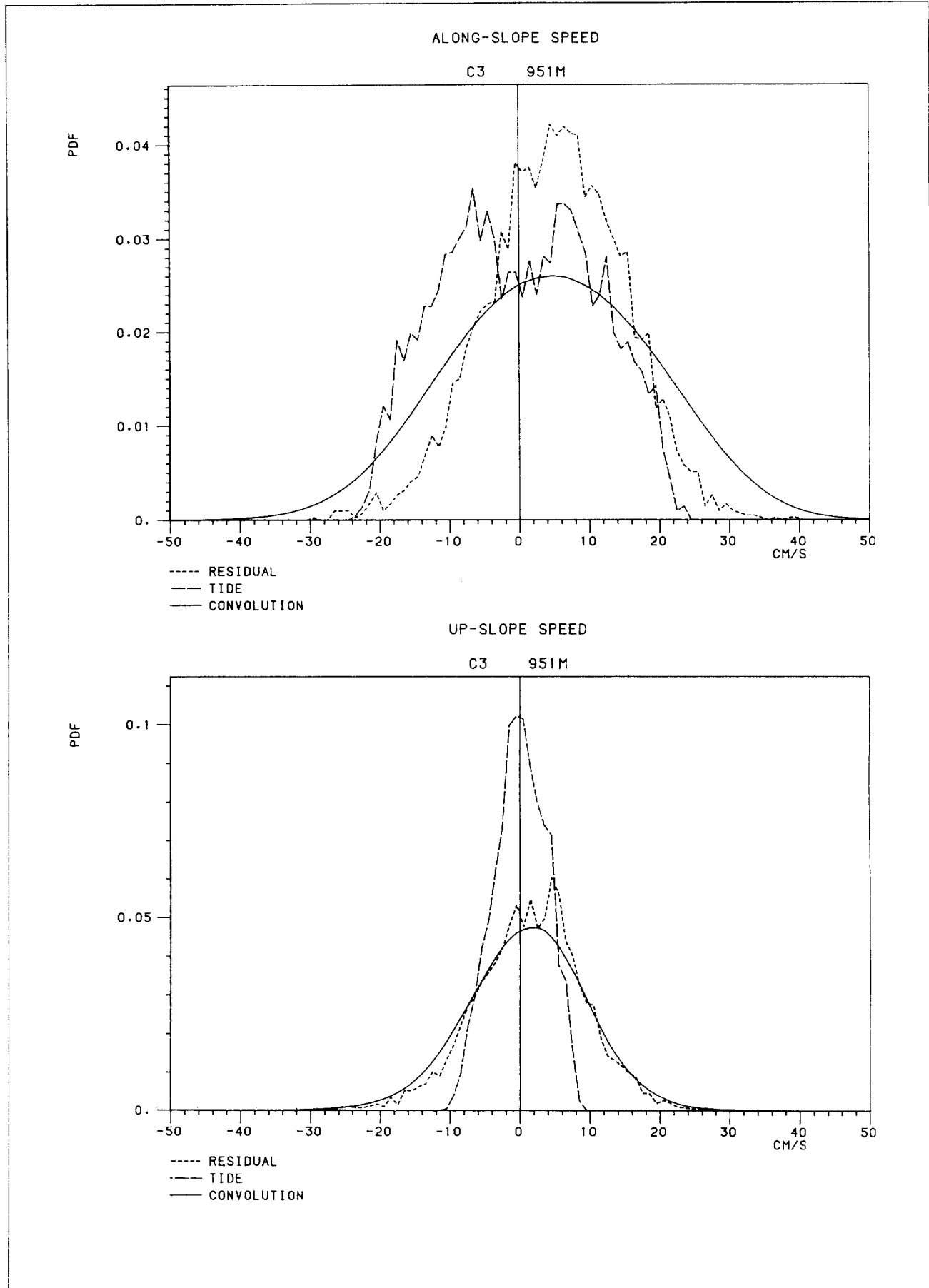


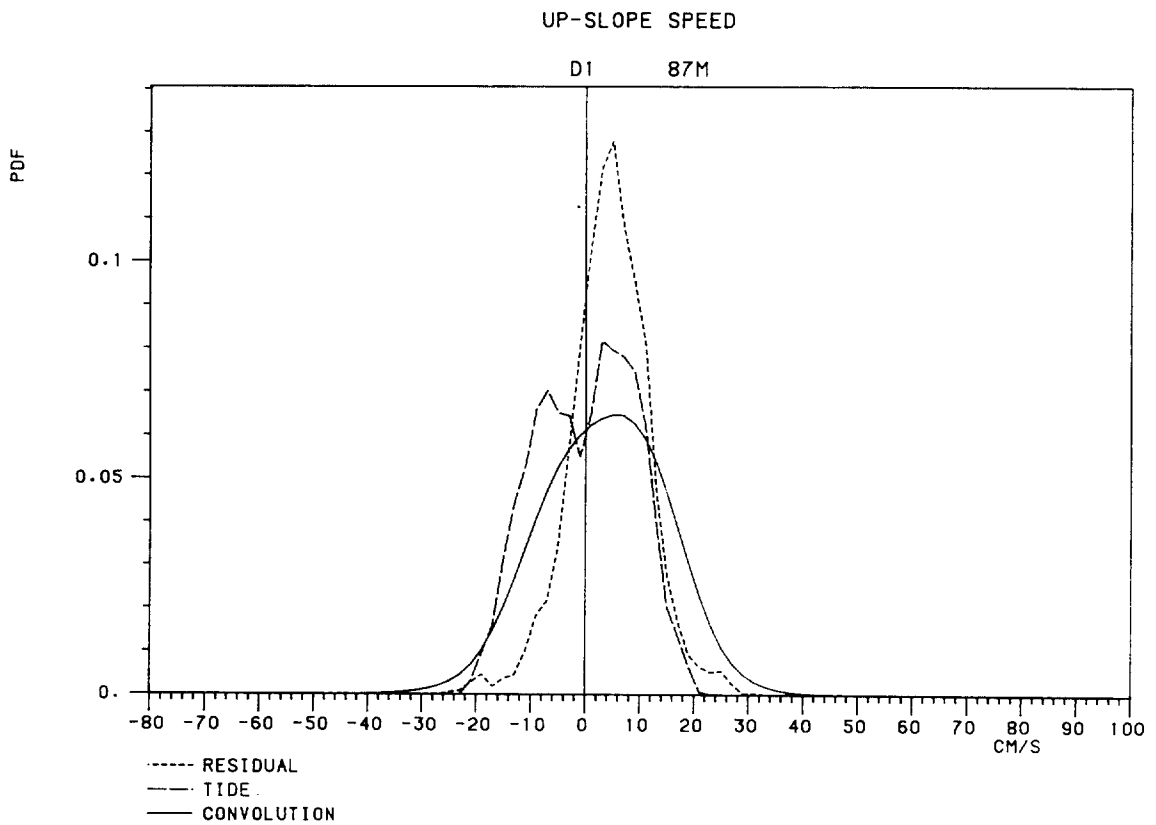
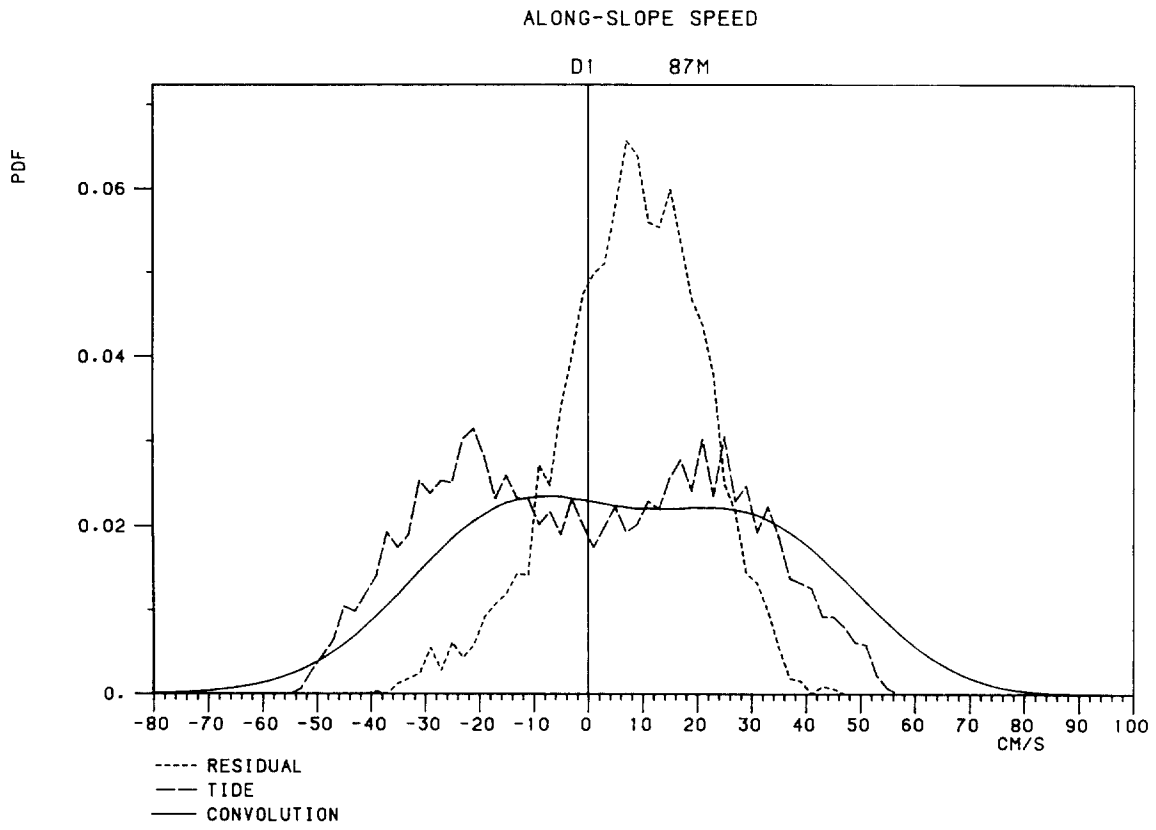


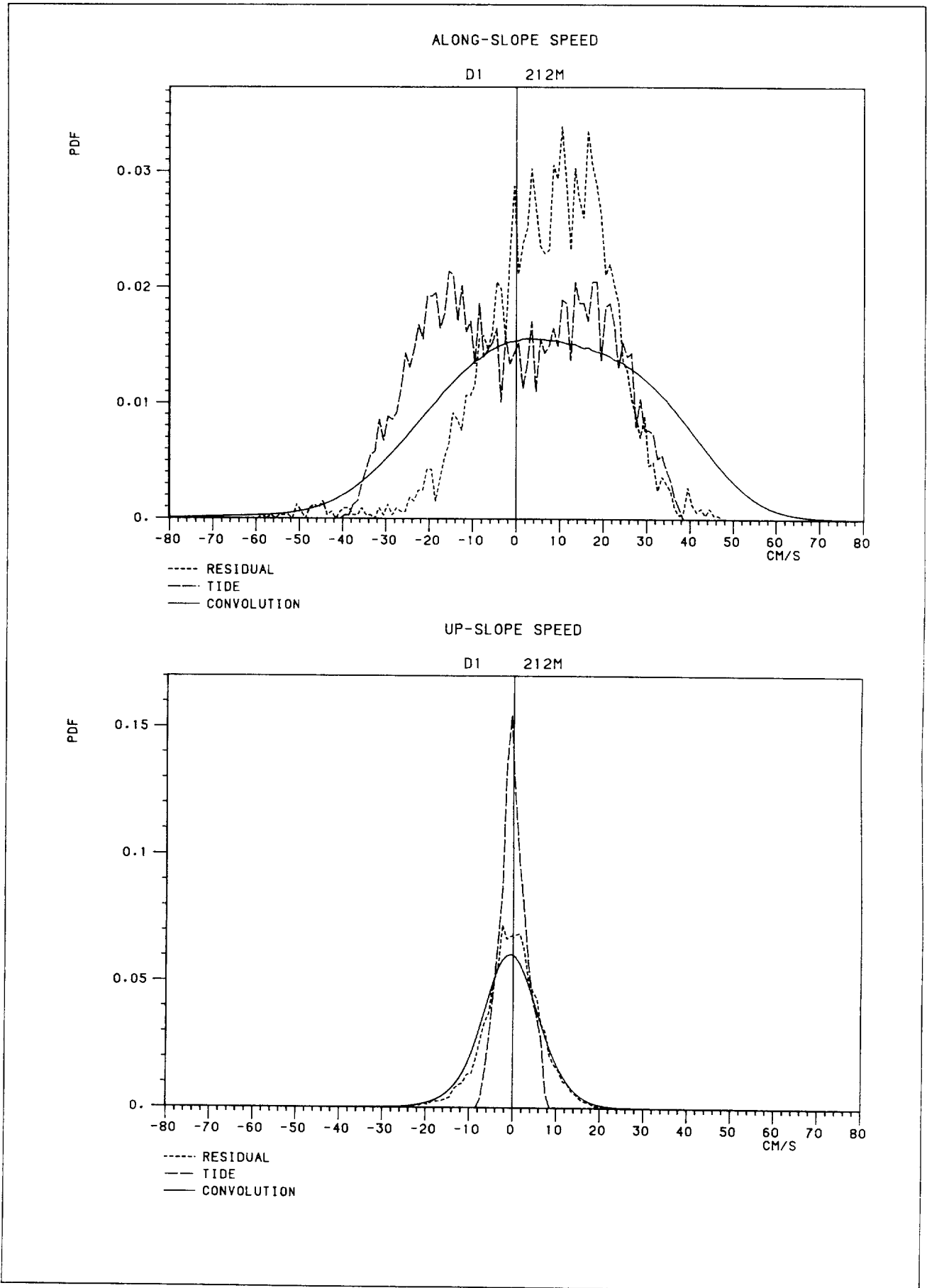


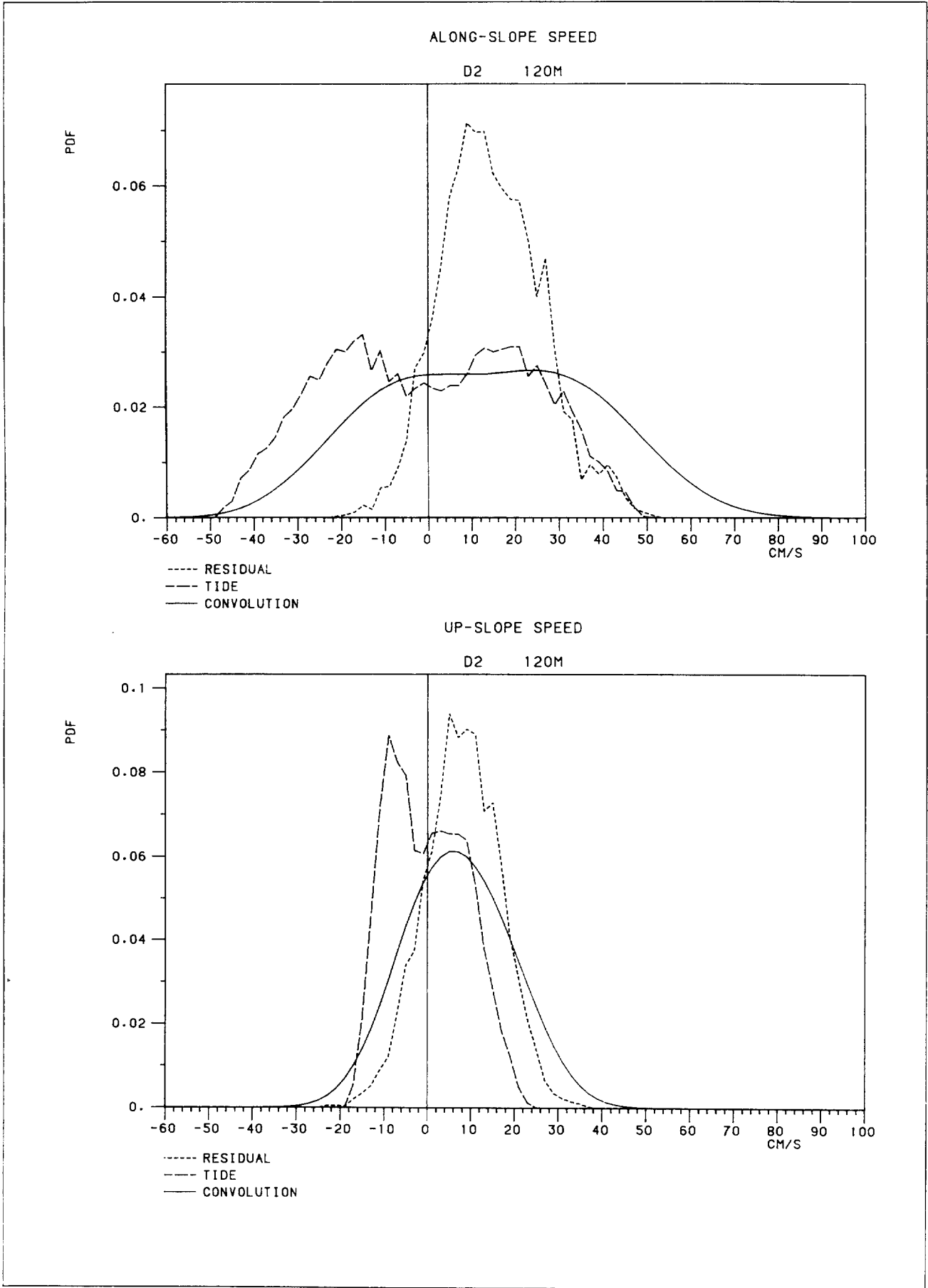


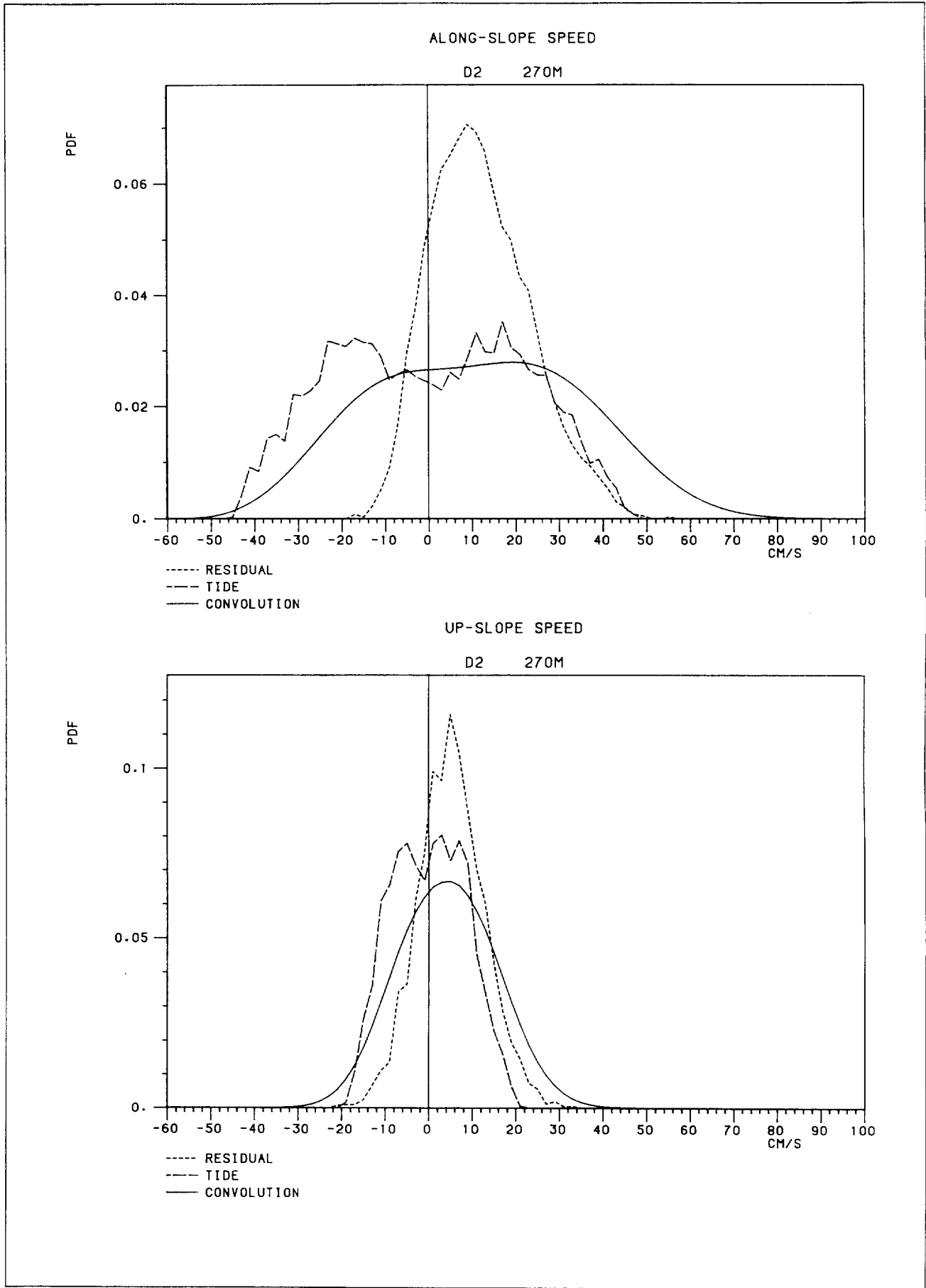


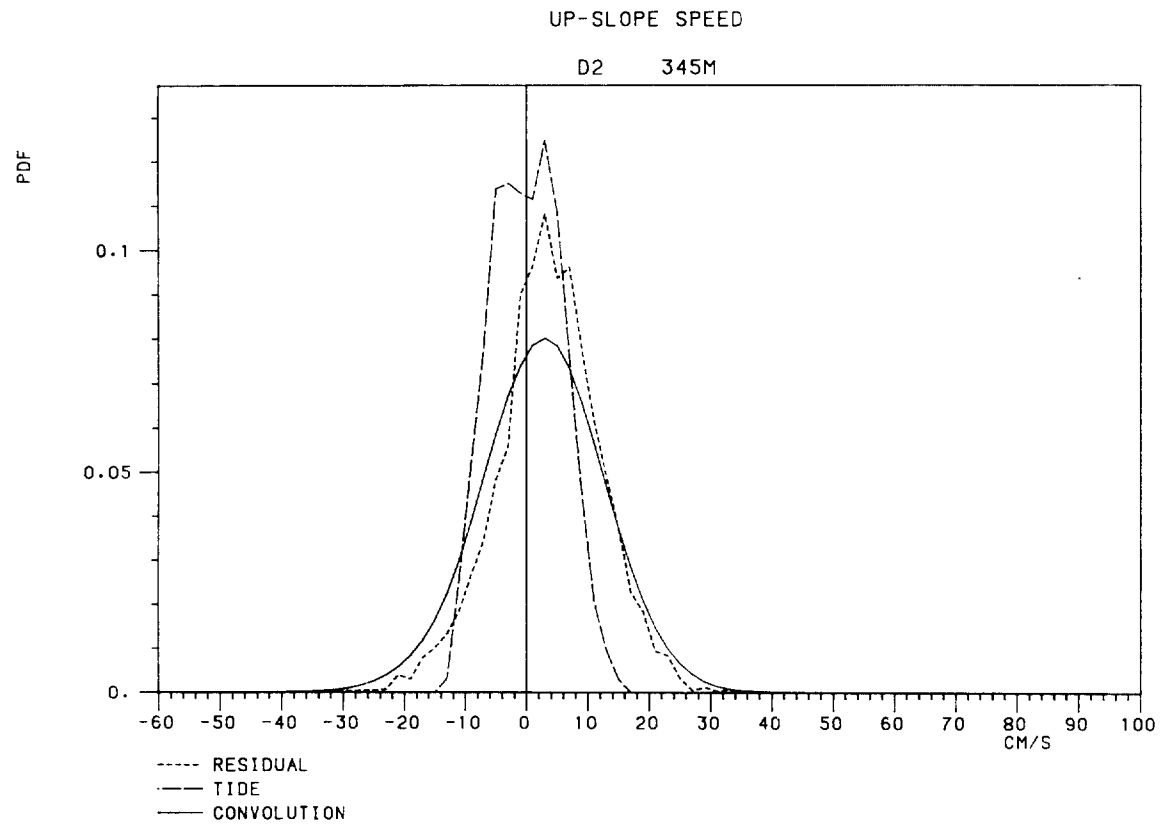
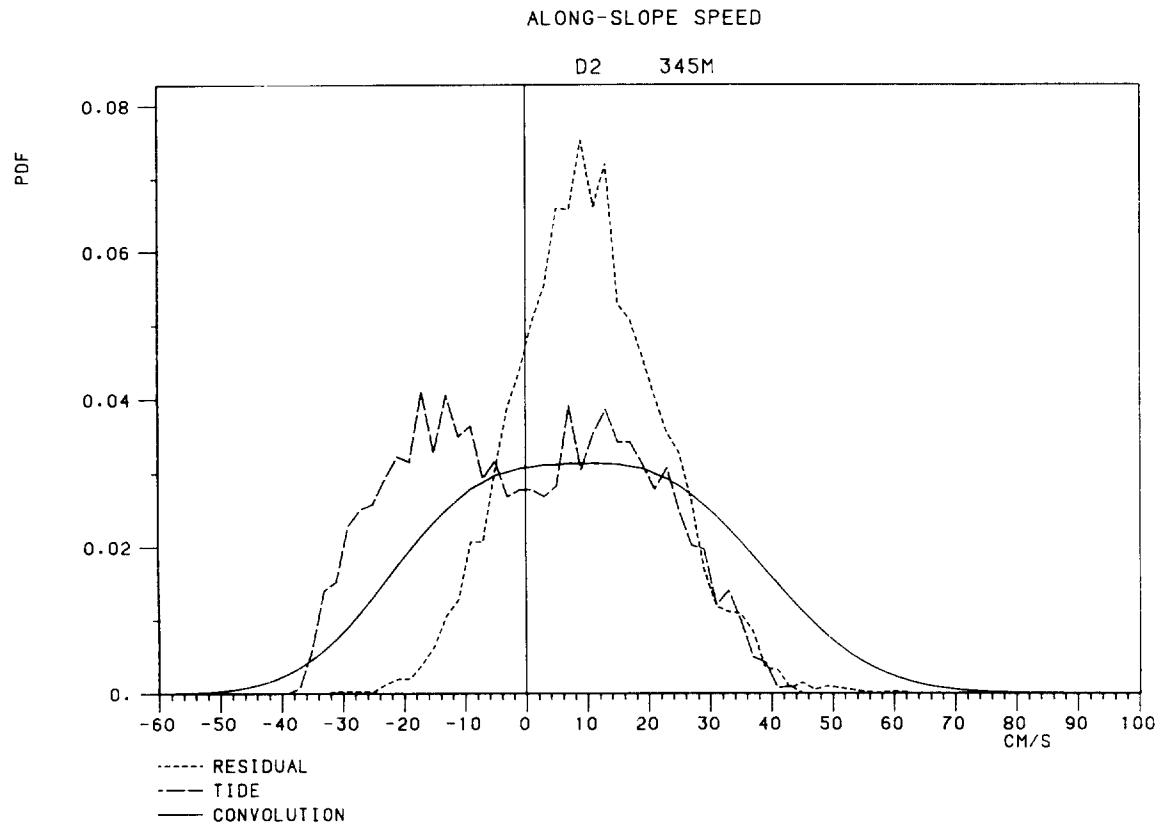


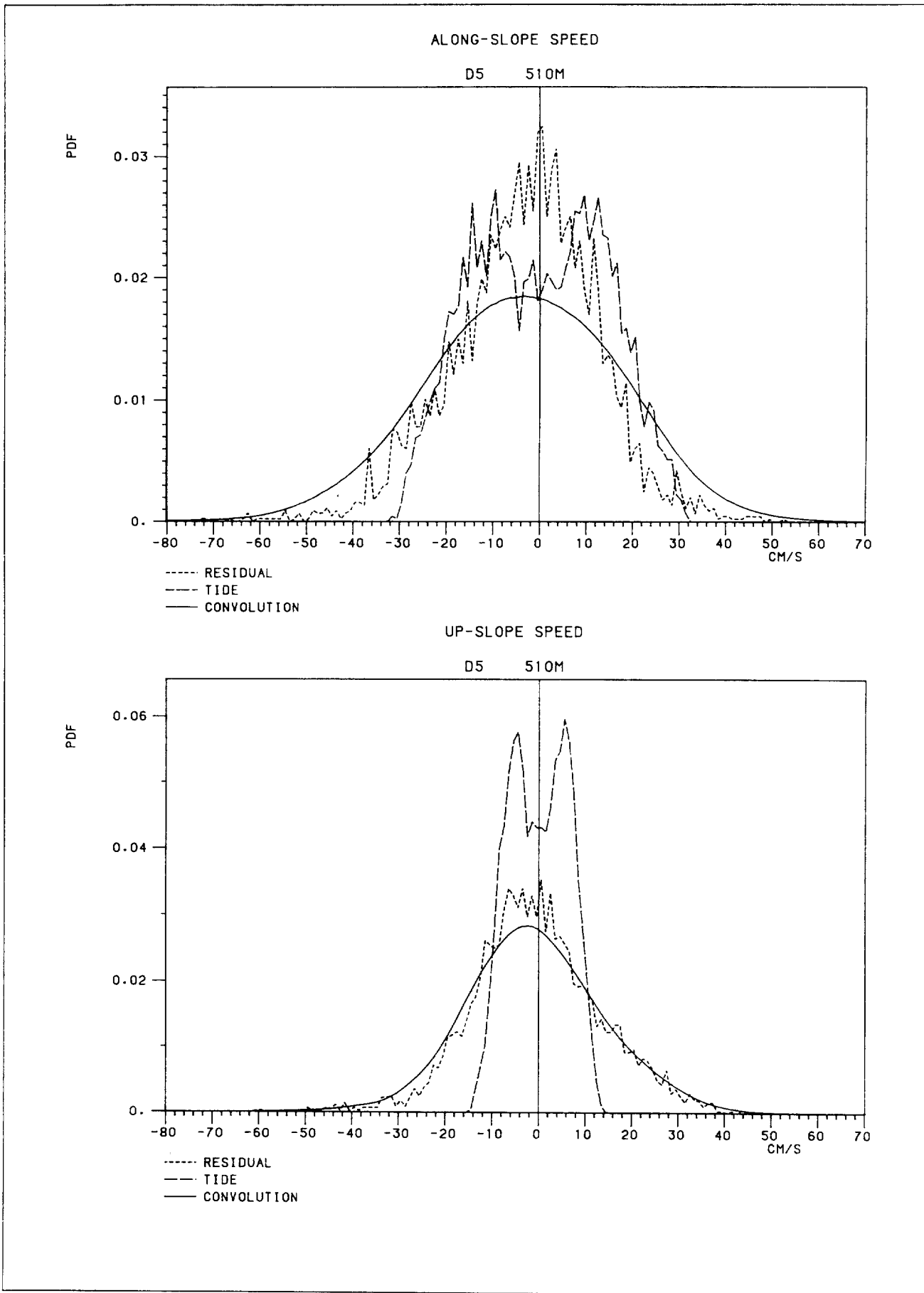






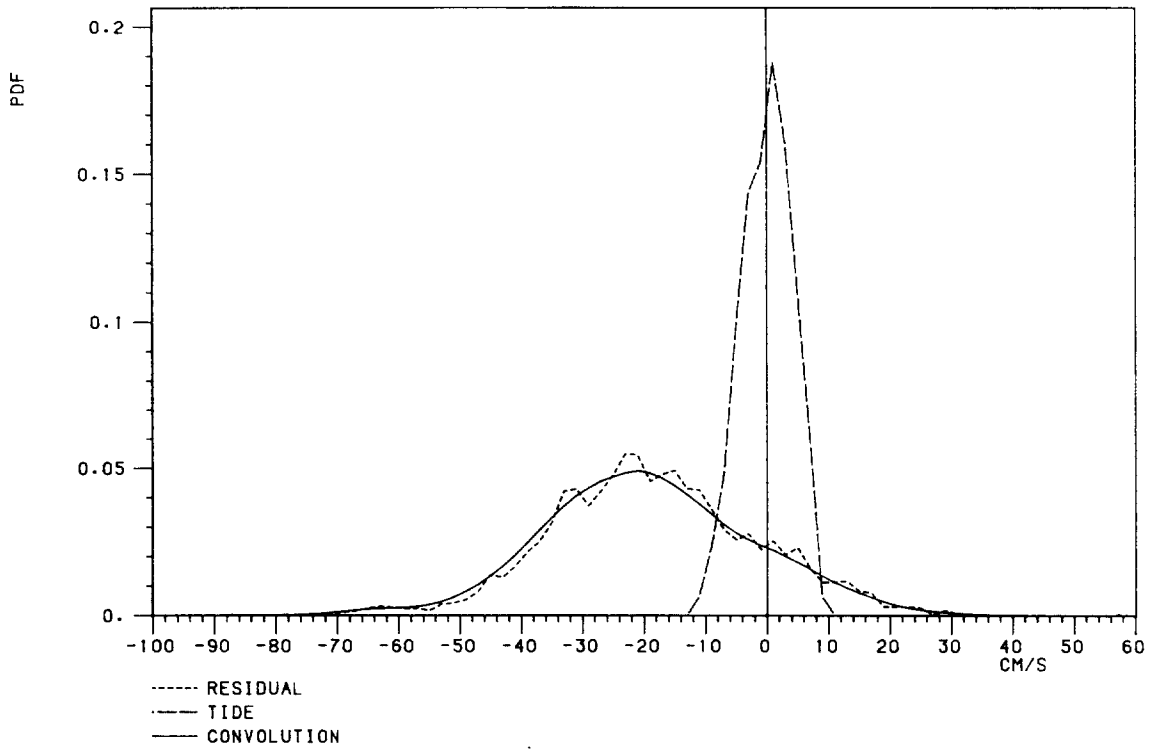






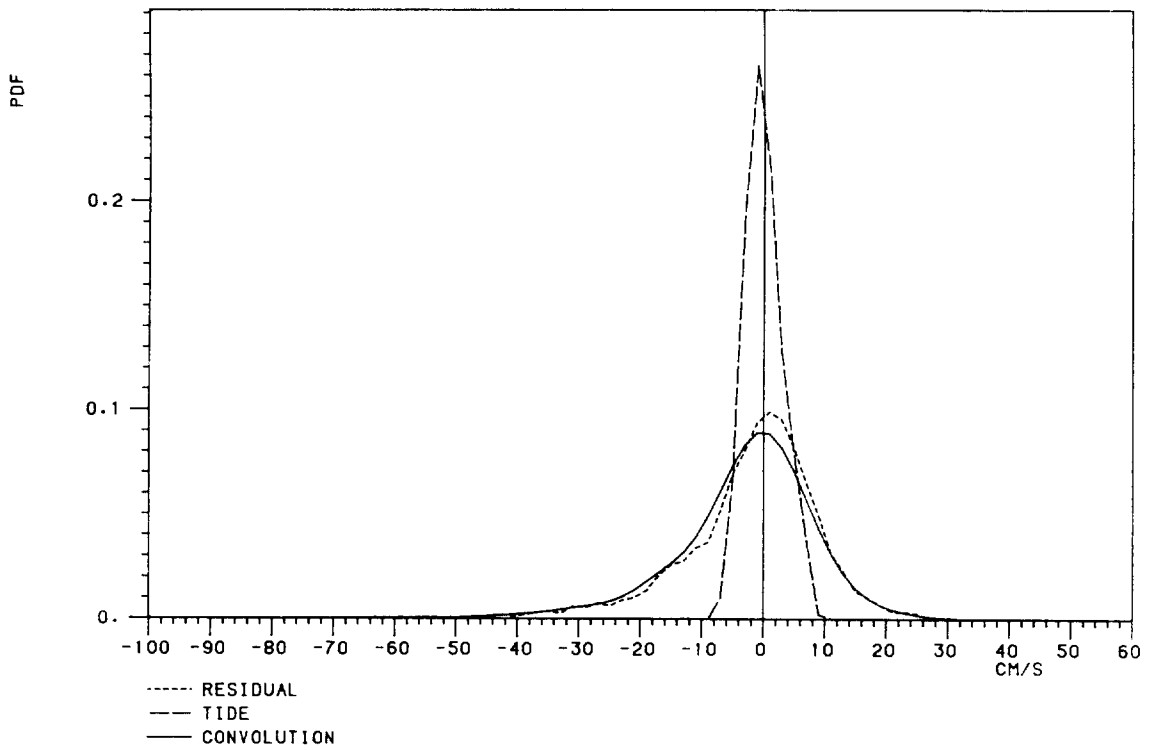
ALONG-SLOPE SPEED

D5 633M



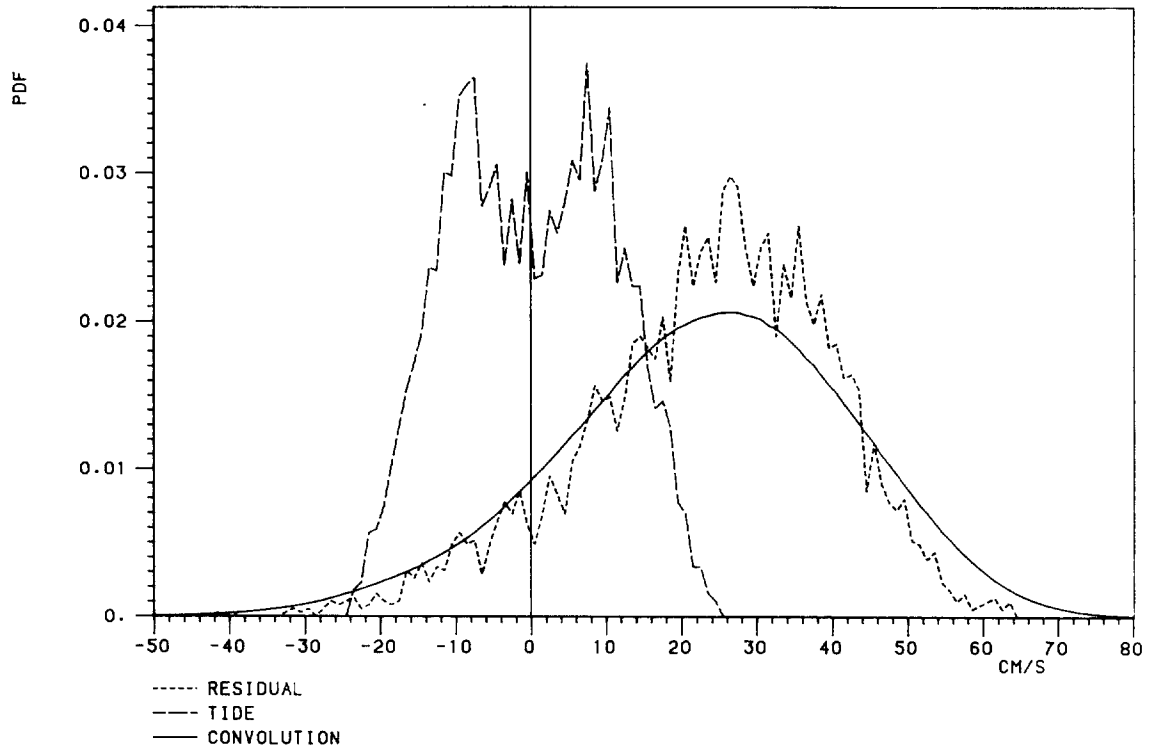
UP-SLOPE SPEED

D5 633M



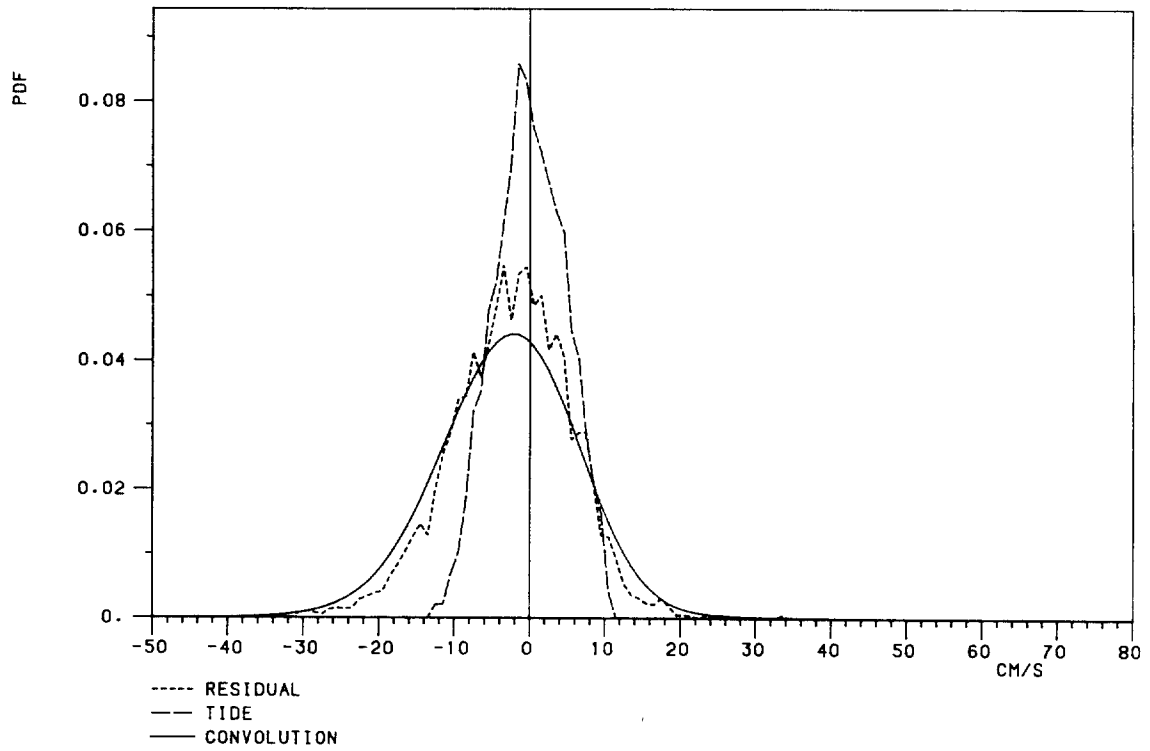
ALONG-SLOPE SPEED

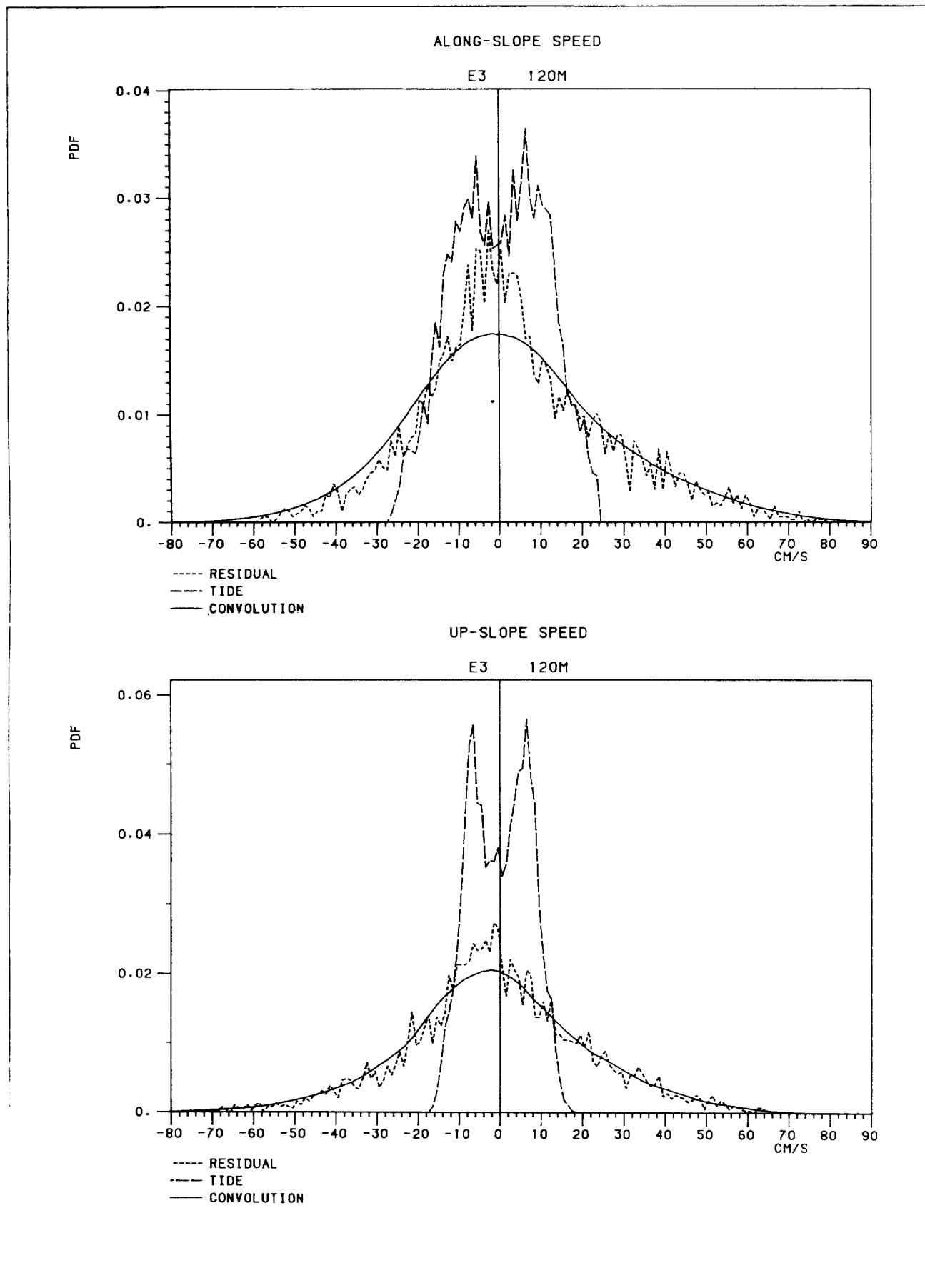
E2 453M

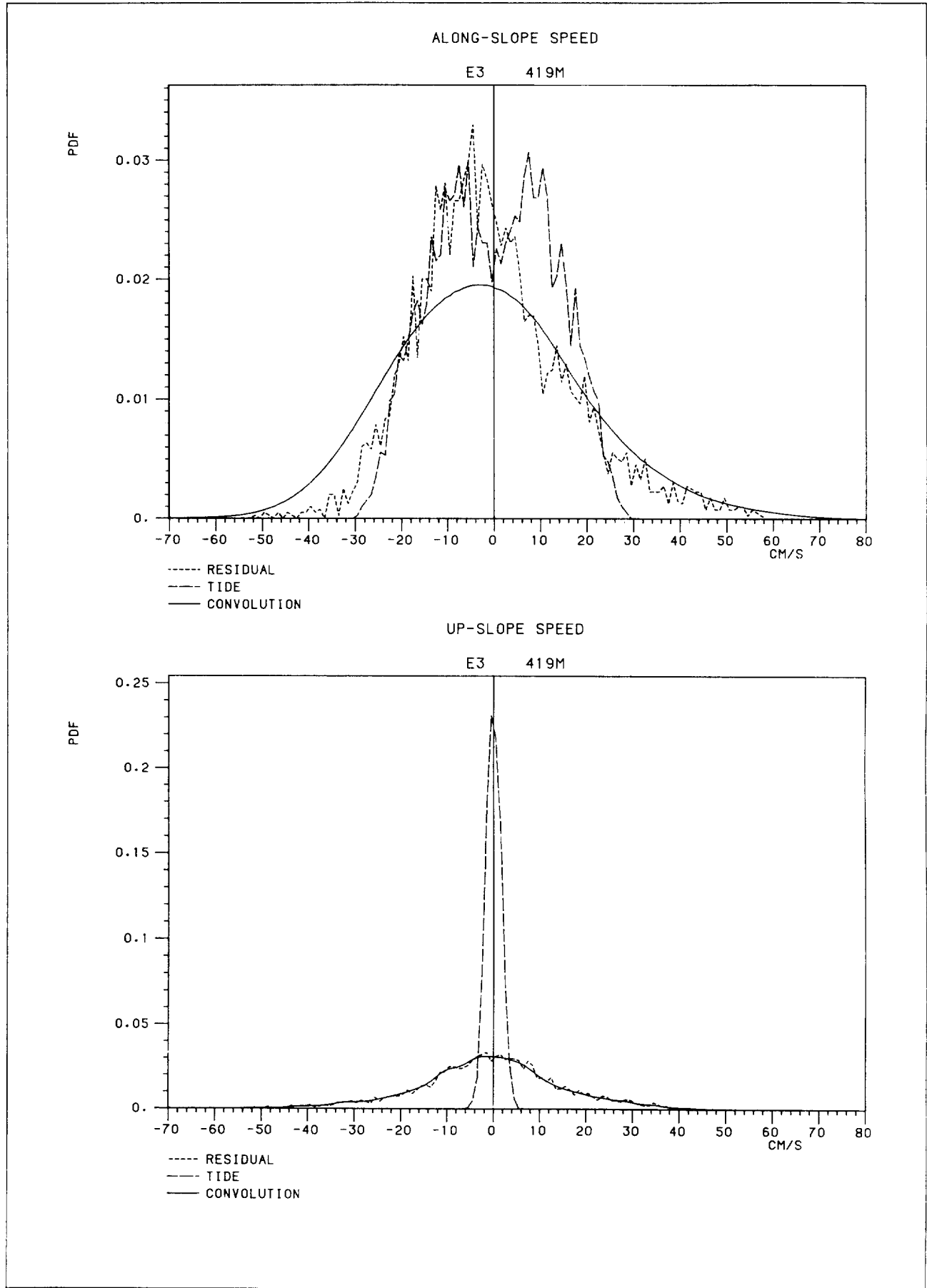


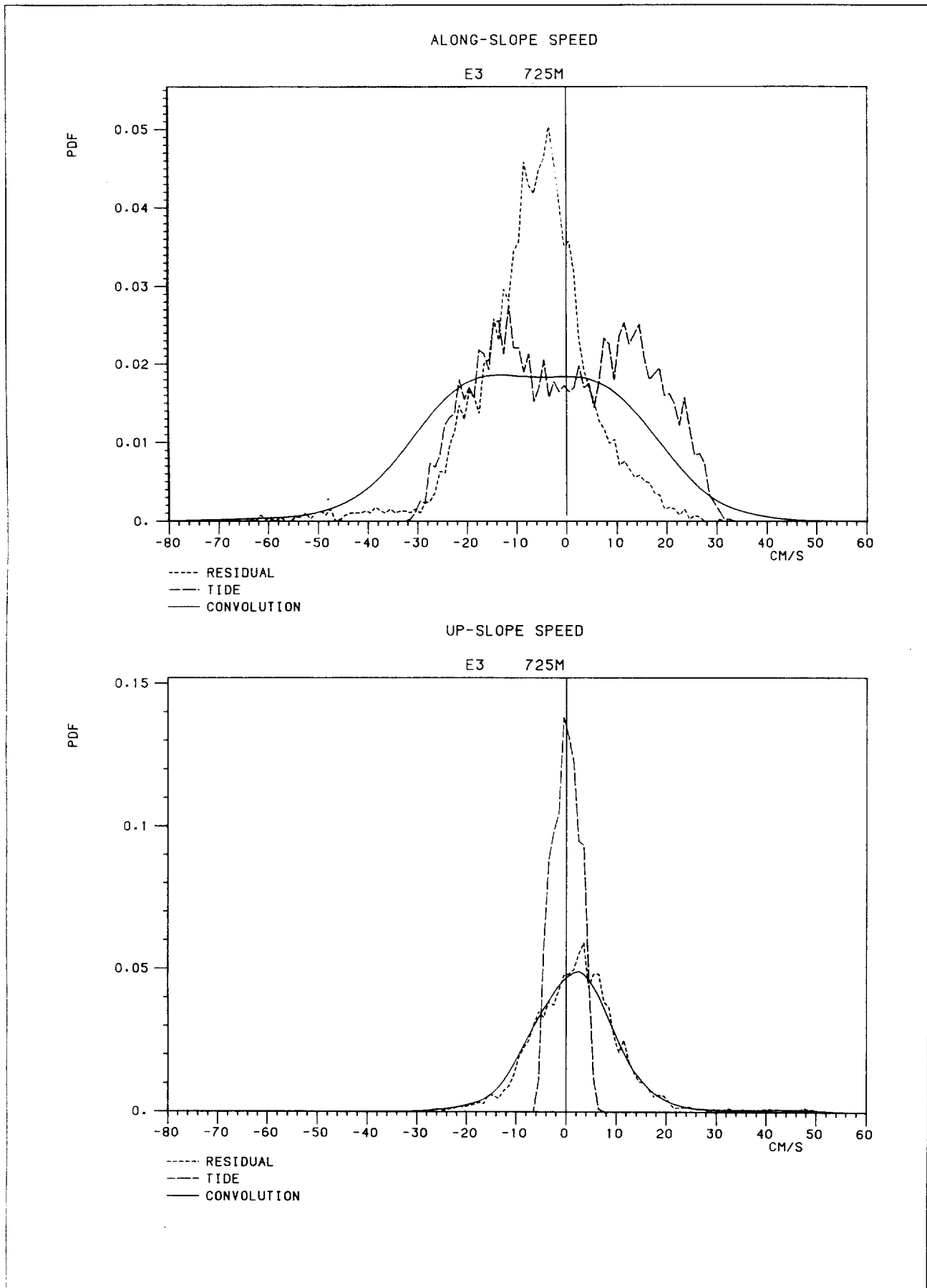
UP-SLOPE SPEED

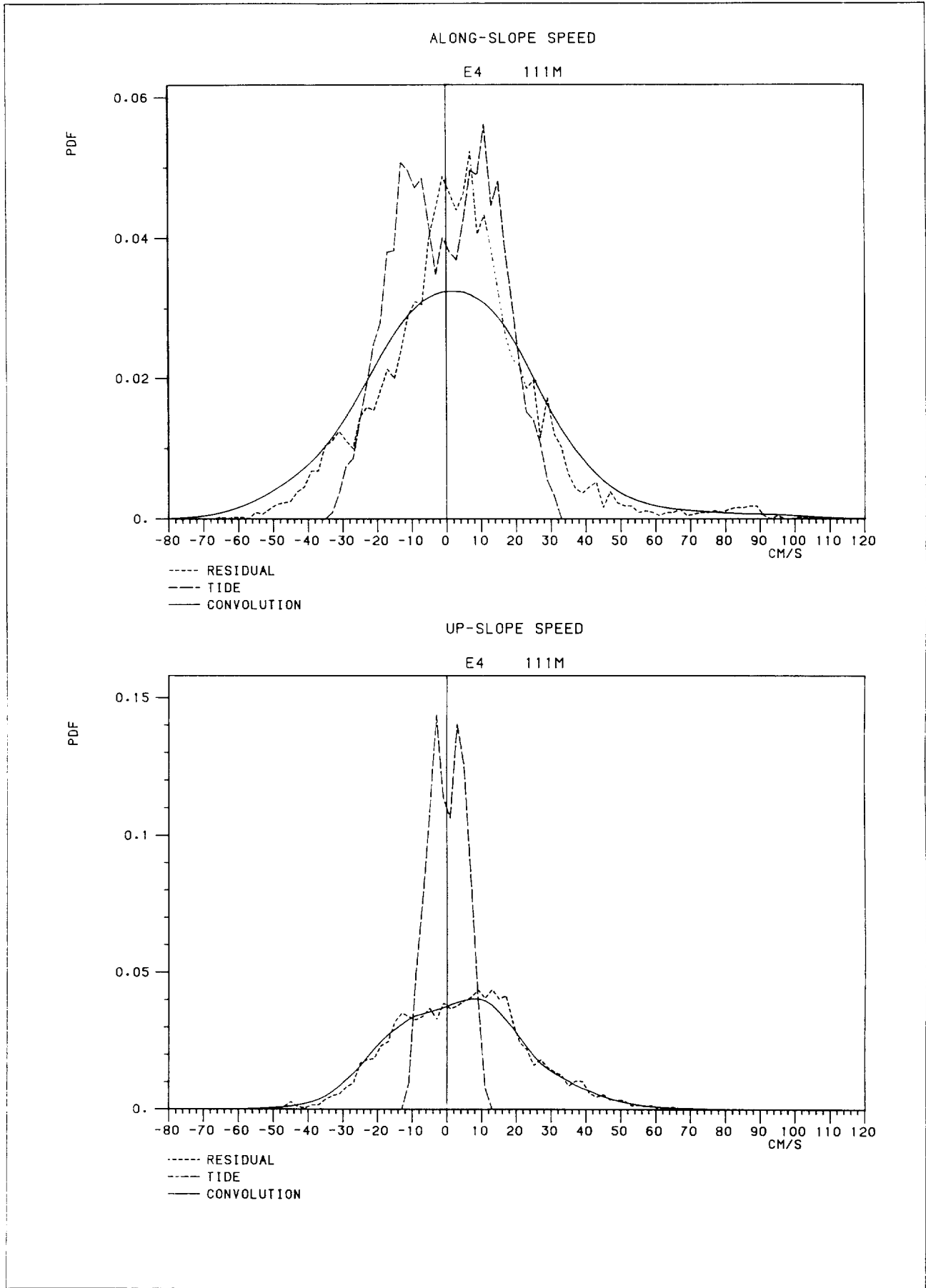
E2 453M

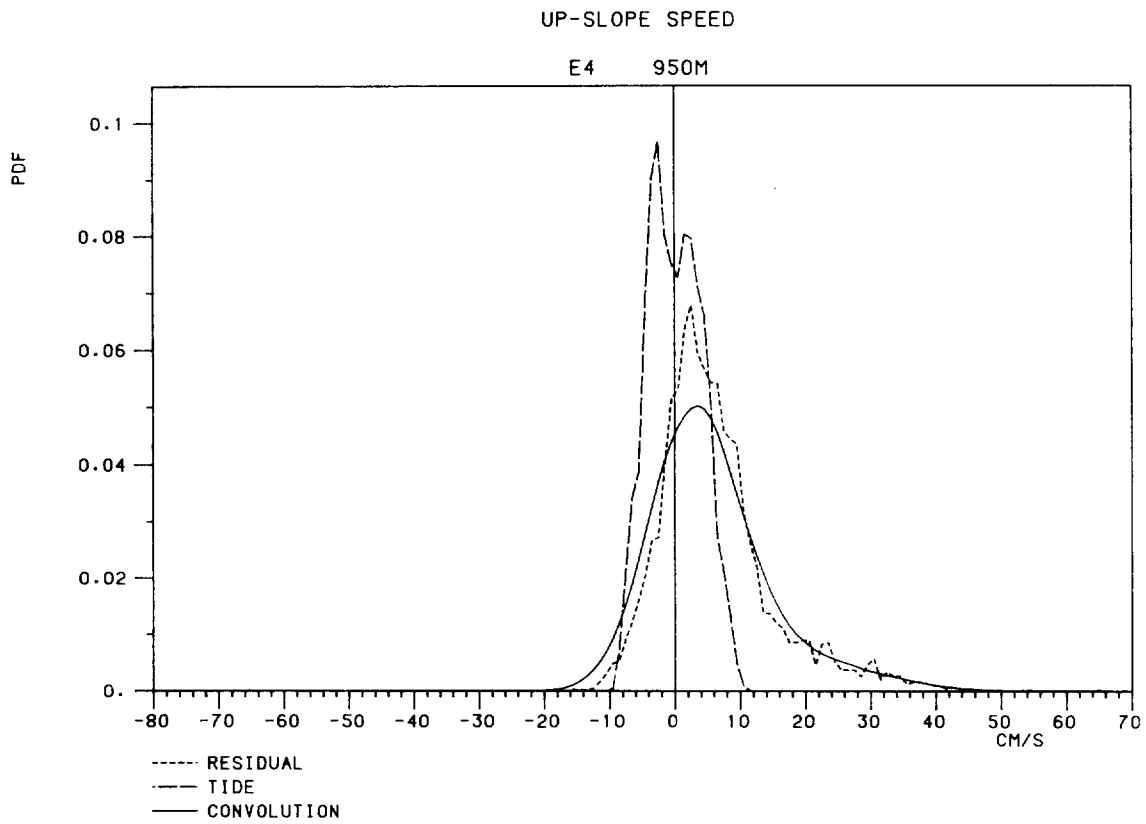
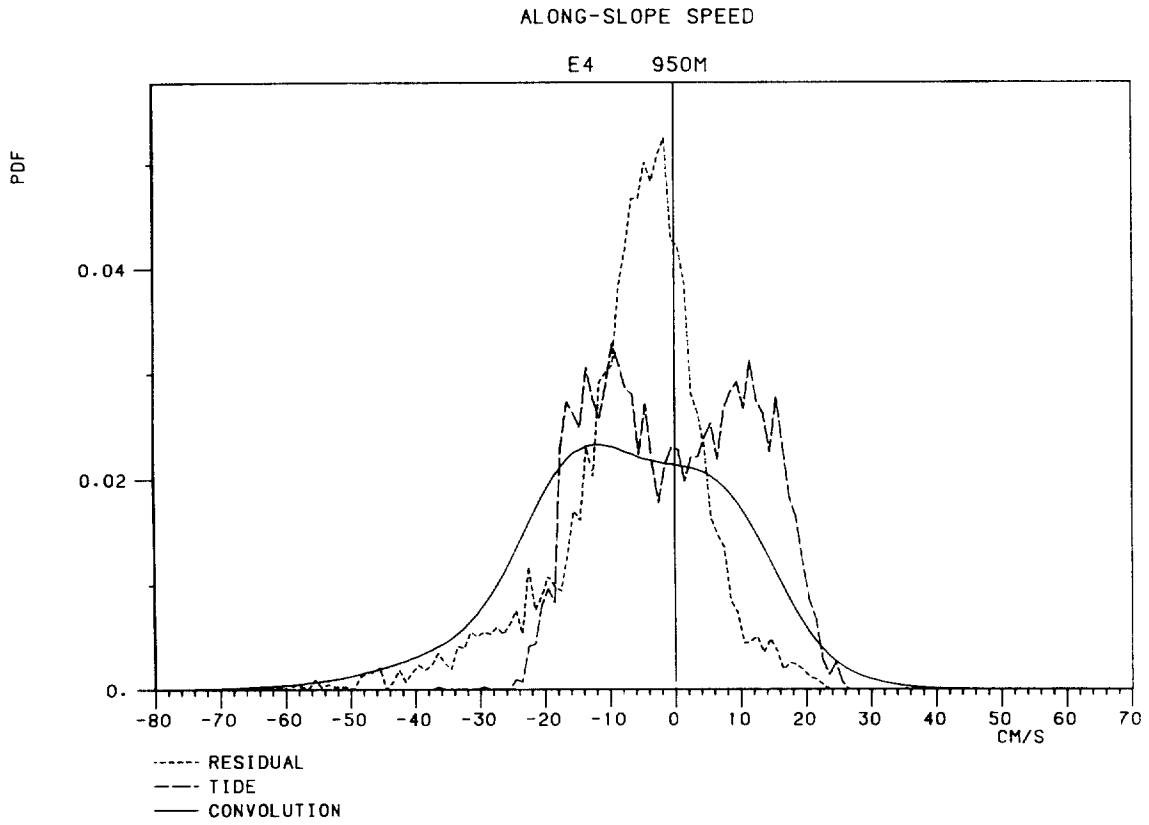


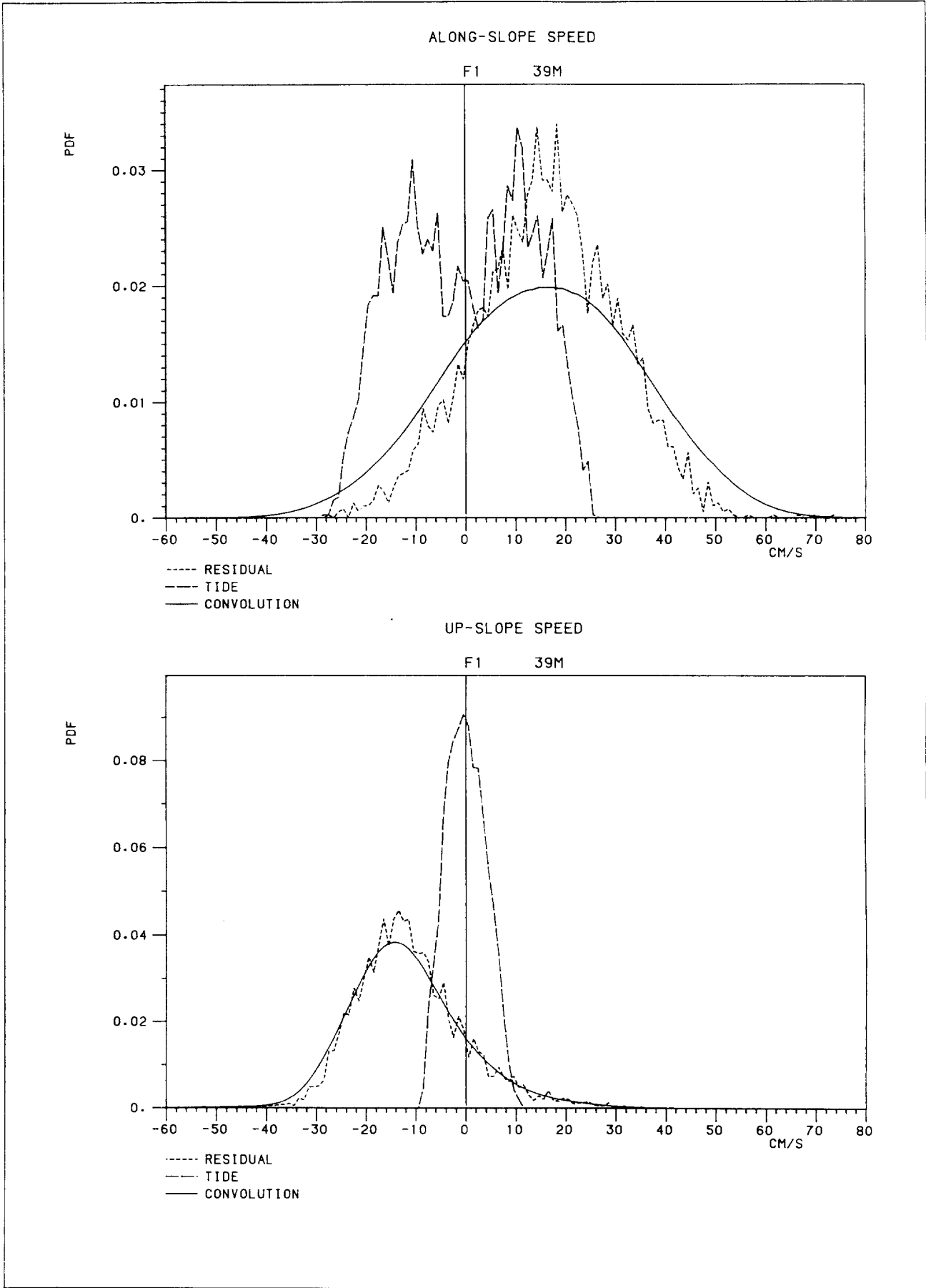


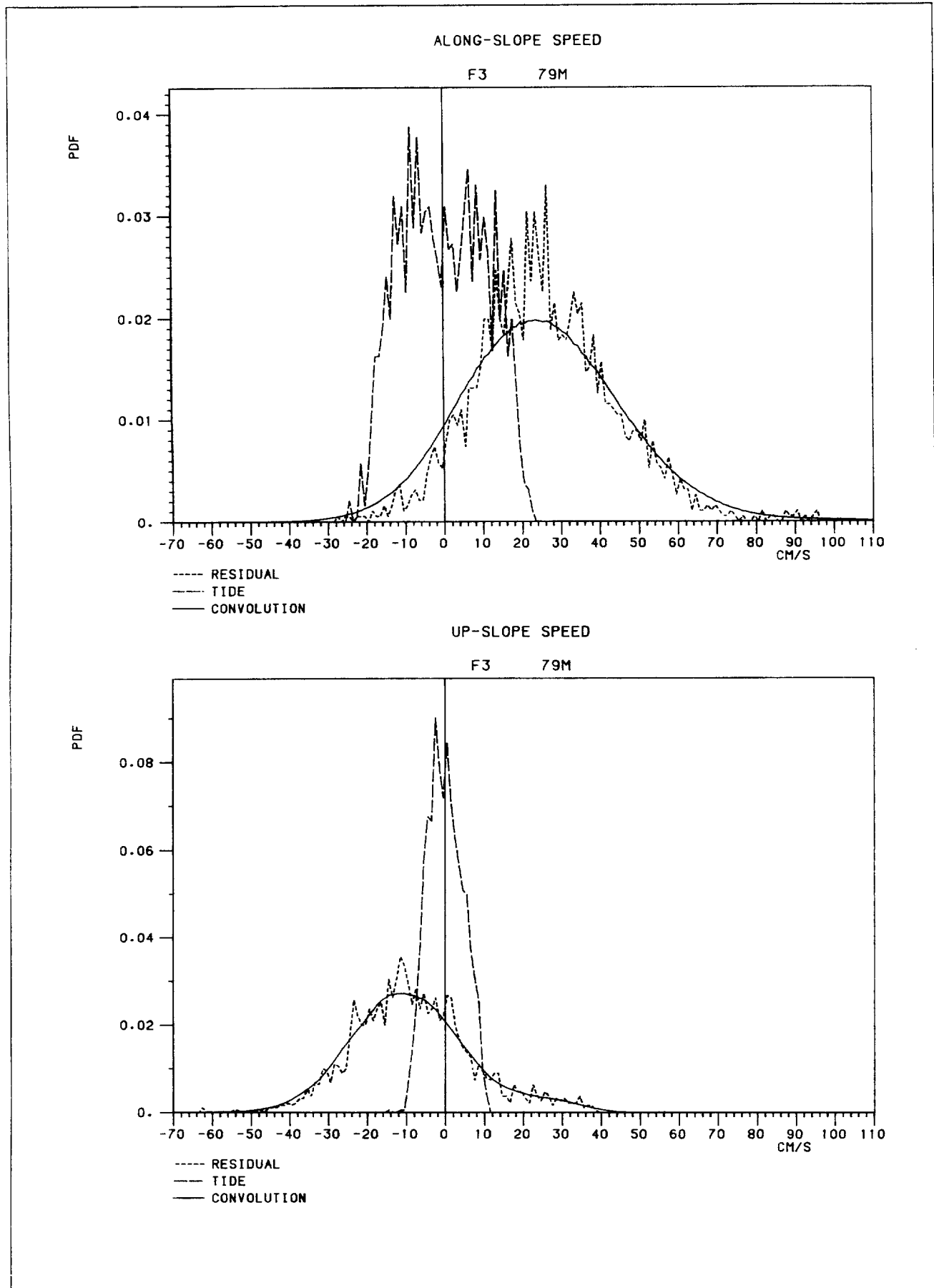


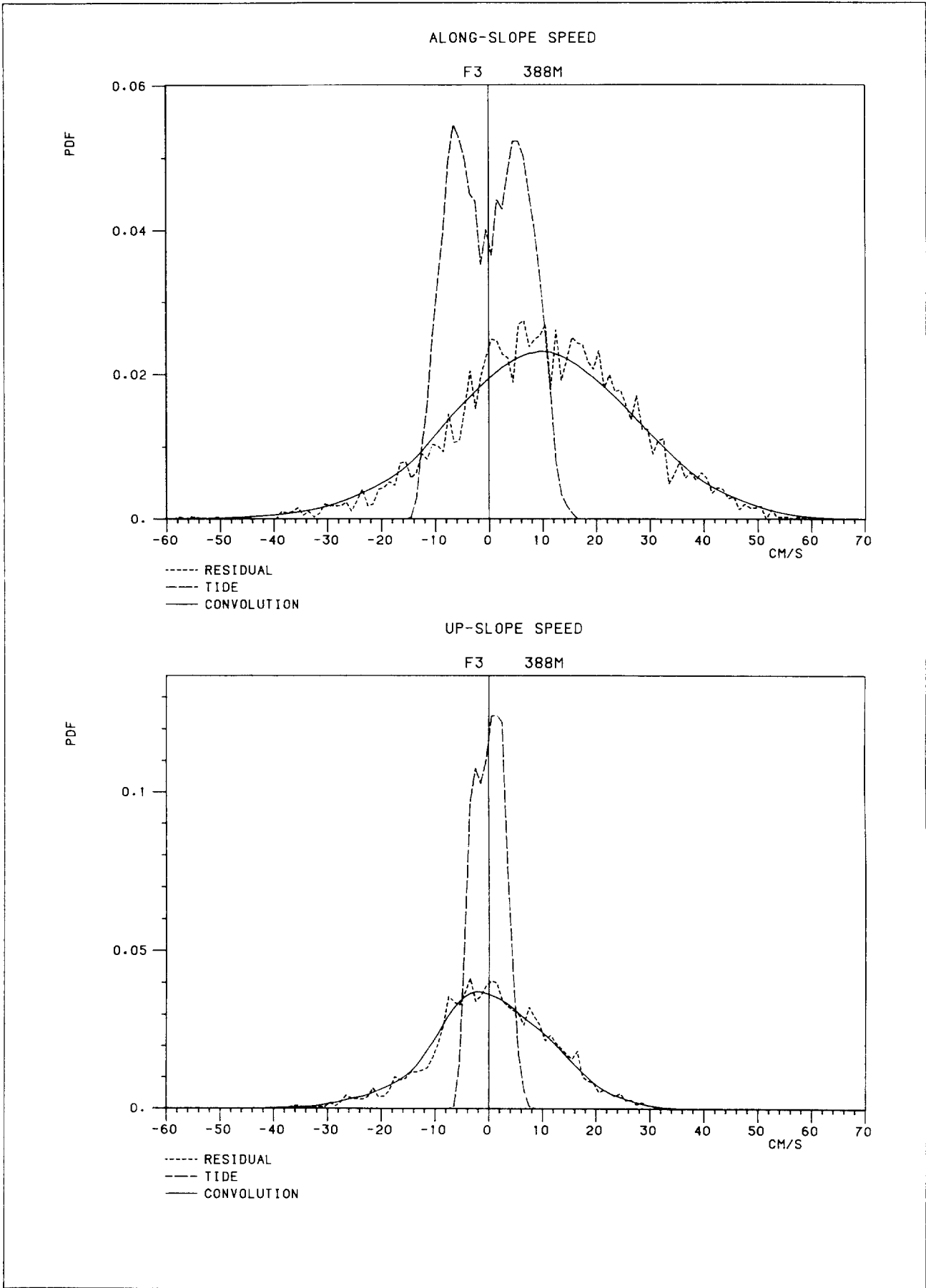


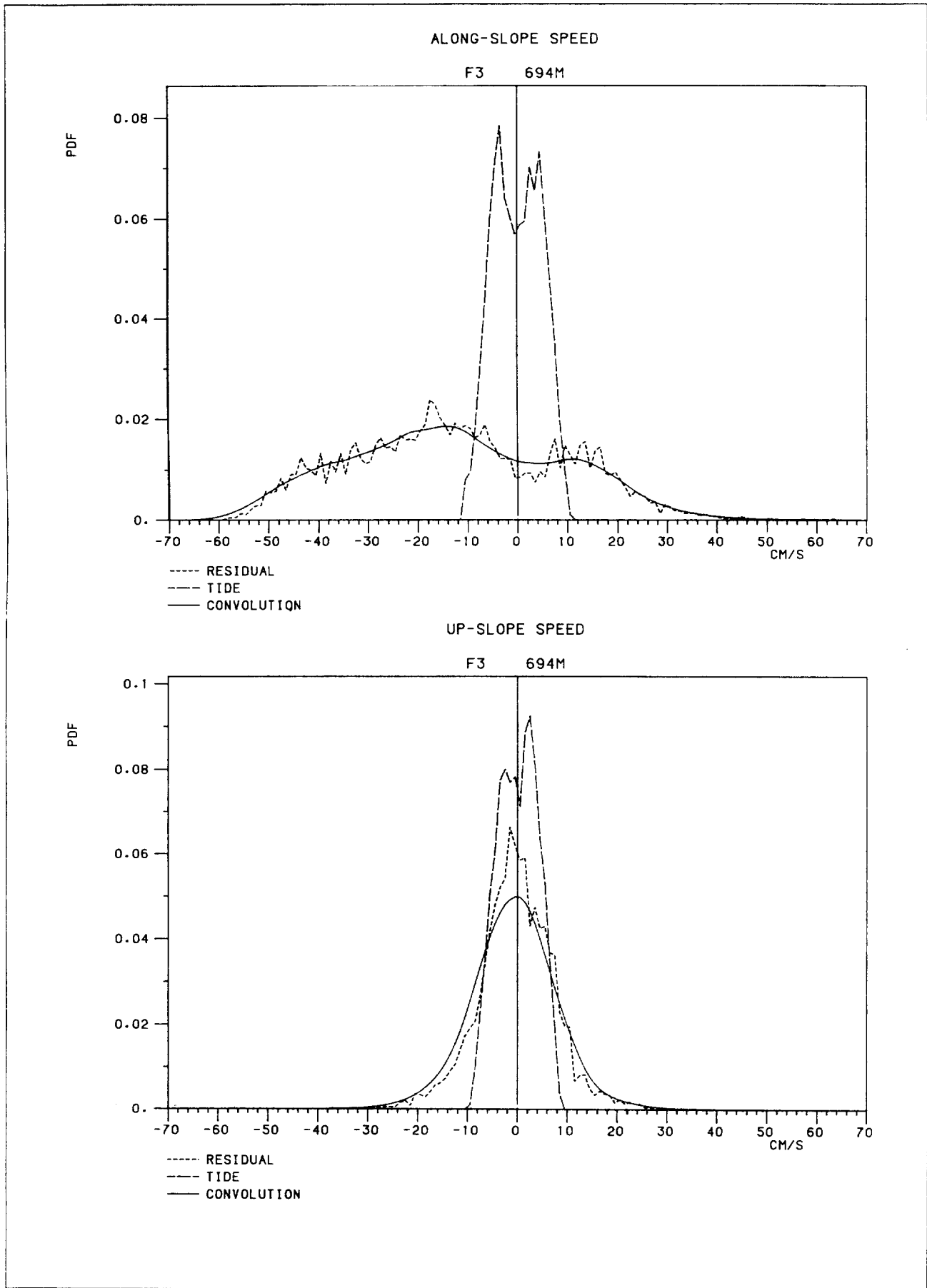


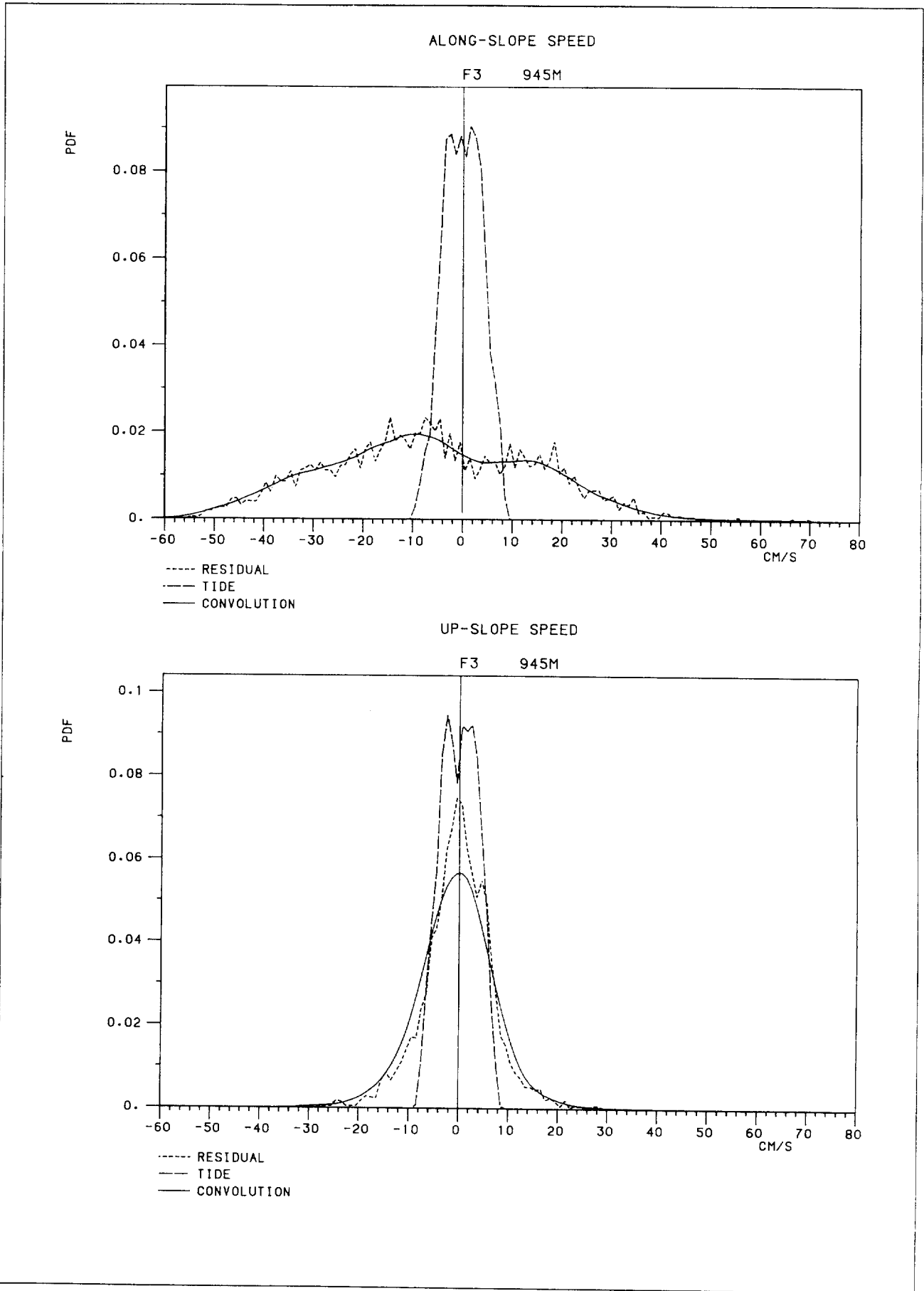






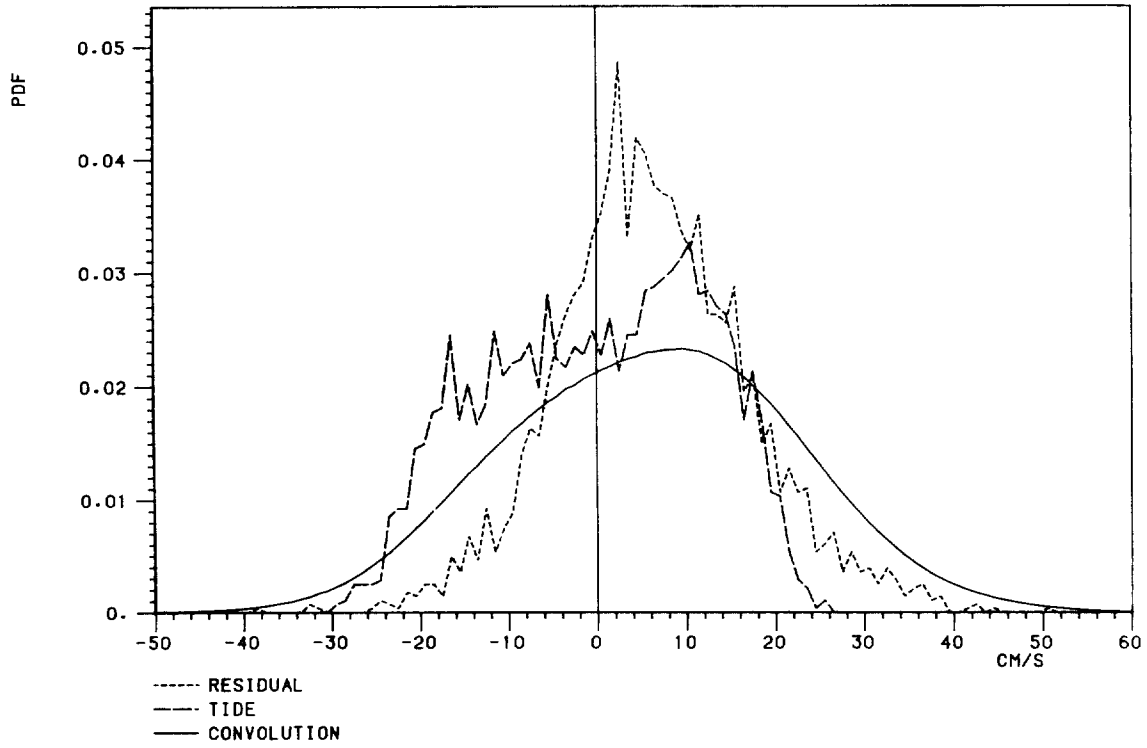






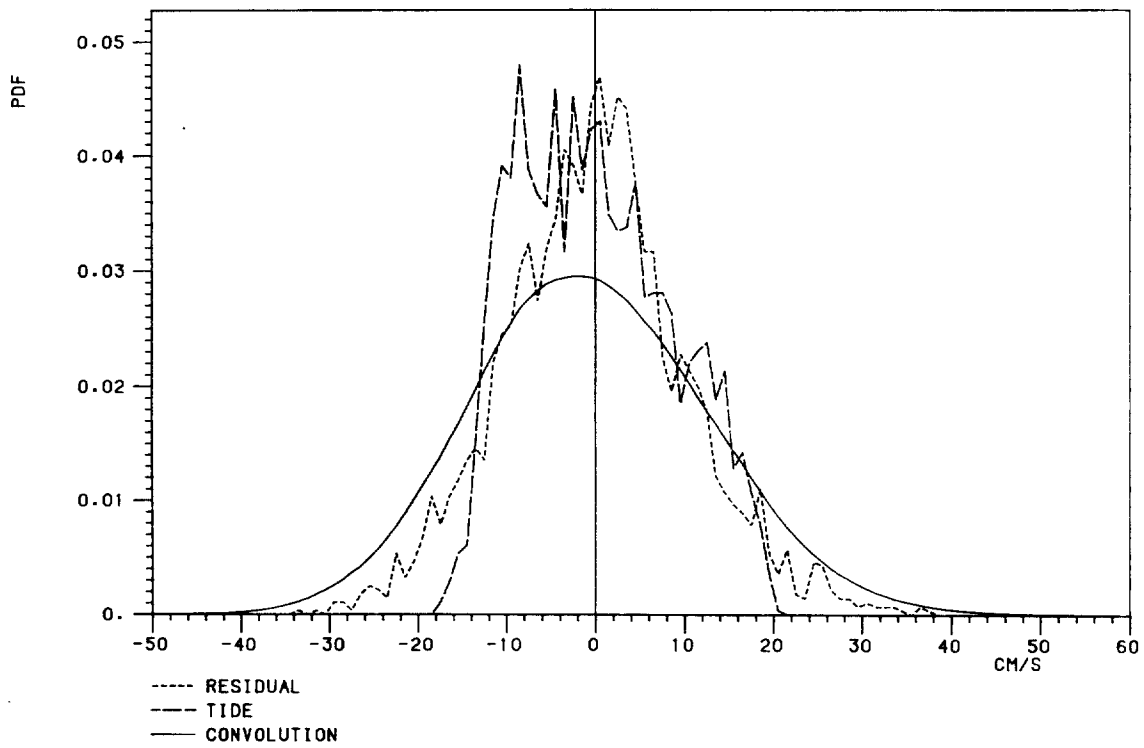
ALONG-SLOPE SPEED

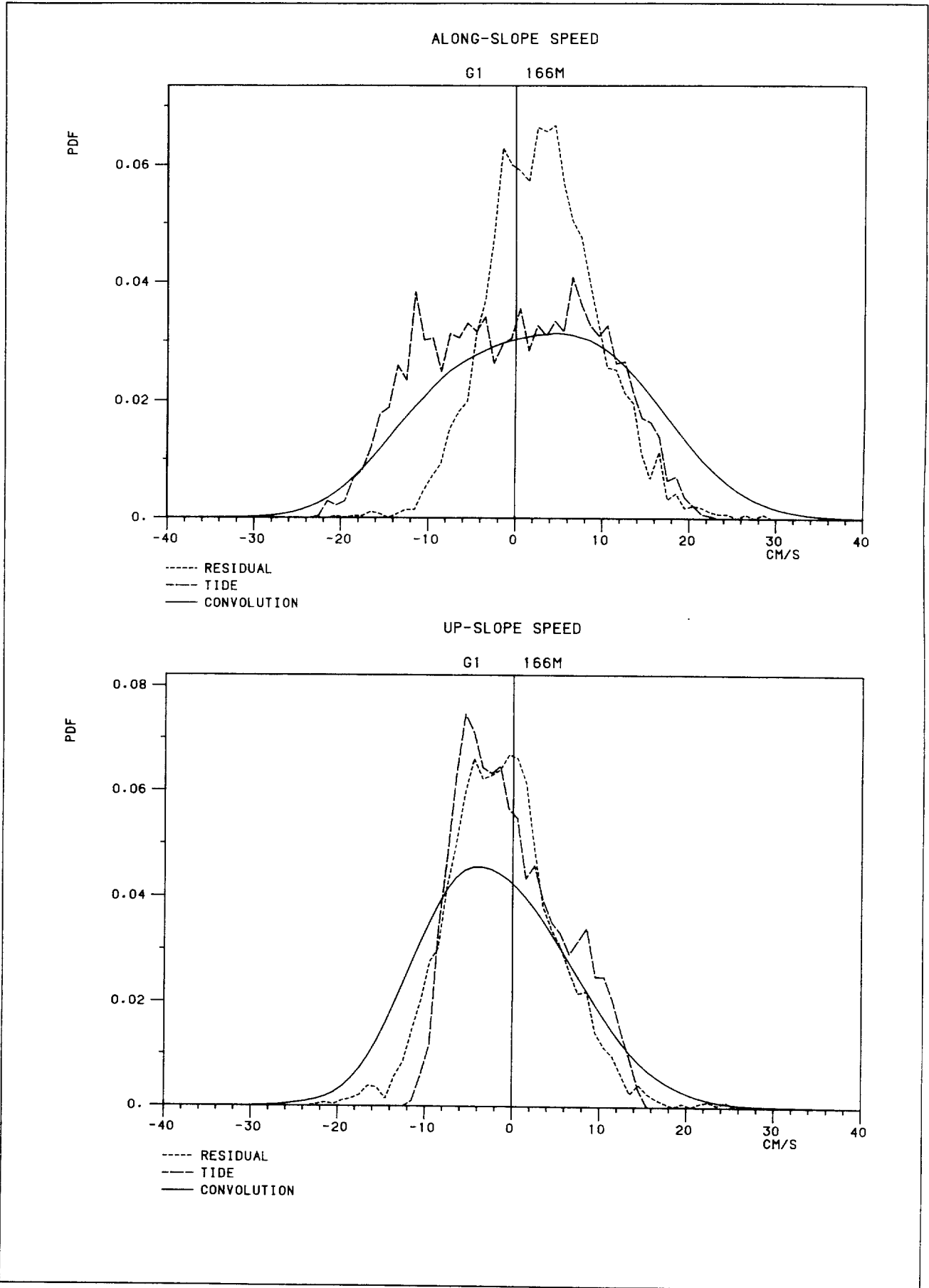
G1 41M



UP-SLOPE SPEED

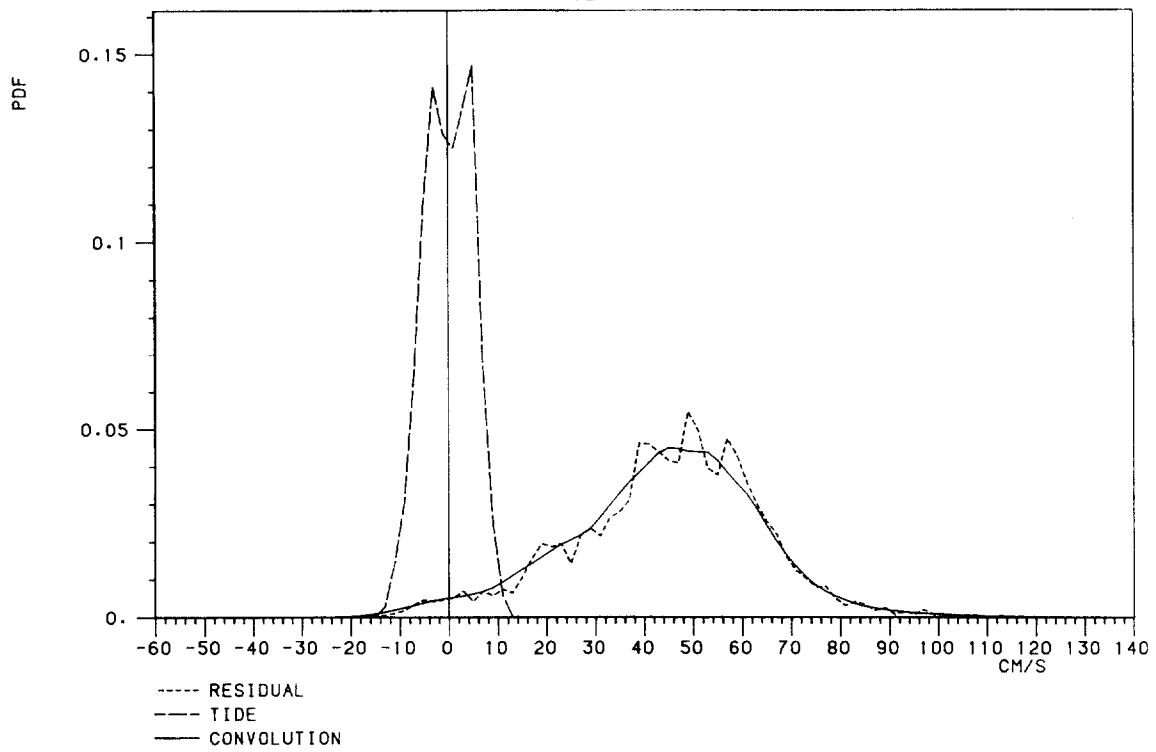
G1 41M





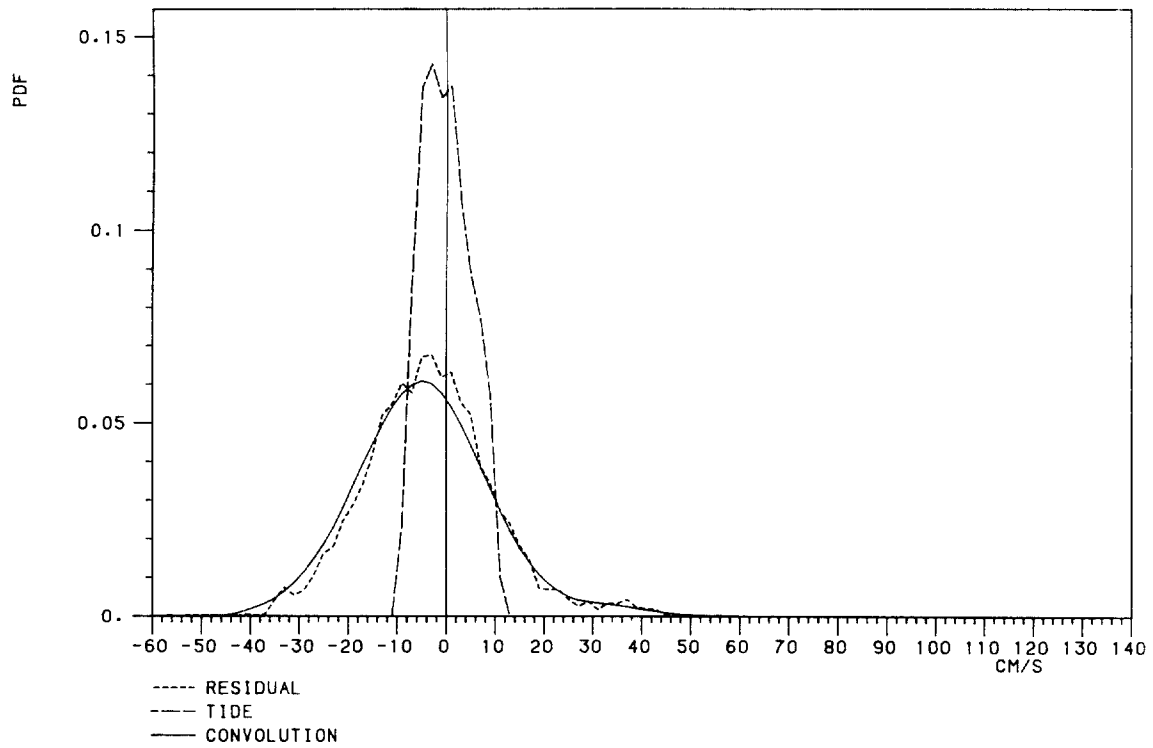
ALONG-SLOPE SPEED

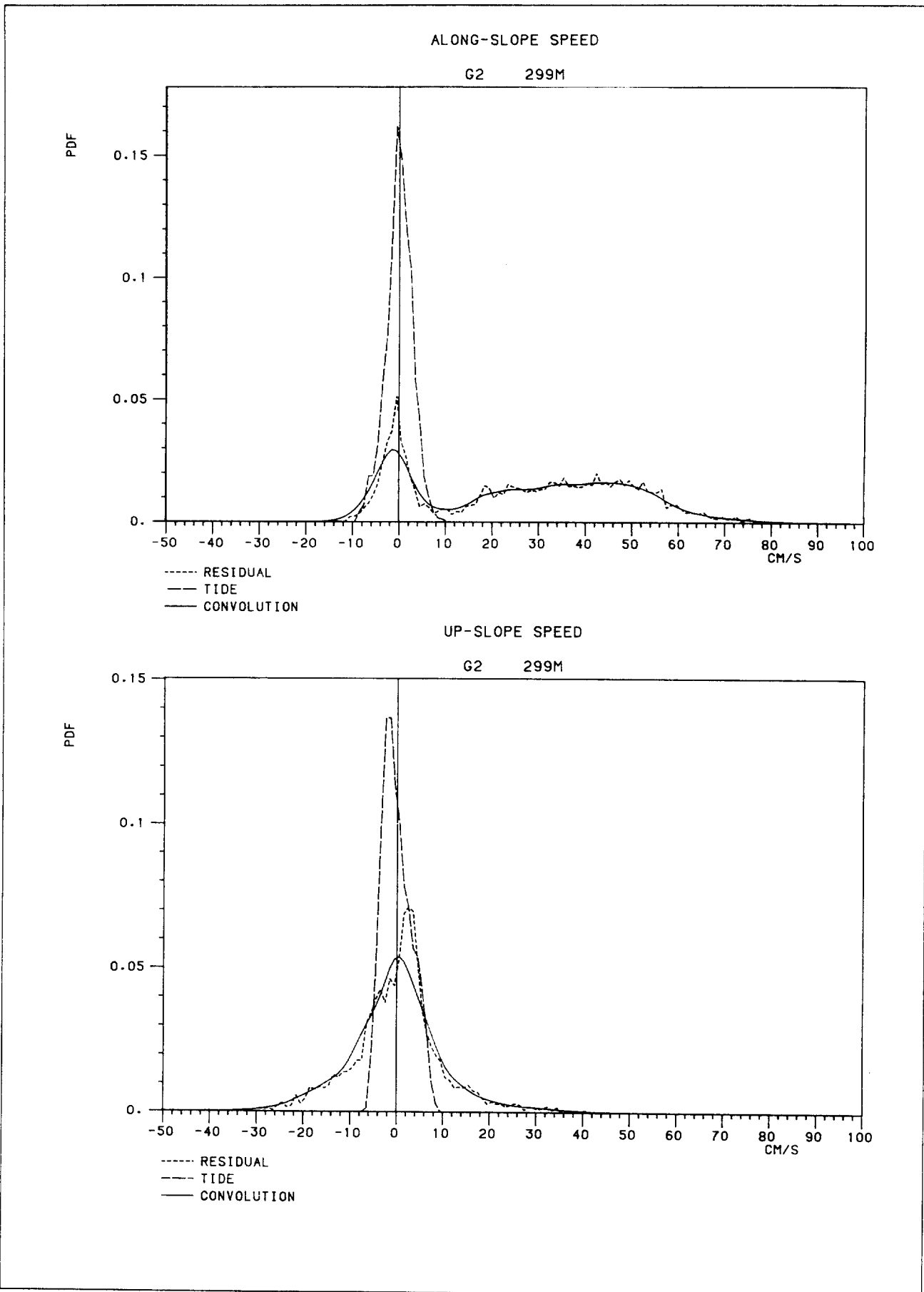
G2 151M

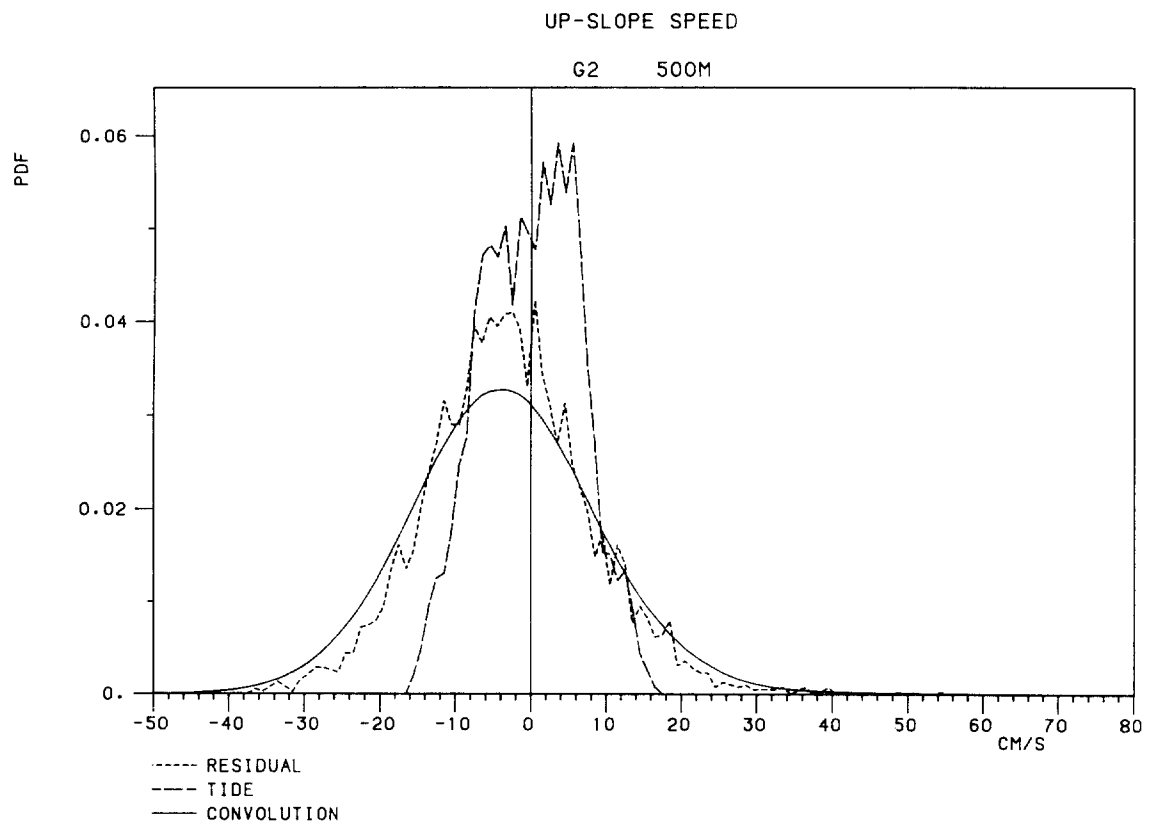
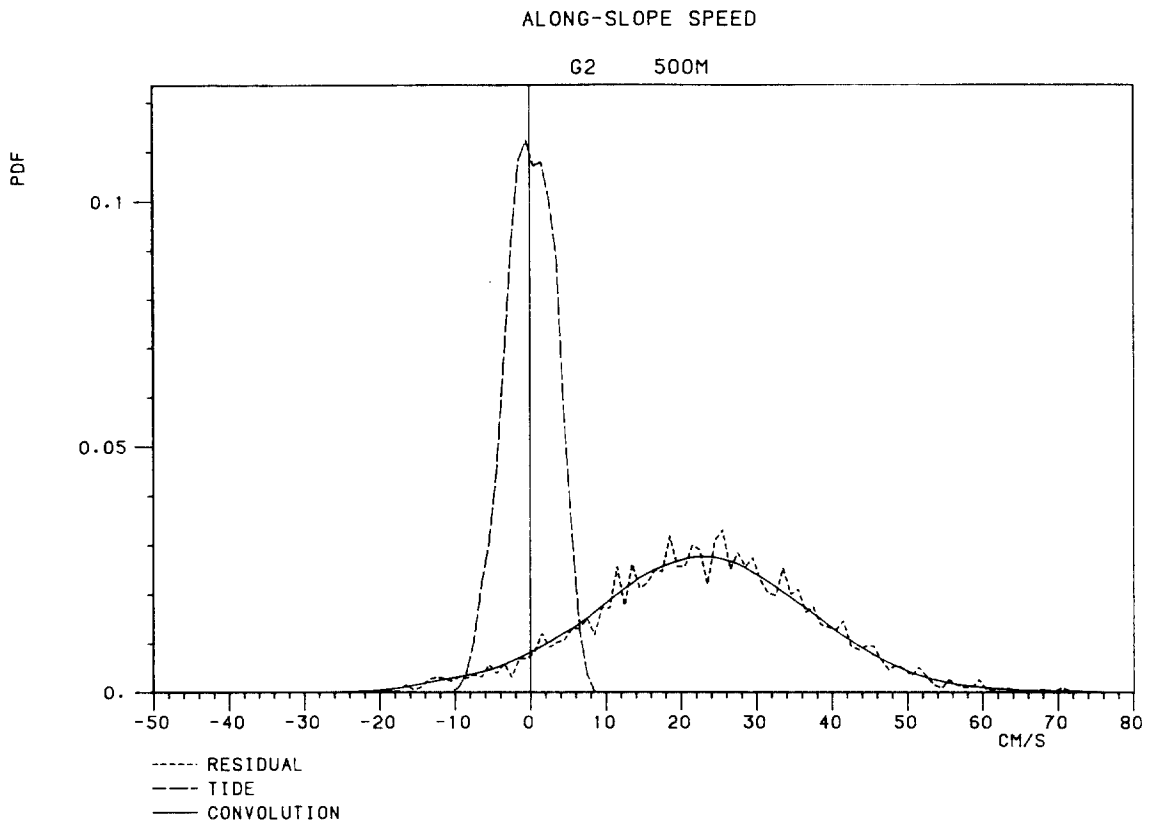


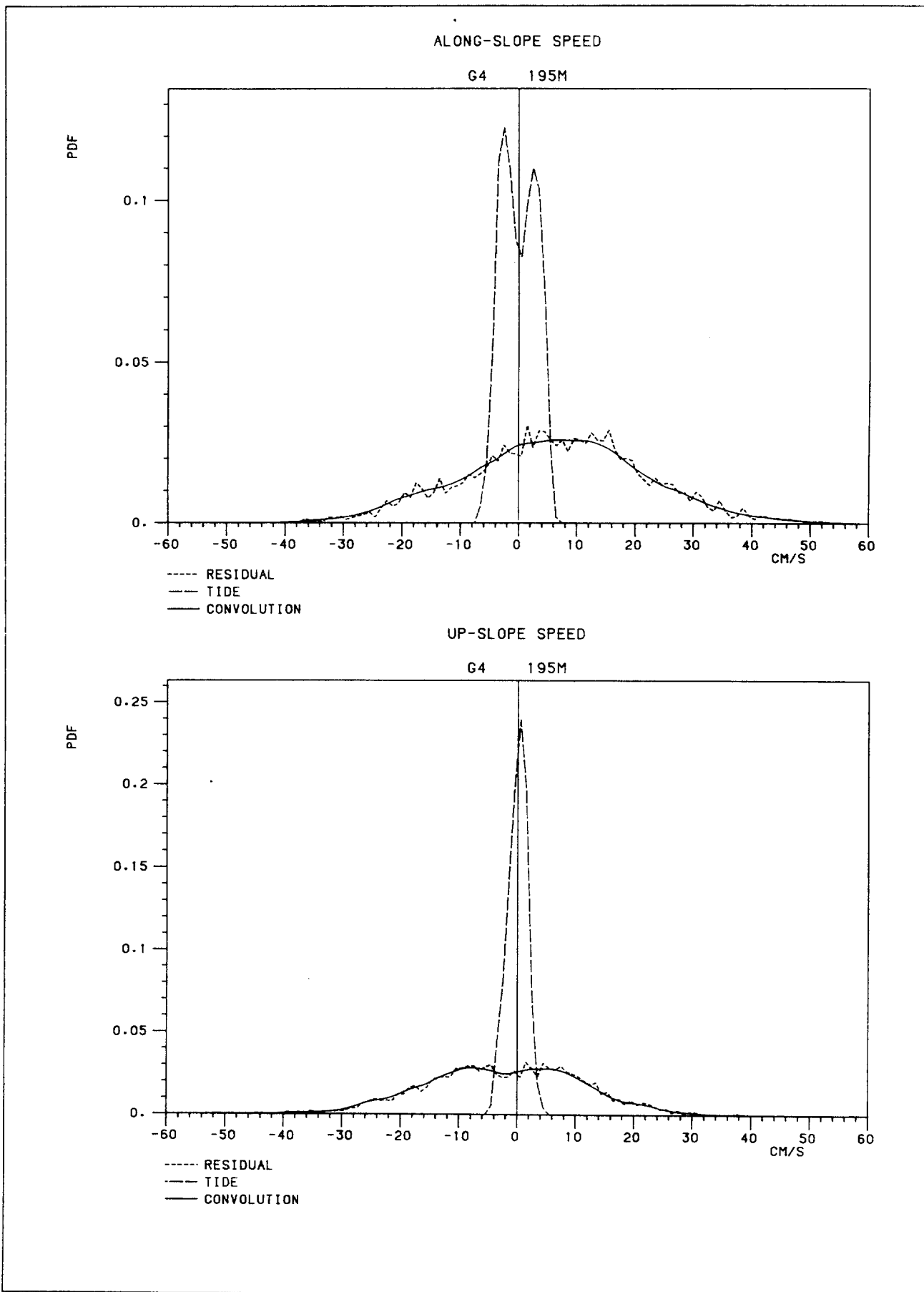
UP-SLOPE SPEED

G2 151M



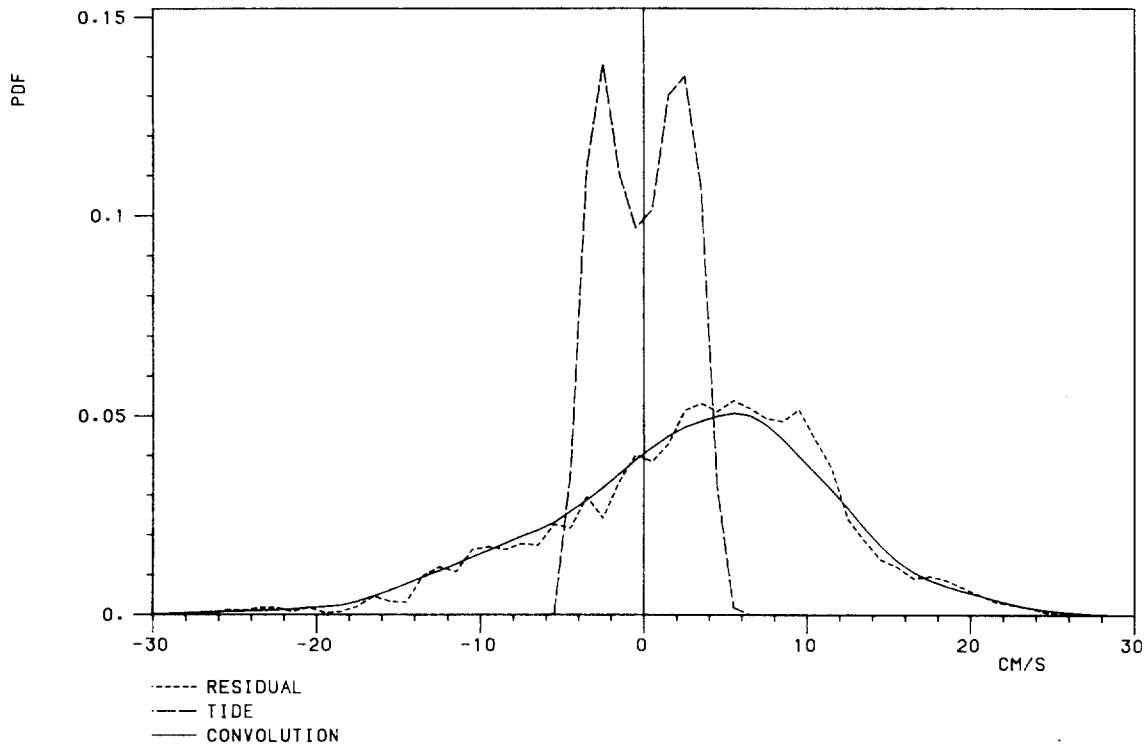






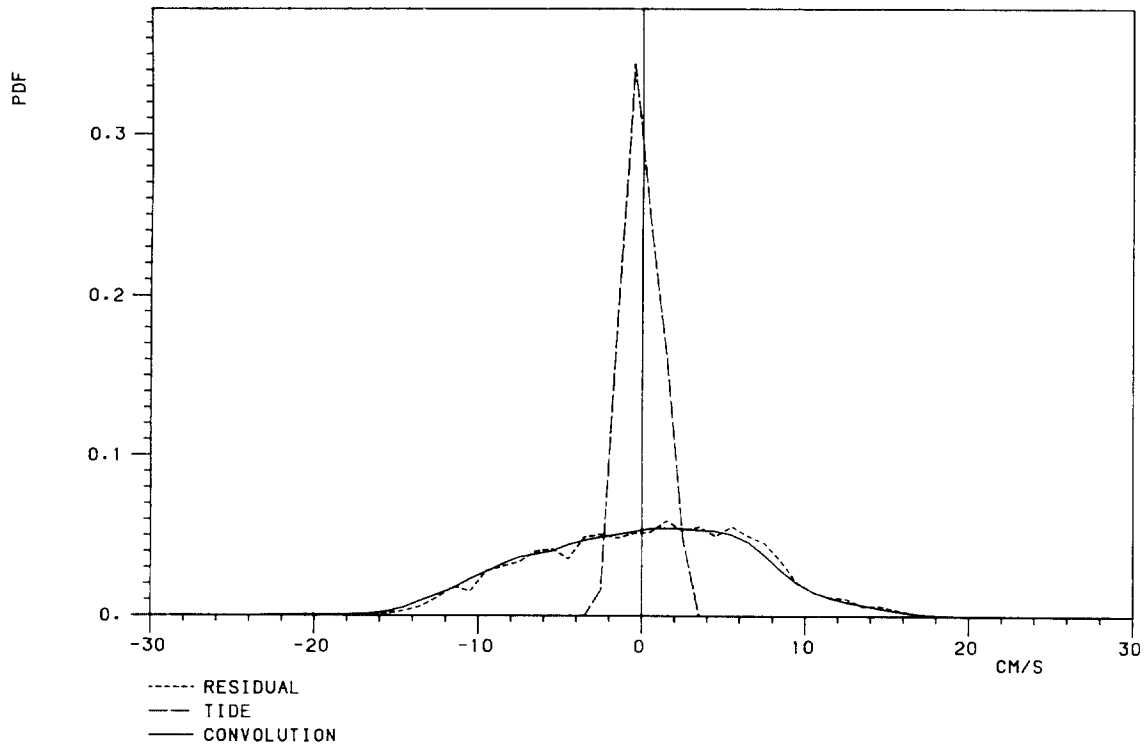
ALONG-SLOPE SPEED

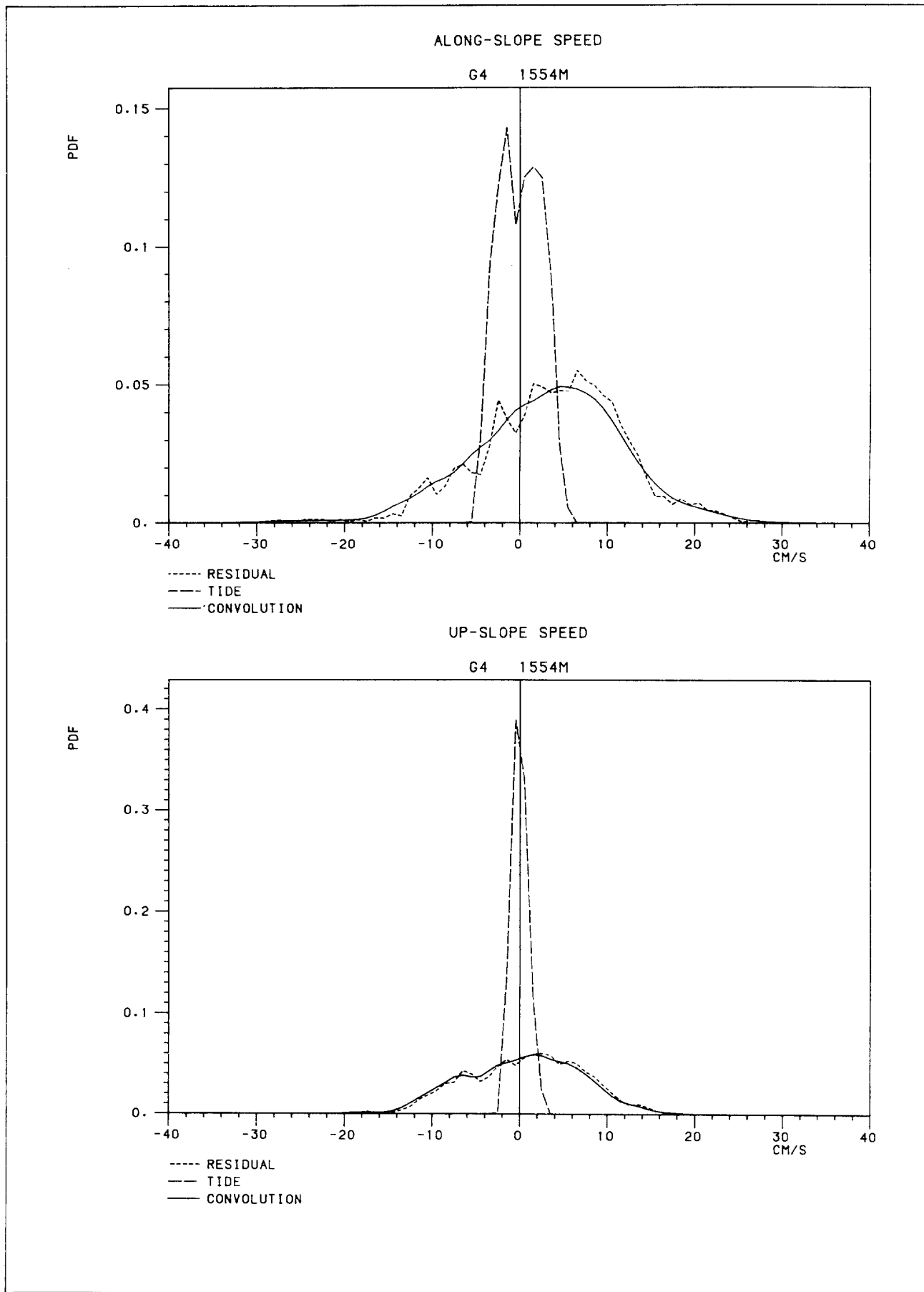
G4 1104M

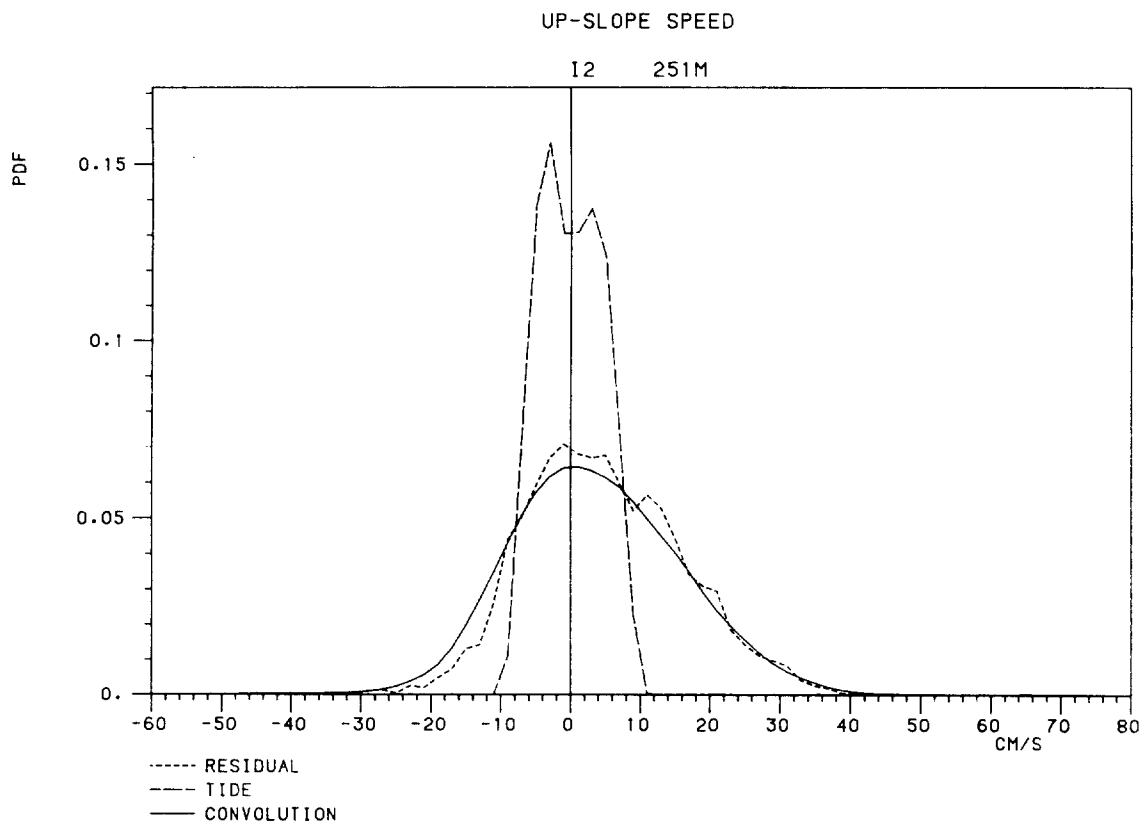
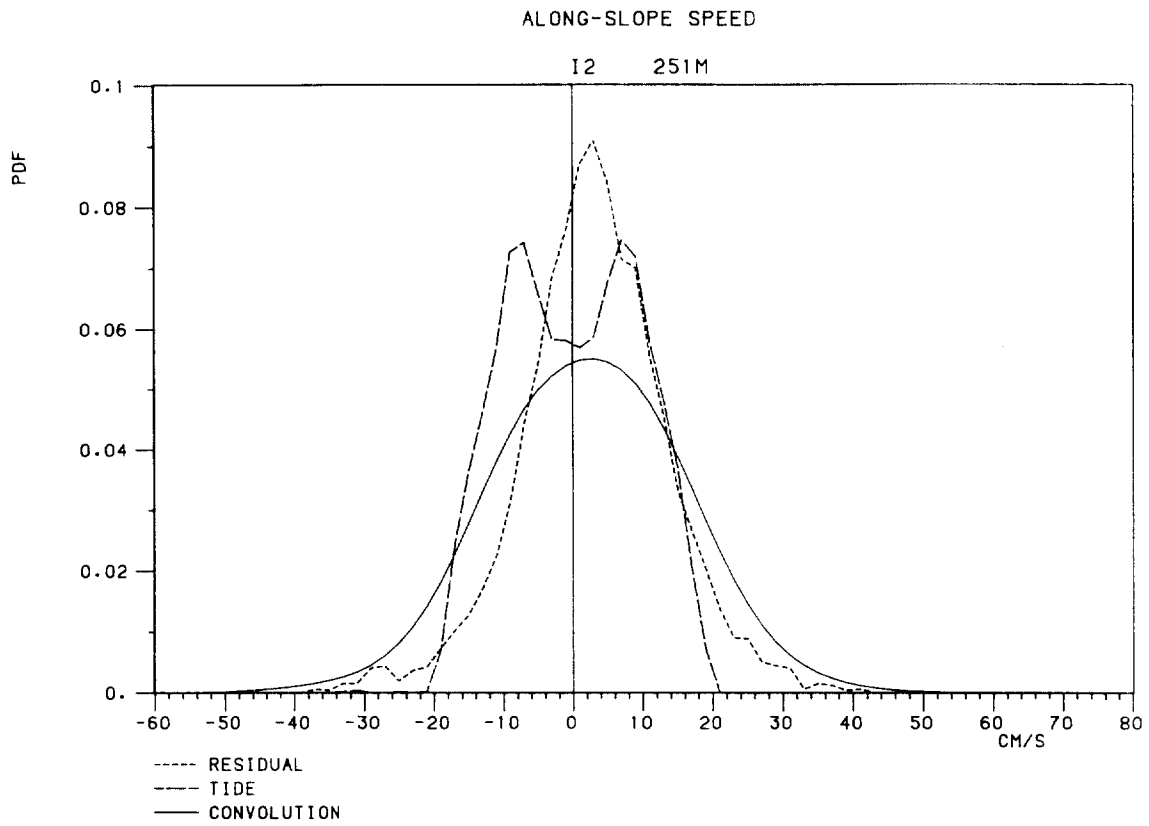


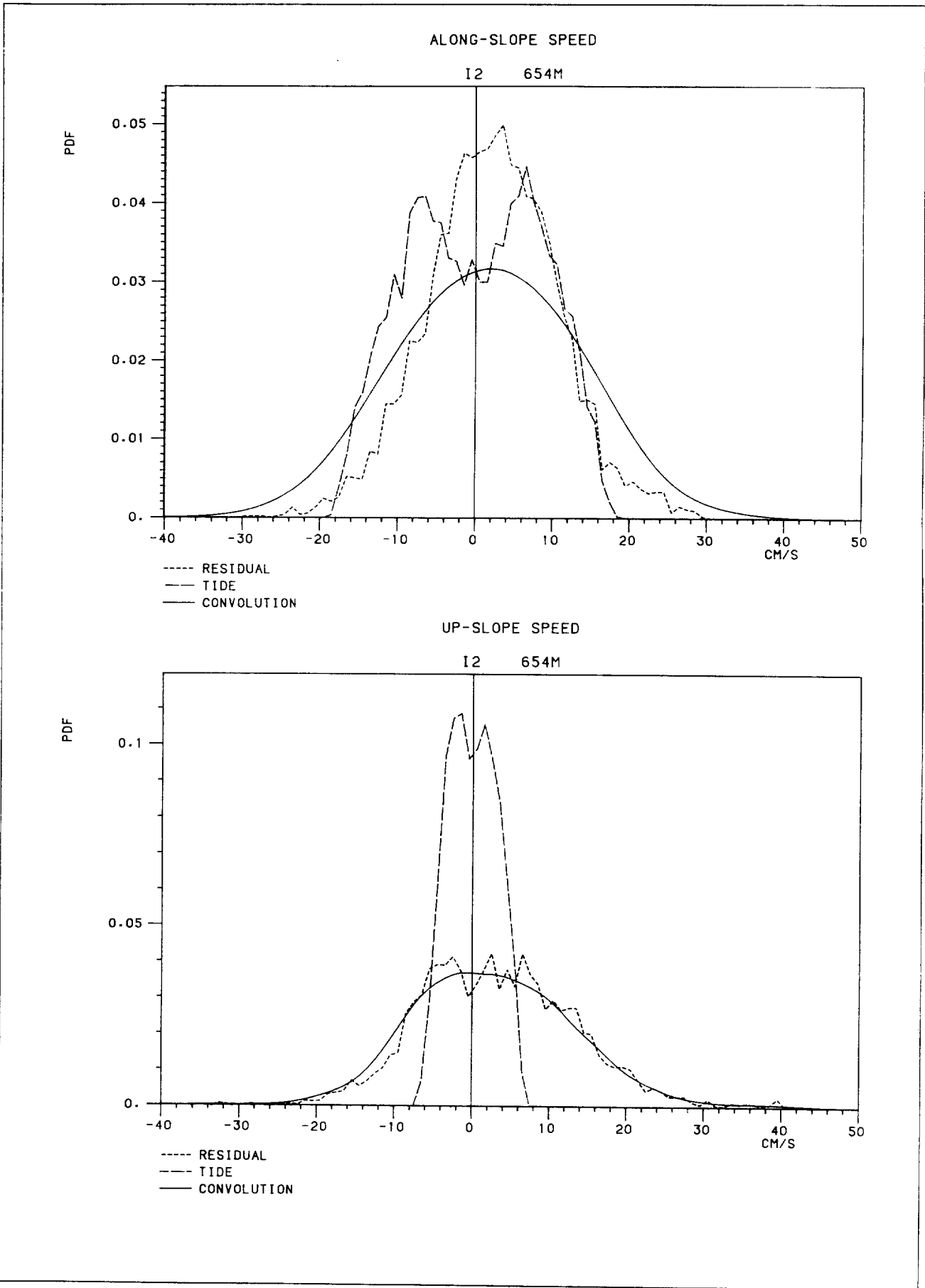
UP-SLOPE SPEED

G4 1104M



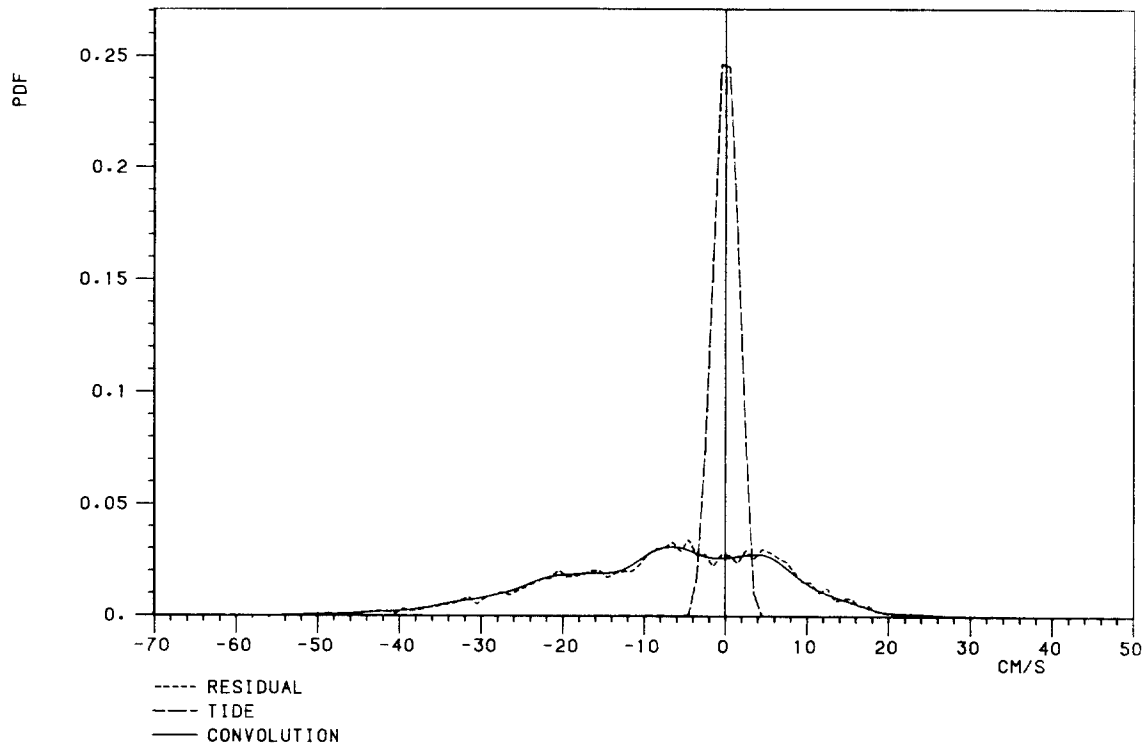






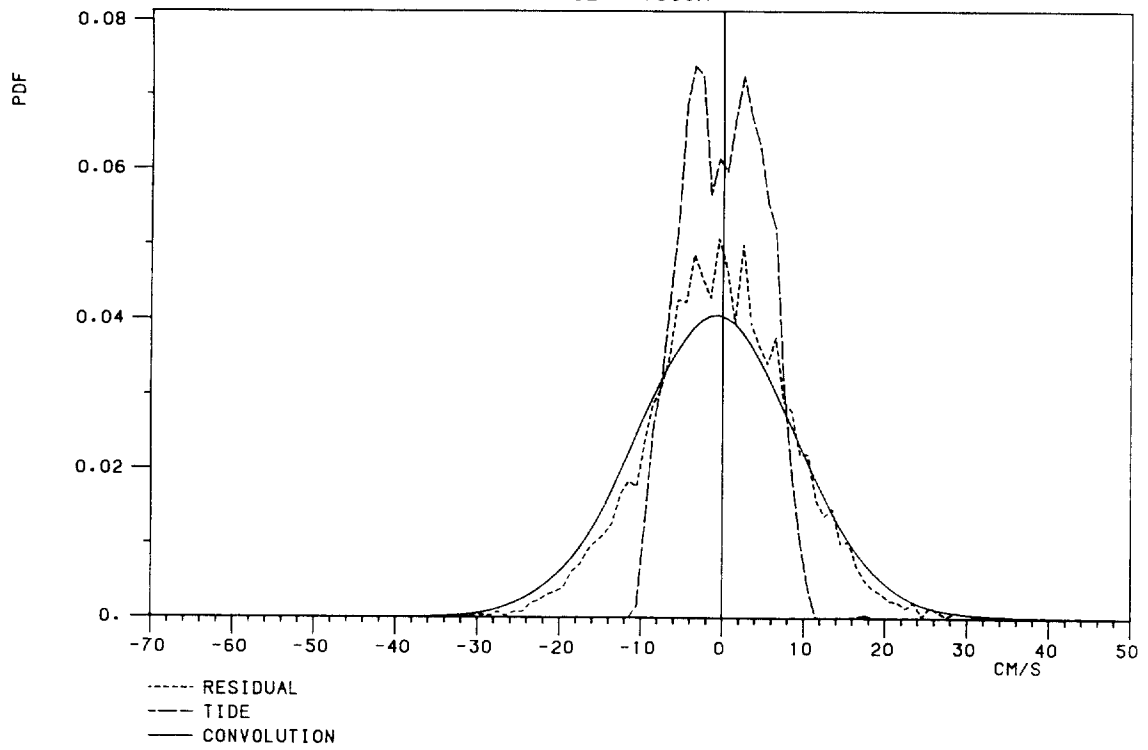
ALONG-SLOPE SPEED

I2 1055M



UP-SLOPE SPEED

I2 1055M



2.2 50-year return value of resolved speed

Defining the 50-year return value of hourly mean speed, U_{50} , as that which is exceeded on average once in 50 years, then it is given by

$$\text{Prob}(U_{50} < U) = 1 - 1/(365.25 \times 24 \times 50)$$

ie.

$$\text{Prob}(U_{50} < U) \approx 0.99999772 \quad (3)$$

Hence U_{50} may be calculated given the distribution p_{t+r} - or rather two values, one from each tail of p_{t+r} , giving the 50-year speed in opposite directions.

With the definition for U_{50} , in terms of only the average interval between exceedances, its value is not affected by any correlation between the data. However, given positive correlation between successive hourly mean values, exceedances of U_{50} will tend to come together, while maintaining the average interval between exceedances of 50 years. So if the 50-year return value is defined as that which is exceeded at least once during one year in 50, then it would have a slightly lower value than that given by (3). However, Pugh and Vassie (1980) examined the effect of correlation upon estimates of return values of surface elevation and decided that any such reduction would in practice be insignificant.

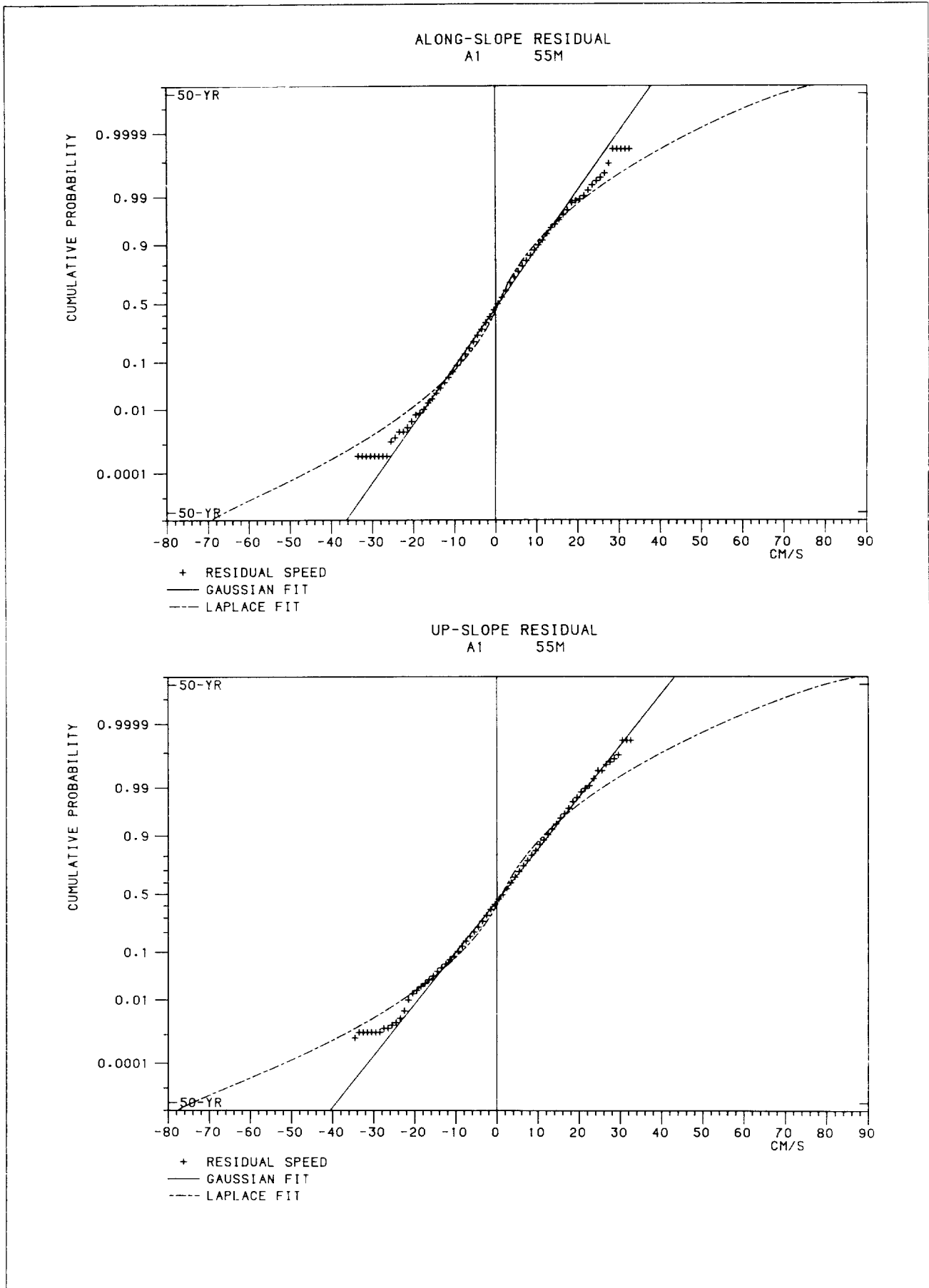
2.3 Probability distribution and extreme value of total speed

Suppose U and V are current speeds resolved orthogonally so that total speed W is given by

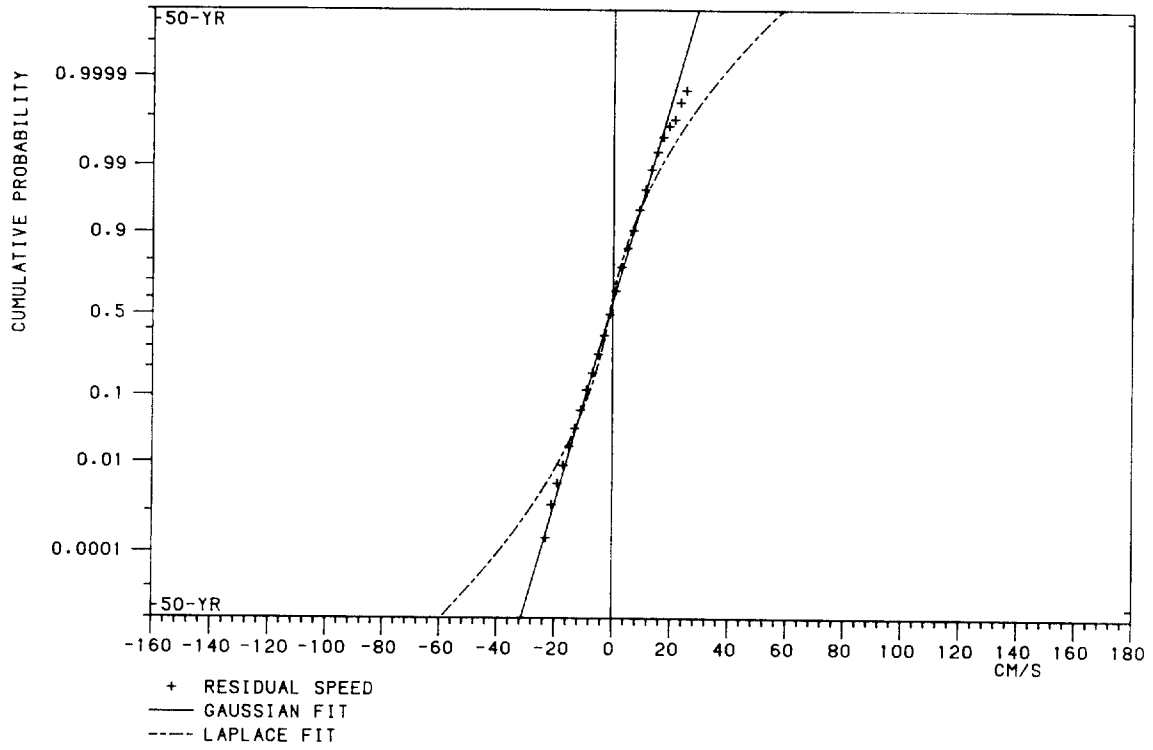
$$W = \sqrt{U^2 + V^2}$$

Fig.3: Cumulative probability distributions of residual current speed along- and up-slope from records at each current meter and fitted Gaussian and Laplacian fits. (The meter is identified by the mooring and by the depth of the meter below the sea surface.)

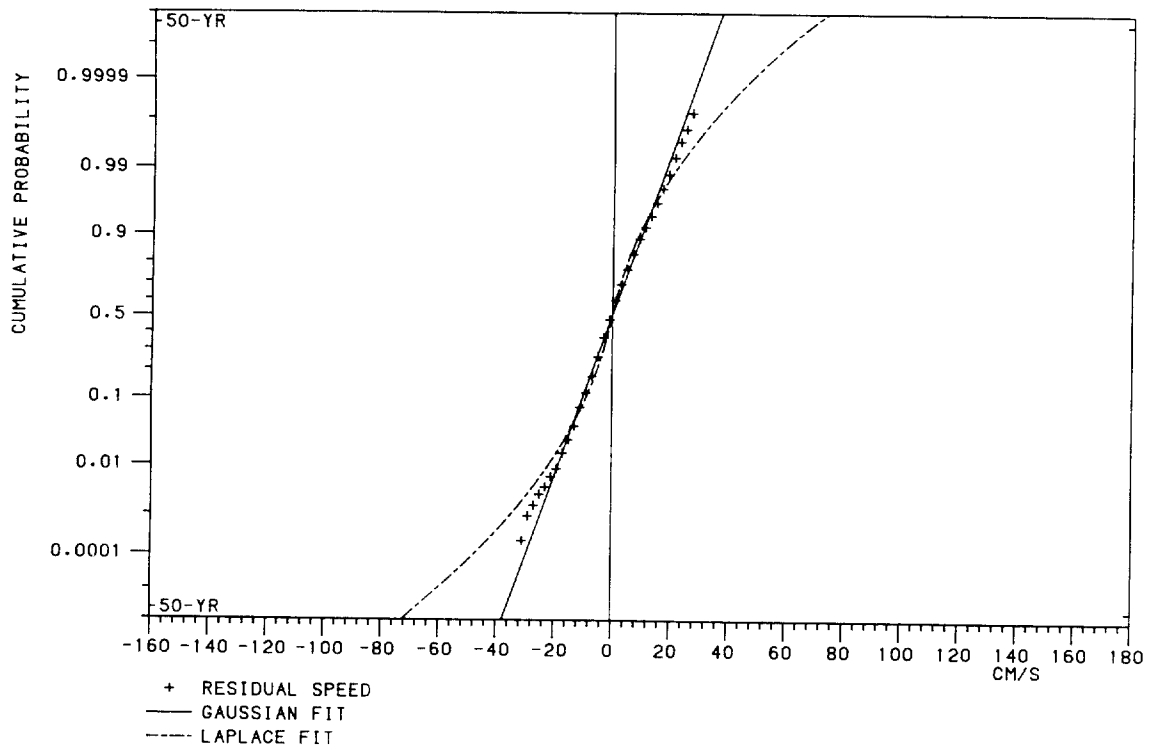


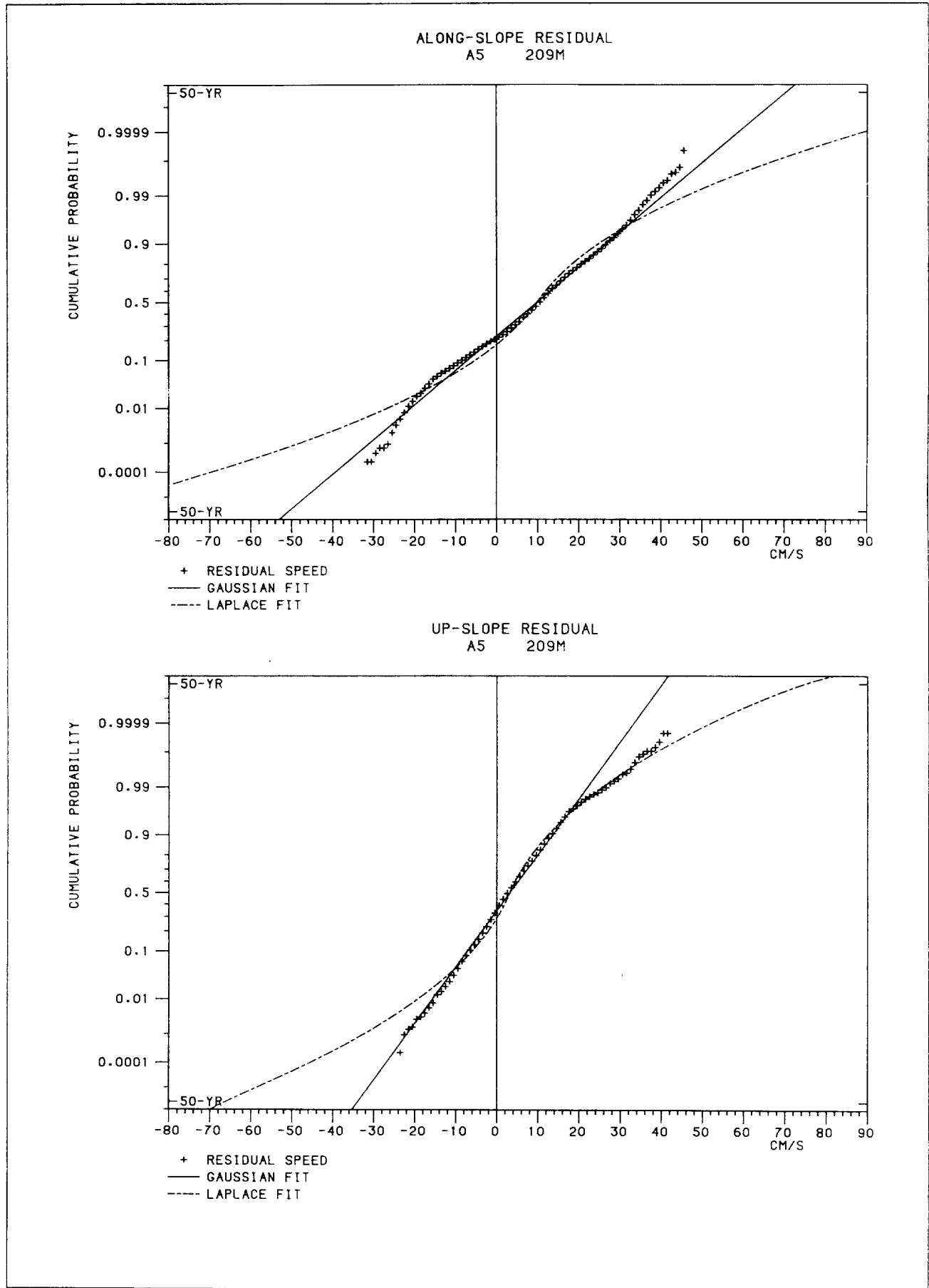


ALONG-SLOPE RESIDUAL
A1 120M

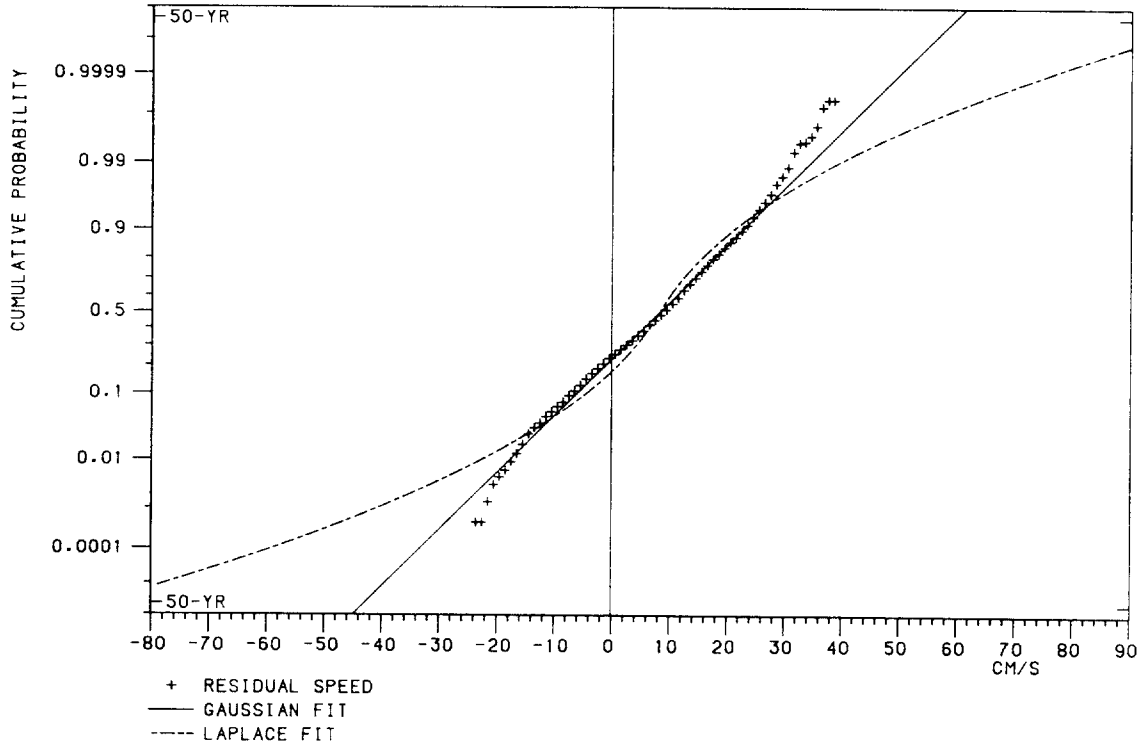


UP-SLOPE RESIDUAL
A1 120M

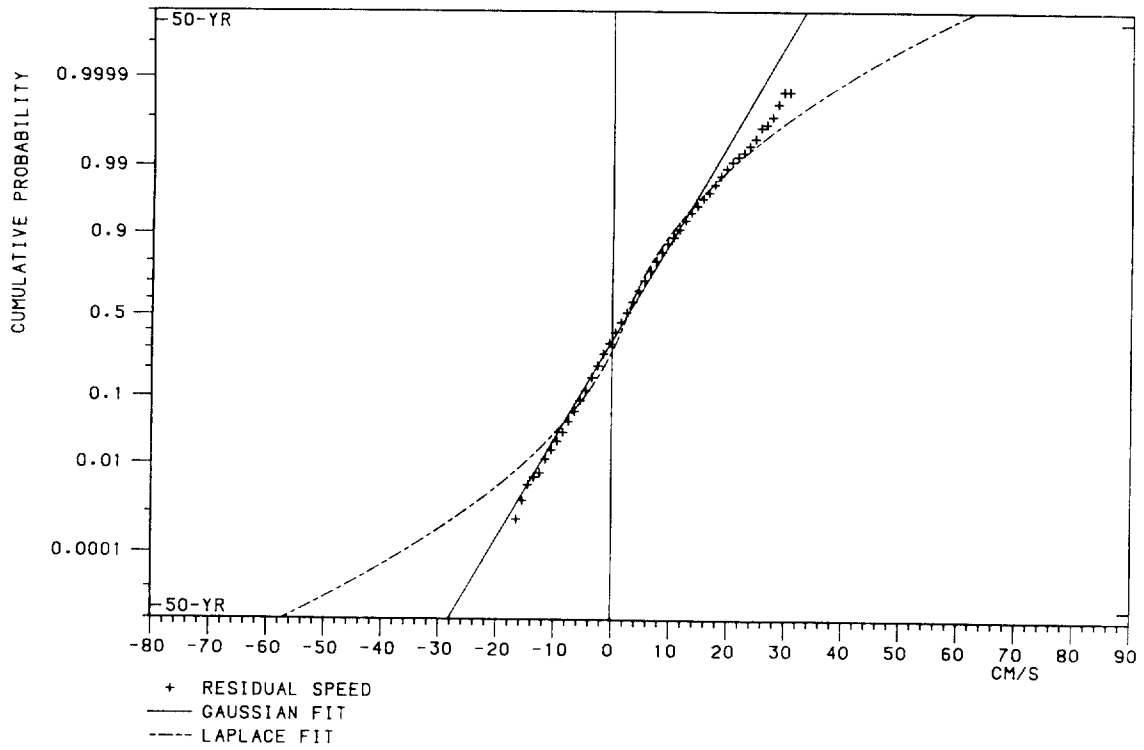


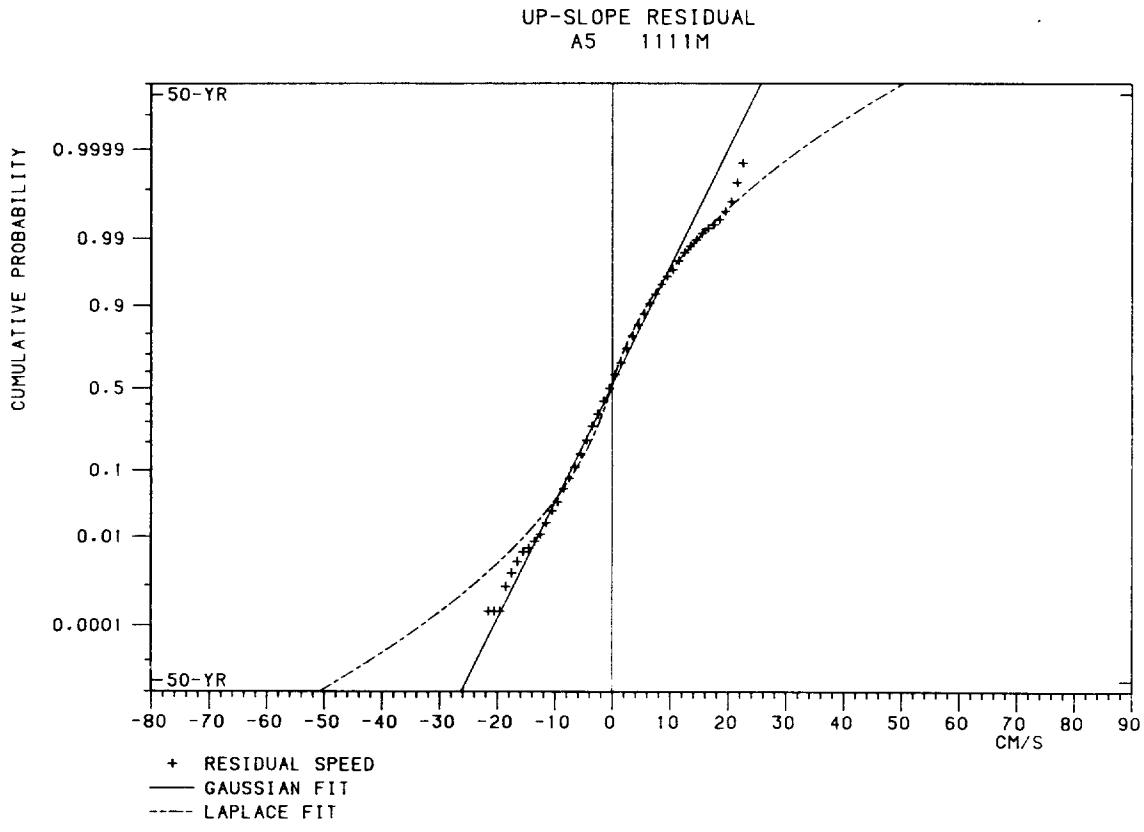
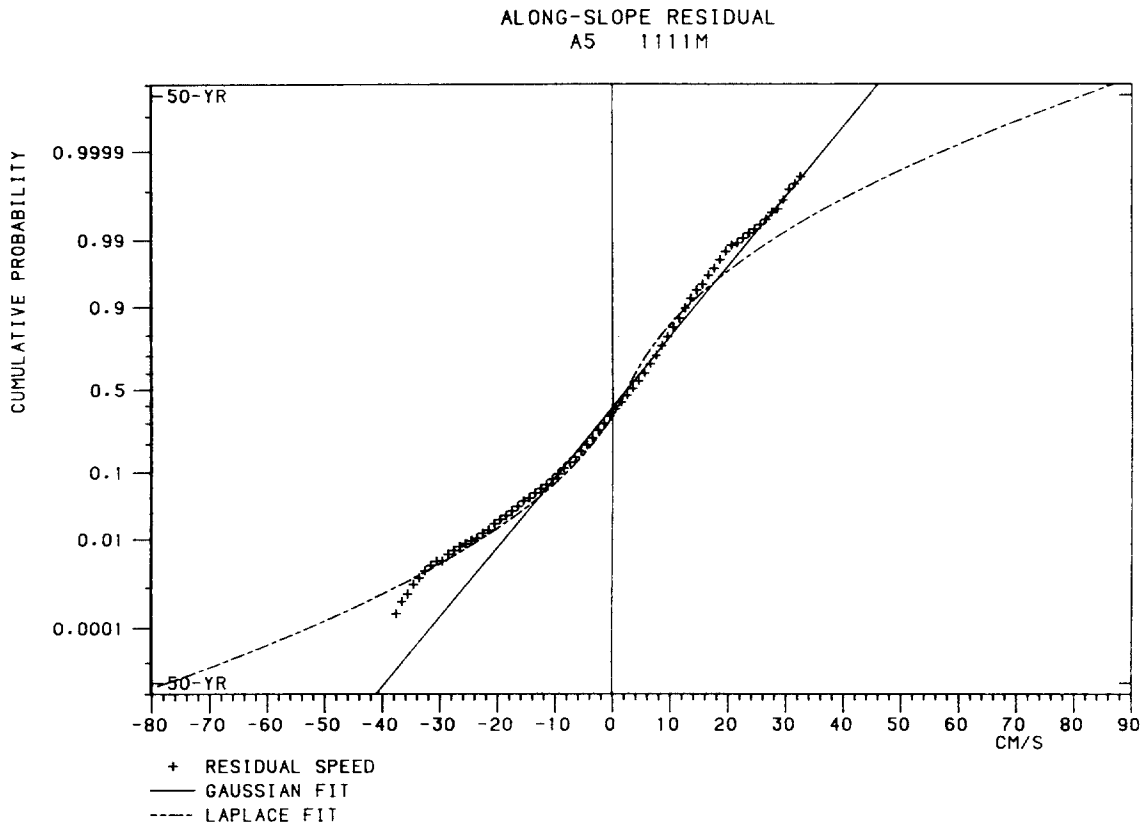


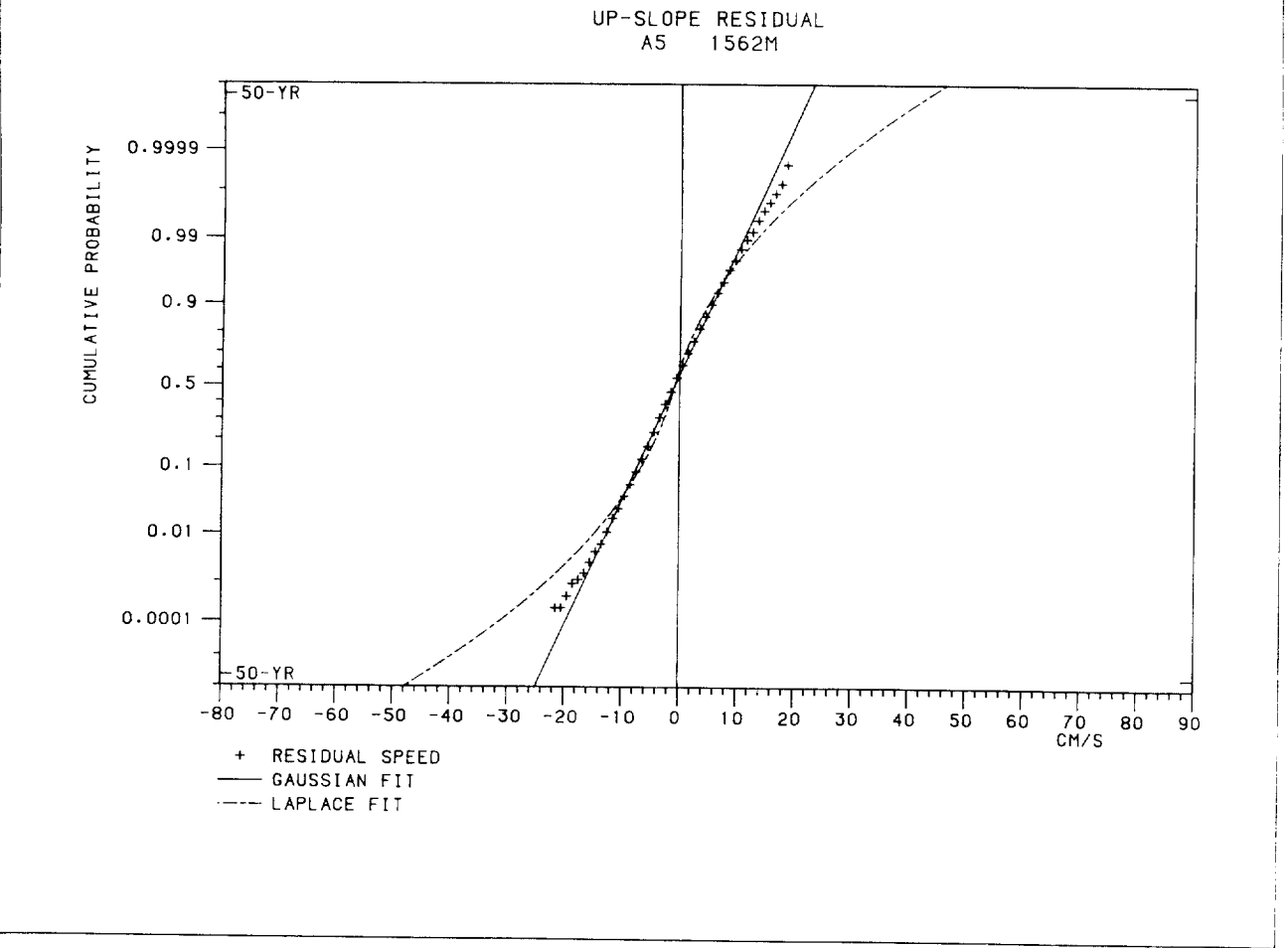
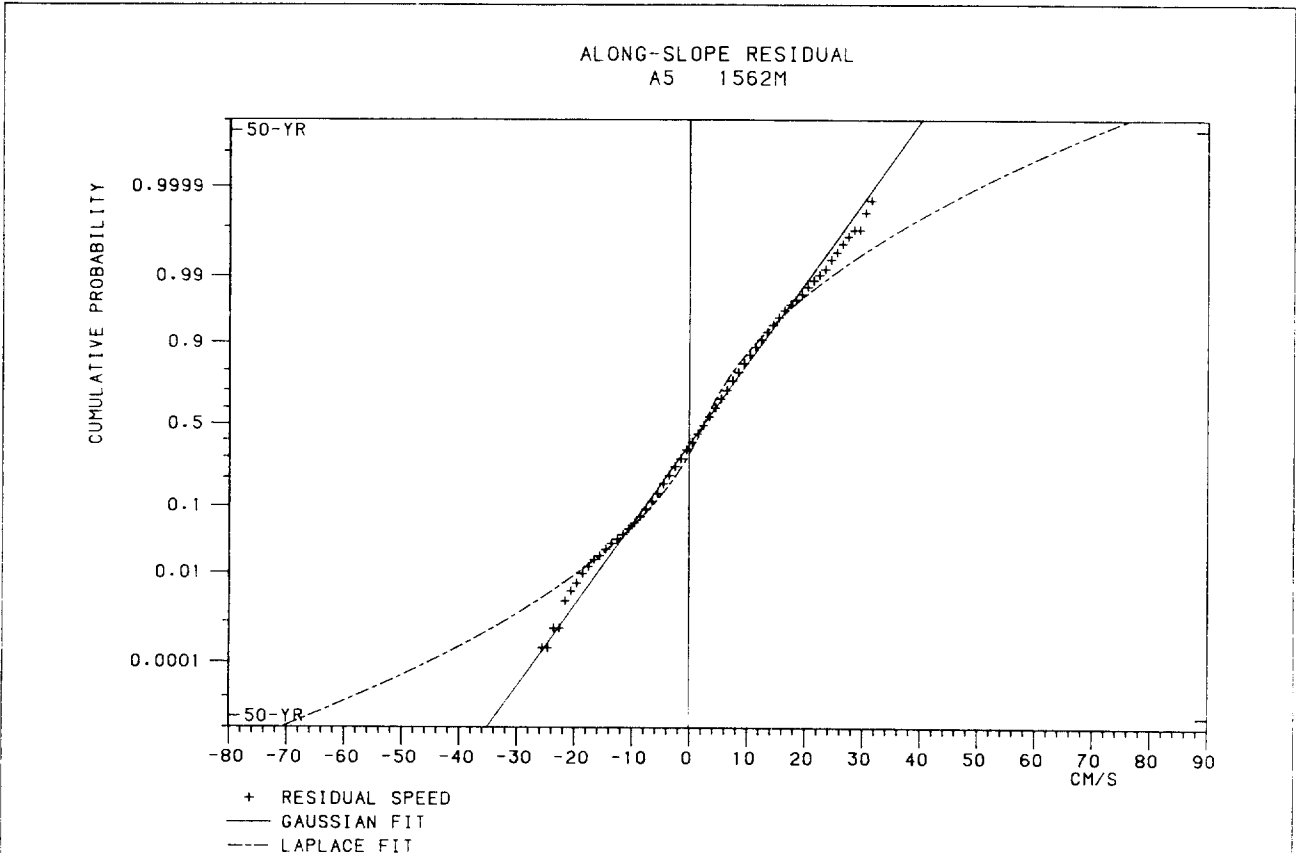
ALONG-SLOPE RESIDUAL
A5 510M

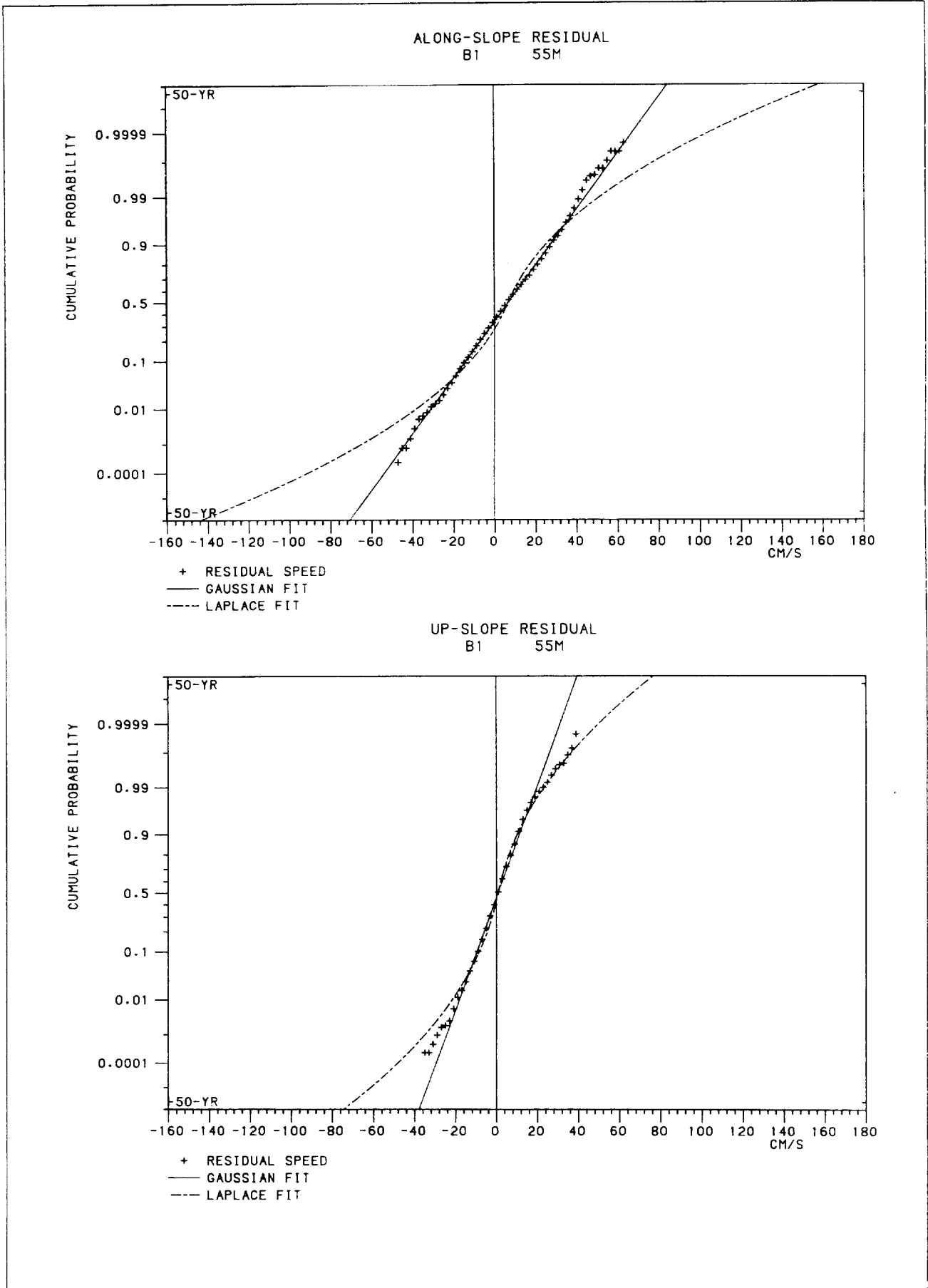


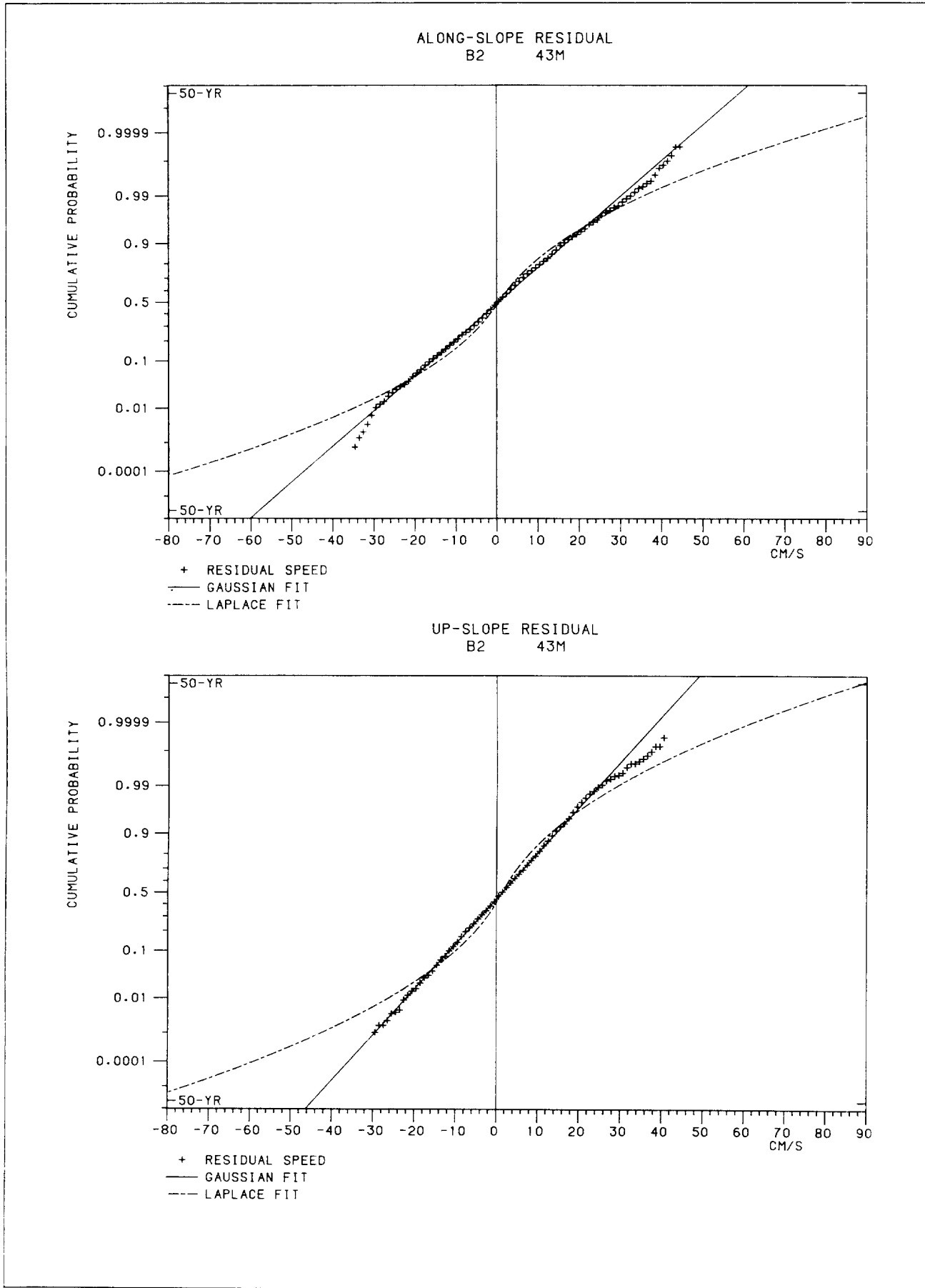
UP-SLOPE RESIDUAL
A5 510M

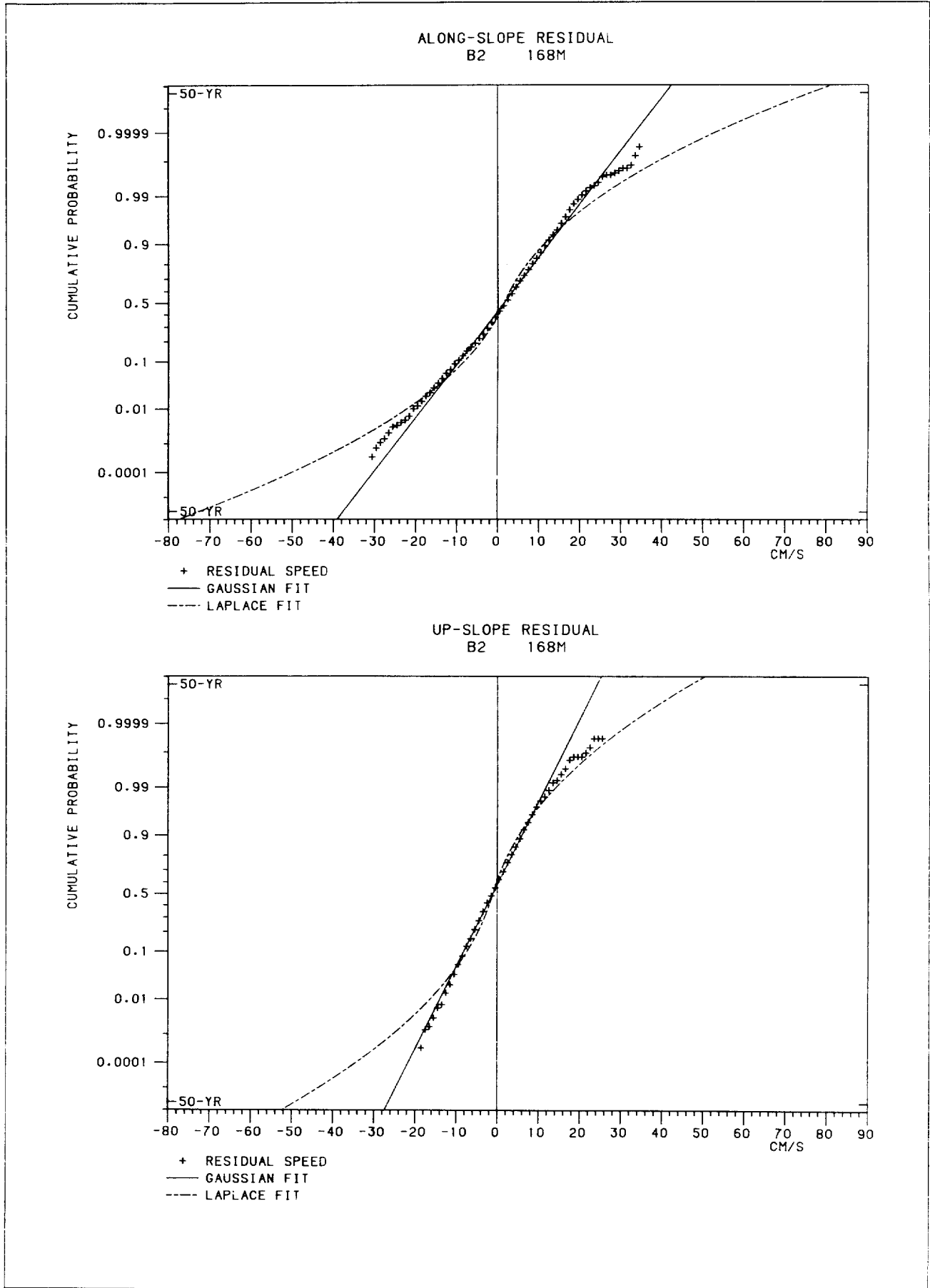




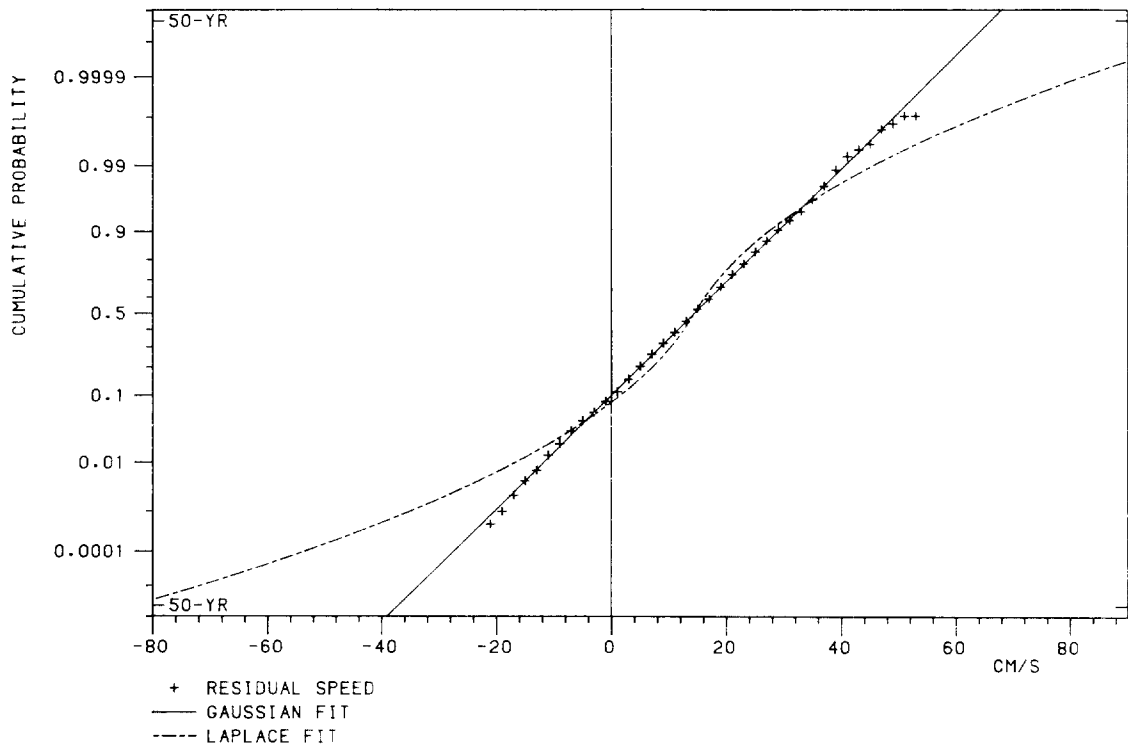




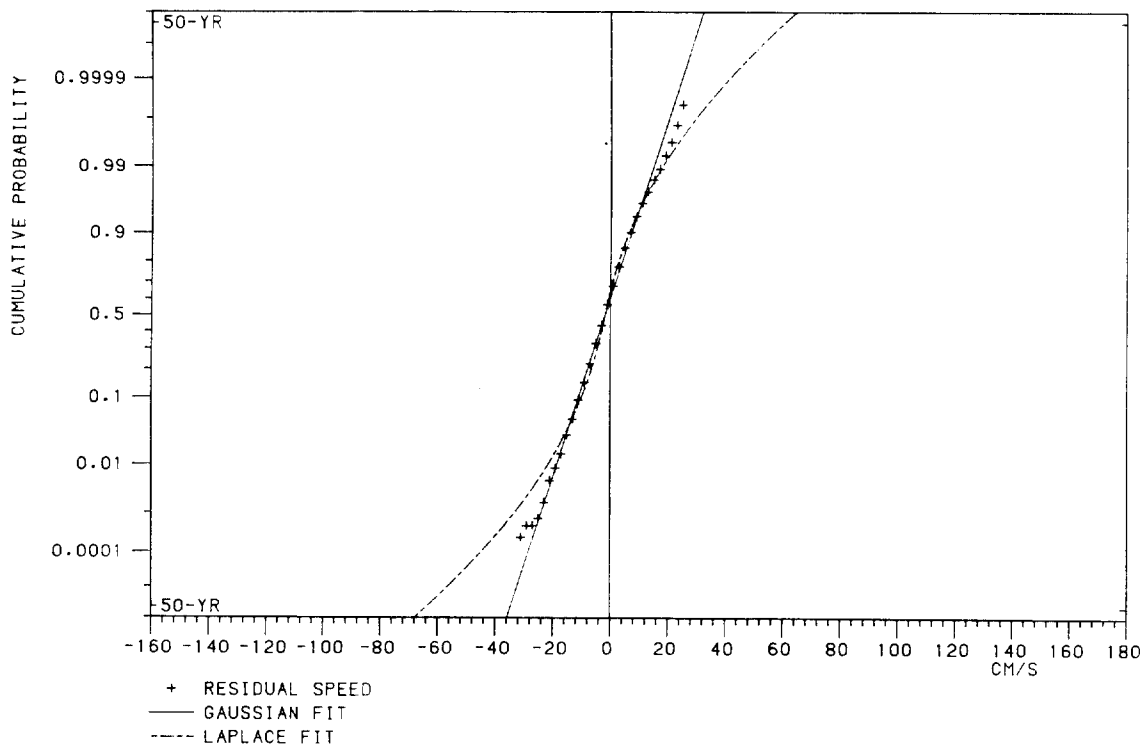




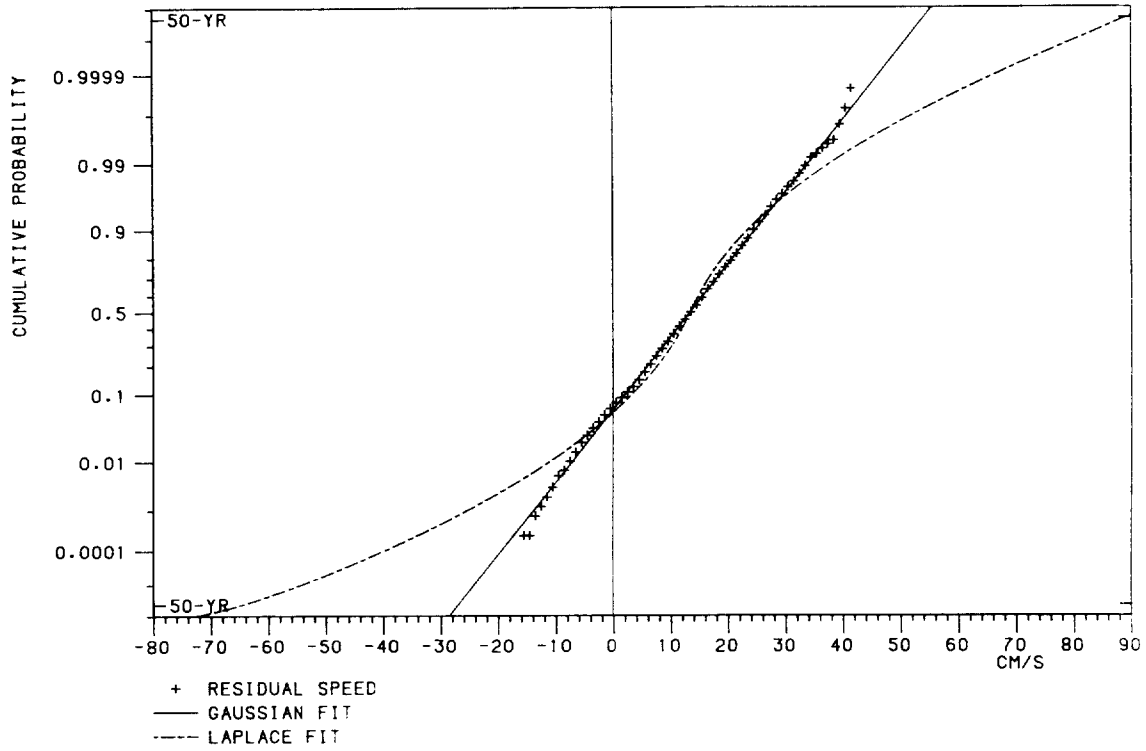
ALONG-SLOPE RESIDUAL
B3 104M



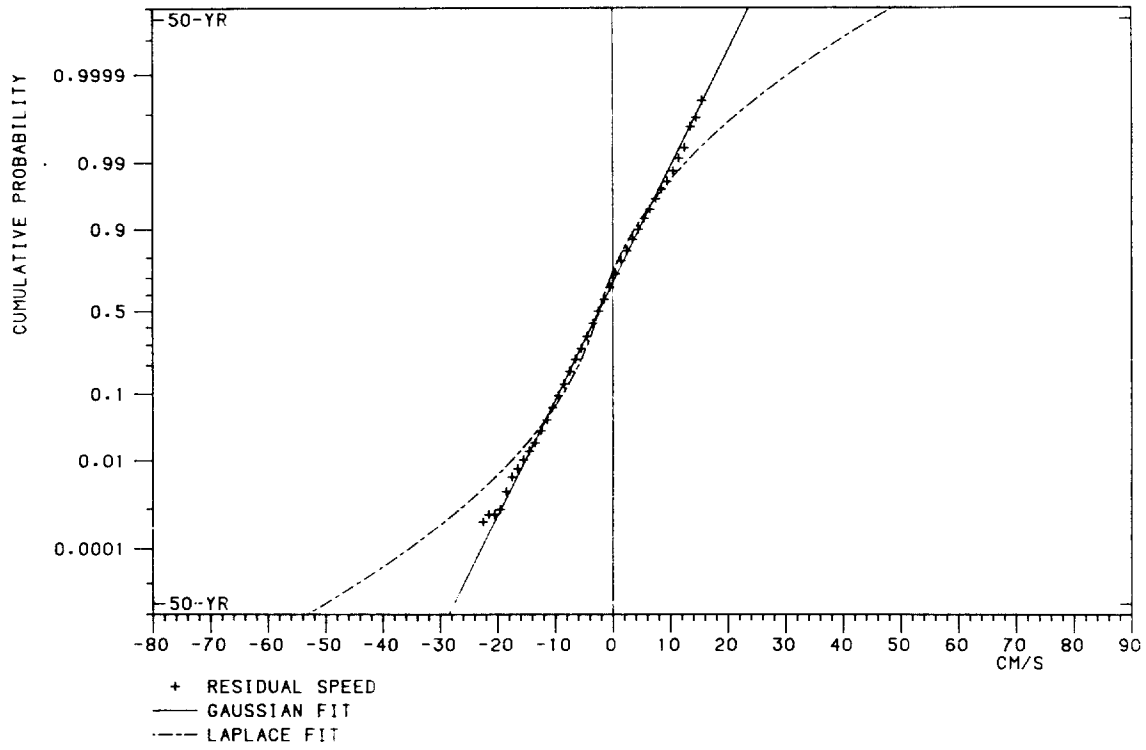
UP-SLOPE RESIDUAL
B3 104M

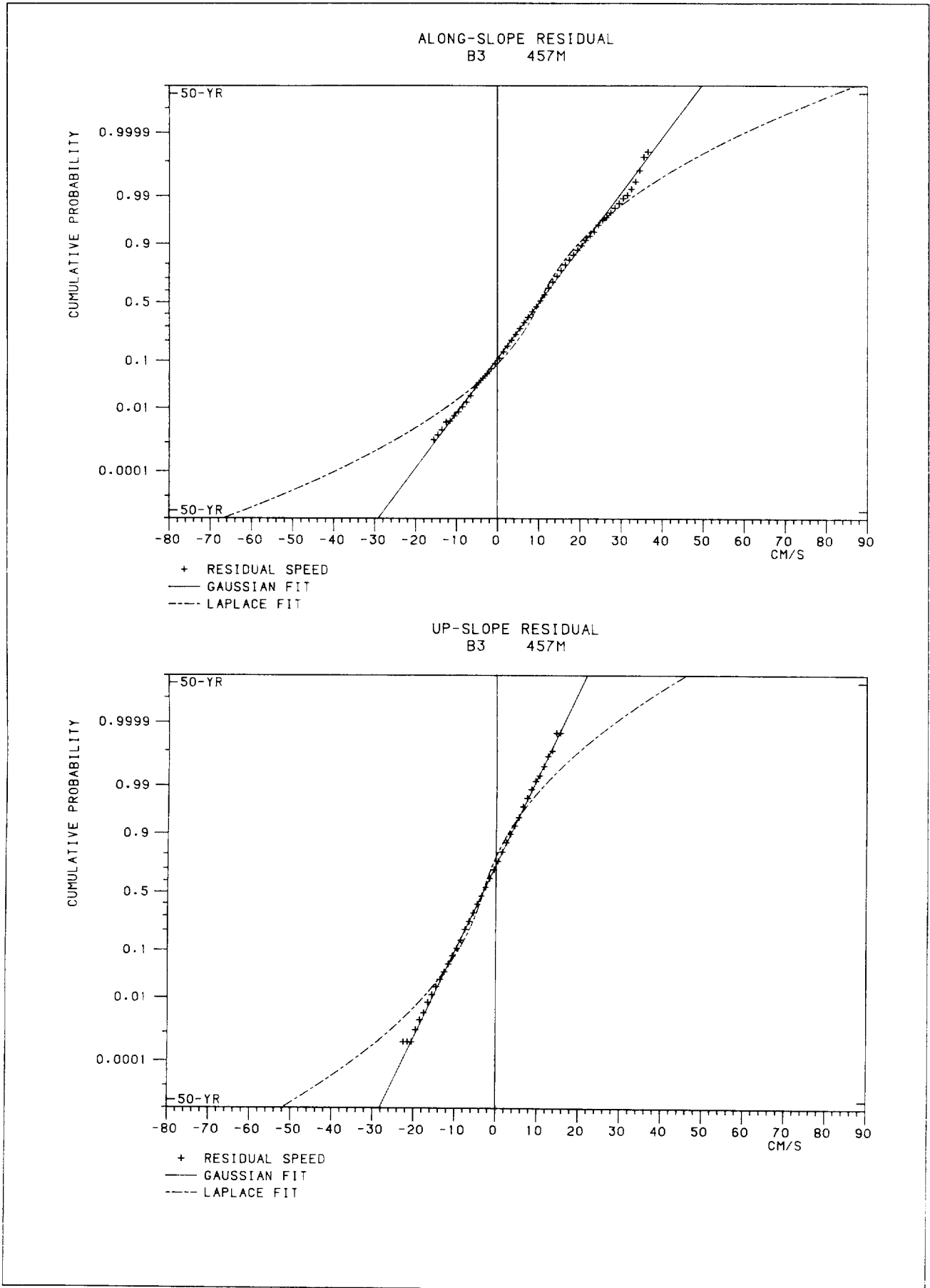


ALONG-SLOPE RESIDUAL
B3 257M

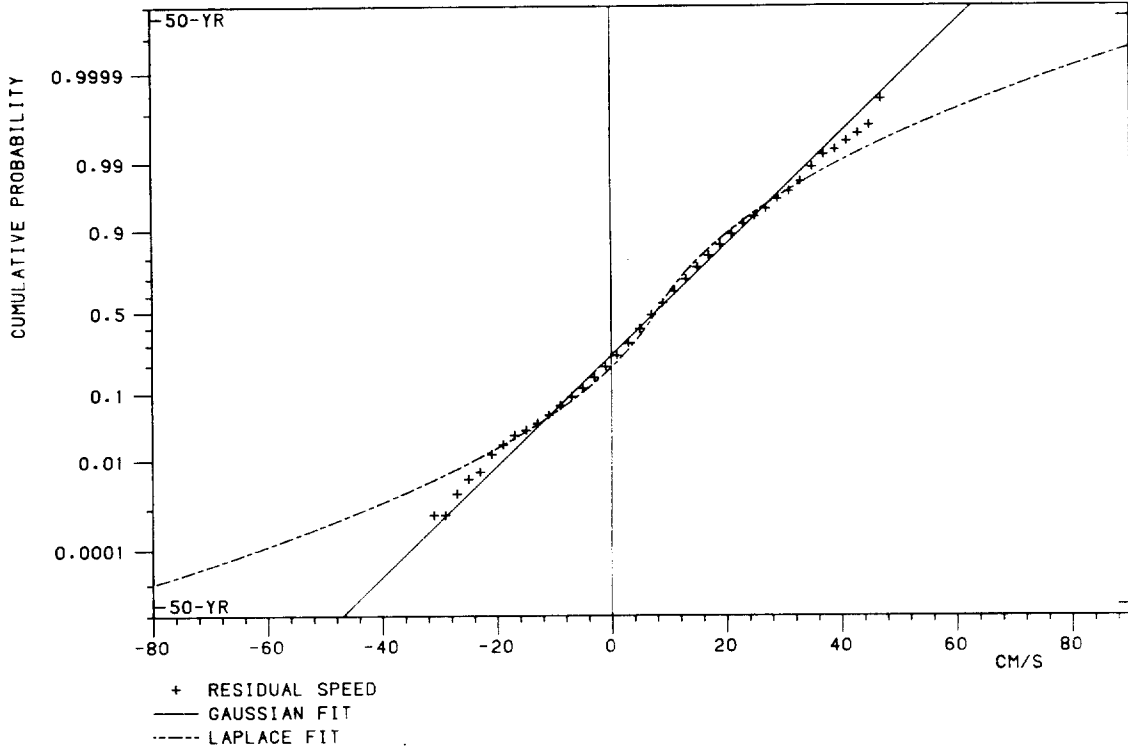


UP-SLOPE RESIDUAL
B3 257M

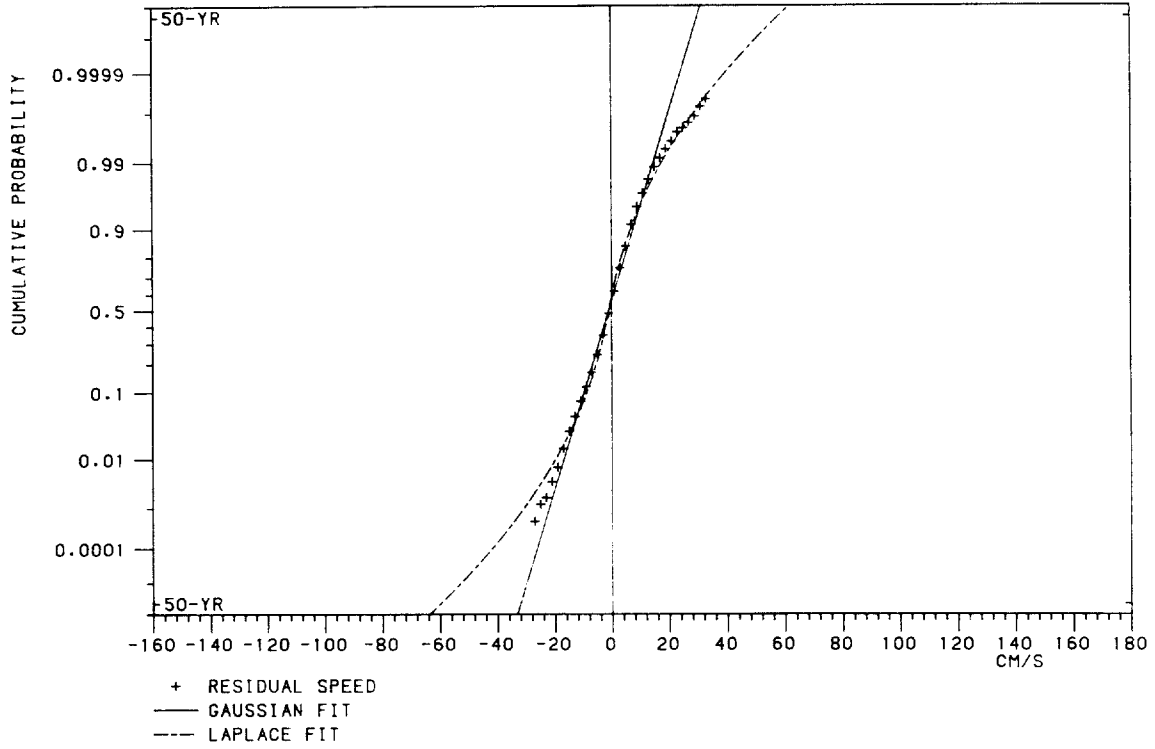


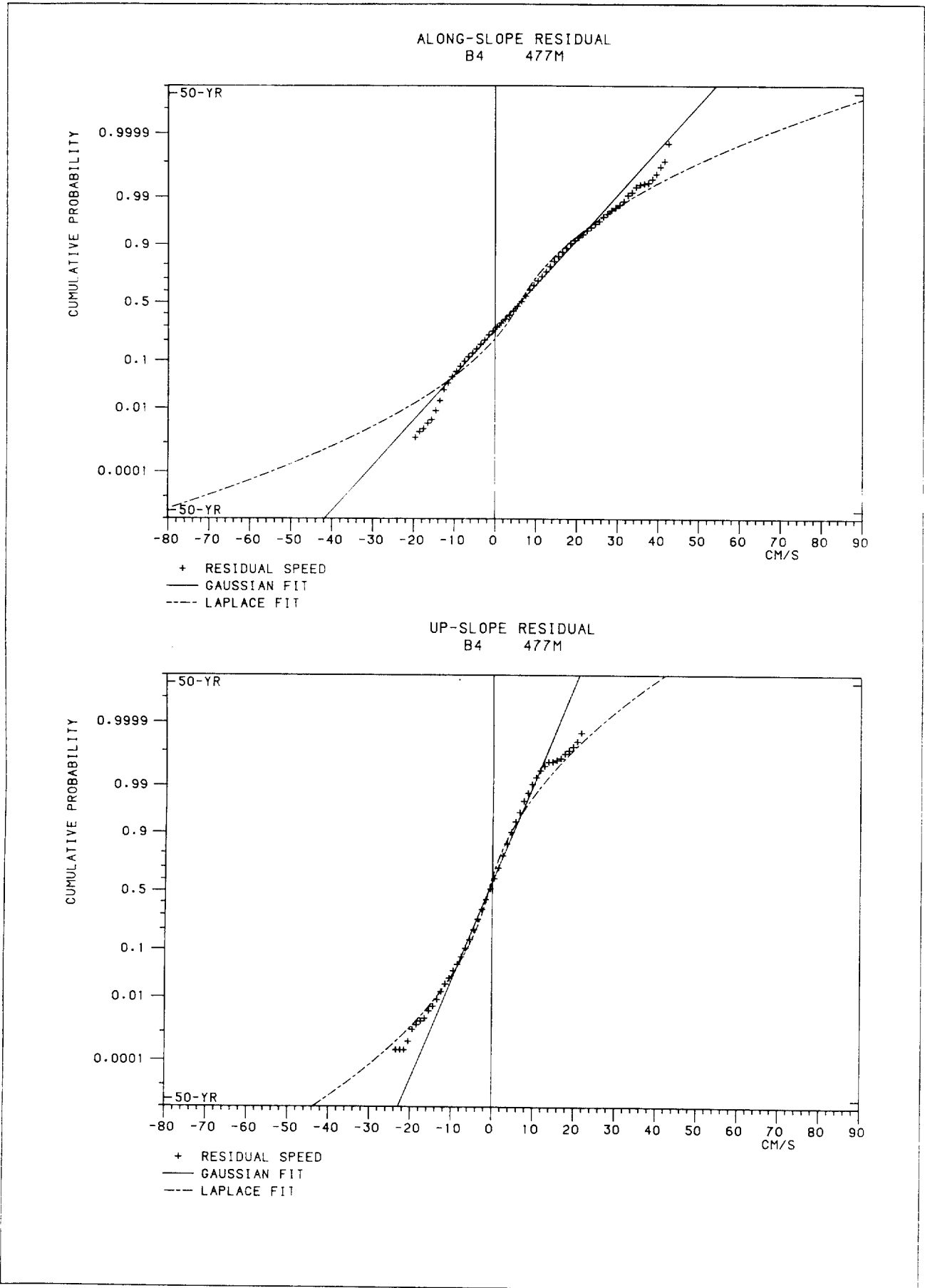


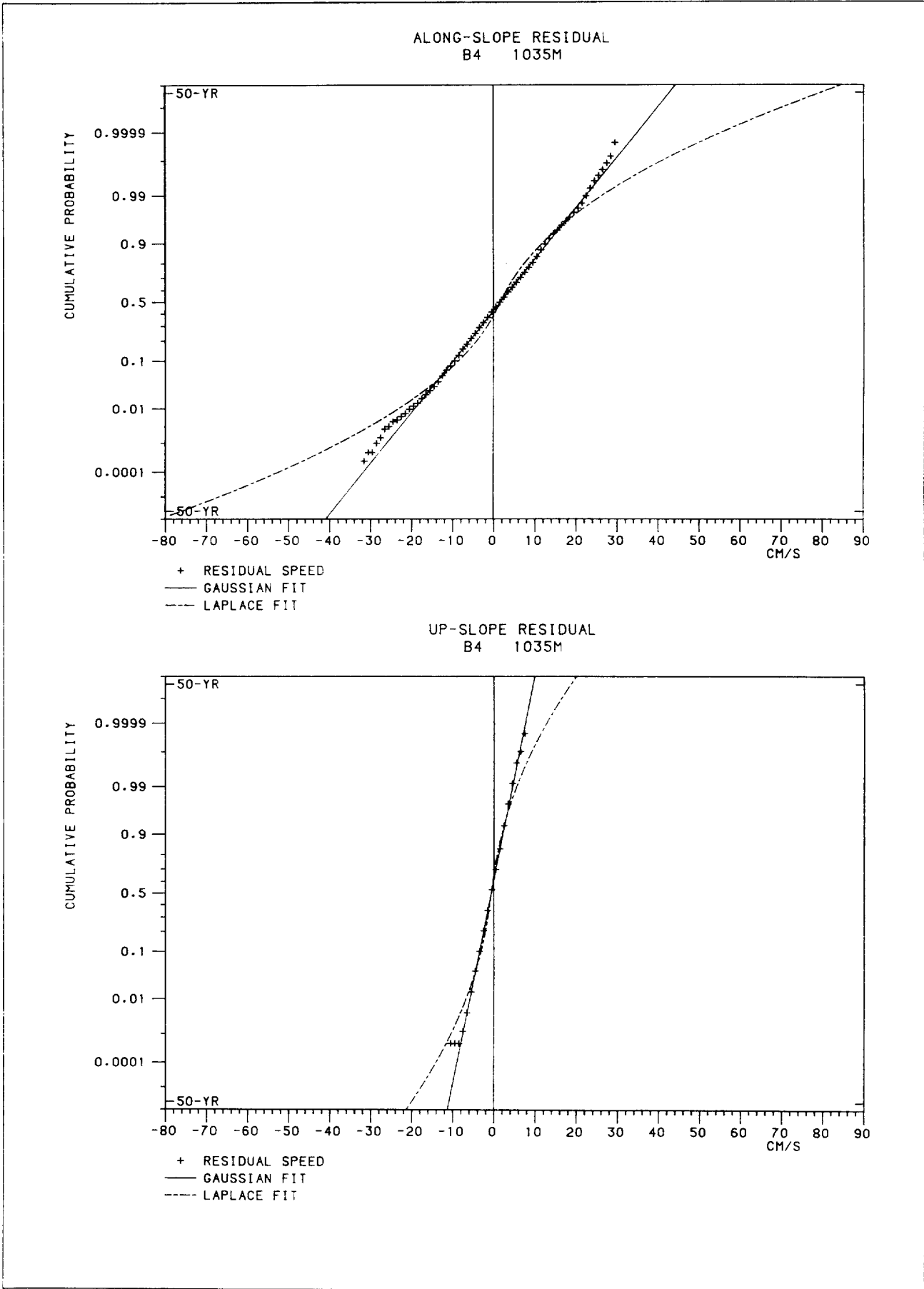
ALONG-SLOPE RESIDUAL
B4 169M



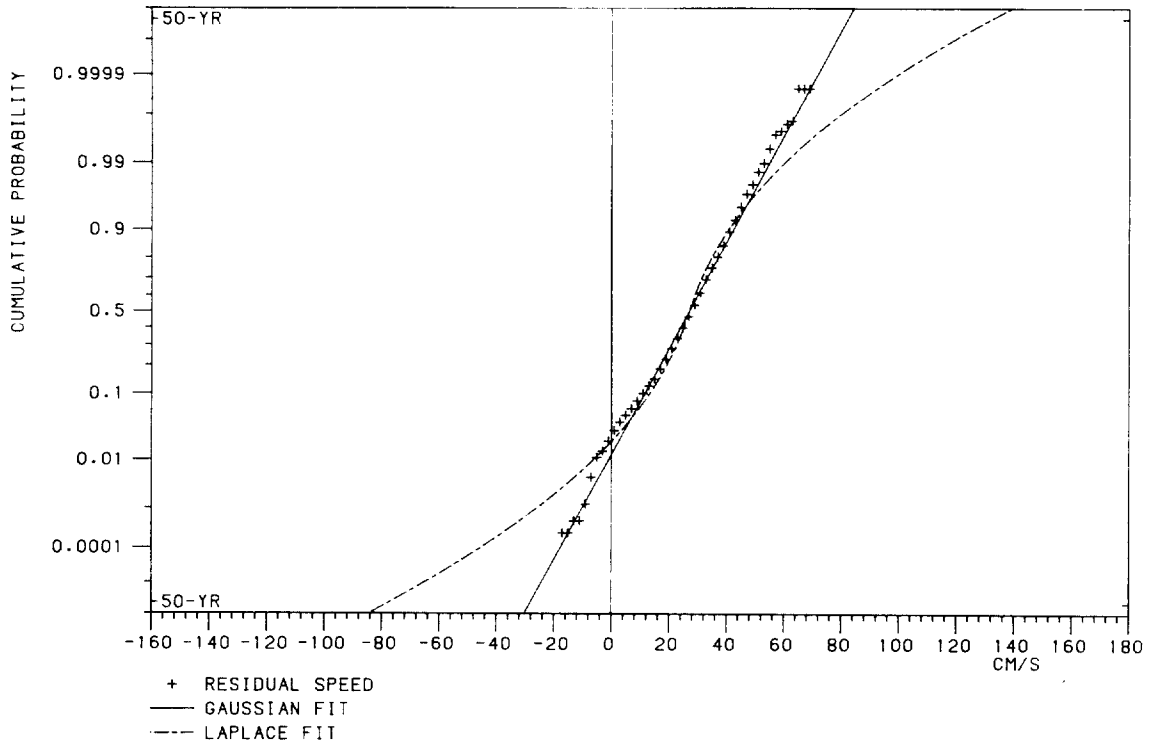
UP-SLOPE RESIDUAL
B4 169M



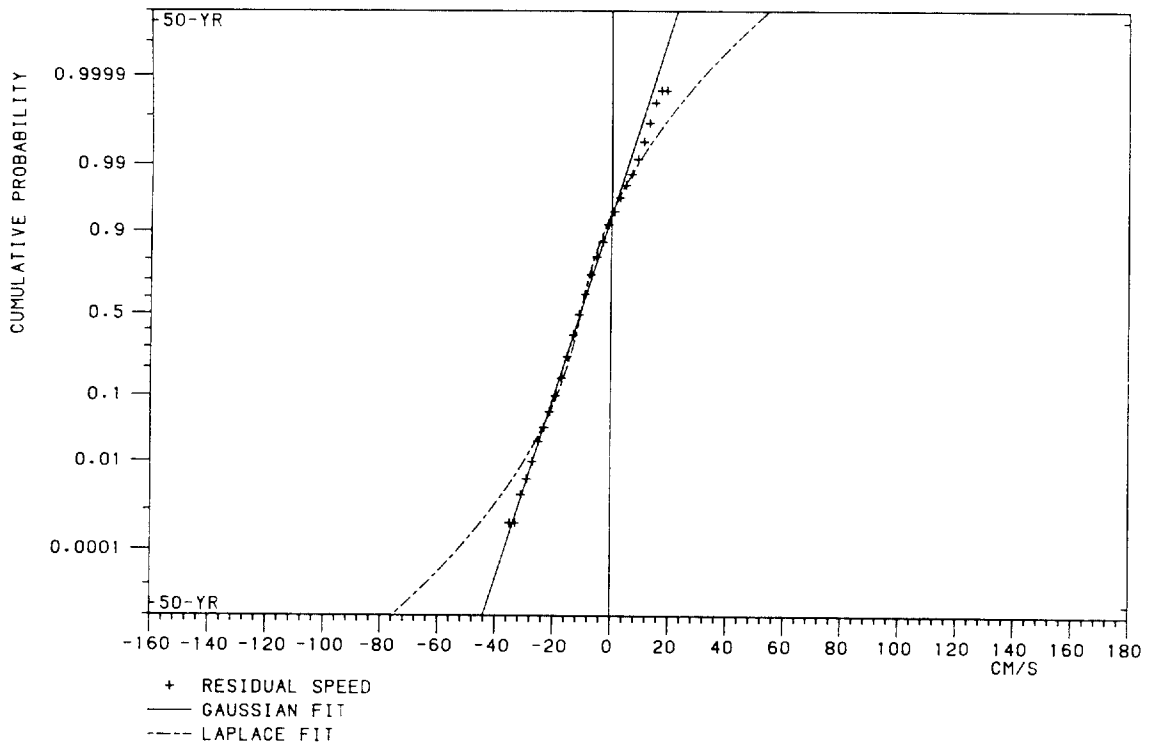


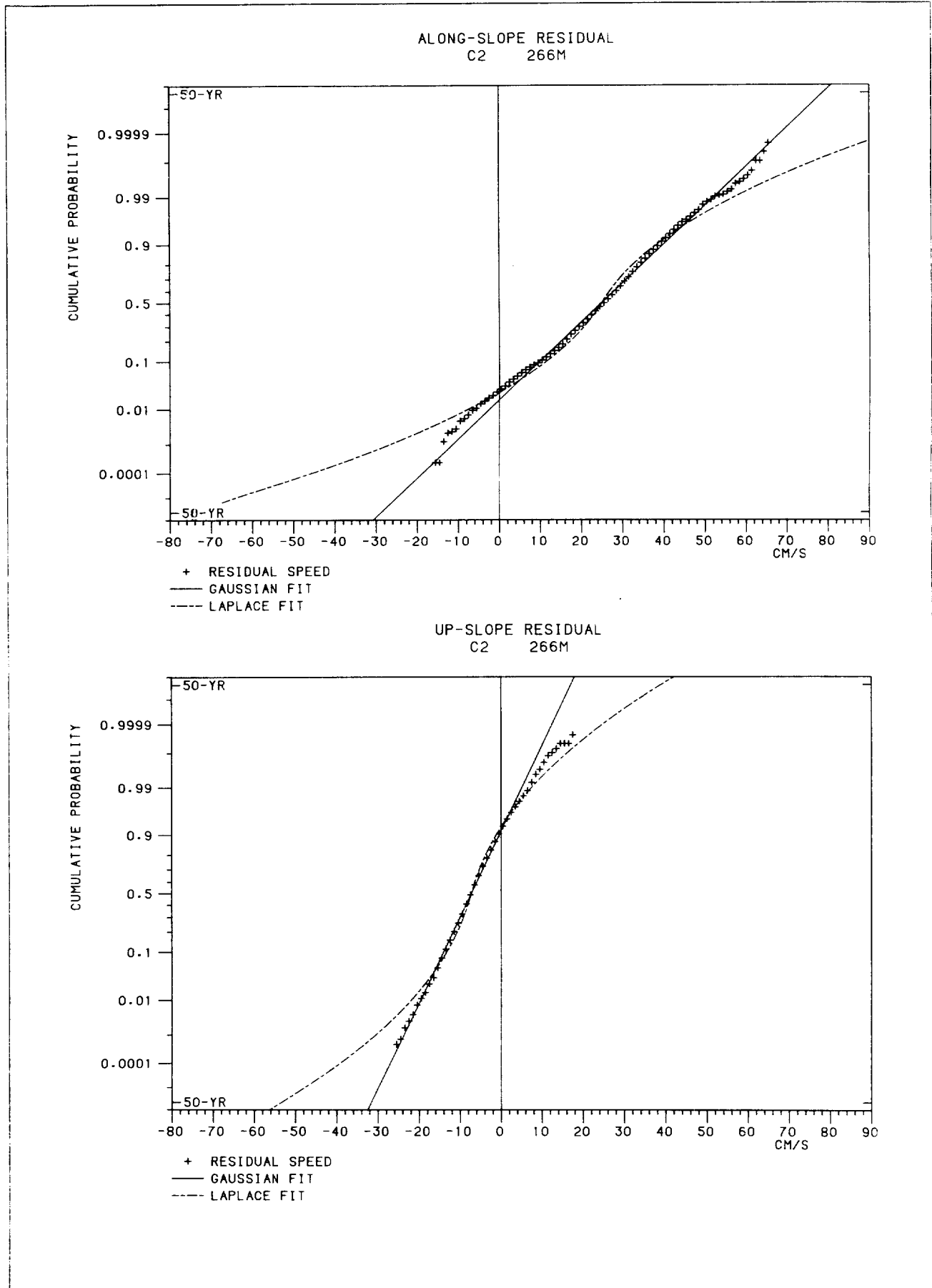


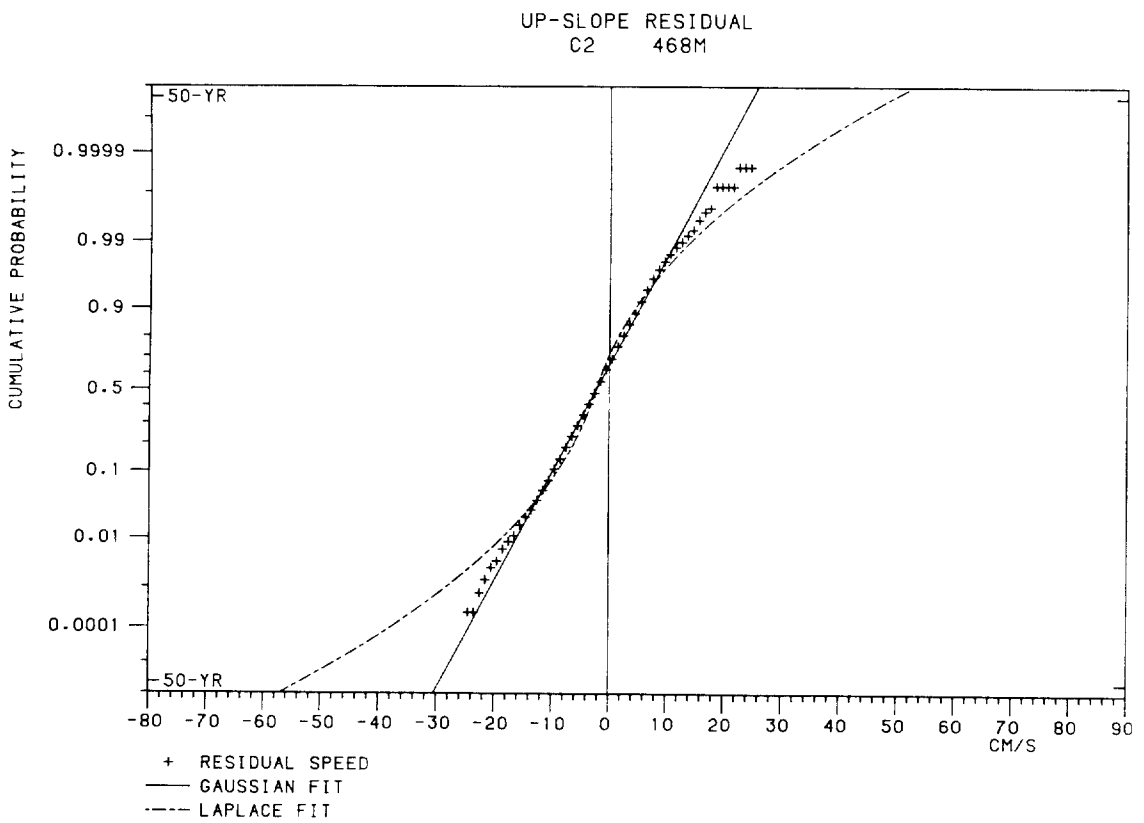
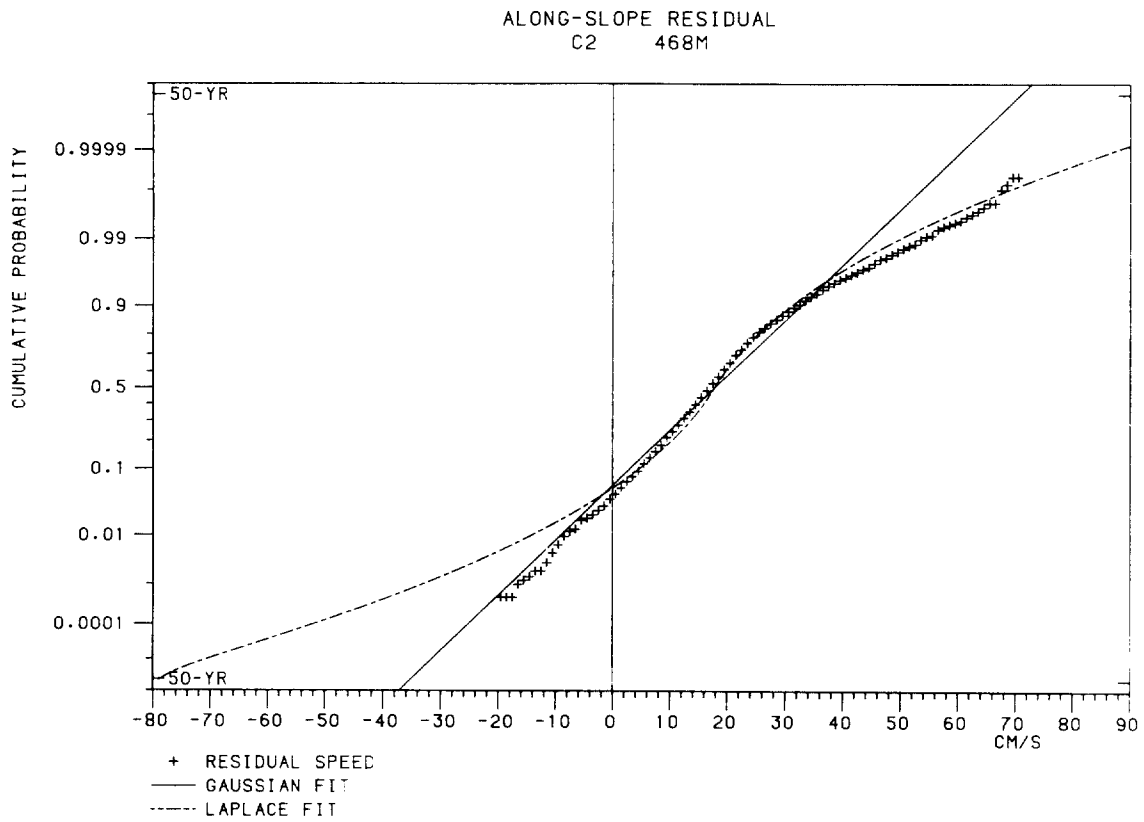
ALONG-SLOPE RESIDUAL
C2 115M

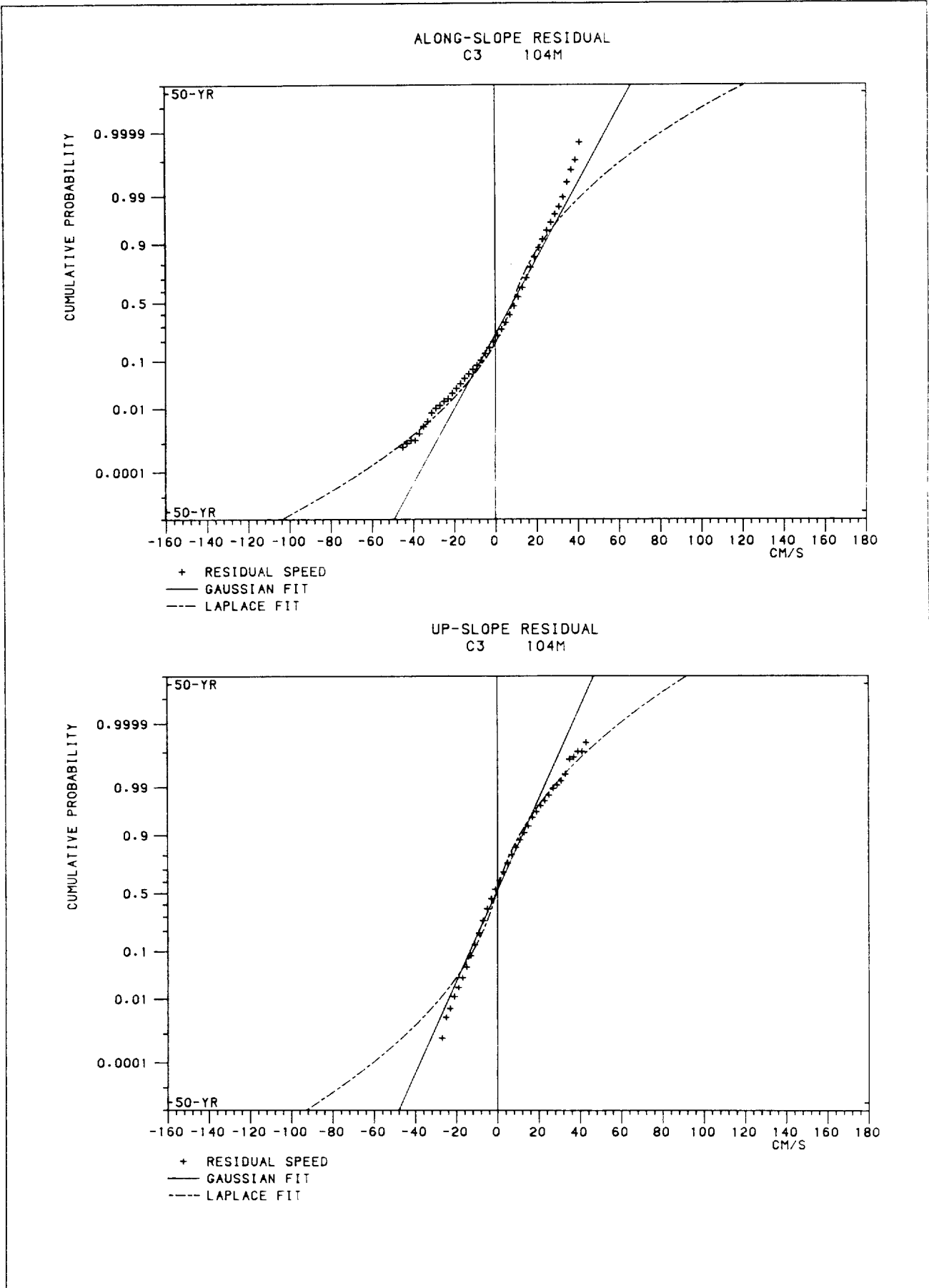


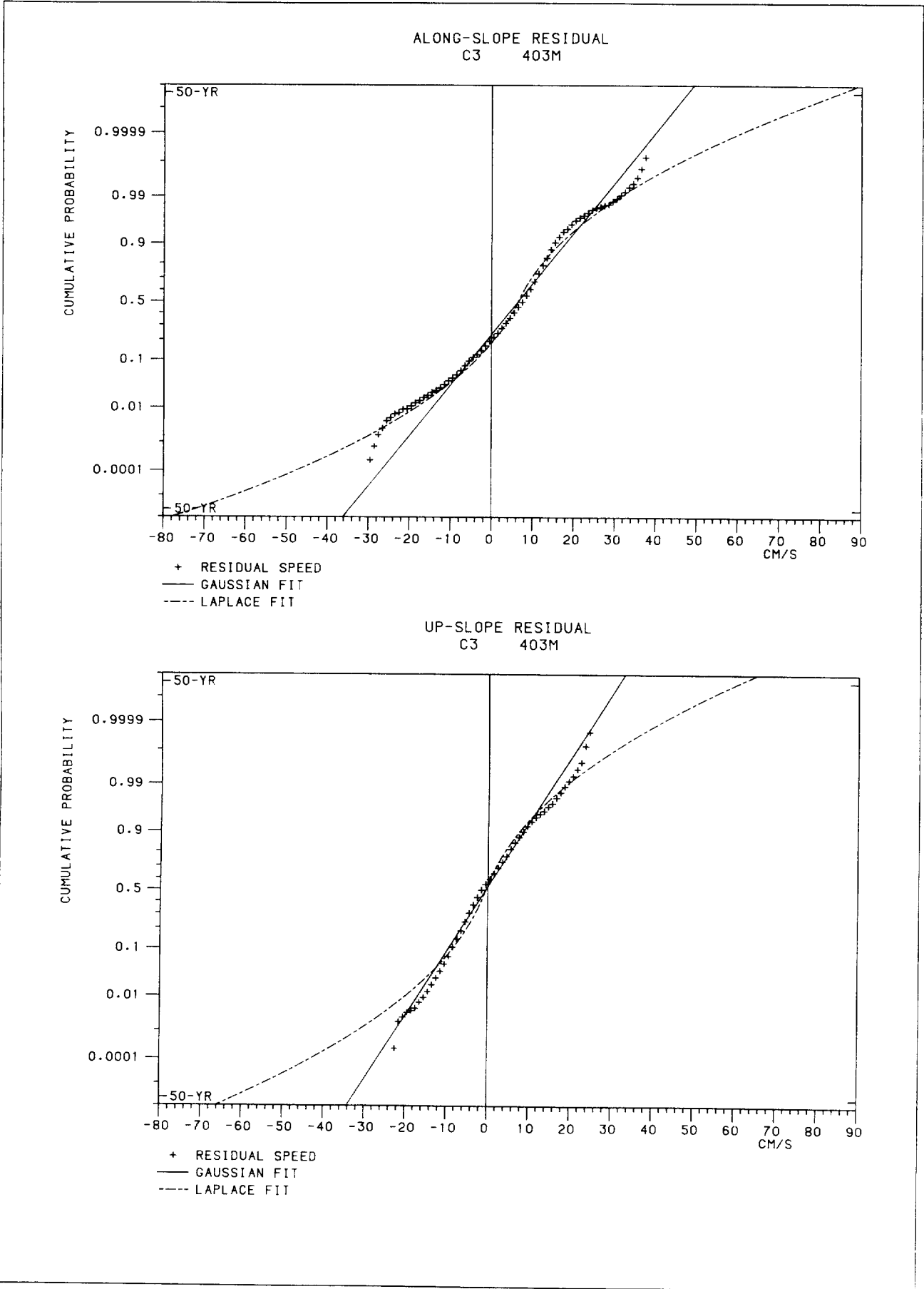
UP-SLOPE RESIDUAL
C2 115M

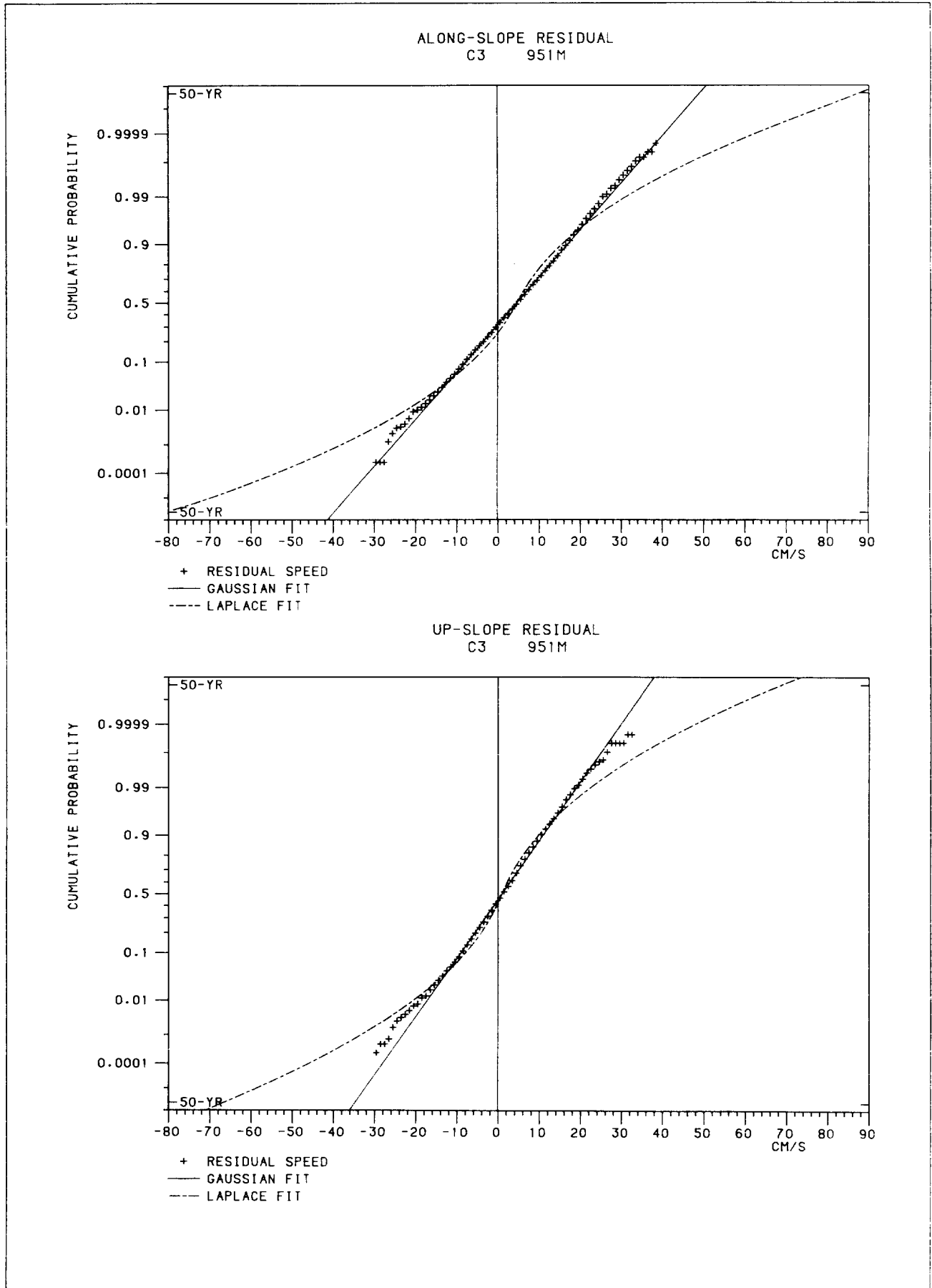




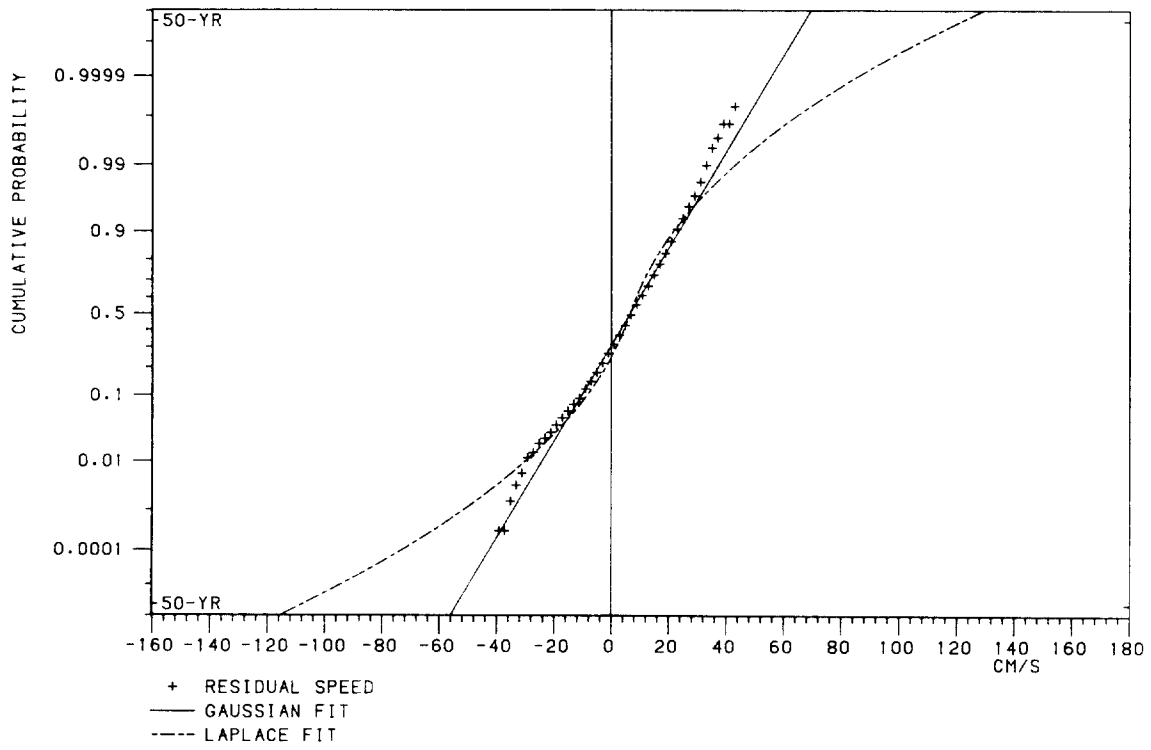




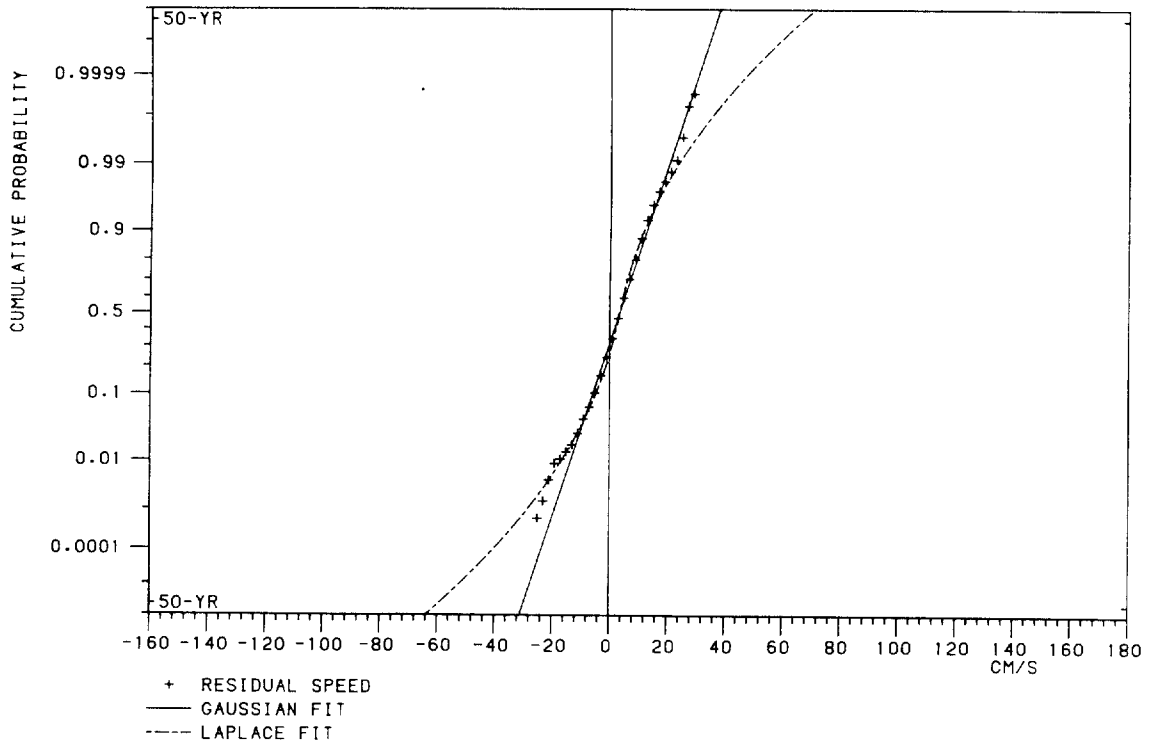




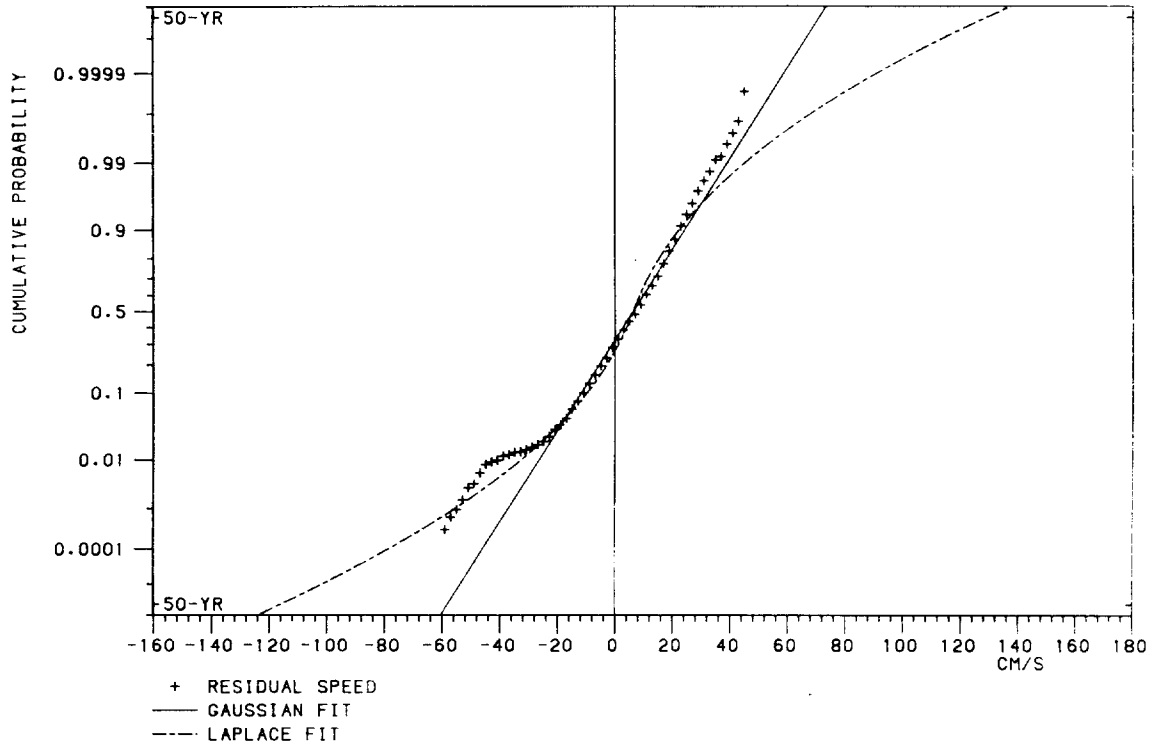
ALONG-SLOPE RESIDUAL
D1 87M



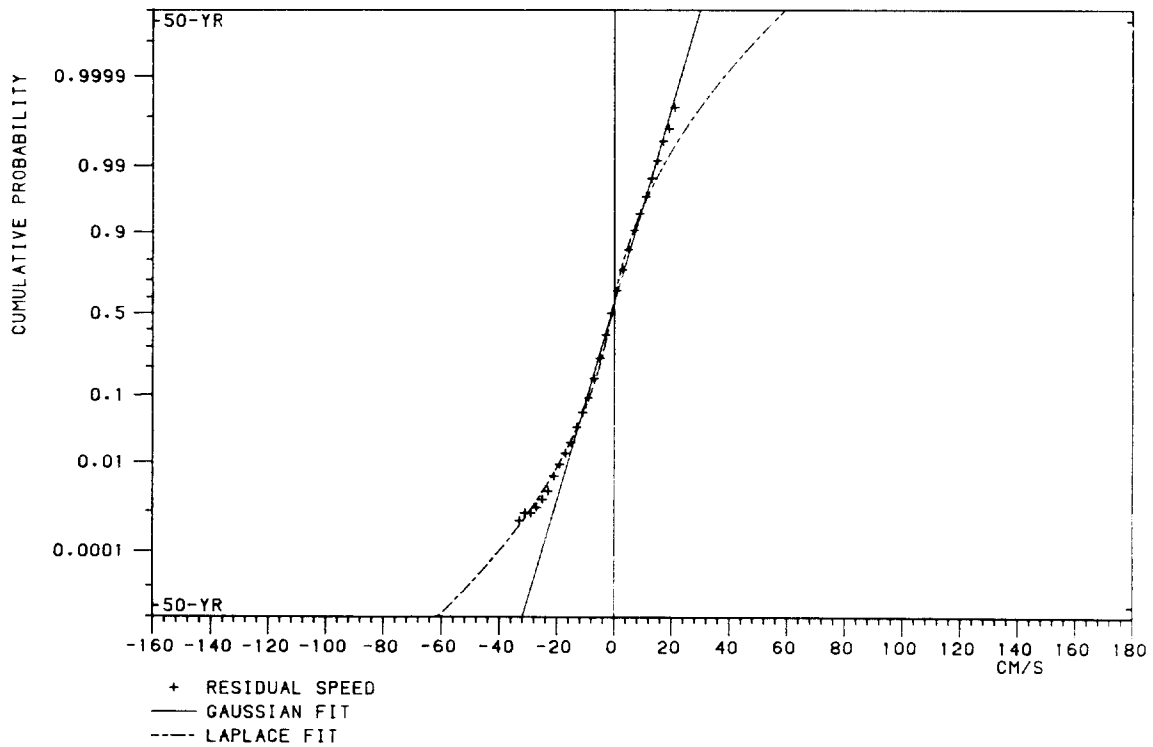
UP-SLOPE RESIDUAL
D1 87M

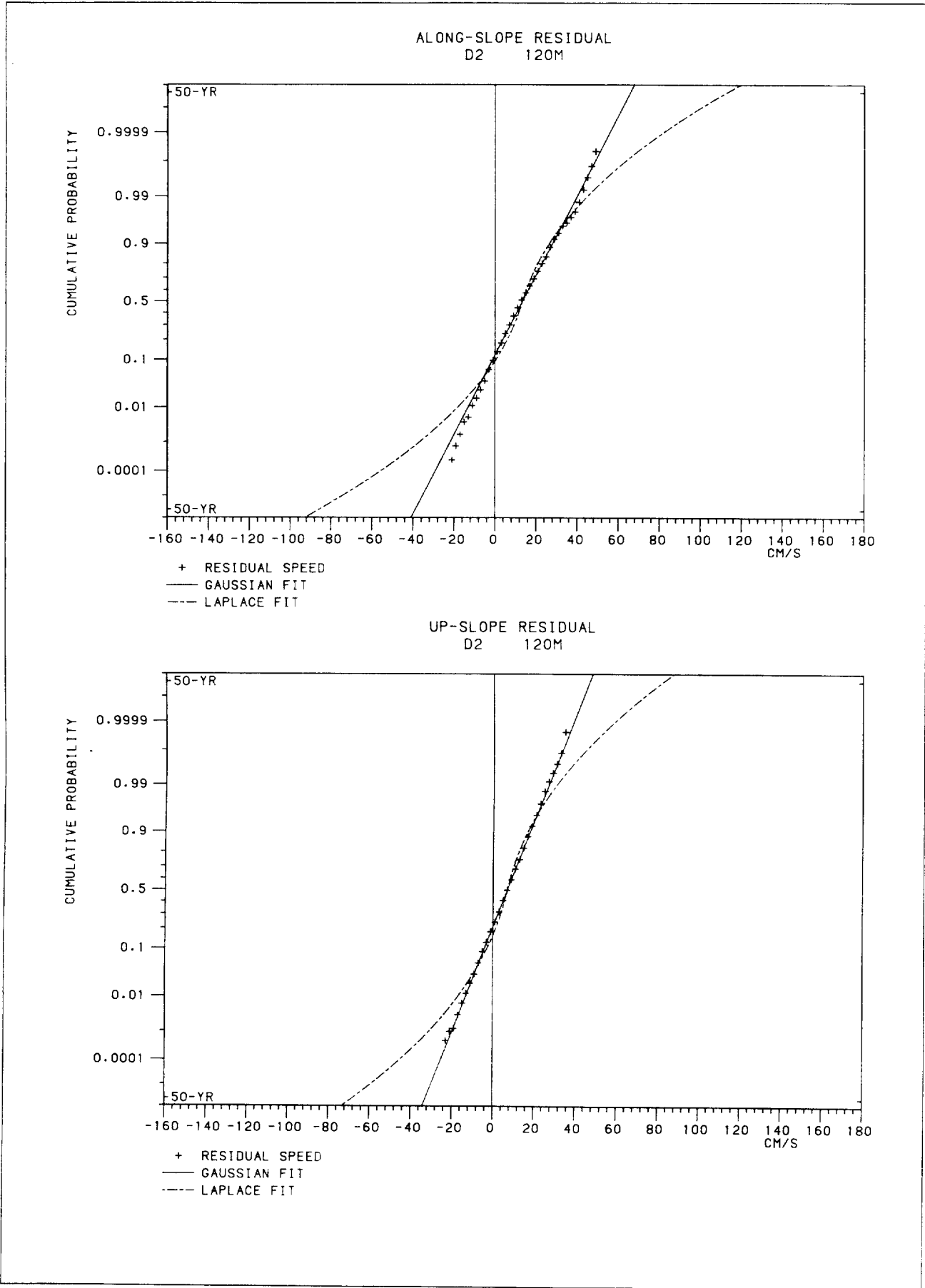


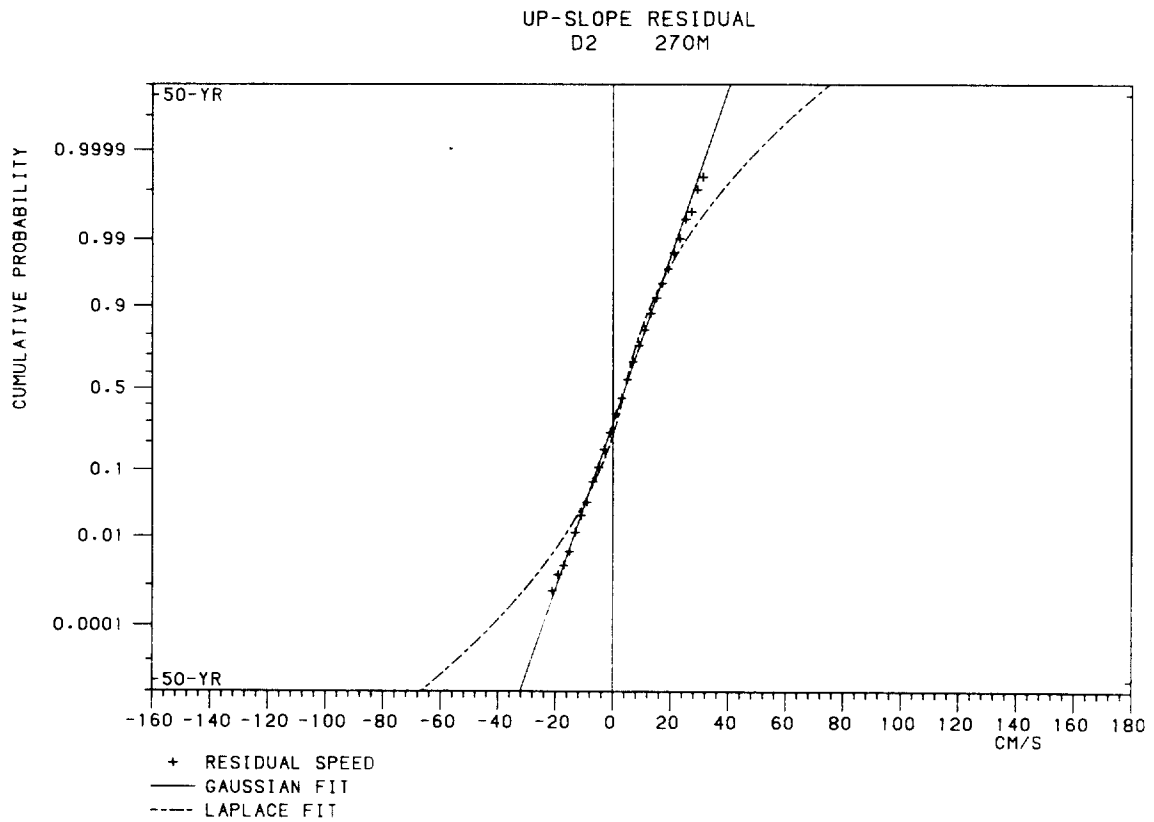
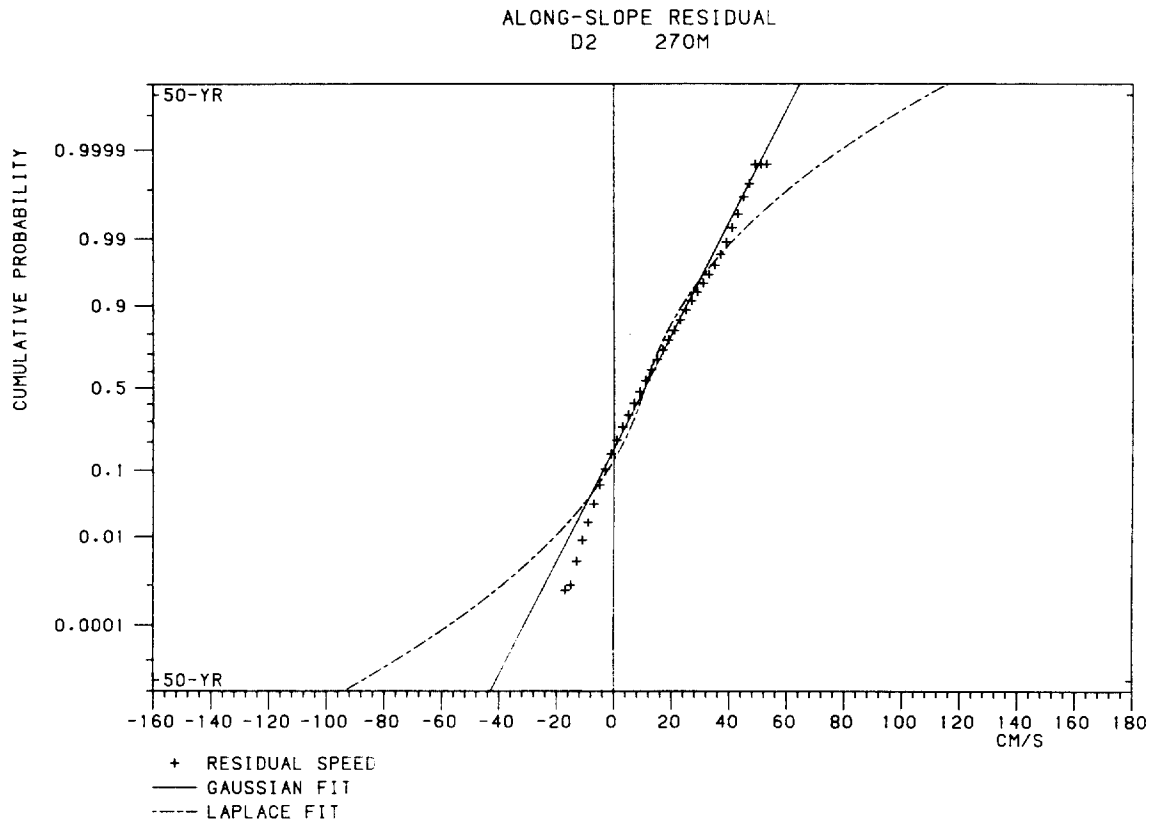
ALONG-SLOPE RESIDUAL
D1 212M

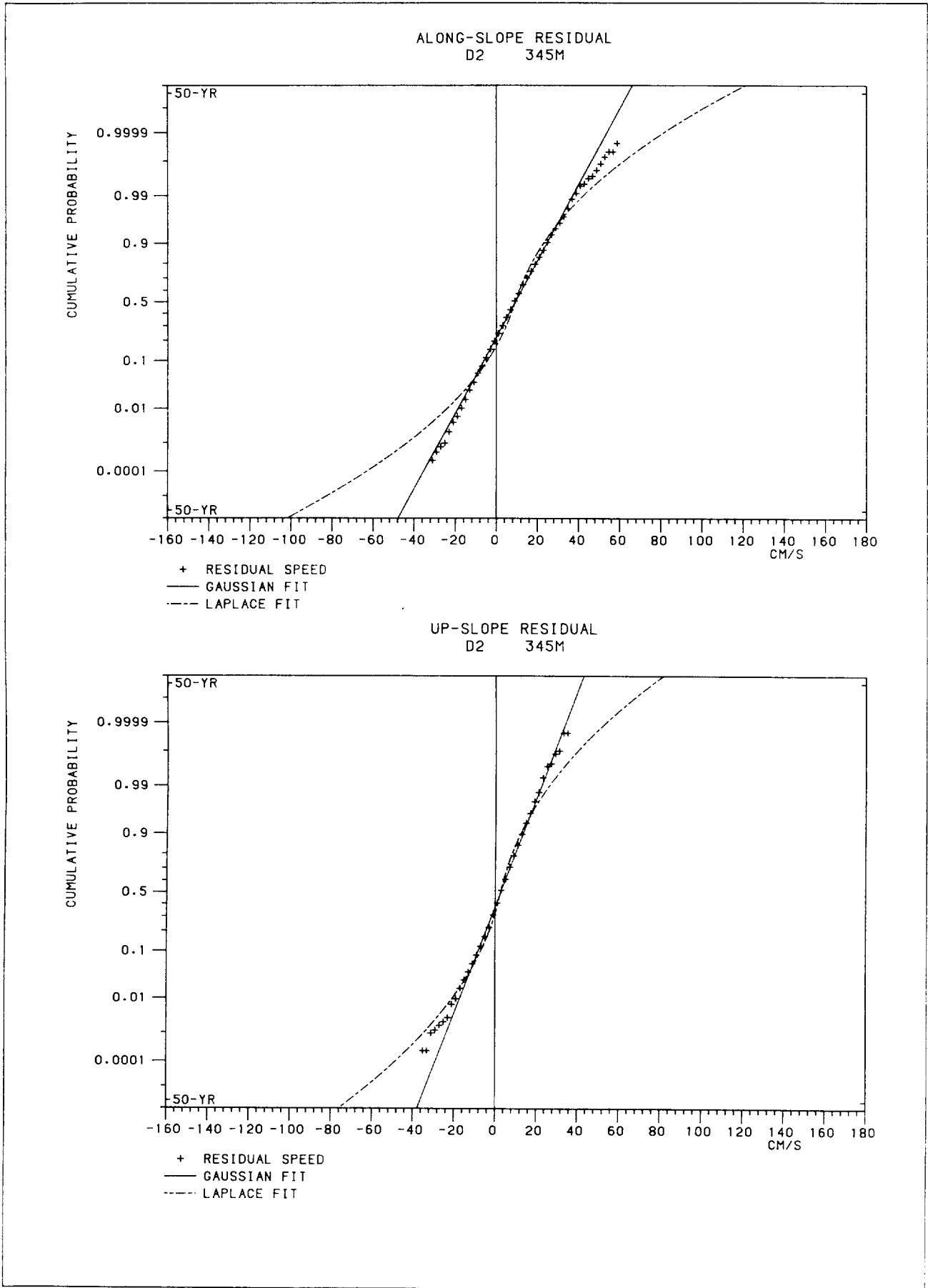


UP-SLOPE RESIDUAL
D1 212M

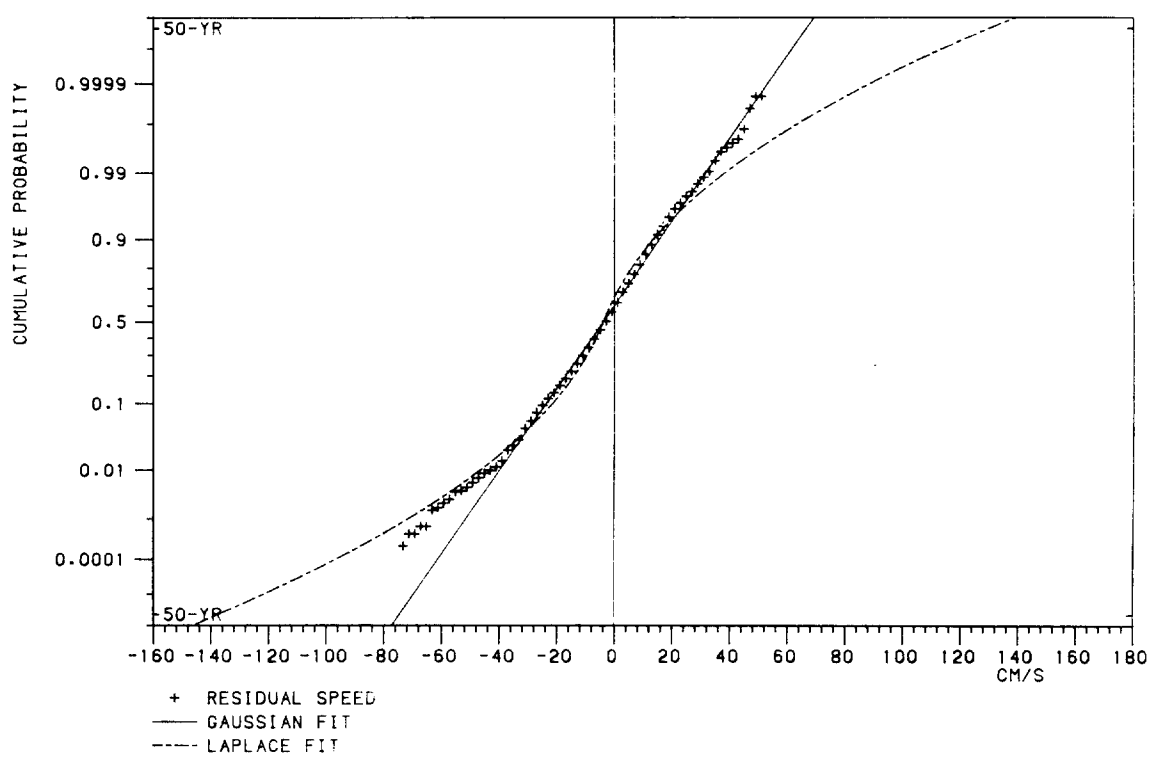




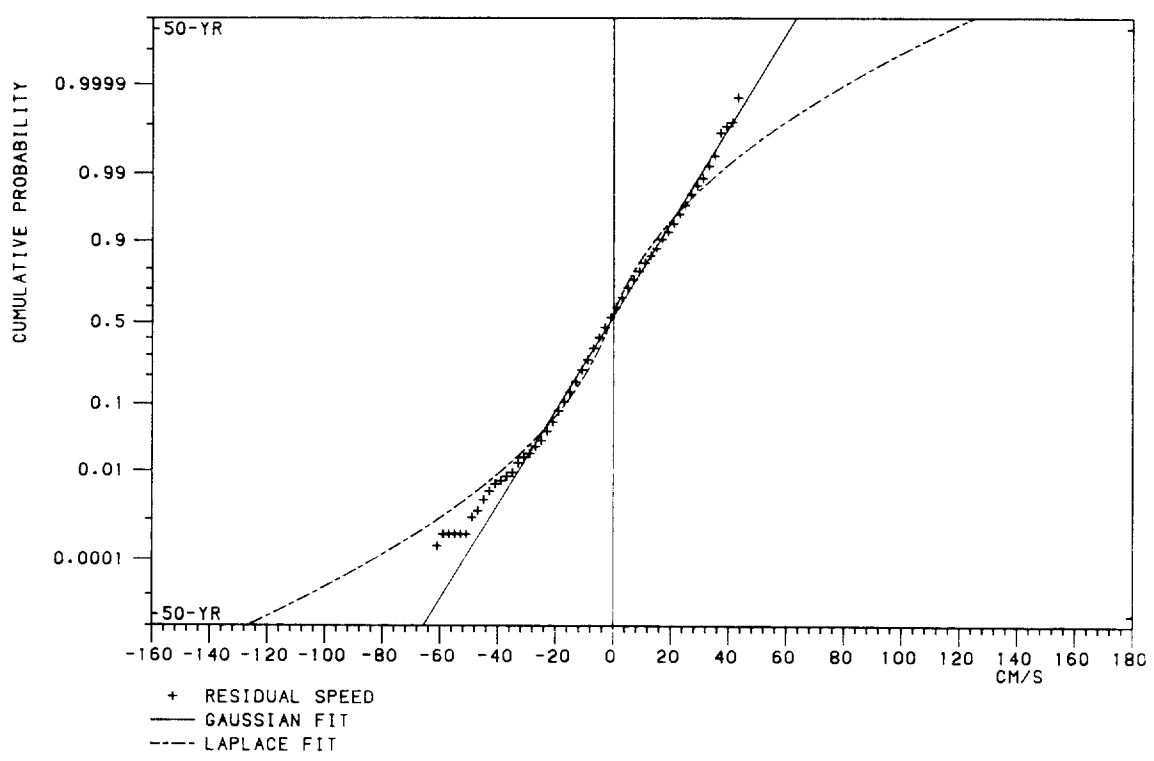


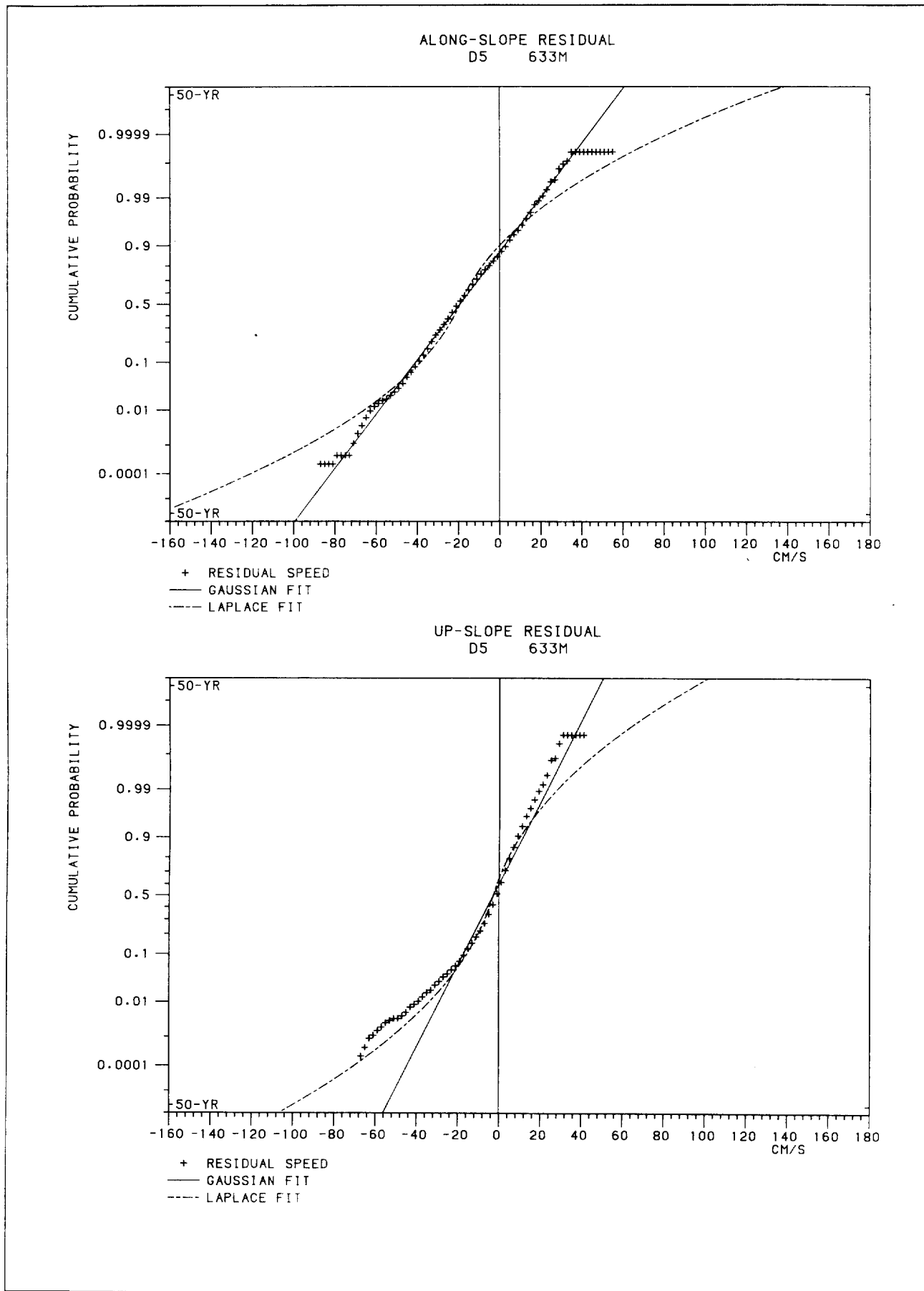


ALONG-SLOPE RESIDUAL
D5 510M

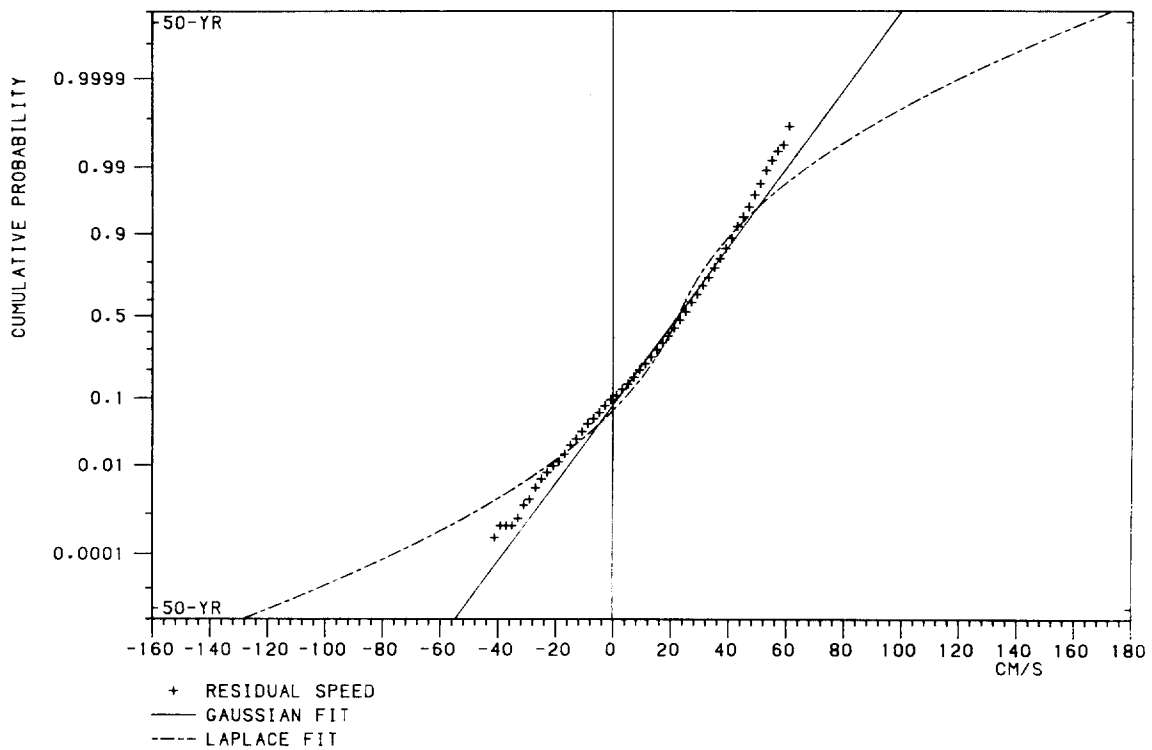


UP-SLOPE RESIDUAL
D5 510M

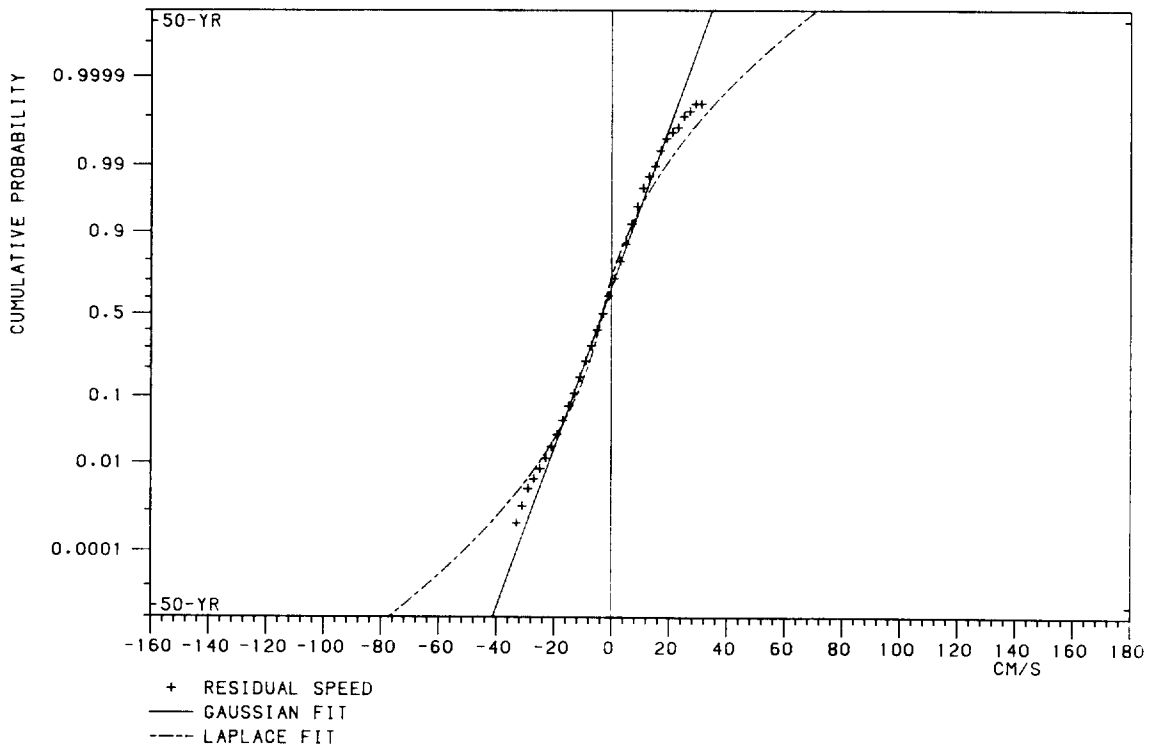


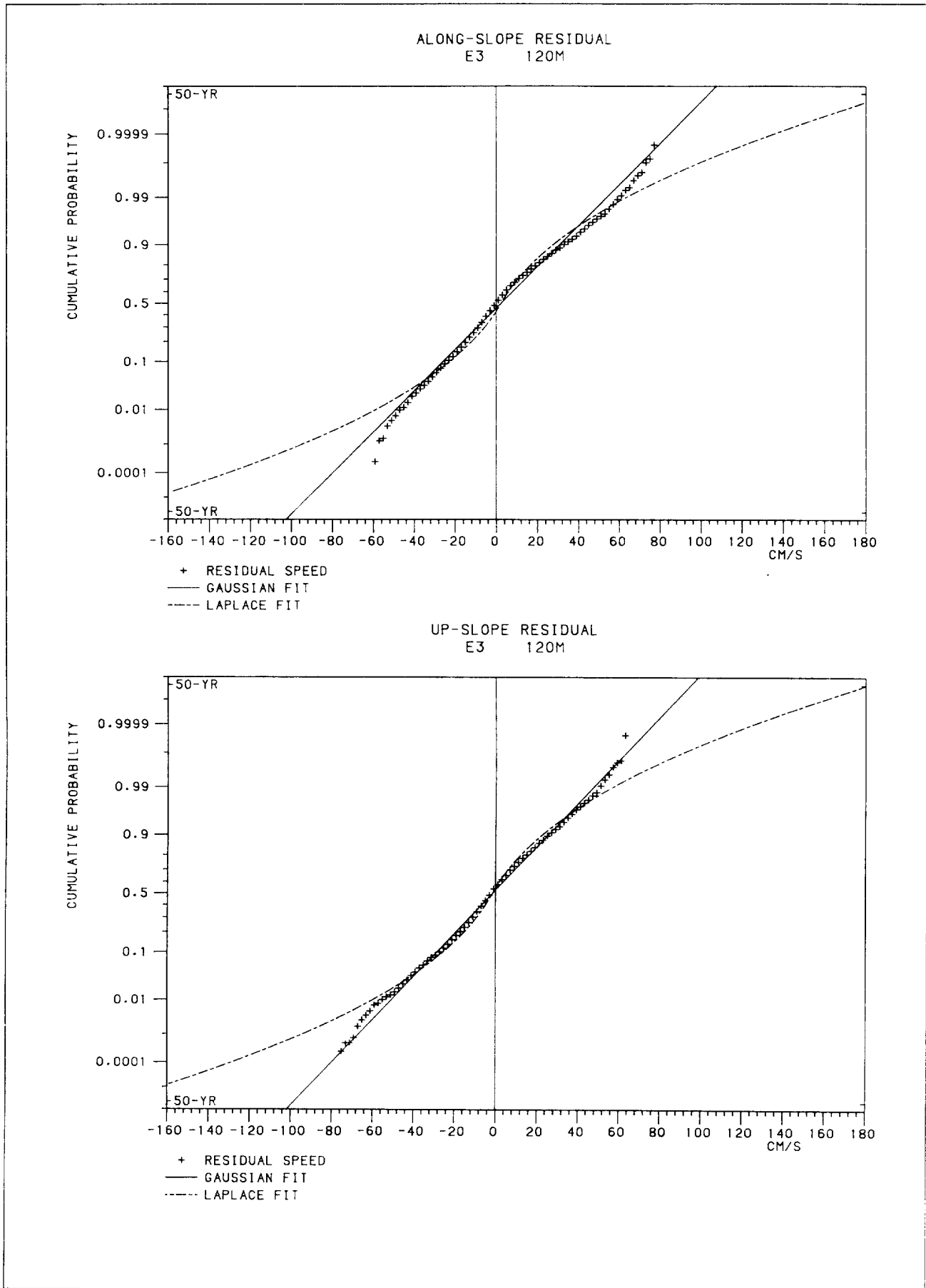


ALONG-SLOPE RESIDUAL
E2 453M

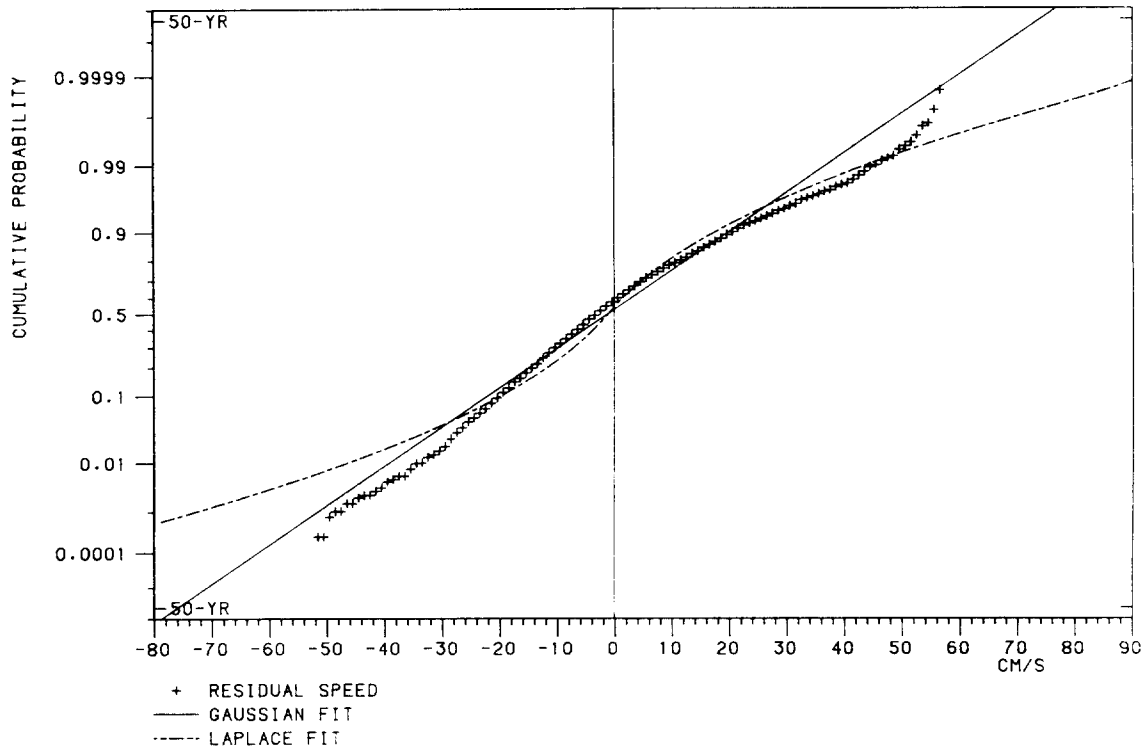


UP-SLOPE RESIDUAL
E2 453M

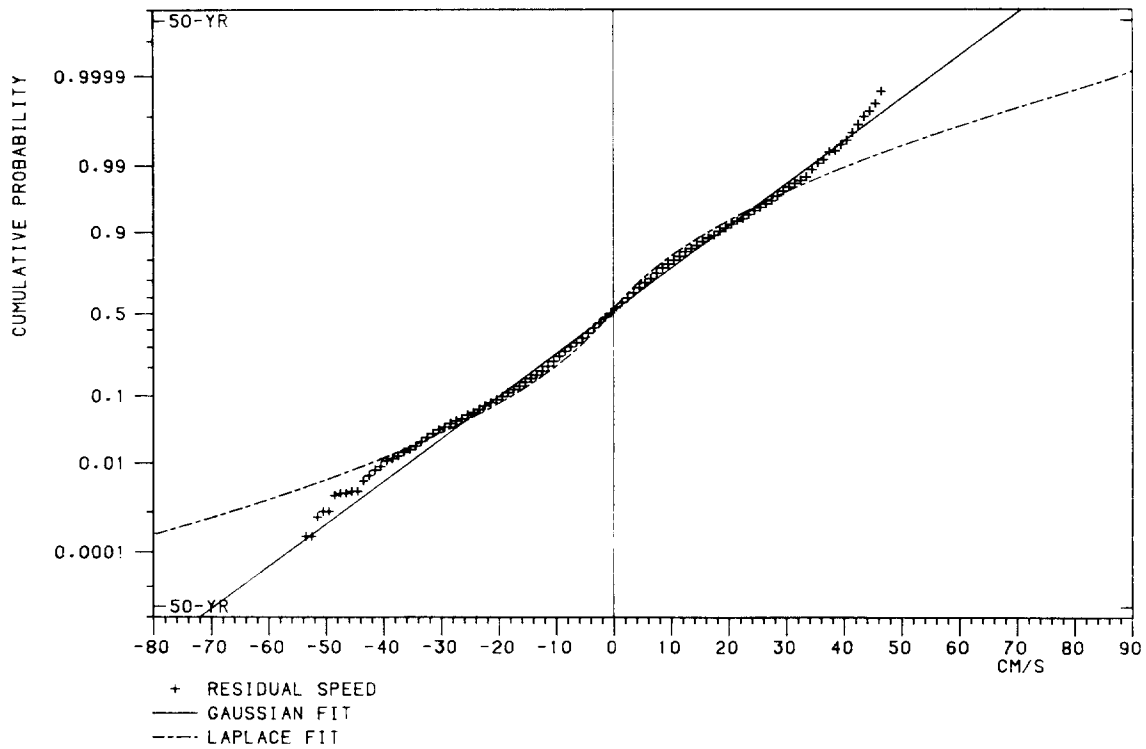




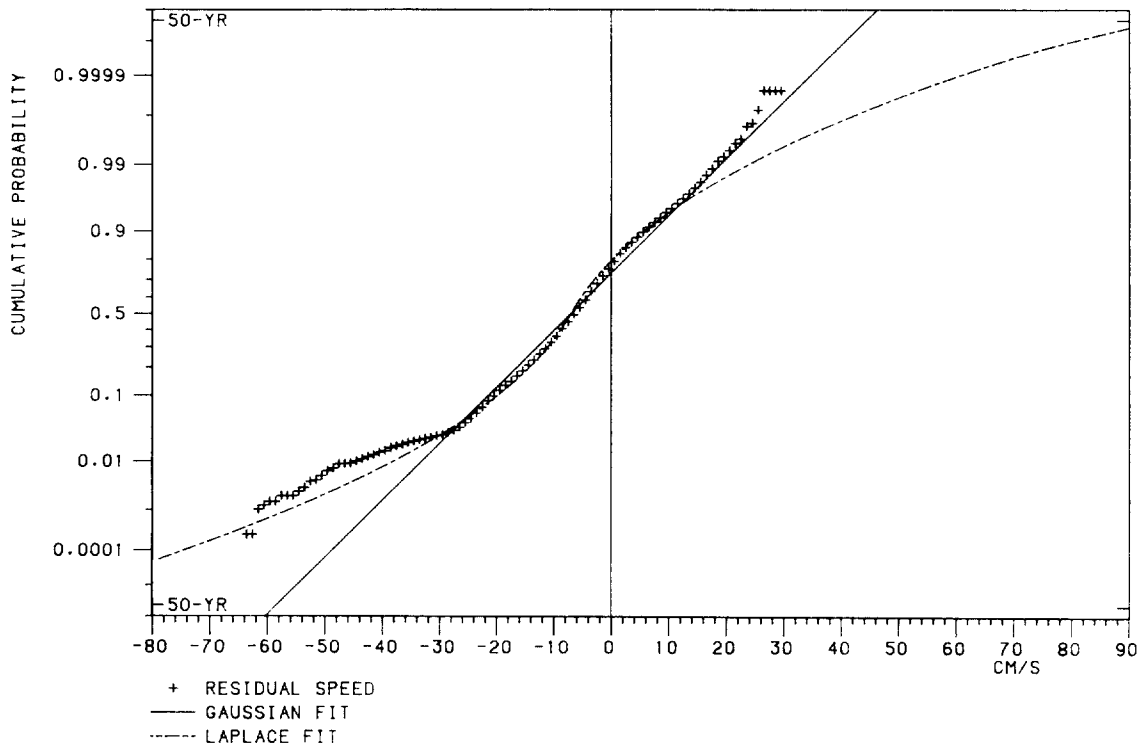
ALONG-SLOPE RESIDUAL
E3 419M



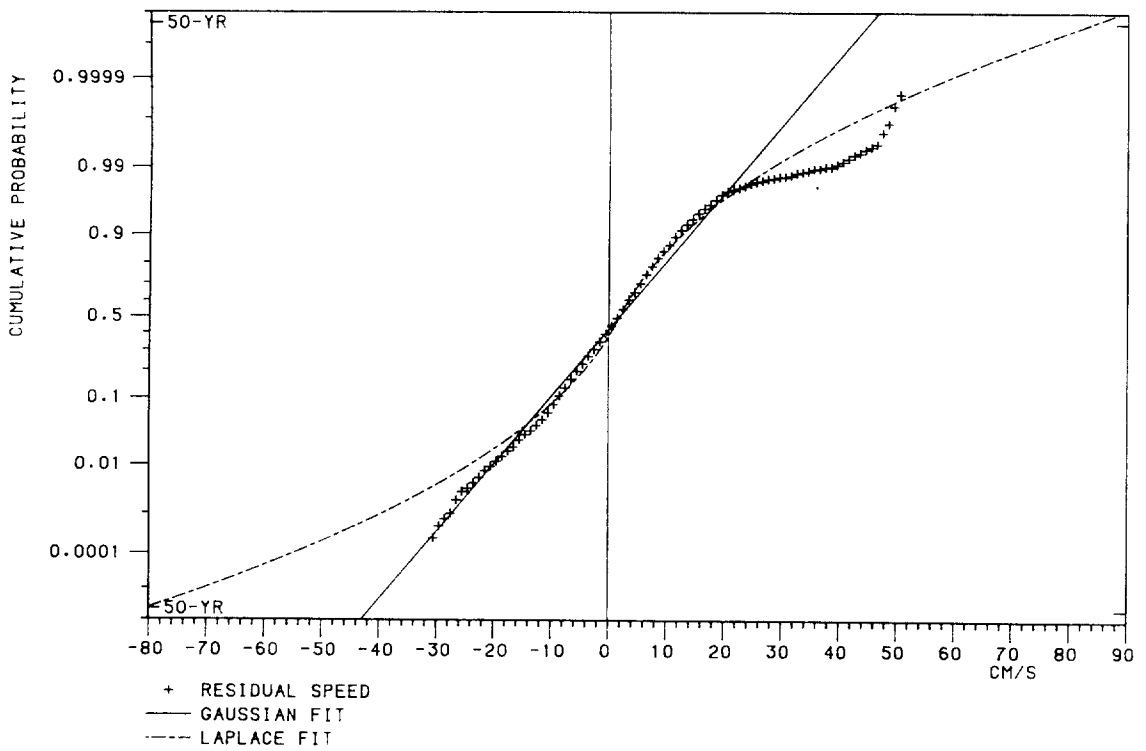
UP-SLOPE RESIDUAL
E3 419M

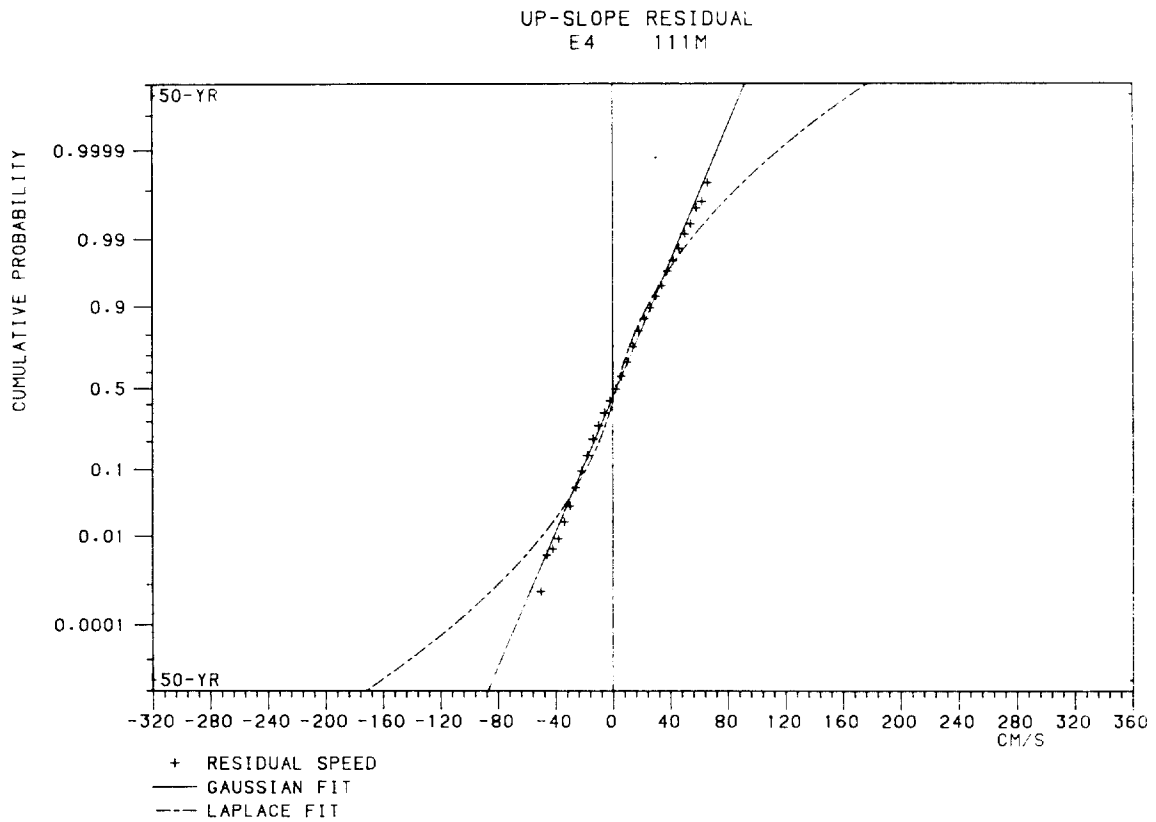
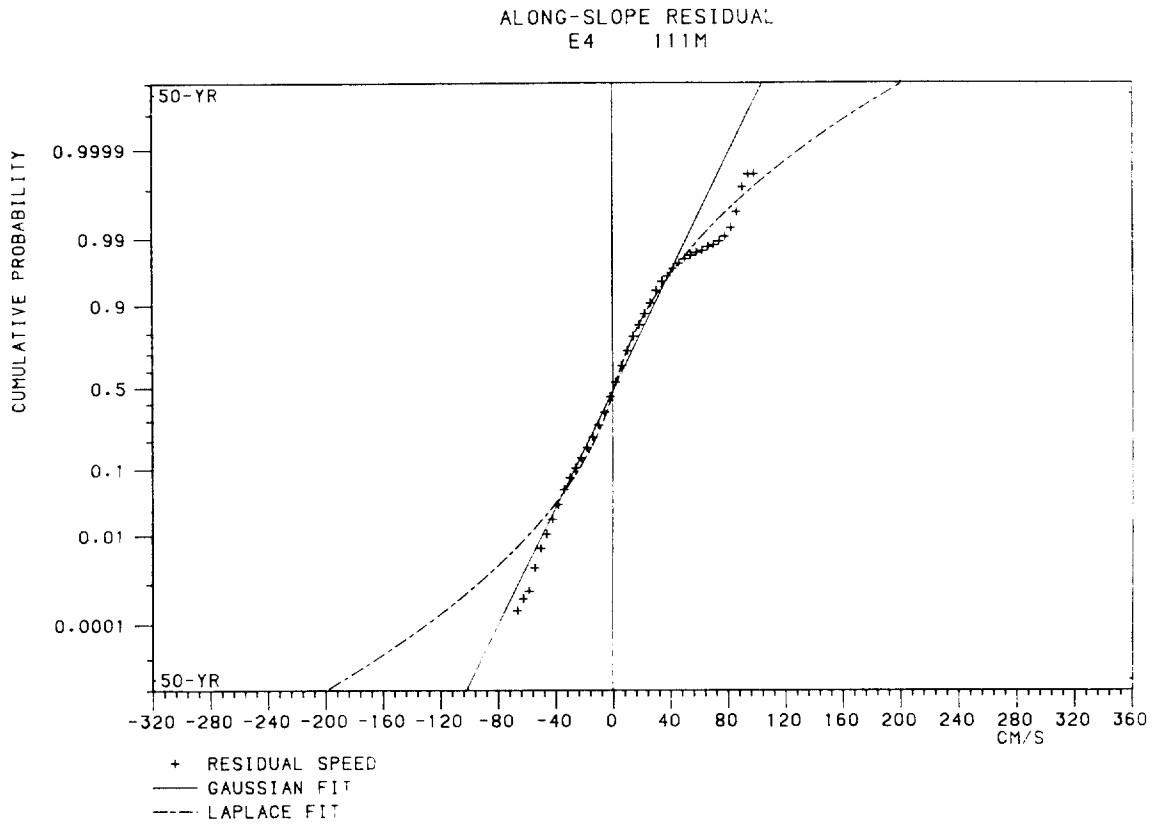


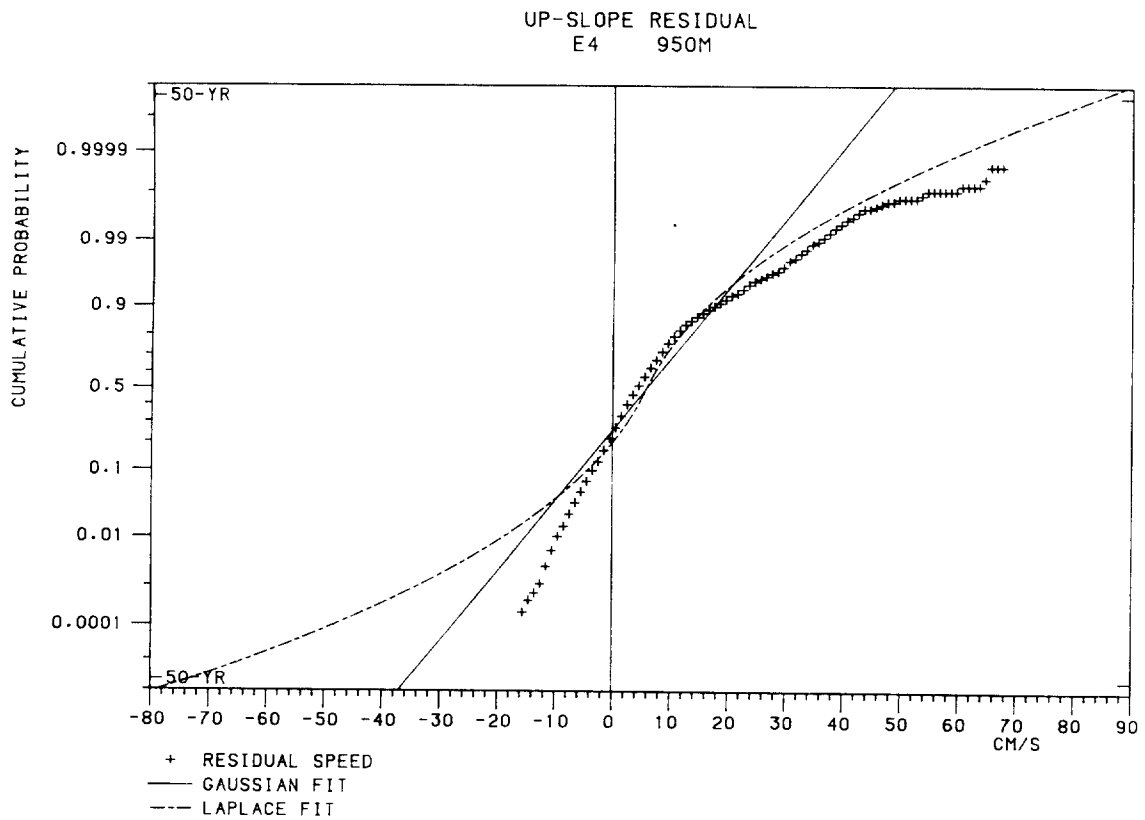
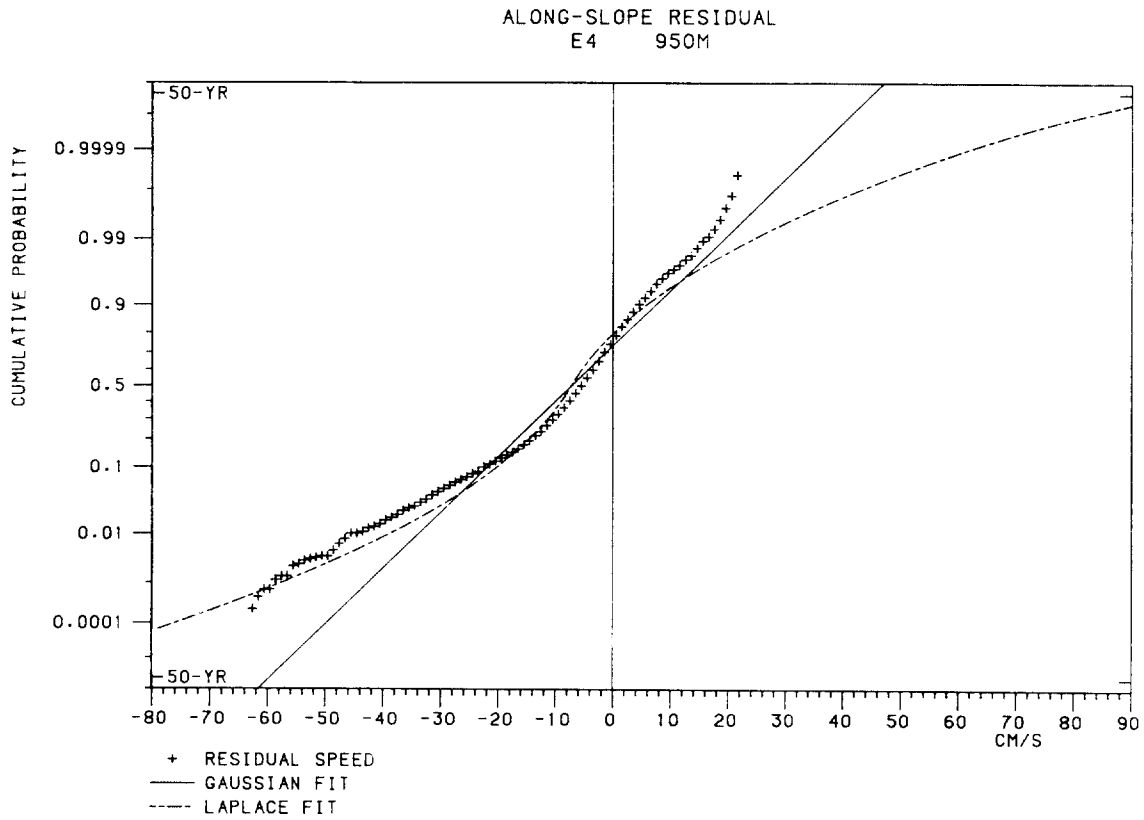
ALONG-SLOPE RESIDUAL
E3 725M

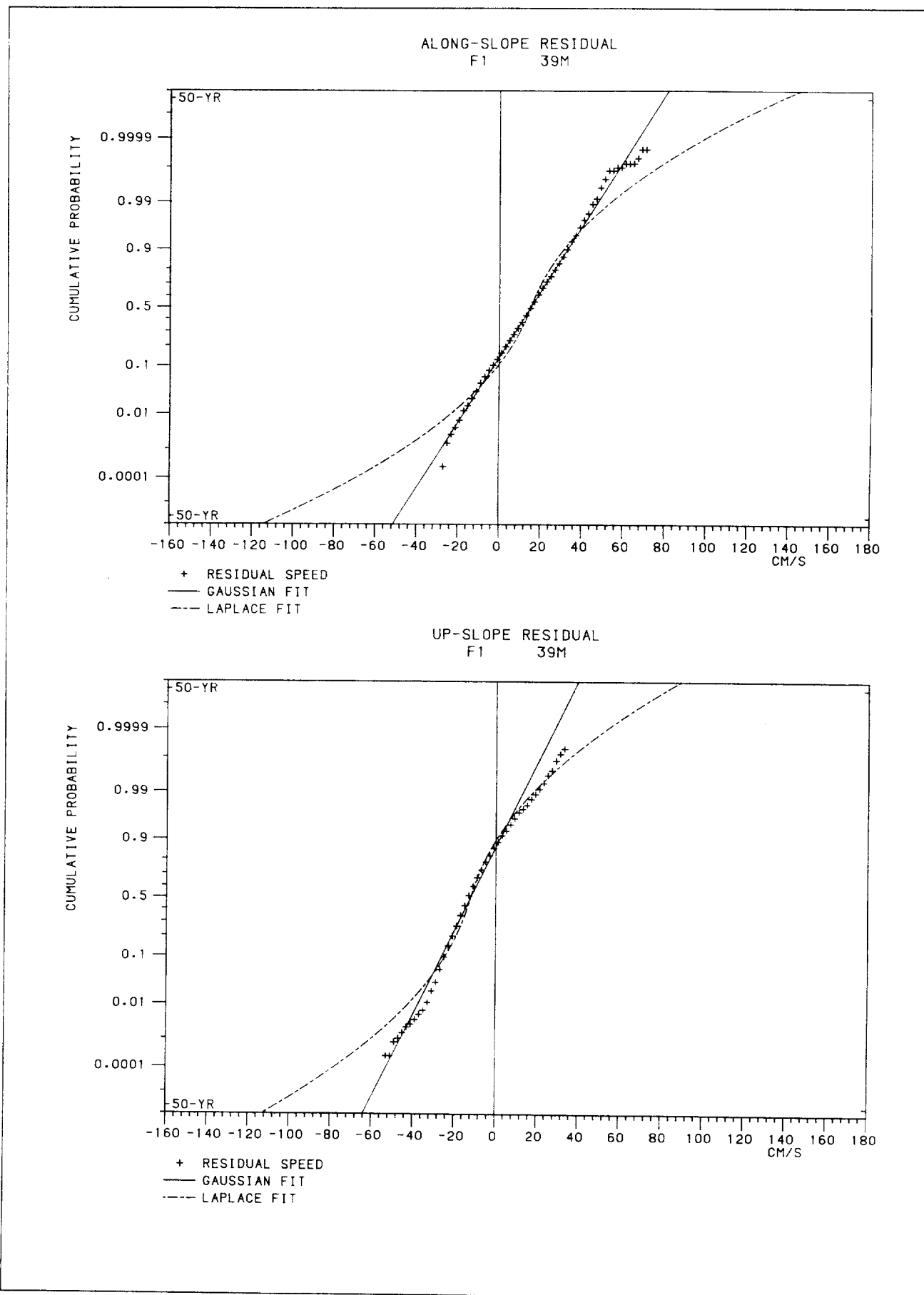


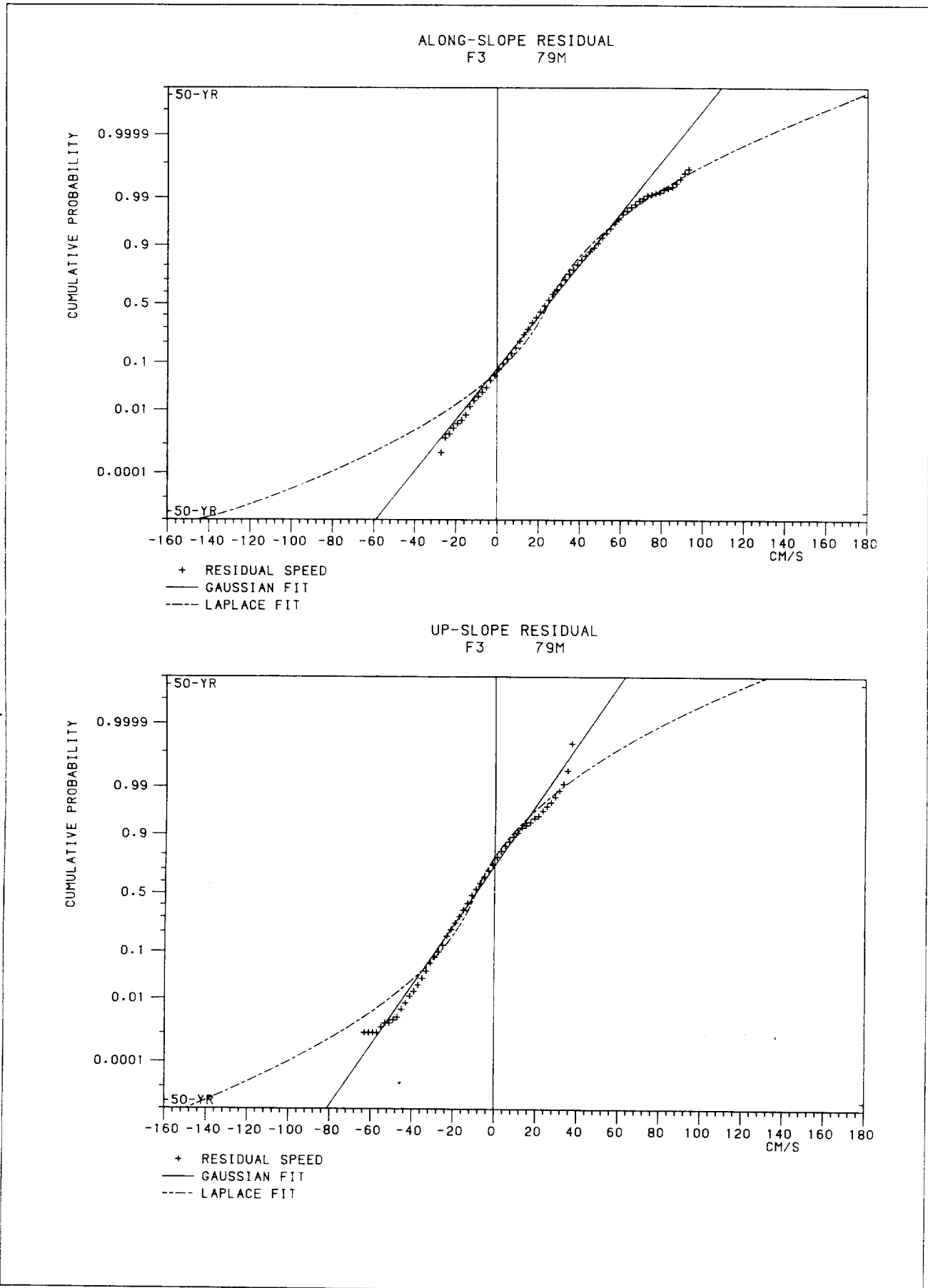
UP-SLOPE RESIDUAL
E3 725M



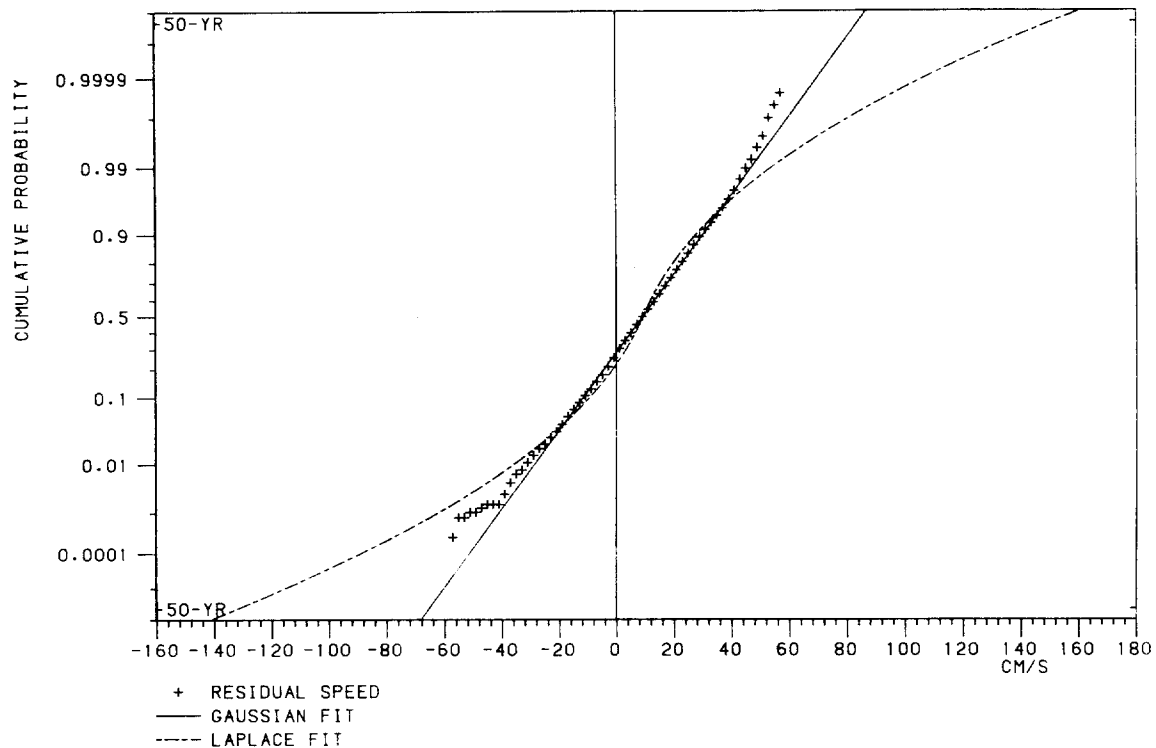




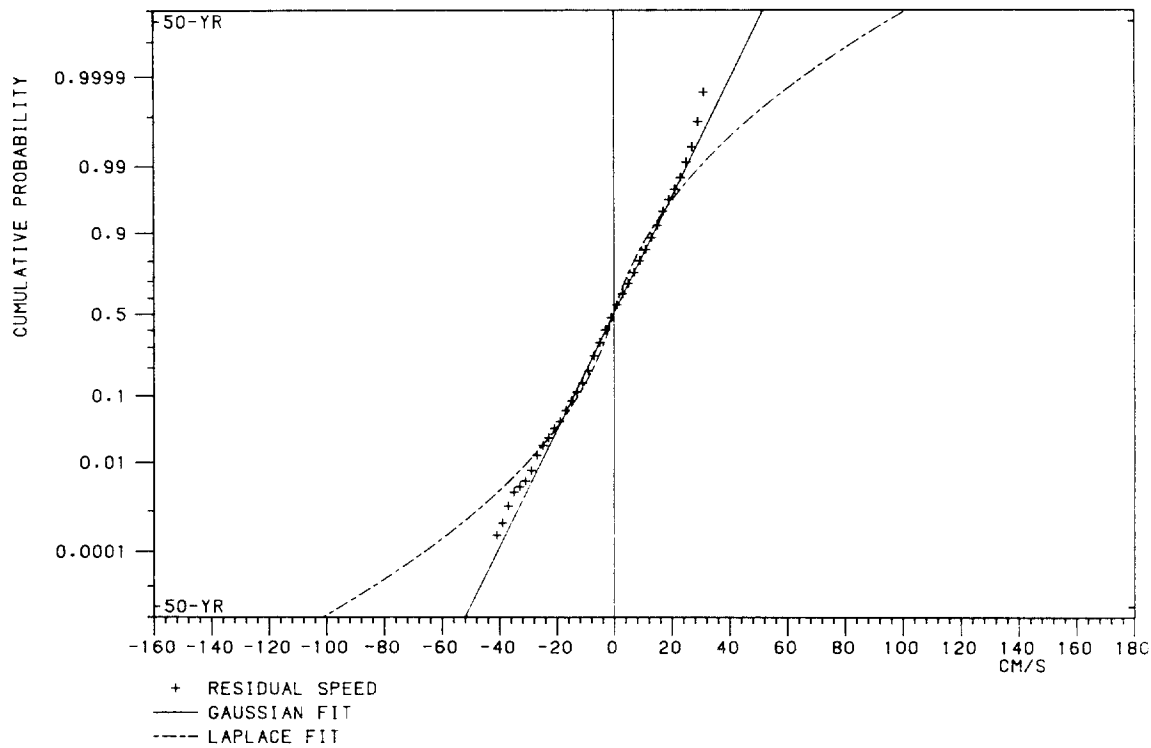


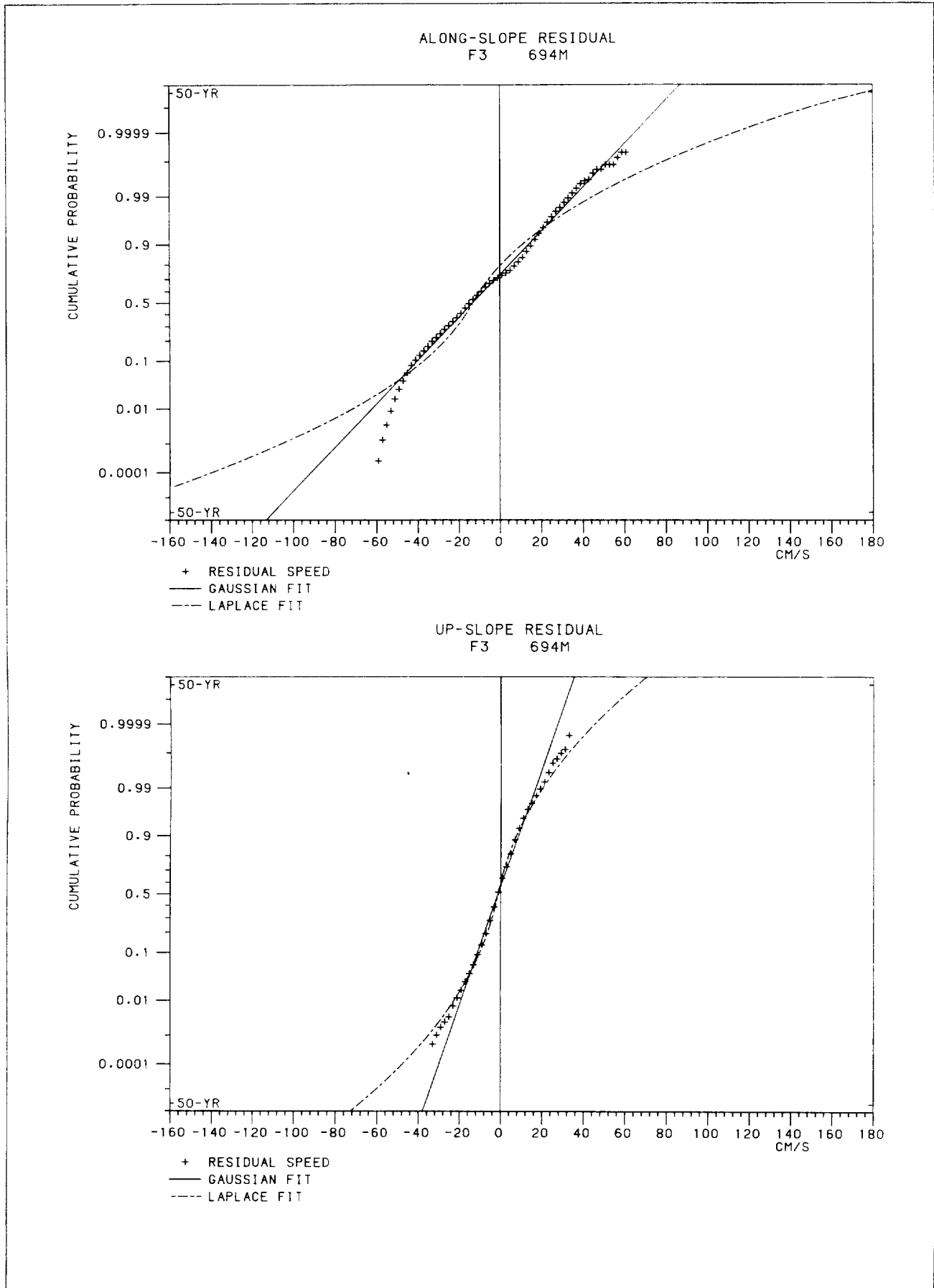


ALONG-SLOPE RESIDUAL
F3 388M

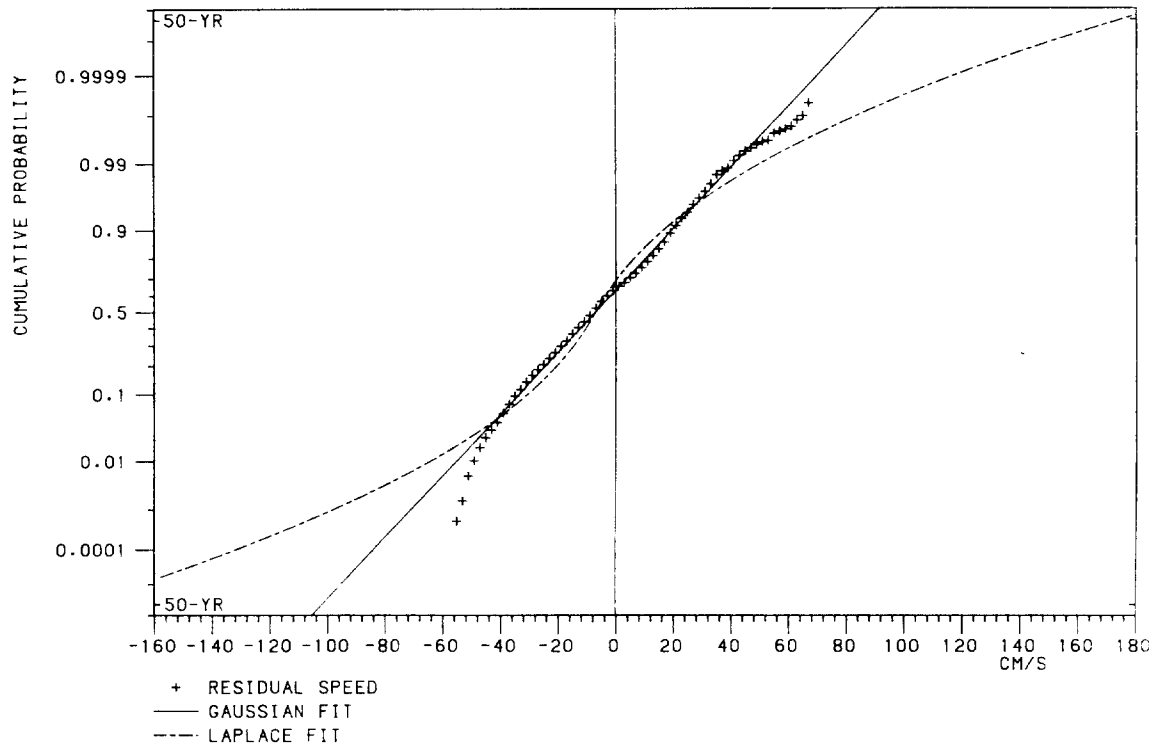


UP-SLOPE RESIDUAL
F3 388M

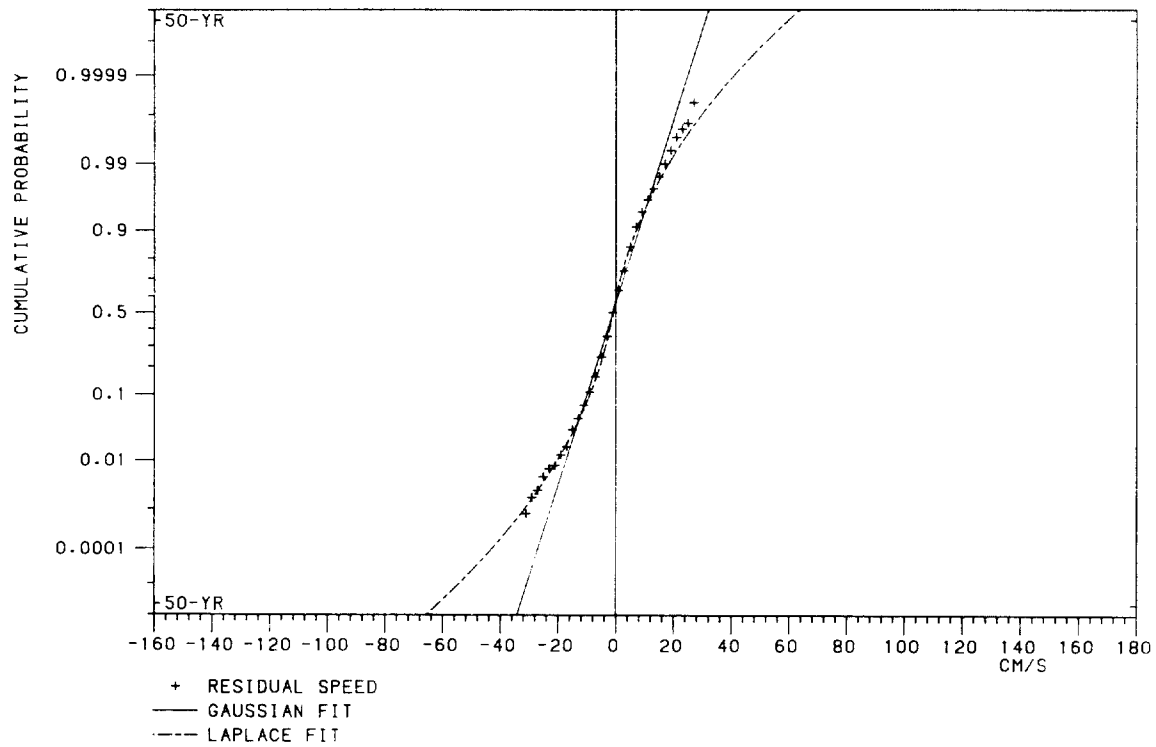


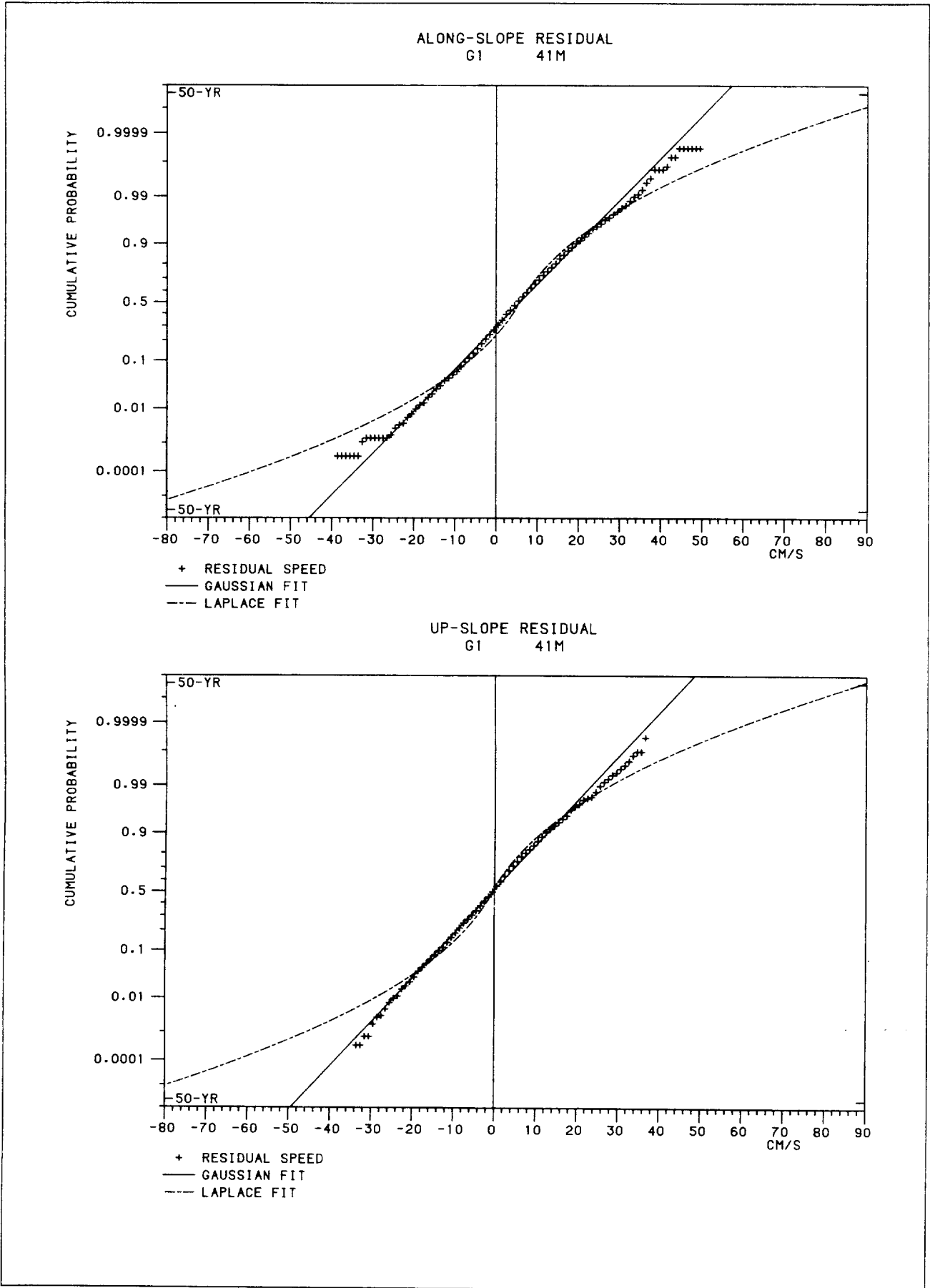


ALONG-SLOPE RESIDUAL
F3 945M

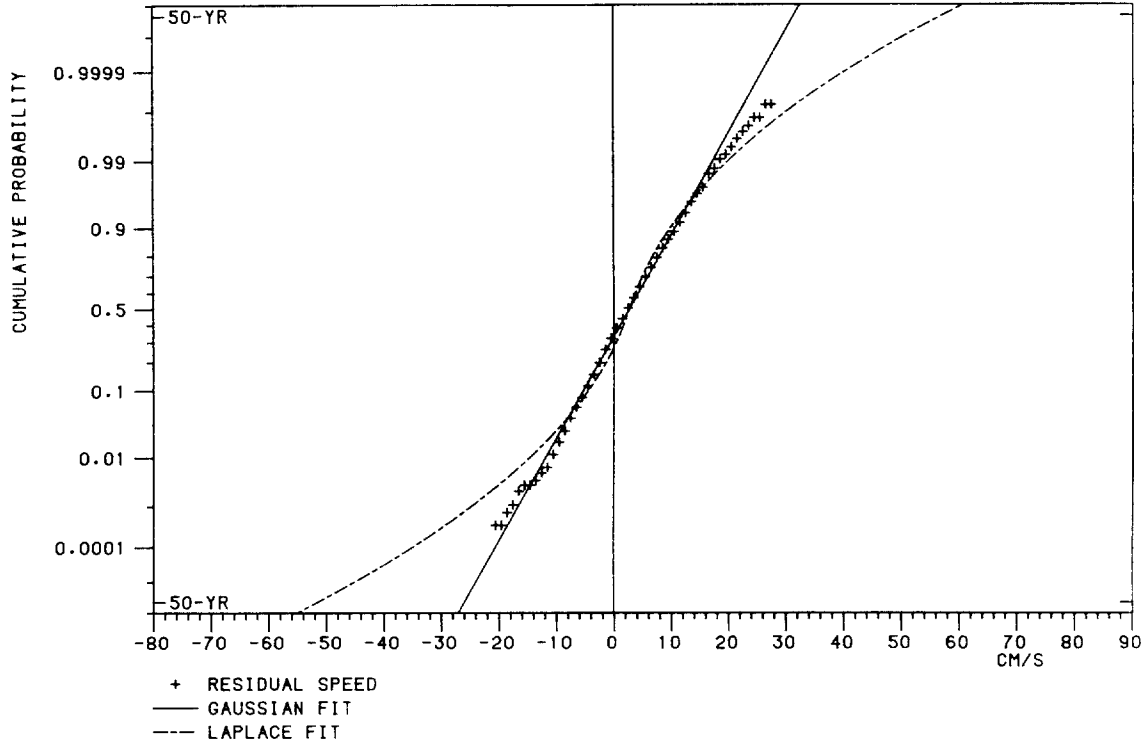


UP-SLOPE RESIDUAL
F3 945M

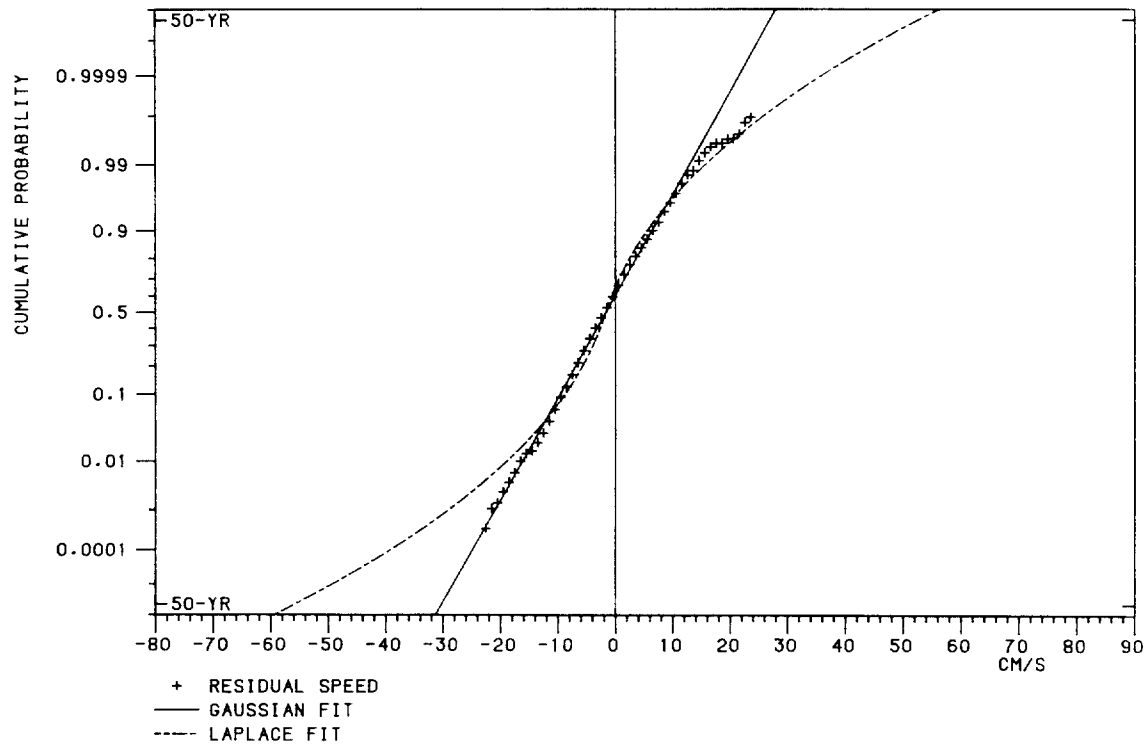


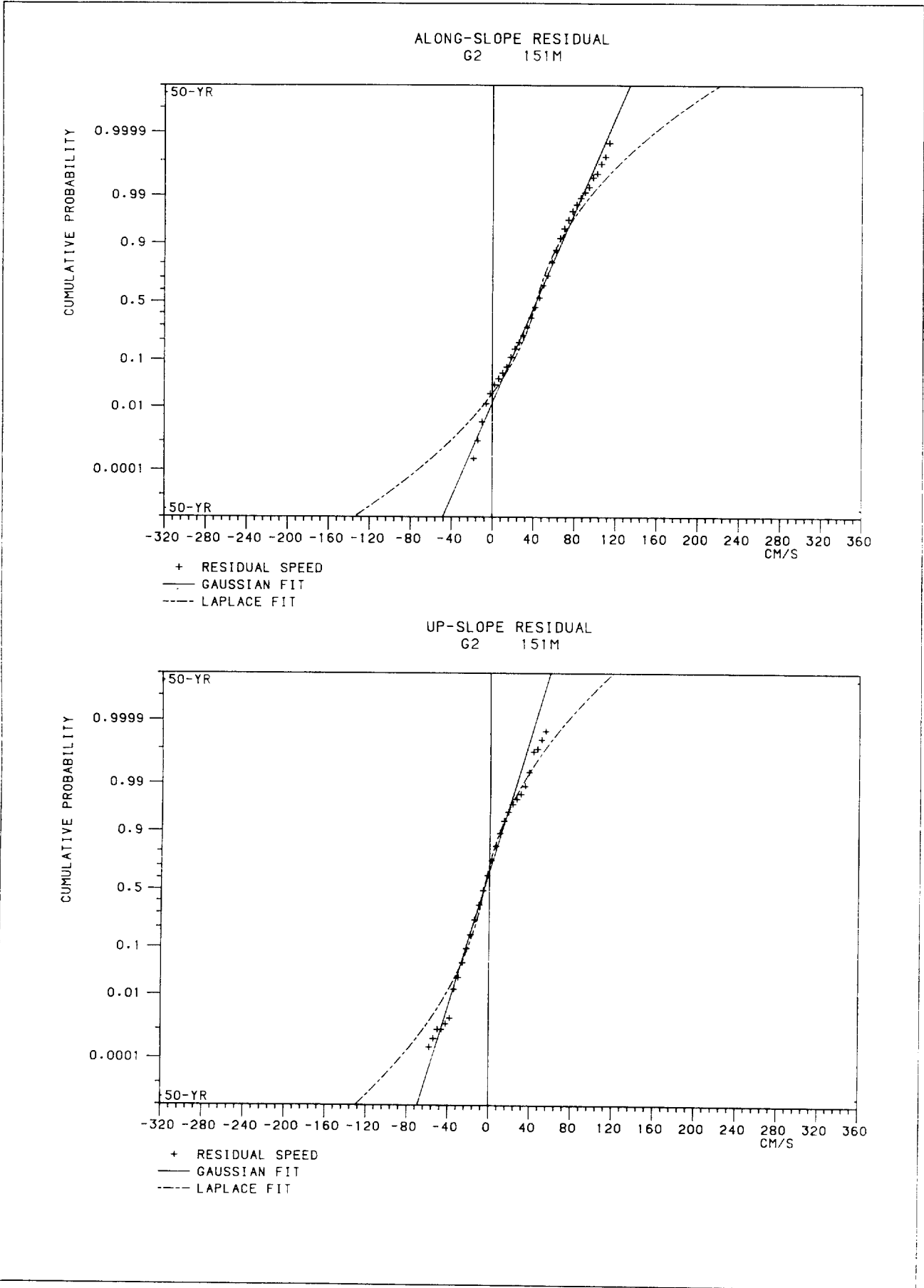


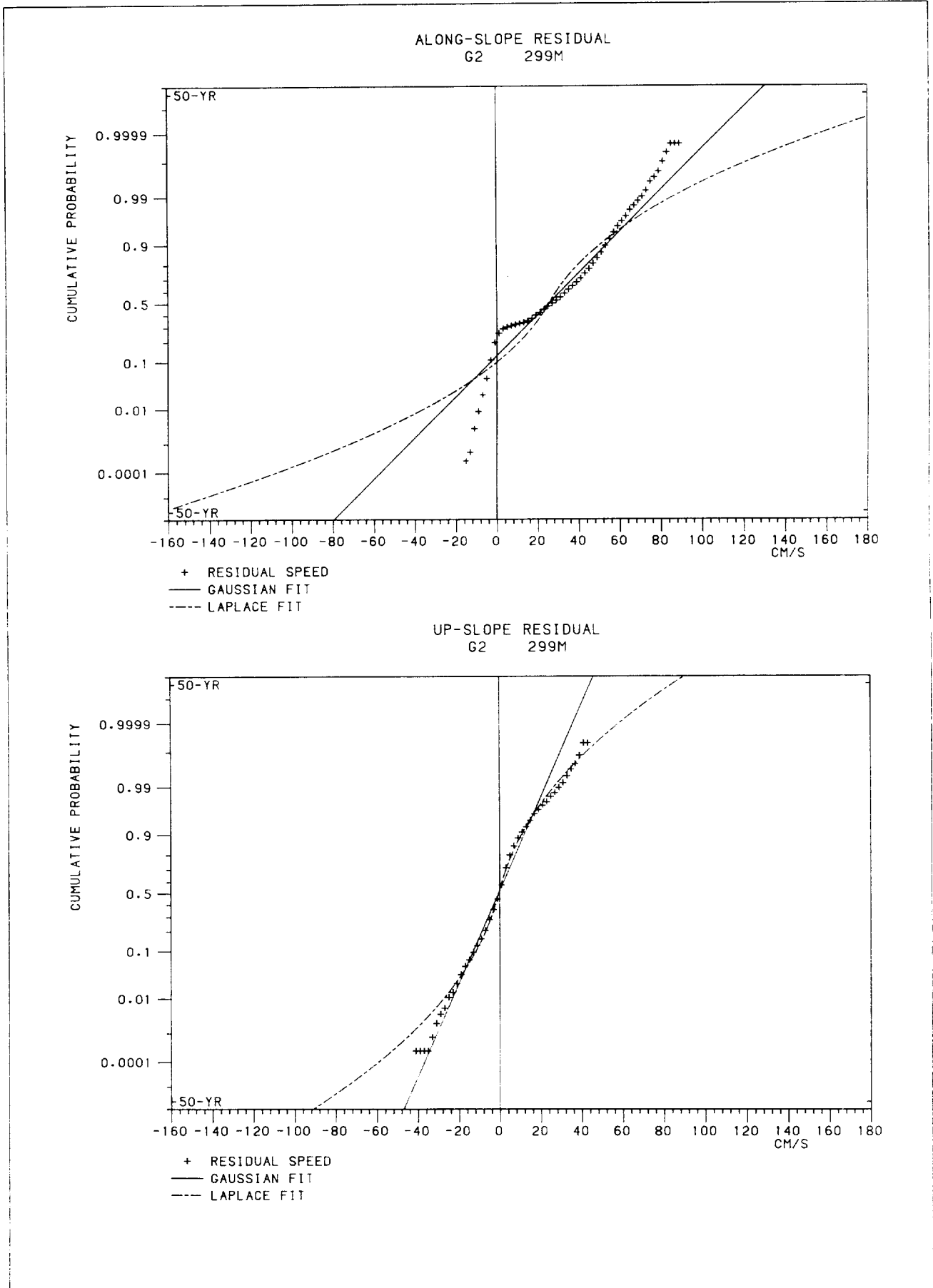
ALONG-SLOPE RESIDUAL
G1 166M

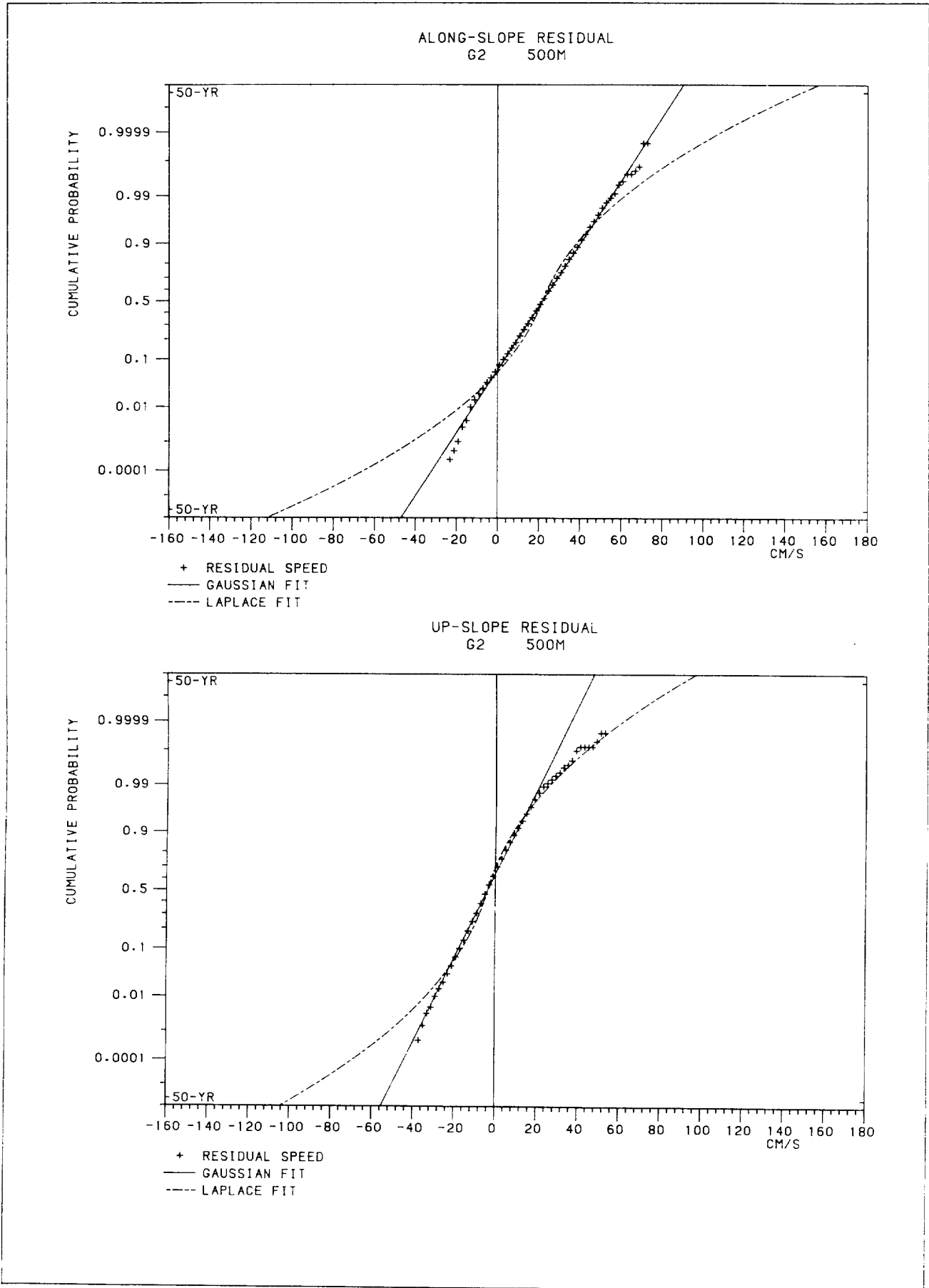


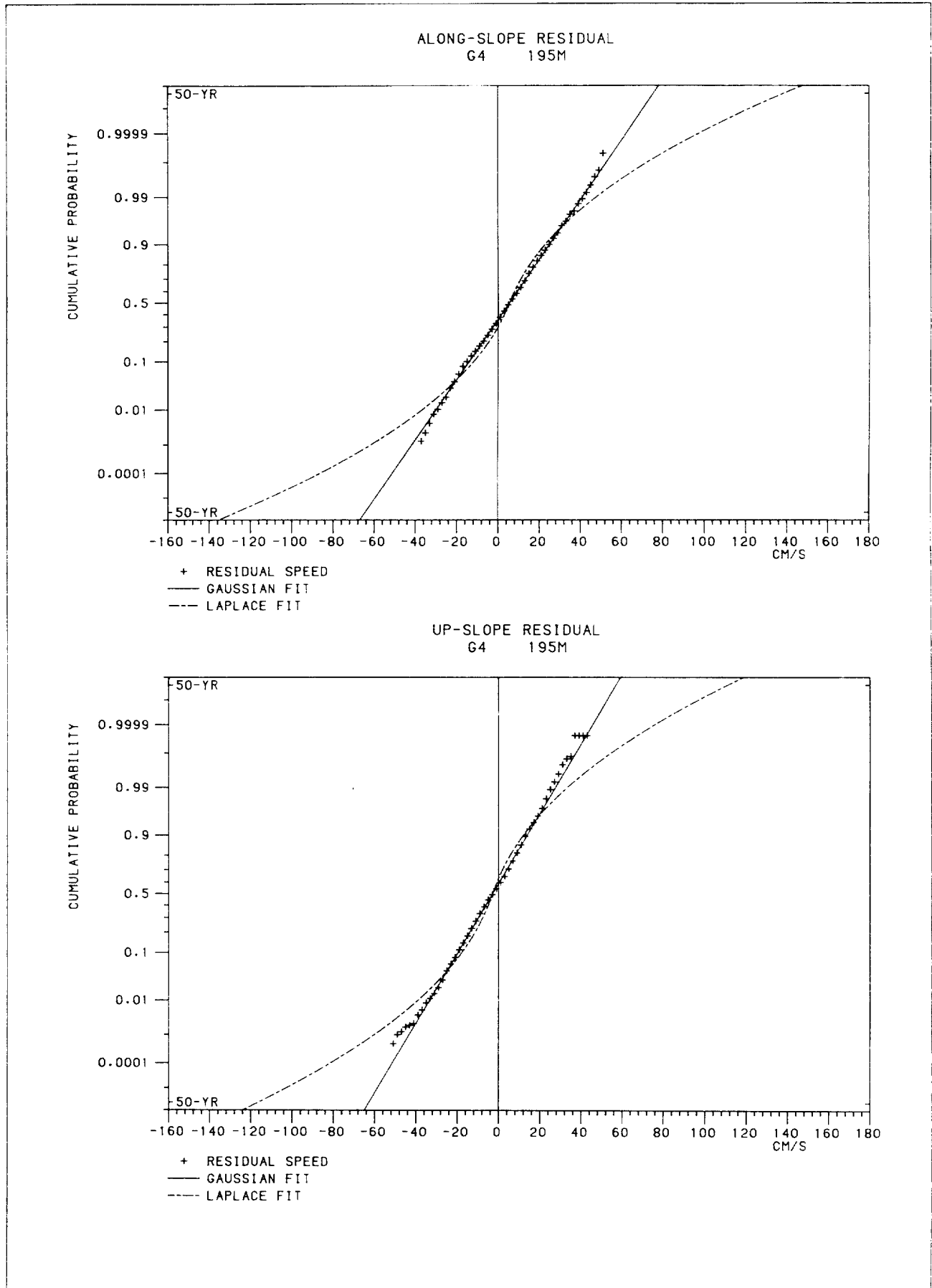
UP-SLOPE RESIDUAL
G1 166M



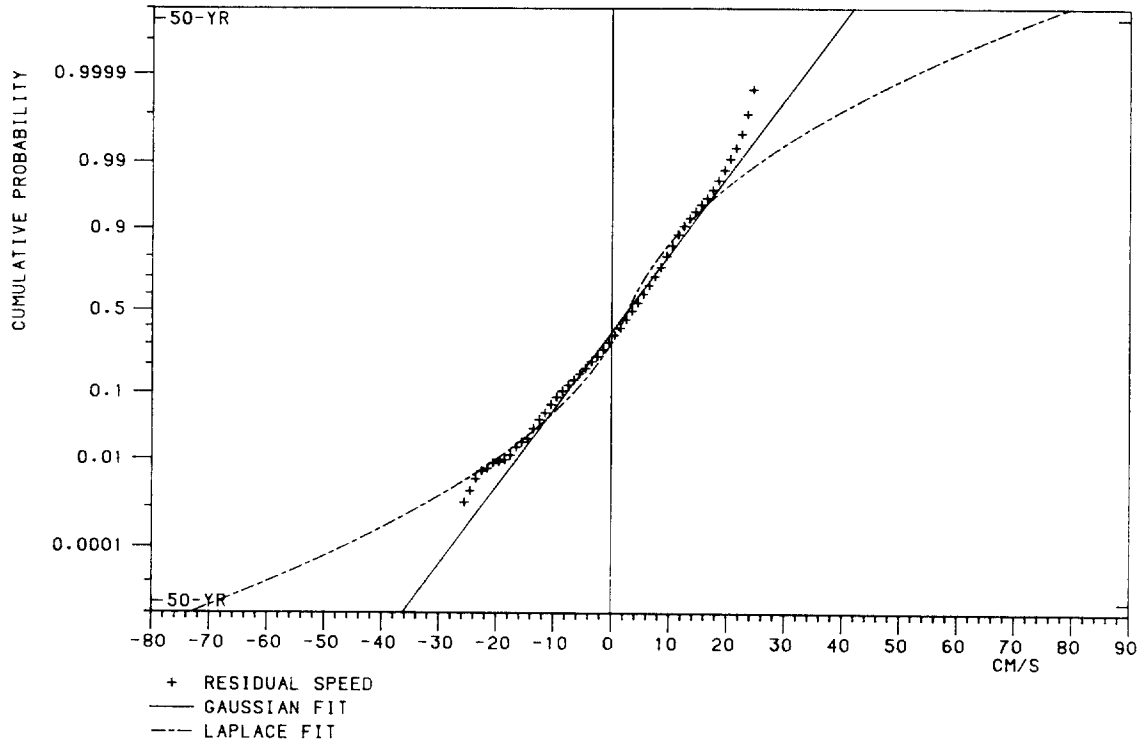




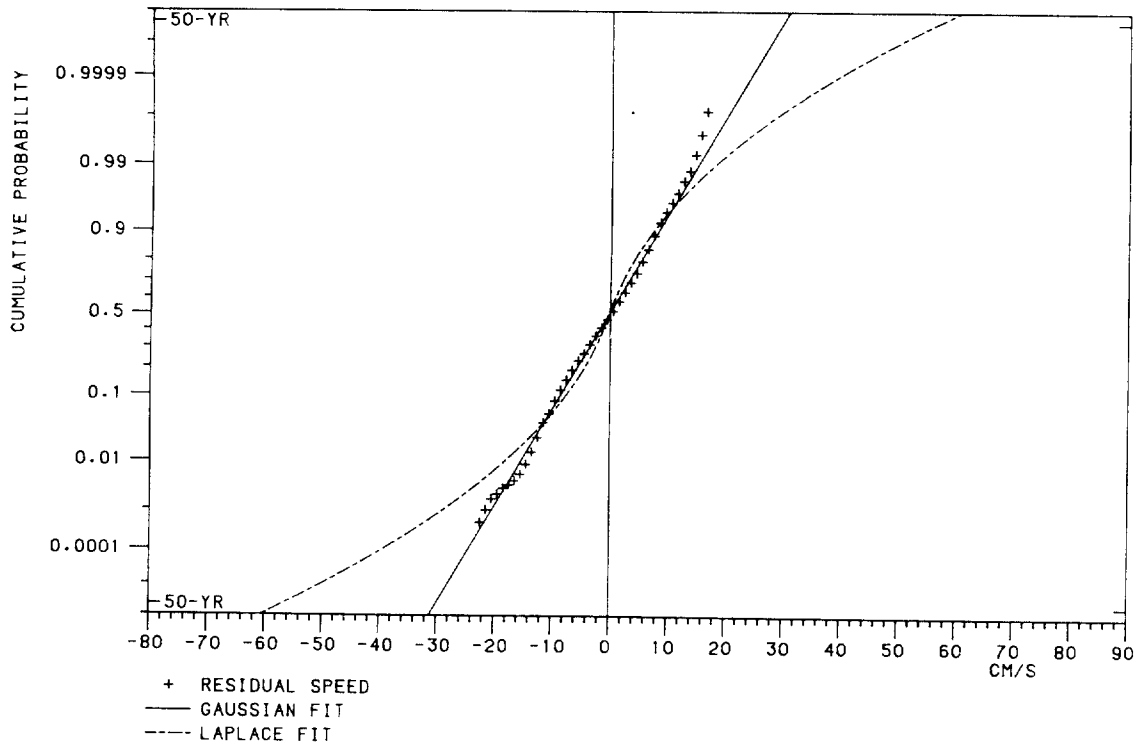




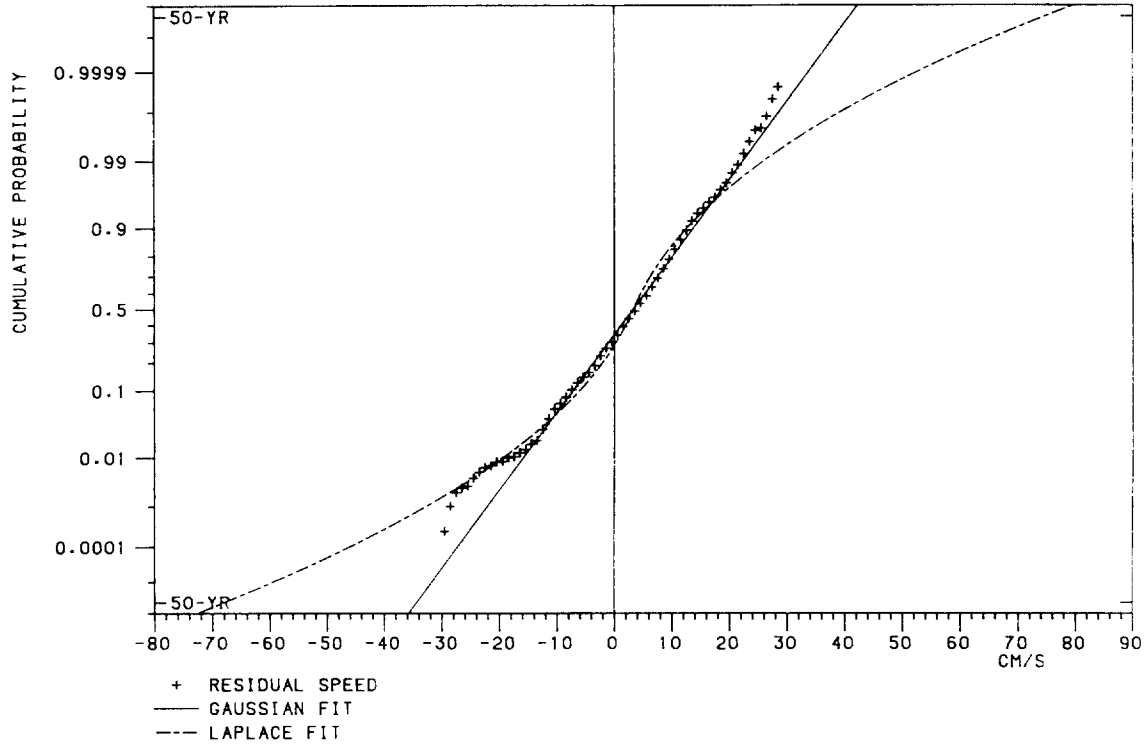
ALONG-SLOPE RESIDUAL
G4 1104M



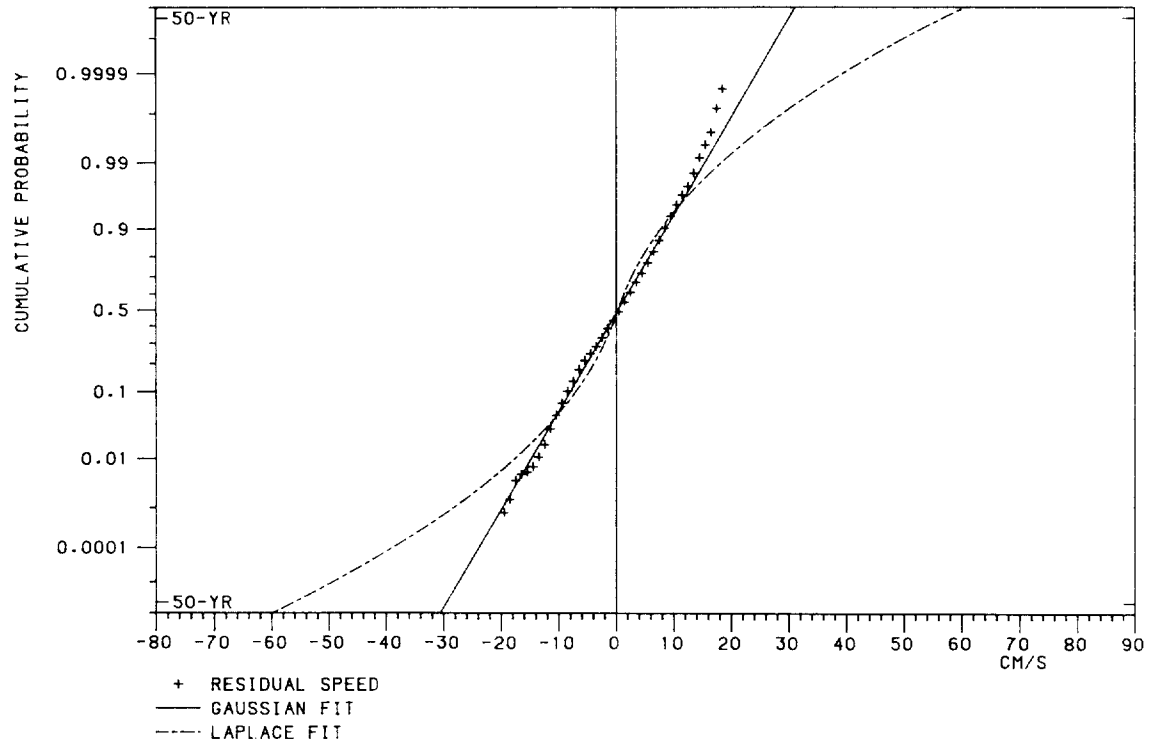
UP-SLOPE RESIDUAL
G4 1104M

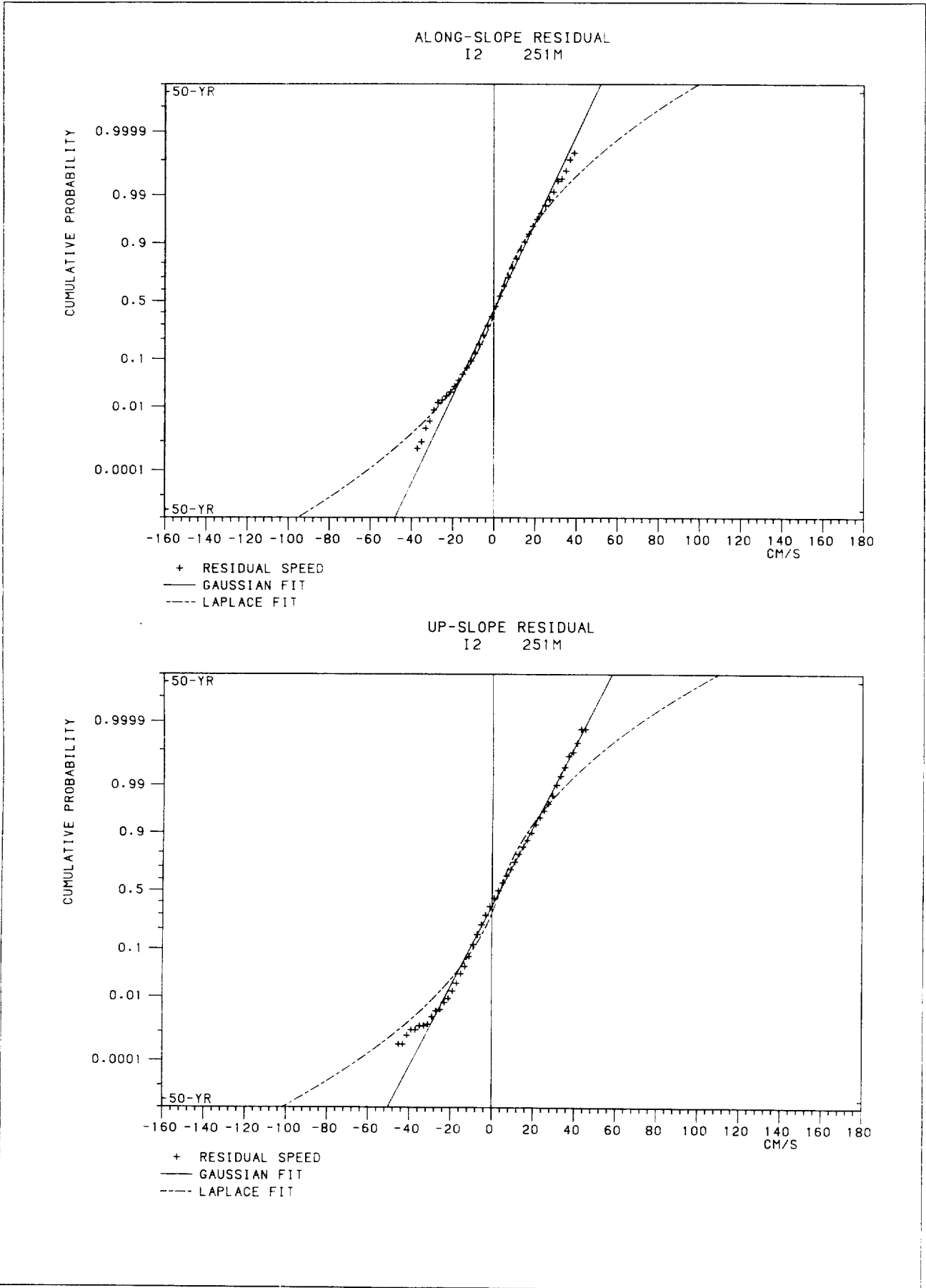


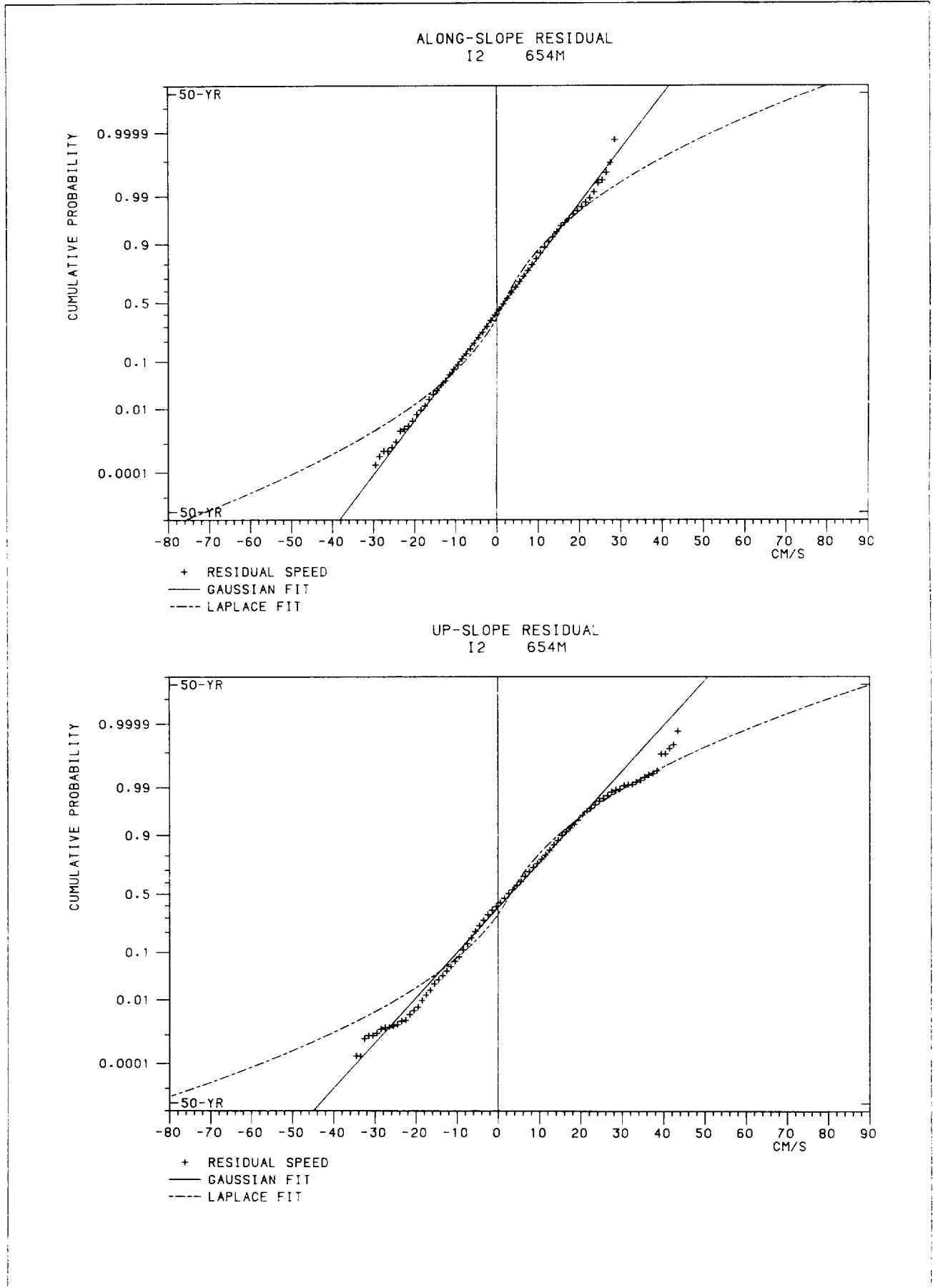
ALONG-SLOPE RESIDUAL
G4 1554M

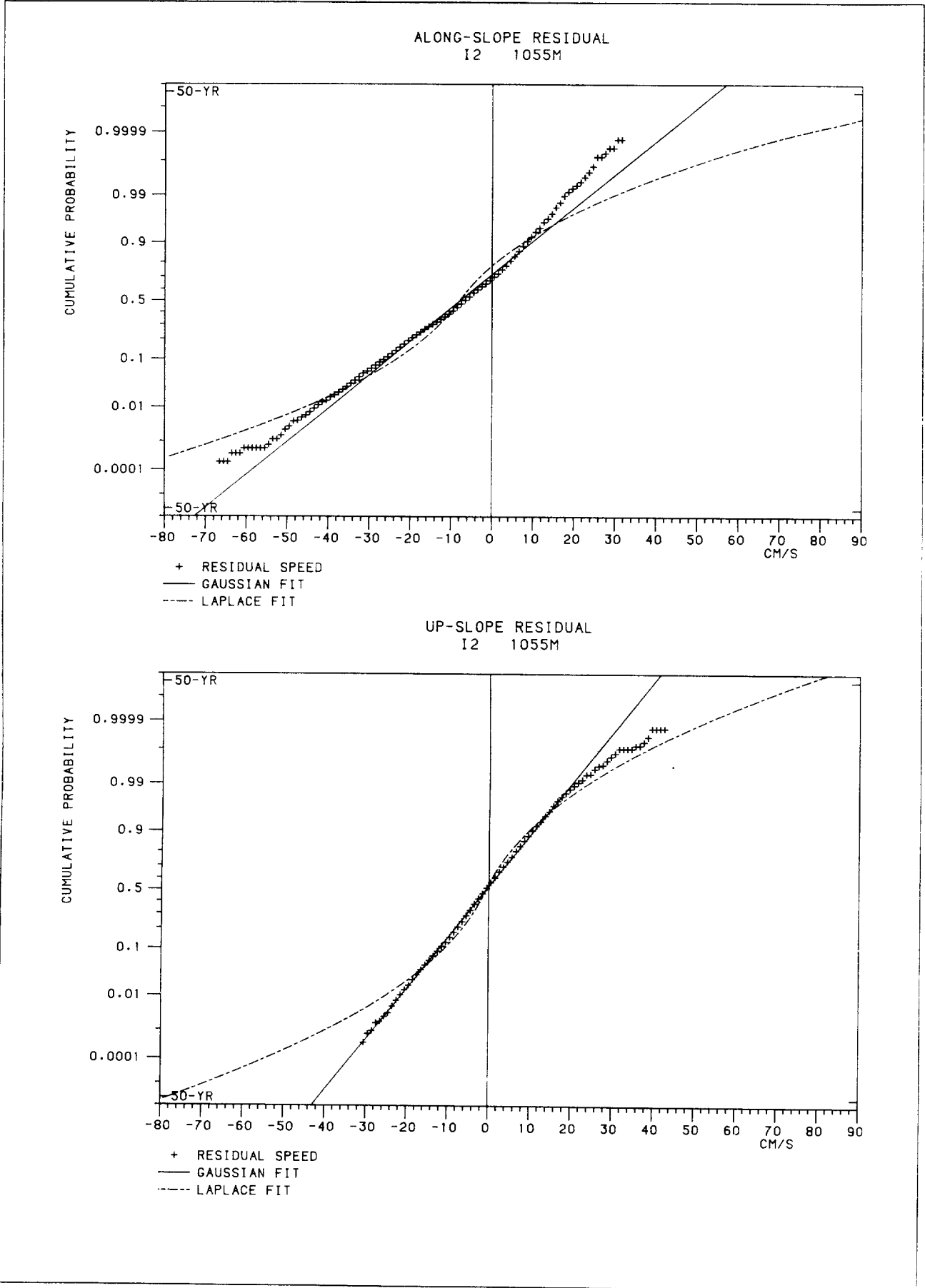


UP-SLOPE RESIDUAL
G4 1554M









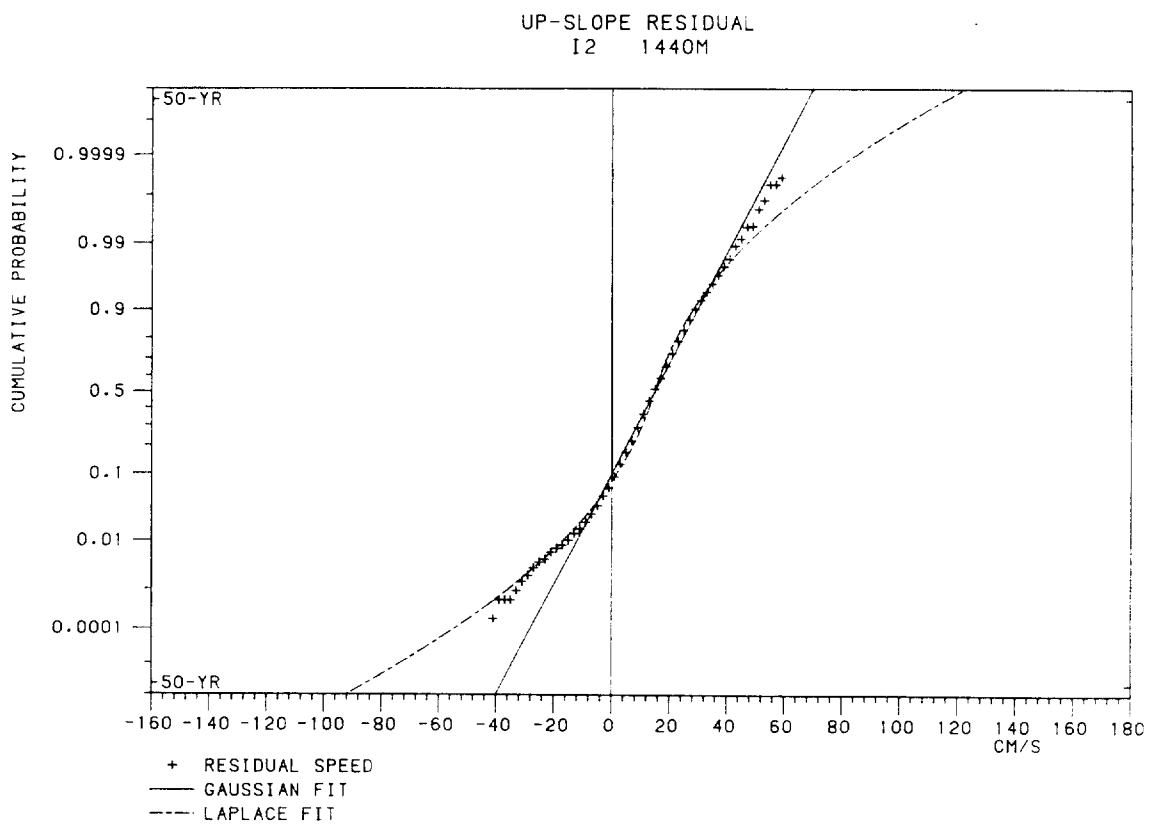
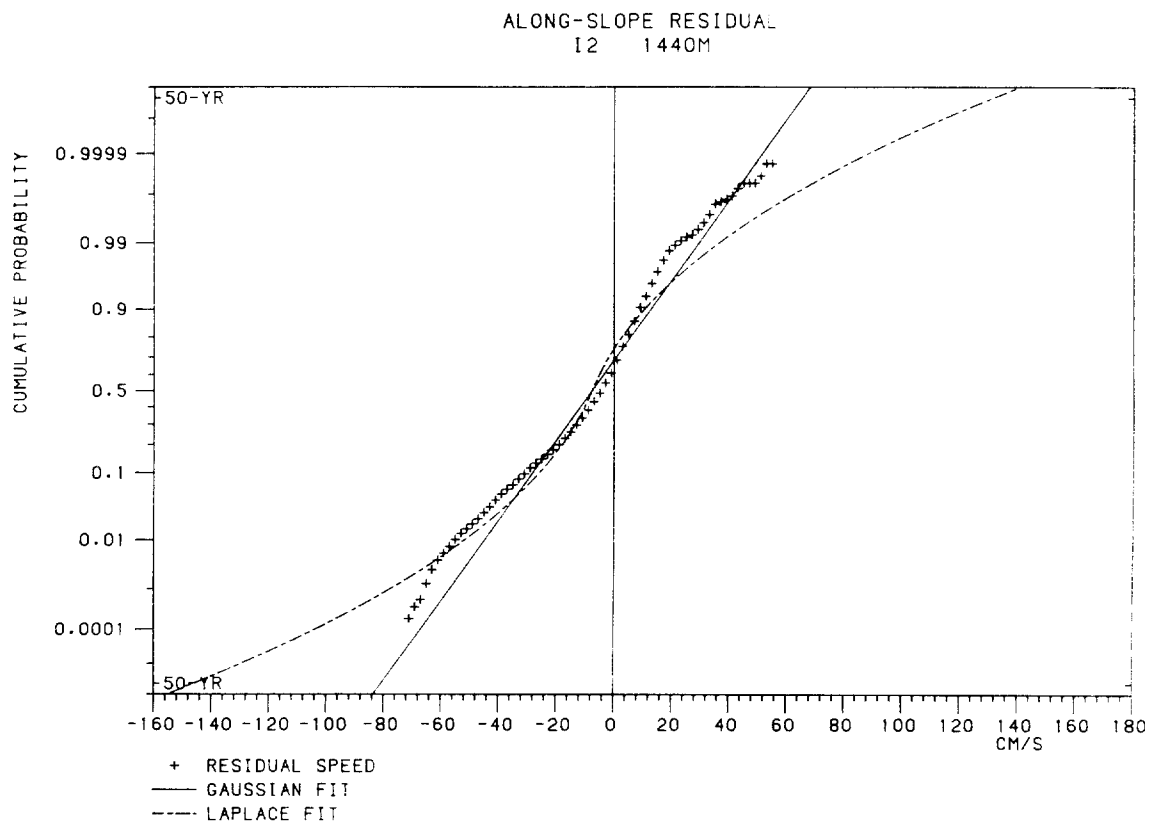
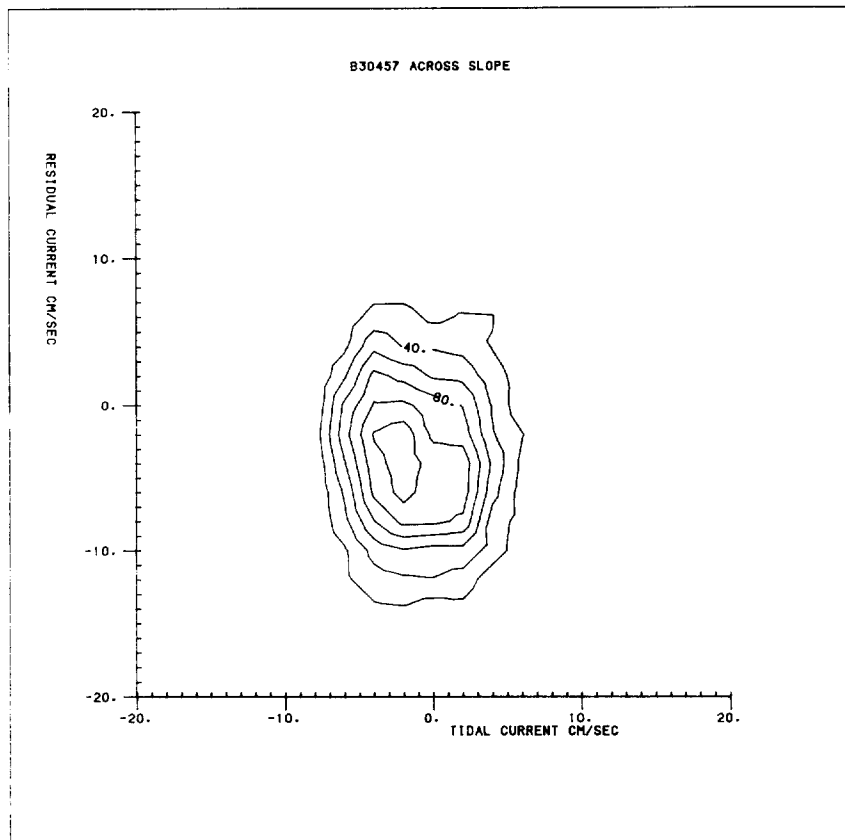
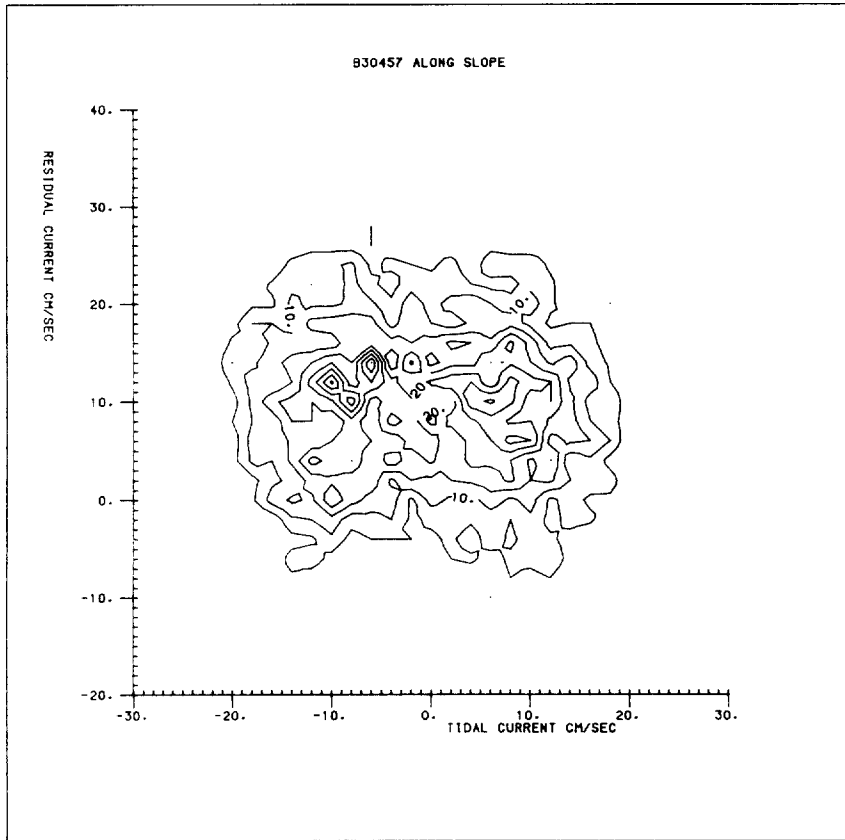
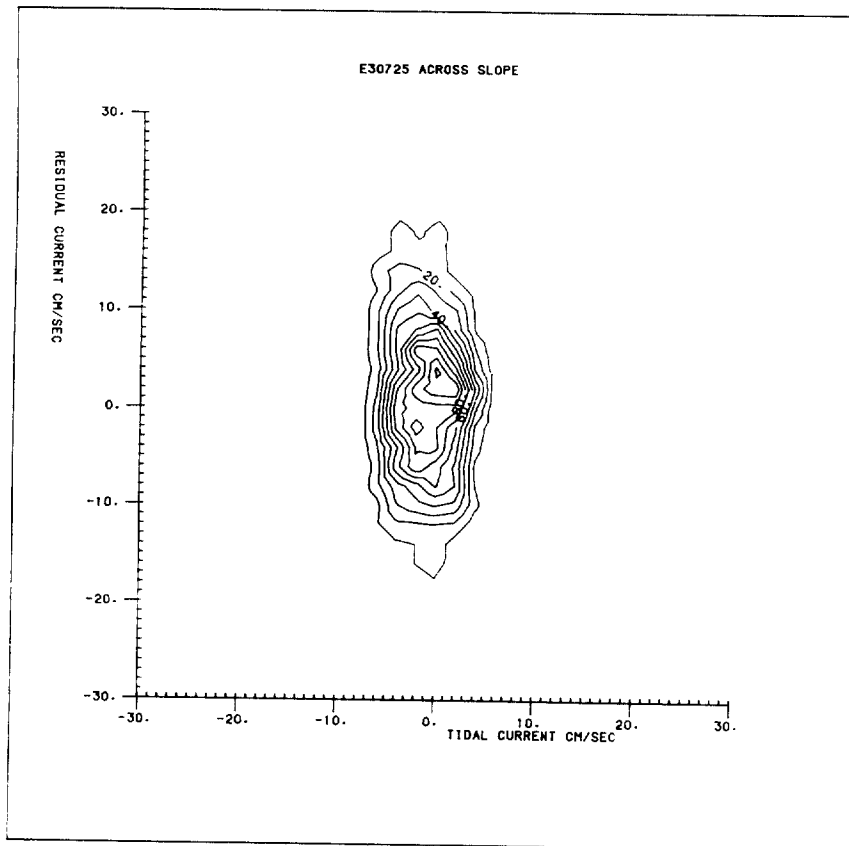
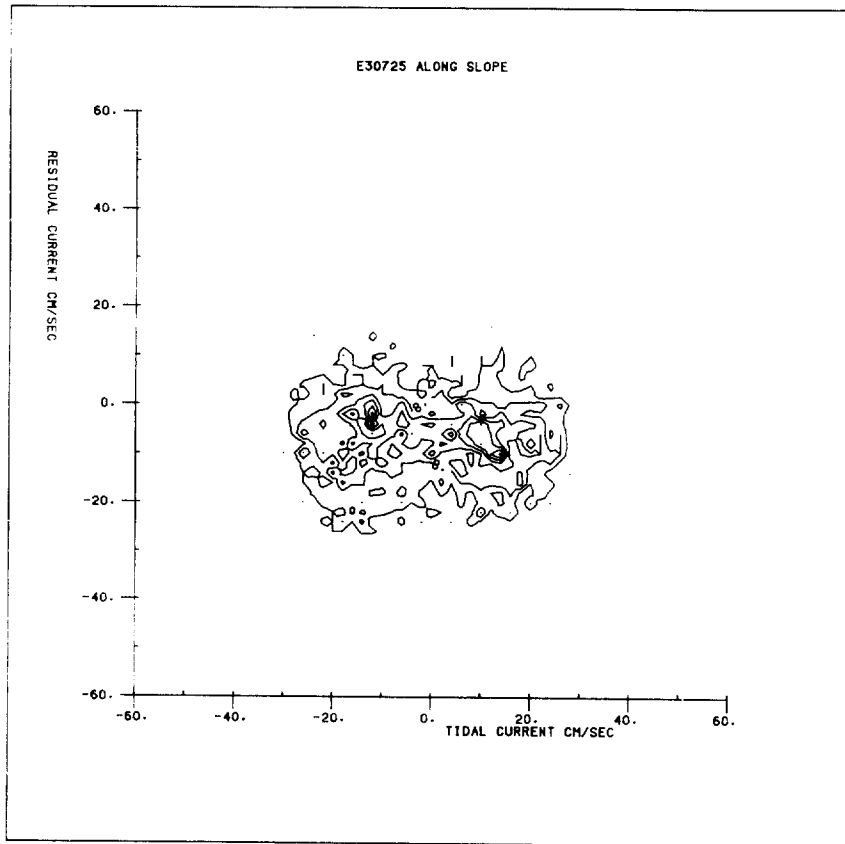
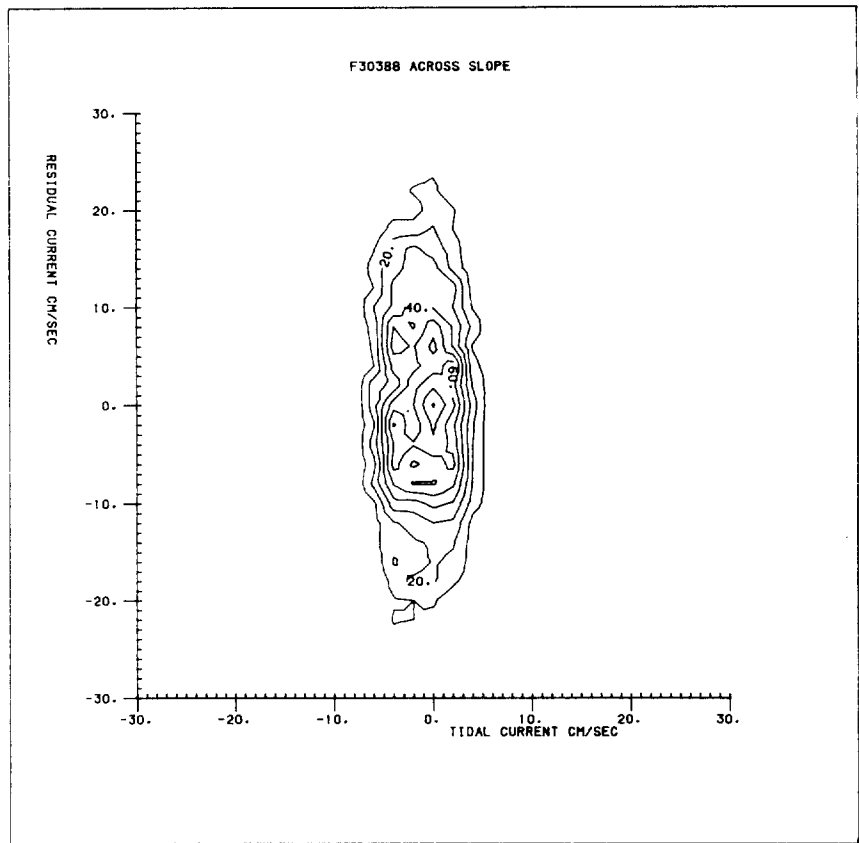
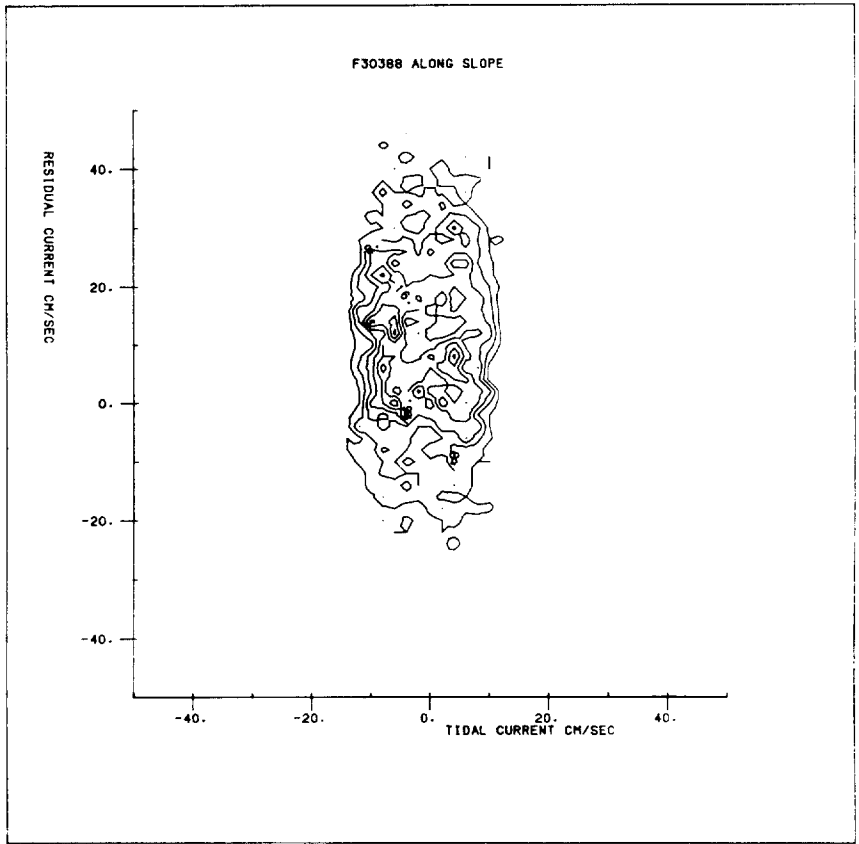


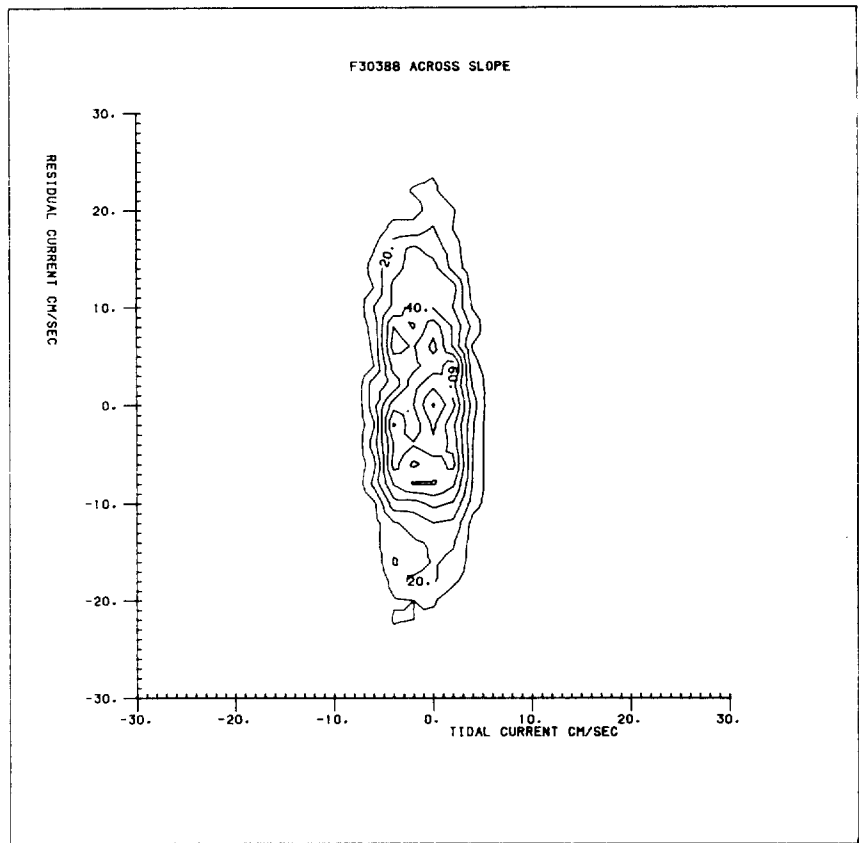
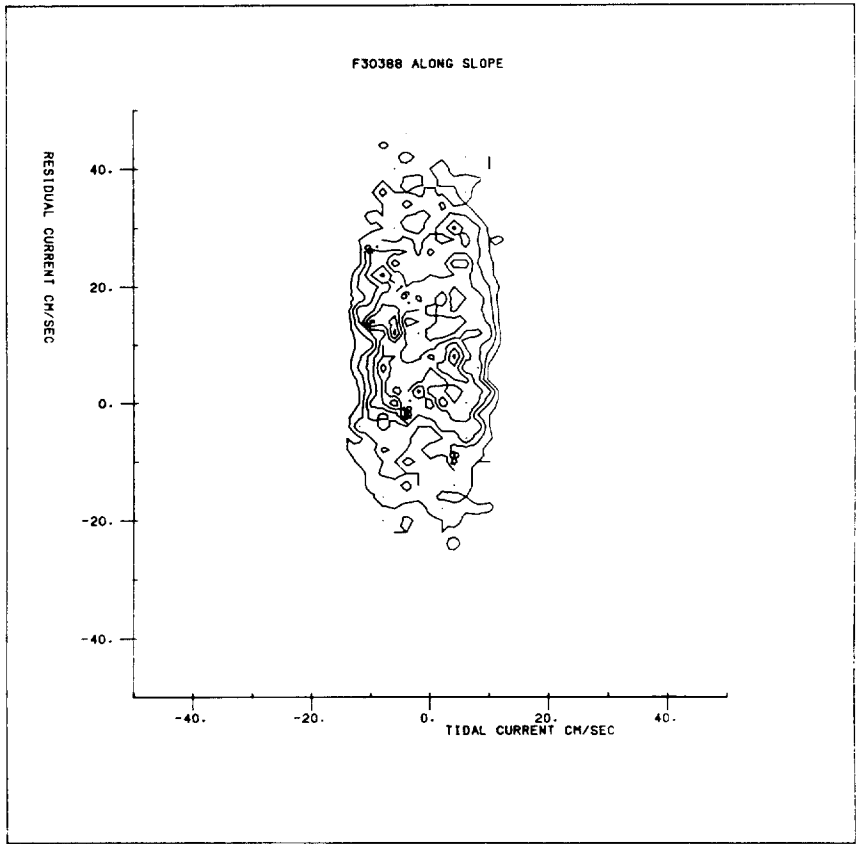
Fig.4: Examples of the joint probability distribution of tidal and residual currents.











I.O.S.

ESTIMATES OF EXTREME CURRENT SPEEDS
OVER THE CONTINENTAL SLOPE OFF SCOTLAND

BY
D.J.T. CARTER, J. LOYNES AND P.G. CHALLENGOR

REPORT NO. 239
1987

NATURAL ENVIRONMENT
INSTITUTE OF OCEANOGRAPHIC SCIENCES
RESEARCH COUNCIL

INSTITUTE OF OCEANOGRAPHIC SCIENCES

WORMLEY

Estimates of extreme current speeds
over the continental slope off Scotland

by

D.J.T. Carter, J. Loynes* and P.G. Challenor

I.O.S. Report No. 239

March 1987

The preparation of this report was supported financially by the Department of Energy.

* *Present address:*

*Cranfield Institute of Technology
School of Management
Cranfield
BEDS. MK43 0AL*

CONTENTS

	<u>Page</u>
SUMMARY	5
1. INTRODUCTION	7
2. METHOD OF ANALYSIS	9
2.1 Probability distribution of resolved speed	9
2.2 50-year return value of resolved speed	11
2.3 Probability distribution and extreme value of total speed	11
3. APPLICATION TO THE CONSLEX DATA	13
3.1 General description of the data sets	13
3.2 Maximum observed current speeds	14
3.3 Probability distributions of current speeds and estimates of return values	15
4. CONCLUSIONS	18
REFERENCES	20
TABLES	
1. CONSLEX mooring sites	21
2. CONSLEX current meter records	22
3. Estimates of 50-year current speeds	24
FIGURES	
1. CONSLEX mooring sites	27-29
2. Probability distribution functions of residual and tidal current speeds	31-83
3. Cumulative probability distributions of residual current speed	85-137
4. Joint probability distributions of tidal and residual currents	139-143

SUMMARY

A method for estimating return values of current speed from time-series data, based upon the convolution of tidal and non-tidal (residual) components, is described. It is applied to the CONSLEX data set of measurements obtained over the Continental Slope to the northwest of the UK during 1982-83, to obtain estimates of 50-year return values of hourly mean speed along-slope, cross-slope and omni-directional.

The method depends upon the speed of the tidal component being at least comparable with the residual component. This condition is found to hold at most CONSLEX sites west of 4°W but usually not at sites to the east of 4°W.

Histograms are presented showing the observed probability distributions of tidal and residual components of current speed and their convolutions along- and cross-slope for each CONSLEX current meter data set.

1. INTRODUCTION

As exploration for offshore oil and gas resources moves into deeper waters, so the need for estimates of extreme currents also extends into them. In particular, designers of offshore structures require estimates of extreme speeds over the continental slope to the West and North of Scotland in order to assess the feasibility and design of rigs there, where water depths are between 200m and 1000m.

Estimating extreme values of environmental parameters (such as the 50-year return value of wind speed or wave height) generally requires many years of measurements or the use of a well-validated model. Neither is available for estimating ocean currents on the UK continental slope. Fortunately, the forcing periods of the tides are well-established and extreme tidal speeds can be calculated from considerably shorter series of measurements.

If the tidal component is a significant portion of the extreme total current speed, then - as pointed out by Pugh and Vassie (1980) - estimates of extreme values can be made from relatively short data sets. This report develops a method for doing so, and applies it to estimate 50-year return values of hourly mean current speed from the Continental Slope Experiment (CONSLEX) measurements obtained between August 1982 and April 1983 from twenty moorings laid on the slope to the West and North of Scotland (Gould, 1982). The locations of these moorings are shown in Figure 1. Their co-ordinates are given, along with the water depth at each mooring, in Table 1.

Estimating extremes from records covering only about seven months is clearly unsatisfactory, particularly as we have only a limited understanding of the physics of some components of the total current. However, the tidal constituents are obtainable, with good accuracy, from the CONSLEX data; so, where the tidal stream contributes a significant portion of the total current, we might expect a reasonable estimate for the extreme speed - although it is not possible to put confidence limits upon the value - but at some current meters the tide turns out to be relatively small and here the estimates are questionable.

2. METHOD OF ANALYSIS

2.1 Probability distribution of resolved speed

Given a data series of current speed resolved in a specified direction, such as the easterly component of mean values at hourly intervals, and assuming the series is sufficiently long to estimate the tidal component, then the total speed in the specified direction at any hour, U , can be expressed as a tidal component, U_t , and a residual U_r :

$$U = U_t + U_r$$

and histograms can be constructed showing estimates for the probability distributions of U_t and U_r , p_t and p_r .

Assuming the tidal and residual components are independent, then the probability distribution of U , p_{t+r} , is given by a convolution of p_t and p_r , defined by

$$p_{t+r} = \int_{-\infty}^{\infty} p_t(x-z) p_r(z) dz \quad (1)$$

(Feller, 1971, p.144)

It readily follows that the Fourier transform of p_{t+r} equals the product of the transforms of p_t and p_r , that is:

$$p_{t+r}^* = p_t^* \cdot p_r^* \quad (2)$$

where $*$ denotes Fourier transform. Equation 2 provides an efficient method for calculating p_{t+r}^* from p_t and p_r , and hence, by an inverse Fourier transform, for calculating p_{t+r} .

An estimate for p_{t+r} might be obtained by constructing the histogram from observations of U . The reason for using the convolution to estimate p_{t+r} is that by assuming independence of tide and residual we can essentially recombine the N observations, assuming random sampling, to give N^2 values from which to estimate p_{t+r} . Hence we obtain a smoother distribution with generally better-defined tails. However, if the tidal component U_t is much less than U_r , so that p_t is a relatively narrow distribution, then the tail of the compounded distribution p_{t+r} is dominated by p_r - or in our case by the histogram approximation for p_r . In this case, a better estimate for the tail of p_{t+r} might be obtained by fitting a distribution to the histogram for p_r and convolving this distribution with p_t . But estimates of extreme currents from the tail will then depend upon the choice of distribution. There is no theoretical or physical justification for using any particular distribution. In practice with the CONSLEX data we found that the Gaussian distribution often appeared a reasonable fit to the residual histogram p_r , but at some sites the histogram tails extended beyond the Gaussian distributions, and were closer to a Laplace distribution although this was not a good fit to the entire histogram (The Laplace distribution consists of two negative exponential distributions 'back-to-back' so is sharply peaked at the mean).

The method of moments was used to fit these distributions. The hourly residual speeds are correlated so there is no simple goodness-of-fit test apart from a visual estimate, and even here with so many data sets being analysed a few poor fits are likely to appear.

2.2 50-year return value of resolved speed

Defining the 50-year return value of hourly mean speed, U_{50} , as that which is exceeded on average once in 50 years, then it is given by

$$\text{Prob}(U_{50} < U) = 1 - 1/(365.25 \times 24 \times 50)$$

ie.

$$\text{Prob}(U_{50} < U) \approx 0.99999772 \quad (3)$$

Hence U_{50} may be calculated given the distribution p_{t+r} - or rather two values, one from each tail of p_{t+r} , giving the 50-year speed in opposite directions.

With the definition for U_{50} , in terms of only the average interval between exceedances, its value is not affected by any correlation between the data. However, given positive correlation between successive hourly mean values, exceedances of U_{50} will tend to come together, while maintaining the average interval between exceedances of 50 years. So if the 50-year return value is defined as that which is exceeded at least once during one year in 50, then it would have a slightly lower value than that given by (3). However, Pugh and Vassie (1980) examined the effect of correlation upon estimates of return values of surface elevation and decided that any such reduction would in practice be insignificant.

2.3 Probability distribution and extreme value of total speed

Suppose U and V are current speeds resolved orthogonally so that total speed W is given by

$$W = \sqrt{U^2 + V^2}$$

Then, the distributions of U and V can be estimated from data as described above. In theory the distributions of U^2 and V^2 can then be estimated and convolved to give the distribution of W^2 and hence of W (assuming U^2 and V^2 are independent). However, the sizes of the arrays to accommodate the histograms for the distributions of U^2 and V^2 are too large for practical FFT procedures. So we estimate the distribution of W using the numerical approximation for

$$\text{Prob}(W < w) = \iint \sqrt{U^2 + V^2} p(U, V) dU dV$$

where integration is over all U, V such that $0 < \sqrt{U^2 + V^2} < w$ and $p(U, V)$ is the joint probability distribution of U and V .

i.e.
$$\text{Prob}(W < w) \approx \sum_{i,j} w_{ij} p(U_i, V_j) \delta U \delta V \quad (4)$$

where δU and δV are the bin sizes of the histogram representation of the distributions of U and V and summation is over all bins (i, j) such that $w_{ij} < w$ where w_{ij} is the speed at the mid-point of the (i, j) bin. Assuming U and V are independent, then

$$p(U_i, V_j) \delta U \delta V = \text{Prob}(U_i < U < U_{i+1}) \text{Prob}(V_j < V < V_{j+1}) \quad (5)$$

The 50-year return value of W , W_{50} , is given by

$$\text{Prob}(W_{50} < w) \approx 0.99999772 \quad (6)$$

An alternative method for obtaining the distribution of W was considered: histograms for the distributions of the tidal and residual components of W , W_t and W_r , could be obtained, where

$$W = W_t + W_r$$

and these histograms convolved to obtain the distribution of W . But this method fails because W_t and W_r are not independent - since W cannot be negative.

3. APPLICATION TO THE CONSLEX DATA

3.1 General description of the data sets

The method of analysis described above was applied to the CONSLEX data set of hourly mean current speeds associated with 'spot' measurements of direction. The data were obtained from the IOS Marine Information and Advisory Service data base, including the results of tidal analysis carried out at IOS (Bidston).

The CONSLEX data consists of 53 sets of recordings made by DAFS, IOS and SMBA from 20 moorings, using Anderaa current meters deployed between 23 August 1982 and 31 April 1983 - measurements at one site (I2) extended into May 1983. The sites of these moorings and the notation identifying them are shown in Fig. 1 together with the approximate orientation, θ , of the maximum variance of current velocity.

This orientation was calculated for each meter by a principal component analysis of the current velocity. In general it was found to lie along the slope; the flow seems to be constrained by topography. The direction of the line of maximum variance is not specified by this analysis. The direction arrows shown in Fig. 1 were specified in order to fix the co-ordinate system. The variation in θ between meters at any one mooring was generally within $\pm 10^\circ$, and an average direction is shown in Fig. 1. Where the spread was greater than $\pm 10^\circ$, the range of θ is shown. The 'cross-slope' axis was taken as positive to the right of the along-slope, ie. up-slope. The data were analysed in a co-ordinate system defined by

the value of θ for the individual meter - thus ensuring zero correlation between resolved current speeds - but directions are referred to as 'along-slope' and 'up-slope'. Further details, including the depth of each instrument and the values of θ , are given in Table 2.

Site I2 is not on the slope, but in the Rockall Trough with a water depth of 1463m. Section D is on the Wyville-Thomson Ridge; currents at D5 in particular appear unlike those on the slope, as indicated by the wide range of θ with depth - similar to that at I2.

Records from the current meter at G4 at 496m cover only 34 days, and at B1 (130m) only 58 days. The other meter at B1 and both meters at B2 had to be replaced during October 1982 - with the loss of some days of records at B2.

3.2 Maximum observed current speeds

The maximum mean hourly current speed recorded by each instrument and associated direction are included in Table 2.

The maximum recorded hourly mean current speed was 117 cm/s at E4 at a depth of 111m. The only other measurement exceeding 100 cm/s was at G2 at 151m. Generally the maximum speeds at each mooring tended to decrease with increasing meter depth; an exception was at E3 where 100 cm/s was recorded at 725m. The direction of the maximum speed was usually within about 20° of the direction given by the principal component analysis; a notable exception was that of 66 cm/s at E4 at 950m which was 79° away (down-slope).

3.3 Probability distributions of current speeds and estimates of return values

Using the data from each meter, except B1 (130m) and G4 (496m) with less than two months data, histograms showing the distribution of tidal and residual current speeds along-slope and up-slope were constructed with a bin size of 1 cm/s, or 2 cm/s if a component speed exceeded 100 cm/s. These histograms, together with their convolution are shown in the set of figures: Fig. 2. (Strictly, the histograms should be drawn as step functions, but joining mid-points of the bin values gives a clearer picture.)

Fig. 2 shows that the along-slope flow is generally considerably stronger than the up-slope. It also shows that the residual current is usually stronger than the tidal component - but not, for example, at A1 (145m) and at D1 and D2. Sometimes the residual is very much stronger than the tidal component particularly for the up-slope flow, and the convolution is then a smoothed version of the residual histogram, so the tails of the convolution are dominated by the few calculated extreme residual values, eg. F3 at 388m. In these cases it seems preferable to fit a distribution to the residual histogram and to convolve this distribution with the tidal histogram. The set of figures, Fig. 3, show the Gaussian and Laplacian fits to the cumulative distribution of residual components - scaled such that the Gaussian distribution is linear. Generally the Gaussian distribution appears to be a reasonable fit to the residuals; occasionally the observations in the tails deviate from the straight line, but these are determined by only a few values so their sampling variance is high. Construction of confidence limits would require an analysis of the

correlation structure of the data; but where the data approaches the long-tailed Laplace distribution the use of the Gaussian distribution must be expected to underestimate extreme values.

The fifty-year return values of current speed up- and down-slope and in both directions along-slope were estimated using equation 3 and the convolutions with the residual histograms and the Gaussian fit. Results are shown in Table 3.

Values are given to the nearest bin size, that is ± 2 cm/s for the higher values and ± 1 cm/s for the lower.

Note that the fifty-year return values are given by interpolation of the convolution. No extrapolation is required.

The convolution only gives the distribution of the sum of the tidal and residual components if these components are independent. There is no entirely satisfactory method for testing independence, but examples of the joint distributions of the tide and residual components plotted in the set: Fig. 4 show no obvious dependence. On physical grounds, one might expect negative correlation between tide and residual in shallow water or at current meters close to the sea bed, but none is apparent in Fig. 4, or in other joint distributions which we examined. If there were negative correlation then the convolution would overestimate the fifty-year return values.

Table 3 also includes fifty-year return values of total speed, U_{50} , calculated from equations (4)-(6), and the maximum observed speeds from

Table 2. The choice of θ from the principal component analysis ensures no correlation between the measured 'up-slope' and 'along-slope' speeds. The requirement of (5) is stronger, requiring independence between the two distributions, but this seems a not-unreasonable assumption.

The values for U_{50} from the residual histogram are given in brackets if Fig. 2 suggests that the dominant tail of the component convolution has a negligible tidal contribution. The value of U_{50} from the Gaussian fit is in brackets if Fig. 3 indicates that the dominant residual component is not Gaussian.

4. CONCLUSIONS

An inspection of the bracketed (more dubious) estimates in Table 3 for the 50-year return value of hourly mean current speed, U_{50} , indicates that the method proposed in this report might be expected to give reasonable results at CONSLEX sites A to E, but further North at F and G (except at F1 and G1 in less than 200m) the method is less satisfactory; the tidal components are here considerably weaker than the residual currents and often these residuals do not appear to be normally distributed.

The highest estimate for U_{50} from the analysis of the CONSLEX data is 133 cm/s for mooring E4 at 111m, with a water depth of 1015m. This was where the highest recorded current speed of 117 cm/s was obtained. Fig. 3 (E4, 111m) shows apparently anomolous residuals along-slope, towards the North East approaching 100 cm/s, which convolve with the along-slope tidal stream exceeding 30 cm/s. The origin of these anomolous residuals, perhaps associated with the oceanic front separating deep and coastal waters, requires further investigation.

Nearby at E3 at 725m, the estimated value of U_{50} is 94 cm/s while the maximum recorded current speed was 100 cm/s; the greatest recorded residual happened to occur within a few hours of the maximum recorded tide.

At the deep water site of I2, which is off the slope in a depth of 1463m, the method does not give satisfactory estimates of U_{50} at the two current meters below 1000m because the tidal components are small compared to the residuals. The method appears to be reasonable at shallower depths.

However, because of our lack of knowledge of all the mechanisms producing extreme currents at sites off the continental shelf including their within-year variability, estimates of the 50-year return value of current speed made from data recorded over only a few months must be viewed with caution. Even where the method suggested in this report appears to be satisfactory, further data are needed to confirm its applicability and to put confidence limits upon the results.

REFERENCES

- Feller, W. 1971. An introduction to probability theory and its applications. Vol. 2 (2nd edition) J. Wiley and Sons.
- Gould, W.J. 1982. Currents on the continental slope. MIAS News Bulletin 5, 3-5.
- Pugh, D.T. 1982. Estimating extreme currents by combining tidal and surge probabilities. Ocean Engng. 9, 361-372.
- Pugh, D.T. and Vassie, J.M. 1980. Applications of the joint probability method for extreme sea level computations. Proc. Instn. Civ. Engrs. Part 2, 69, 959-975.

Table 1: CONSLEX mooring sites

Mooring	Latitude (N)	Longitude	Water depth (m)
A1	57° 20.7'	9° 07.2'W	145
A5	57° 18.6'	9° 40.4'W	1614
B1	57° 56.3'	8° 51.0'W	155
B2	58° 00.7'	9° 07.7'W	193
B3	58° 06.5'	9° 33.1'W	504
B4	58° 08.3'	9° 41.2'W	1082
C2	59° 05.4'	7° 27.0'W	514
C3	59° 08.5'	7° 42.4'W	998
D1	59° 39.8'	6° 02.5'W	237
D2	59° 46.7'	6° 10.8'W	370
D5	60° 09.9'	7° 44.5'W	637
E2	60° 13.3'	4° 31.8'W	478
E3	60° 31.2'	4° 56.8'W	1035
E4	60° 46.4'	4° 49.4'W	1015
F1	61° 09.3'	1° 31.7'W	189
F3	61° 24.8'	2° 06.1'W	995
G1	61° 30.7'	0° 02.5'E	191
G2	62° 06.1'	0° 03.9'E	550
G4	63° 08.8'	0° 00.9'W	1611
I2	60° 12.7'	9° 13.3'W	1463

Table 2: CONSLEX current meter records

Mooring	meter depth (m)	days of records	max. recorded speed (cm/s)	hr mean vely. dir ⁿ towards (° from N)	dir ⁿ princ. component (θ°)
A1	55	106	59	031	046
	120	181	44	307	042
A5	209	179	57	347	333
	510	179	45	340	333
	1111	179	49	186	343
	1562	179	33	339	341
B1	55	173	70	033	032
	130	58	61	194	031
B2	43	120	53	023	036
	168	120	47	033	033
B3	104	172	63	035	025
	257	172	54	028	025
	457	169	50	043	036
B4	169	172	53	023	017
	477	172	50	014	019
	1035	172	38	184	013
C2	115	172	82	043	051
	266	172	77	050	048
	468	172	76	037	035
C3	104	172	58	199	041
	403	172	52	049	046
	951	172	46	027	008
D1	87	136	80	054	049
	212	136	82	227	050
D2	120	169	86	078	061
	270	169	79	074	065
	345	169	69	057	066
D5	510	186	88	208	051
	633	186	85	194	007

Table 2 continued

Mooring	meter depth (m)	days of records	max. recorded hr speed (cm/s)	hr mean vely. dir ⁿ towards (° from N)	dir ⁿ princ. component (θ°)
E2	453	162	77	033	047
E3	120	164	95	92	063
	419	164	83	027	052
	725	164	100	212	055
E4	111	184	117	063	053
	950	181	66	158	057
F1	39	163	88	076	081
F3	79	80	89	084	063
	388	161	66	046	035
	694	161	60	244	049
	945	161	66	030	044
G1	41	117	48	133	108
	166	117	33	117	107
G2	151	162	114	073	073
	299	162	89	069	062
	500	162	84	106	079
G4	195	164	64	98	053
	496	34	26	021	028
	1104	164	32	212	051
	1554	164	34	206	044
I2	251	216	60	331	022
	654	222	45	106	038
	1055	216	67	182	020
	1440	222	75	144	343

Table 3: Estimates of 50-year current speeds (cm/s)

Mooring	meter depth (m)	Residual Histogram				TOTAL SPEED	Gaussian fit				TOTAL SPEED	MAX. OBS. SPEED
		Along-slope +	up-slope -	up-slope +	up-slope -		Along-slope +	up-slope -	up-slope +	up-slope -		
A1	55	65	66	51	58	69	62	60	53	54	66	59
	120	52	50	44	47	55	49	51	45	46	54	44
A5	209	58	43	47	29	(63)	75	55	42	36	75	57
	510	47	32	36	23	(50)	63	46	34	29	63	45
	1111	46	50	29	27	50	52	46	28	28	(52)	49
	1562	39	33	27	29	(40)	42	37	27	29	42	33
B1	55	95	75	54	47	96	99	83	45	43	101	70
B2	43	79	69	56	45	81	81	79	55	51	83	53
	168	63	54	34	27	63	60	52	29	30	60	47
B3	104	73	41	32	37	74	77	48	33	36	77	63
	257	59	33	21	28	59	64	38	25	29	65	54
	457	57	36	24	30	58	62	41	25	31	62	50
B4	169	64	48	38	31	65	70	53	32	33	70	53
	477	59	38	26	28	60	62	50	22	24	62	50
	1035	42	44	10	13	44	49	46	10	12	49	38
C2	115	97	45	27	45	97	101	45	25	47	101	82
	266	88	38	24	33	89	93	42	20	35	93	77
	468	90	37	31	32	91	81	44	28	33	(82)	76
C3	104	67	71	52	35	72	80	62	48	49	(80)	58
	403	59	51	29	27	60	61	48	33	34	(62)	52
	951	60	51	41	39	62	63	54	40	39	64	46
D1	87	95	89	49	45	97	107	91	49	43	107	80
	212	82	94	30	41	94	95	83	31	33	(95)	82
D2	120	95	65	57	41	97	99	73	59	43	101	86
	270	95	61	51	39	97	95	73	51	41	97	79
	345	97	65	49	47	99	93	71	49	43	93	69
D5	510	81	101	57	74	102	83	91	65	69	(91)	88
	633	65	103	49	75	(103)	59	102	51	57	102	85

Table 3 continued

Mooring	meter depth (m)	Residual Histogram				TOTAL SPEED	Gaussian fit				TOTAL SPEED	MAX. OBS. SPEED
		Along-slope +	-	up-slope +	-		Along-slope +	-	up-slope +	-		
E2	453	87	64	43	46	88	109	63	37	45	109	77
E3	120	101	84	79	91	113	113	109	99	103	119	95
	419	83	78	51	58	89	87	91	69	71	93	83
	725	58	93	57	37	94	65	78	47	43	(78)	100
E4	111	131	95	79	63	133	115	111	93	85	(119)	117
	950	46	86	77	24	92	60	75	51	39	(75)	66
F1	39	97	53	44	61	98	94	64	42	65	96	88
F3	79*	117	51	48	73	(121)	115	67	63	81	(117)	89
	388	71	71	38	47	(74)	90	70	52	52	91	66
	694	73	69	43	43	(74)	85	111	37	41	(111)	60
	945	78	64	36	40	(78)	89	102	35	37	(102)	66
G1	41	73	65	57	49	75	71	60	59	56	73	48
	166	50	40	40	33	50	47	40	37	36	47	33
G2	151	128	29	67	67	(129)	134	47	61	69	135	114
	299	98	23	53	47	(100)	127	77	47	47	(127)	89
	500	81	31	68	52	(87)	90	46	54	60	92	84
G4	195	58	44	49	57	(71)	78	65	59	63	79	64
	1104	30	31	20	26	(35)	42	37	31	31	(43)	32
	1554	34	35	22	22	(37)	43	36	31	30	(44)	34
I2	251	59	63	103	55	103	61	59	103	51	103	60
	654	46	47	50	41	58	51	48	52	46	(56)	45
	1055	35	71	53	41	(73)	55	71	45	46	(71)	67
	1440	69	85	68	49	(92)	71	86	71	40	(89)	75

* F3(79m): only 80 days of records.

Fig.1: CONSLEX mooring sites and direction of axis determined by principal component analysis of current records. (A range is shown where directions from each meter on a mooring differed by more than 10° .)

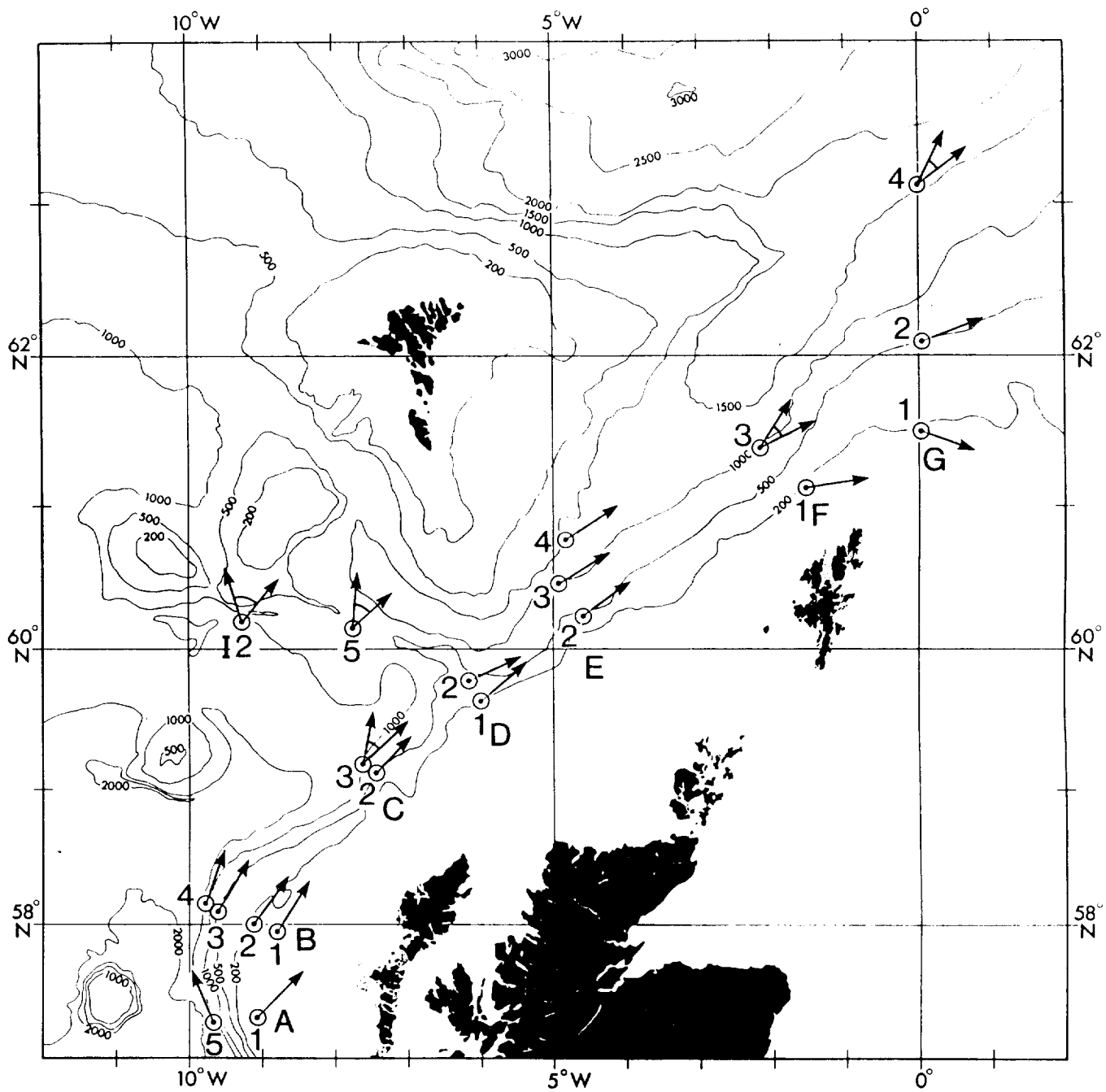
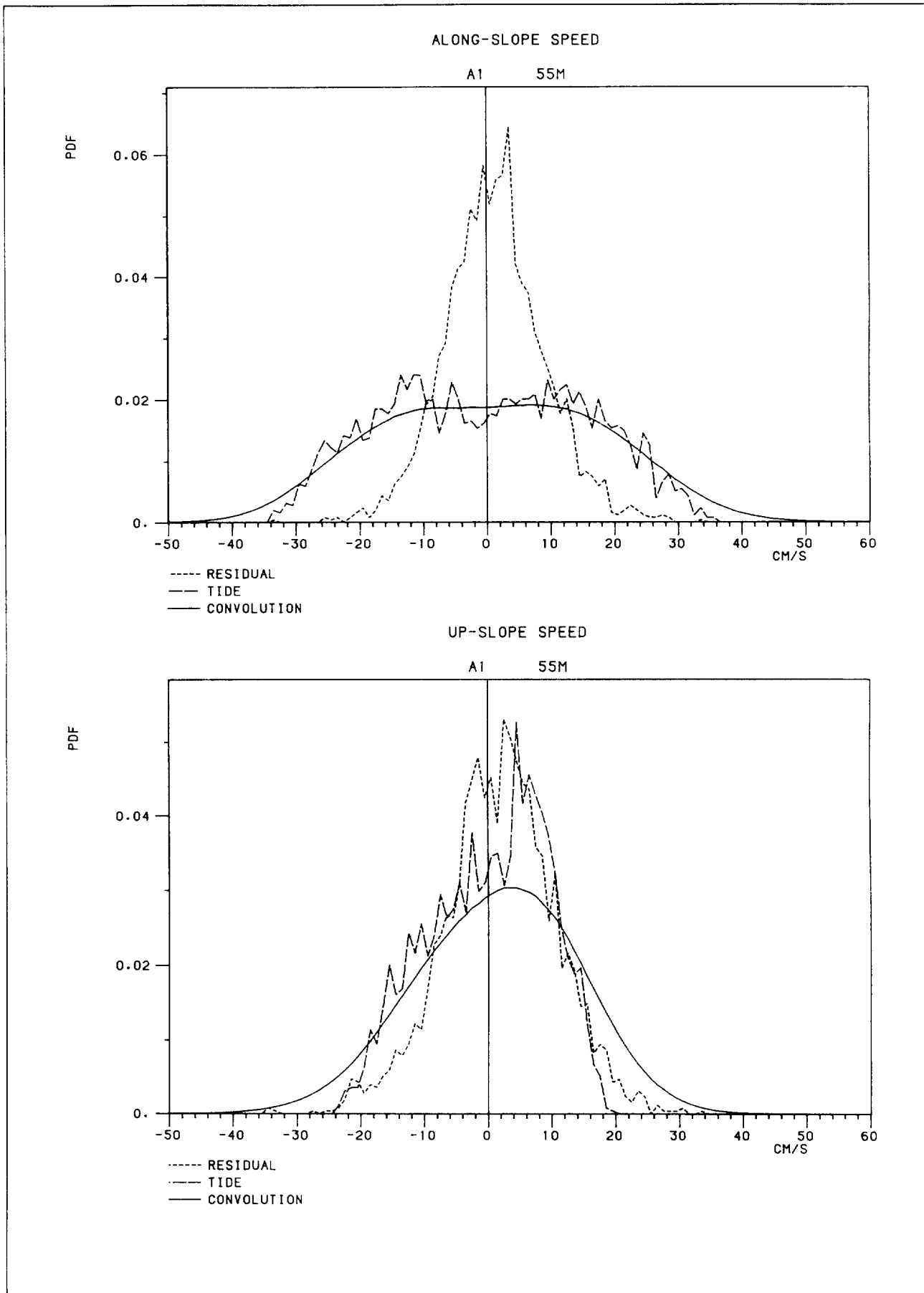
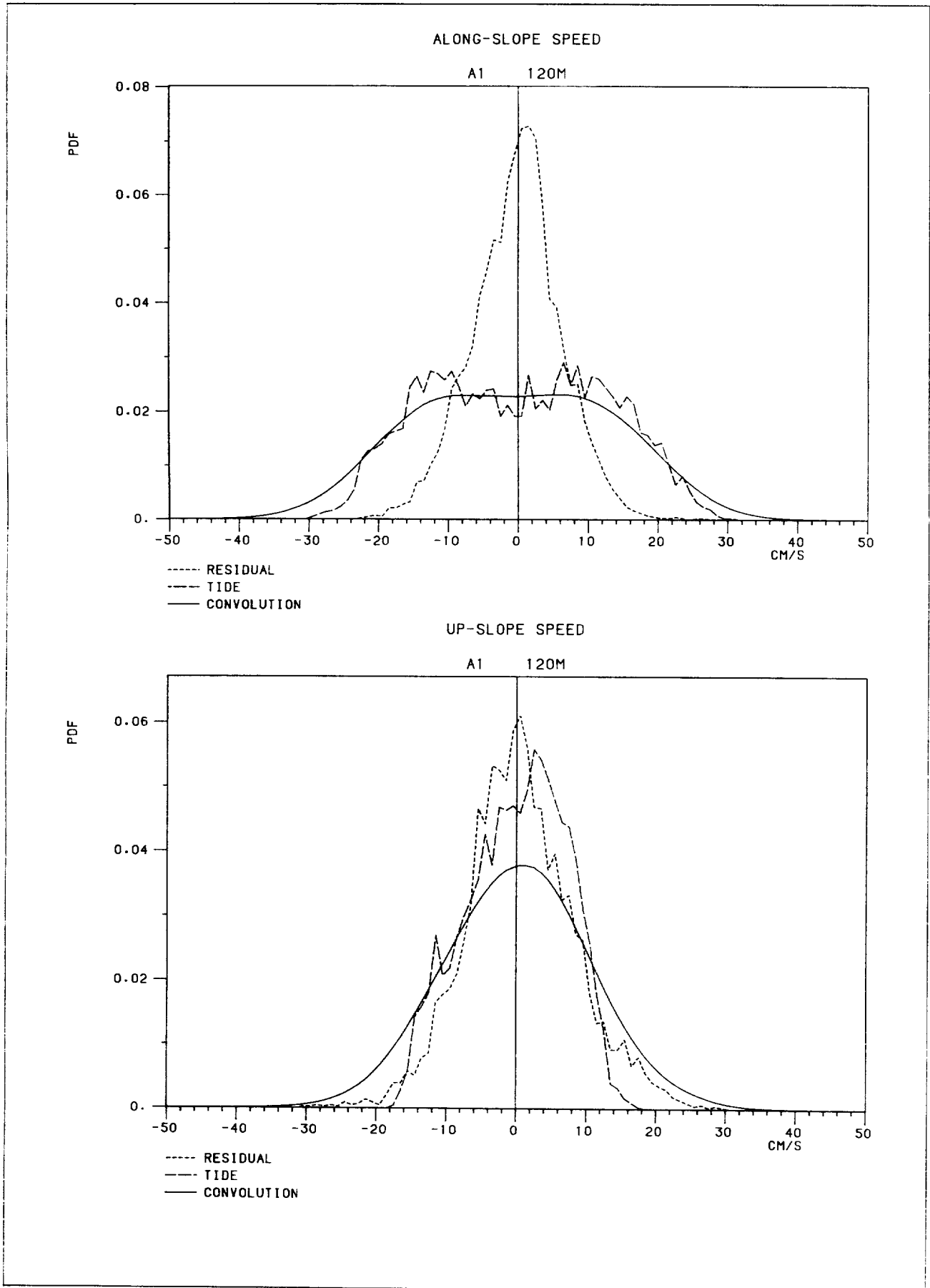
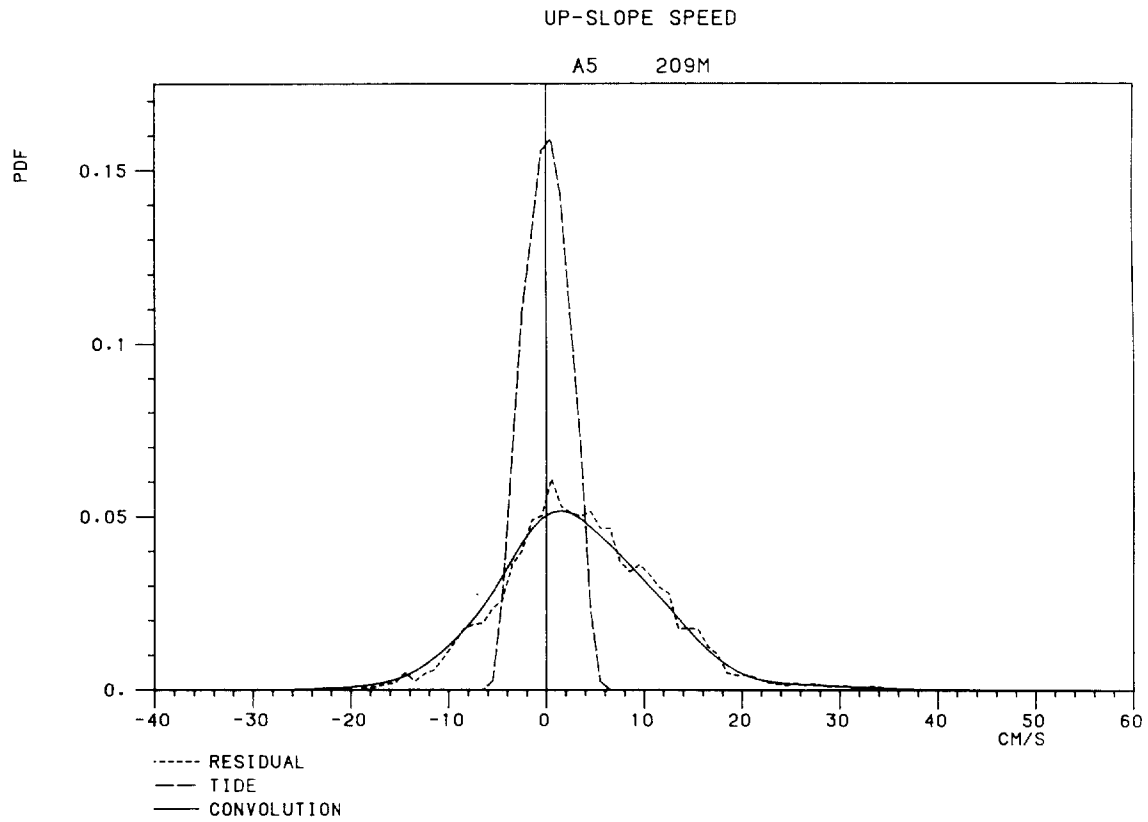
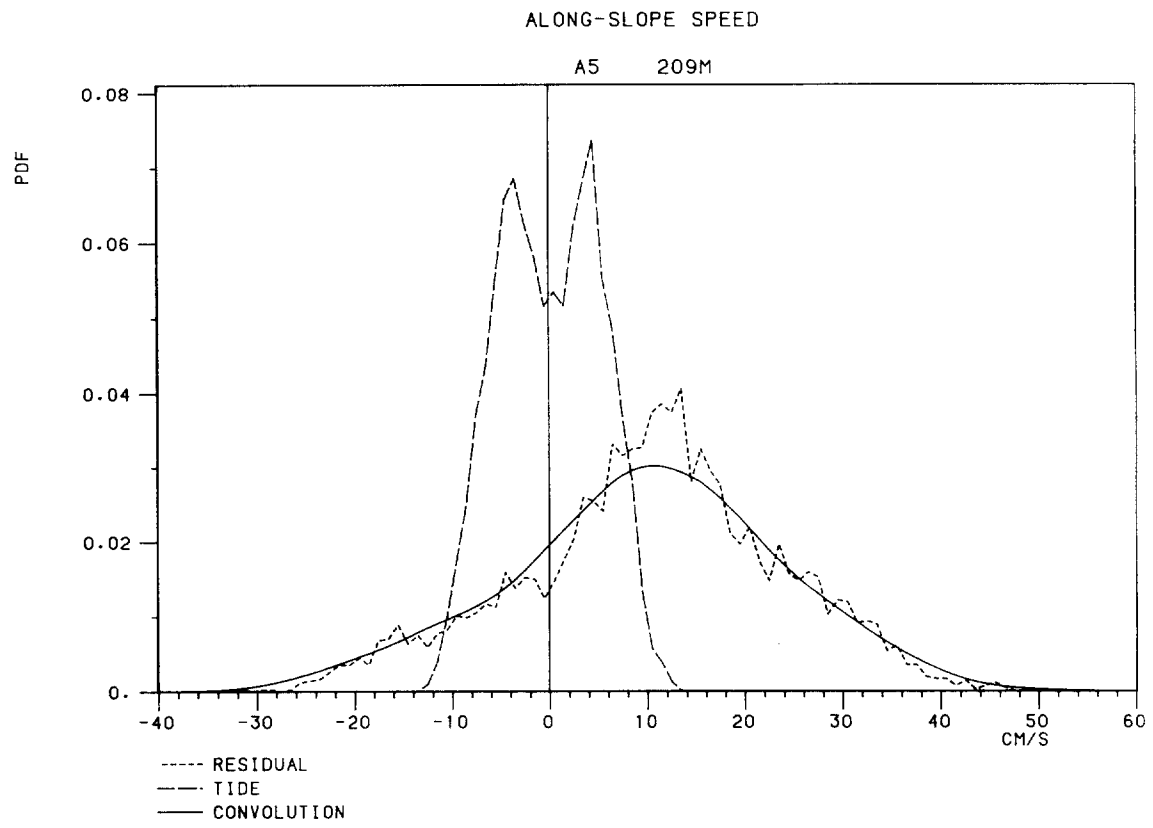


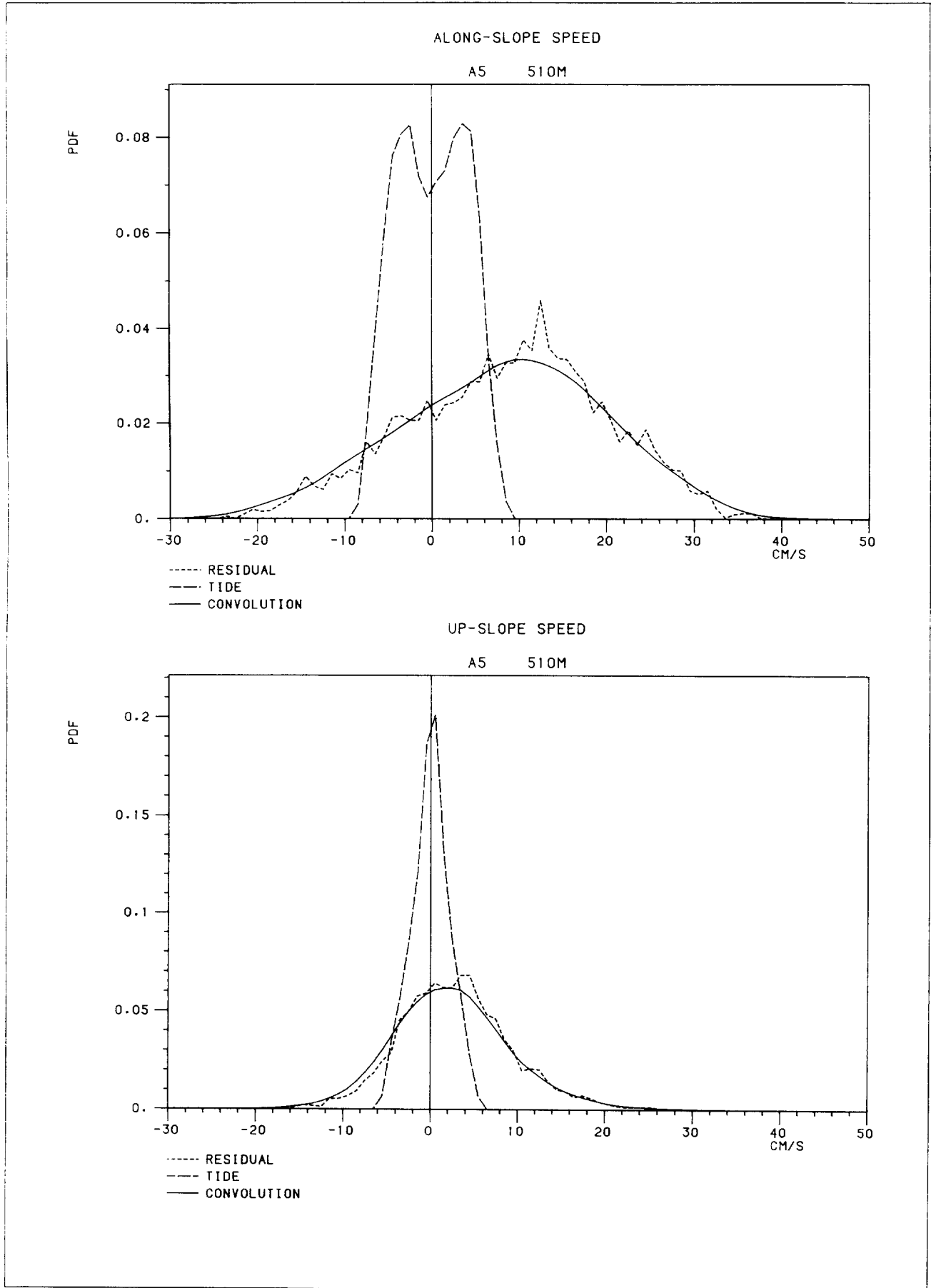
Fig.2: Probability distribution functions of residual and tidal current speeds along- and up-slope from speeds recorded by each current meter and their convolutions. (The meter is identified by the mooring and by the depth of the meter below the sea surface.)





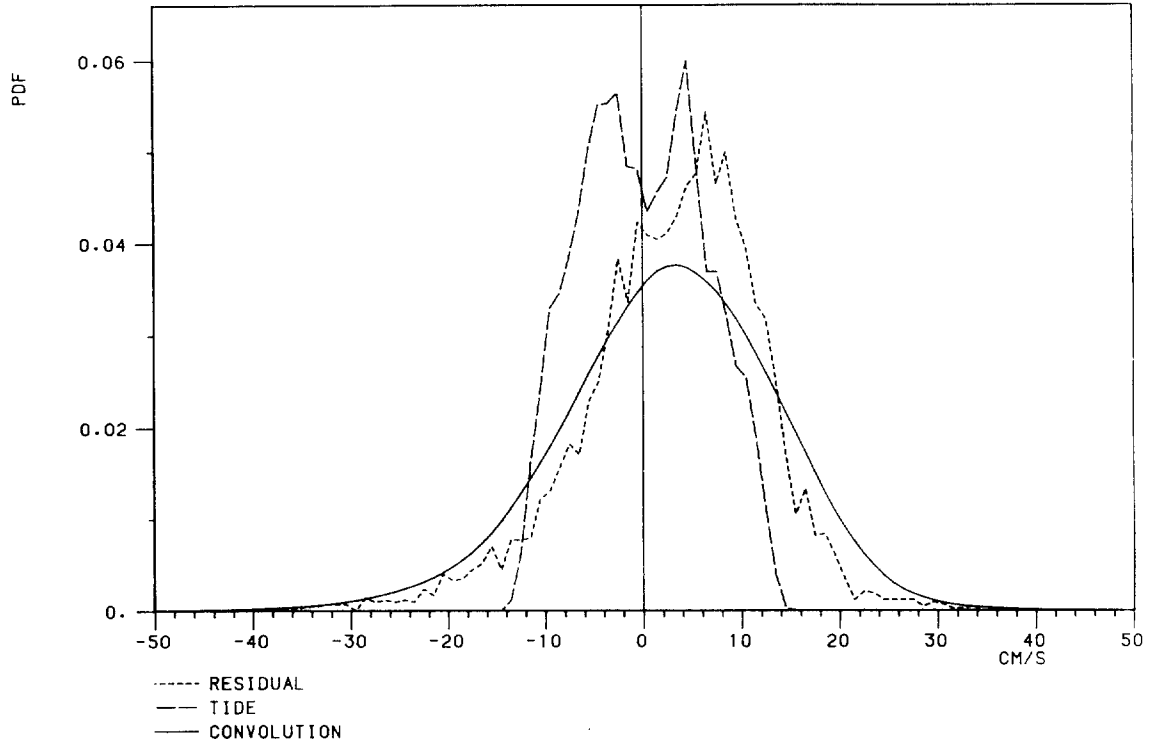






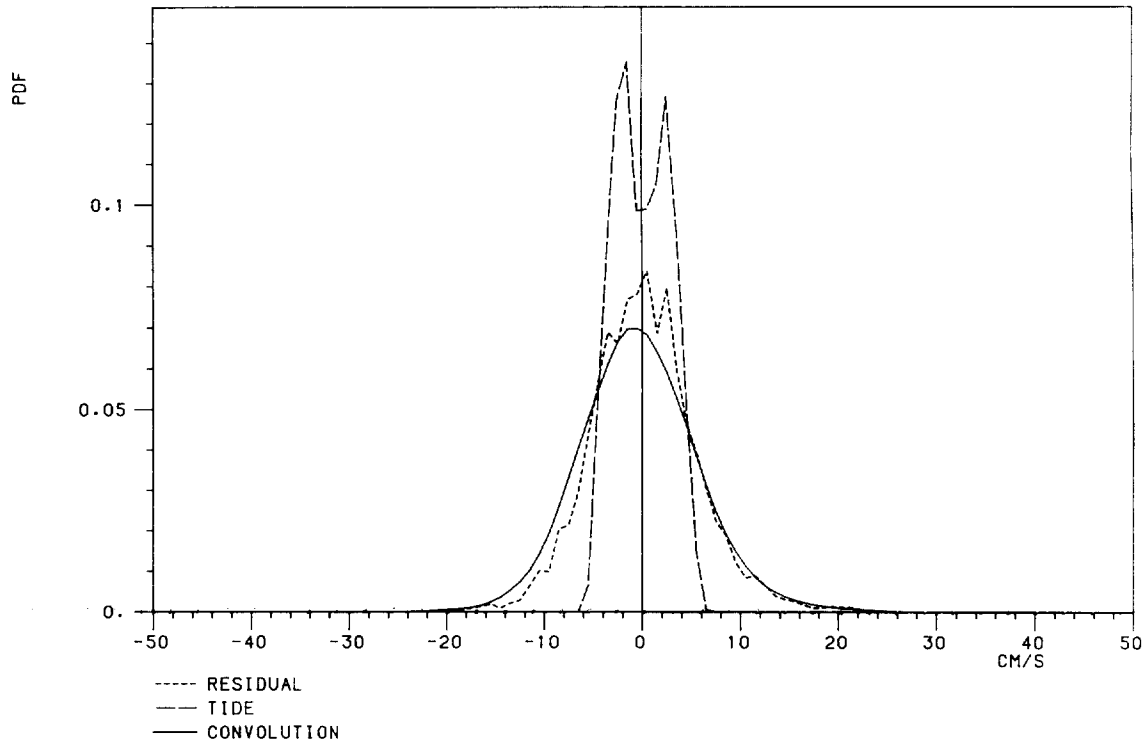
ALONG-SLOPE SPEED

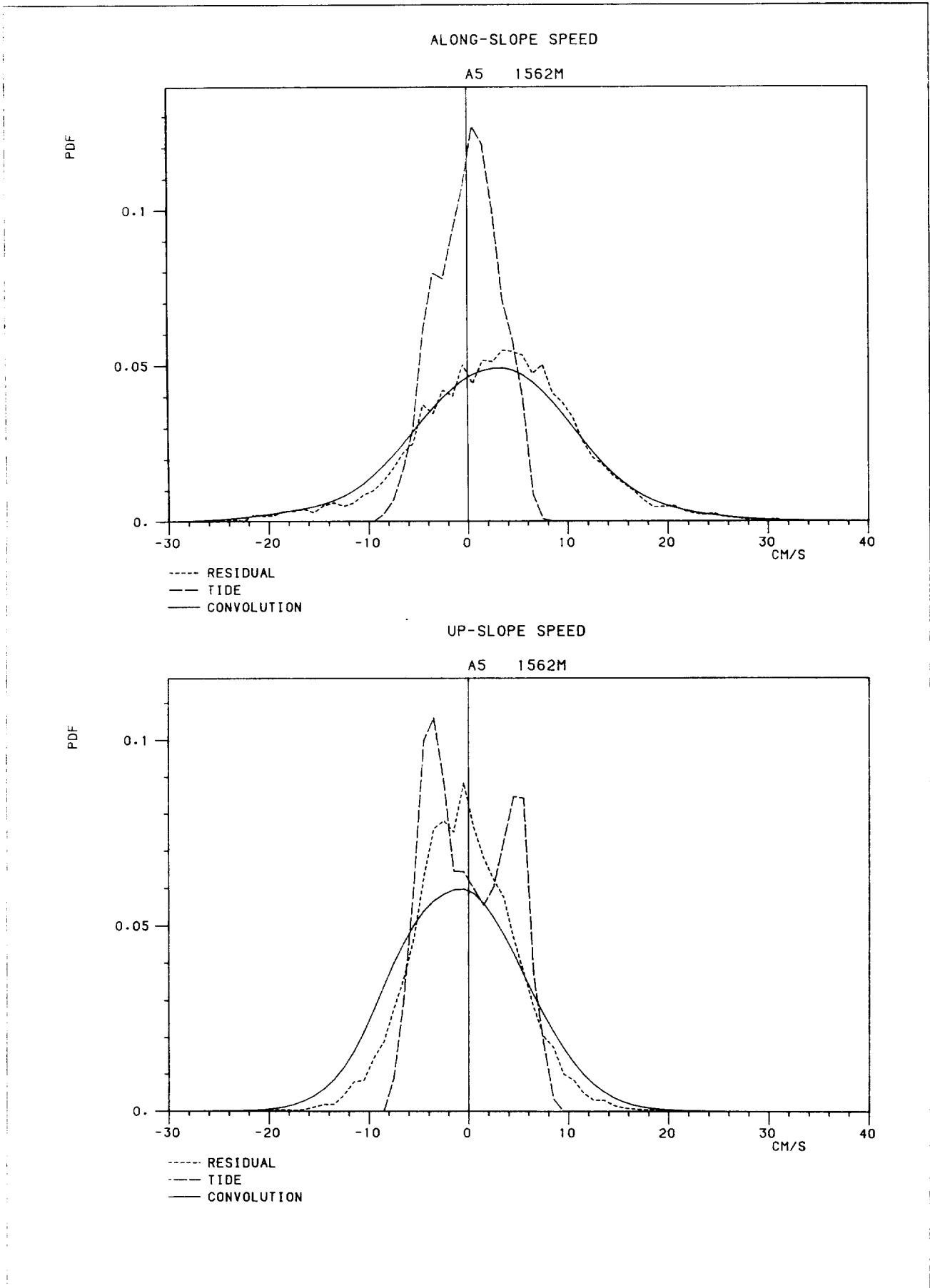
A5 1111M

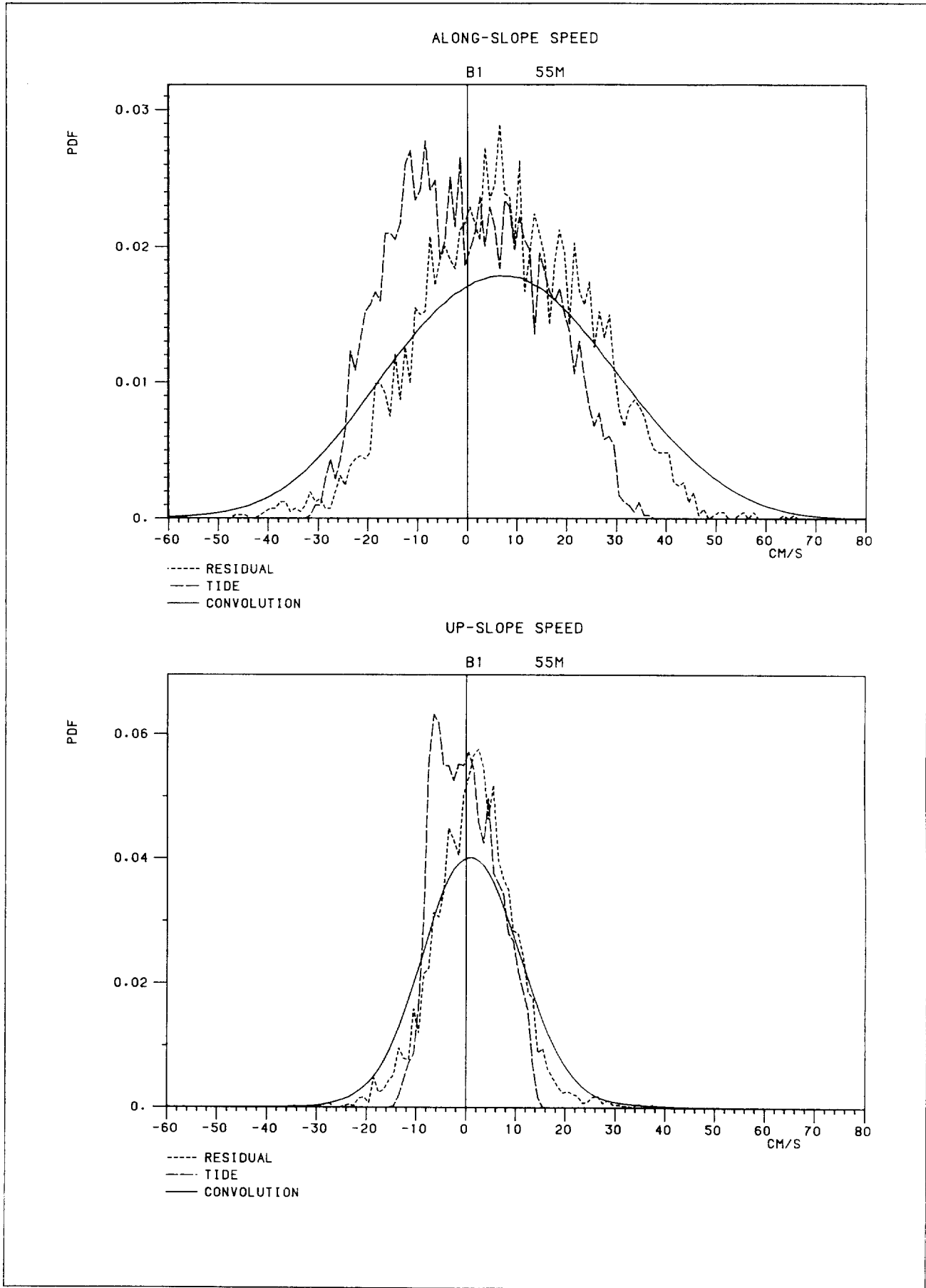


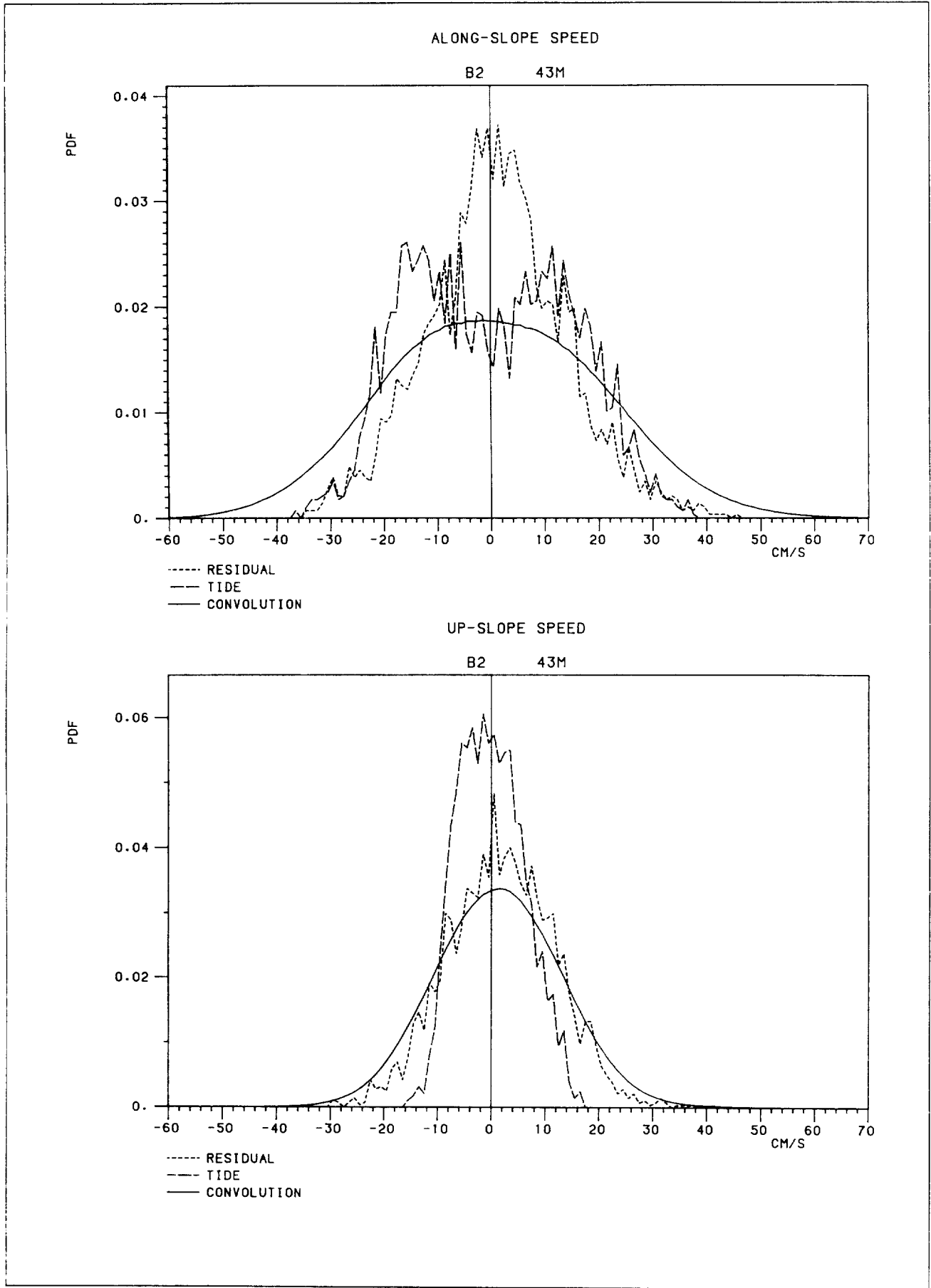
UP-SLOPE SPEED

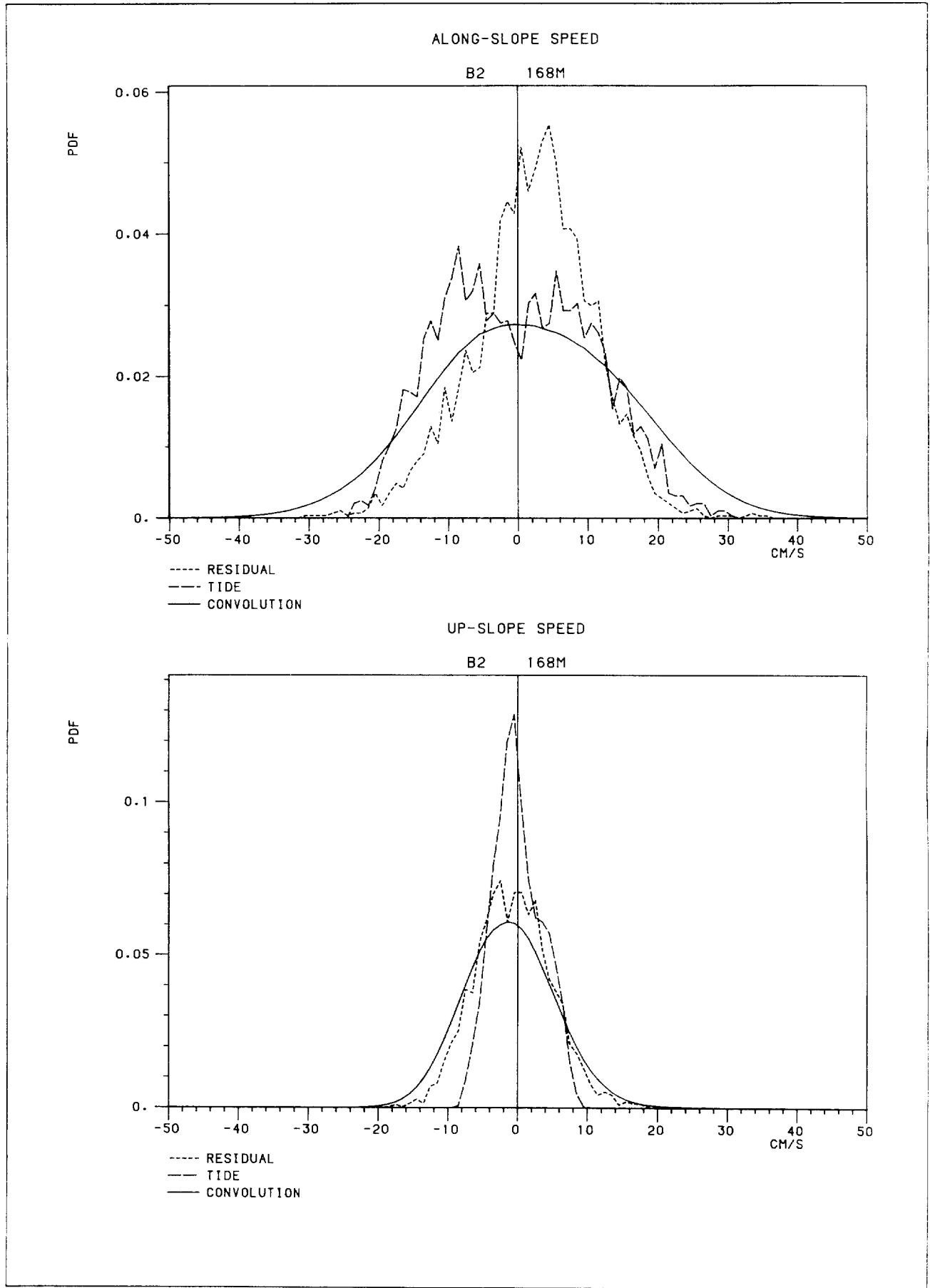
A5 1111M

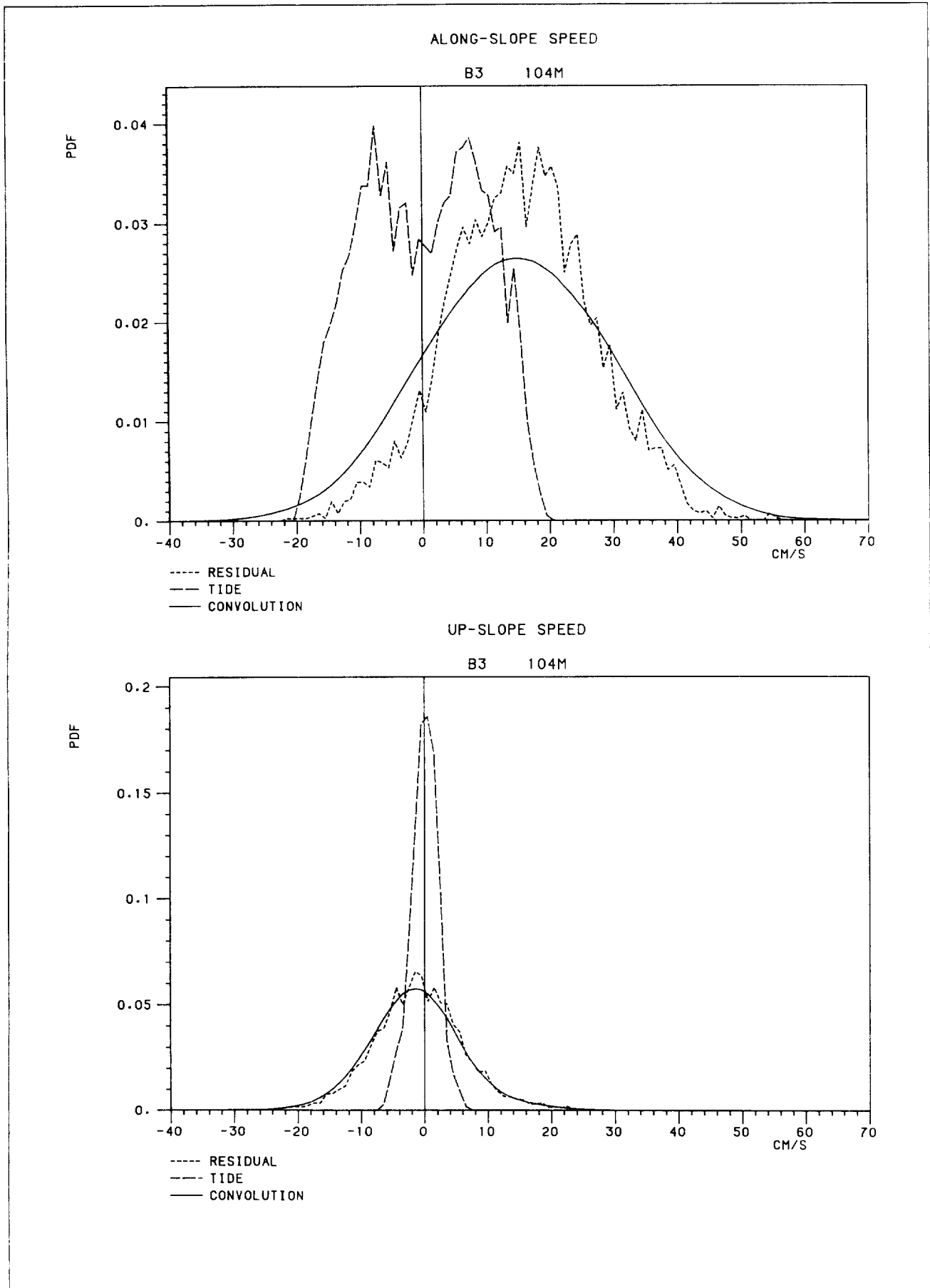


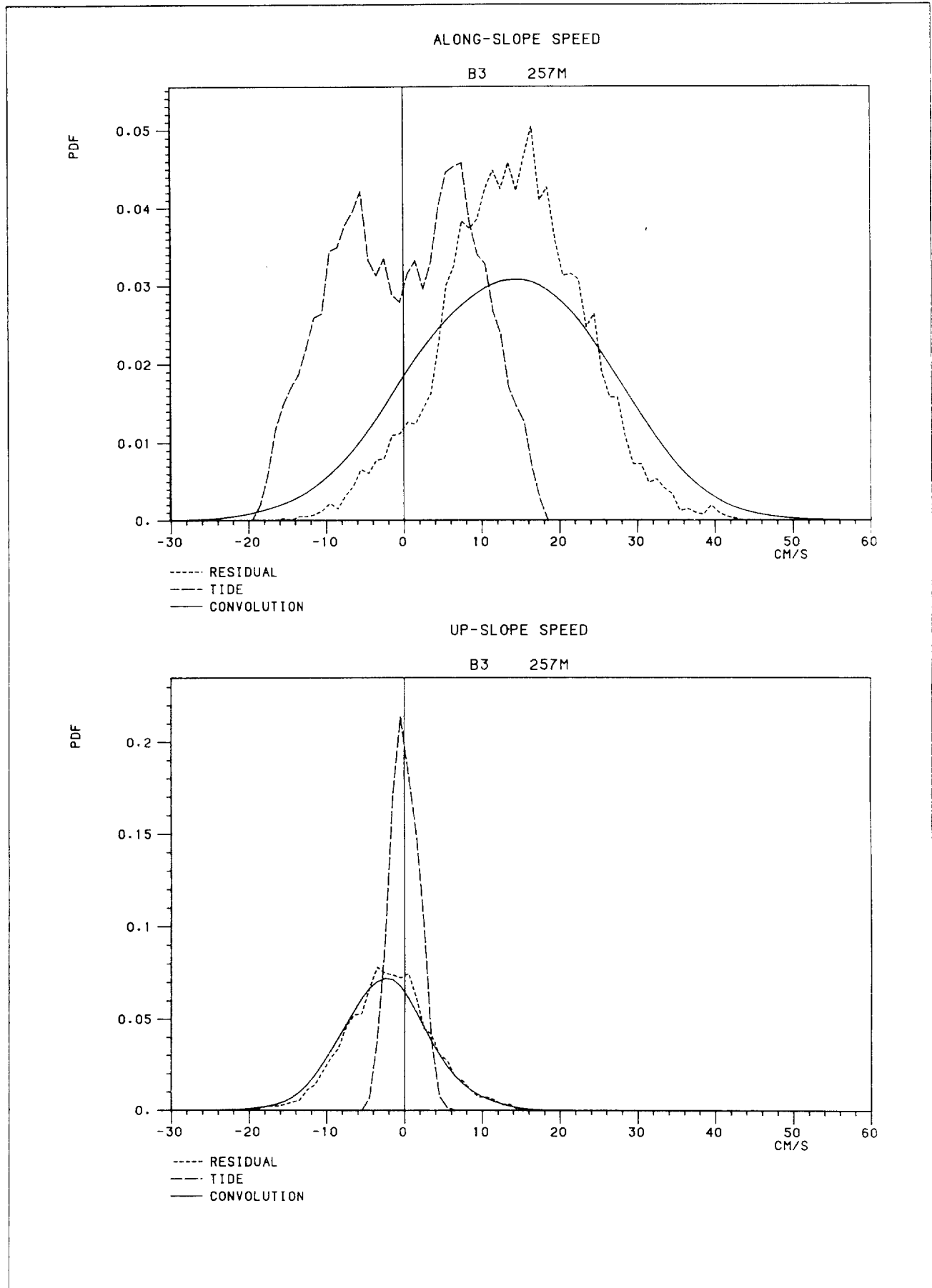


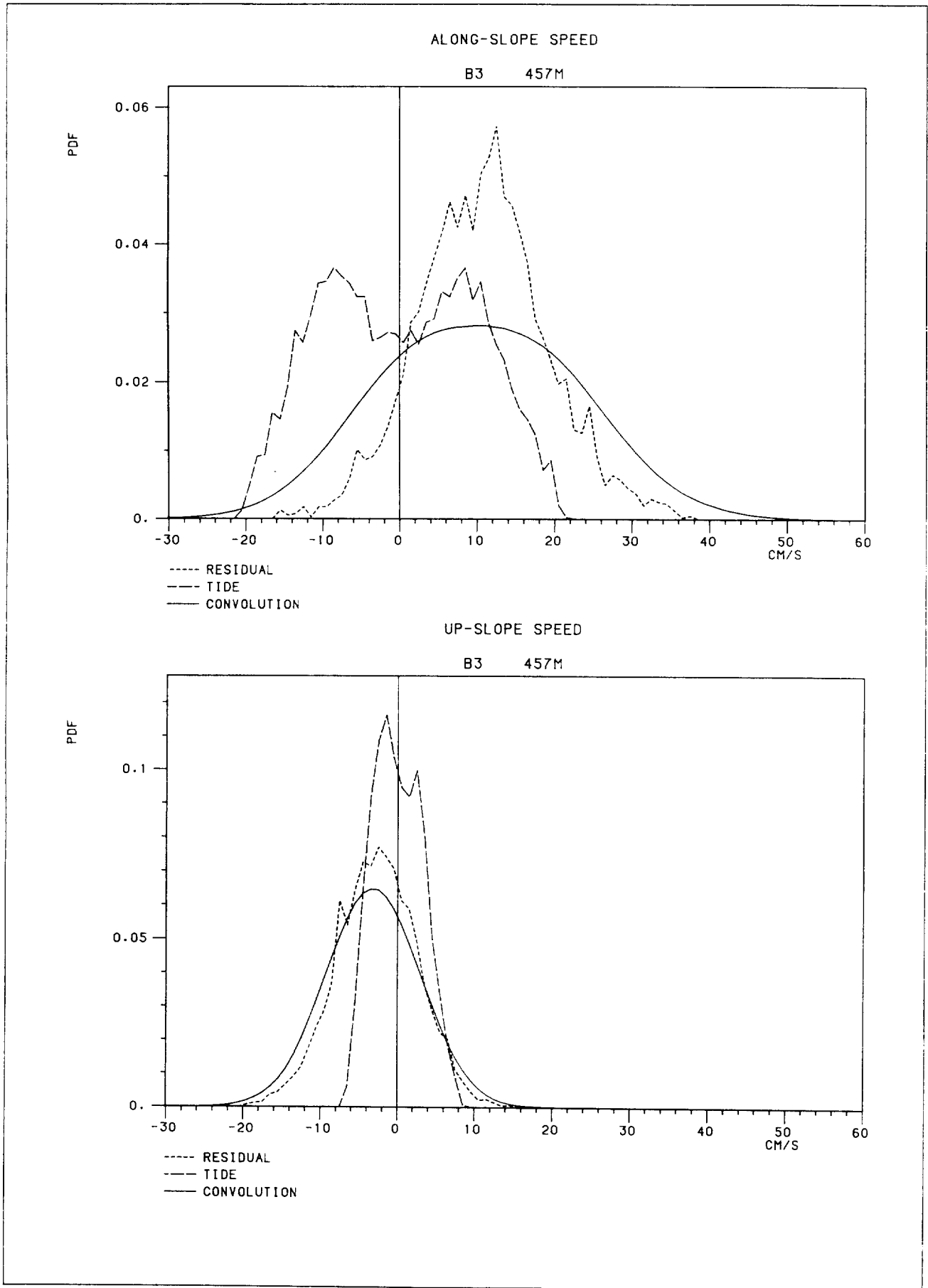


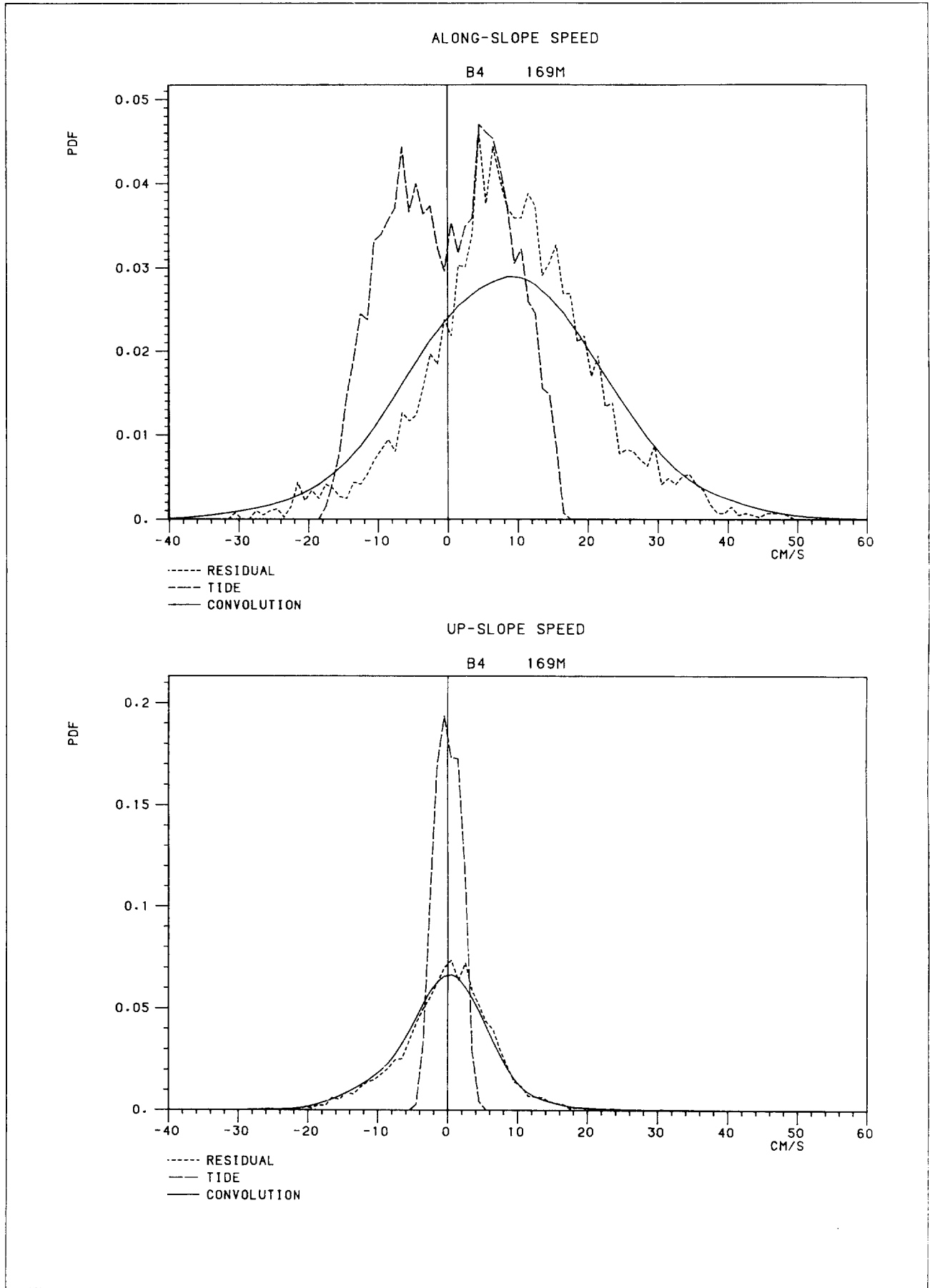






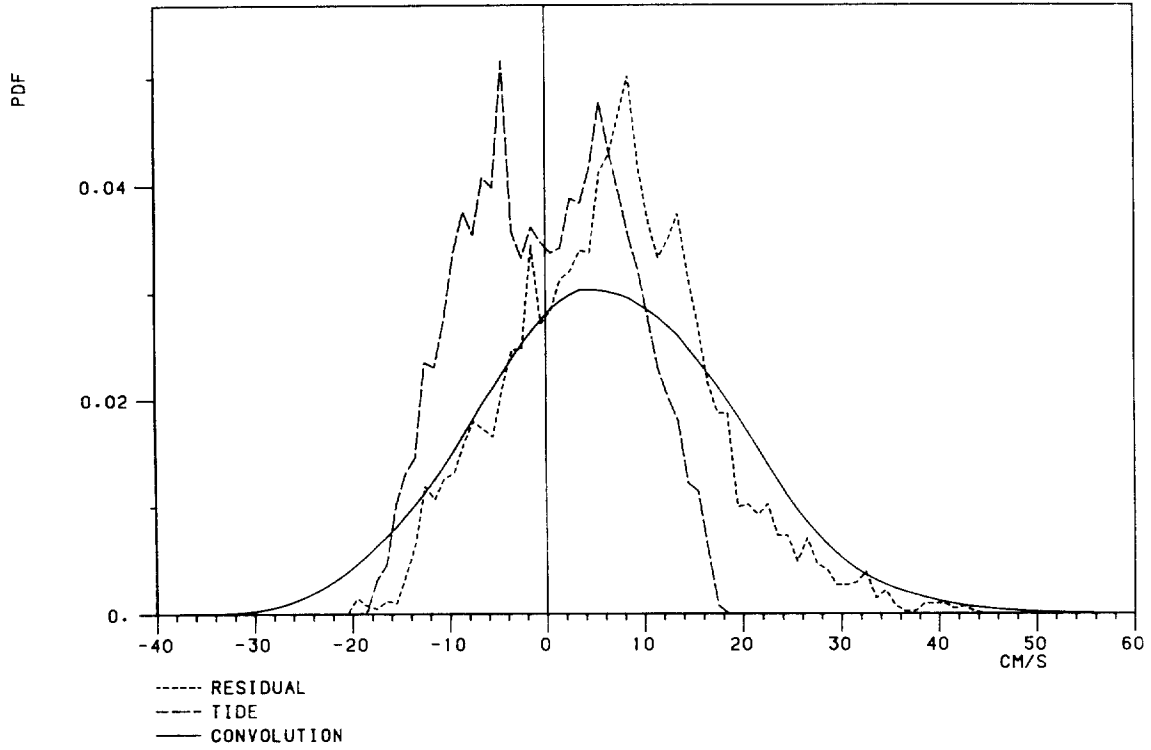






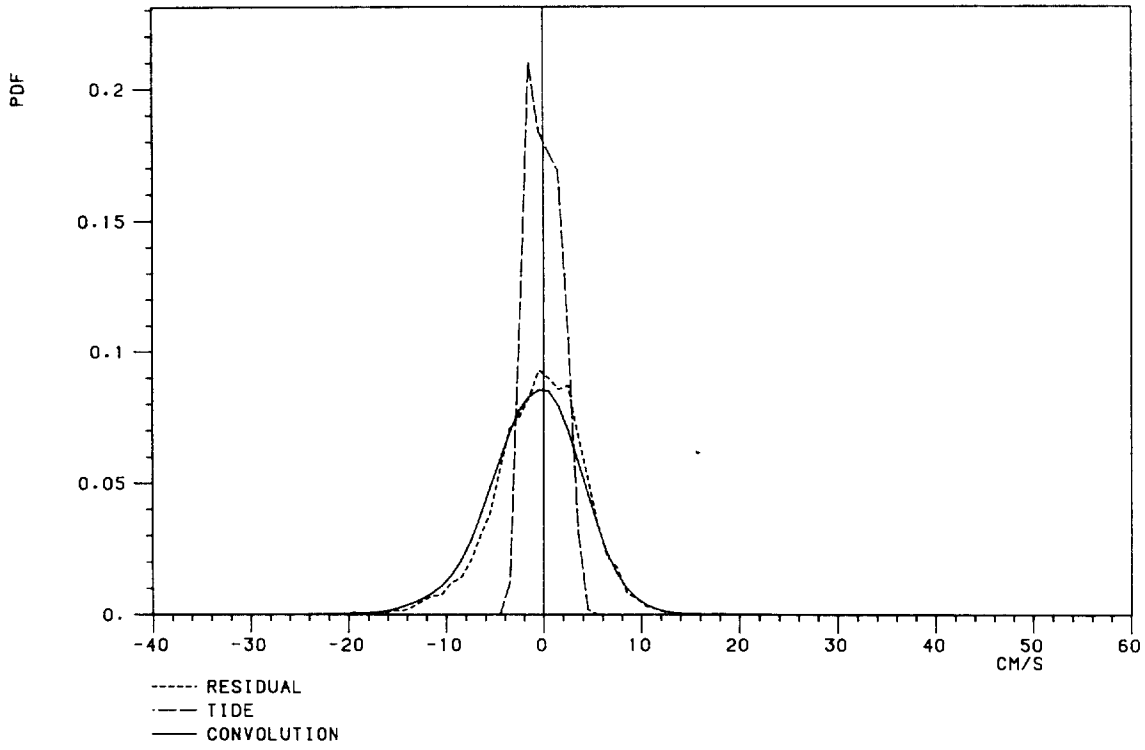
ALONG-SLOPE SPEED

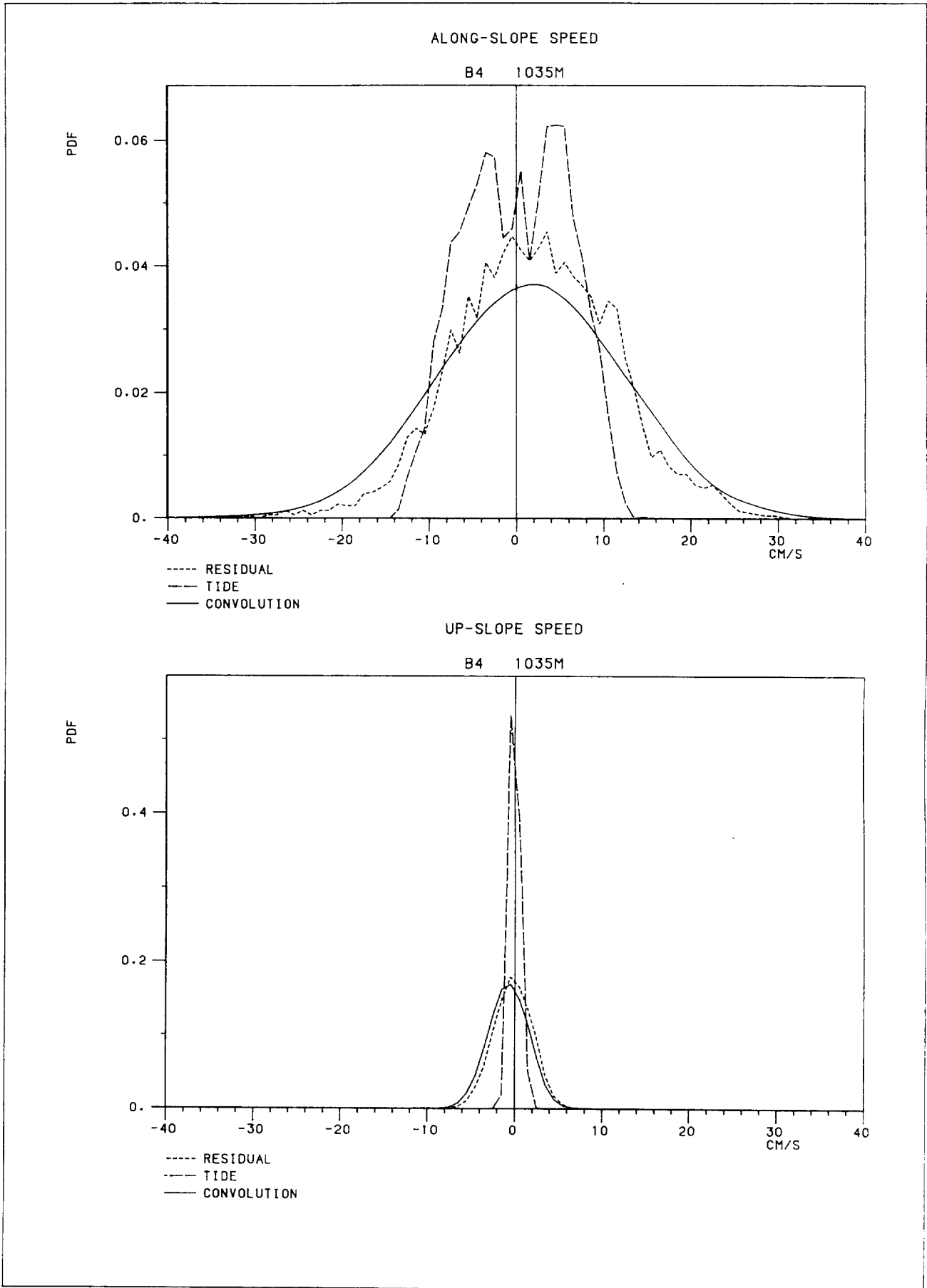
B4 477M



UP-SLOPE SPEED

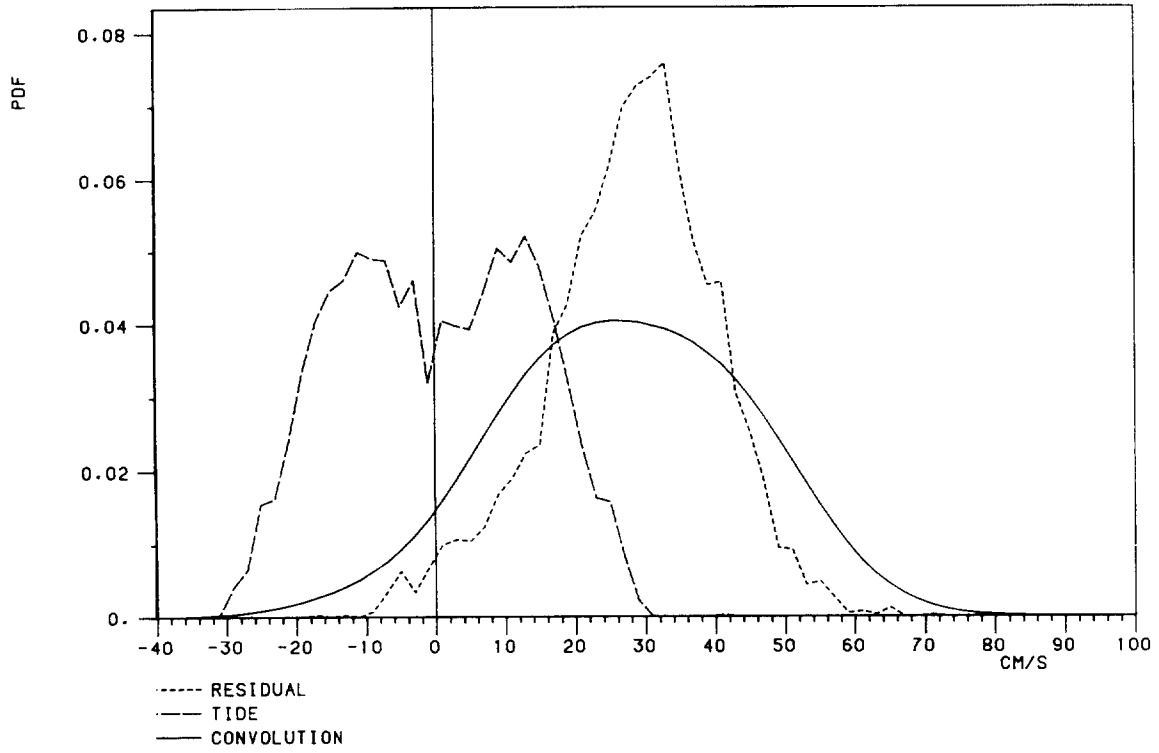
B4 477M





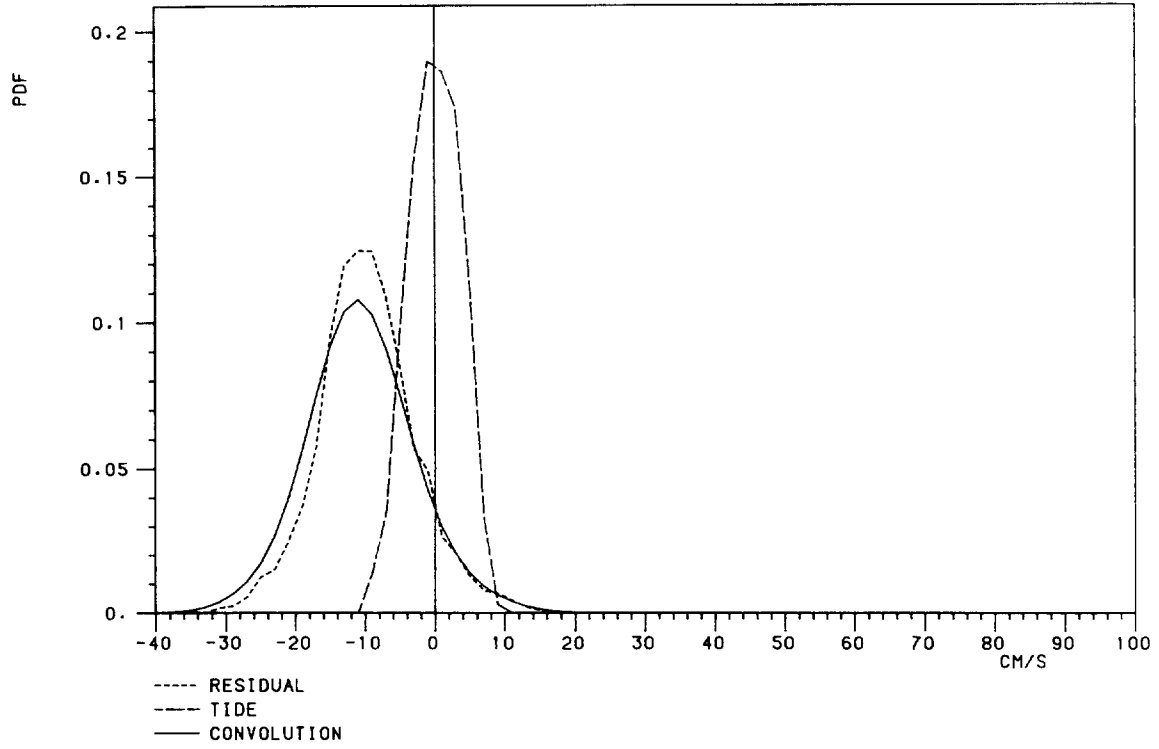
ALONG-SLOPE SPEED

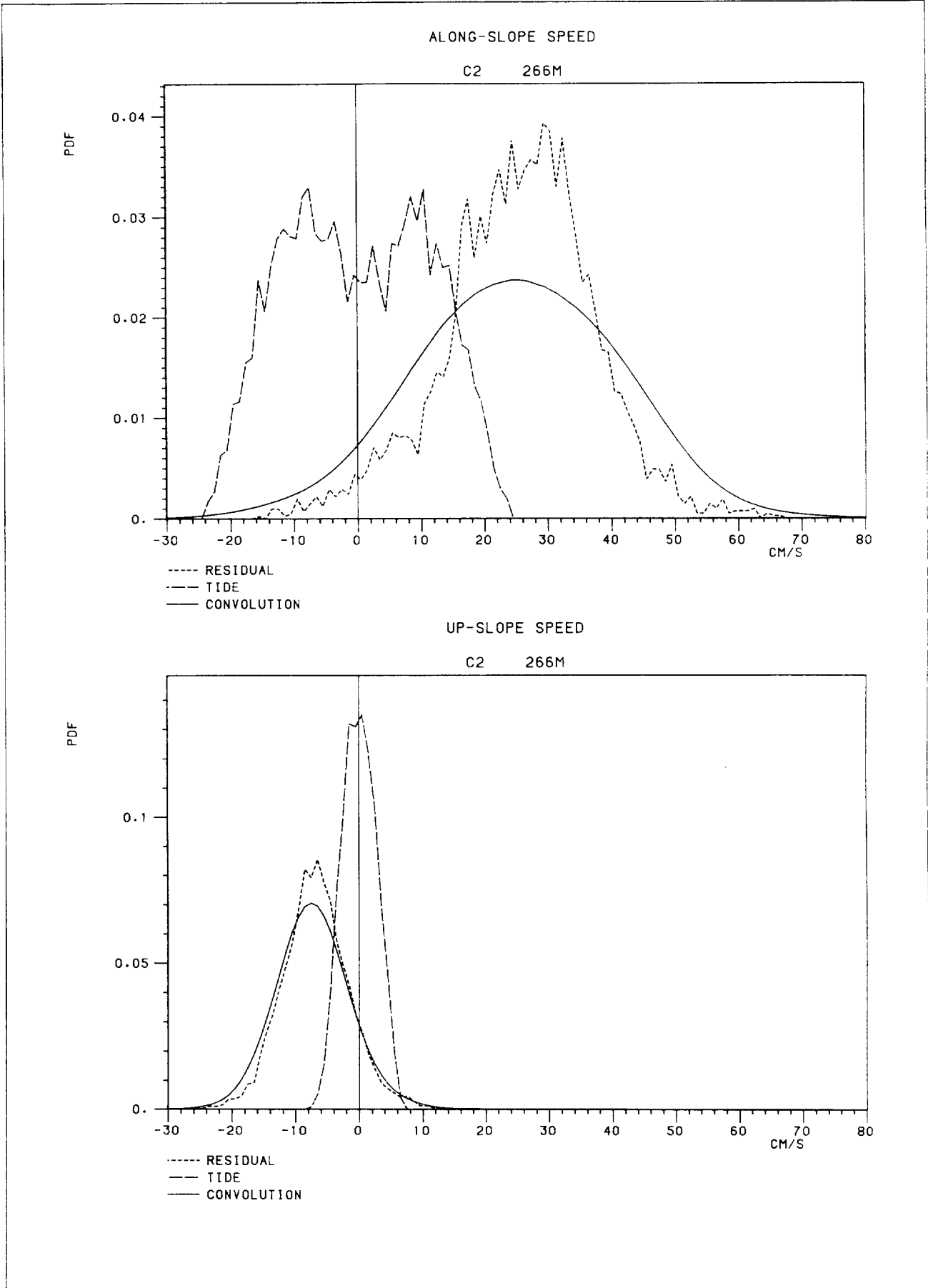
C2 115M

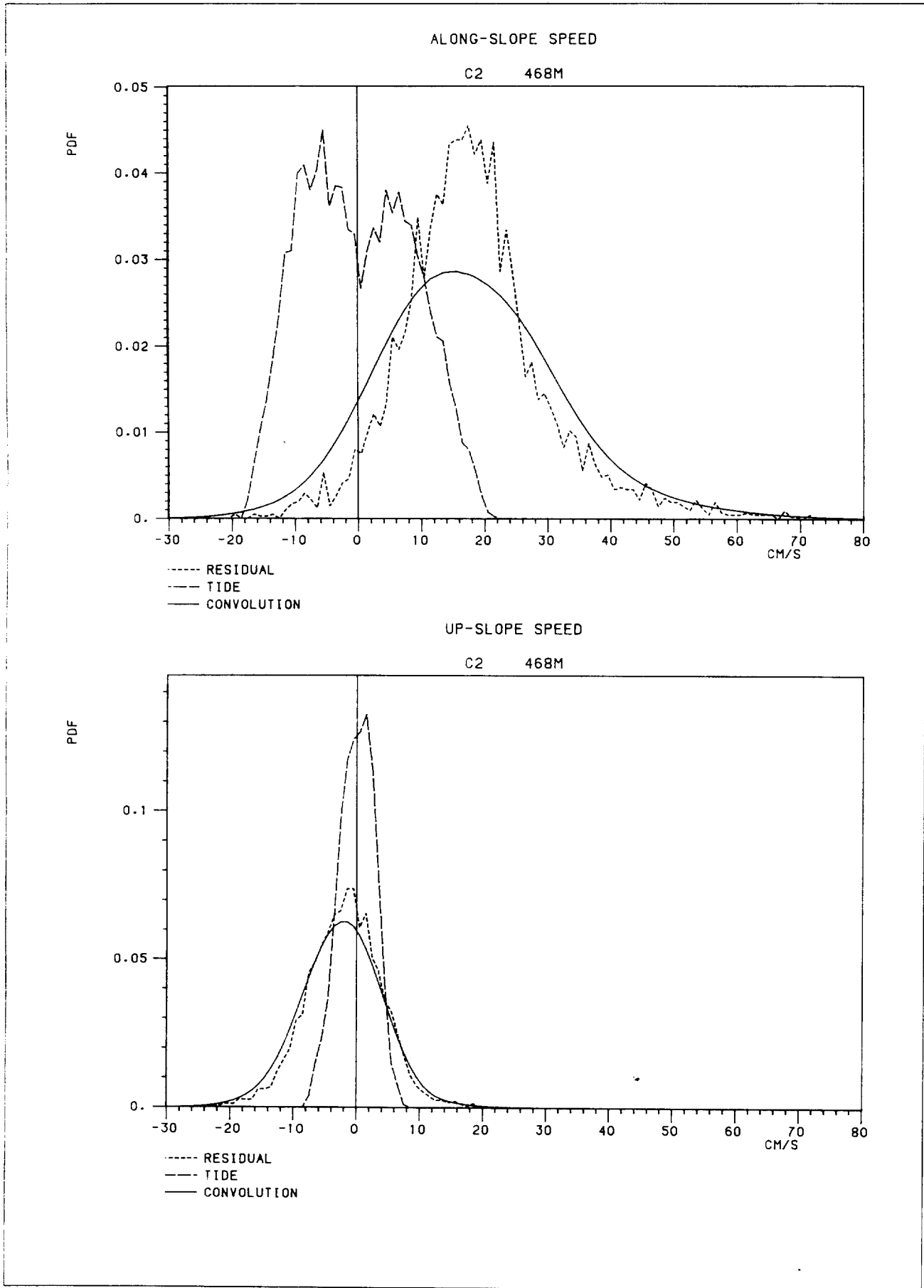


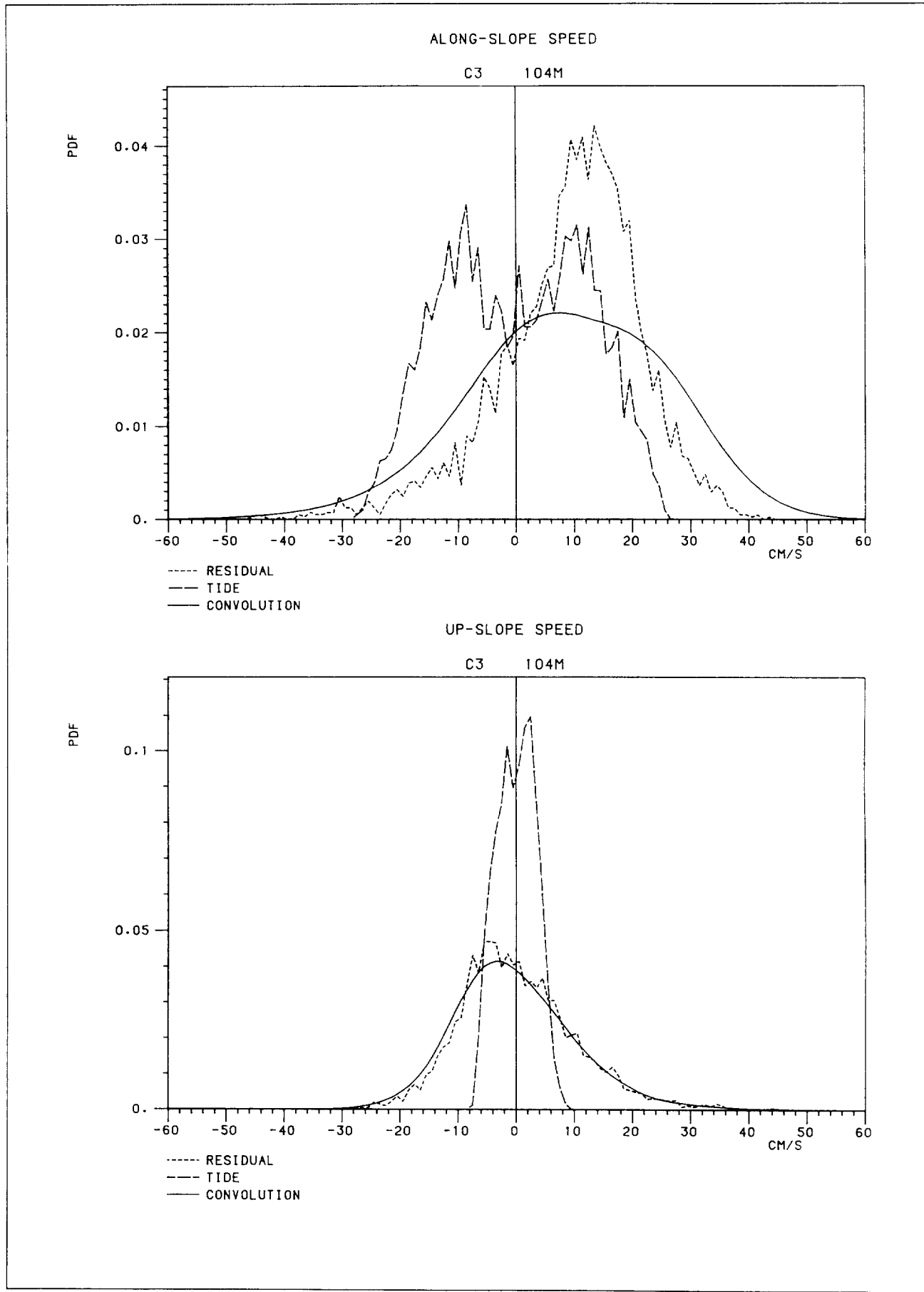
UP-SLOPE SPEED

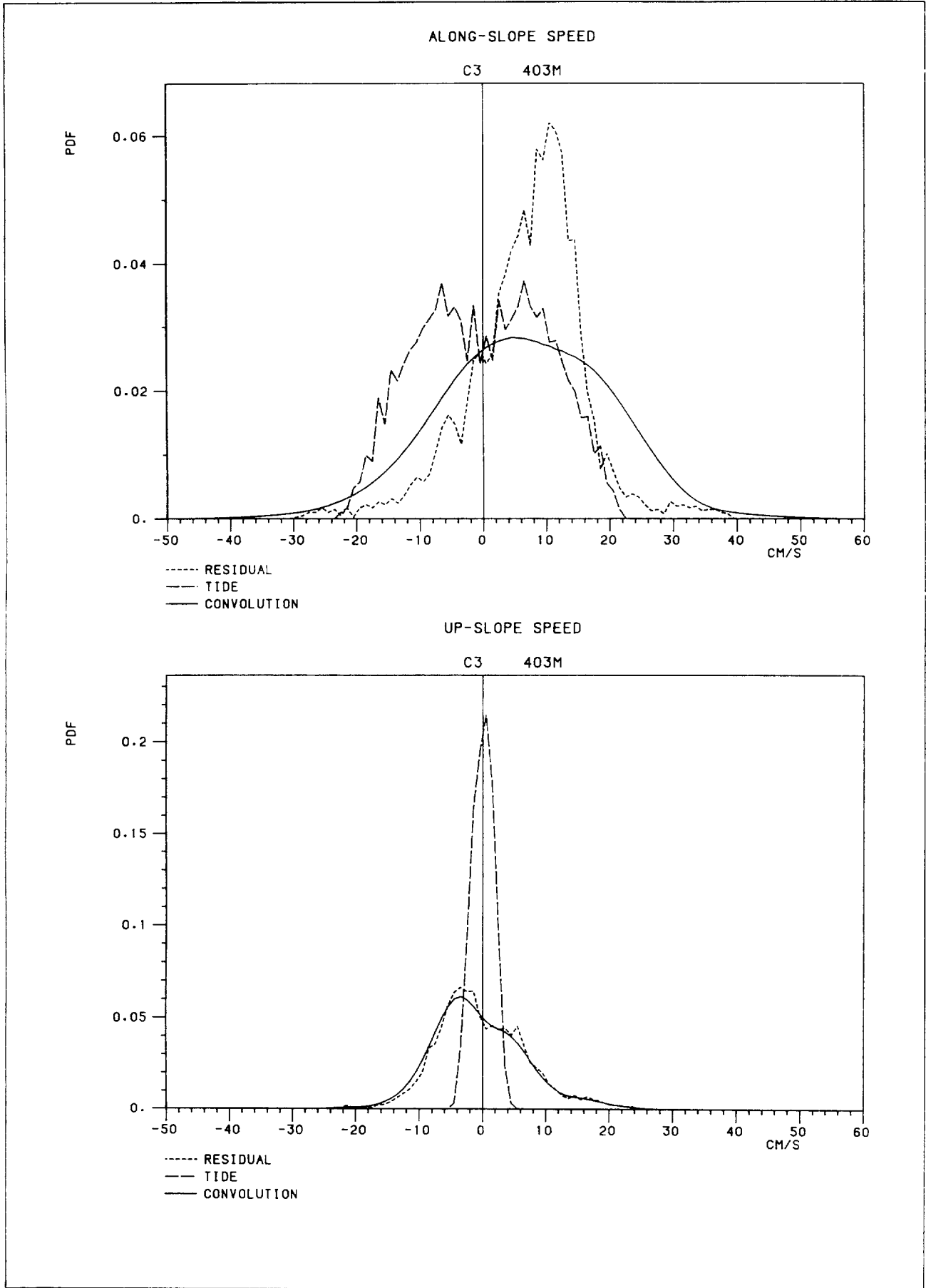
C2 115M

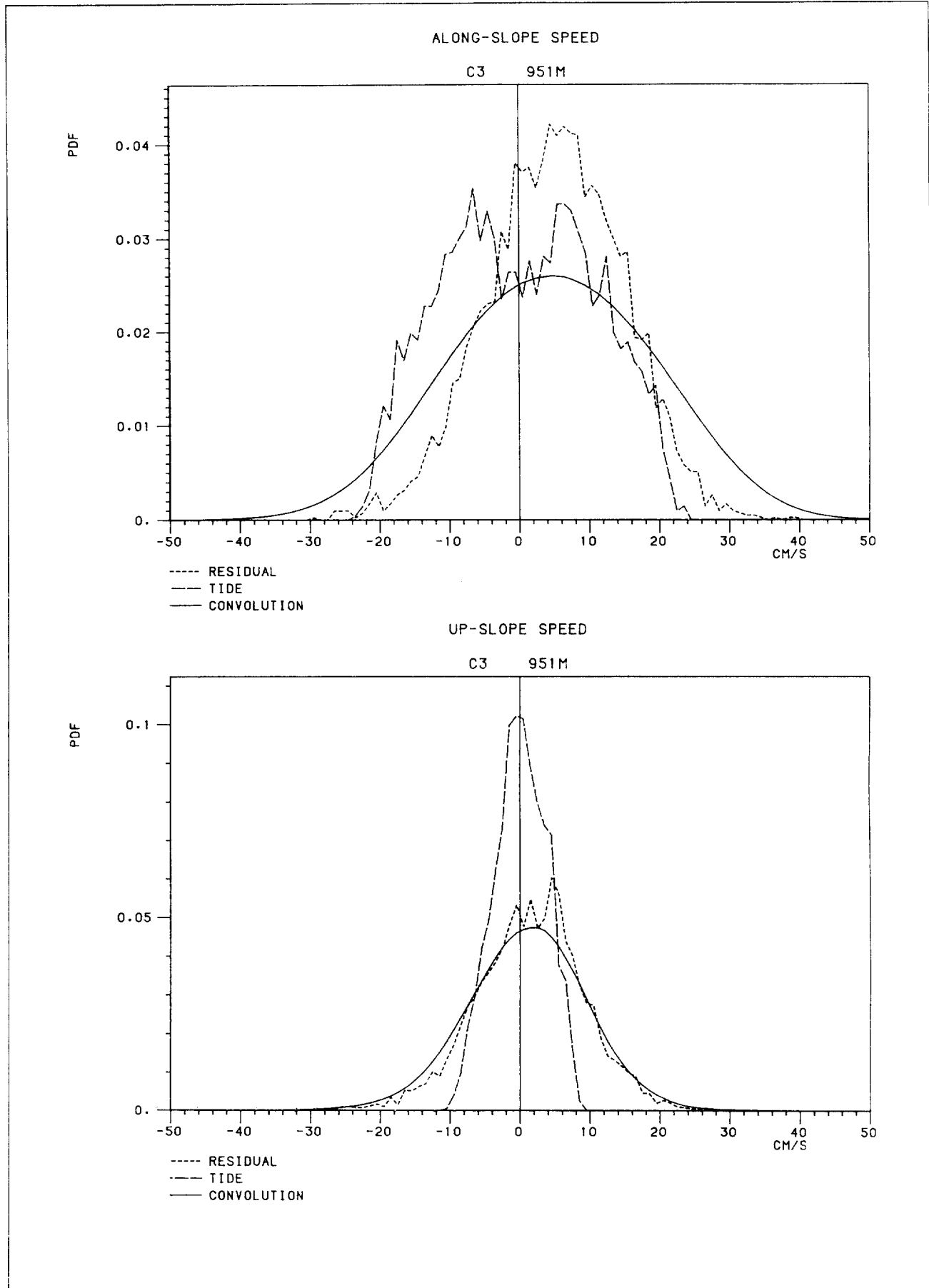


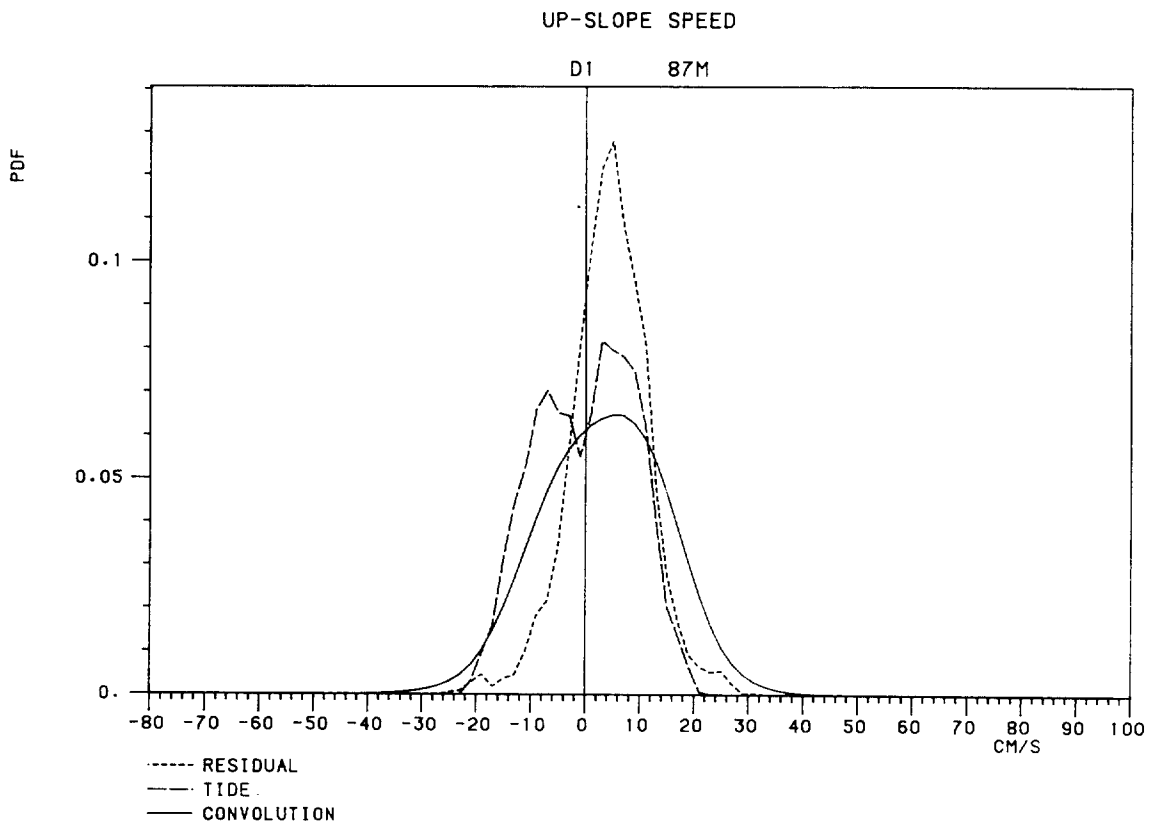
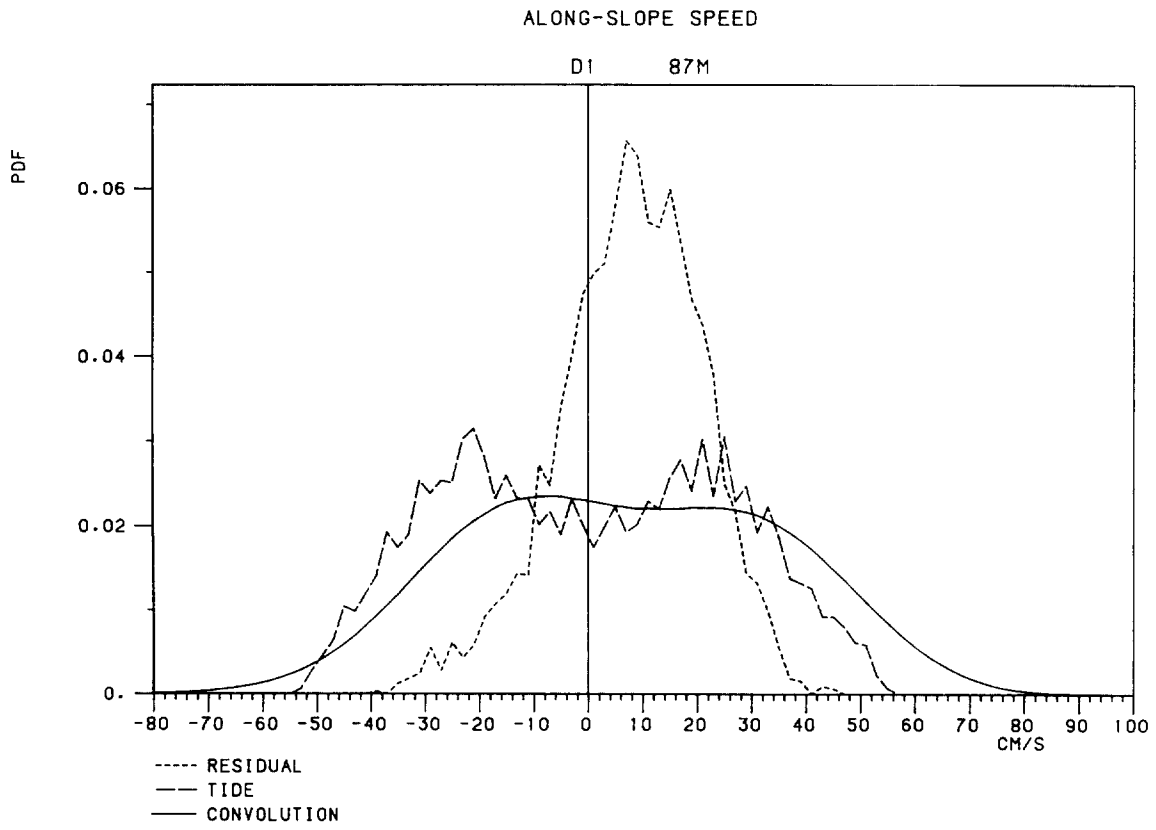


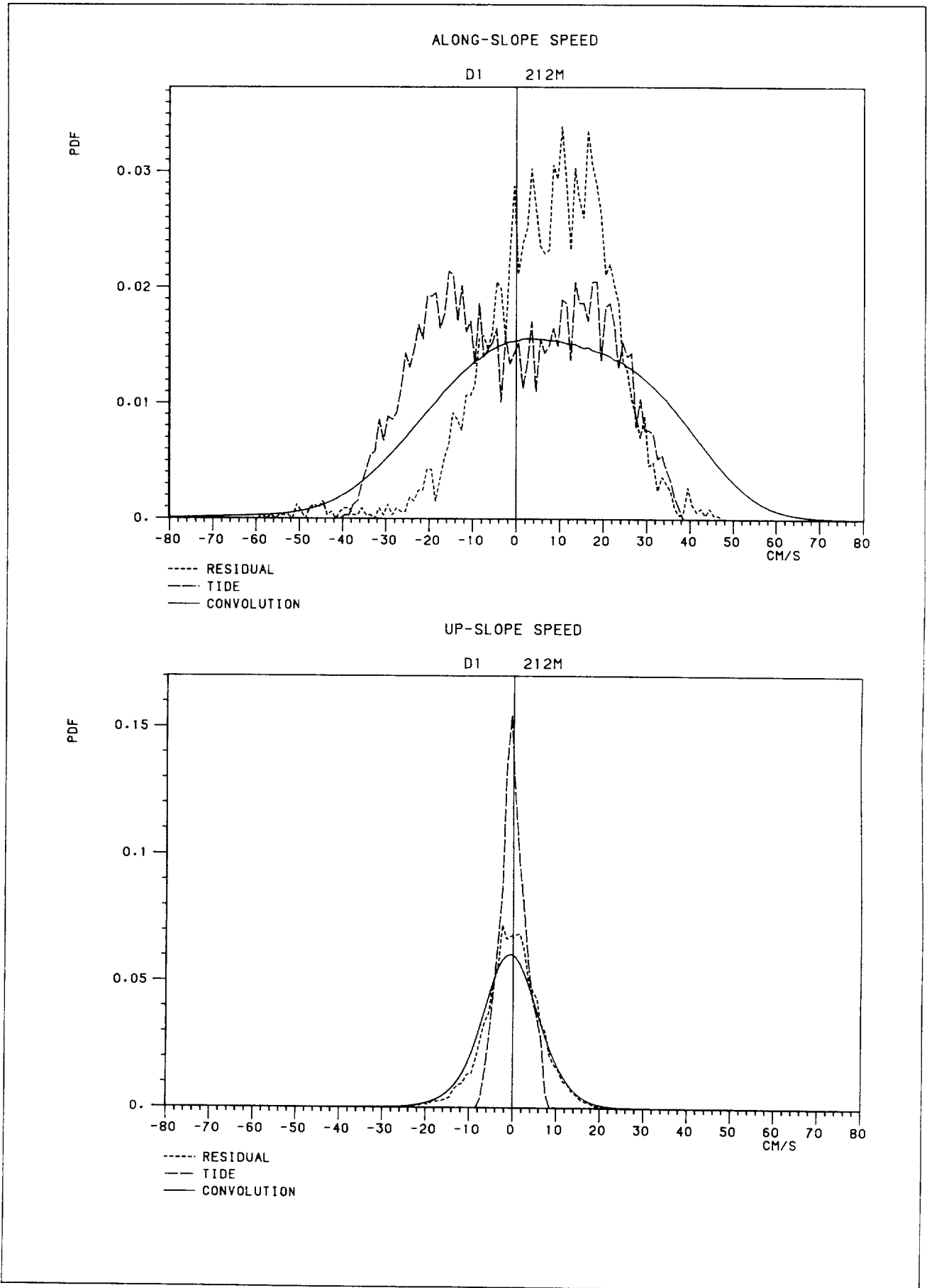


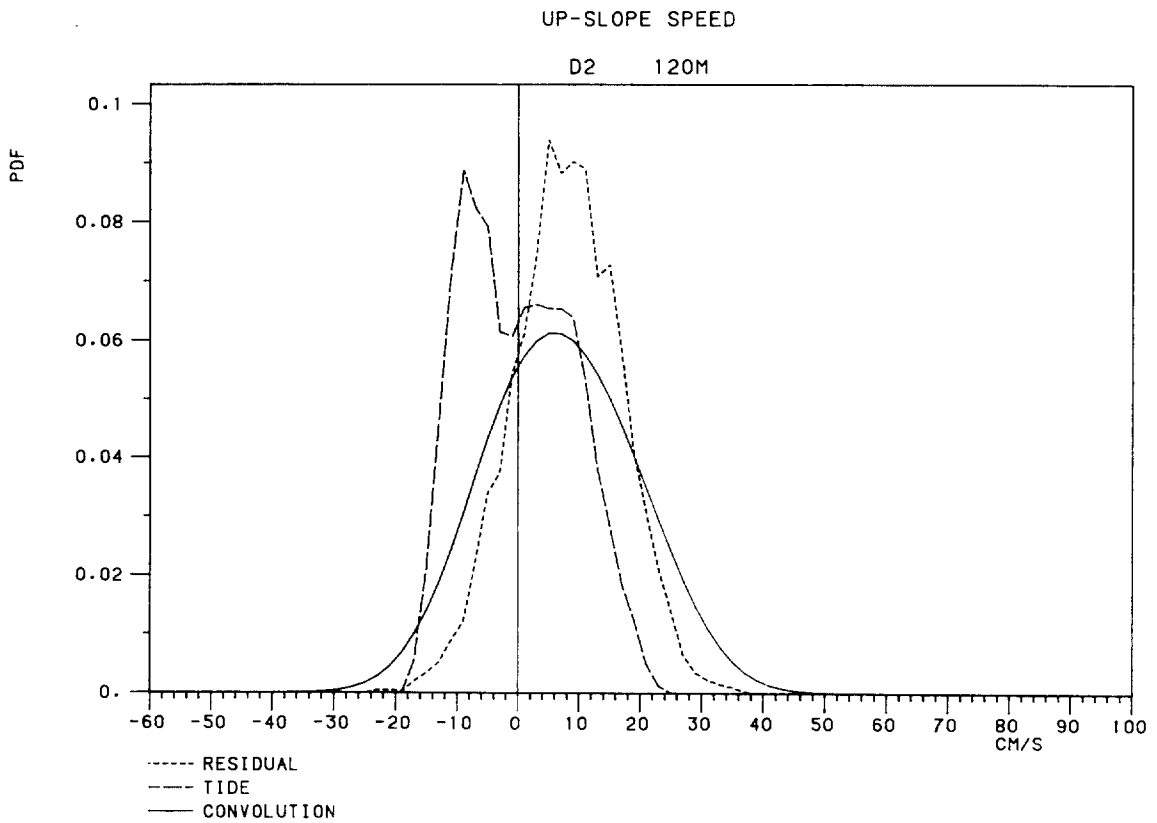
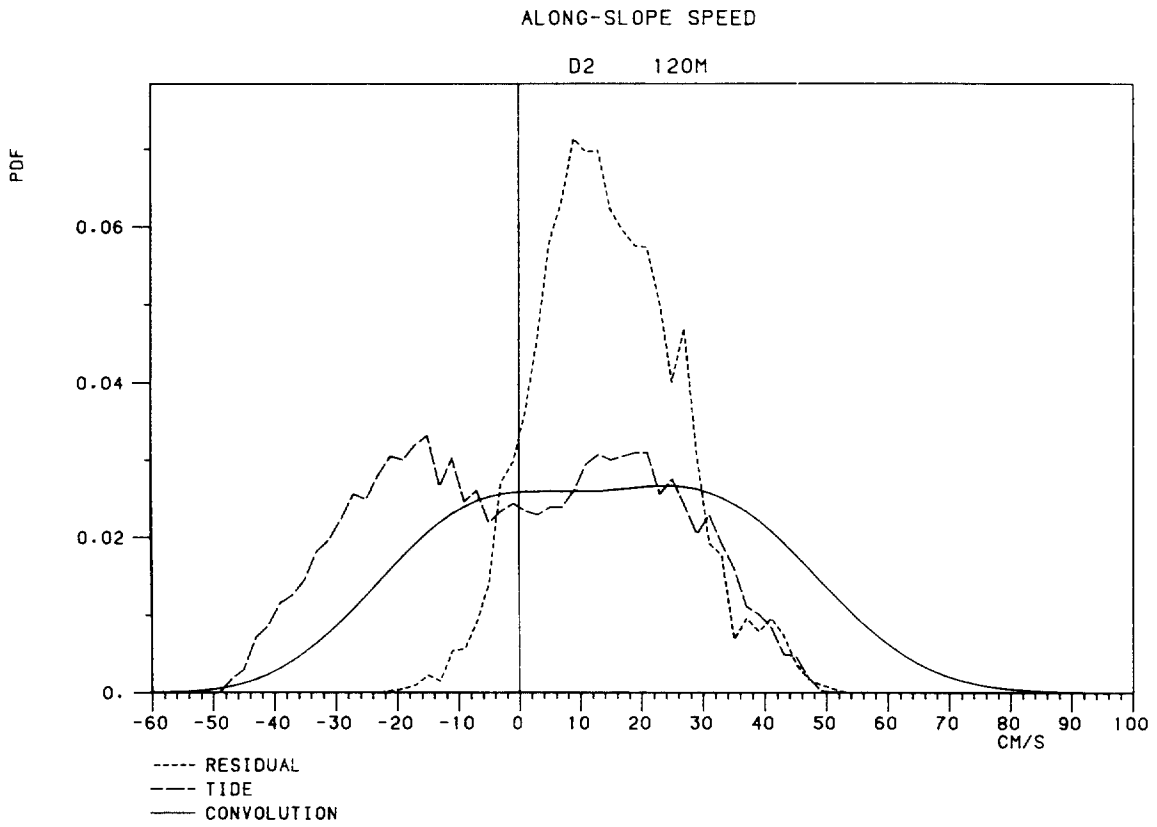


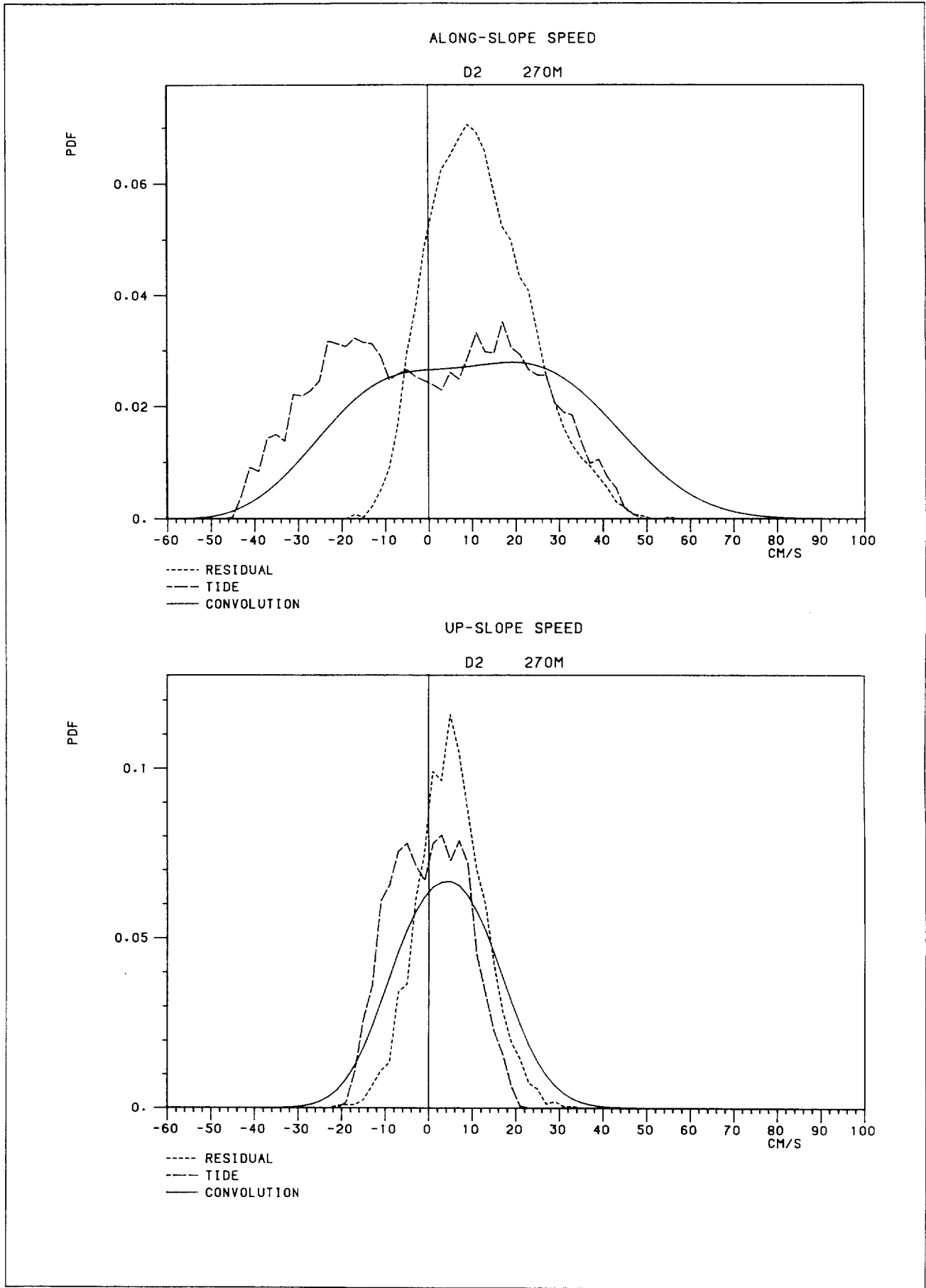


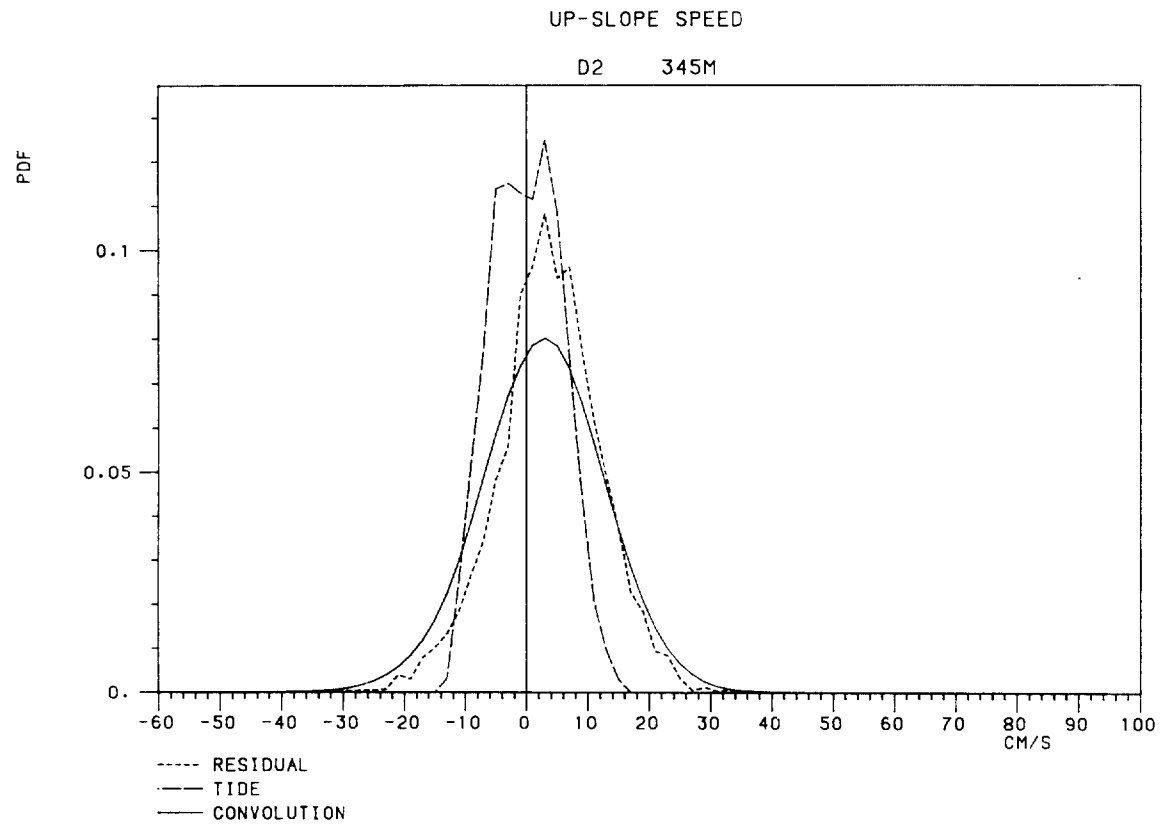
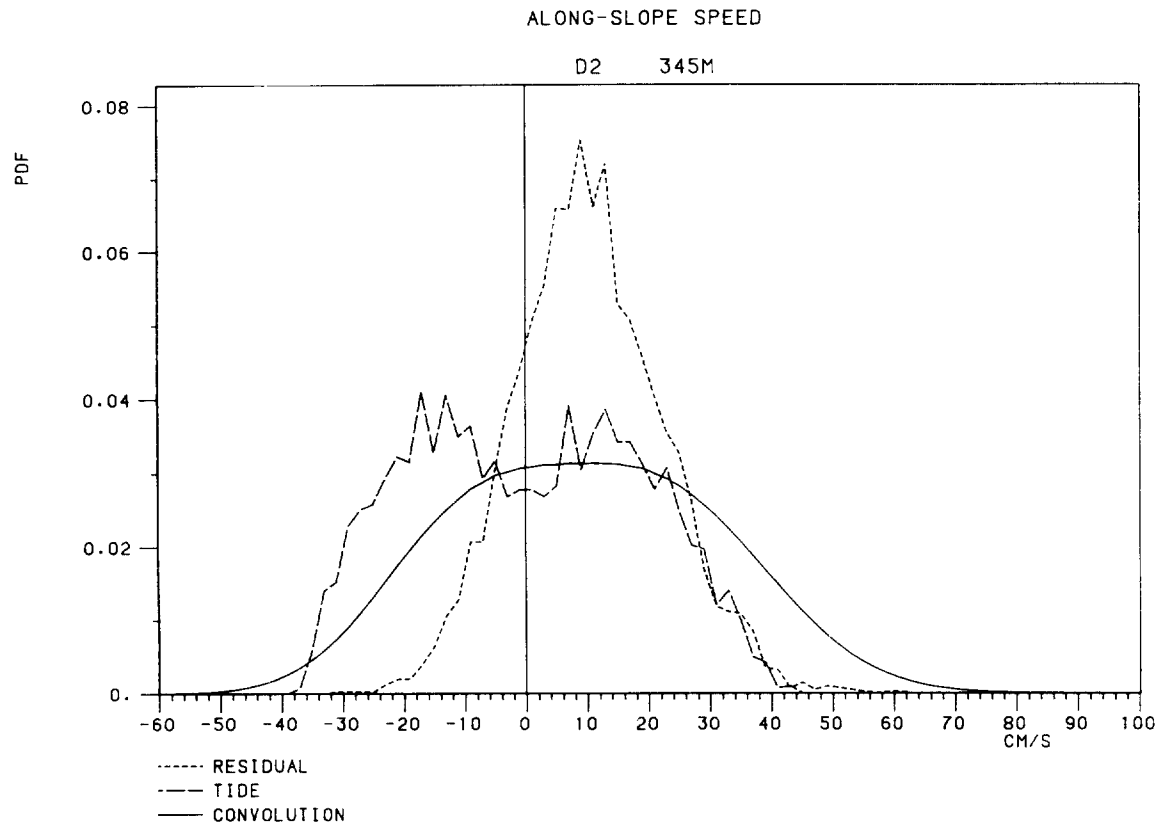


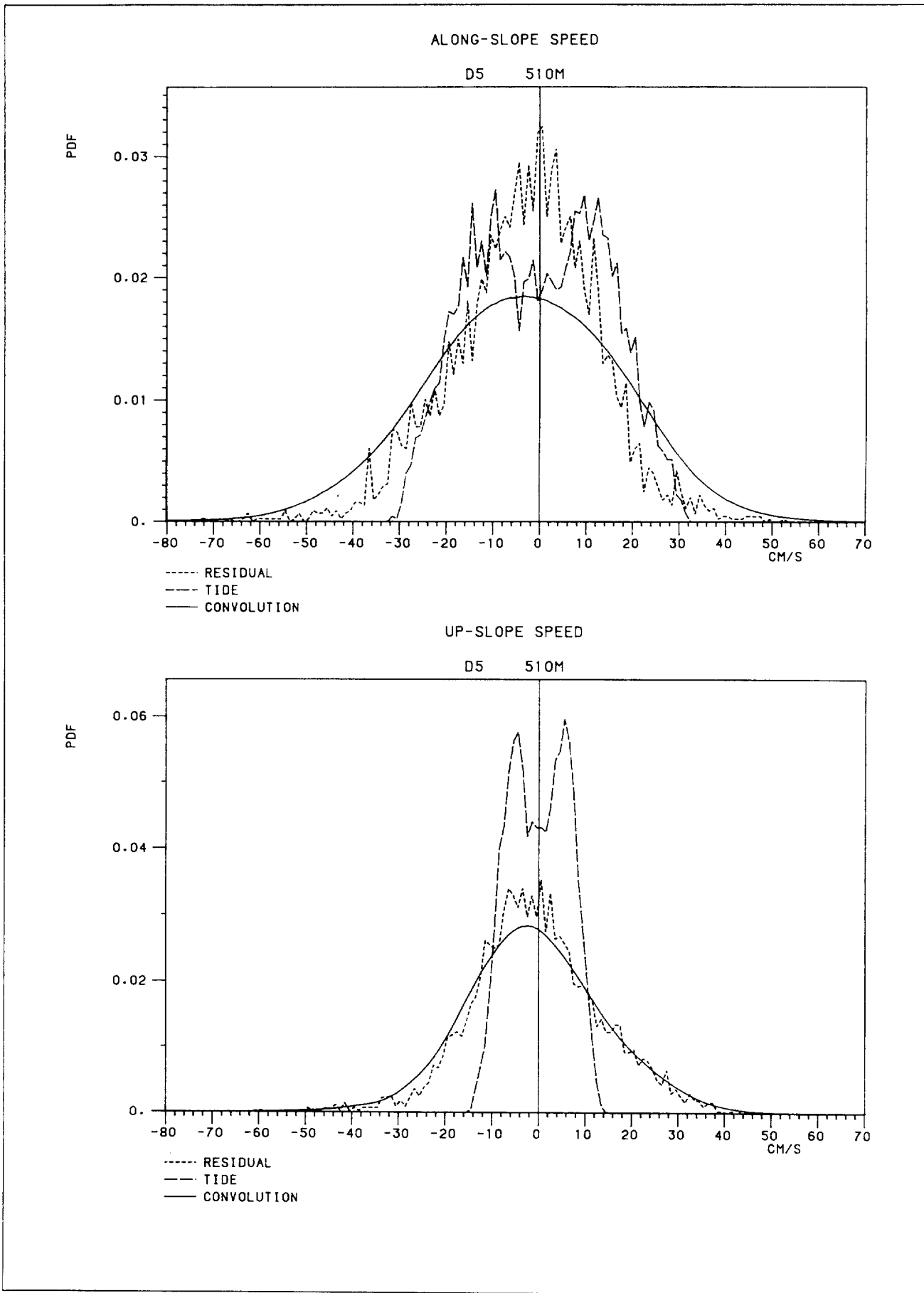






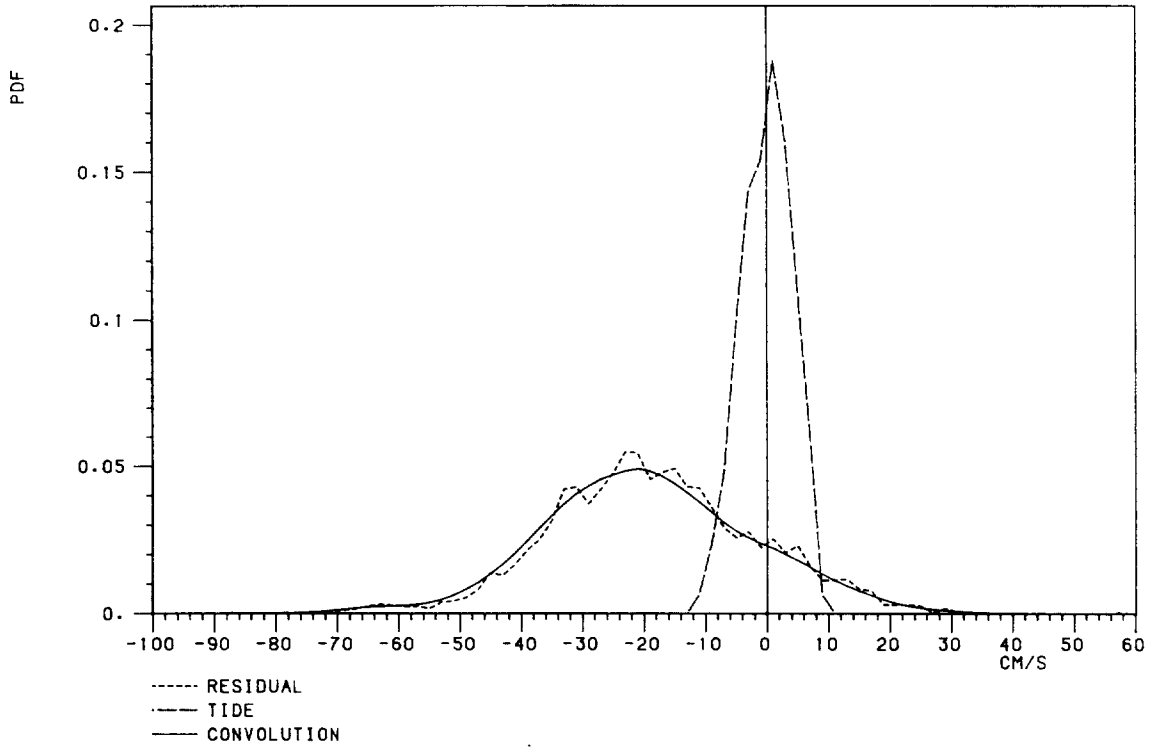






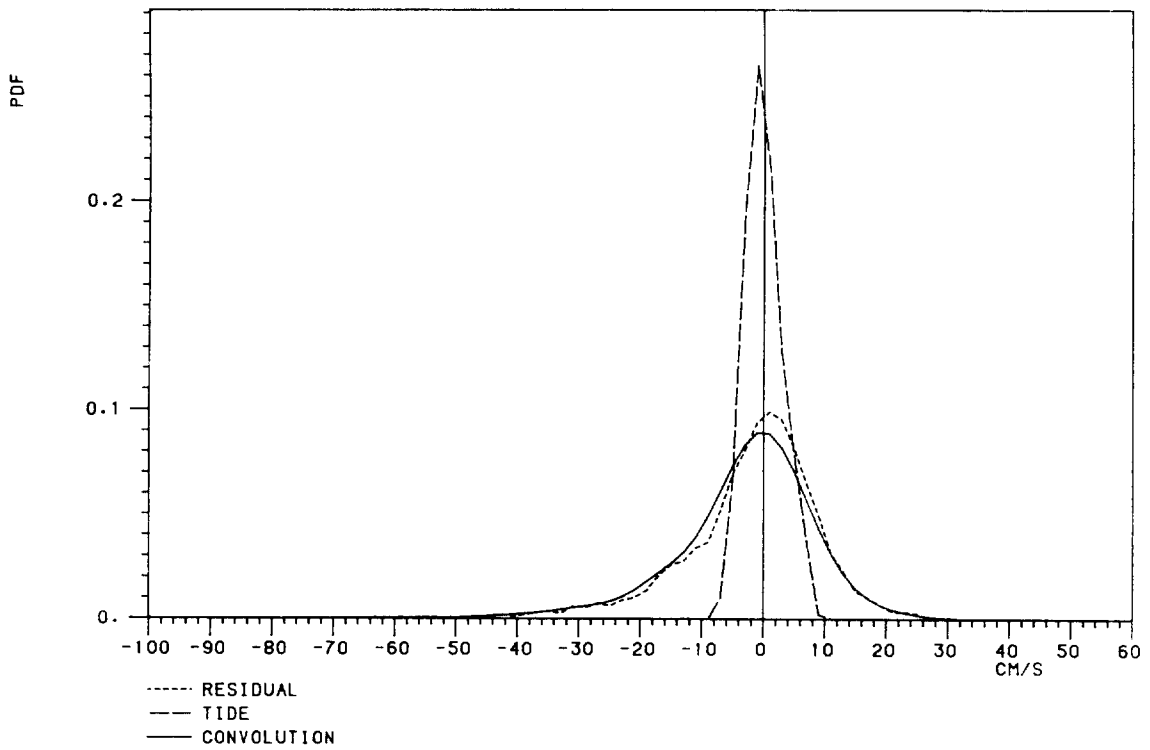
ALONG-SLOPE SPEED

D5 633M



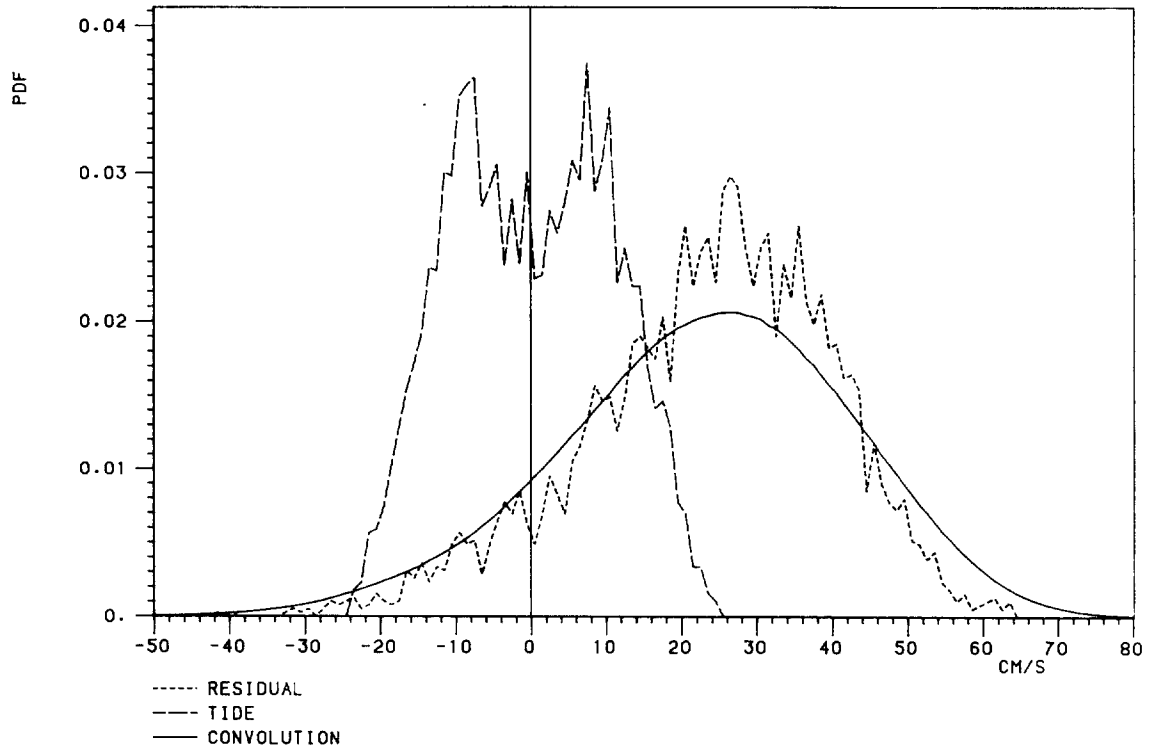
UP-SLOPE SPEED

D5 633M



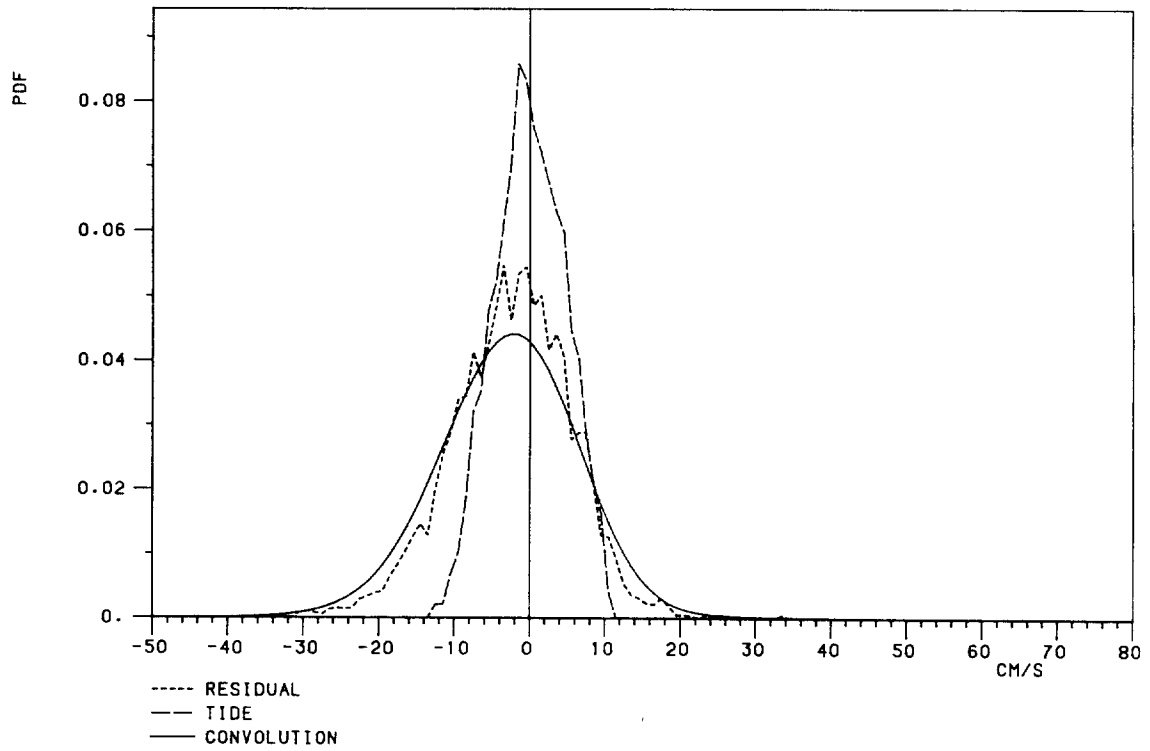
ALONG-SLOPE SPEED

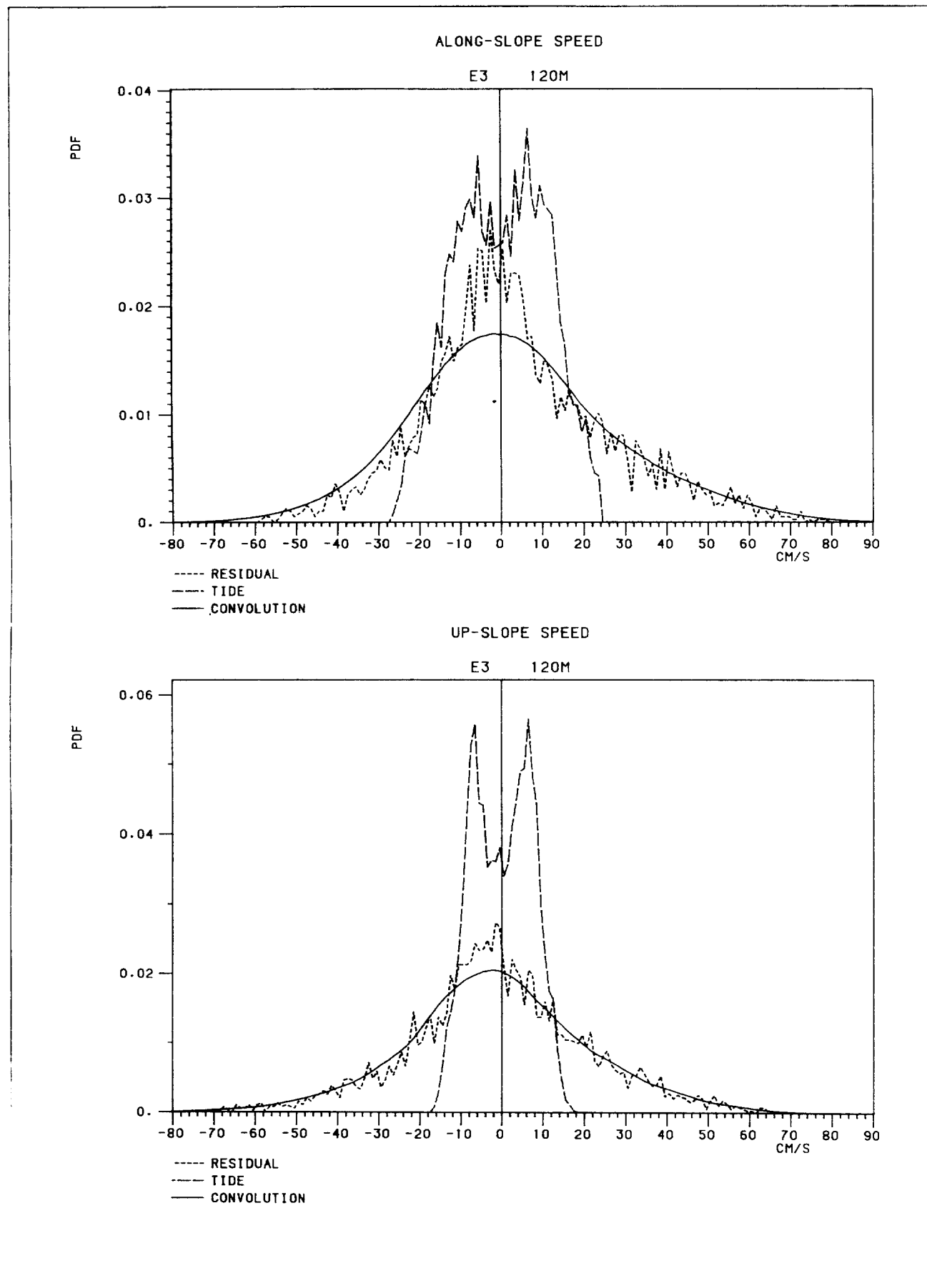
E2 453M

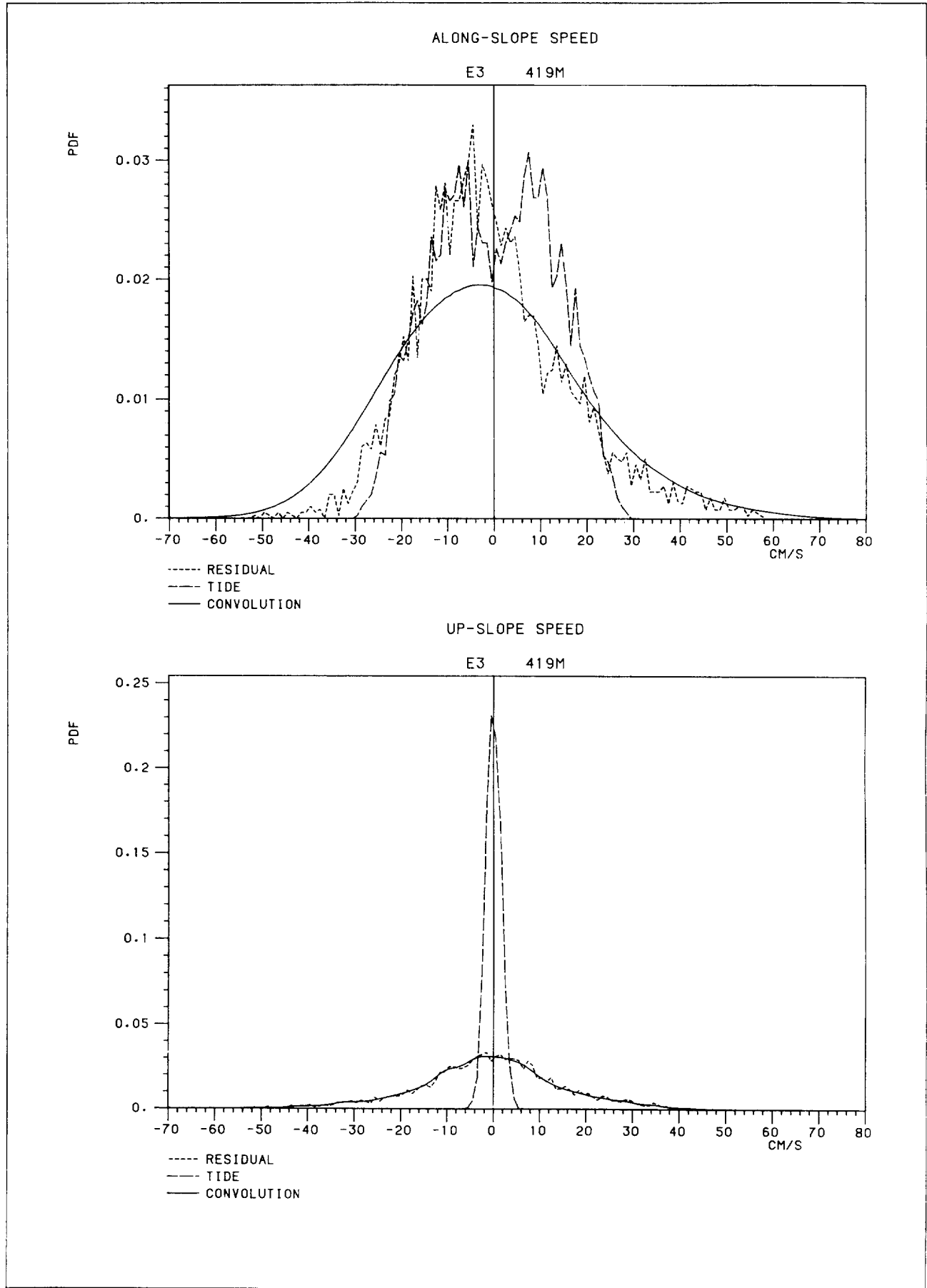


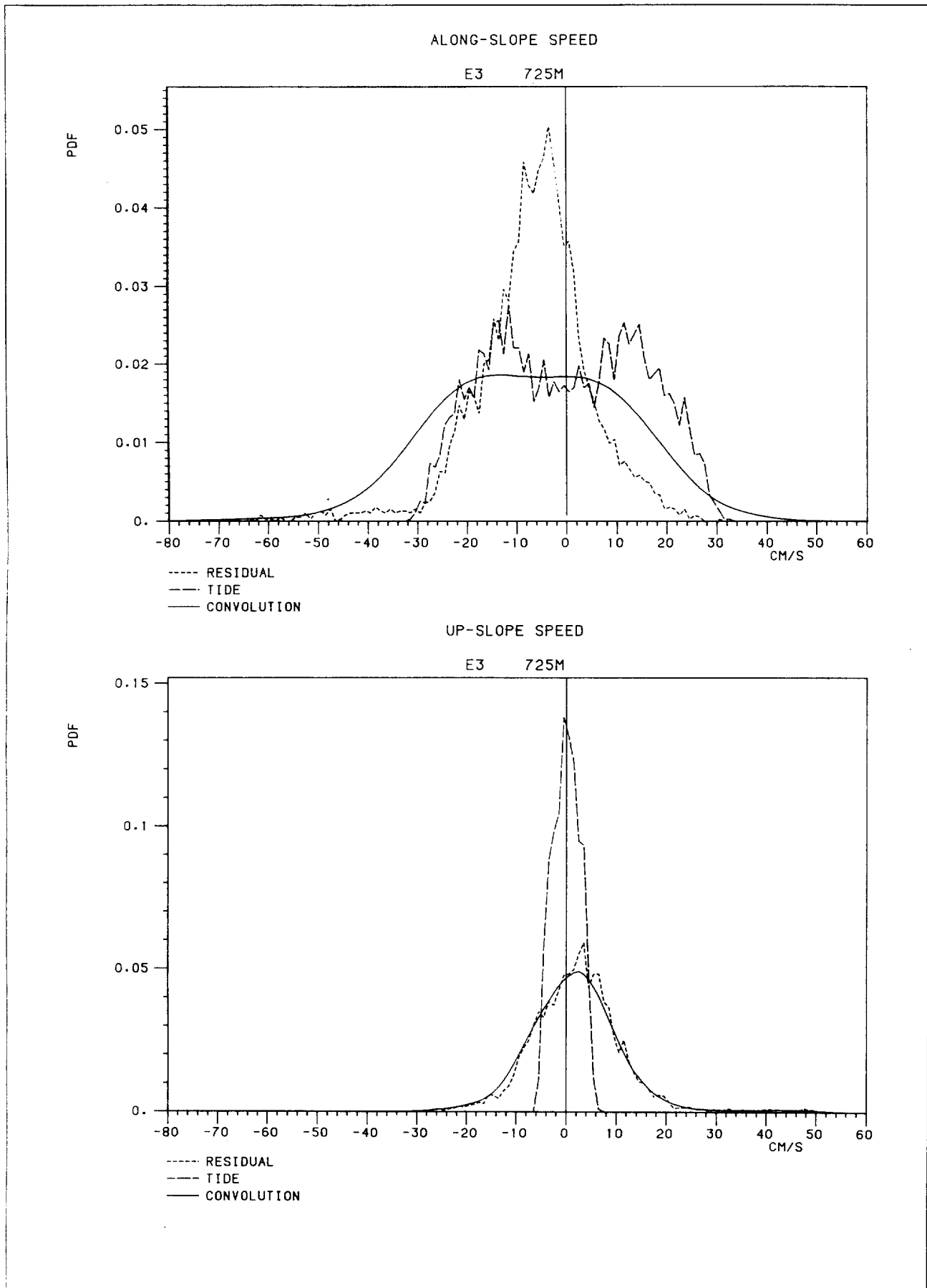
UP-SLOPE SPEED

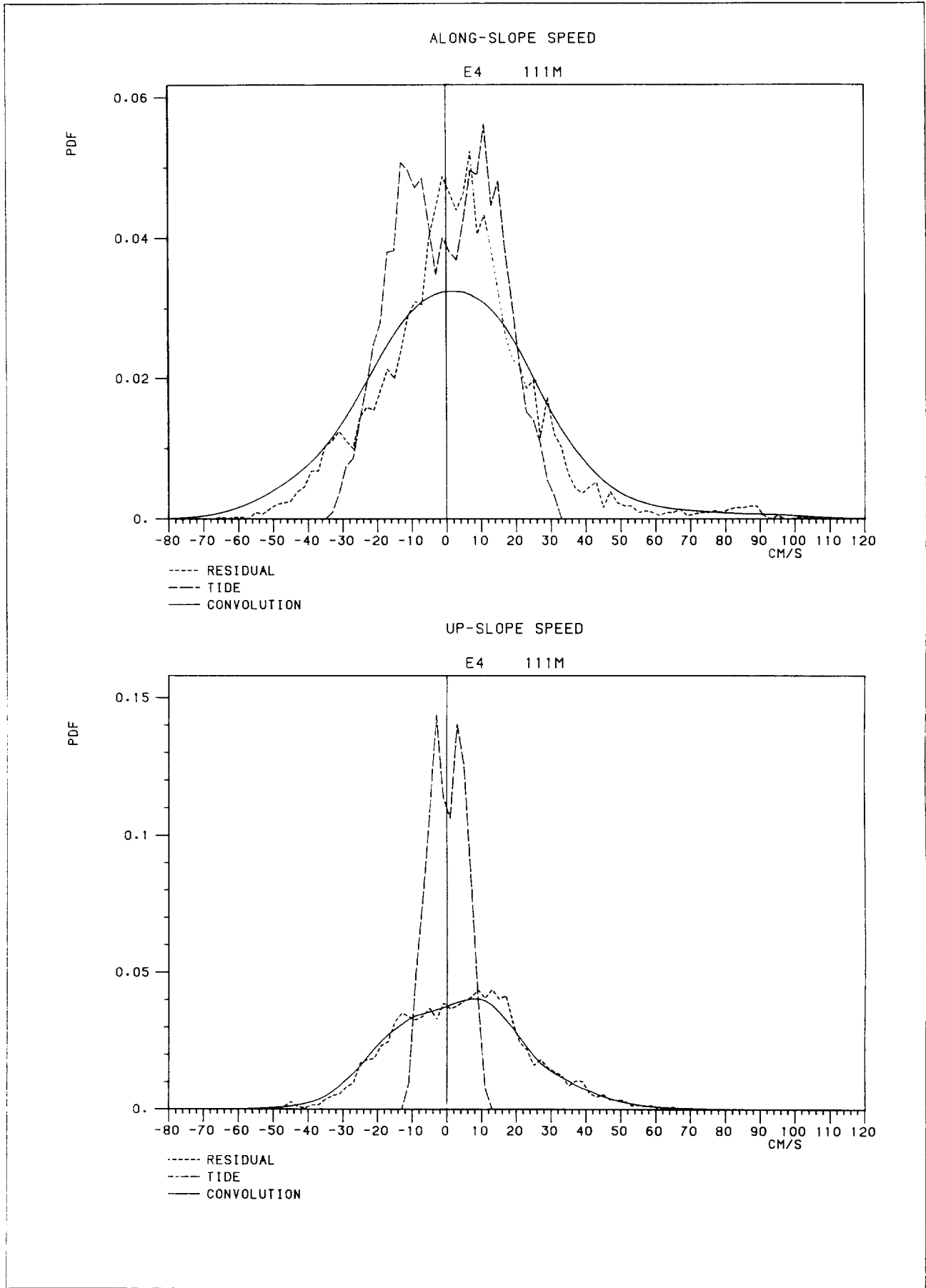
E2 453M

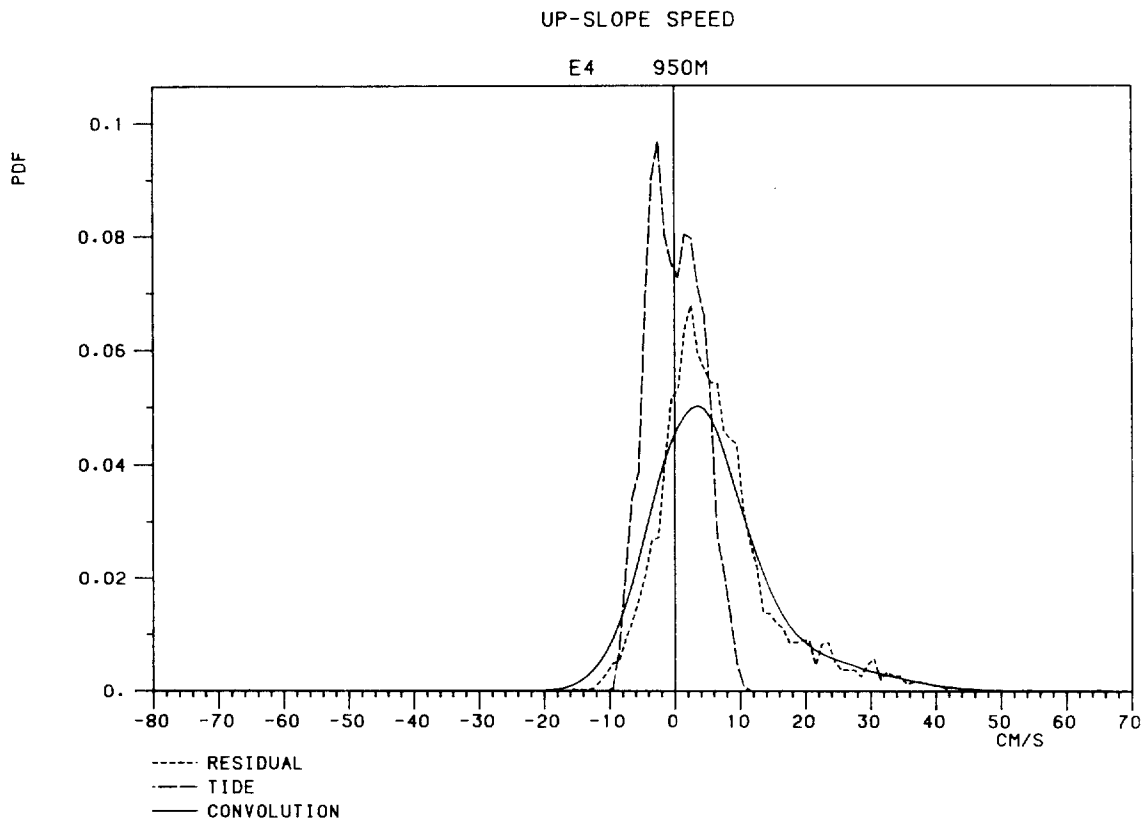
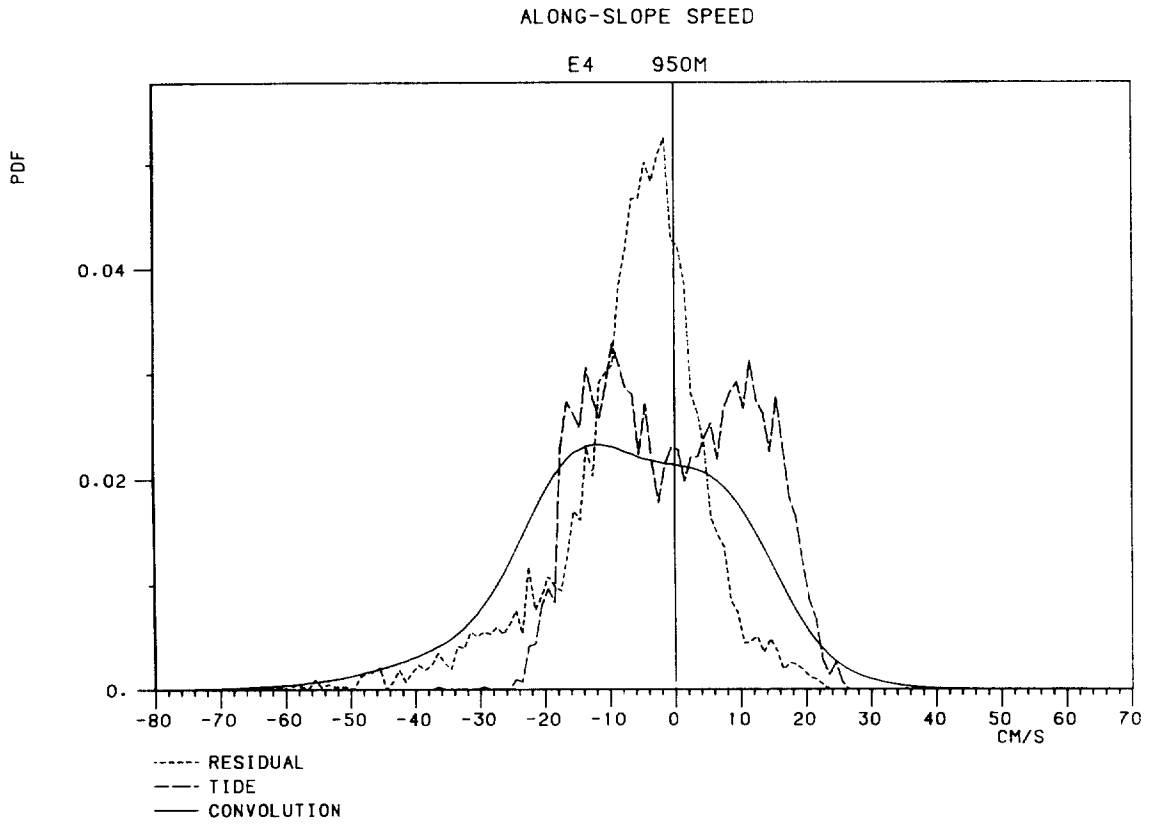


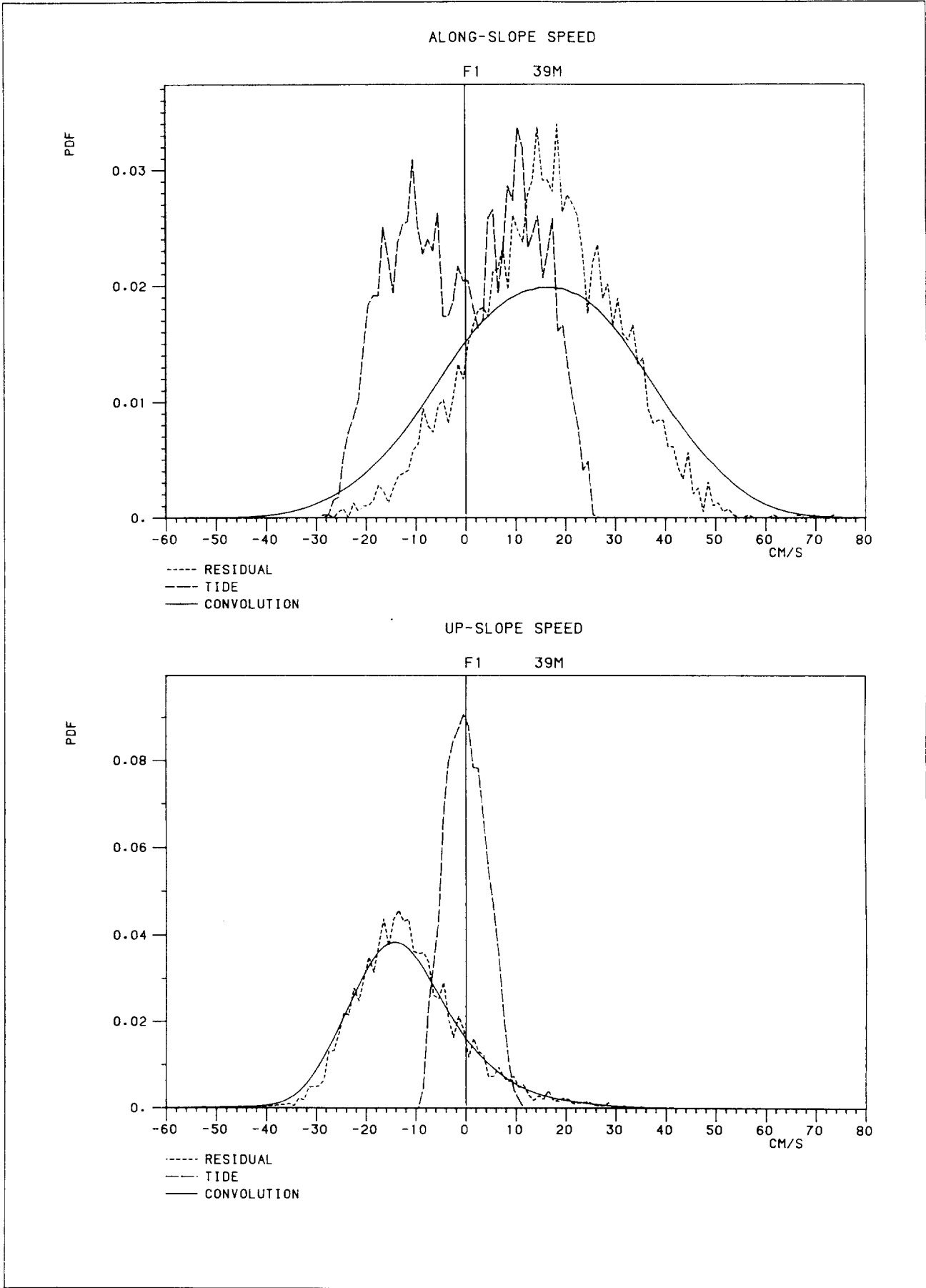


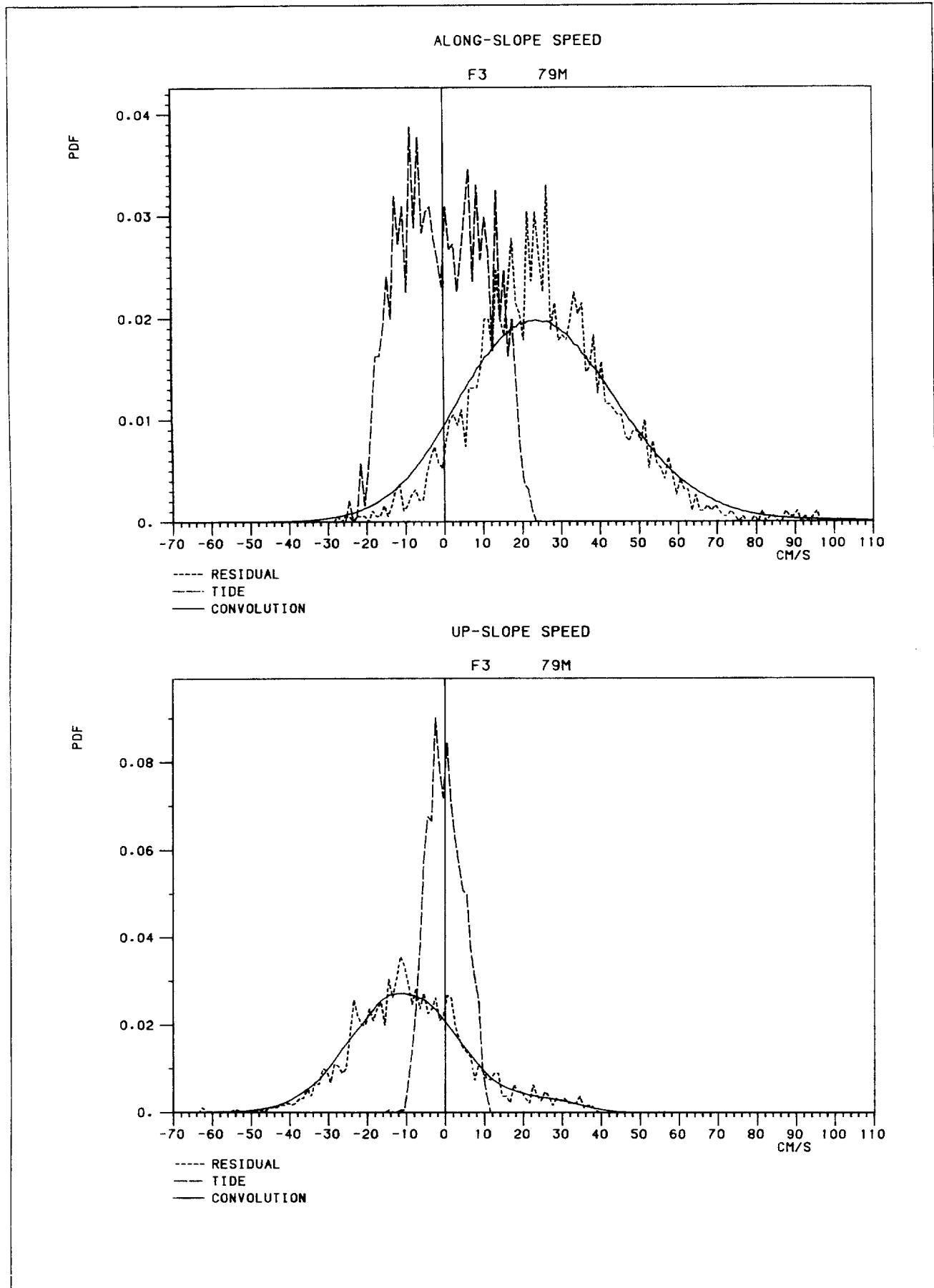


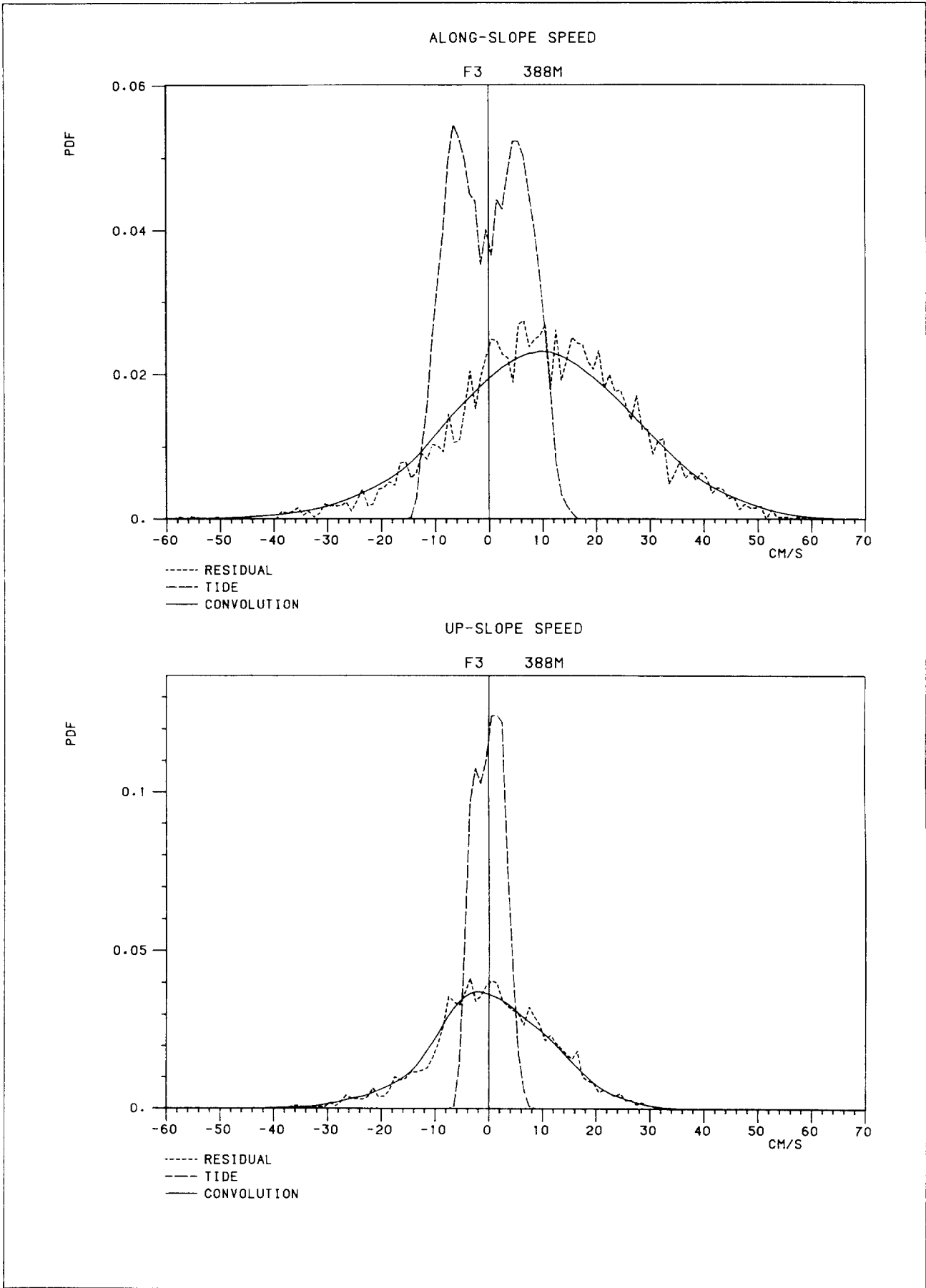


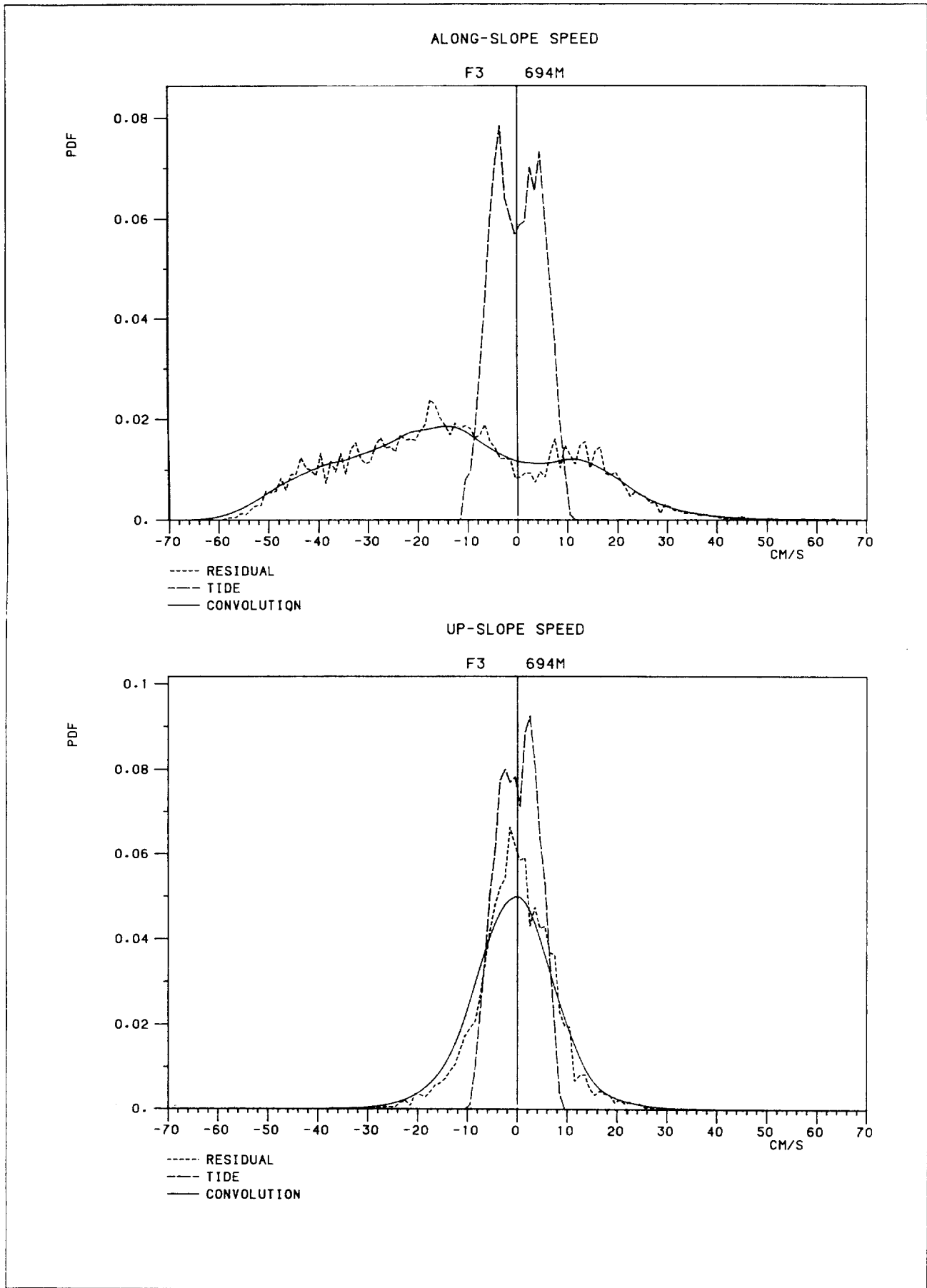


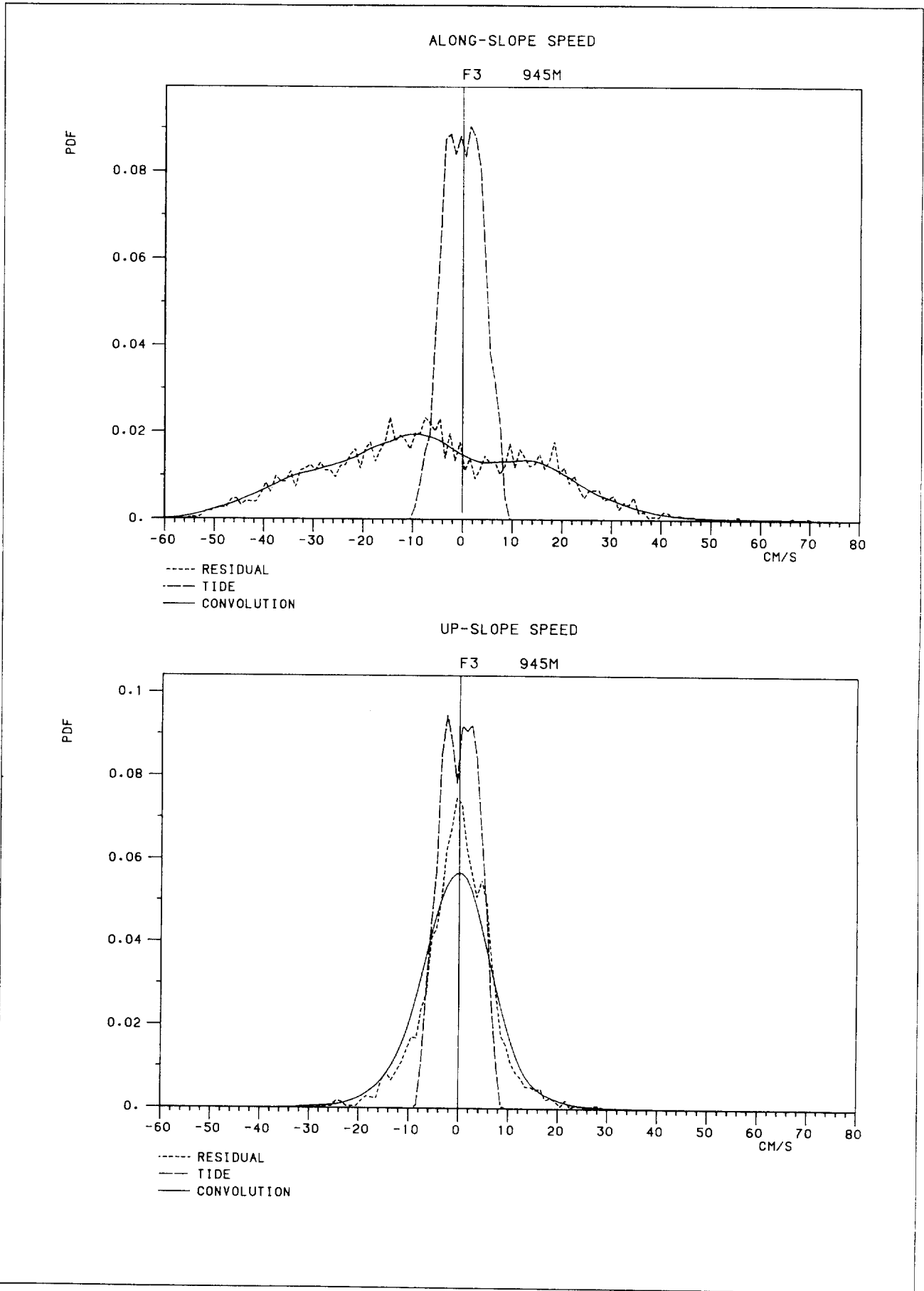






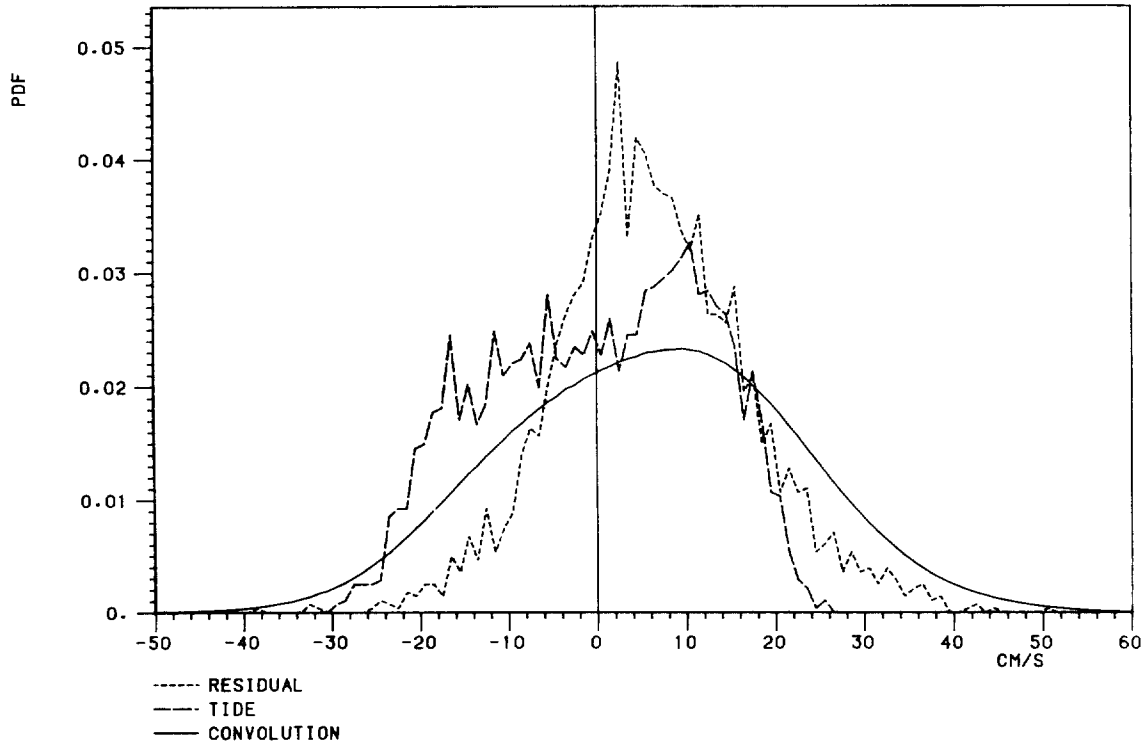






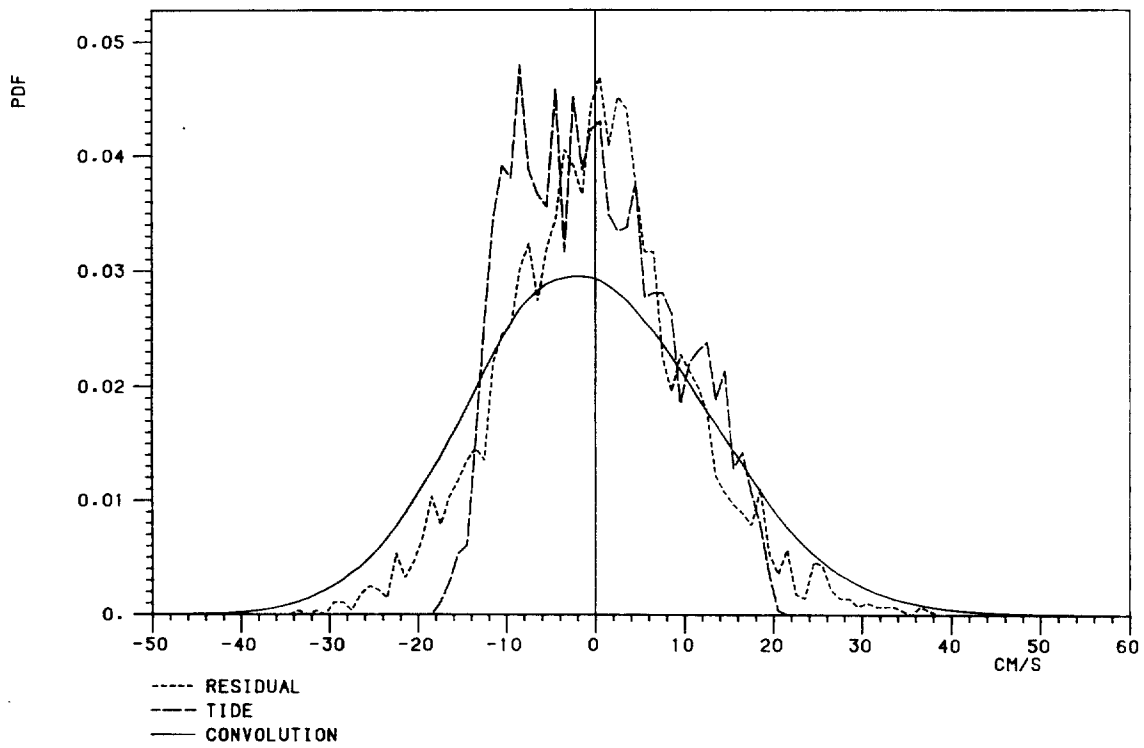
ALONG-SLOPE SPEED

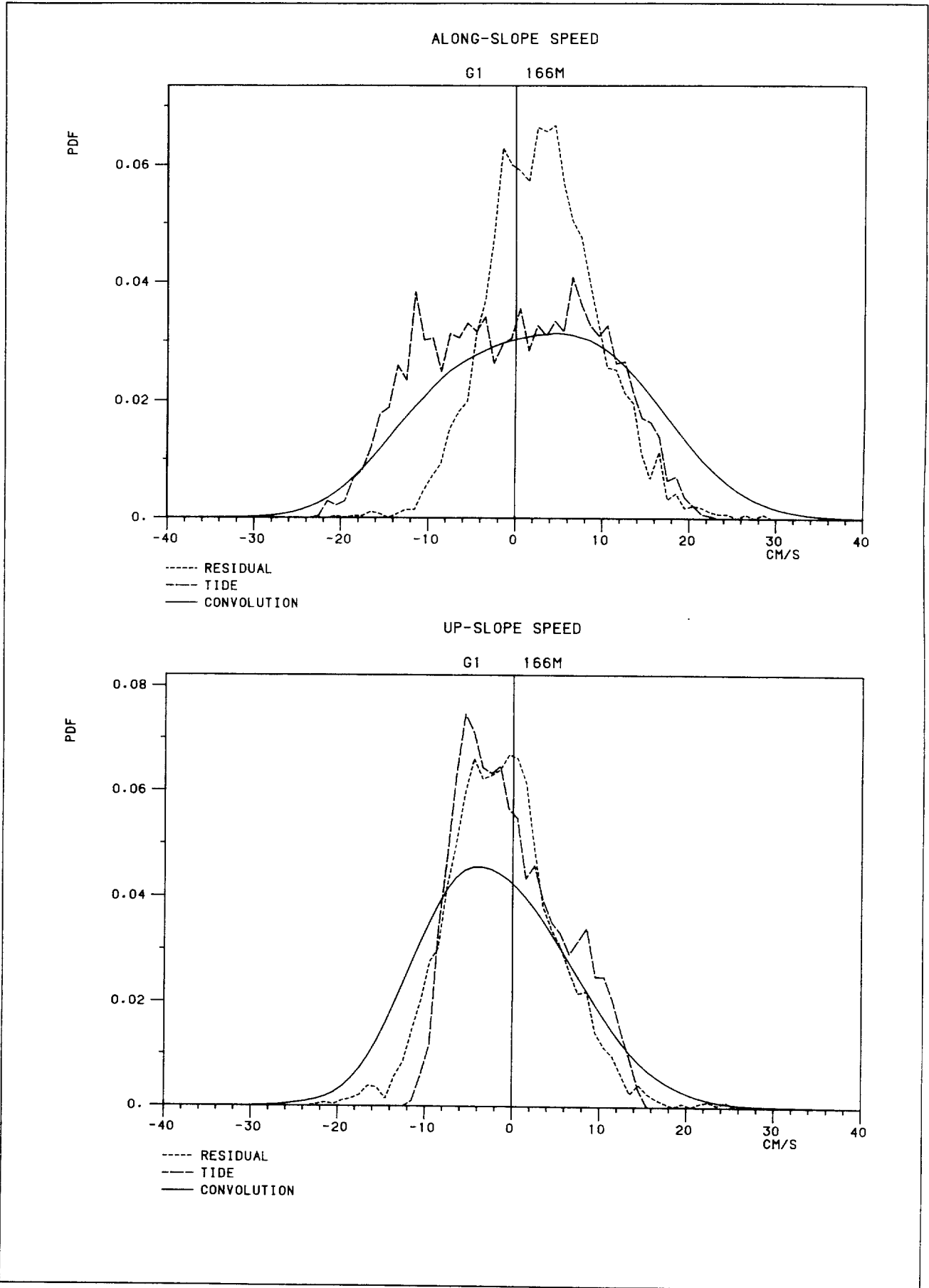
G1 41M



UP-SLOPE SPEED

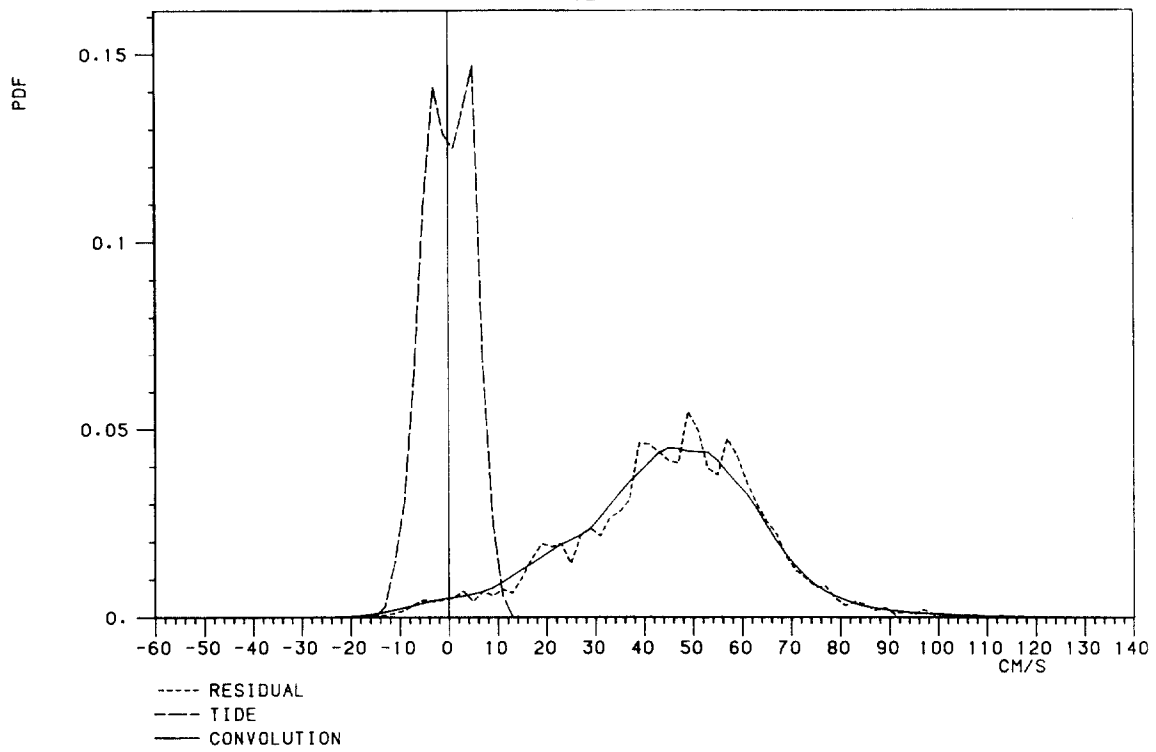
G1 41M





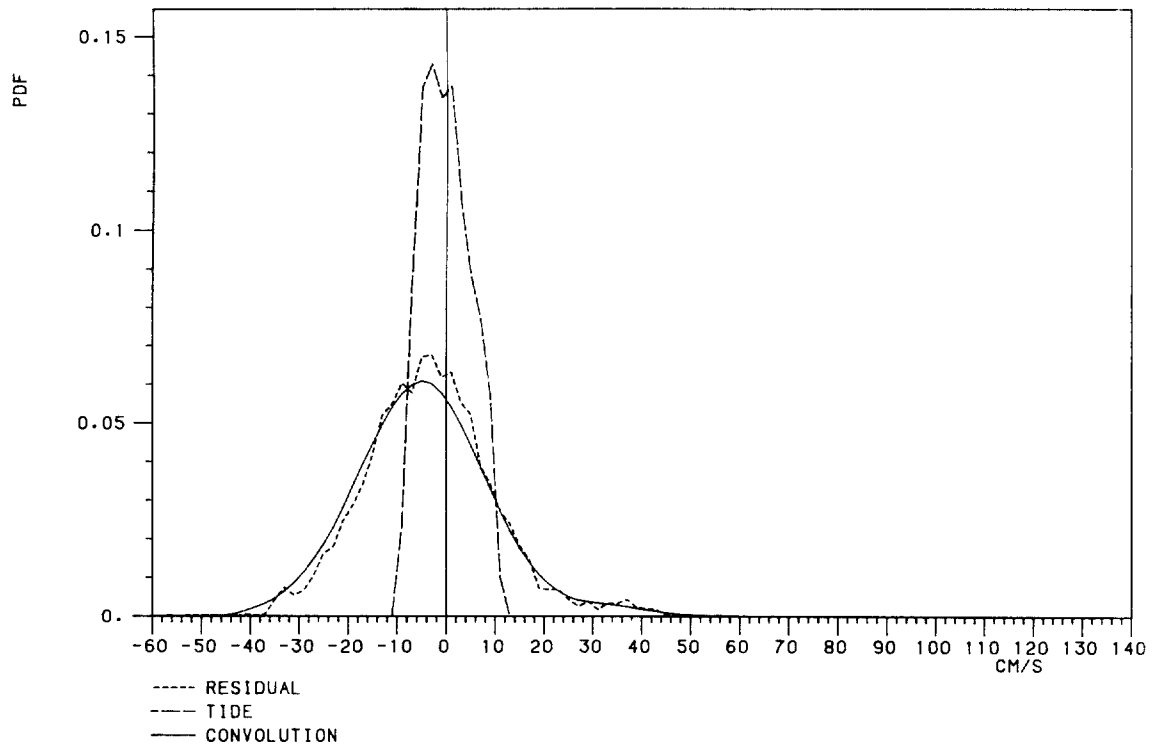
ALONG-SLOPE SPEED

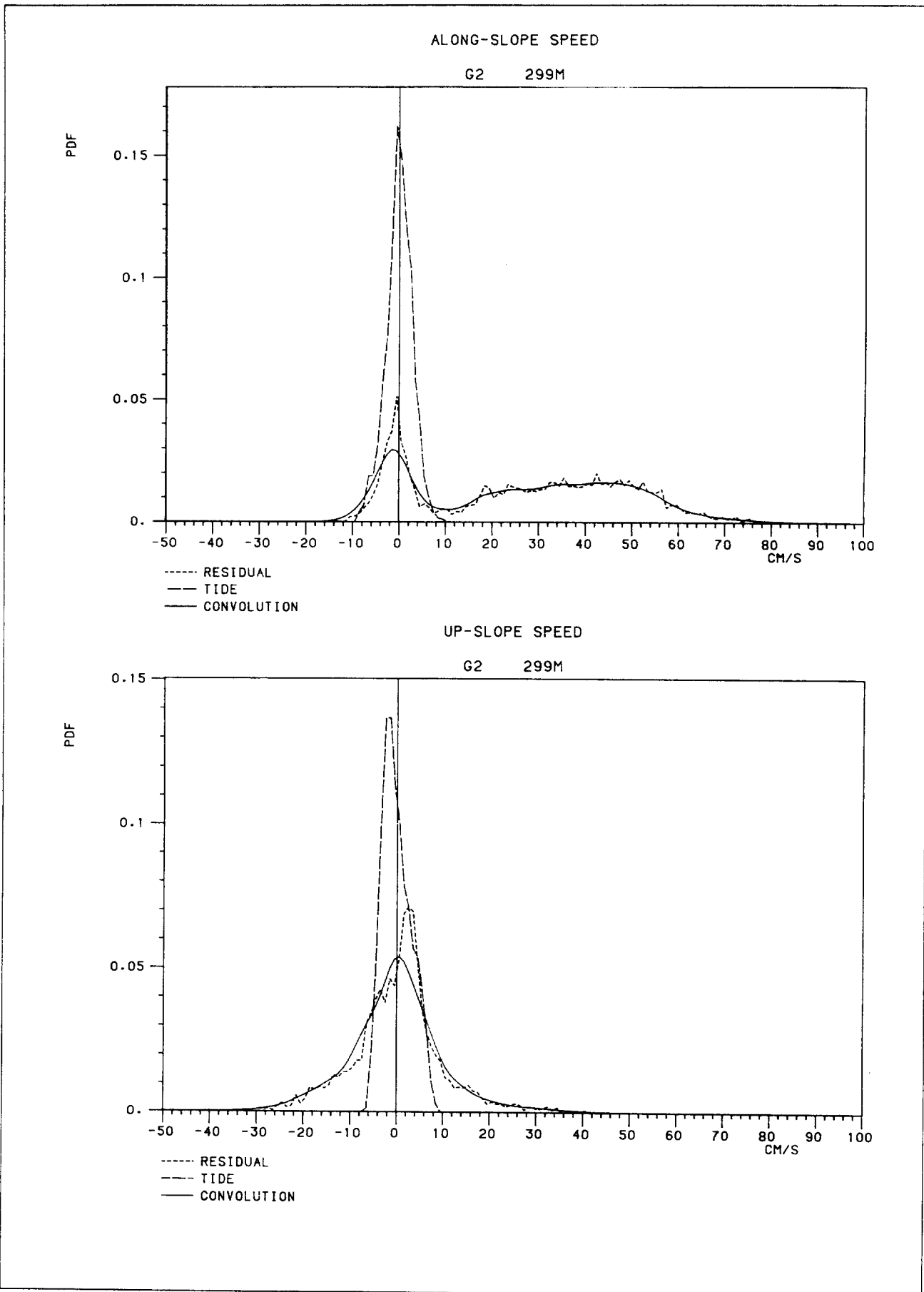
G2 151M



UP-SLOPE SPEED

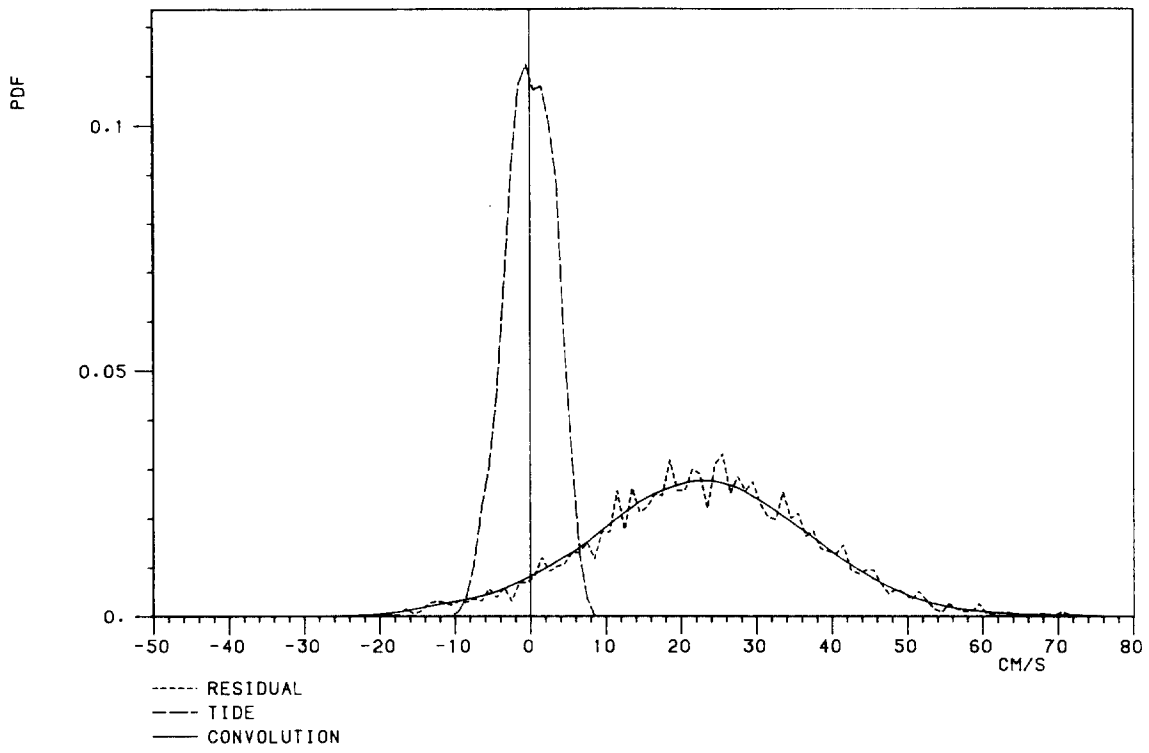
G2 151M





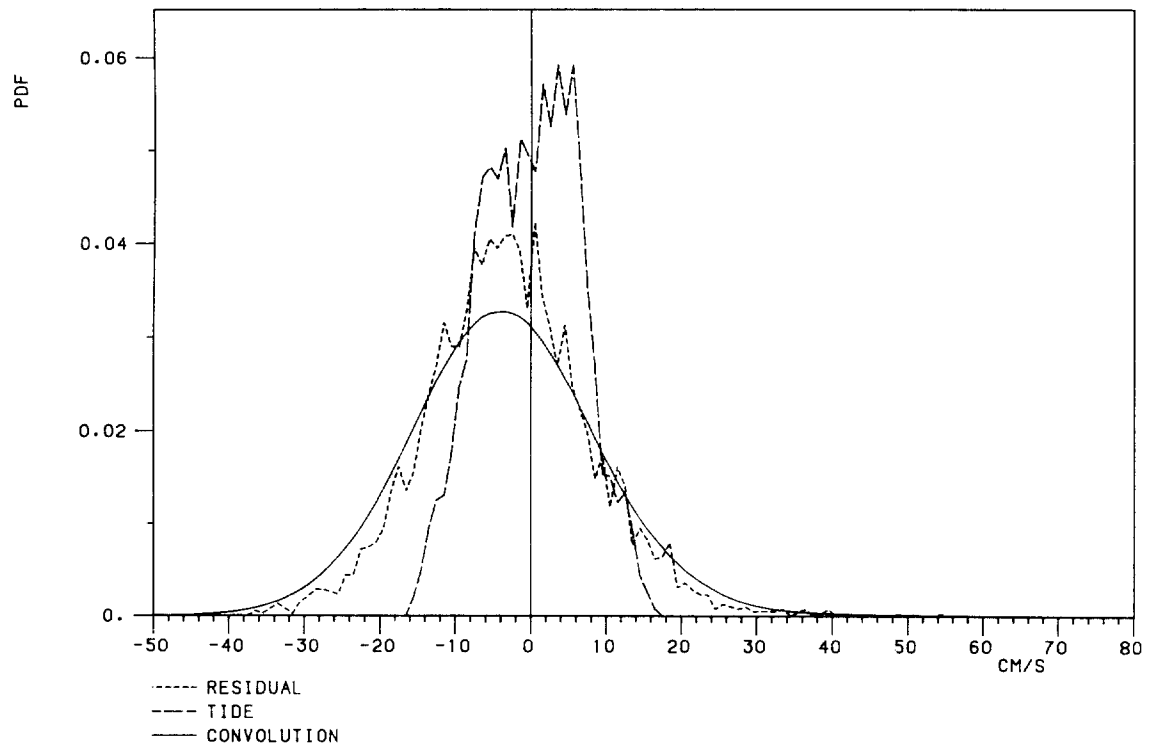
ALONG-SLOPE SPEED

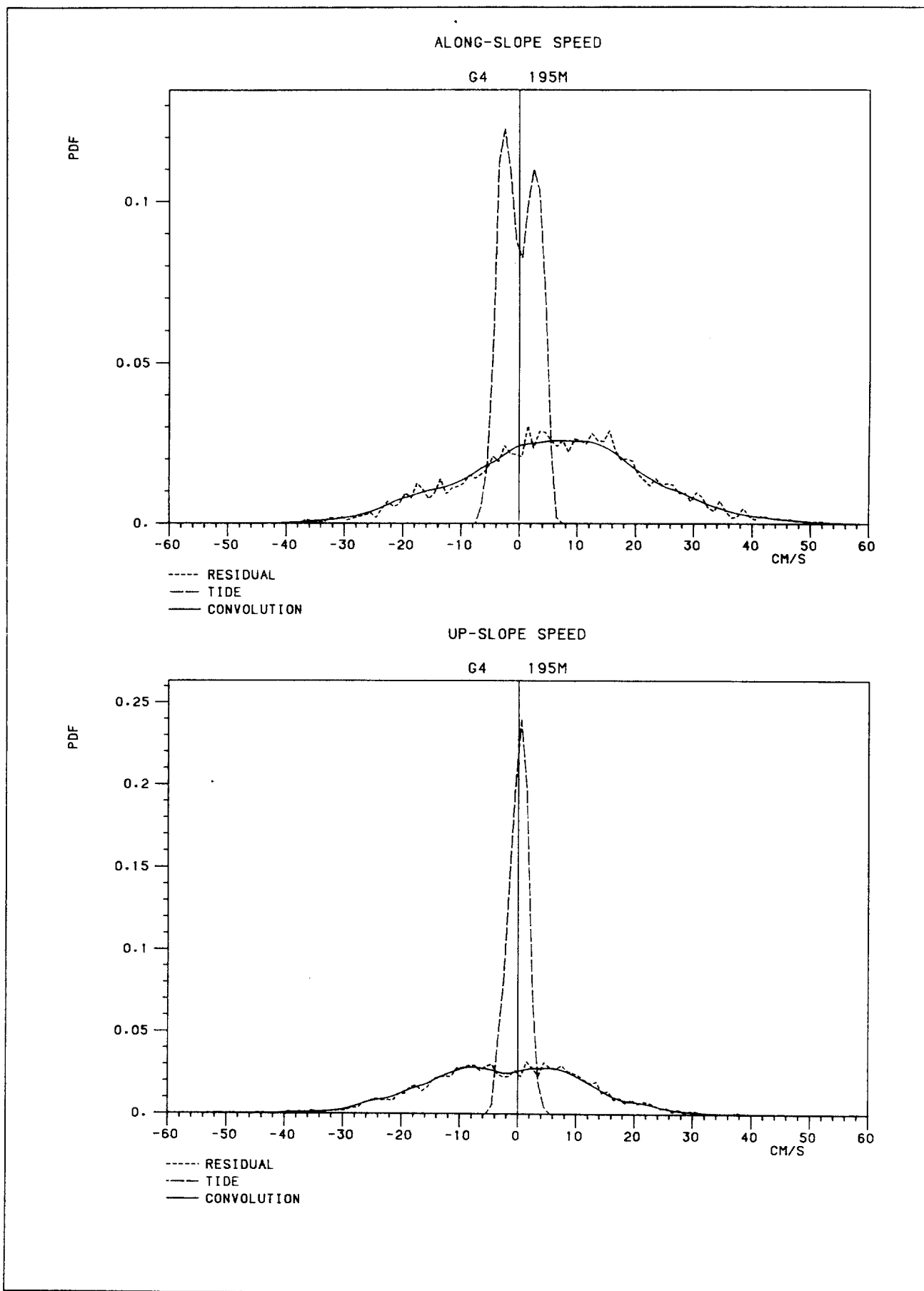
G2 500M



UP-SLOPE SPEED

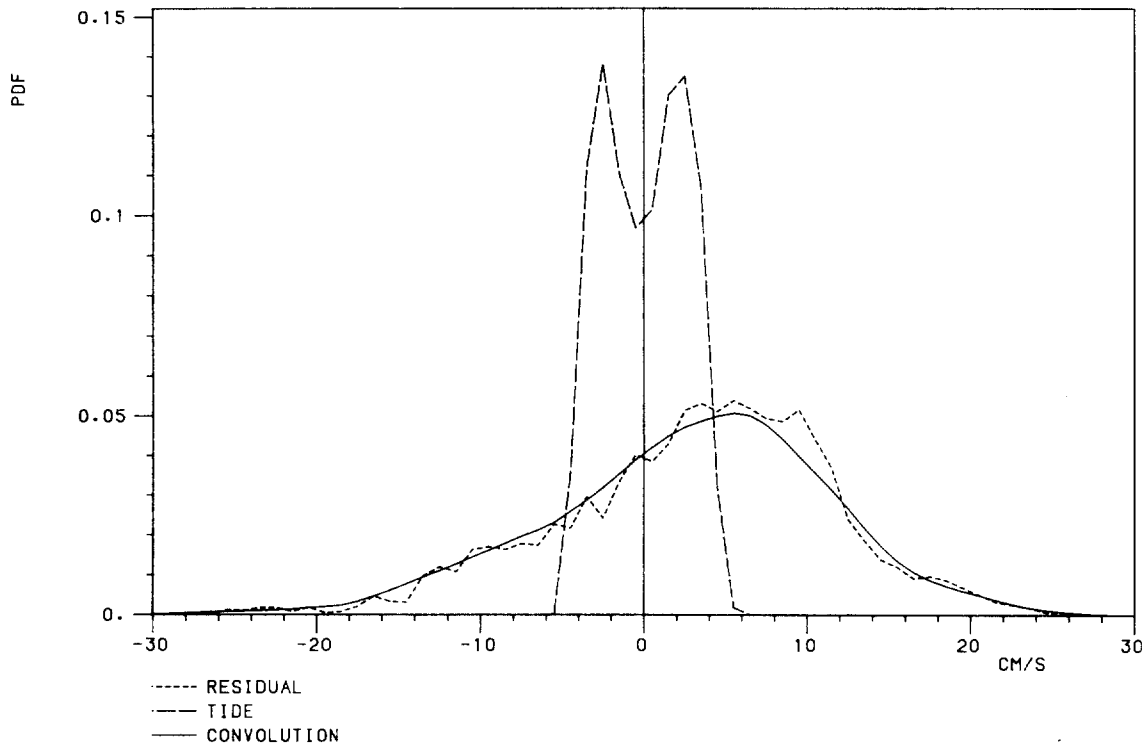
G2 500M





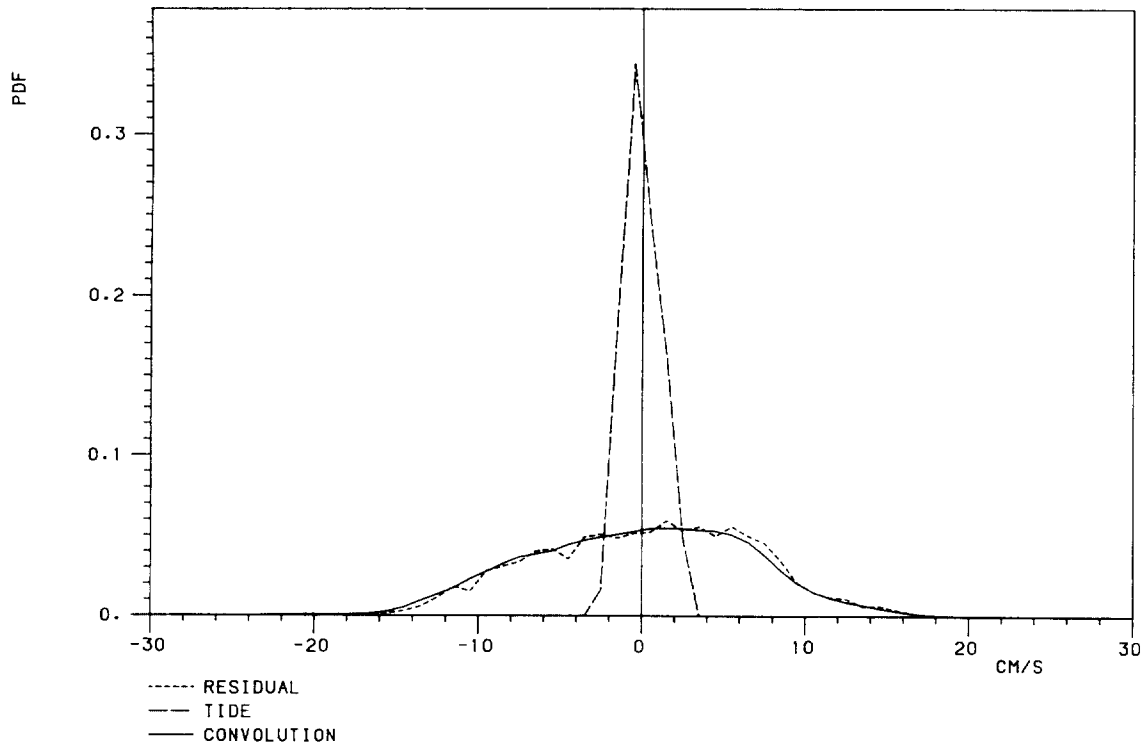
ALONG-SLOPE SPEED

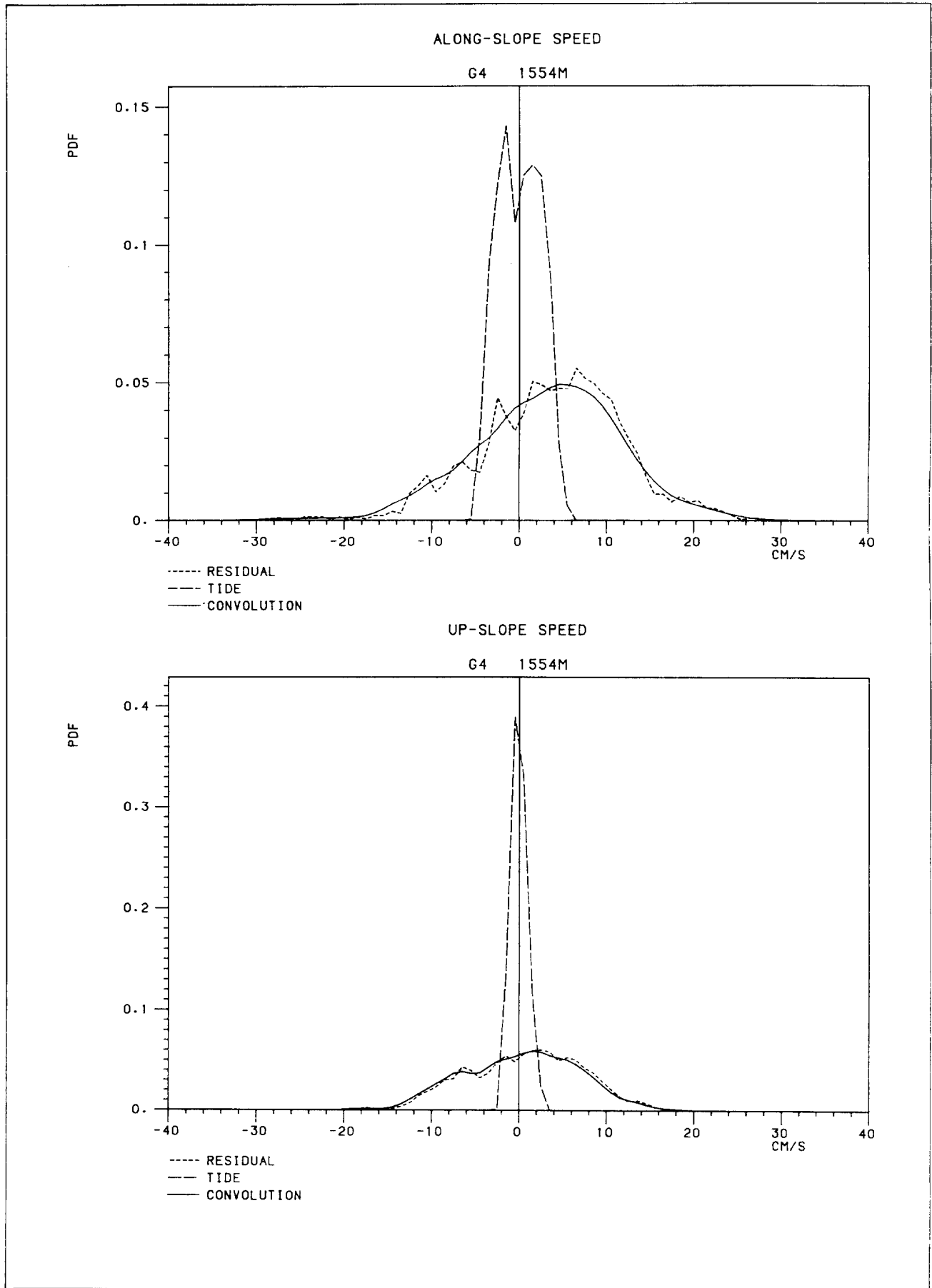
G4 1104M

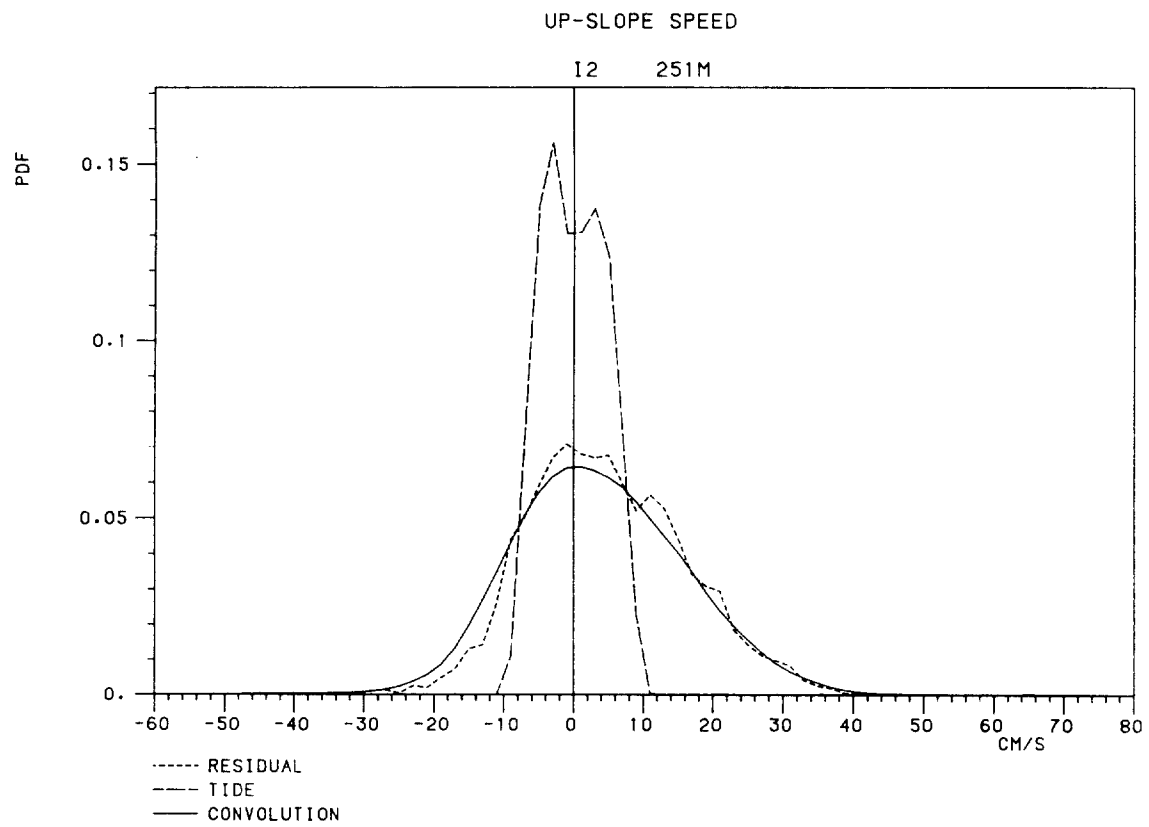
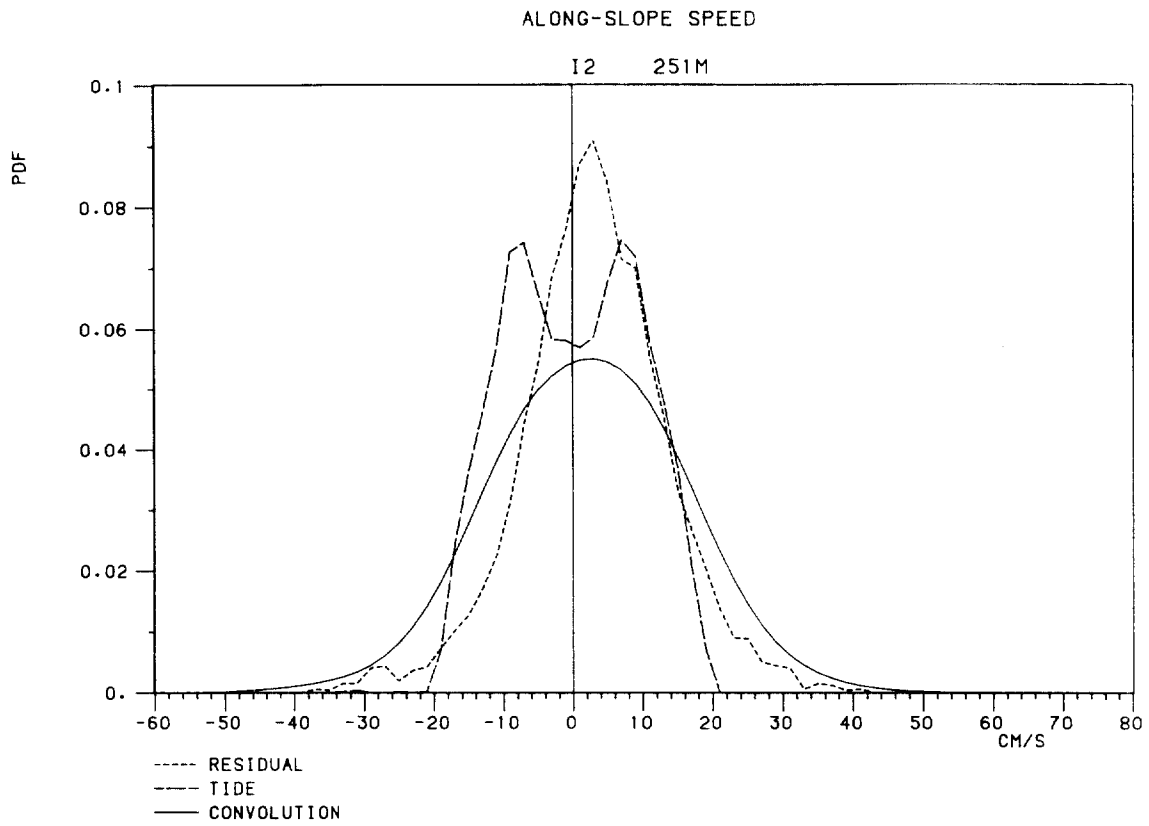


UP-SLOPE SPEED

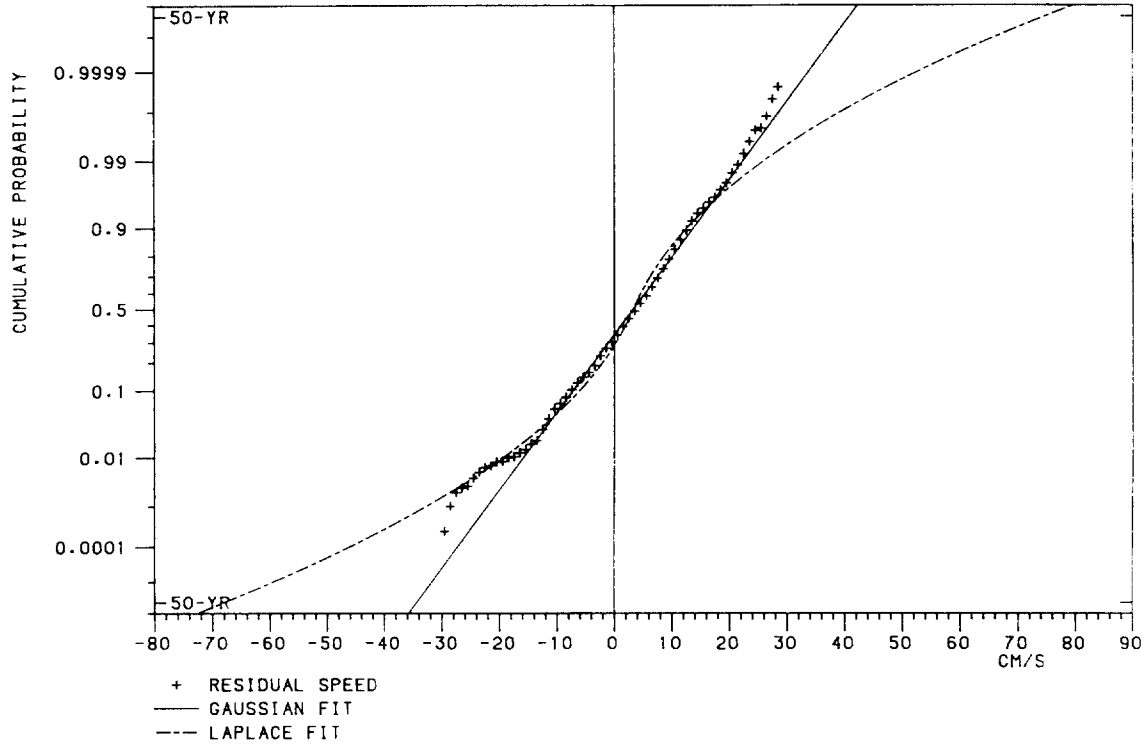
G4 1104M



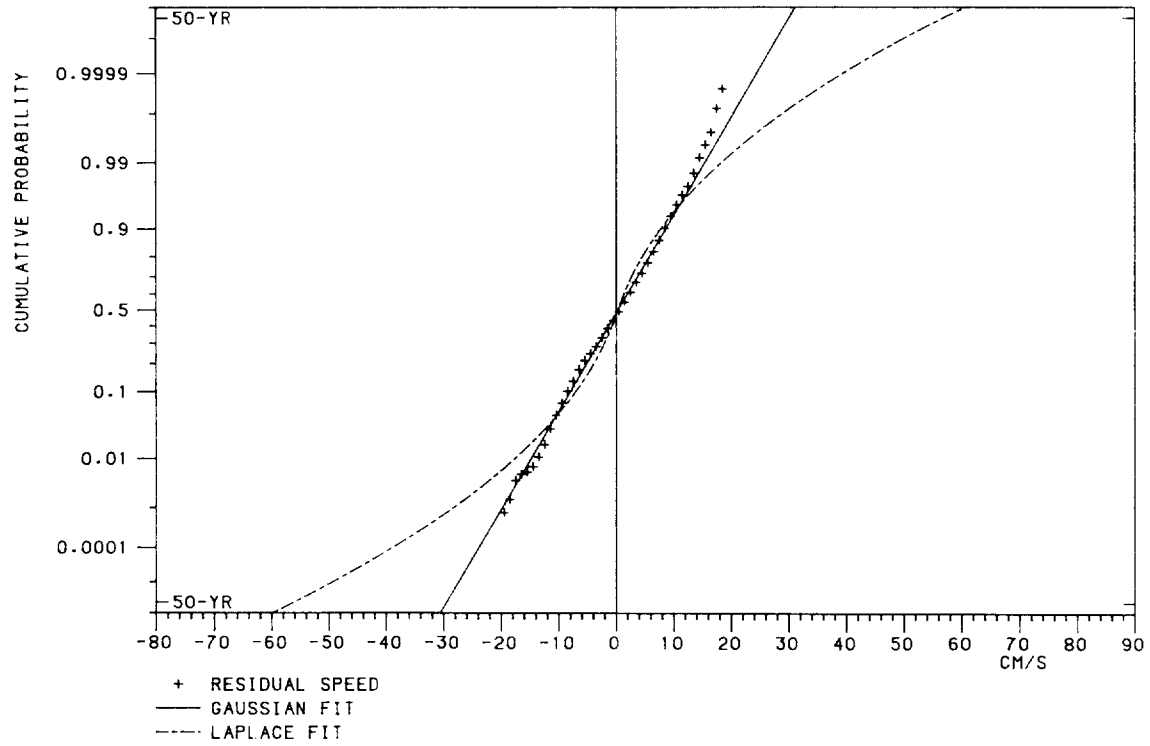




ALONG-SLOPE RESIDUAL
G4 1554M

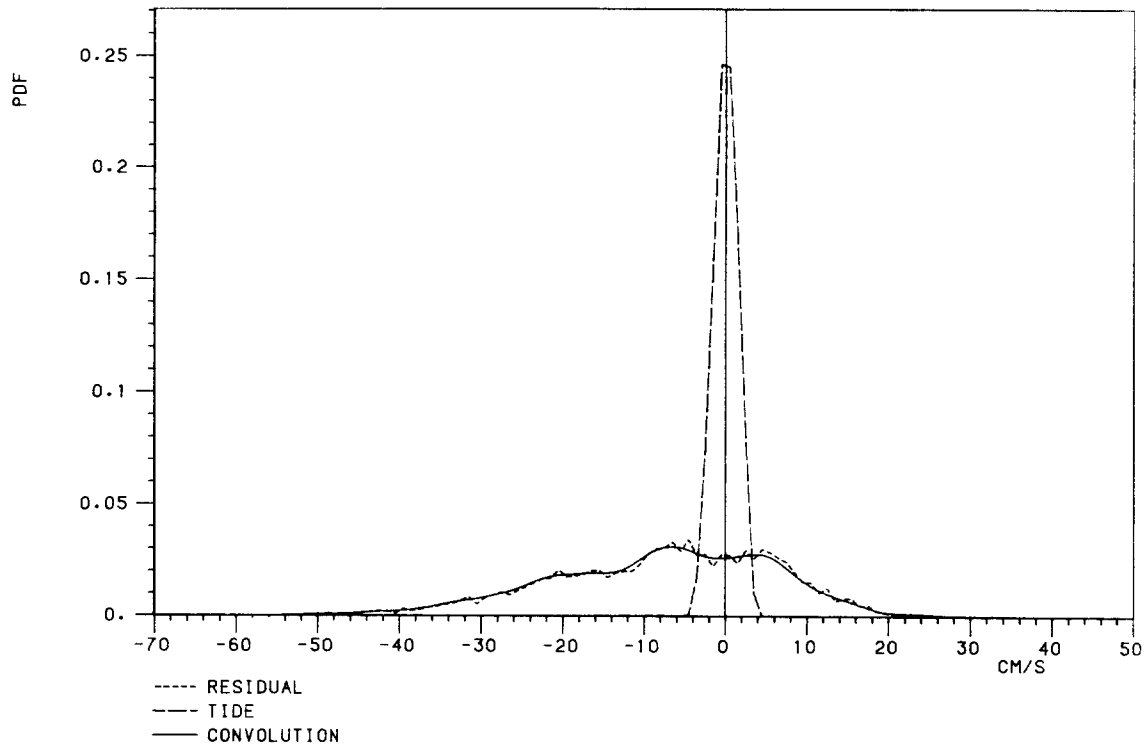


UP-SLOPE RESIDUAL
G4 1554M



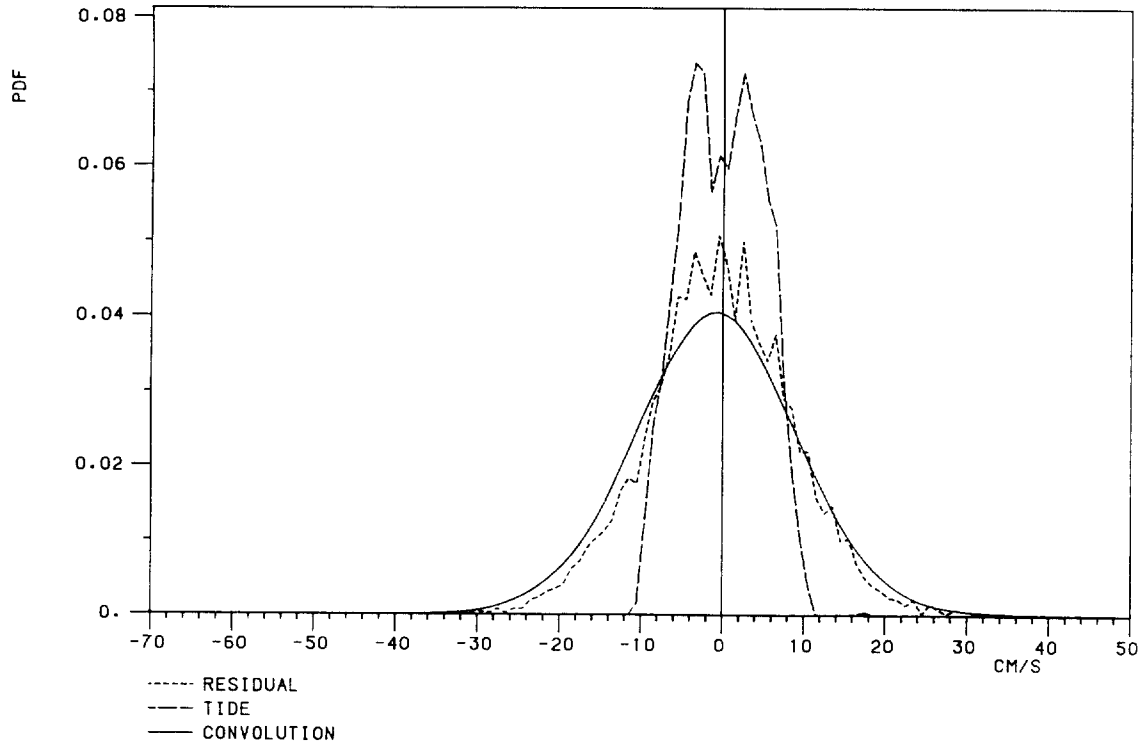
ALONG-SLOPE SPEED

I2 1055M



UP-SLOPE SPEED

I2 1055M



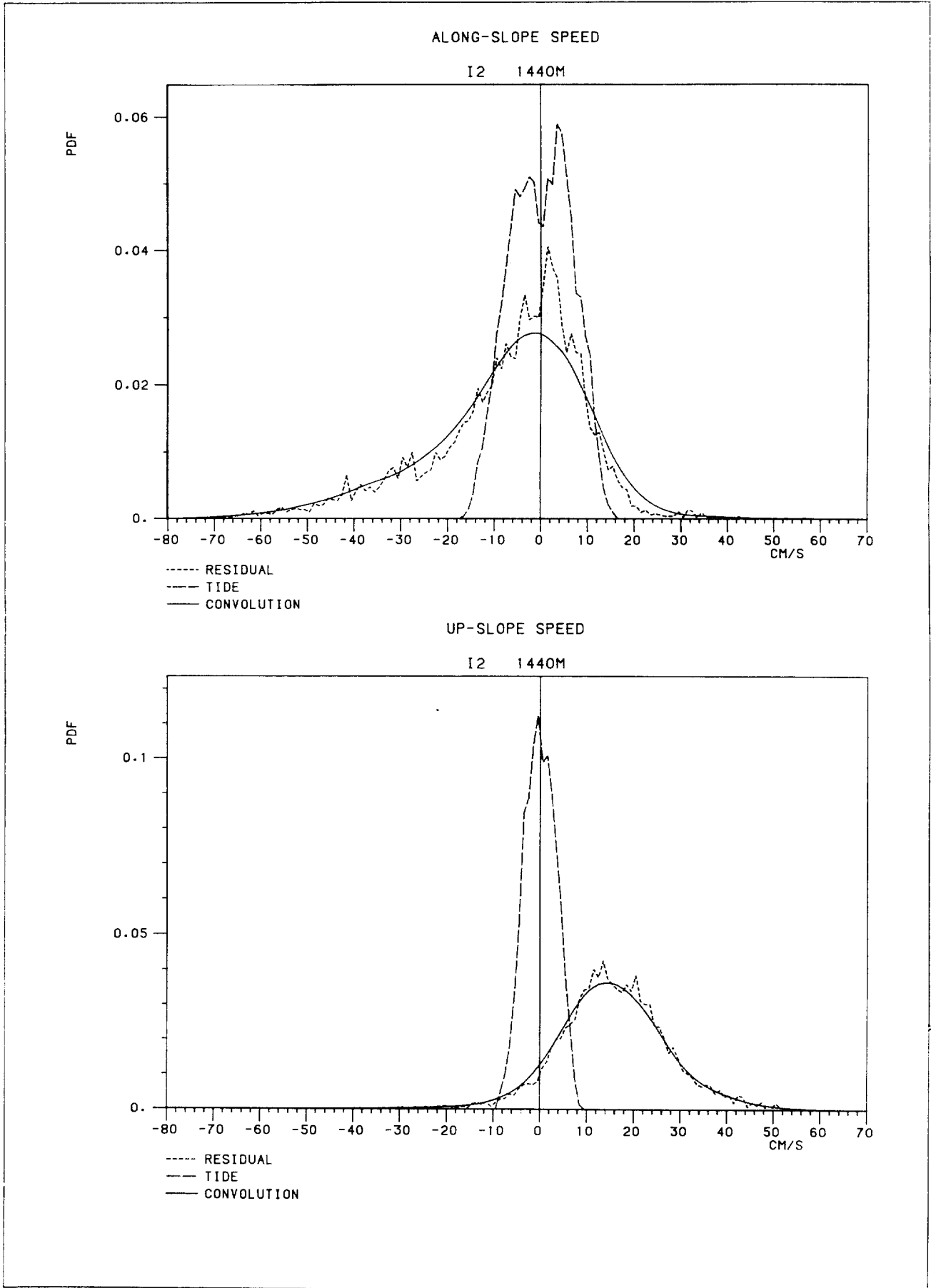
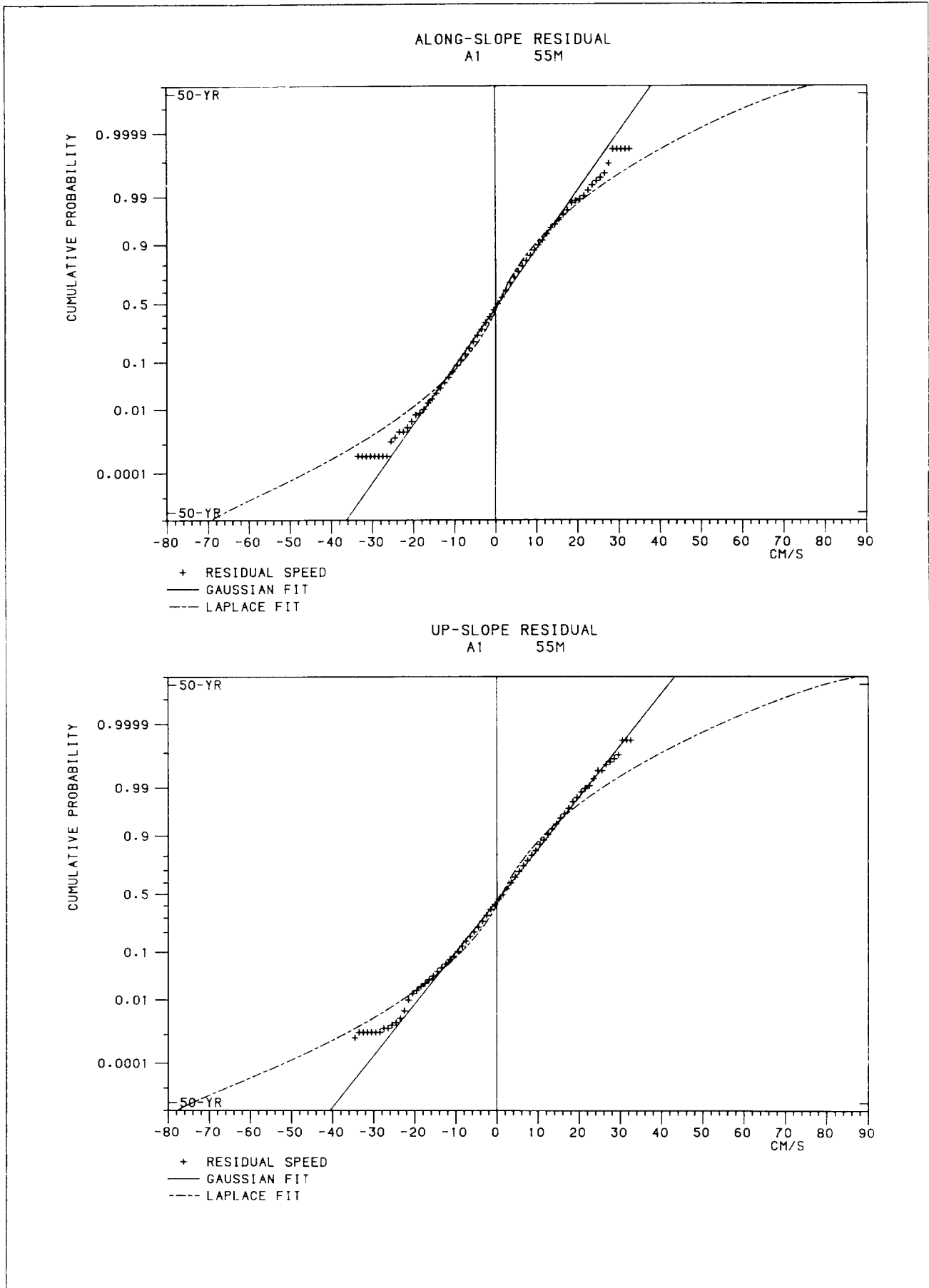
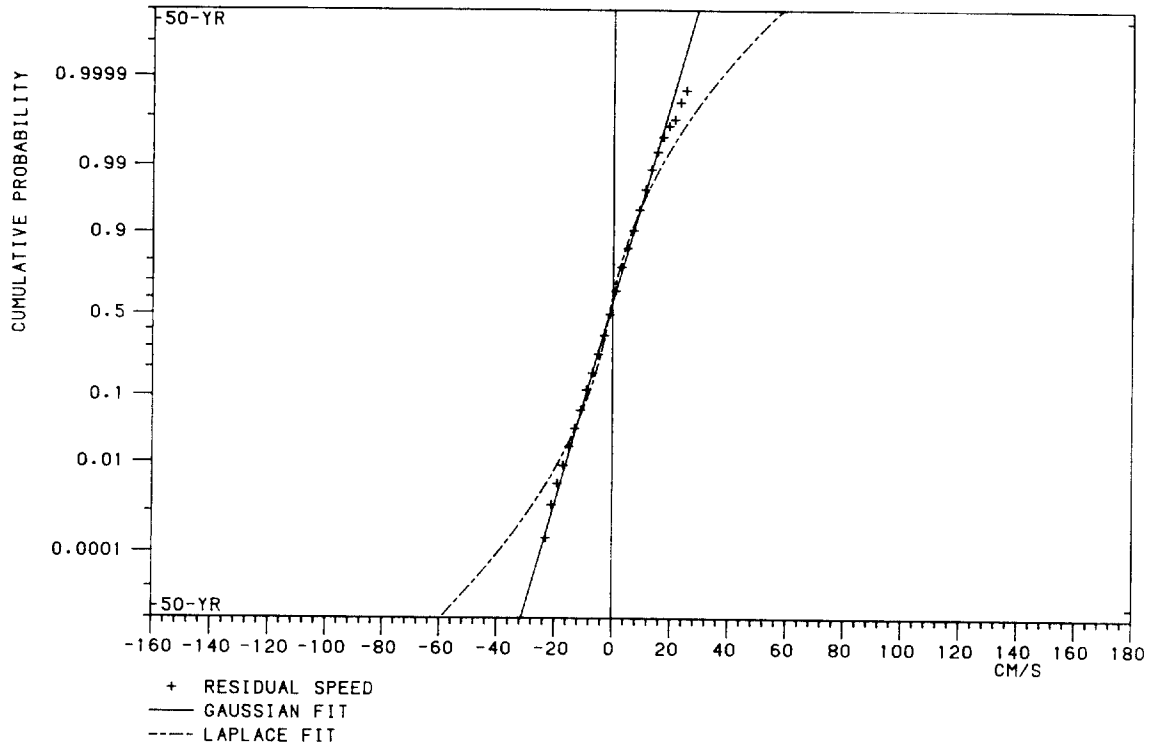


Fig.3: Cumulative probability distributions of residual current speed along- and up-slope from records at each current meter and fitted Gaussian and Laplacian fits. (The meter is identified by the mooring and by the depth of the meter below the sea surface.)

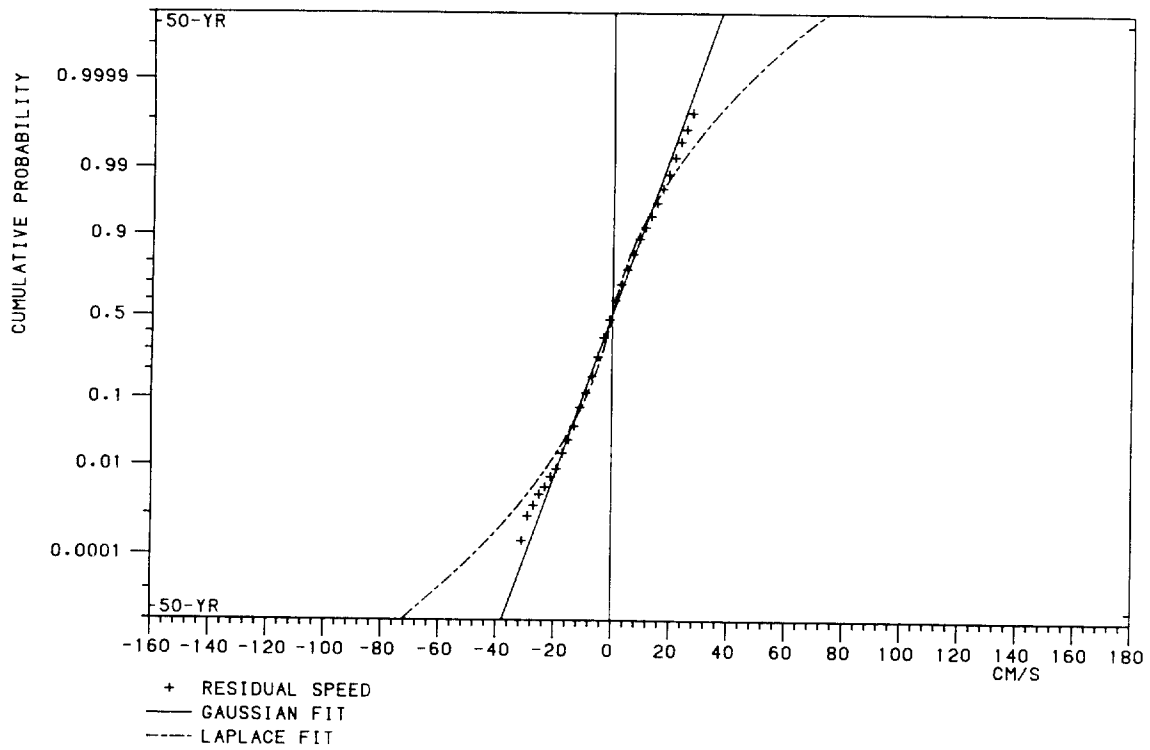


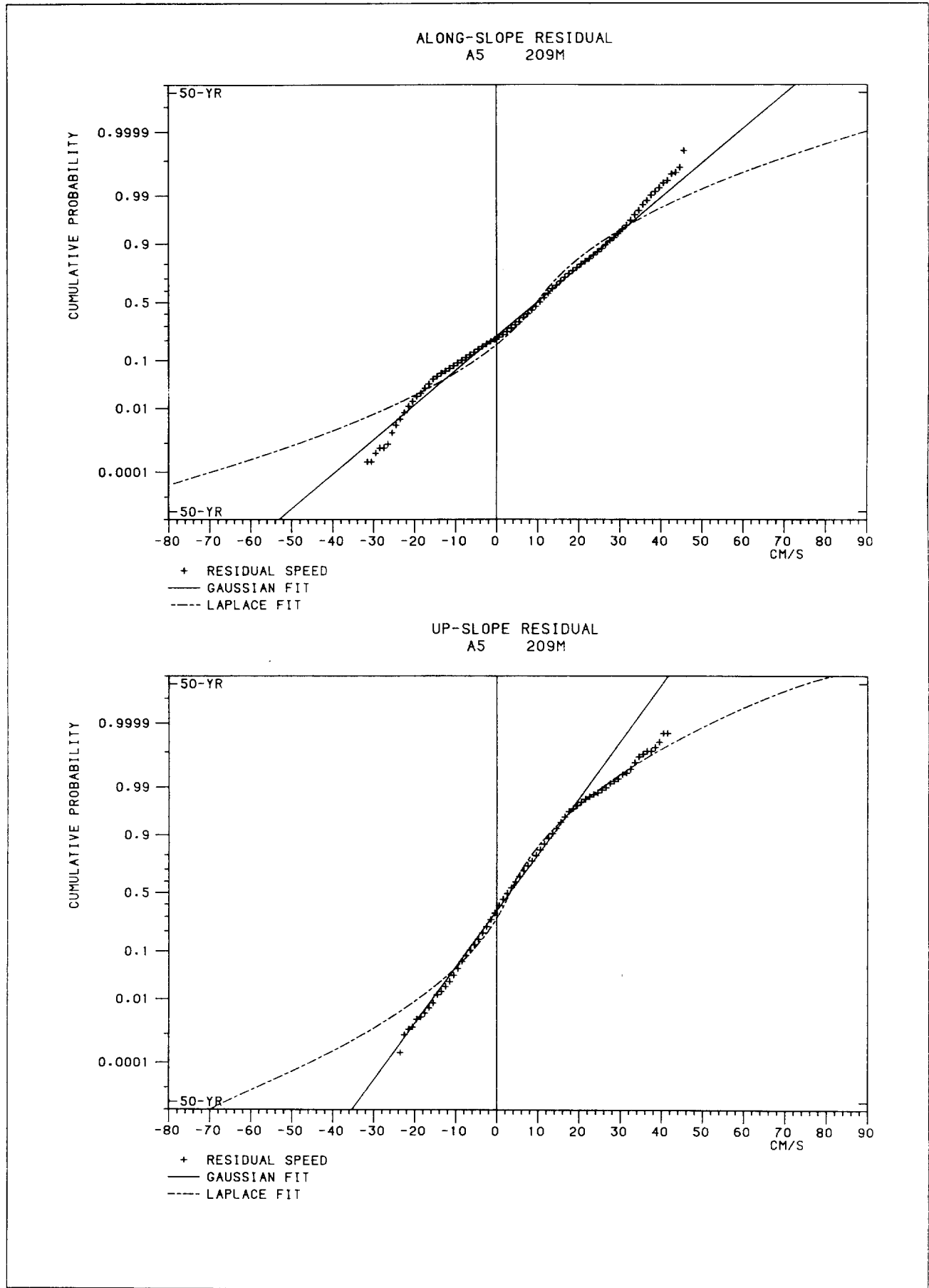


ALONG-SLOPE RESIDUAL
A1 120M

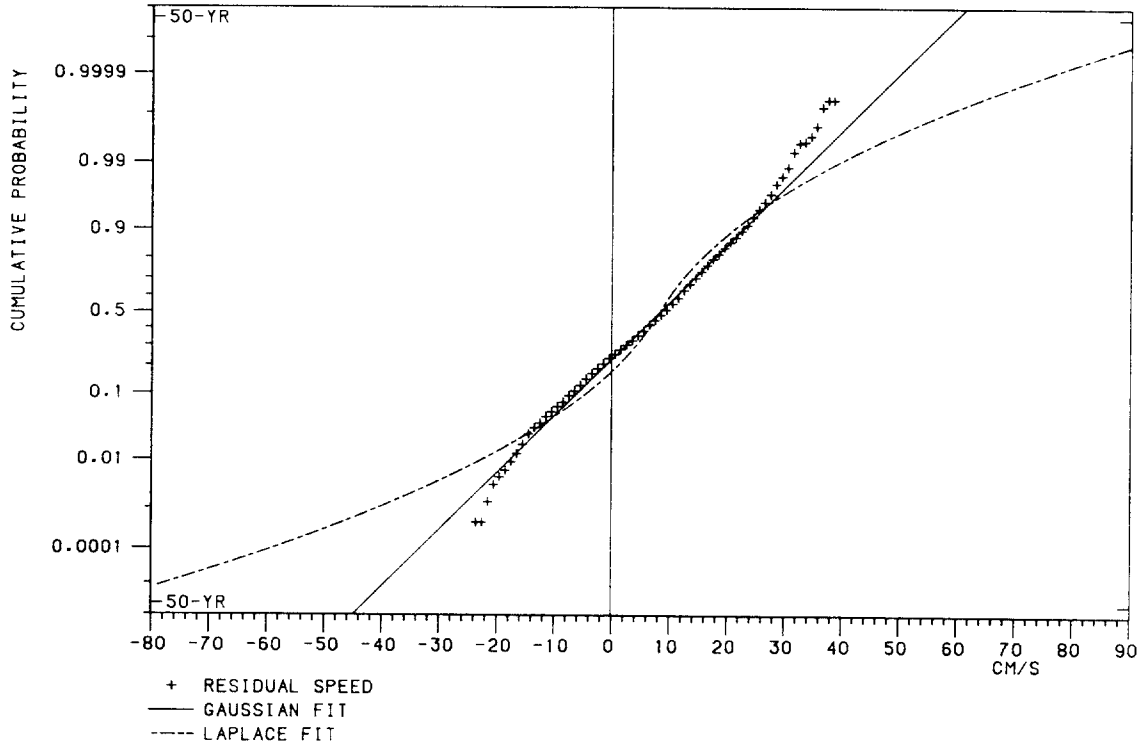


UP-SLOPE RESIDUAL
A1 120M

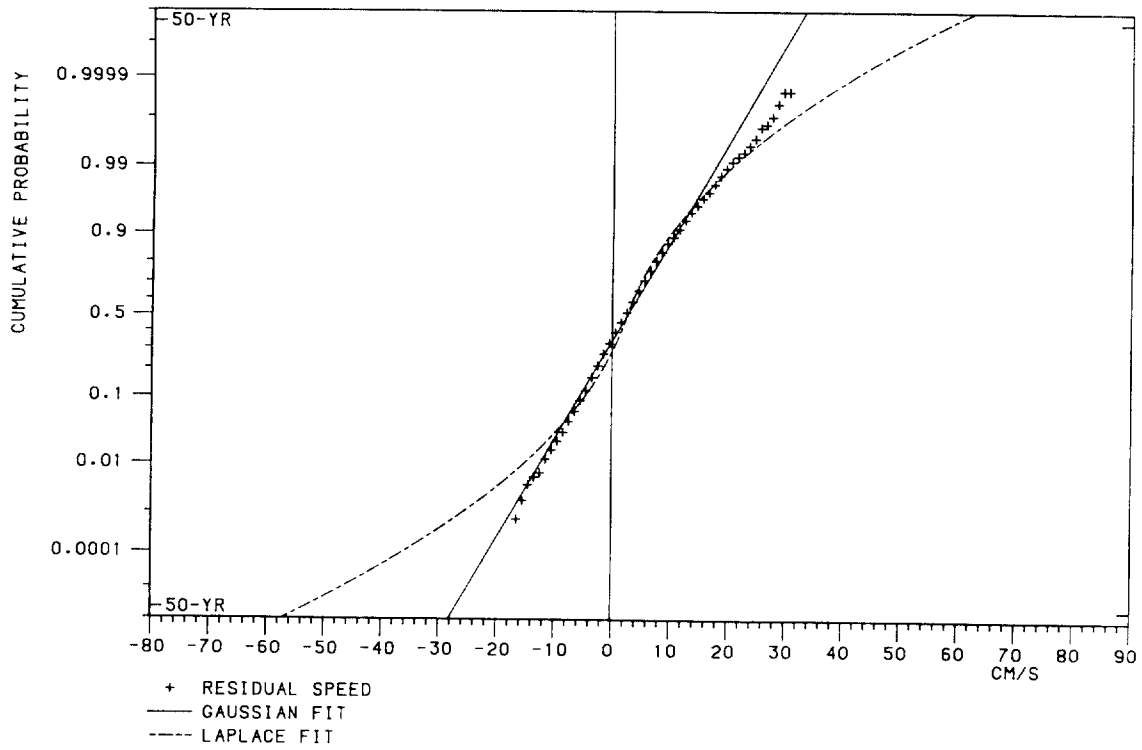




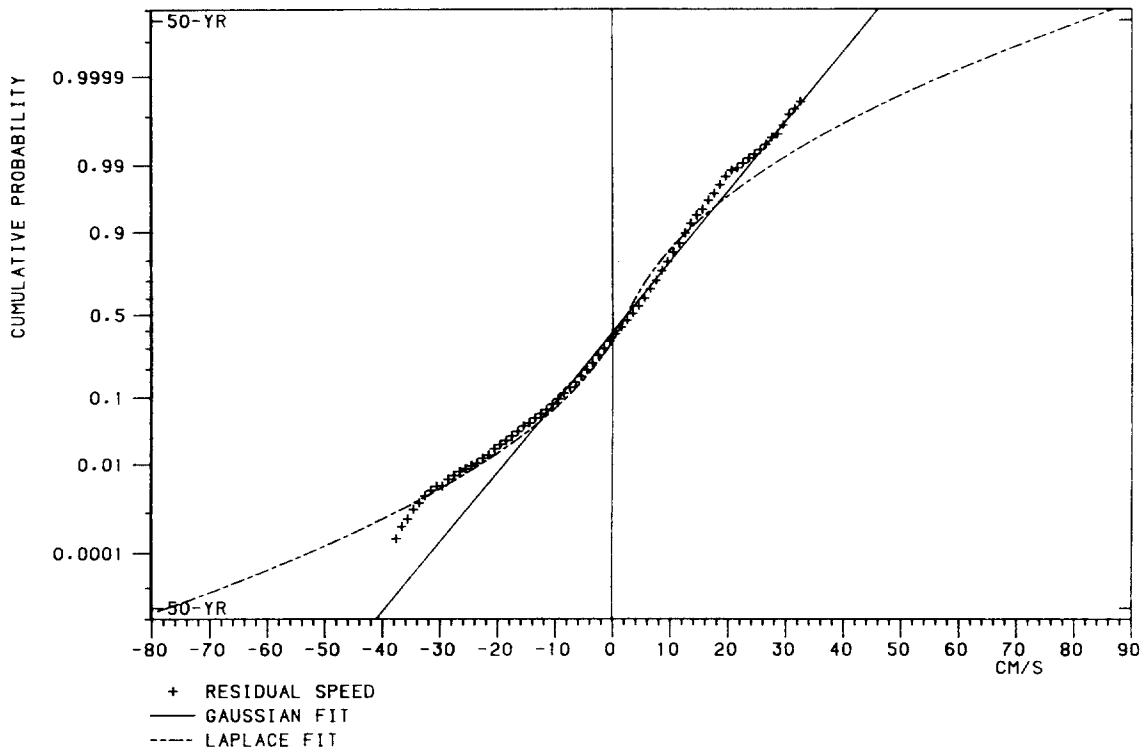
ALONG-SLOPE RESIDUAL
A5 510M



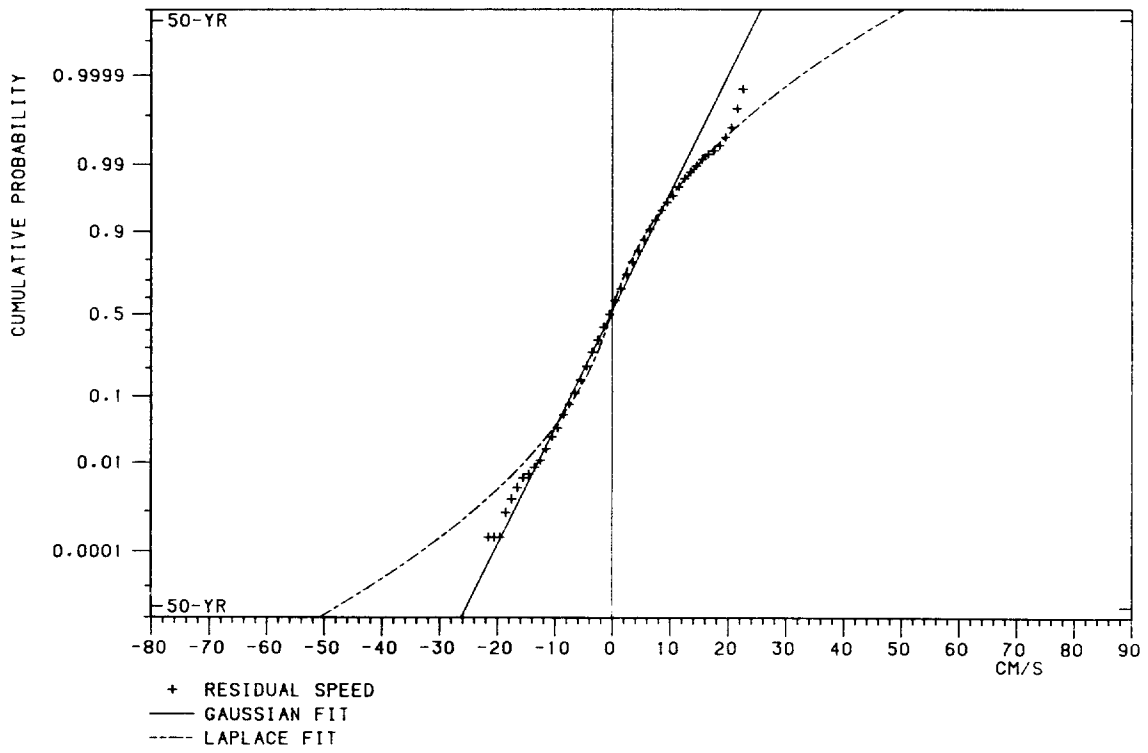
UP-SLOPE RESIDUAL
A5 510M



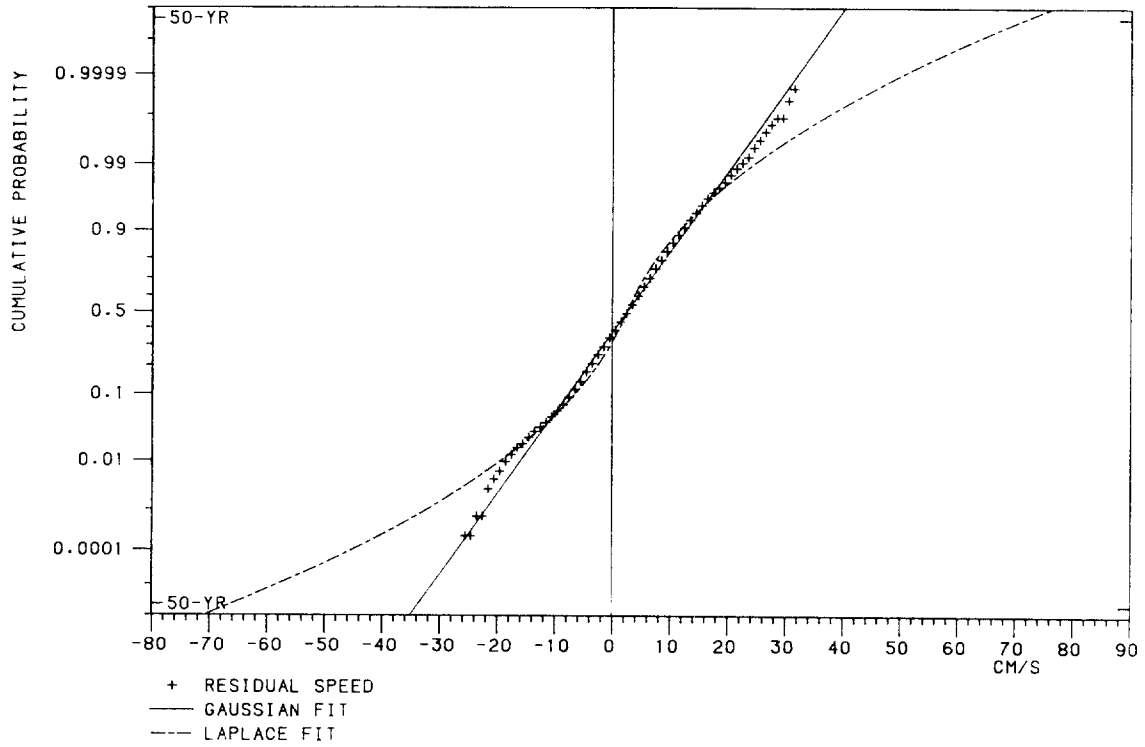
ALONG-SLOPE RESIDUAL
A5 1111M



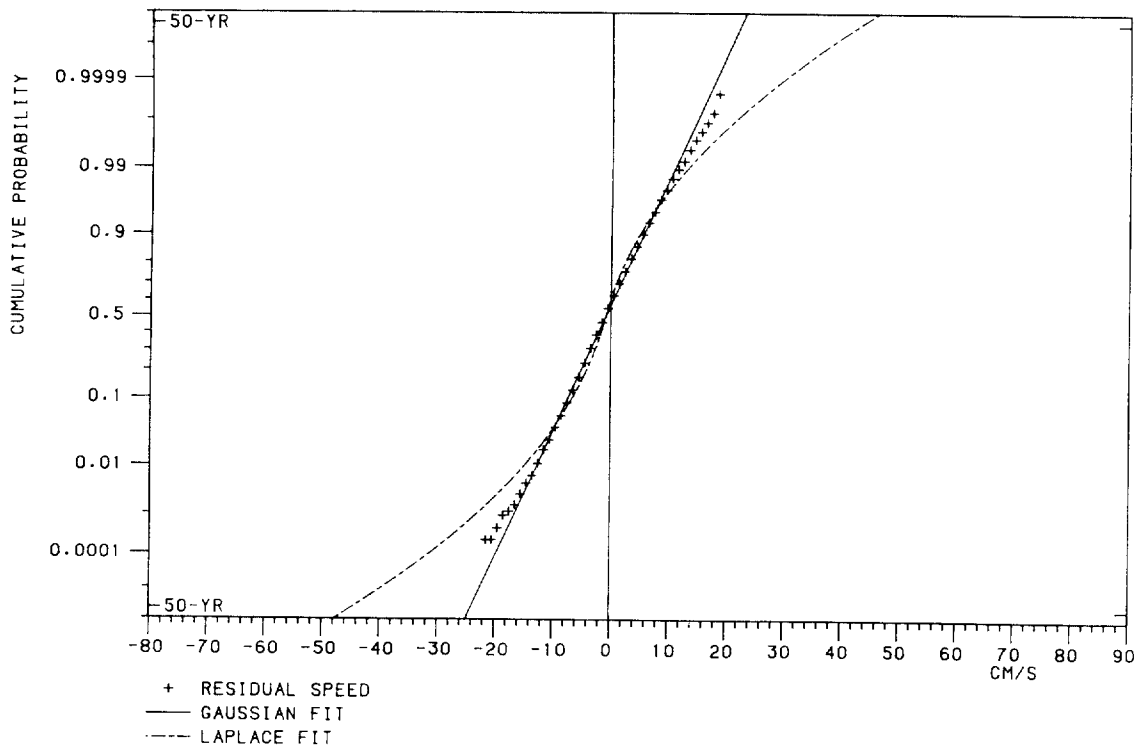
UP-SLOPE RESIDUAL
A5 1111M

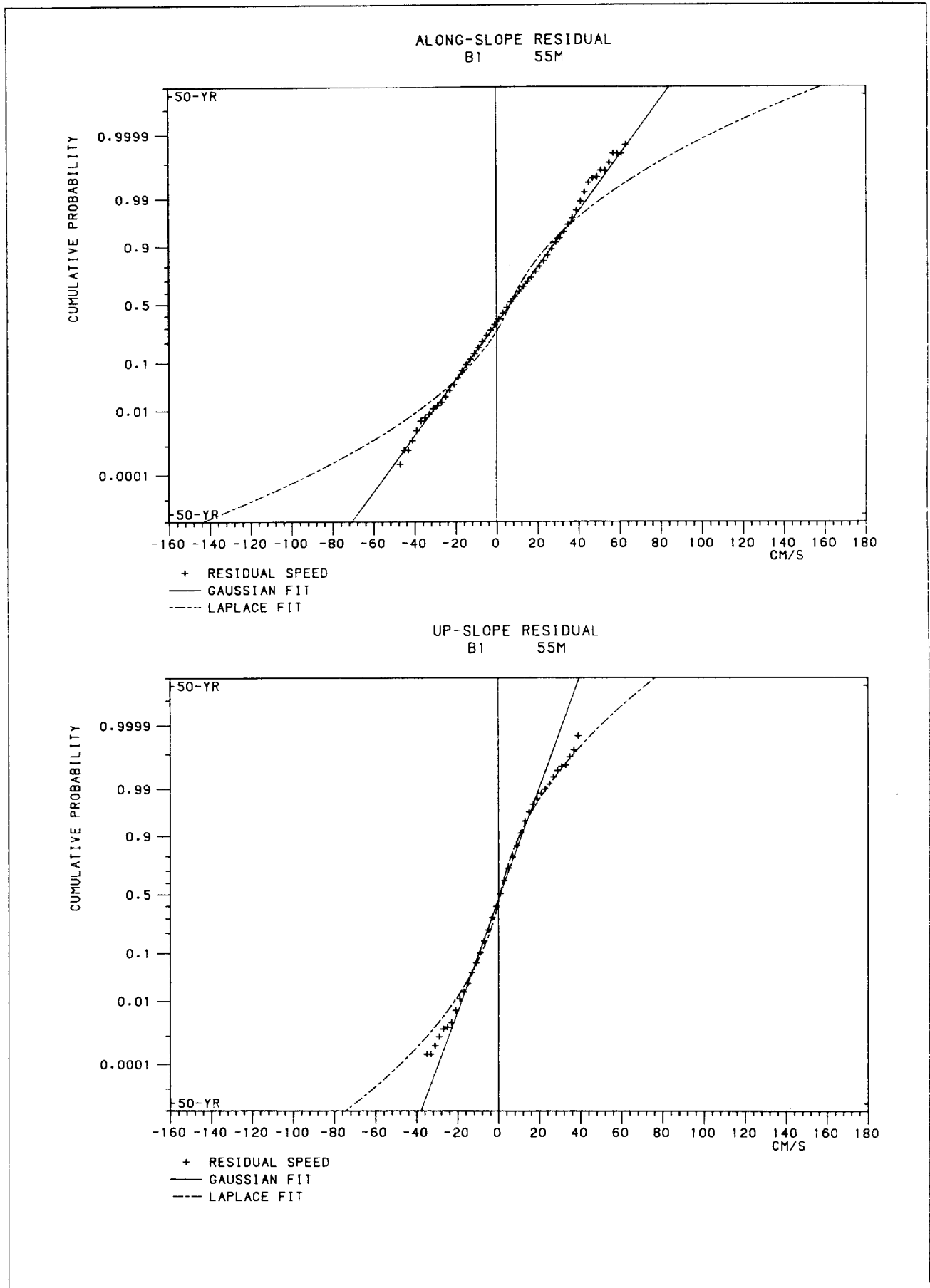


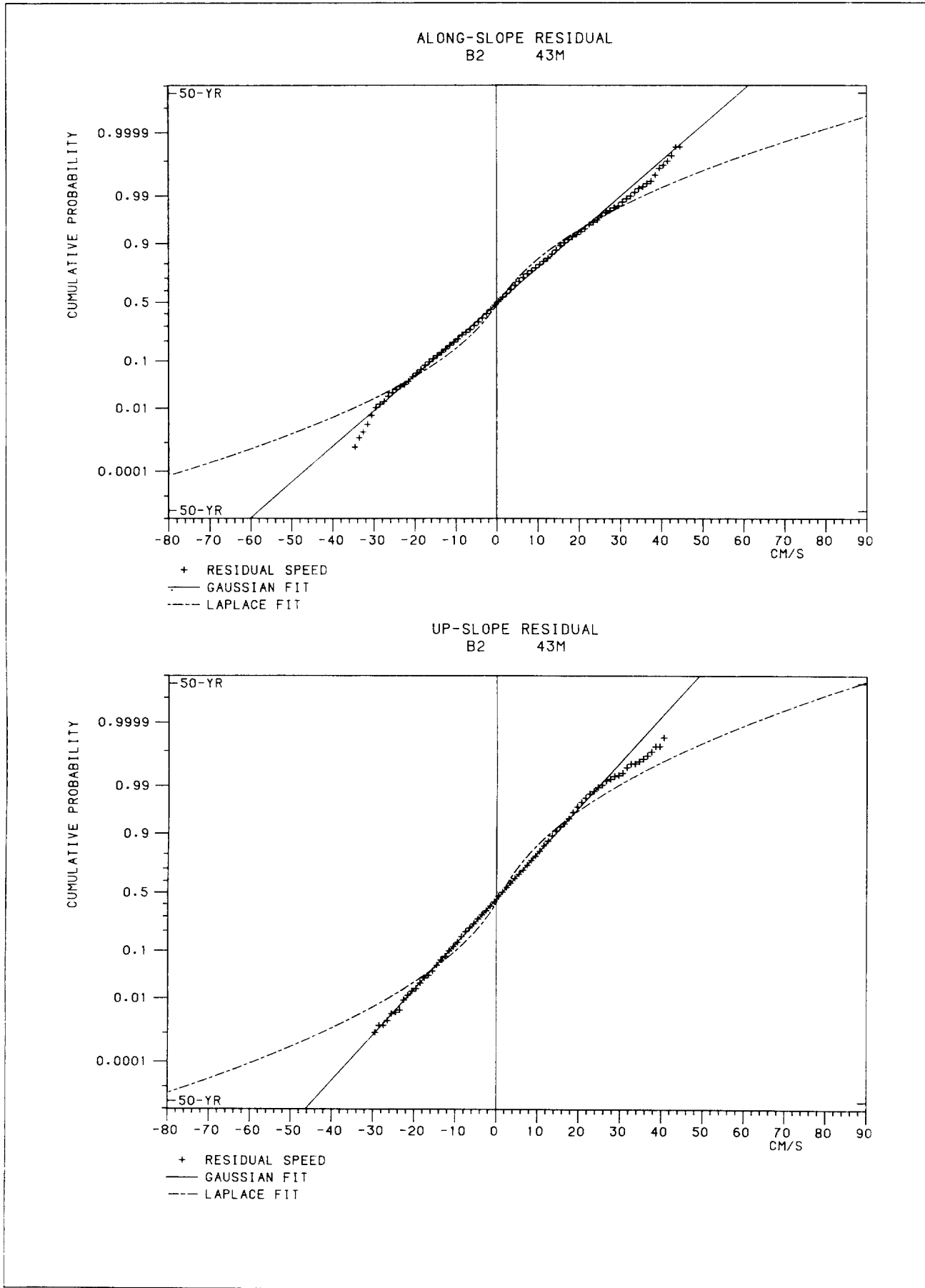
ALONG-SLOPE RESIDUAL
A5 1562M

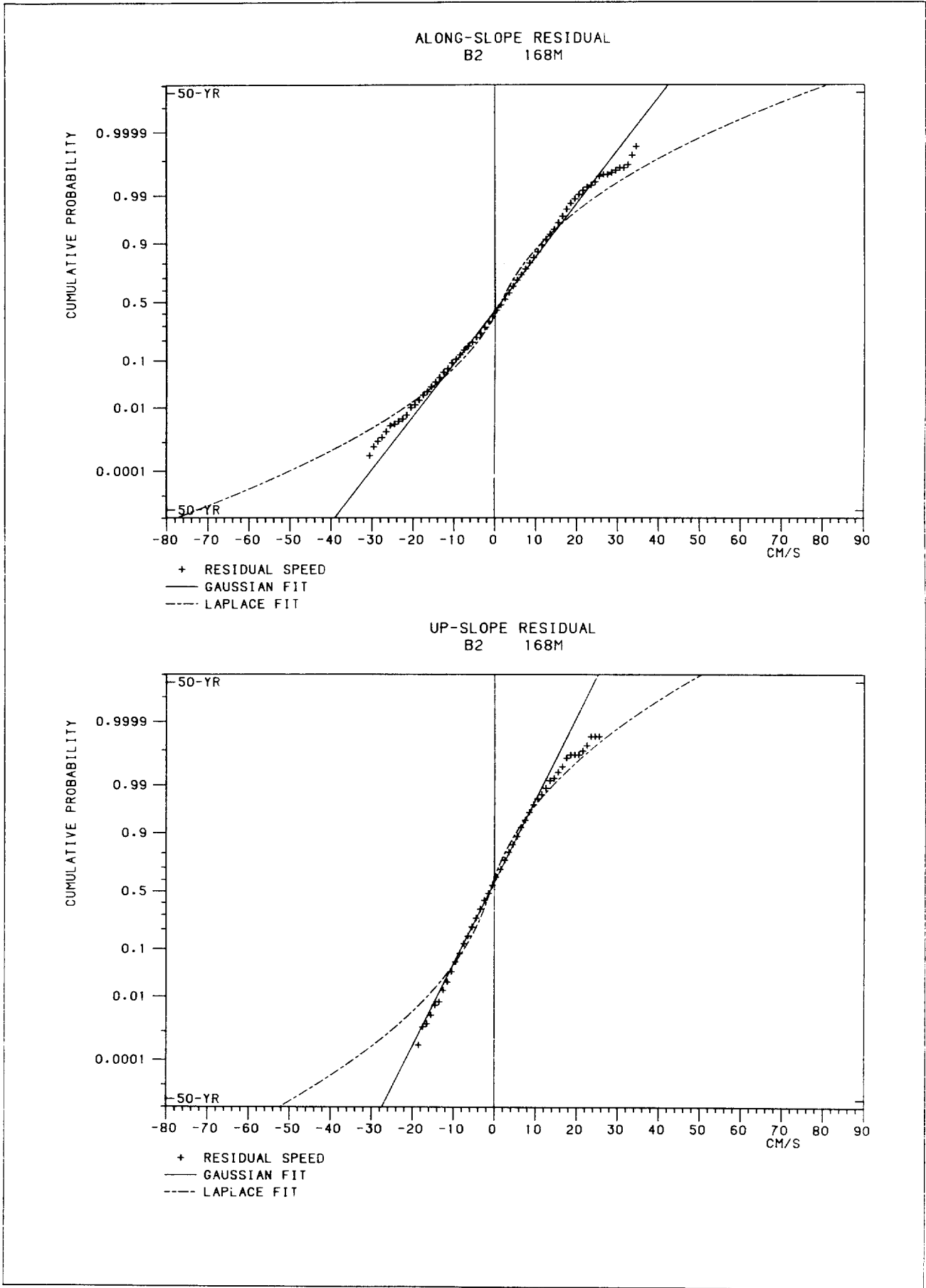


UP-SLOPE RESIDUAL
A5 1562M

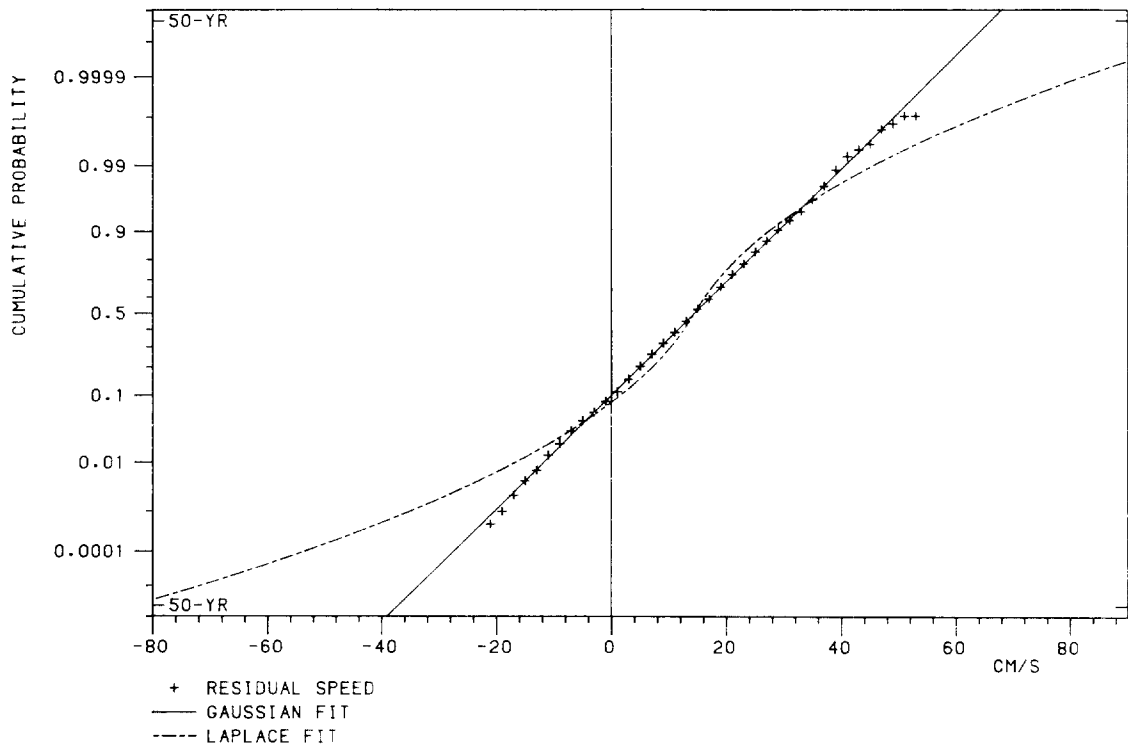




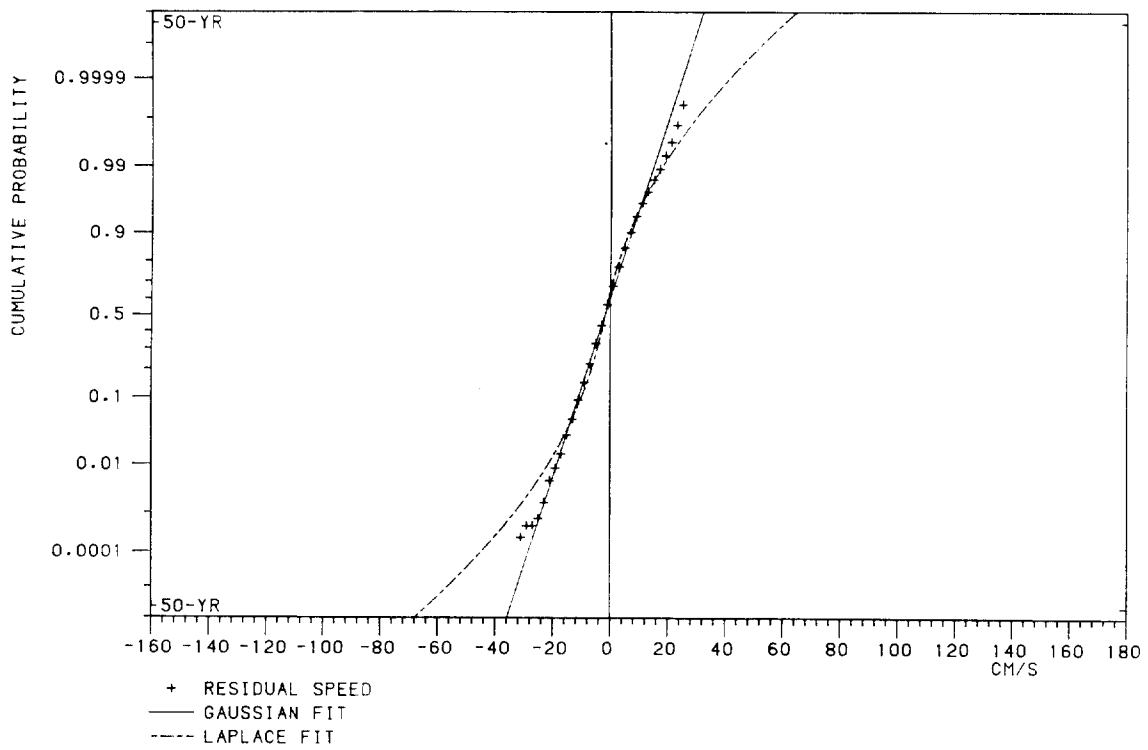




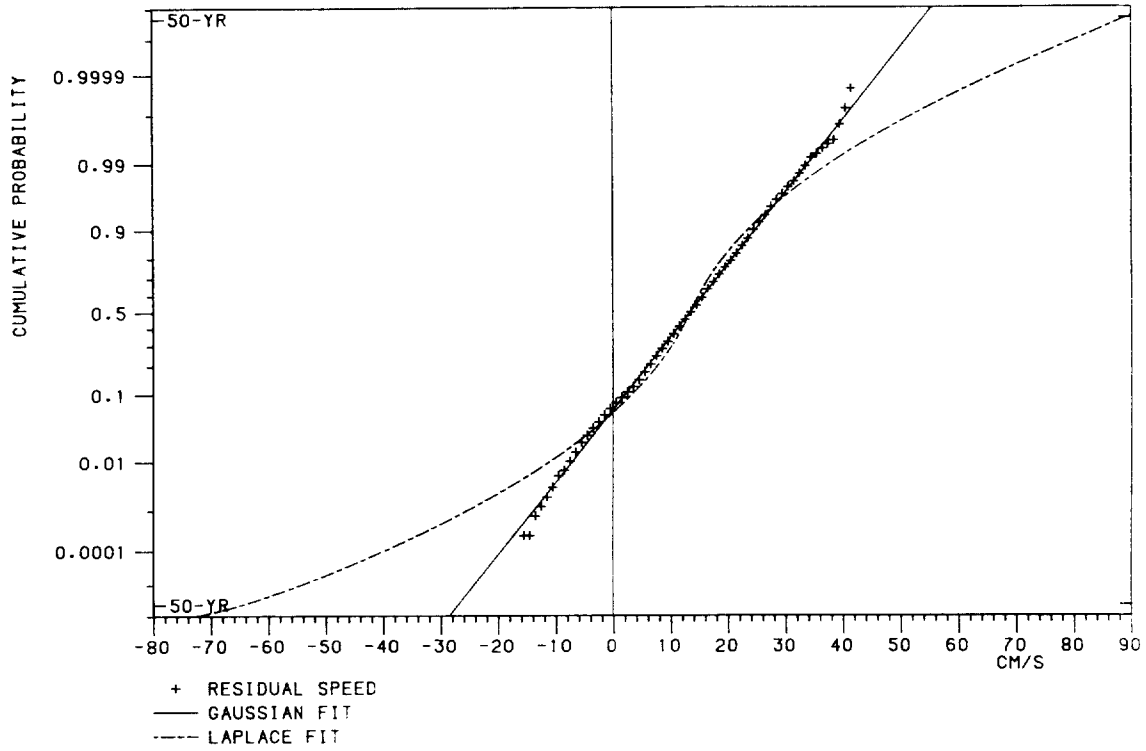
ALONG-SLOPE RESIDUAL
B3 104M



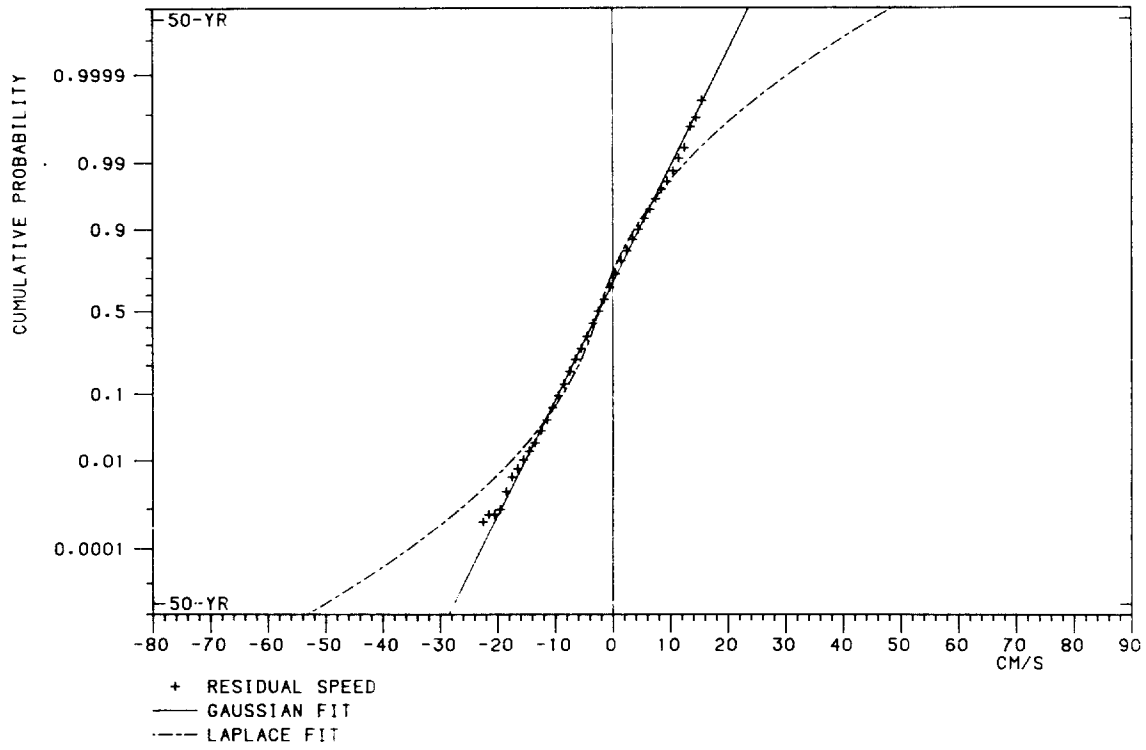
UP-SLOPE RESIDUAL
B3 104M

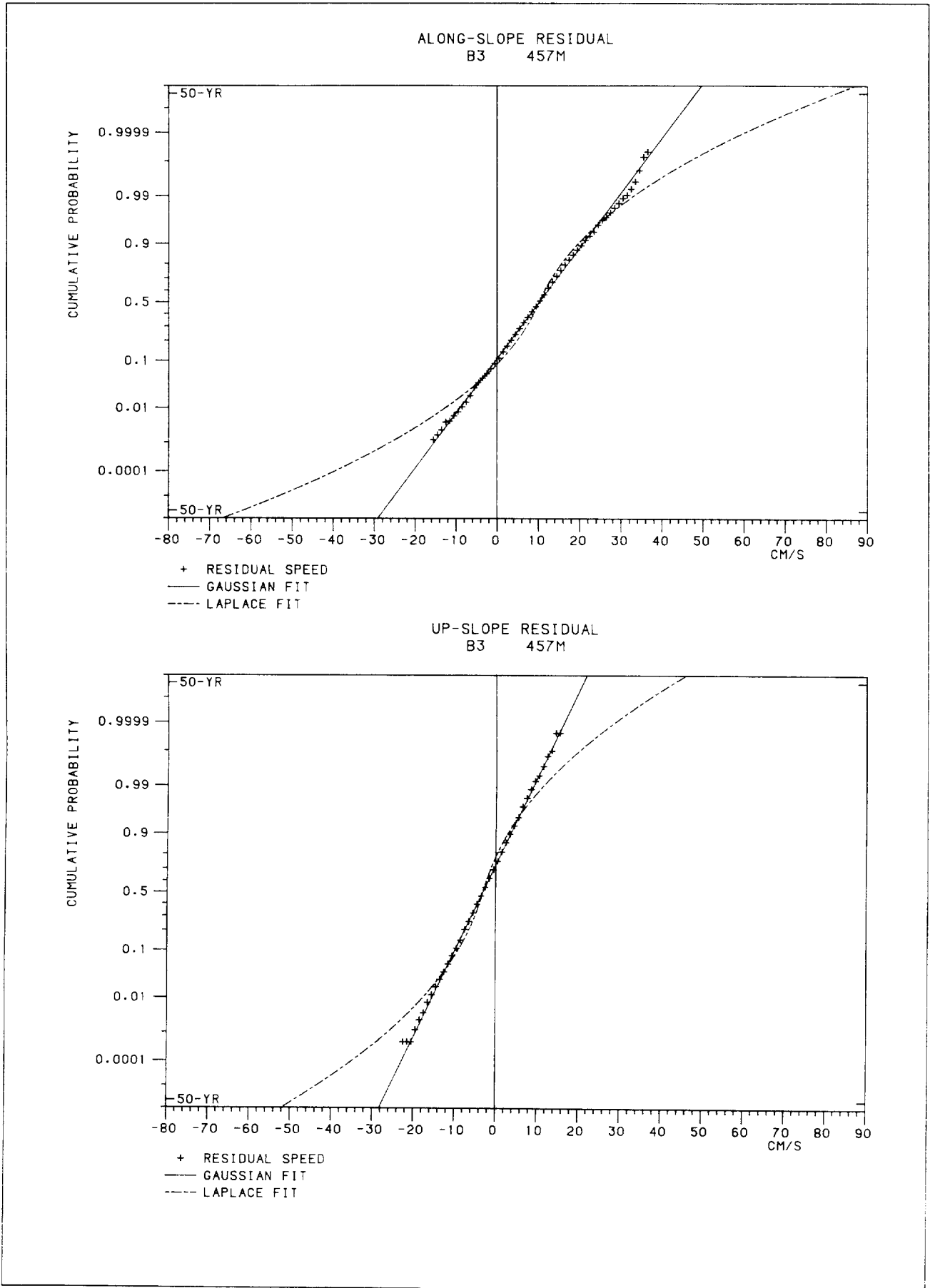


ALONG-SLOPE RESIDUAL
B3 257M

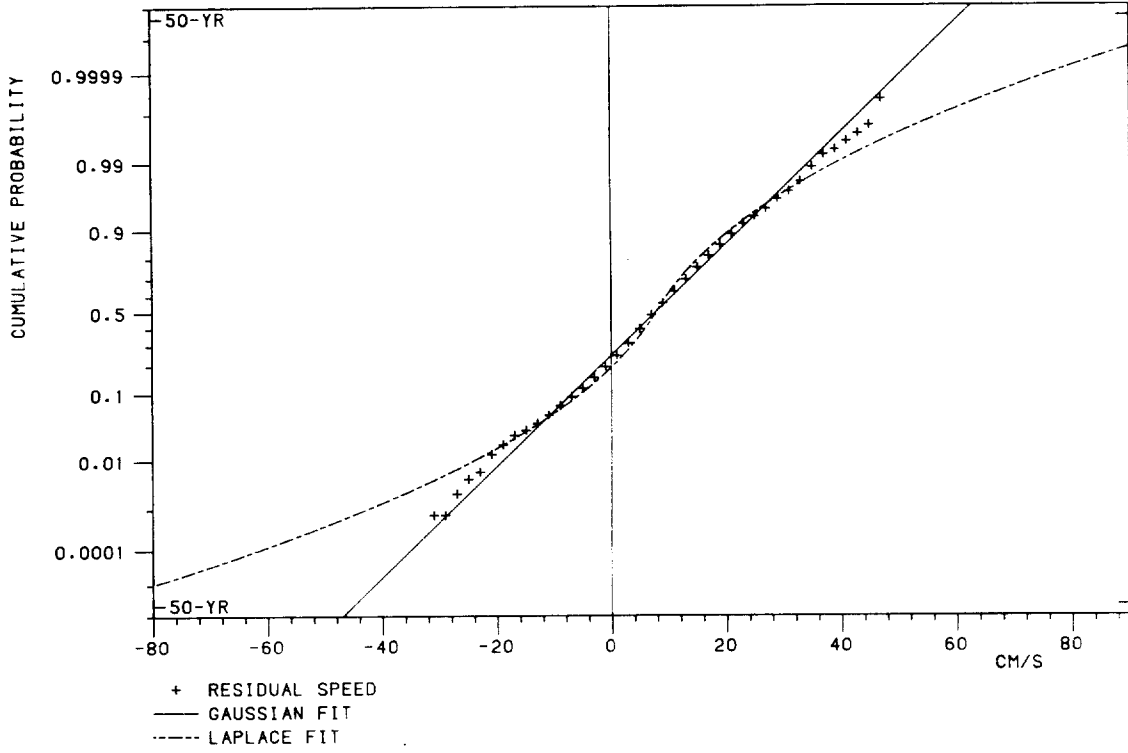


UP-SLOPE RESIDUAL
B3 257M

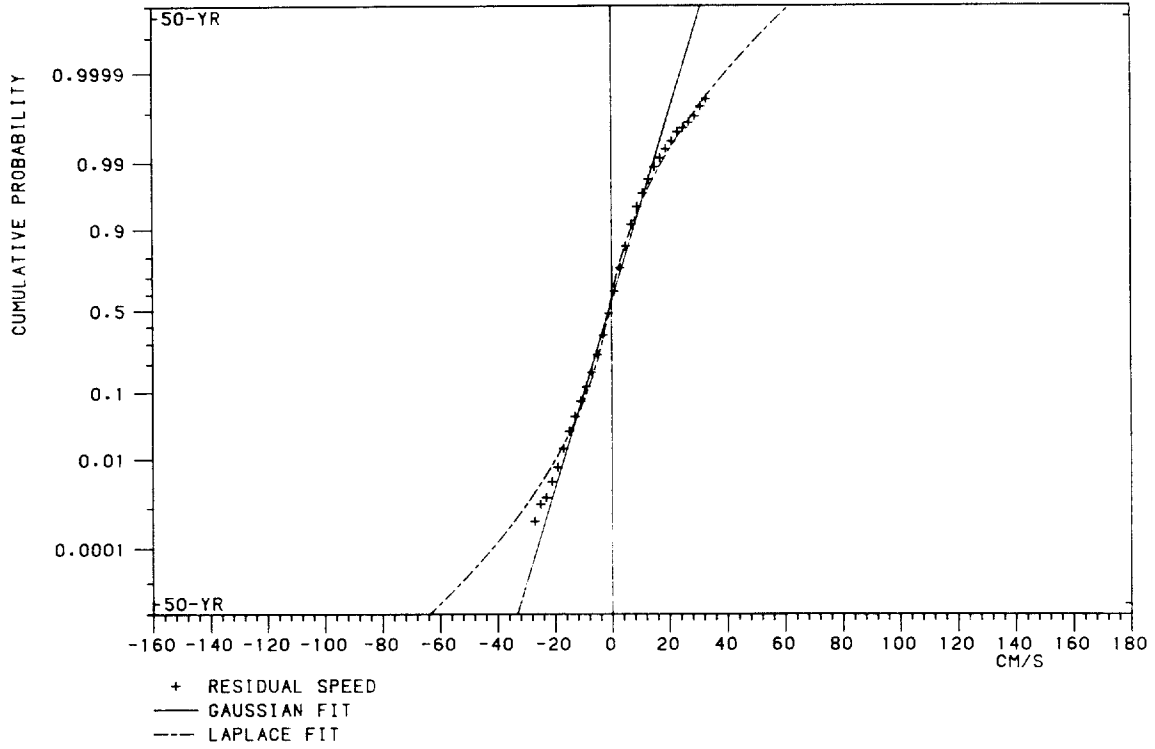


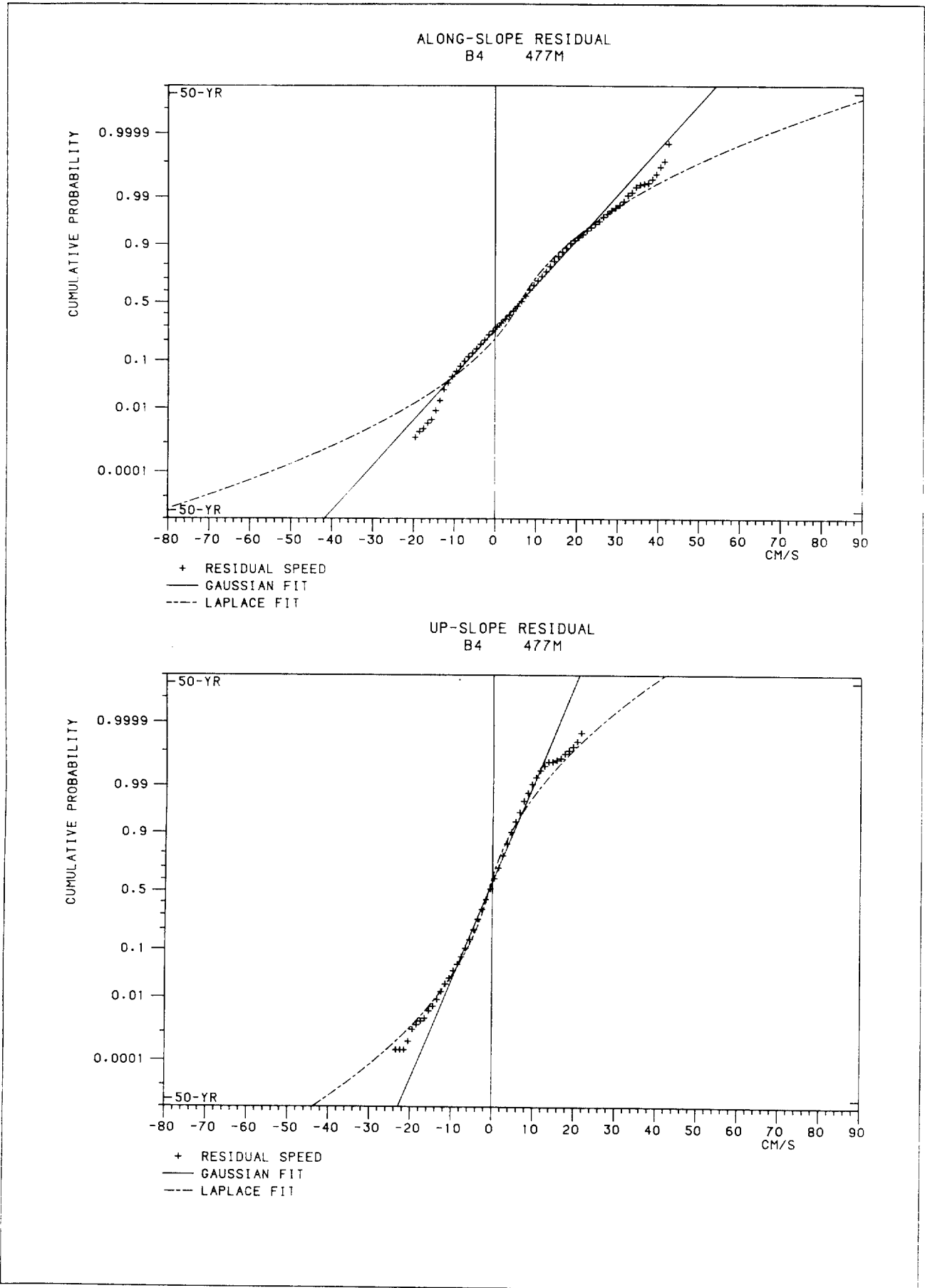


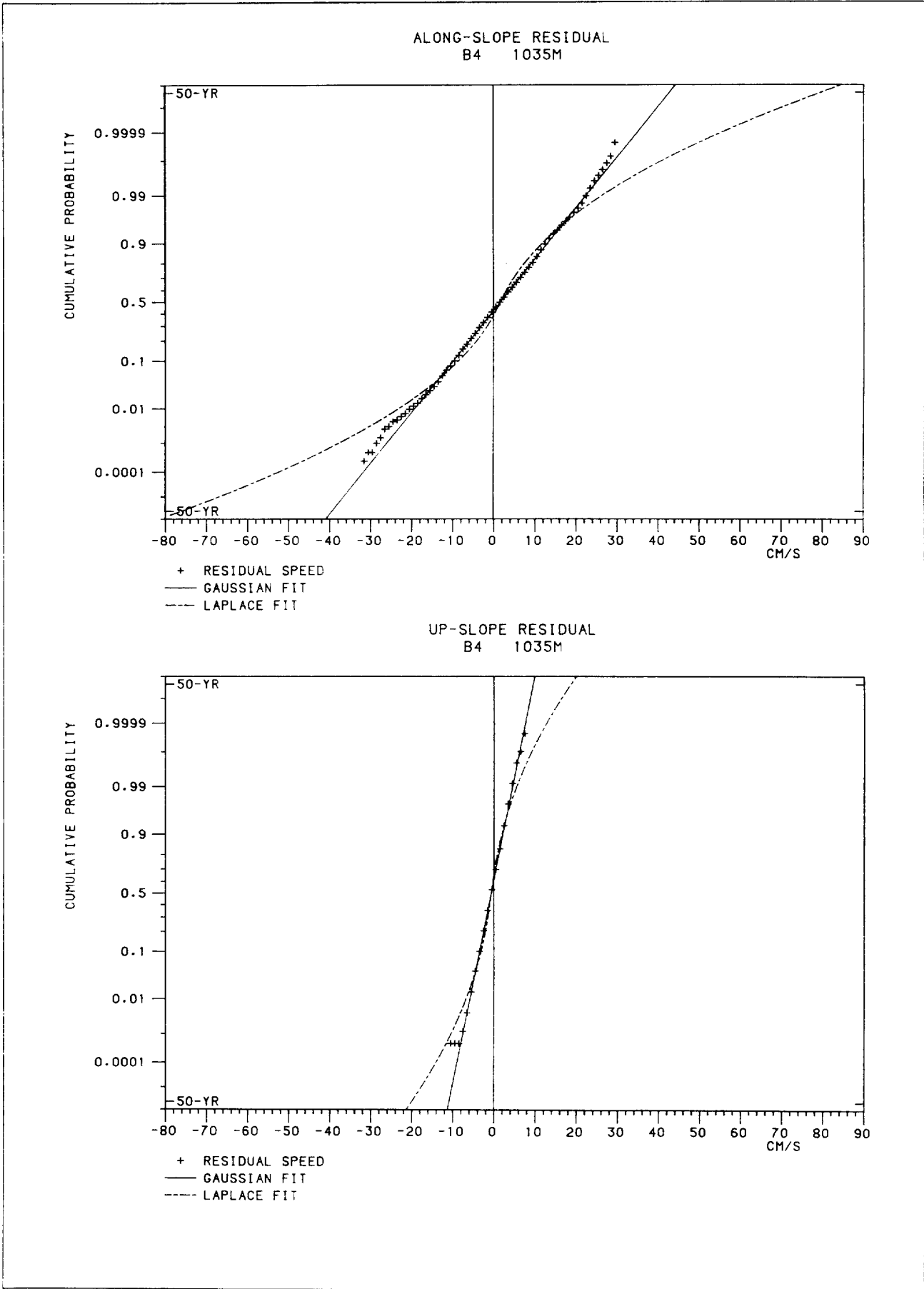
ALONG-SLOPE RESIDUAL
B4 169M



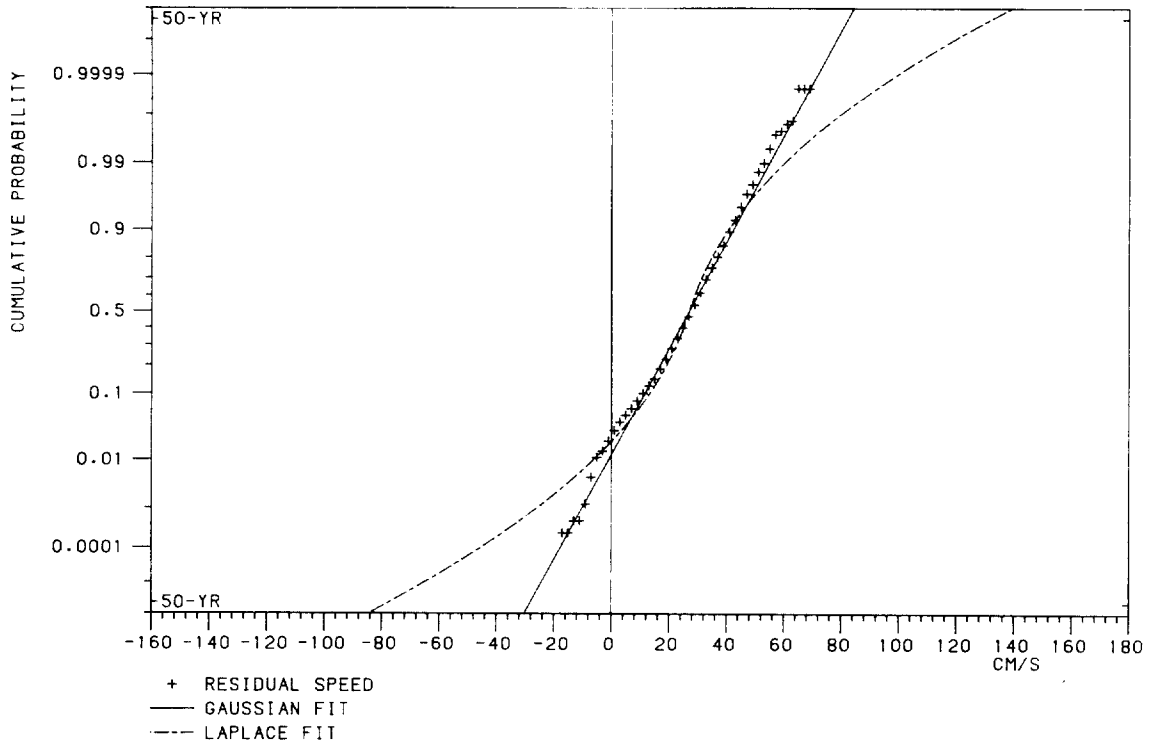
UP-SLOPE RESIDUAL
B4 169M



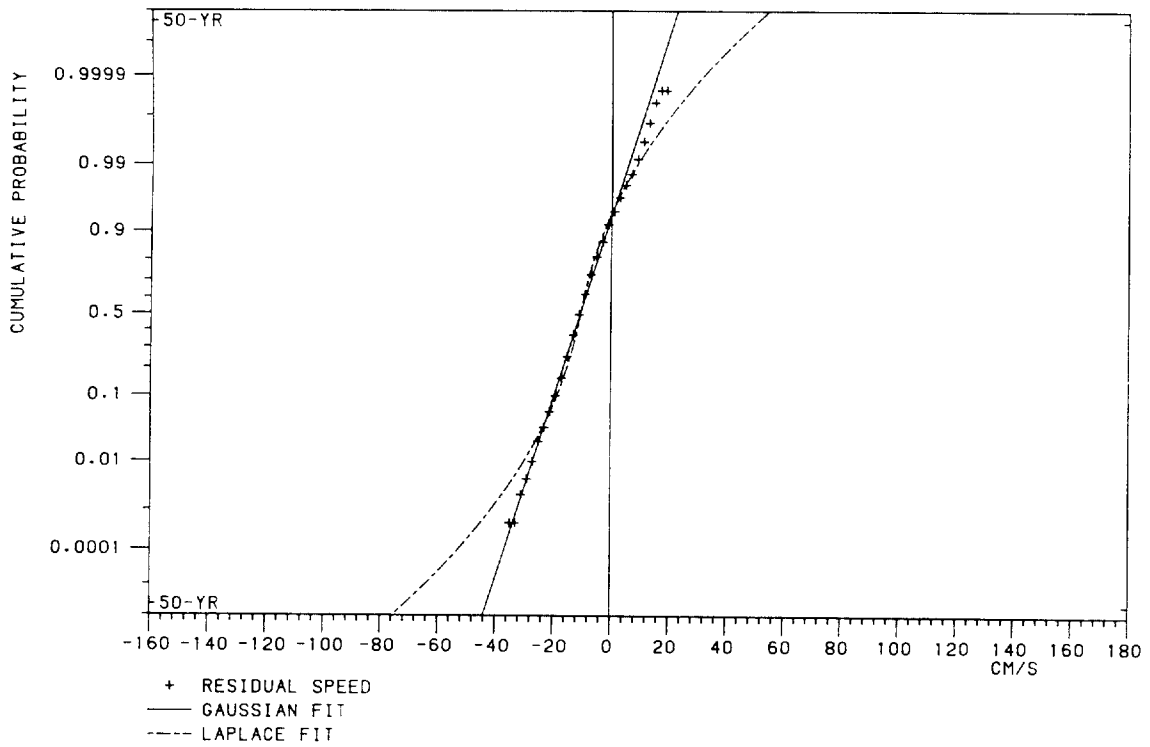


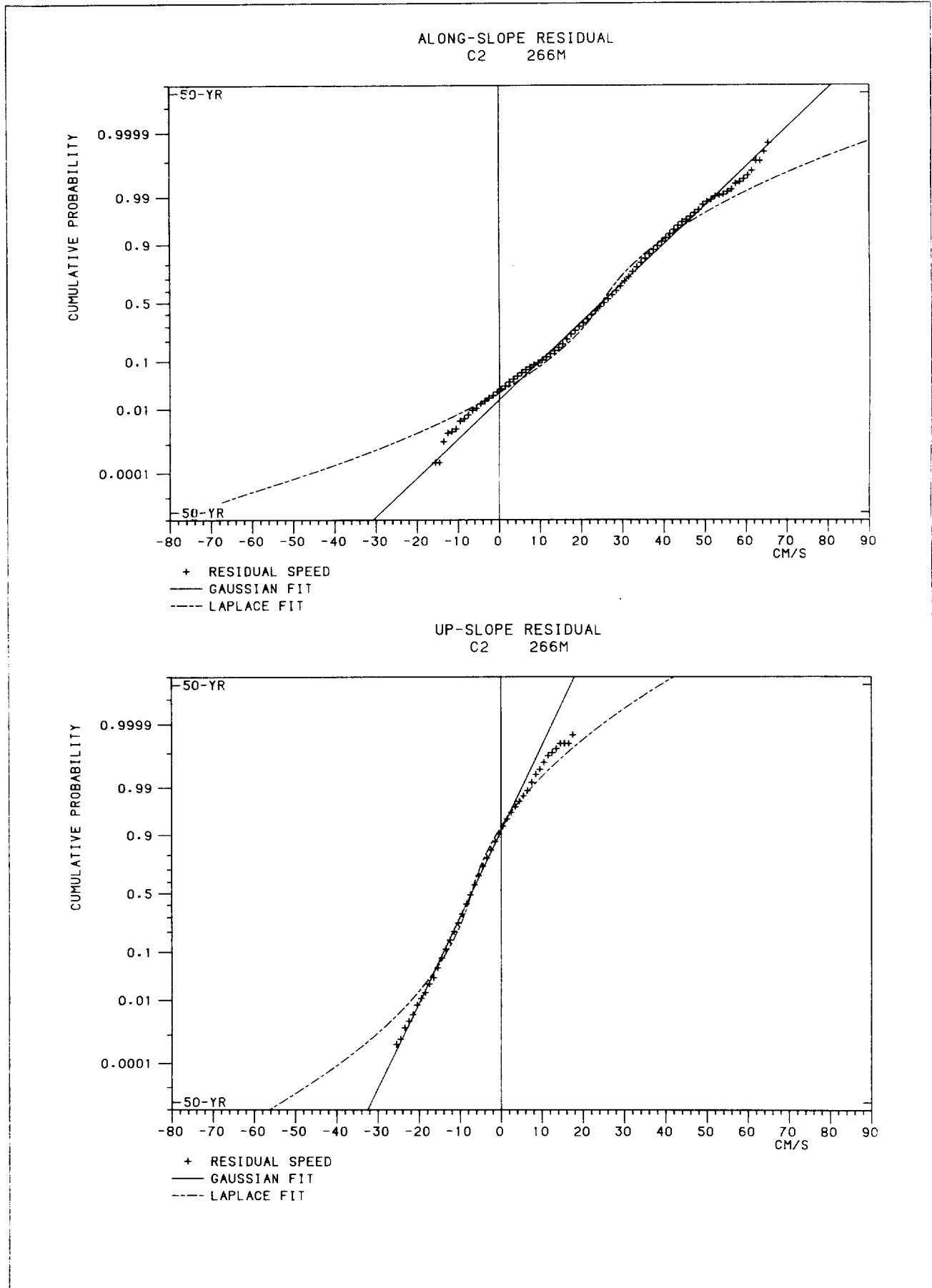


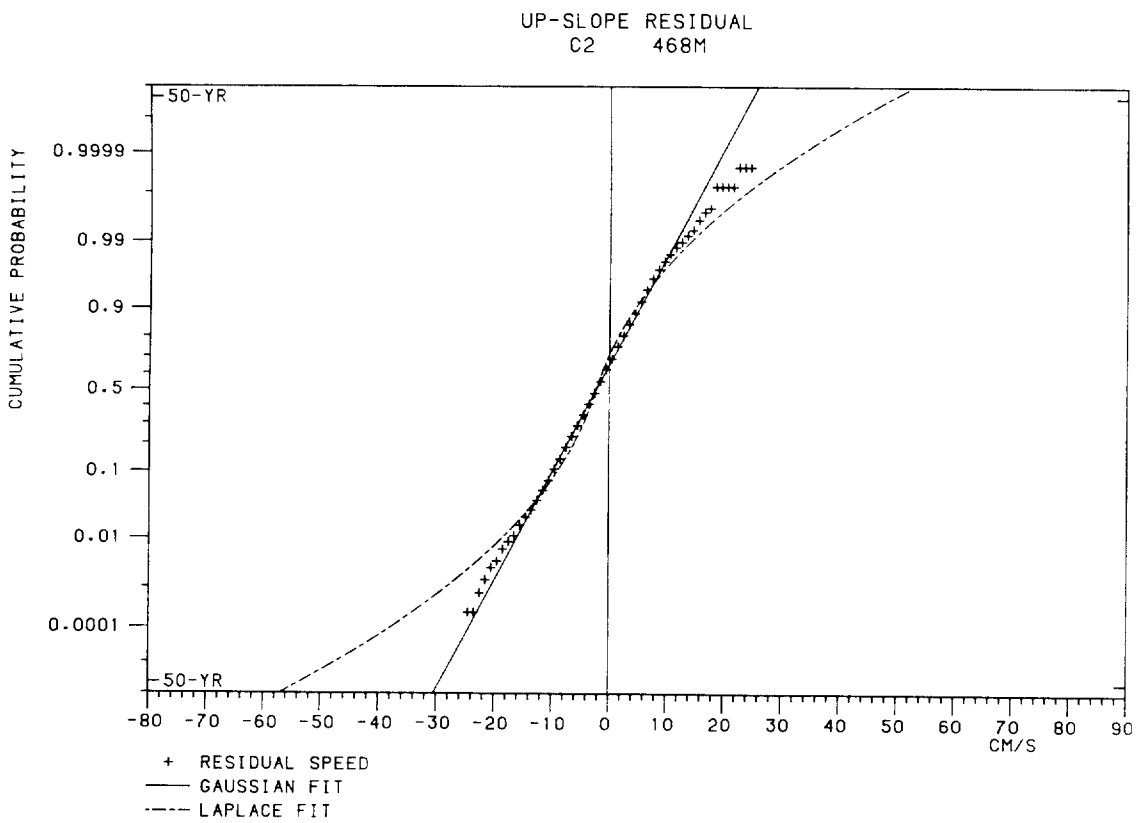
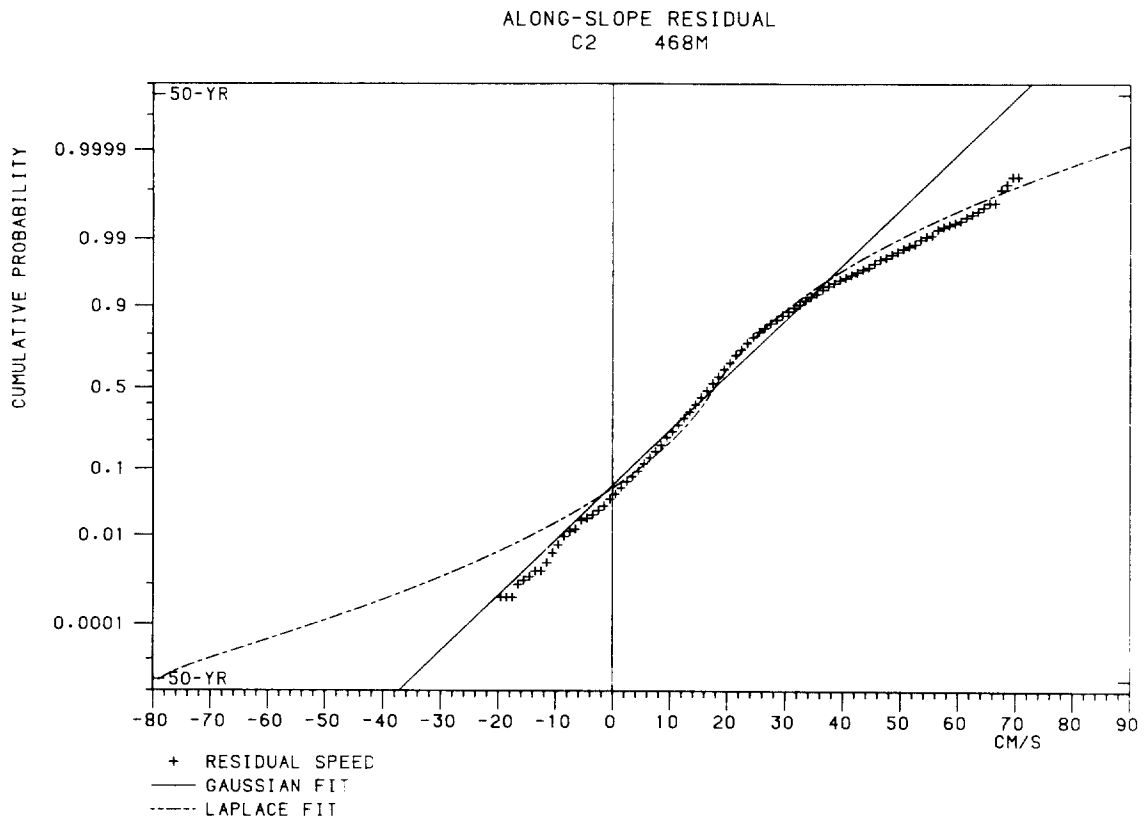
ALONG-SLOPE RESIDUAL
C2 115M

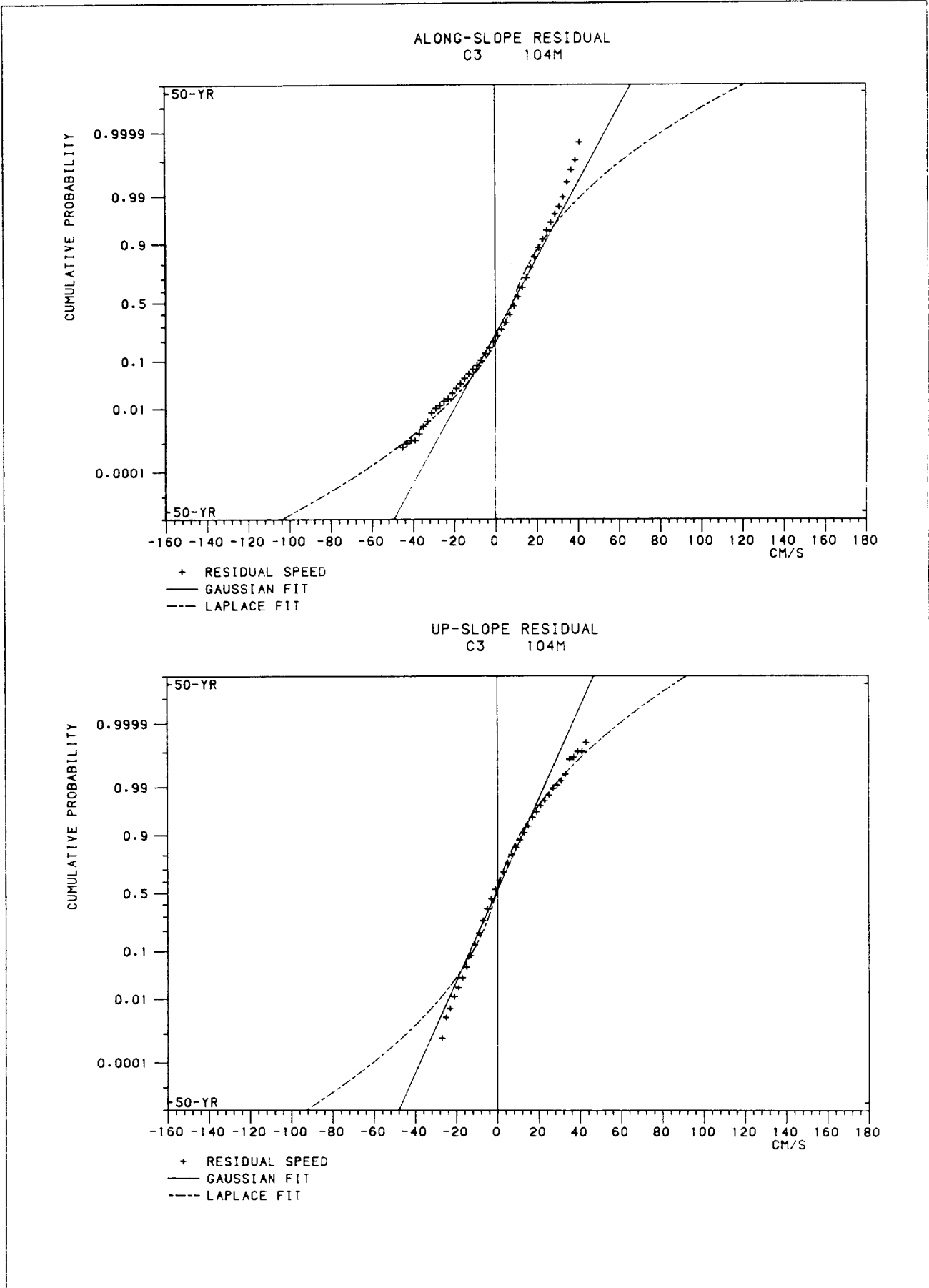


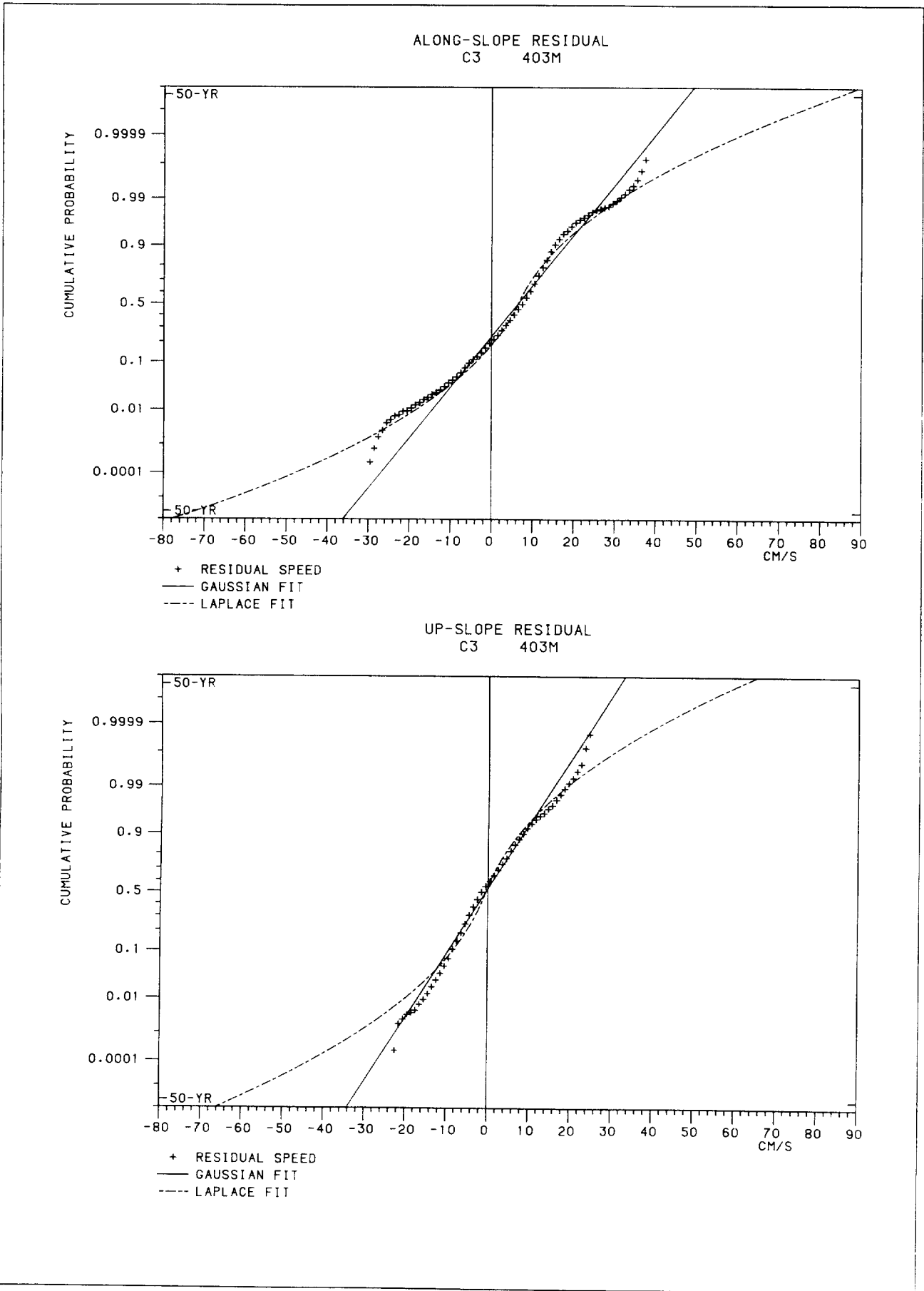
UP-SLOPE RESIDUAL
C2 115M

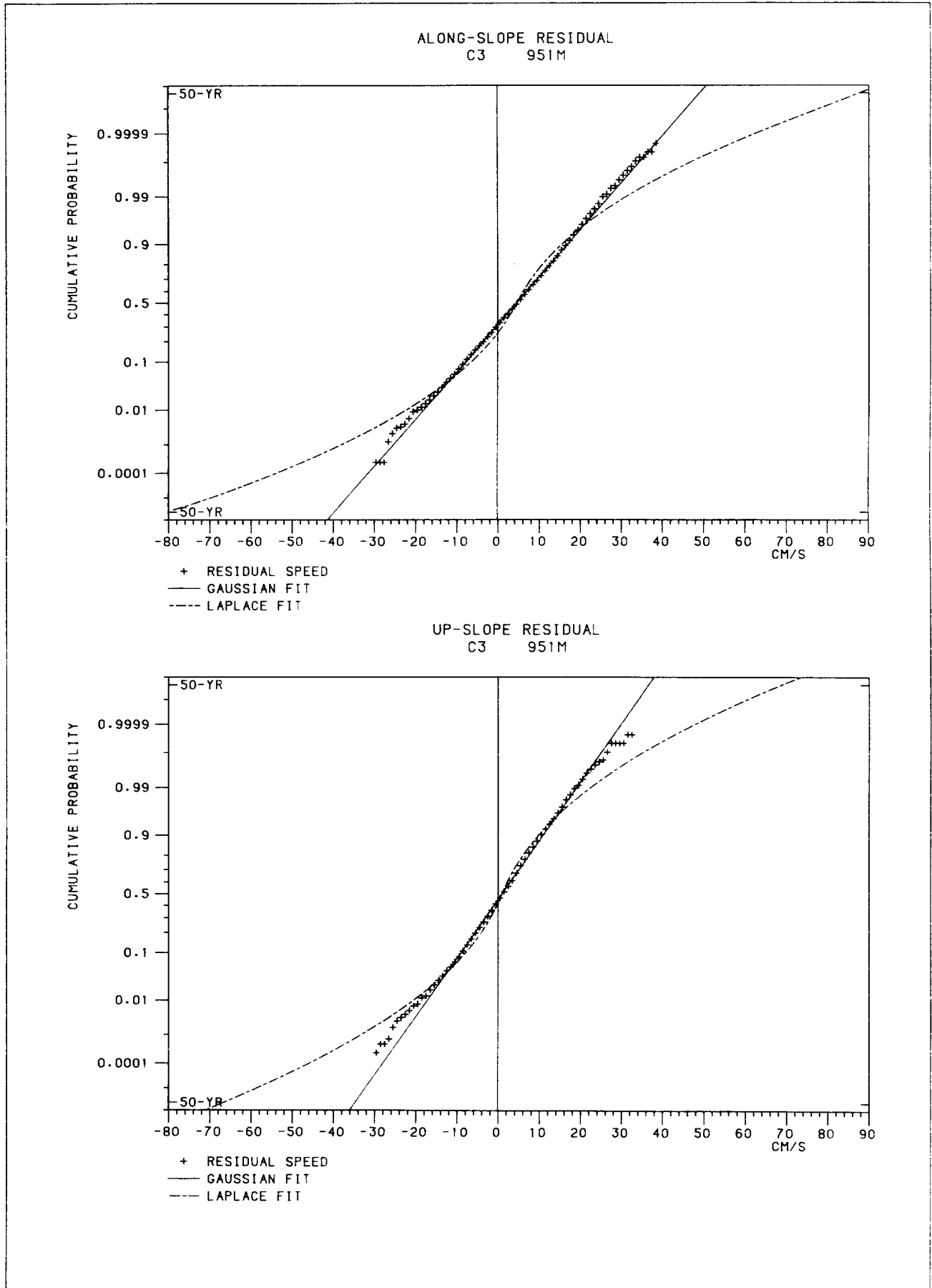




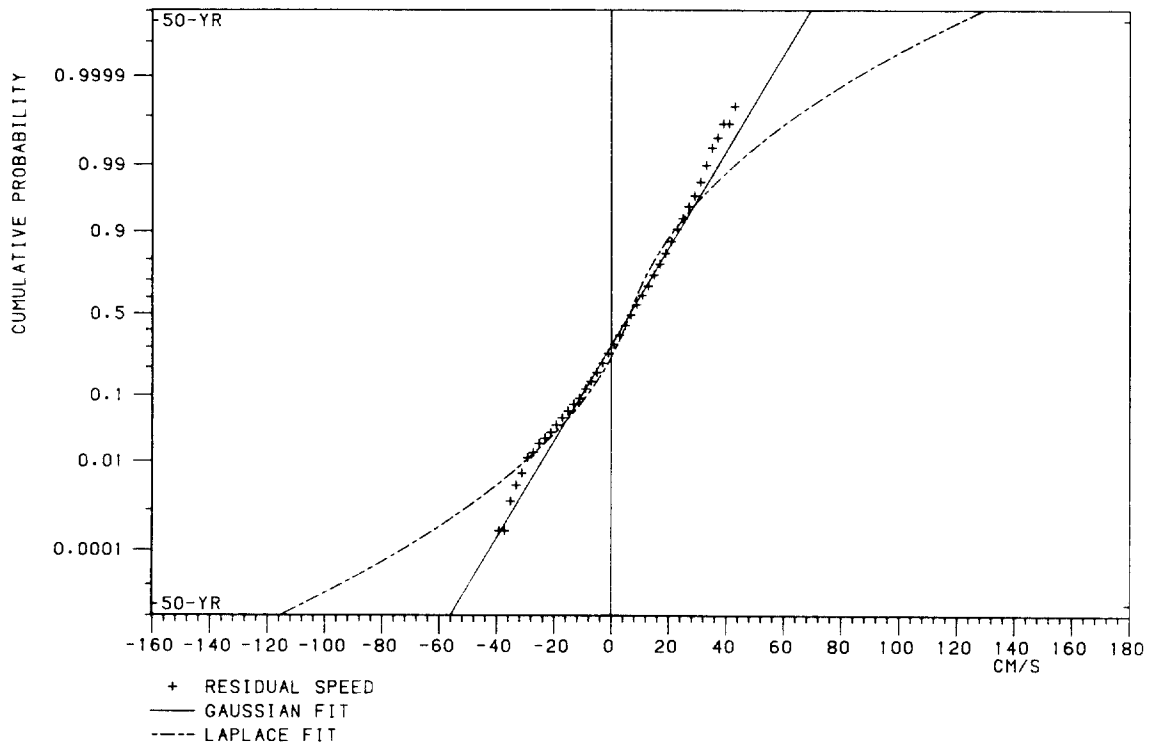




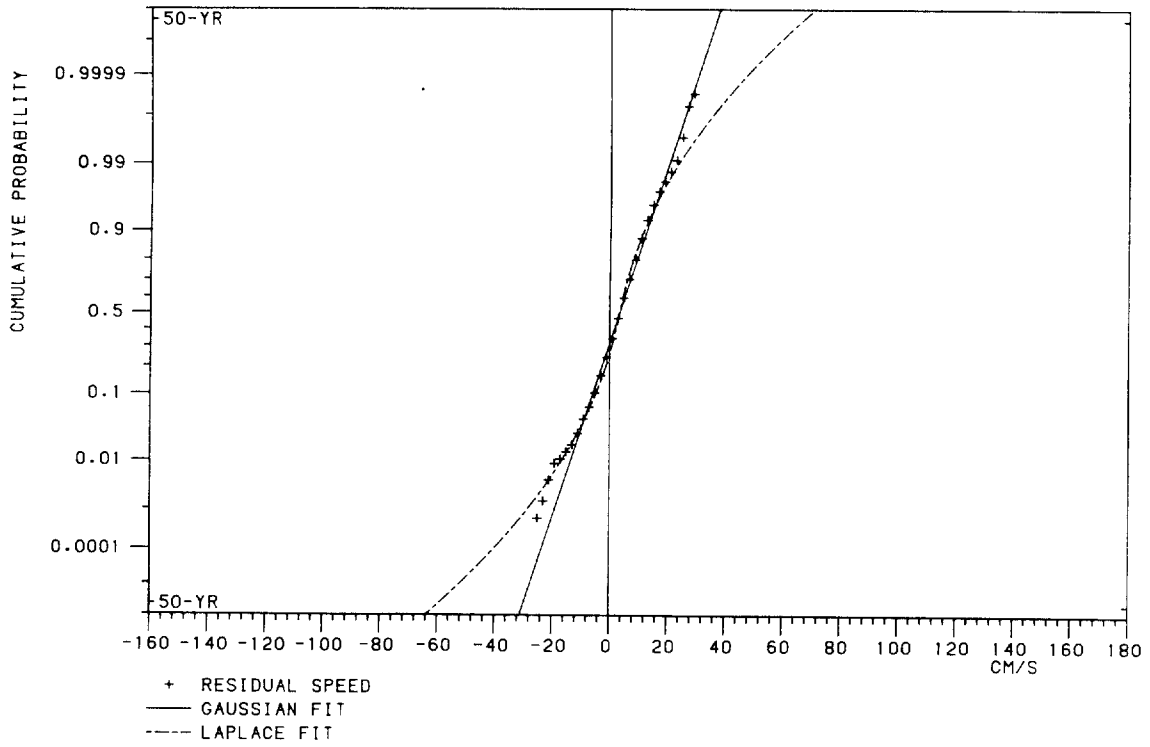




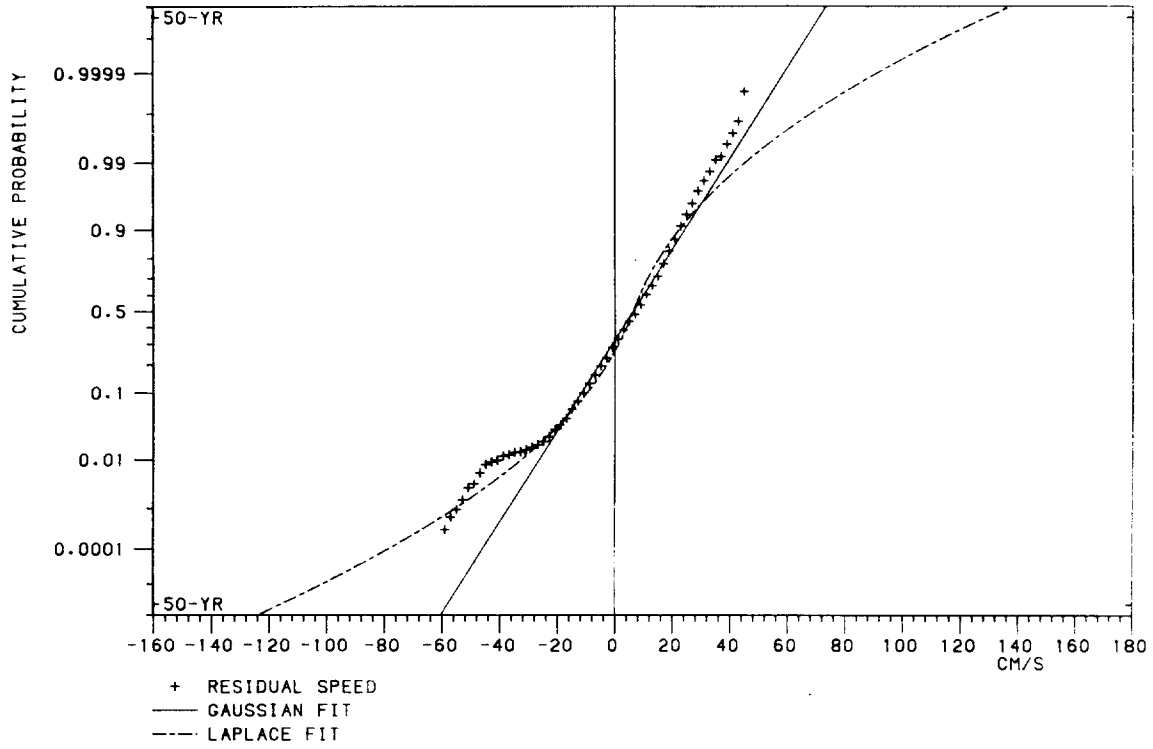
ALONG-SLOPE RESIDUAL
D1 87M



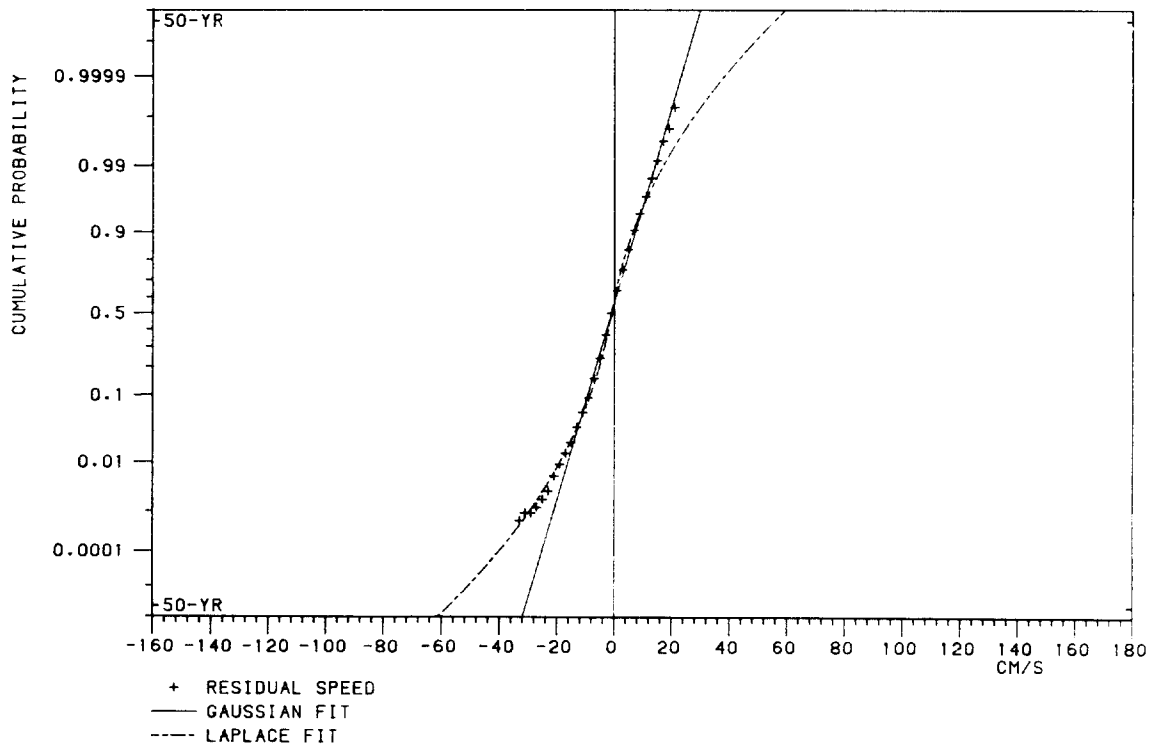
UP-SLOPE RESIDUAL
D1 87M

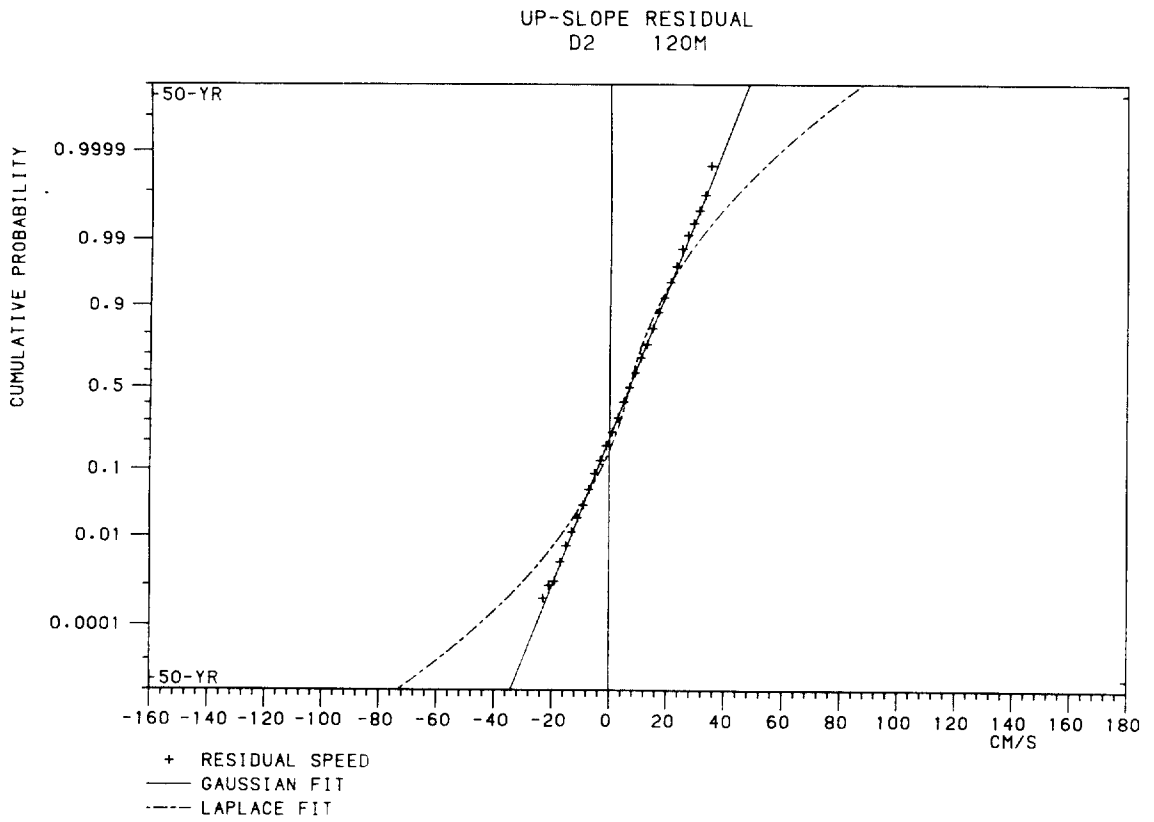
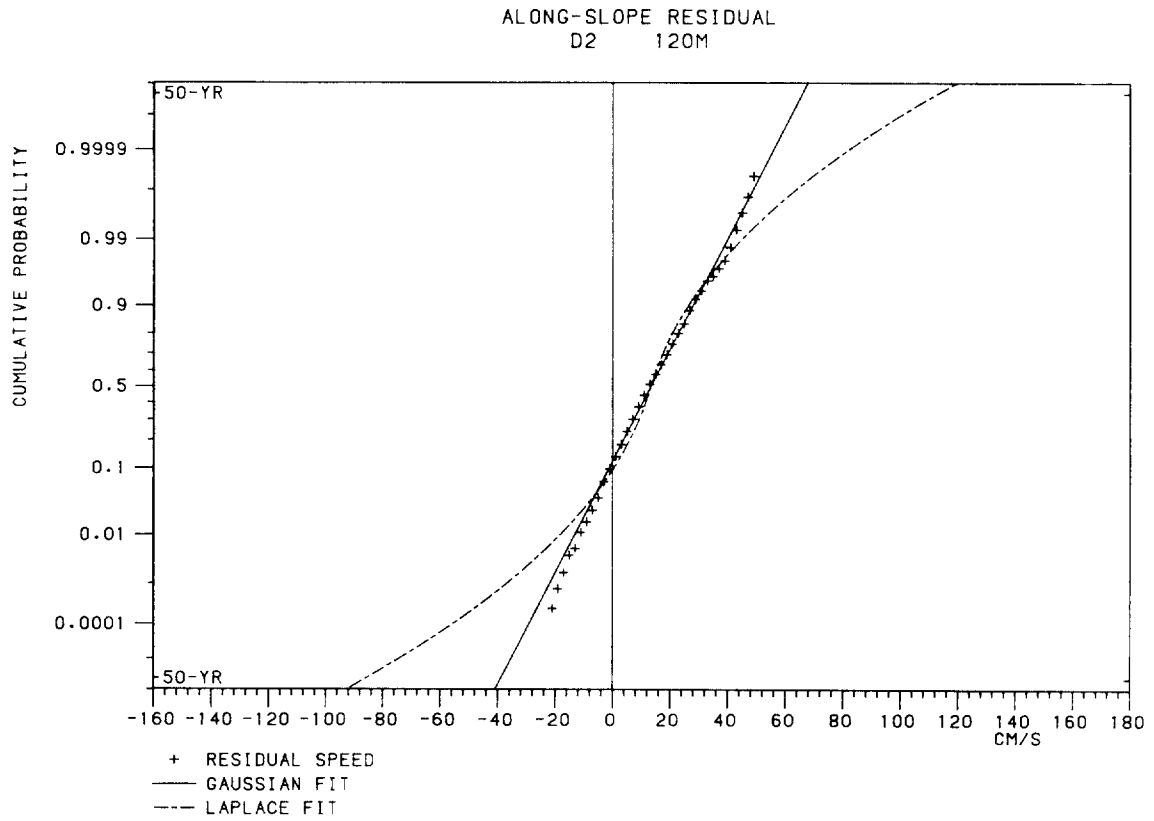


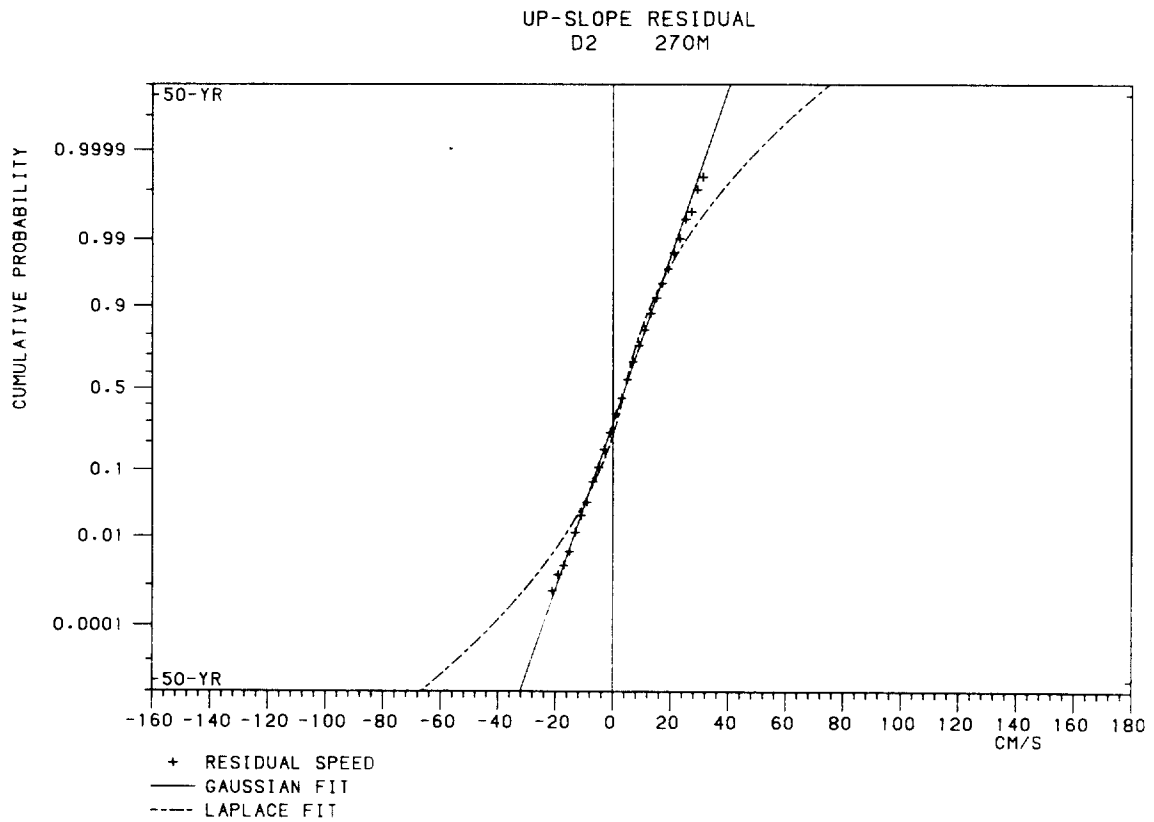
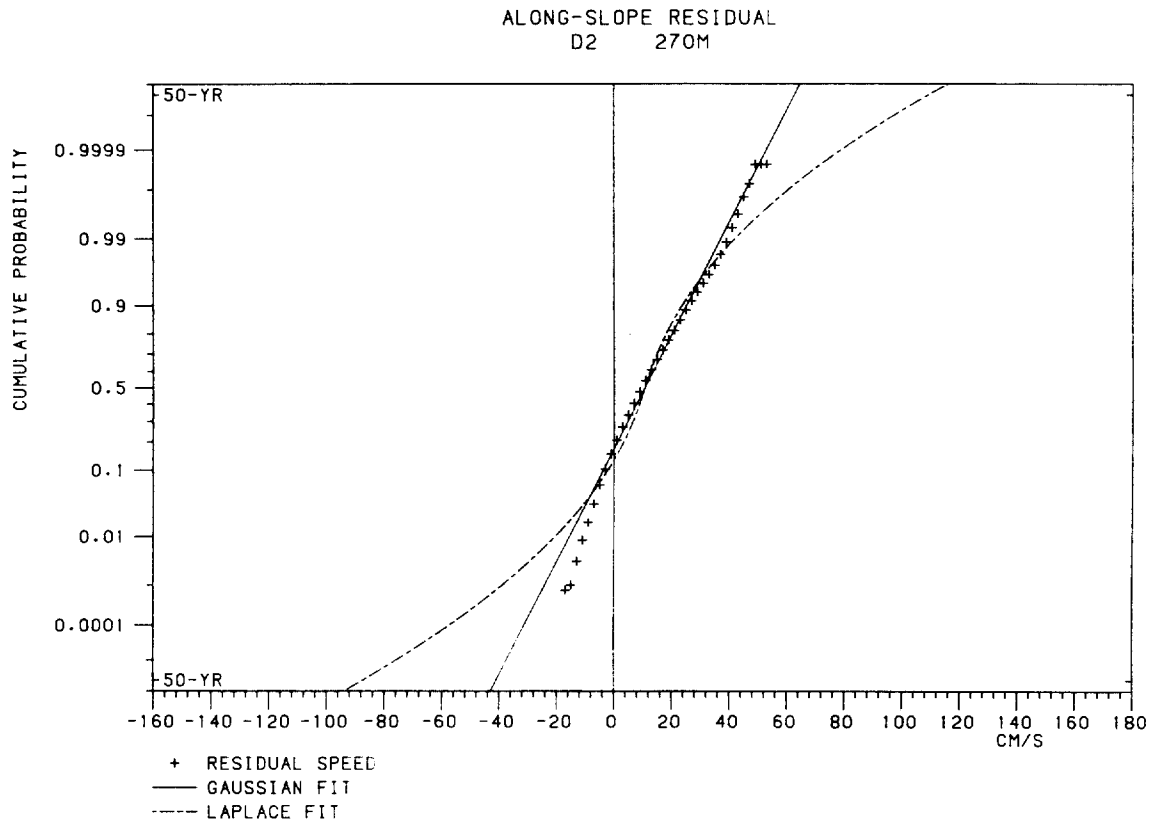
ALONG-SLOPE RESIDUAL
D1 212M

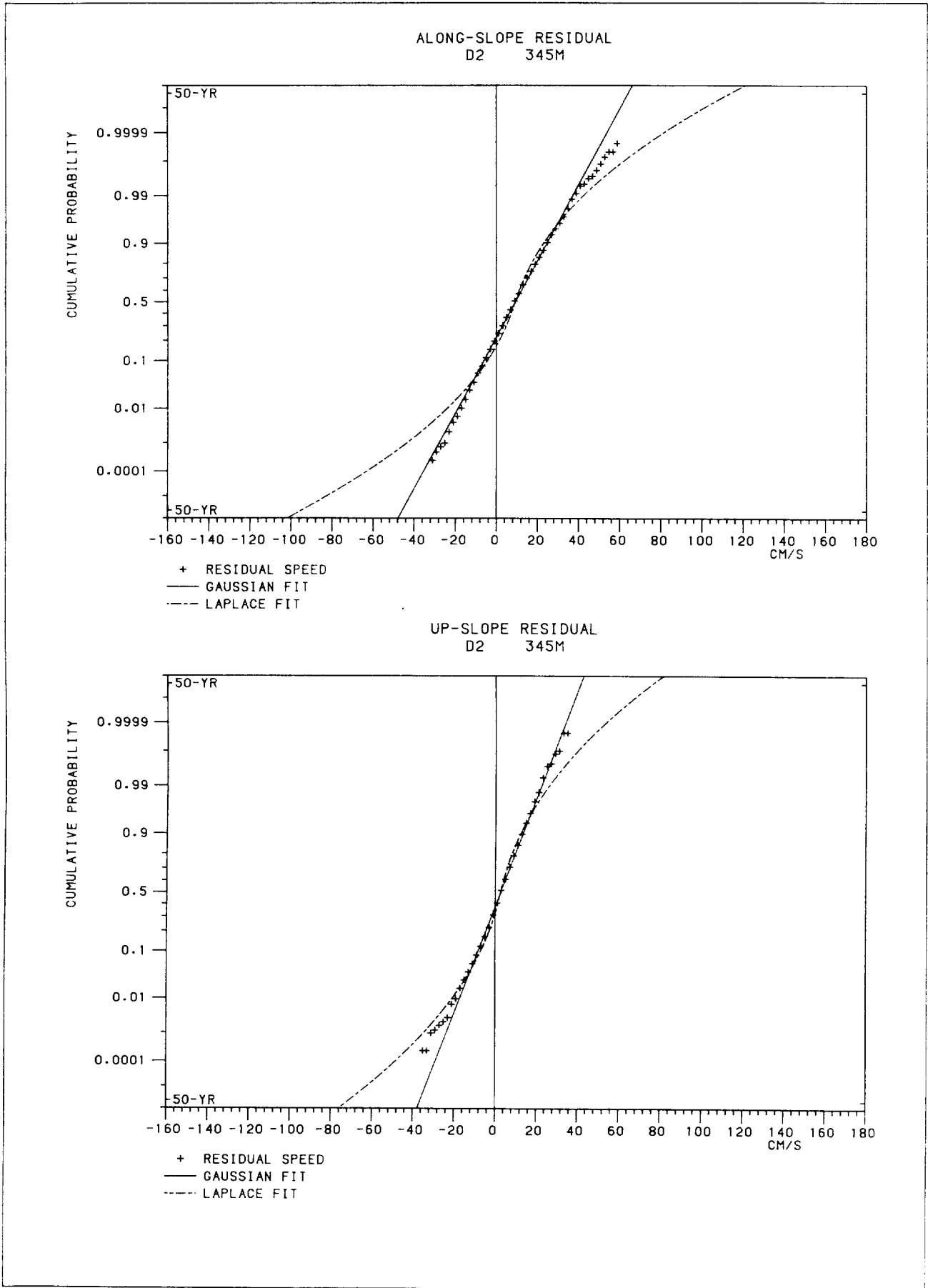


UP-SLOPE RESIDUAL
D1 212M

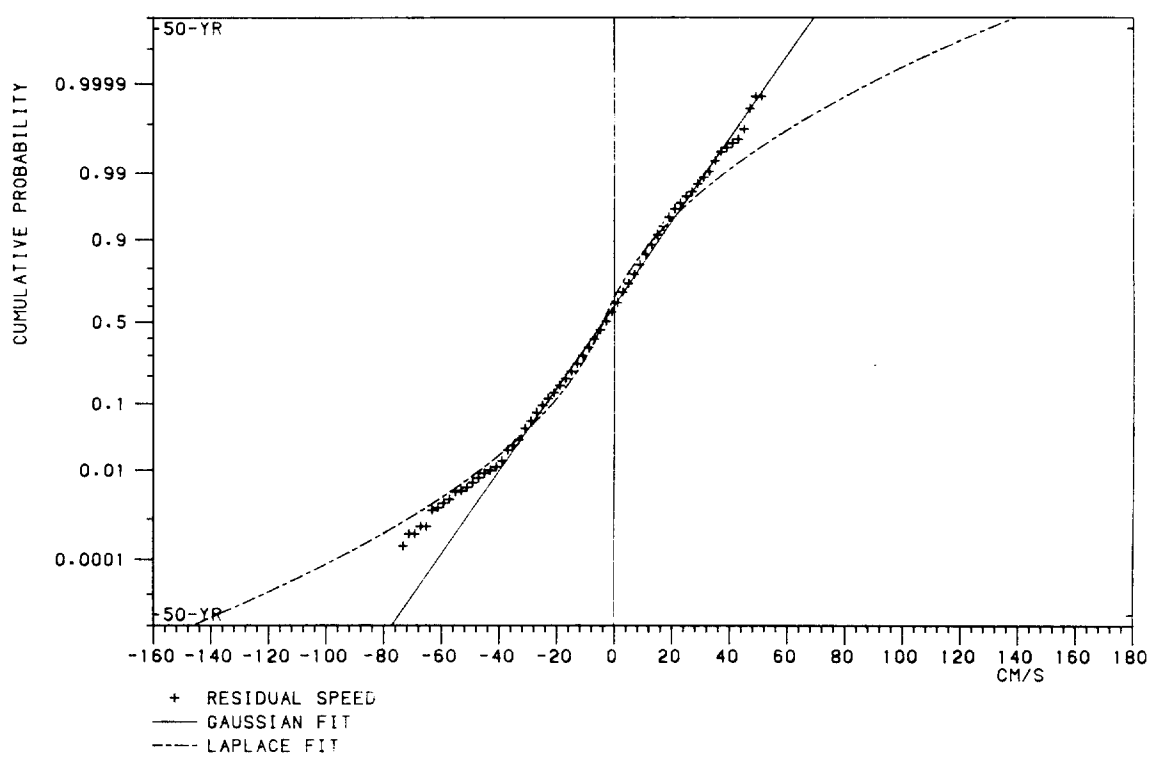




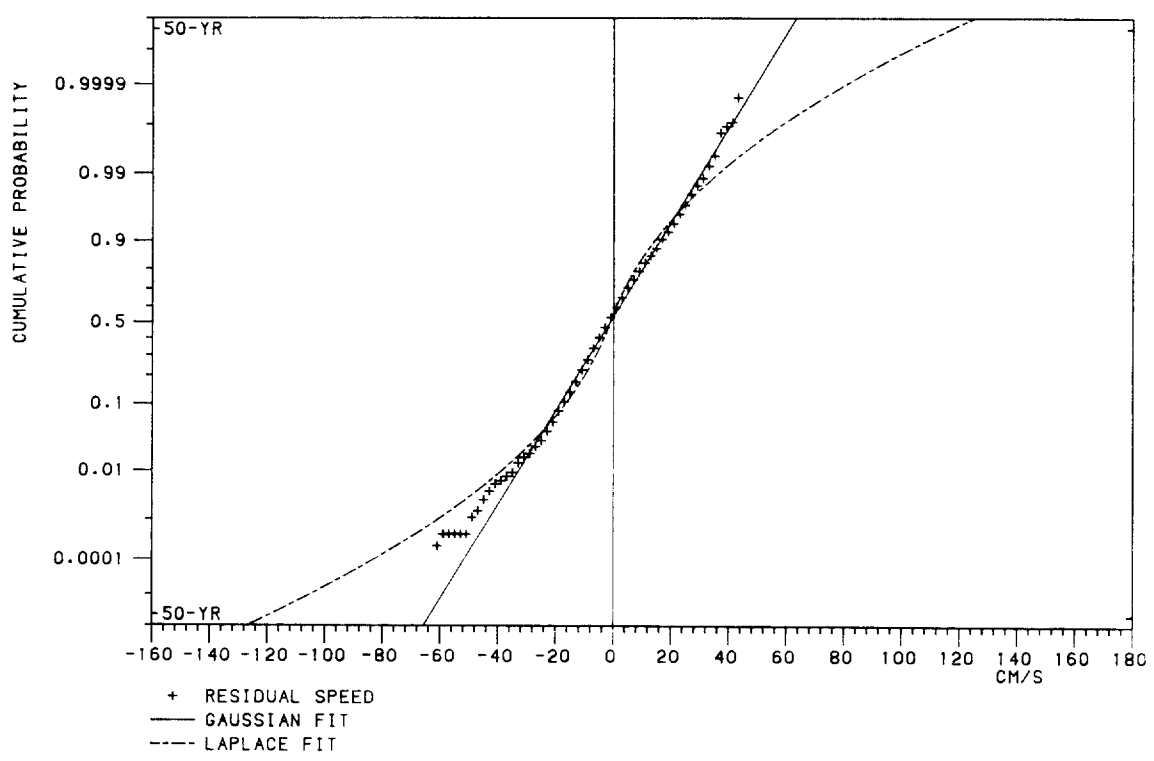


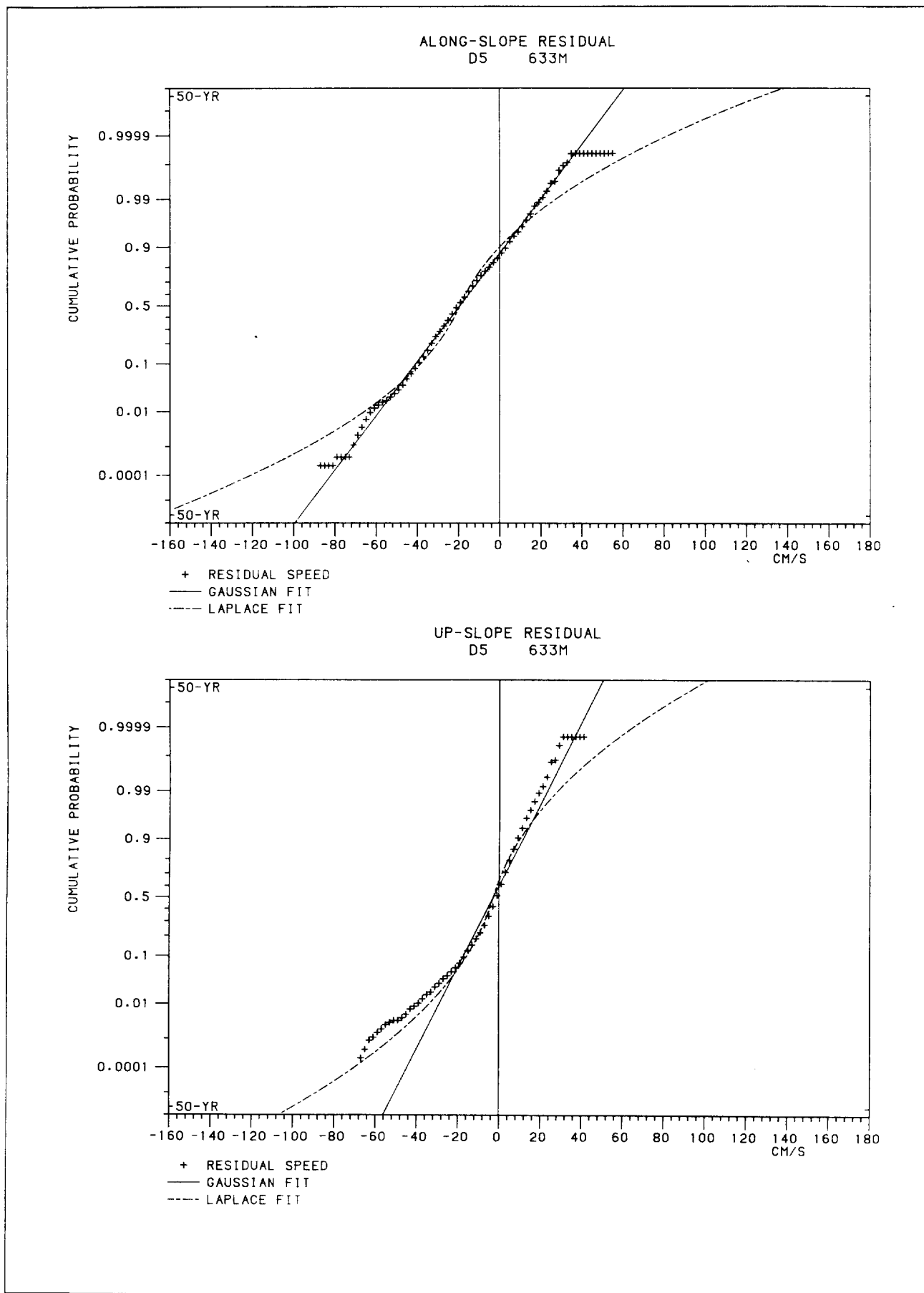


ALONG-SLOPE RESIDUAL
D5 510M

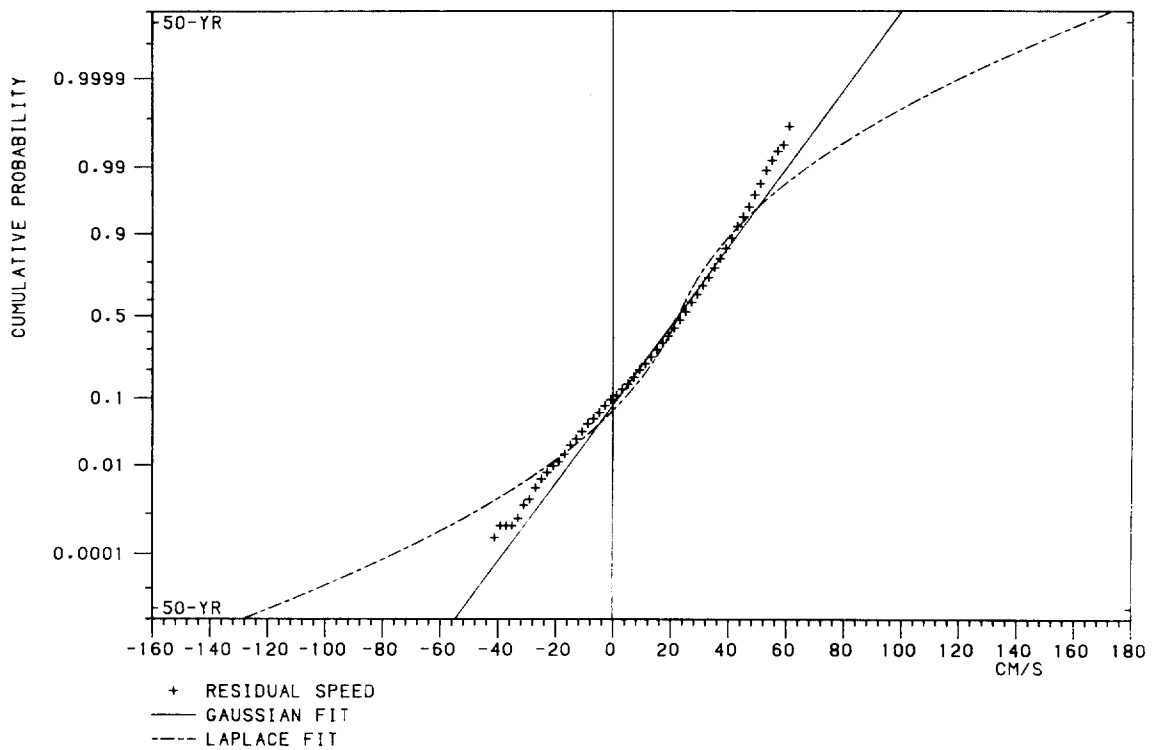


UP-SLOPE RESIDUAL
D5 510M

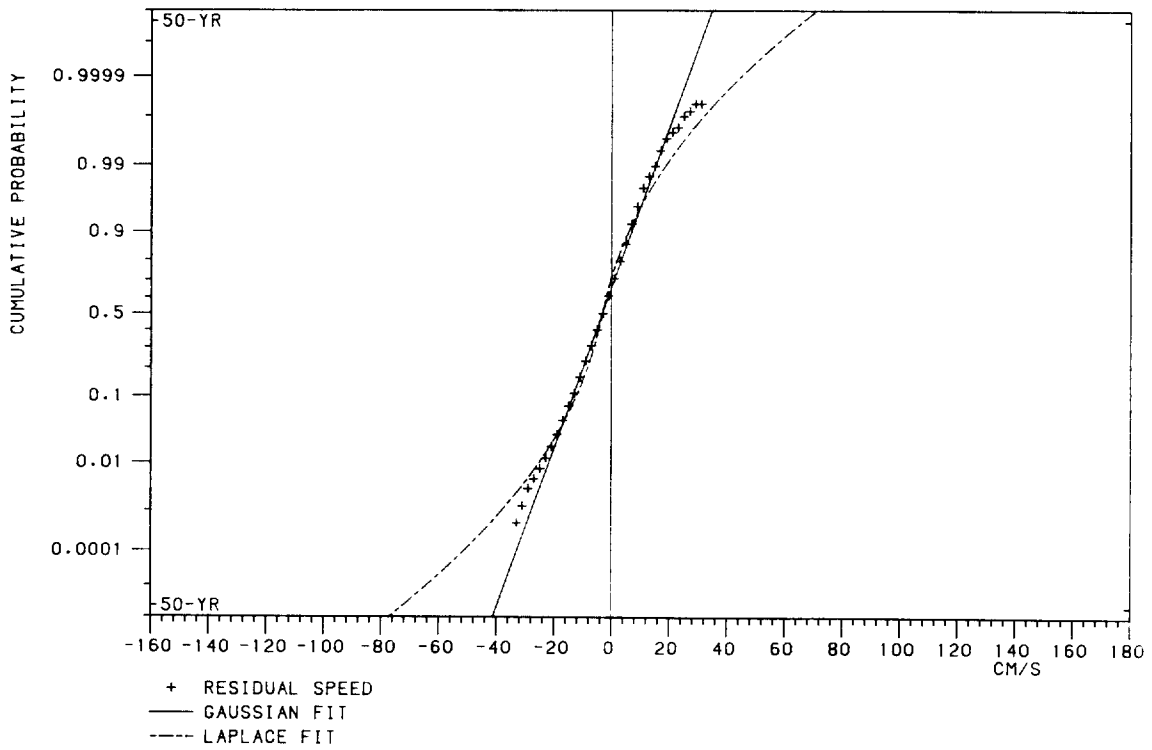


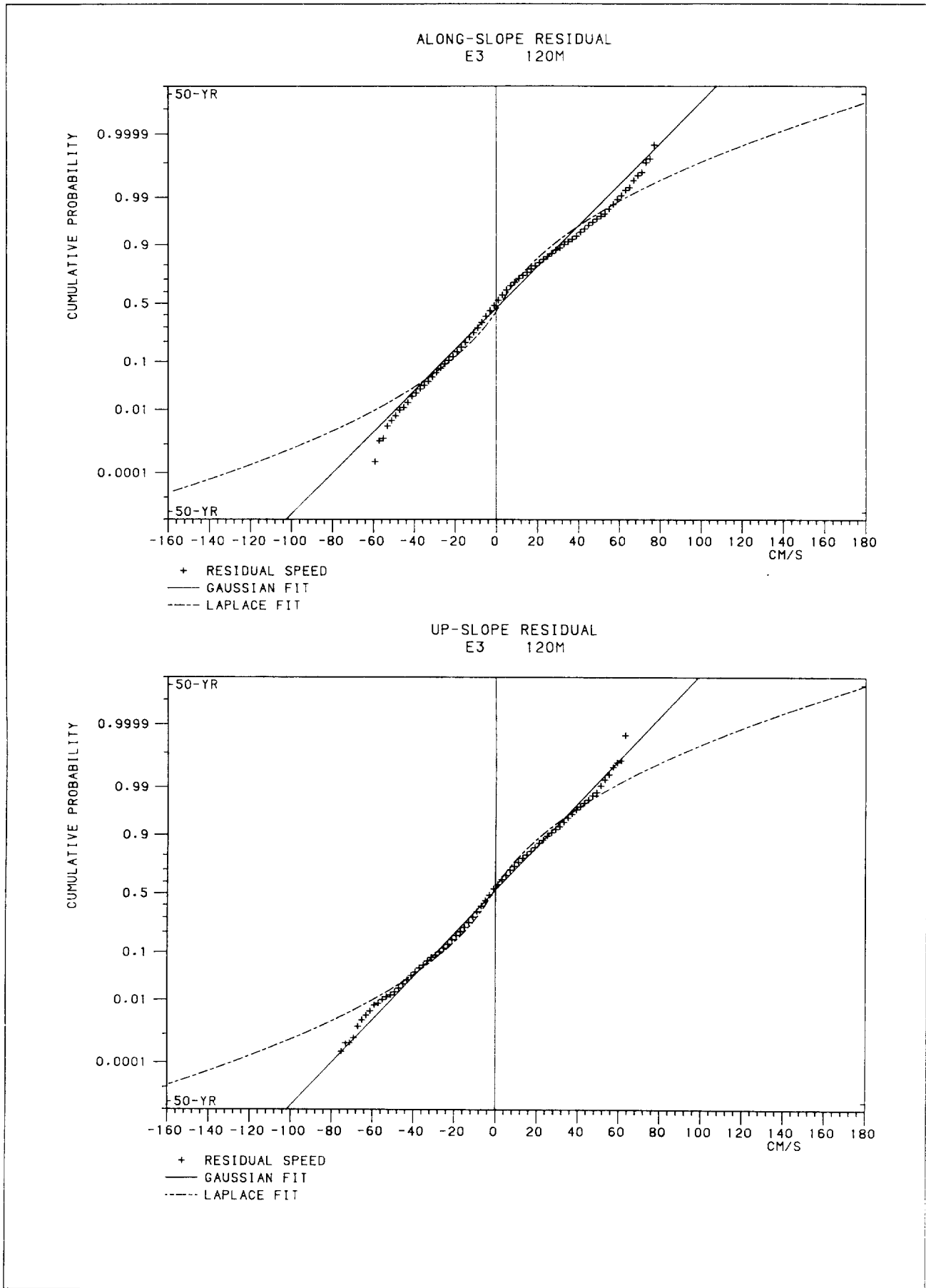


ALONG-SLOPE RESIDUAL
E2 453M

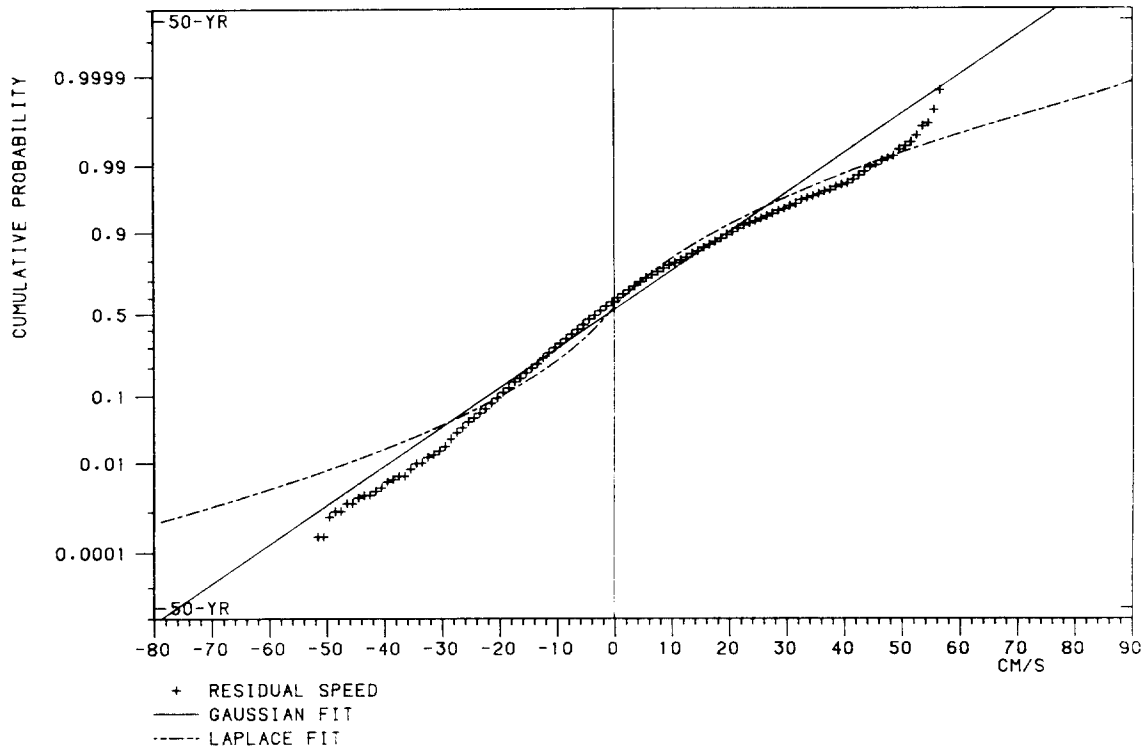


UP-SLOPE RESIDUAL
E2 453M

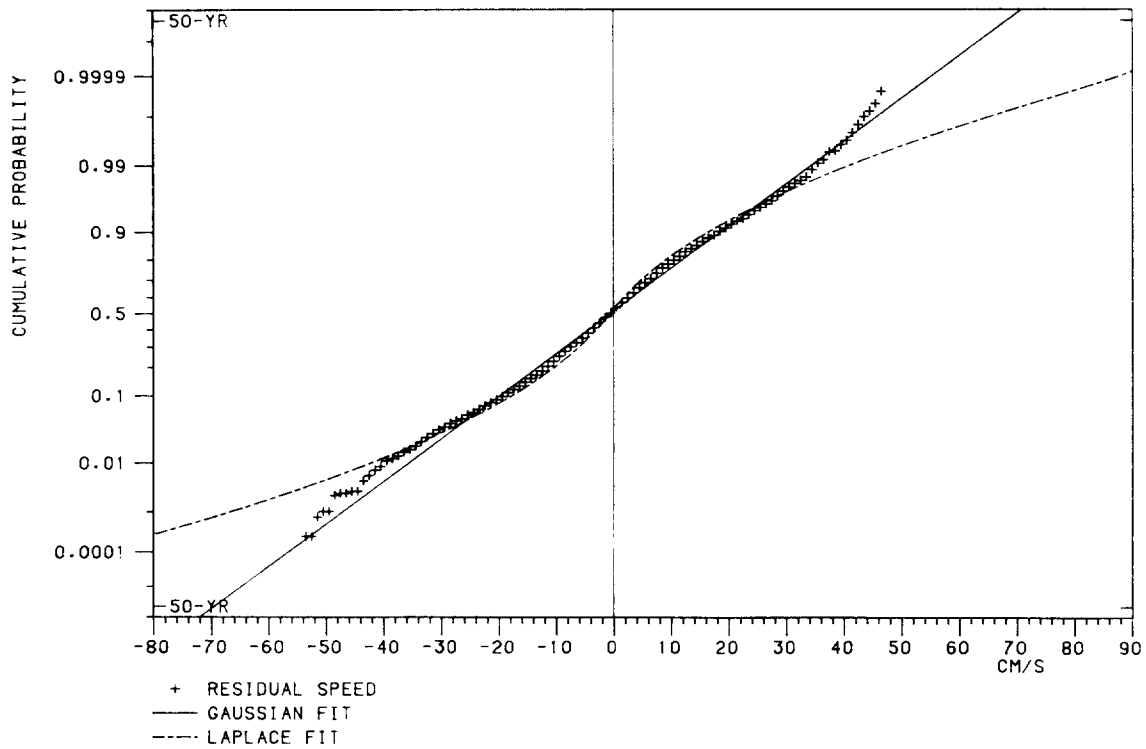




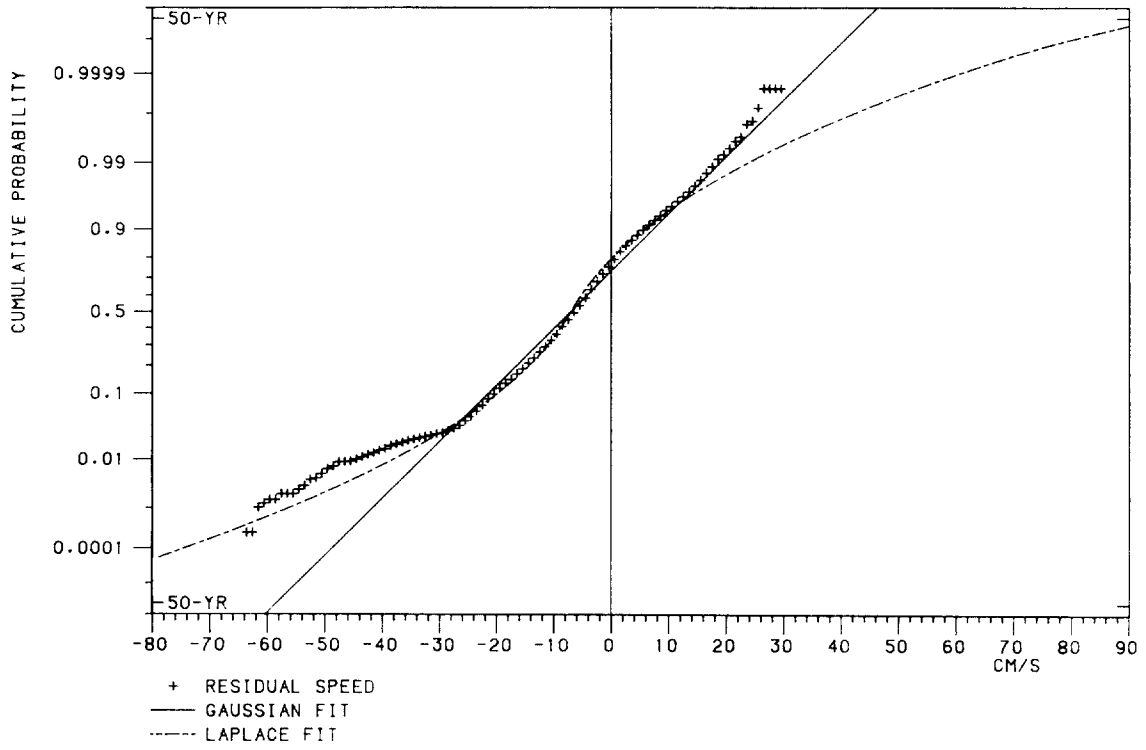
ALONG-SLOPE RESIDUAL
E3 419M



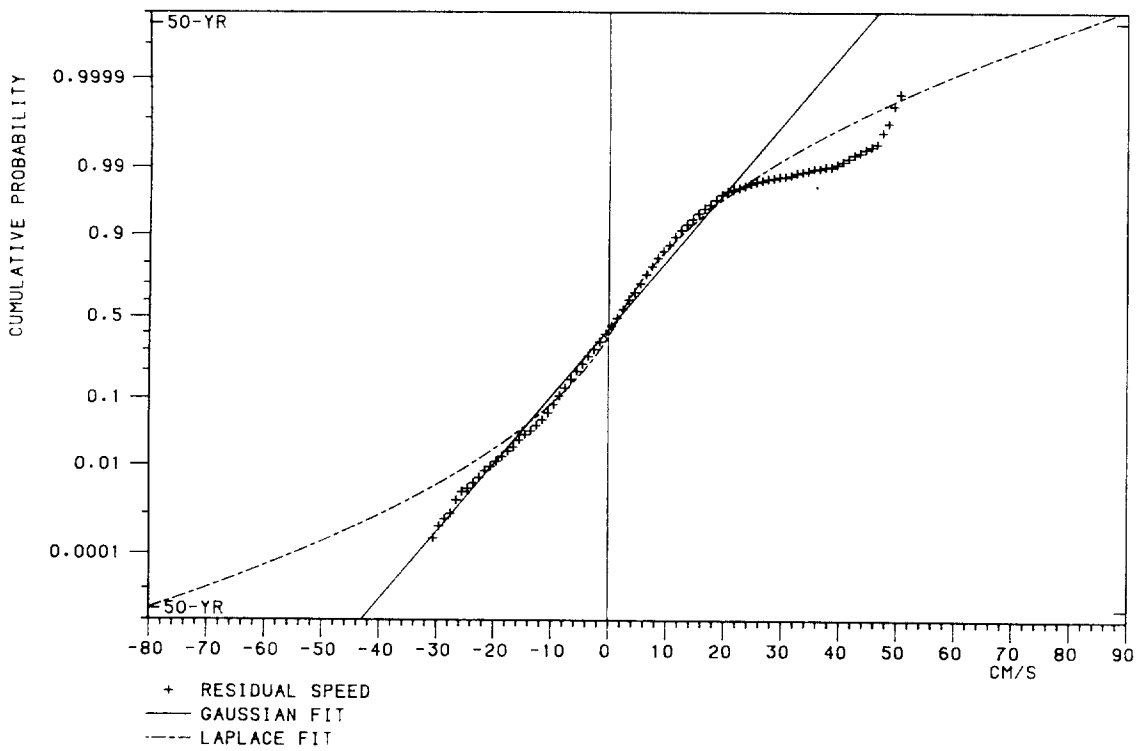
UP-SLOPE RESIDUAL
E3 419M

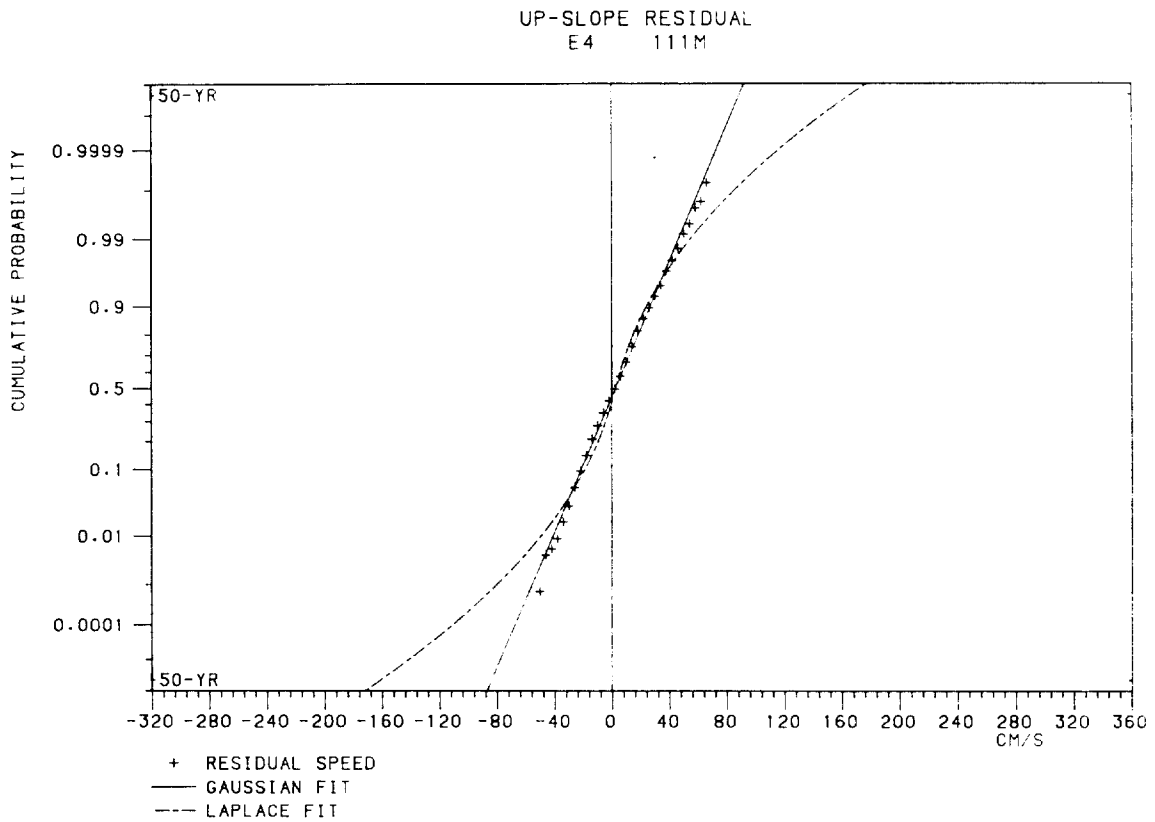
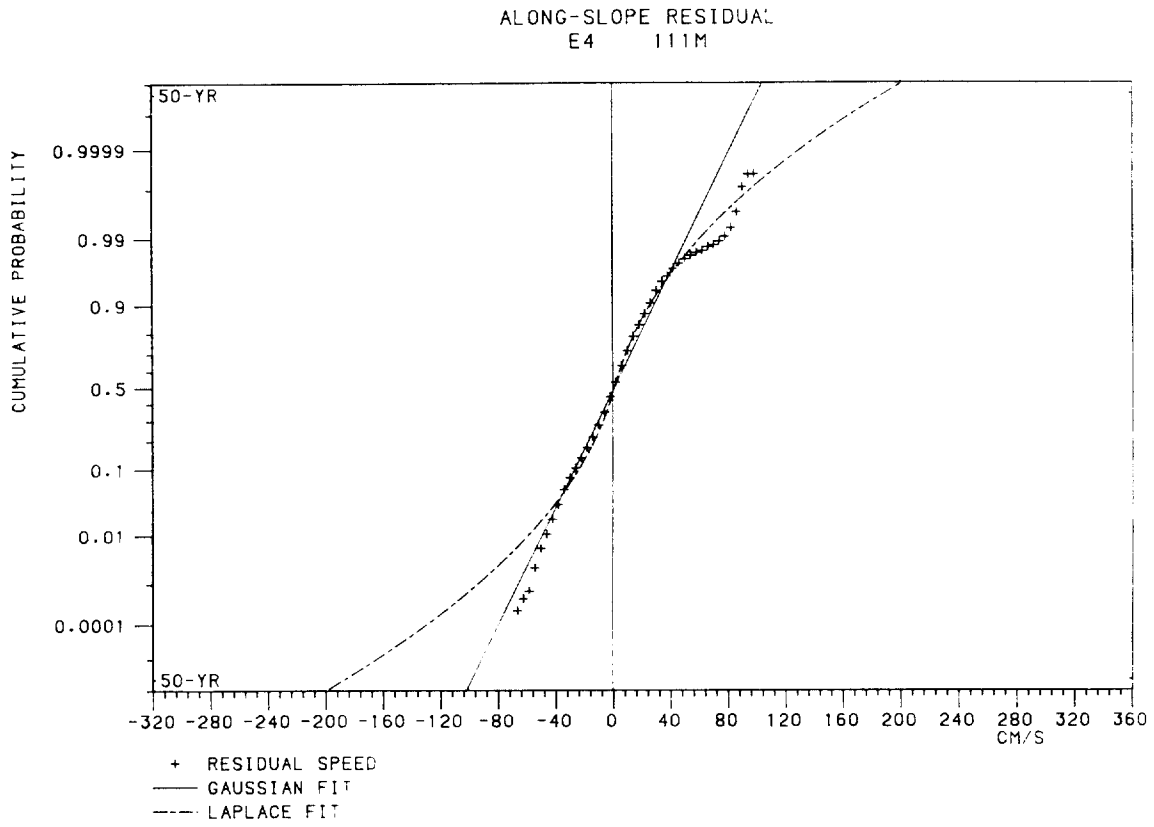


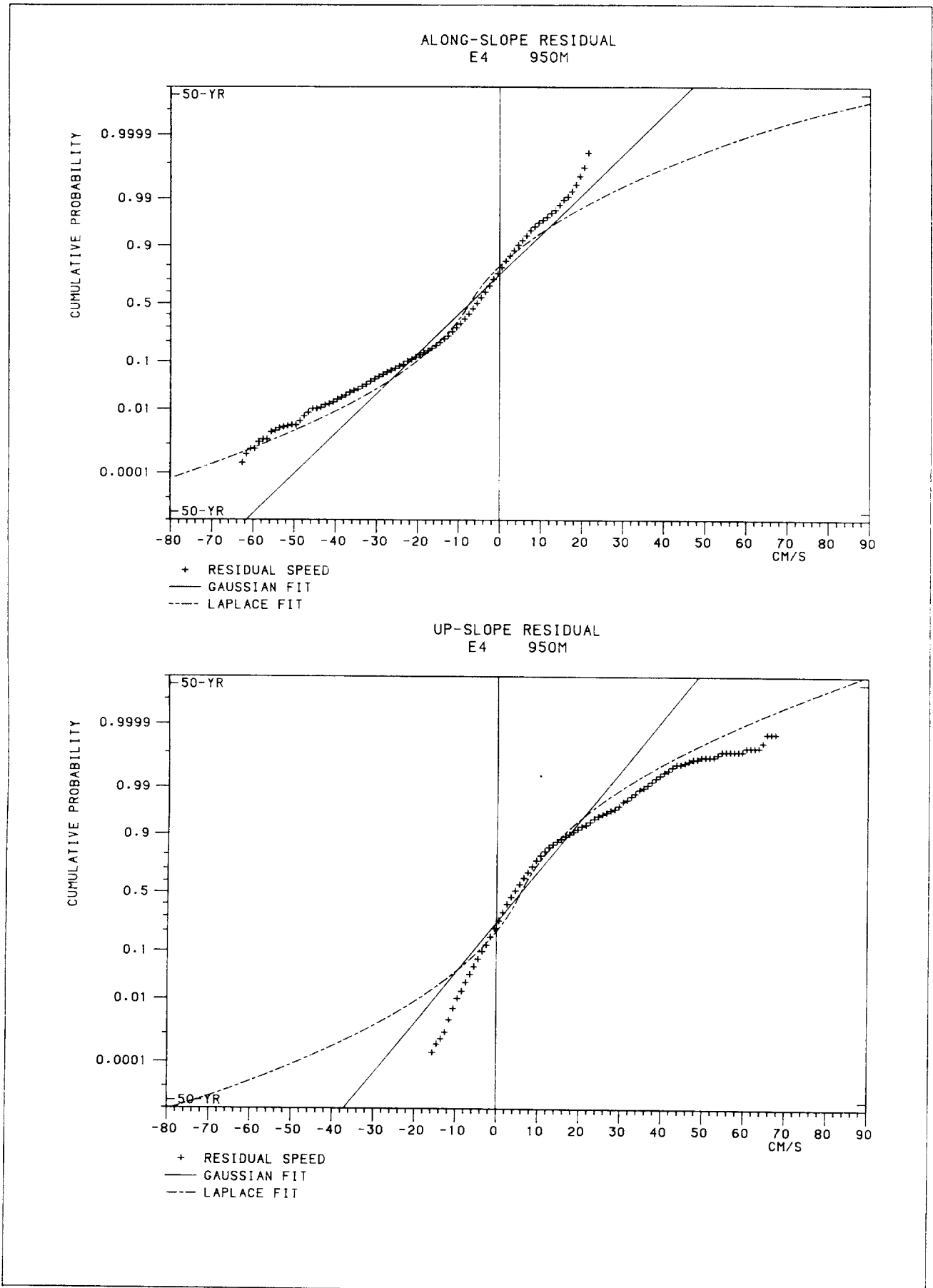
ALONG-SLOPE RESIDUAL
E3 725M

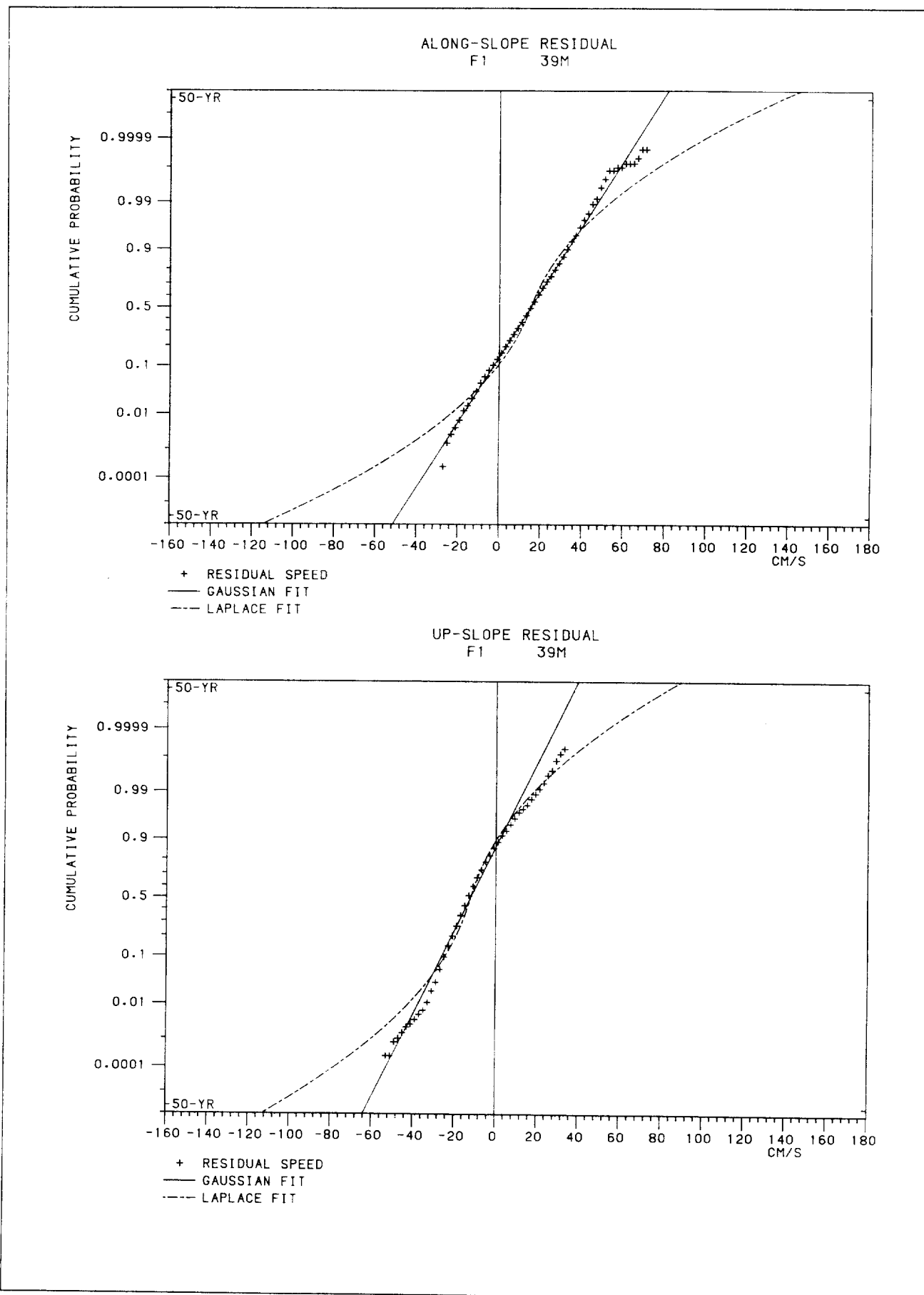


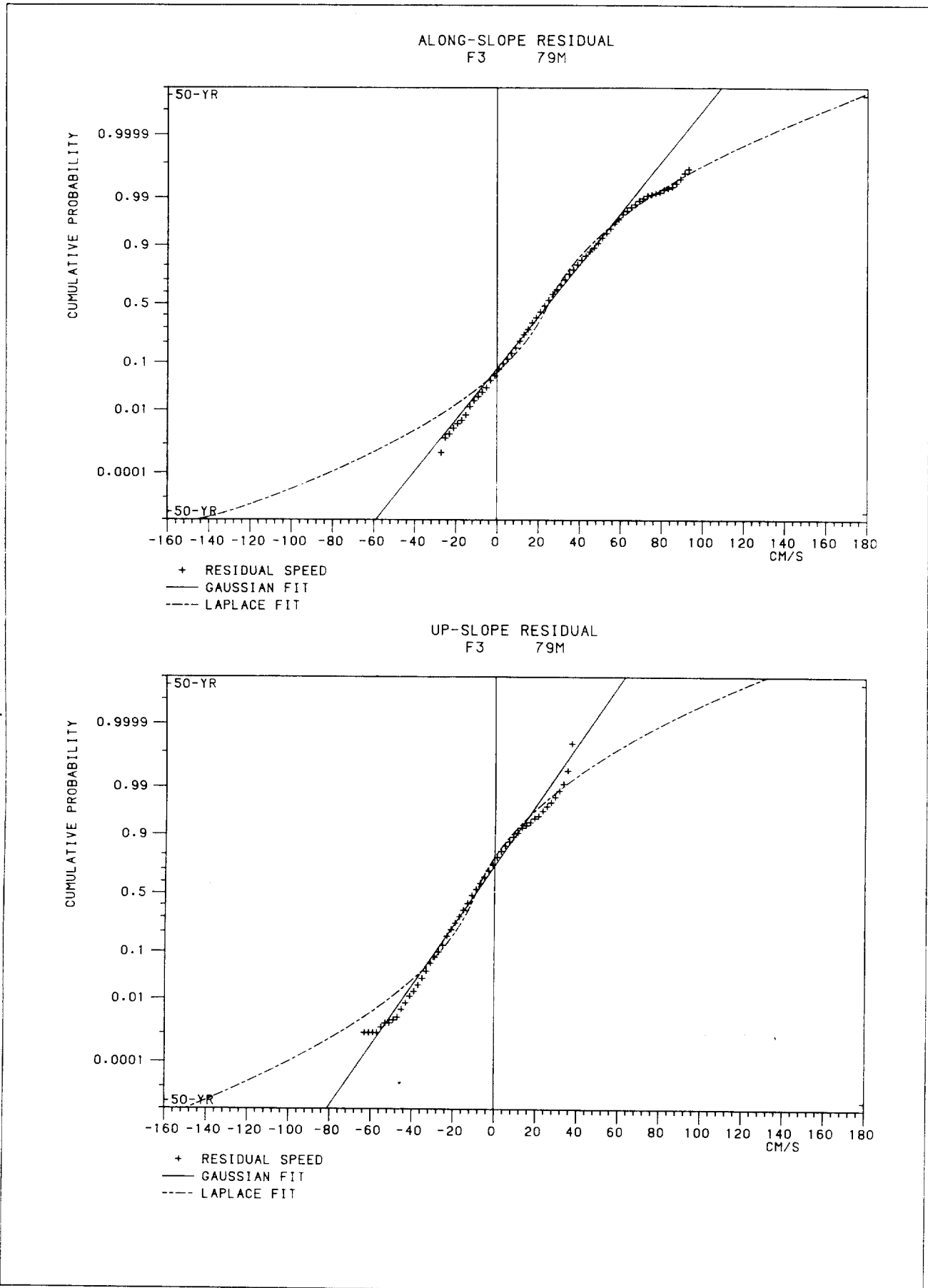
UP-SLOPE RESIDUAL
E3 725M



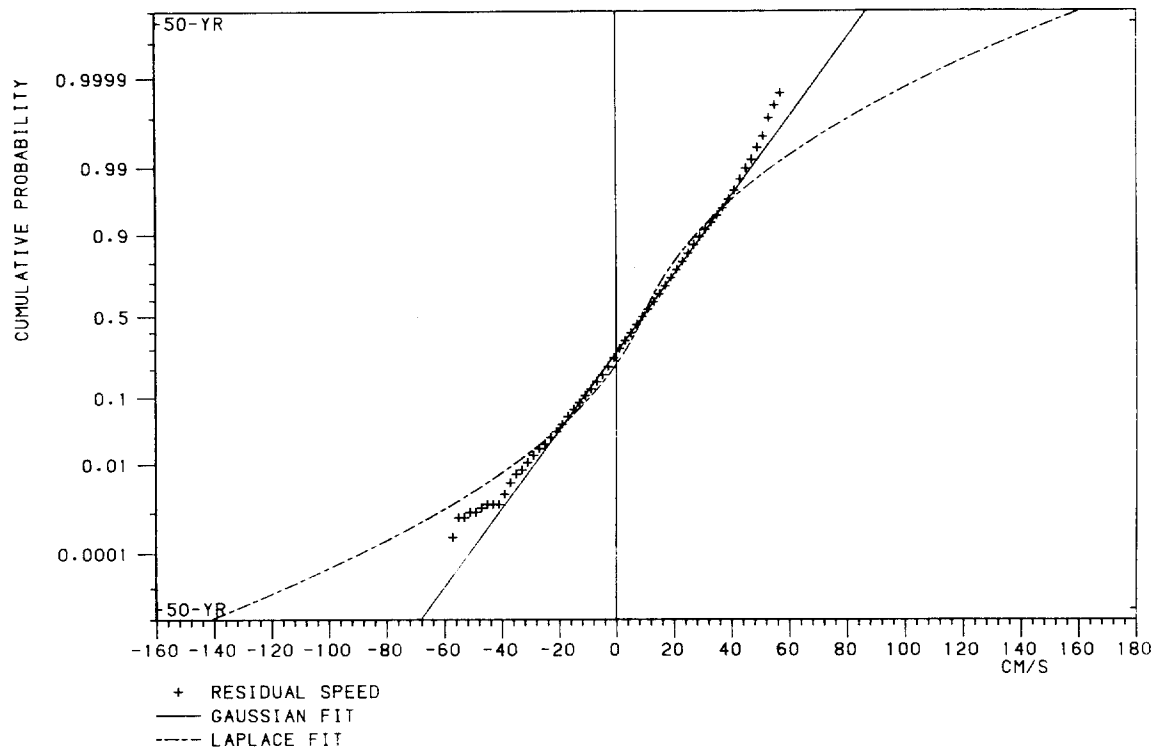




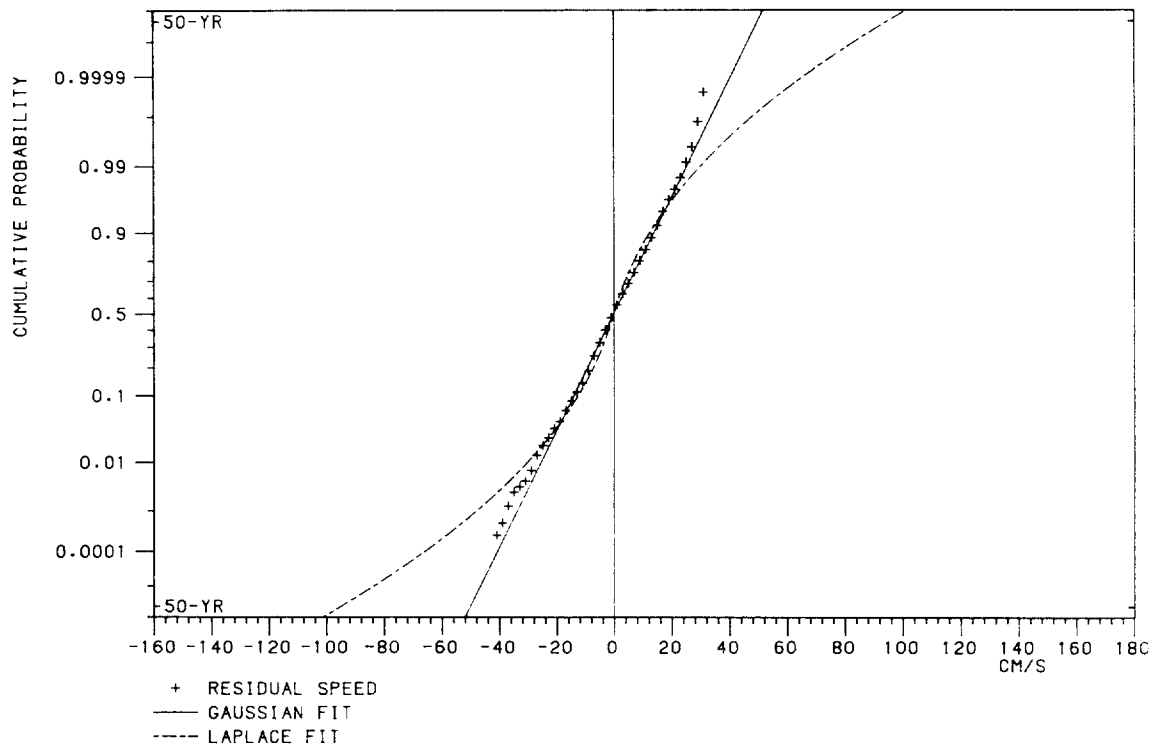


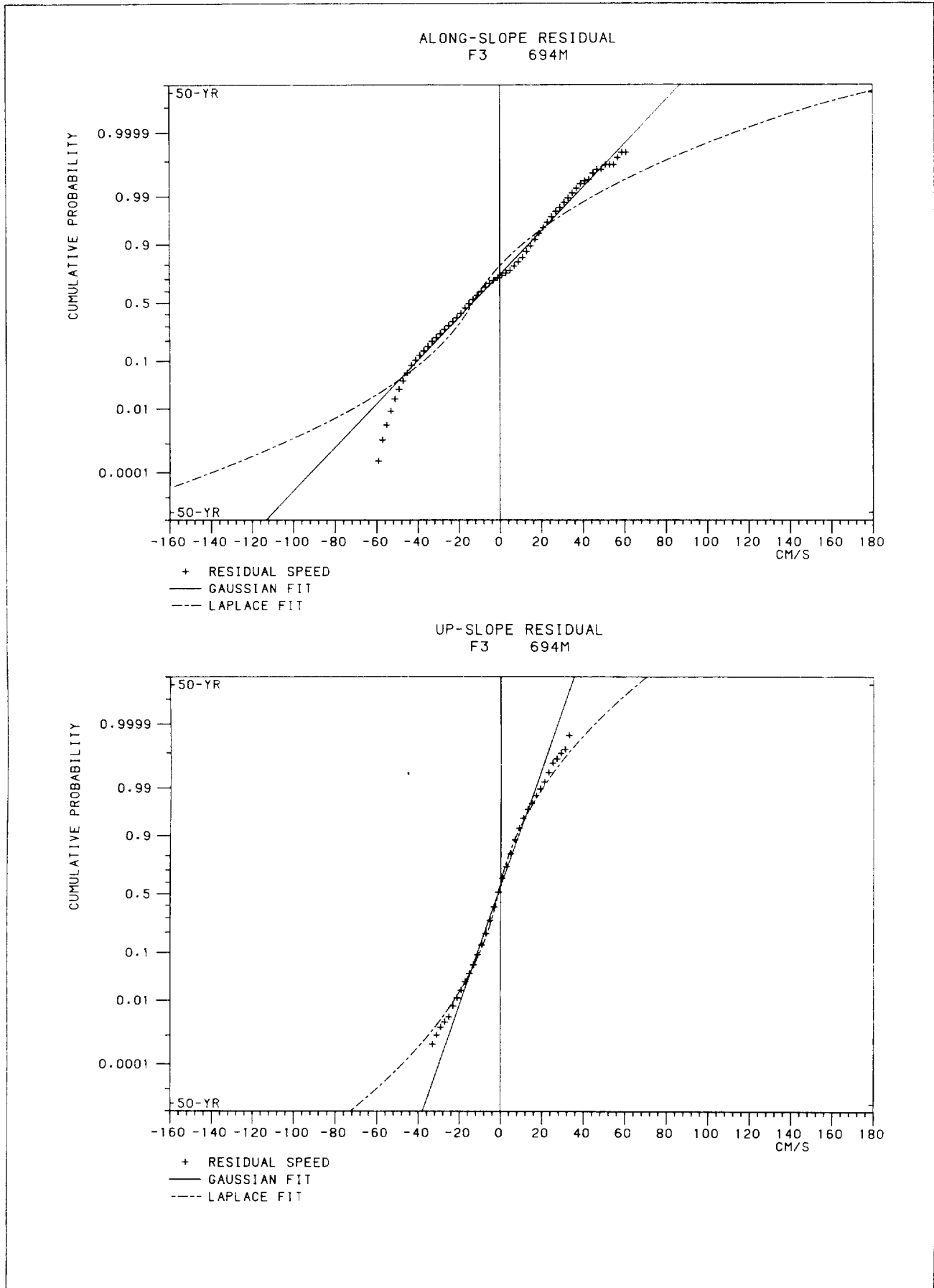


ALONG-SLOPE RESIDUAL
F3 388M

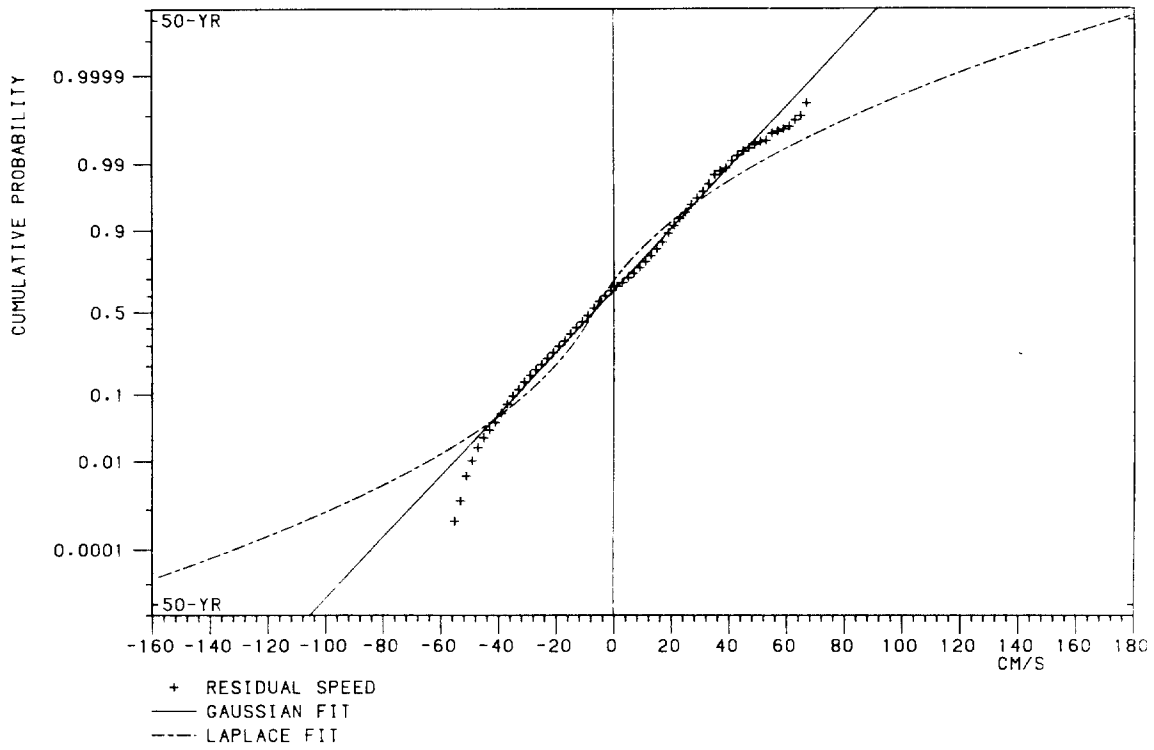


UP-SLOPE RESIDUAL
F3 388M

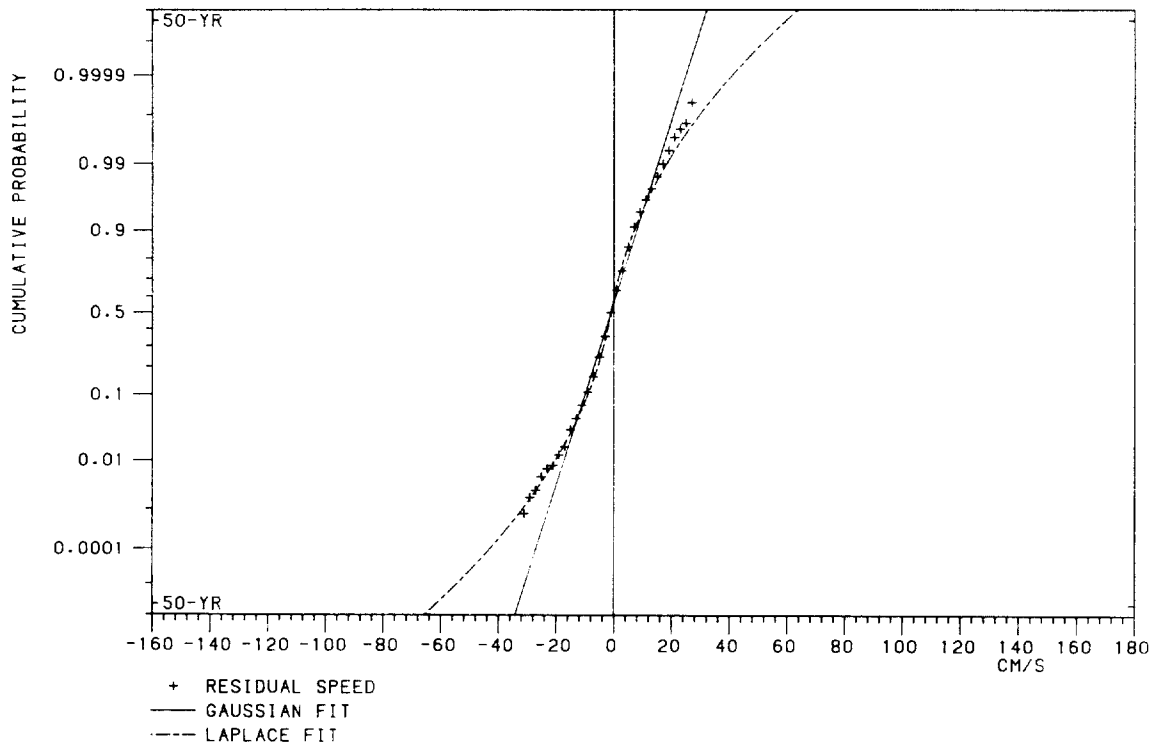


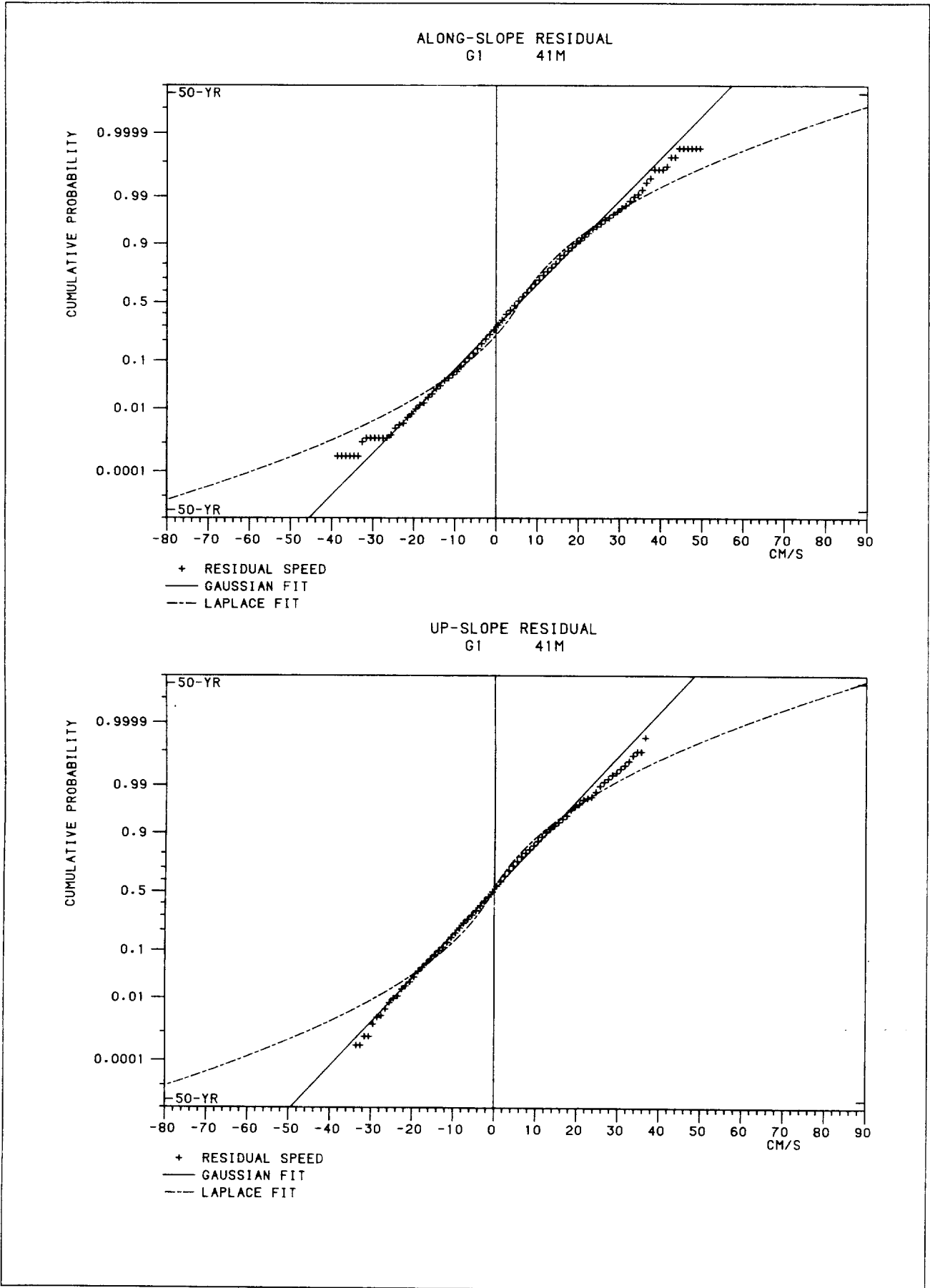


ALONG-SLOPE RESIDUAL
F3 945M

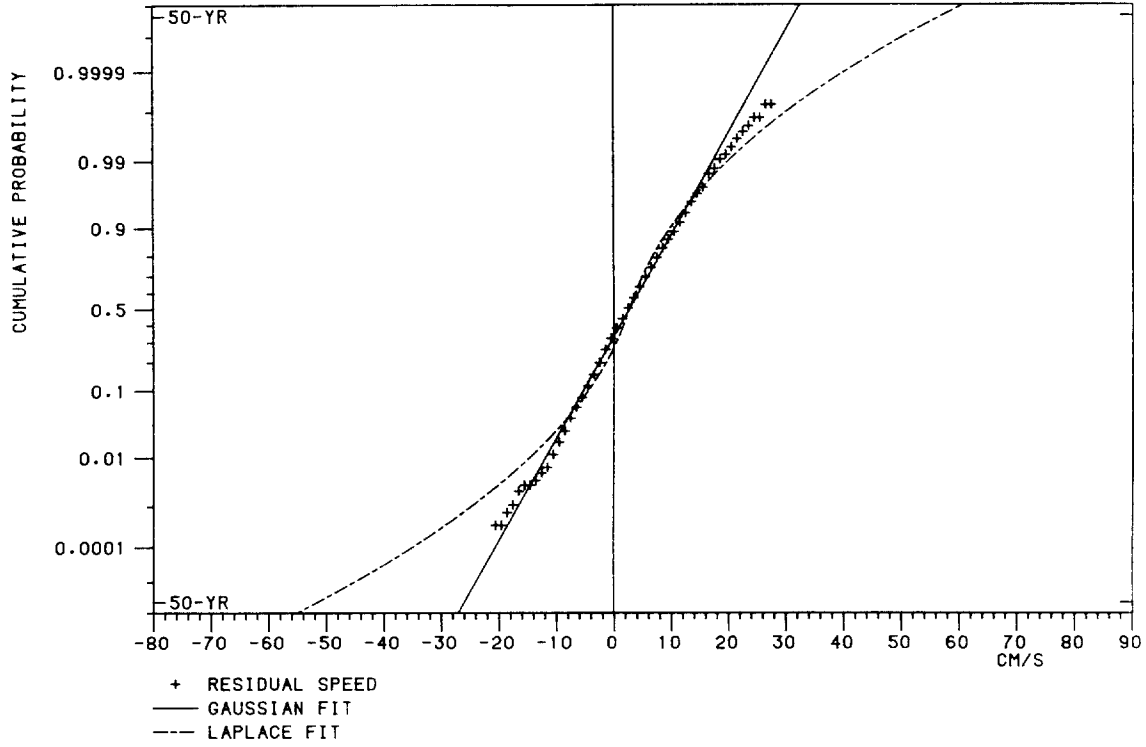


UP-SLOPE RESIDUAL
F3 945M

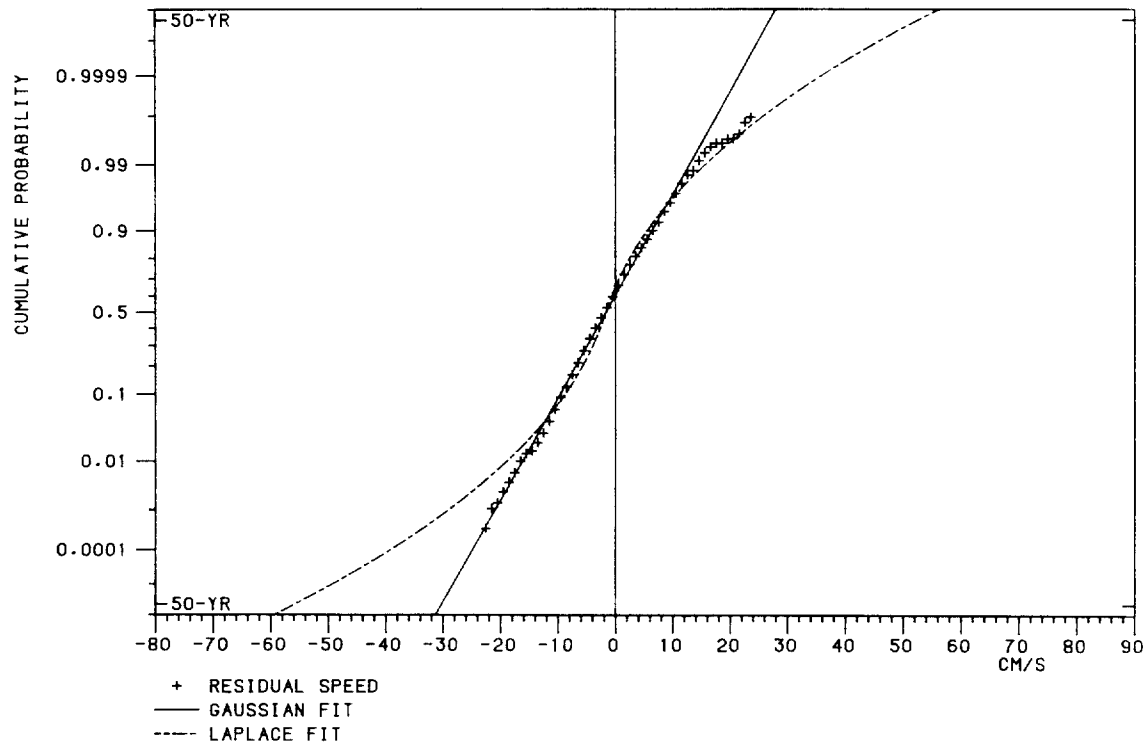


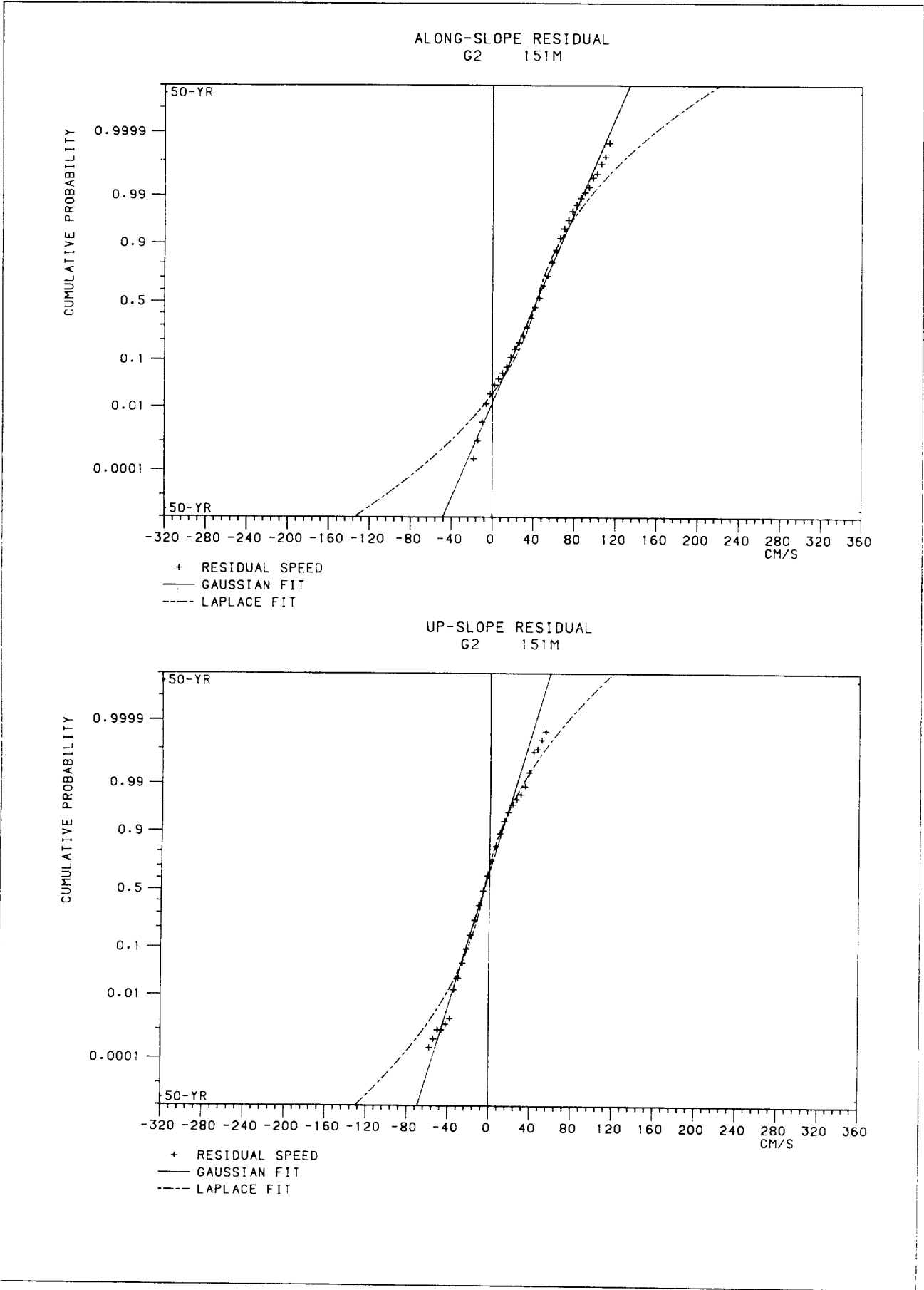


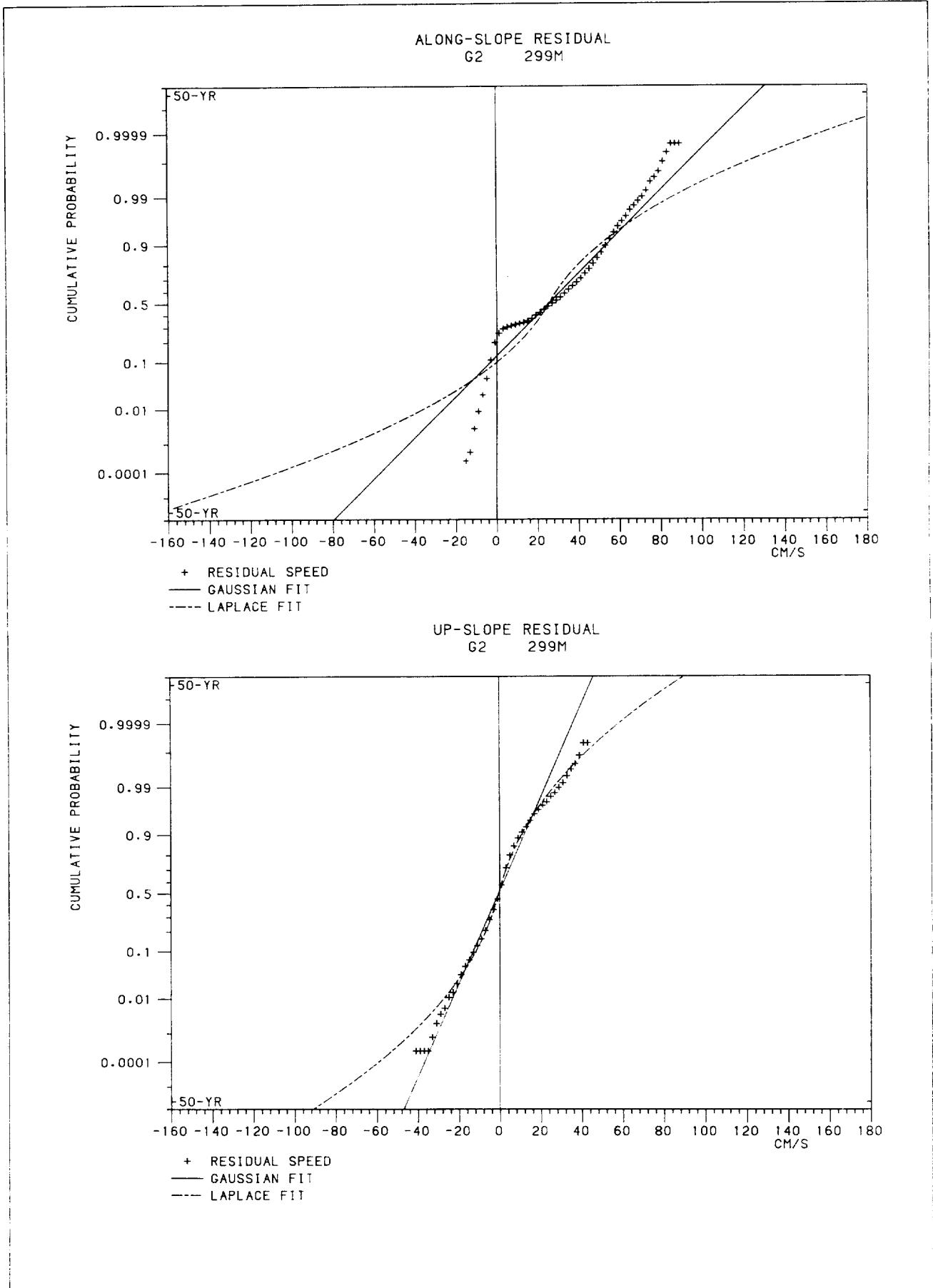
ALONG-SLOPE RESIDUAL
G1 166M

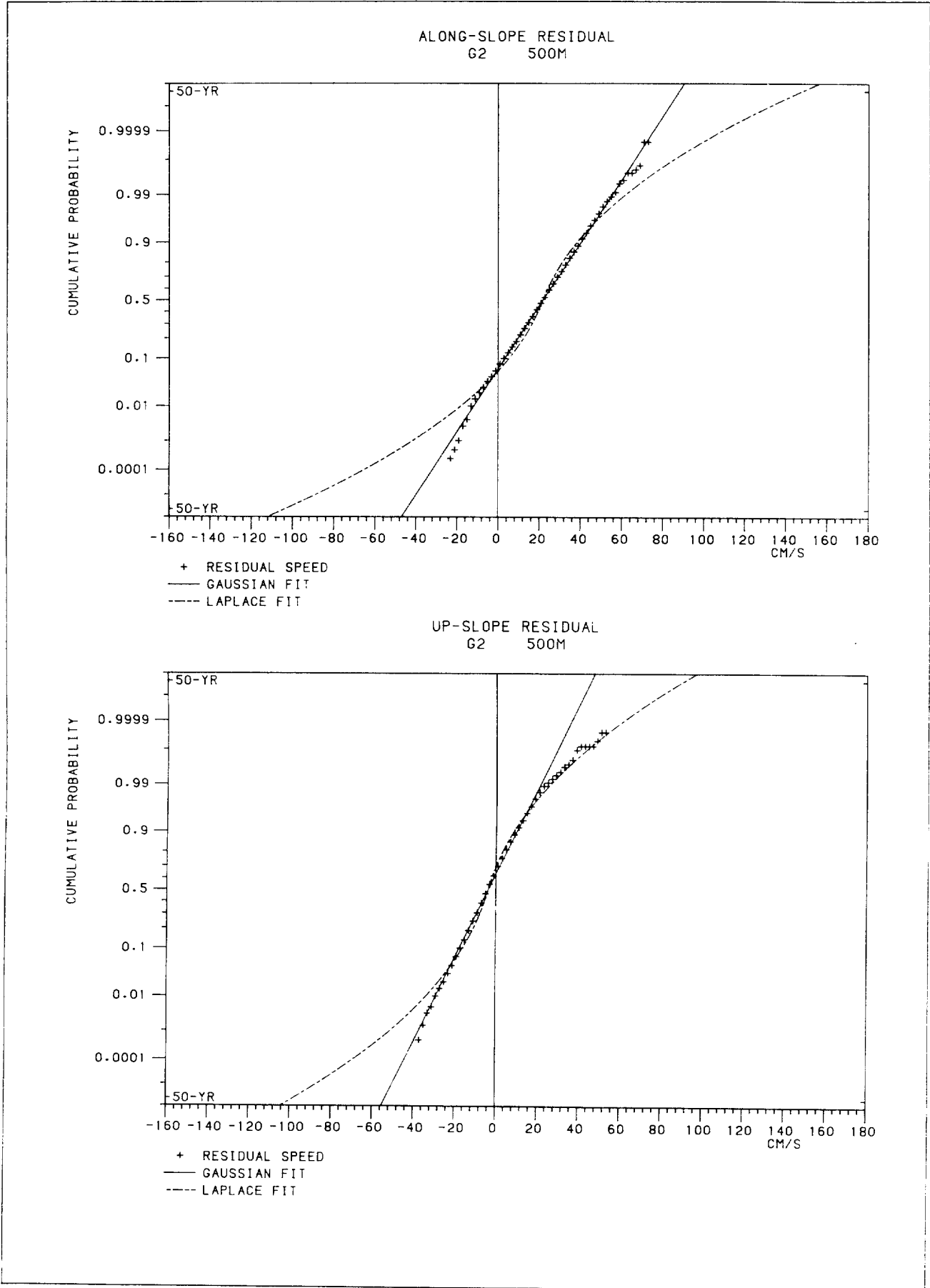


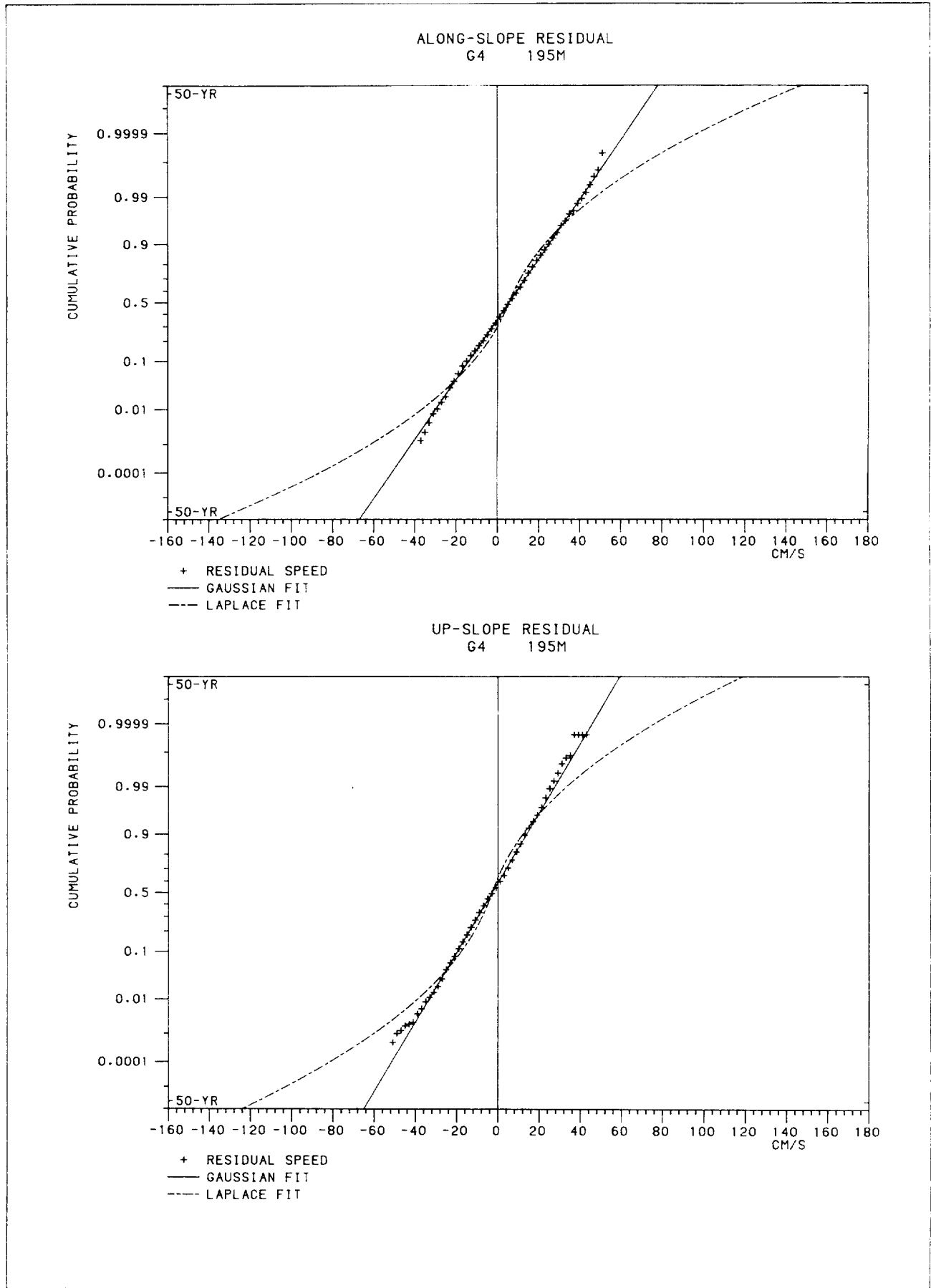
UP-SLOPE RESIDUAL
G1 166M



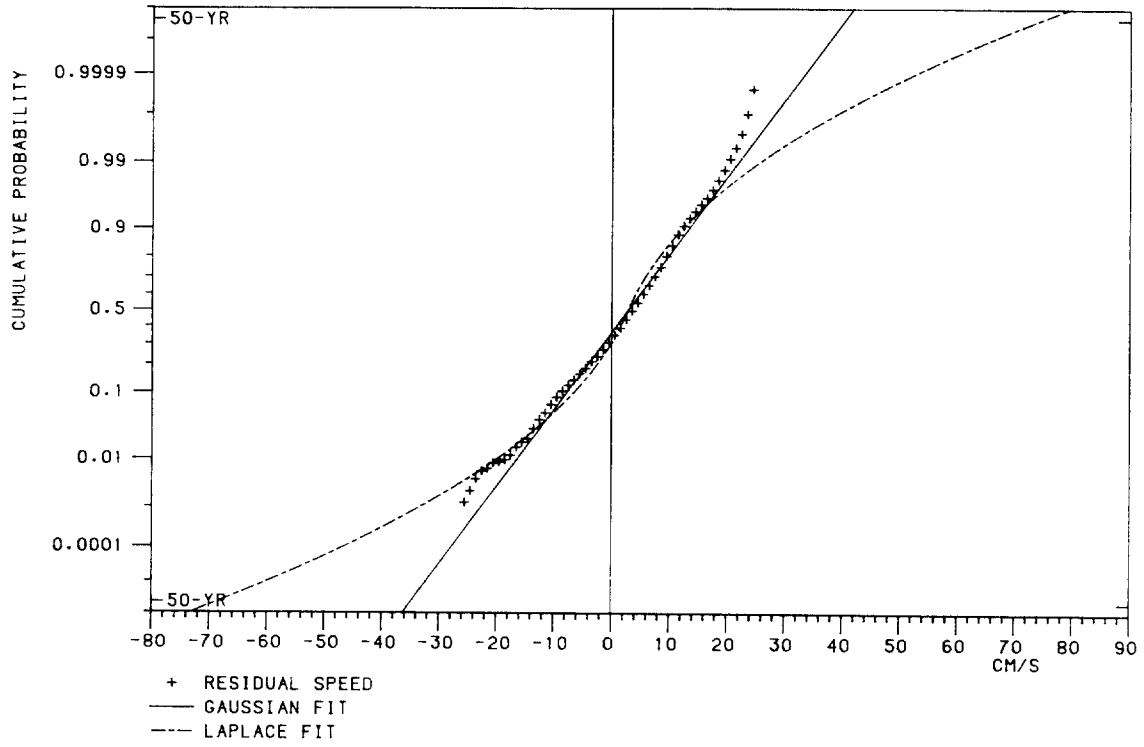




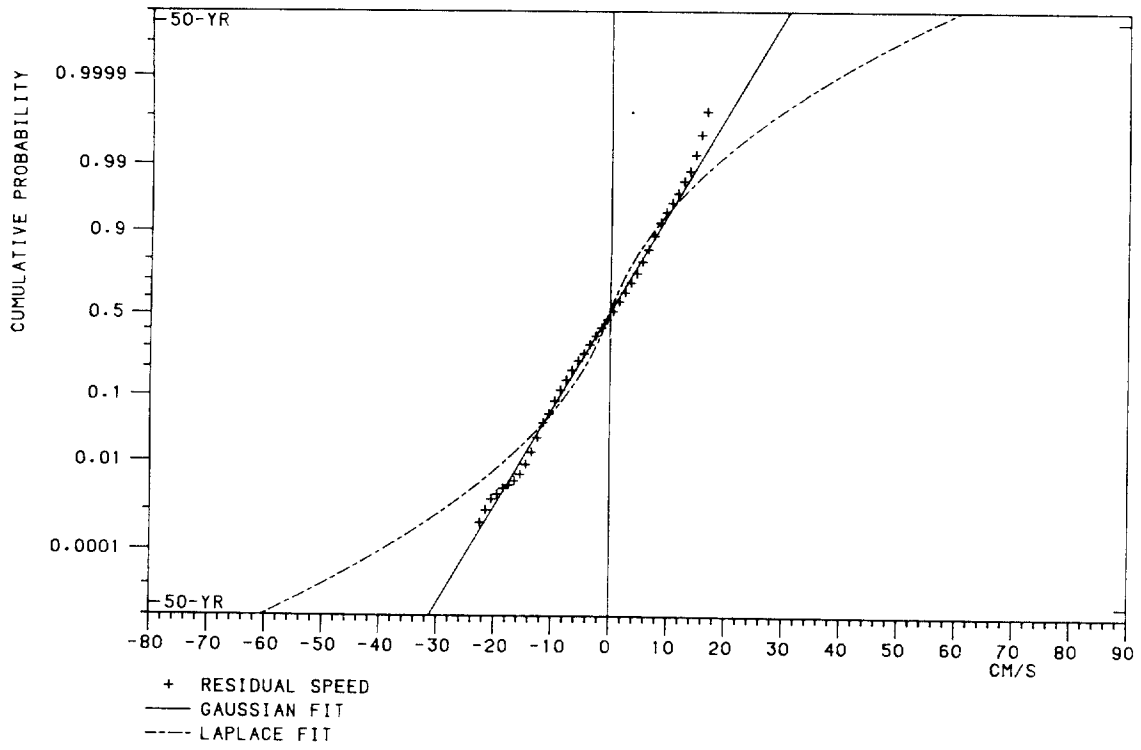




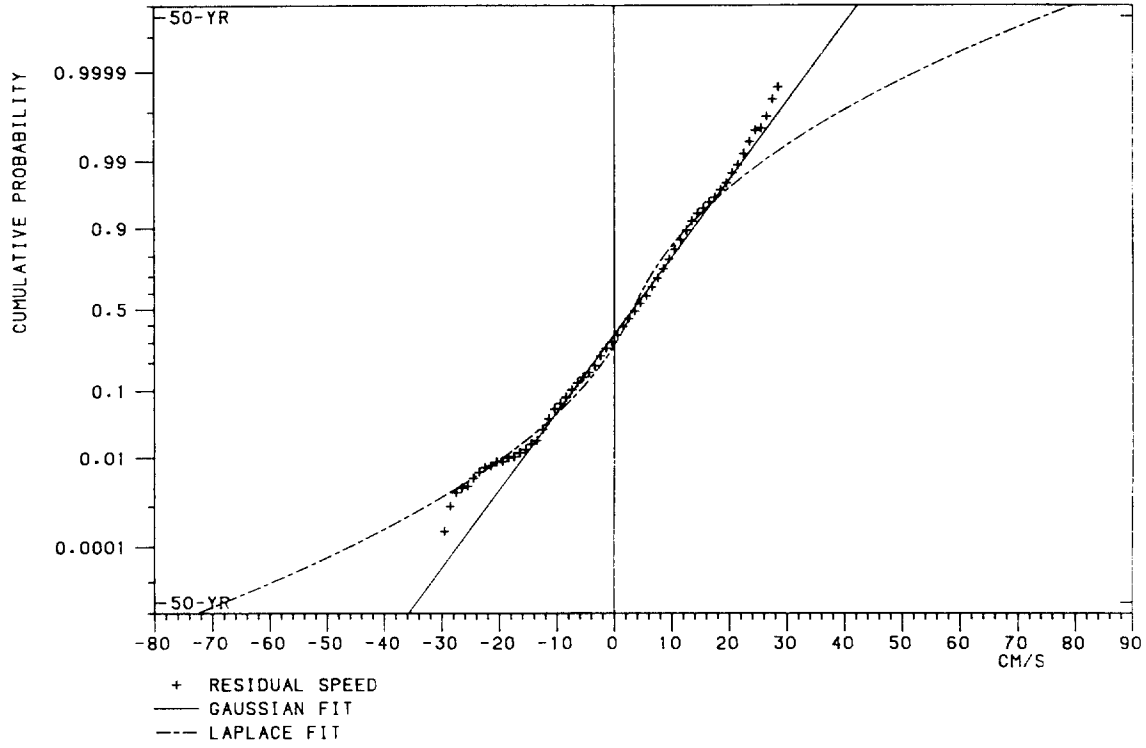
ALONG-SLOPE RESIDUAL
G4 1104M



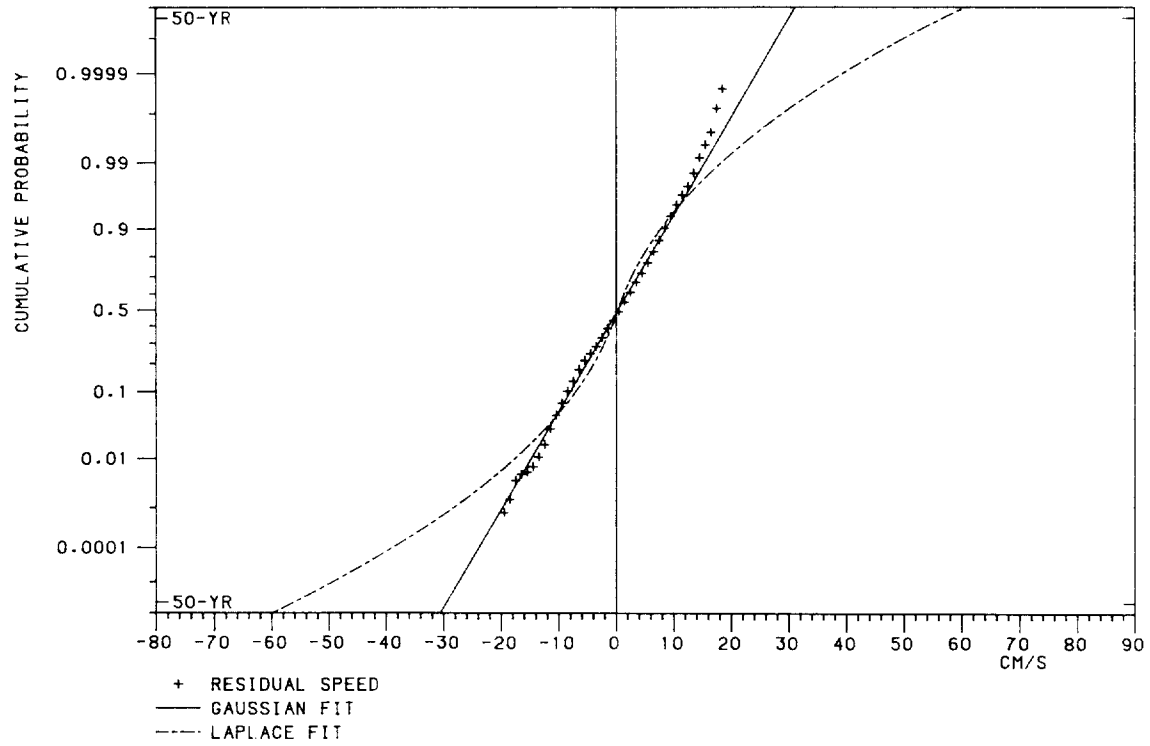
UP-SLOPE RESIDUAL
G4 1104M

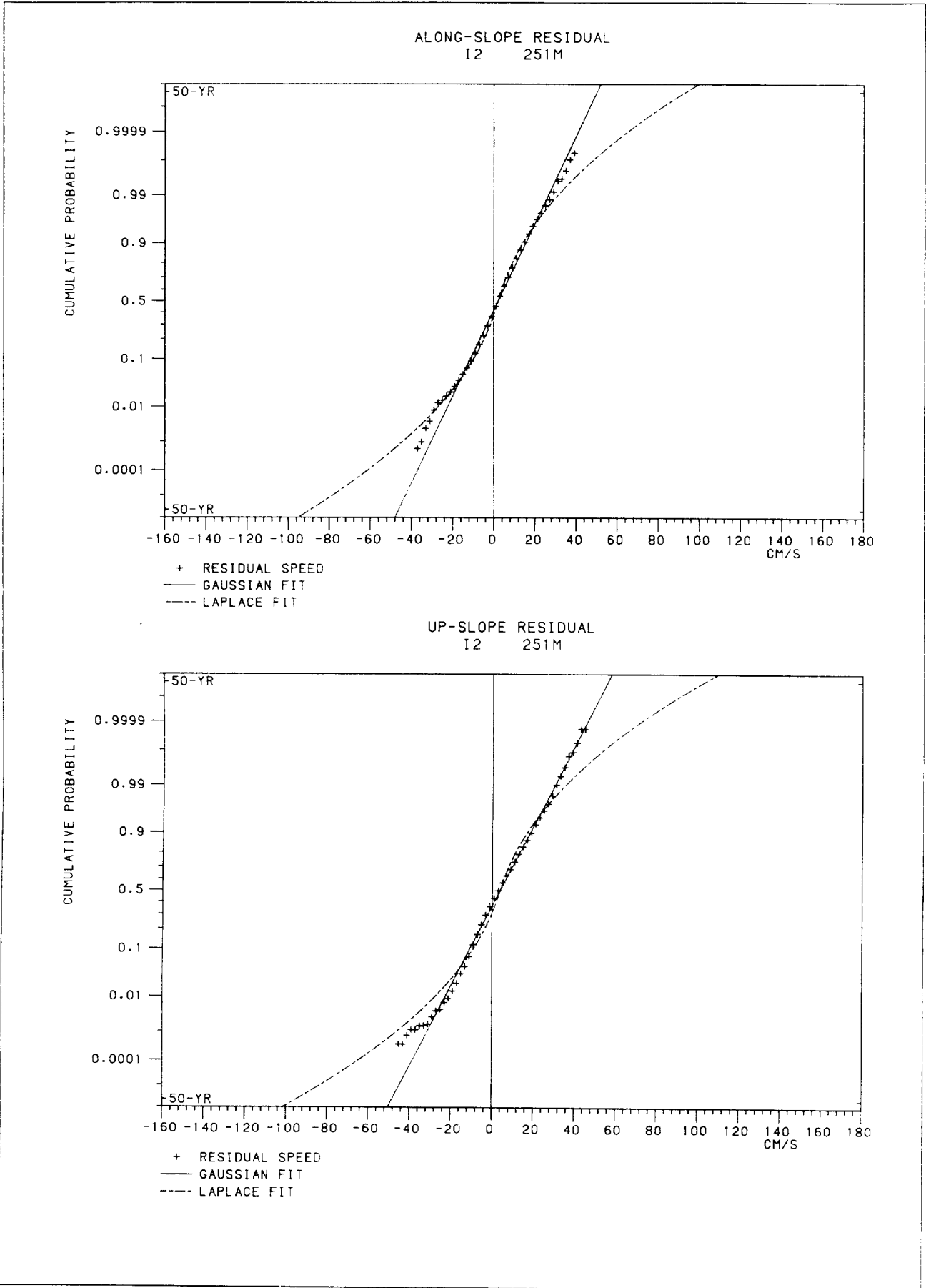


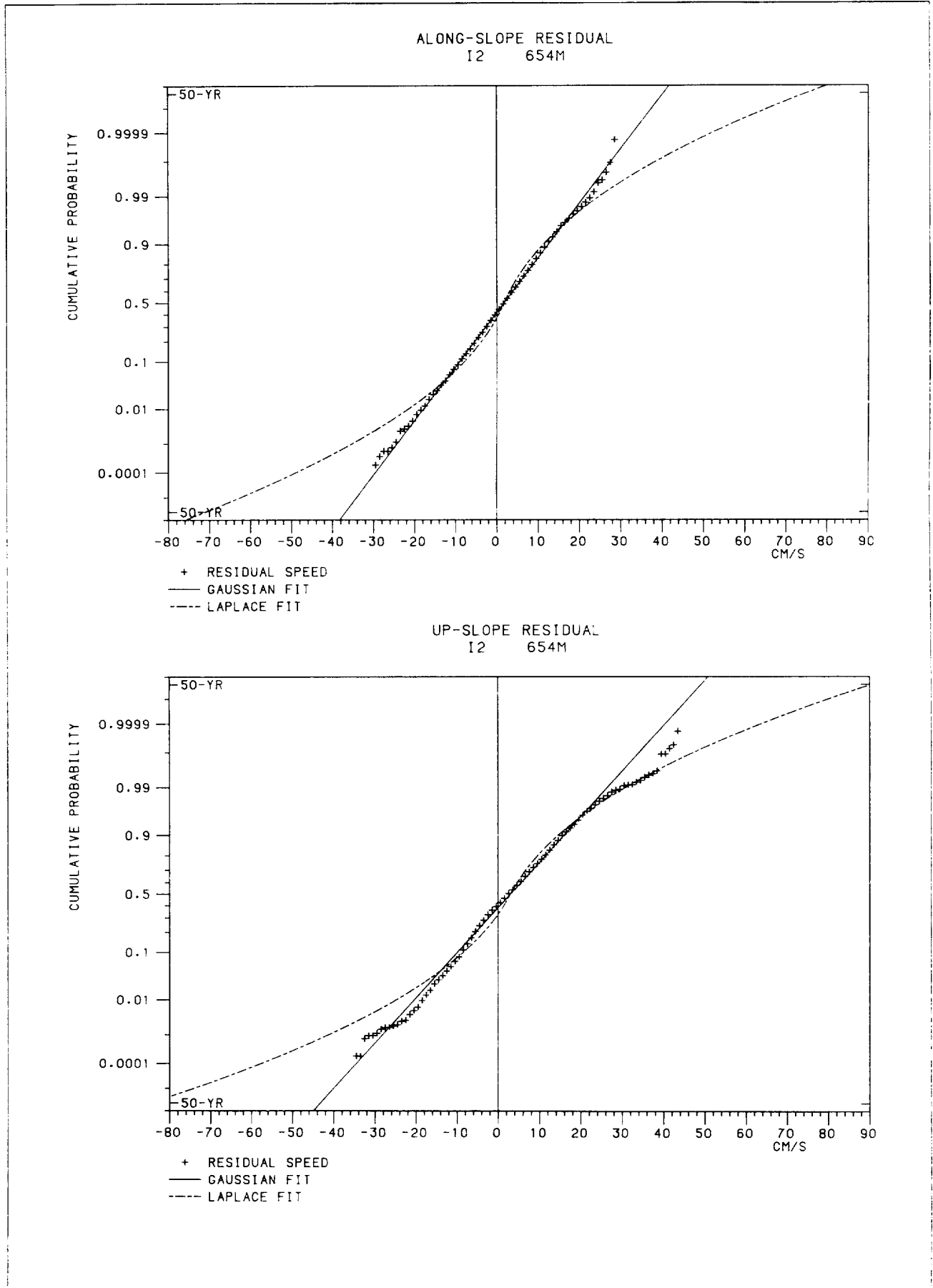
ALONG-SLOPE RESIDUAL
G4 1554M

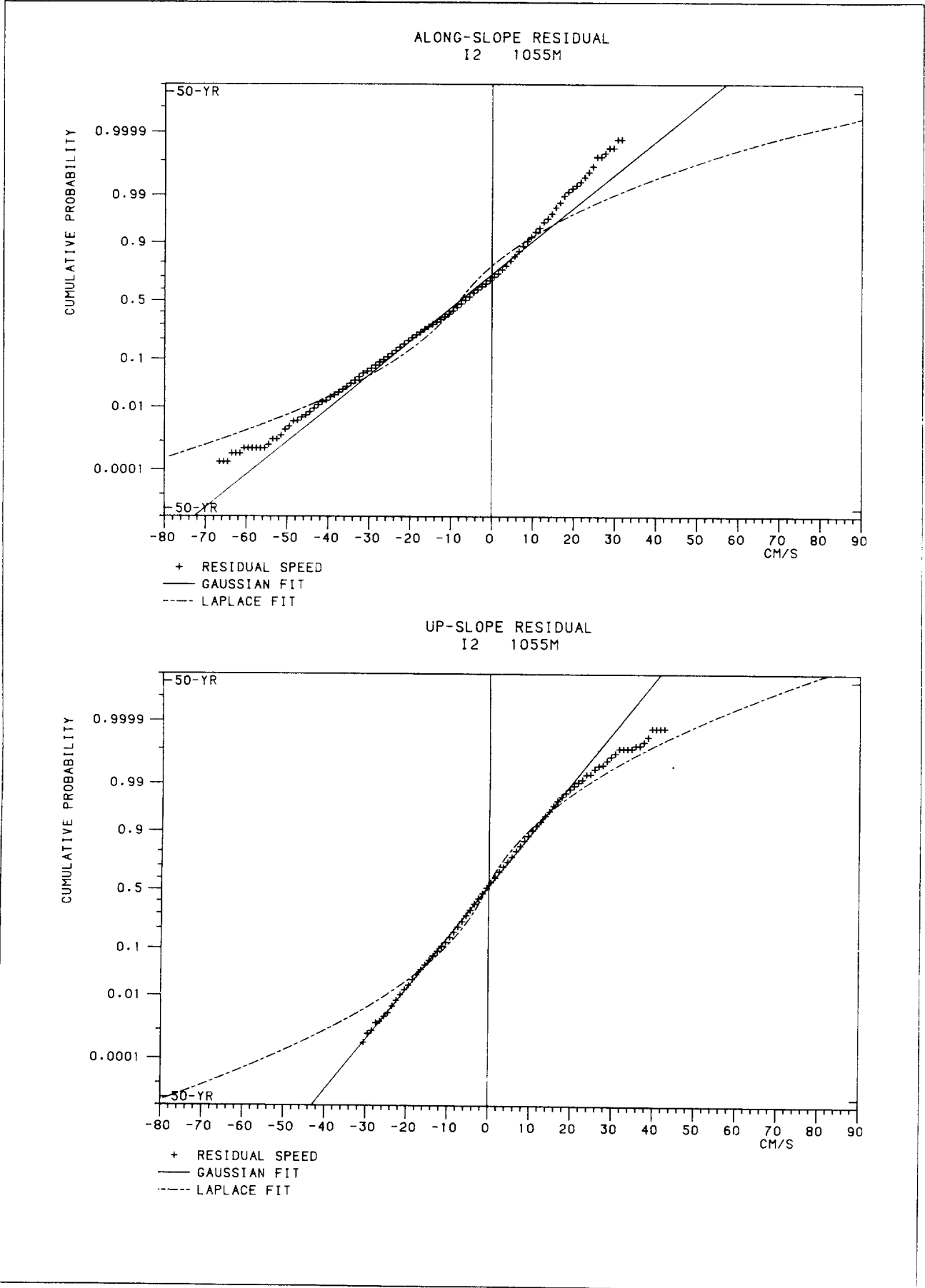


UP-SLOPE RESIDUAL
G4 1554M









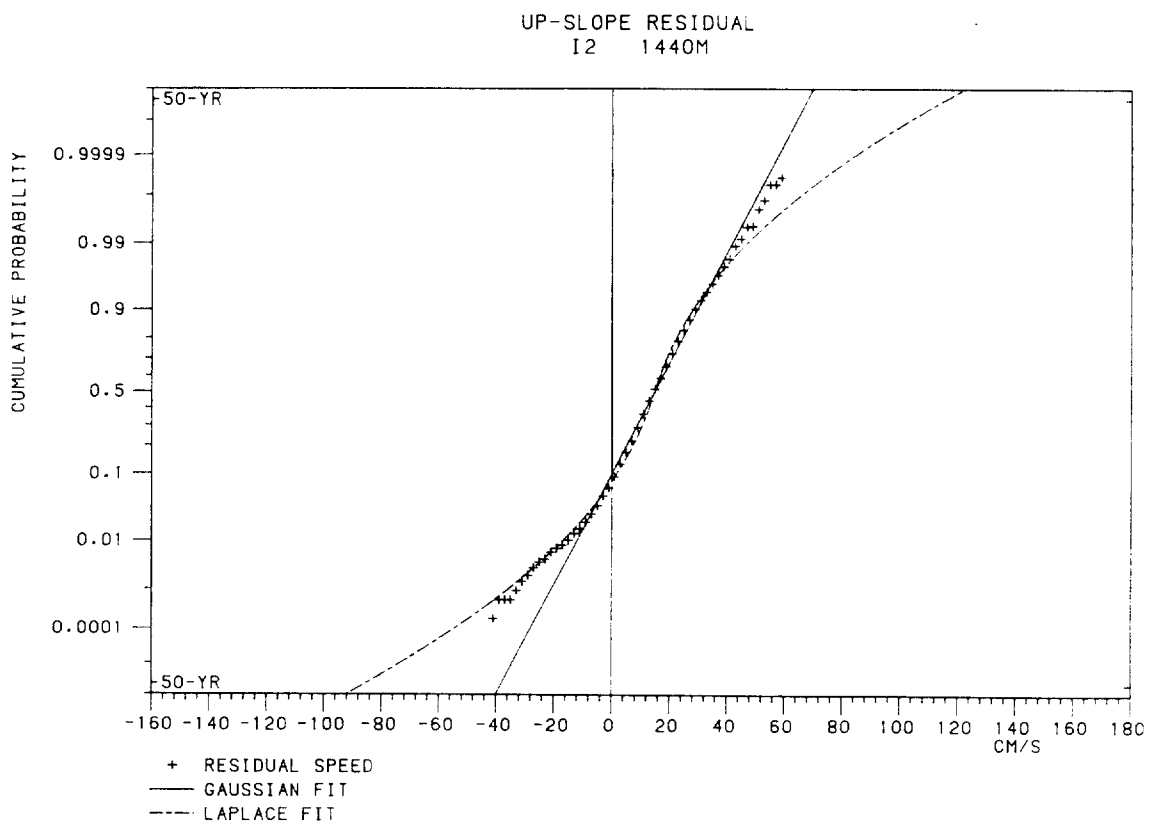
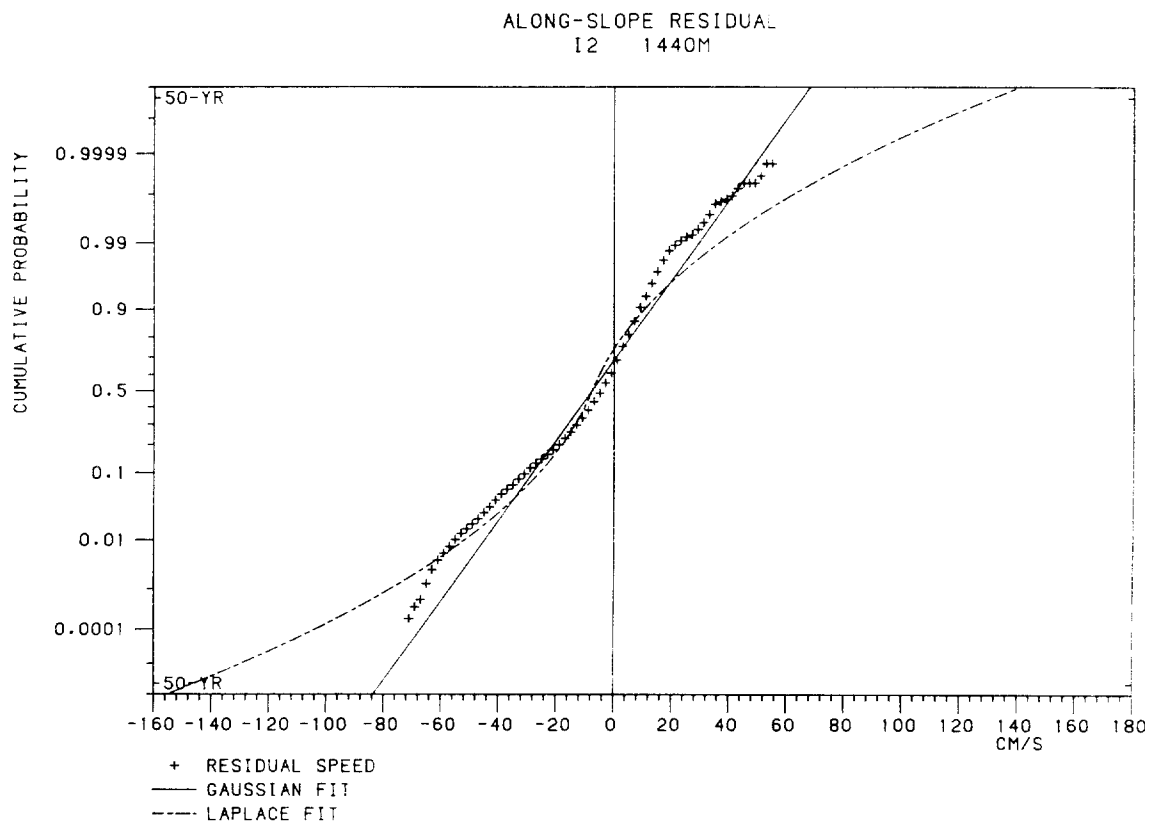


Fig.4: Examples of the joint probability distribution of tidal and residual currents.



